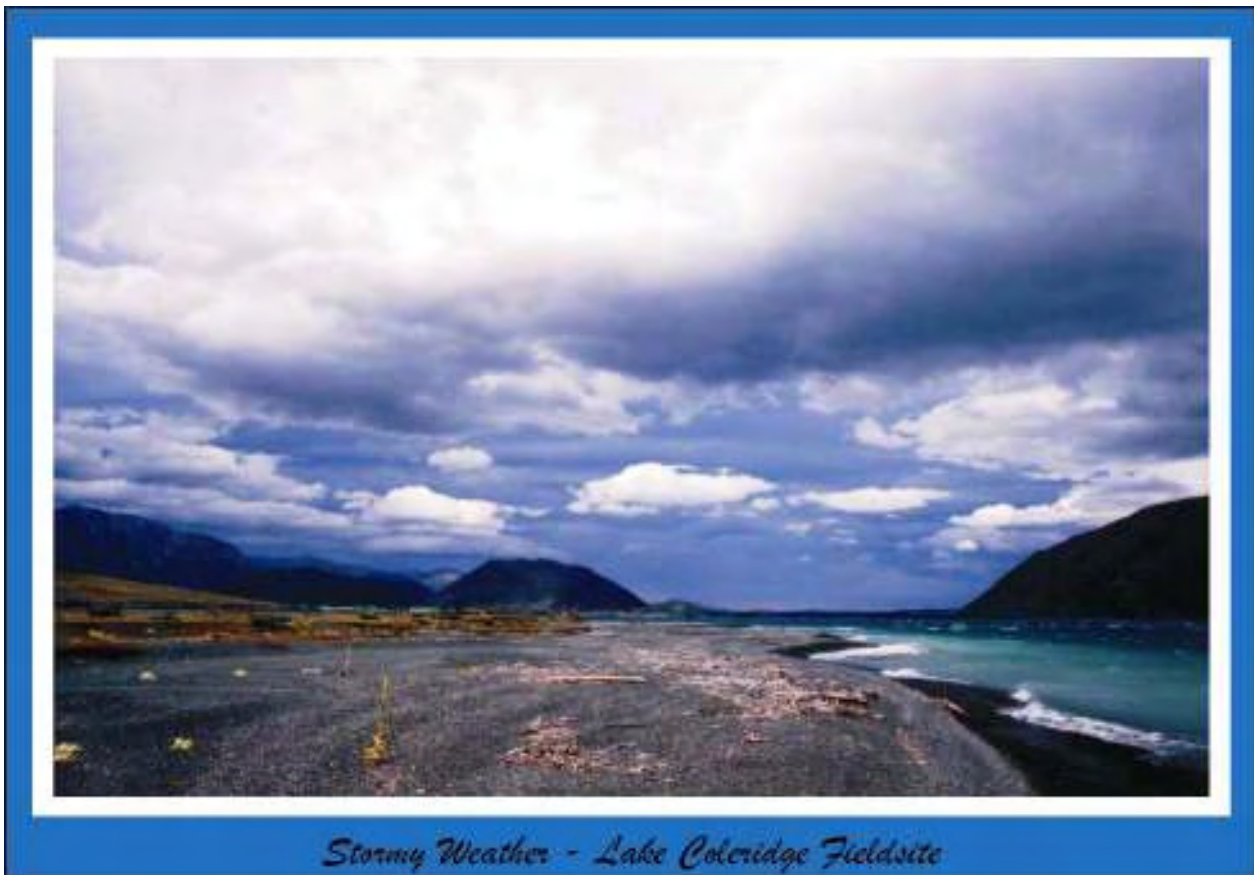

LONGSHORE SEDIMENT TRANSPORT ON A MIXED SAND AND GRAVEL LAKESHORE

**A THESIS SUBMITTED IN FULFILMENT
OF THE REQUIREMENTS FOR THE DEGREE OF
DOCTOR OF PHILOSOPHY IN GEOGRAPHY
IN THE UNIVERSITY OF CANTERBURY,
CHRISTCHURCH, NEW ZEALAND**

**BY
IAIN NICHOLAS DAWE**

**DEPARTMENT OF GEOGRAPHY
UNIVERSITY OF CANTERBURY
2006**

FRONTISPIECE



FOR MICHELLE

ABSTRACT

This thesis examines the processes of longshore sediment transport in the swash zone of a mixed sand and gravel shoreline, Lake Coleridge, New Zealand. It focuses on the interactions between waves and currents in the swash zone and the resulting sediment transport. No previous study has attempted to concurrently measure wave and current data and longshore sediment transport rates on a mixed sand and gravel lakeshore beach in New Zealand. Many of these beaches, in both the oceanic and lacustrine environments, are in net long-term erosion. It is recognised that longshore sediment transport is a part of this process, but very little knowledge has existed regarding rates of sediment movement and the relationships between waves, currents and swash activity in the foreshore of these beach types.

A field programme was designed to measure a comprehensive range of wind, wave, current and morphological variables concurrently with longshore transport. Four electronic instruments were used to measure both waves and currents simultaneously in the offshore, nearshore and swash zone. In the offshore area, an InterOcean S4ADW wave and current meter was installed to record wave height, period, direction and velocity. A WG-30 capacitance wave gauge measured the total water surface variation. A pair of Marsh-McBirney electromagnetic current meters, measuring current directions and velocities were installed in the nearshore and swash zone. Data were sampled for 18 minutes every hour with a Campbell Scientific CR23x data-logger. The wave gauge data was sampled at a rate of 10 Hz (0.1 s) and the two current meters at a rate of 2 Hz (0.5 s). Longshore sediment transport rates were investigated with the use of two traps placed in the nearshore and swash zone to collect sediment transported under wave and swash action. This occurred concurrently with the wave measurements and together yielded over 500 individual hours of high quality time series data.

Important new insights were made into lake wave processes in New Zealand's alpine lakes. Measured wave heights averaged 0.20-0.35 m and ranged up to 0.85 m. Wave height was found to be strongly linked to the wind and grew rapidly to increasing wind strength in an exponential fashion. Wave period responded more slowly and required time and distance for the wave length to develop. Overall, there was a narrow band of wave periods with means ranging from 1.43 to 2.33 s. The wave spectrum was found to be more mixed and complicated than had previously been assumed for lake environments. Spectral band width parameters were large, with 95% of the values between 0.75 and 0.90. The wave regime attained the characteristics of a storm wave spectrum. The waves were characteristically steep and capable of obtaining far greater steepness than oceanic wind-waves. Values ranged from 0.010 to 0.074, with an average of 0.051. Waves were able to progress very close to shore without modification and broke in water less than 0.5 m deep. Wave refraction from deep to shallow water only caused wave angles to be altered in the order of 10%. The two main breaker types were spilling and plunging. However, rapid increases in beach slope near the shoreline often caused the waves to plunge immediately landward of the swash zone, leading to a greater proportion of plunging waves. Wave energy attenuation was found to be severe. Measured velocities were some 10 times less at two thirds the water depth beneath the wave. Mean orbital velocities were 0.30 m s^{-1} in deep water and 0.15 m s^{-1} in shallow water. The ratio difference between the measured deep water orbital velocities and the nearshore orbital velocities was just under one half ($u_s/u_o = 0.58$), almost identical to the predicted phase velocity difference by Linear wave theory. In general Linear wave theory was found to provide good approximations of the wave conditions in a small lake environment.

The swash zone is an important area of wave dissipation and it defines the limits of sediment transport. The width of the swash zone was found to be controlled by the wave height, which in turn determined the quantity of sediment transported through the swash zone. It ranged in width from 0.05 m to 6.0 m and widened landward in response to increased wave height and lakeward in response to the wave length. Slope was found to be an important secondary control on swash zone width. In low energy conditions, swash zone slopes were typically steep. At the onset of wave activity the swash zone becomes scoured by swash activity and the beach slope grades down. An equation was developed, using the wave height and beach slope that provides close estimates of the swash zone width under a wide range of conditions. Run-up heights were calculated using the swash zone width and slope angle. Run-up elevations ranged from 0.01 m to 0.73 m and were strongly related to the wave height and the beach slope. On average, run-up exceeds the deep water wave height by a factor of $1.16H$. The highest run-up elevations were found to occur at intermediate slope angles of between 6° – 8° . Above 8° , the run-up declined in response to beach porosity and lower wave energy conditions. A generalised run-up equation for lake environments has been developed, that takes into account the negative relationship between beach slope and run-up. Swash velocities averaged 0.30 m s^{-1} but maximum velocities averaged 0.98 m s^{-1} . After wave breaking, swash velocities quickly reduced through dissipation by approximately one half. Swash velocity was strongly linked to wave height and beach slope. Maximum velocities occurred at beach slopes of 5° , where incident swash dominated. At slopes between 6° and 10° , swash velocities were hindered by turbulence, but the relative differences between the swash and backswash flows were negligible. At slope angles above 10° there was a slight asymmetry to the swash/backswash flow velocities due to beach porosity absorbing water at the limits of the swash zone. Three equations were developed for estimating the mean and maximum swash velocity flows. From an analysis of these interactions, a process-response model was developed that formalises the morphodynamic response of the swash zone to wave activity.

Longshore sediment transport occurred exclusively in the swash zone, landward of the breaking wave in bedload. The sediments collected in transit were a heterogeneous mix of coarse sands and fine-large gravels. Hourly trapped rates ranged from 0.02 to $214.88 \text{ kg hr}^{-1}$. Numerical methods were developed to convert trapped mass rates into volumetric rates that use the density and porosity of the sediment. A sediment transport flux curve was developed from measuring the distribution of longshore sediment transport across the swash zone. Using numerical integration, the area under this curve was calculated and an equation written to accurately estimate the total integrated transport rates in the swash zone. The total transport rates ranged from a minimum of $1.10 \times 10^{-5} \text{ m}^3 \text{ hr}^{-1}$ to a maximum of $1.15 \text{ m}^3 \text{ hr}^{-1}$. The mean rate was $7.36 \times 10^{-2} \text{ m}^3 \text{ hr}^{-1}$. Sediment transport was found to be most strongly controlled by the wave height, period, wave steepness and mean swash velocity. Transport is initiated when waves break at an oblique angle to the shoreline. No relationships could be found between the grain size and transport rates. Instead, the critical threshold velocities of the sediment sizes were almost always exceeded in the turbulent conditions under the breaking wave. The highest transport rates were associated with the lowest beach slopes. It was found that this was linked to swash high velocities and wave heights associated with foreshore scouring. An expression was developed to estimate the longshore sediment transport, termed the LEXSED formula, that divides the cube of the wave height and the wave length and multiplies this by the mean swash velocity and the wave approach angle. The expression performs well across a wide range of conditions and the estimates show very good correlations to the empirical data. LEXSED was used to calculate an accurate annual sediment transport budget for the field site beaches. LEXSED was compared to 16 other longshore sediment transport formulas and performed best overall. The underlying principles of the model make its application to other mixed sand and gravel beaches promising.

ACKNOWLEDGMENTS

There are many people I would like to thank who helped me at various stages through the task of researching and writing this thesis.

My supervising team deserve special thanks. Prof. Bob Kirk, Honorary Fellow, Department of Geography, University of Canterbury, always made time in his busy schedule. His ideas, many discussions, proof reading, support and encouragement over the years has been greatly appreciated. Thank you for introducing me to Lake Coleridge and visiting me in the field. Dr. Deirdre Hart, Department of Geography, University of Canterbury, kept me on track and encouraged me to keep going through the hard grind of writing a thesis. Her proof reading and constructive criticism was always helpful. Dr. Jon Allan, Oregon Department of Geology and Mineral Industries, was enormously helpful, tirelessly answering many questions regarding data analysis and the use of field equipment.

Conducting a PhD can be expensive and both the University of Canterbury and the Geography Department must be acknowledged for their generous financial support. In particular, financial support was provided by the University of Canterbury in the form of a Doctoral Scholarship, without which this work never would have happened. The Coastal Engineering Conference fund provided assistance to attend international coastal conferences in Rotorua and China. Special thanks must also go to the Department of Geography equipment grants committee for providing funds to buy the CR23x data logger. Without this piece of equipment the, the wave and current sampling would have been nearly impossible.

Heartfelt thanks go to the survey field assistants, Rob Leppard, Justin Harrison and Jason Harbrow for enduring long days of peering through a prism through all the *delightful* weather that Lake Coleridge has to offer. Also, Grant Cosslett for help in building the concrete mooring blocks for the S4. My brother Paul, for visiting me in the long and lonely days of field work. He said Lake Coleridge must be the one of the windiest places on earth. At this stage I can confirm; it is *the* windiest place on earth.

Particular thanks and acknowledgement go to Mike and Karen Meares from Ryton Station at Lake Coleridge, for generously allowing free access on farm vehicle tracks and camping at the field site. Also at Lake Coleridge, John Dignan, TrustPower generation manager for providing information about the Lake Coleridge power scheme operations and water-level data.

Many instruments were used in course of this study and I am grateful to all the people who provided advice concerning the operation and deployment of this equipment. Dr. David Mitchell, University of Sydney, Dr. Rob Brander, University of New South Wales and Prof. Kevin Parnell, Auckland University, for advice and discussion on using wave gauges and wave analysis software. Further advice and information on using the wave gauge was provided by Michael Skafel from the National Water Research Institute, Canada. Dr. Rachel Spronken-Smith, Otago University, Prof. Andy Sturman, University of Canterbury and Dr. Andrew Oliphant, Atmospheric Science Program, Indiana University all generously gave advice for using and programming data loggers. Dr. Anna Taylor gave excellent advice and information about using the Marsh-McBirney current meters.

One cannot forget the Geography department techies, Justin Harrison, Walter Gallagher, Gary Smith and Nick Key for their advice and patience in answering many questions regarding the use of field equipment and for repairing it, when it all went wrong. Graham Furniss for patiently

helping me out with numerous computer problems, answering my seemingly simple questions and securing Lake Coleridge wind data from the dark recesses of the Niwa digital archives. Steven Sykes for solving curly computer glitches for ‘gently coaxing’ windows software to do what it’s told. Janet Bray, former department librarian, for obtaining air photo information for Lake Coleridge.

Thanks must go to the staff at NIWA in Christchurch. Dr. Ian Hawes for generously providing time series wind data from research at Lake Coleridge. Dr. Murray Hicks for freely providing time for discussion and ideas in the formative stages of the research. Graham Elley and Warren Thompson also provided information the use of the S4 and other technical equipment.

During the analysis stage I called on the help of a number of people. I would like to thank Prof. Paul Komar, Oregon State University, for advice on developing my sediment transport equation and for providing ideas and discussion regarding sediment transport and in developing mathematical formulas in general. Dr Nicolai Speranski, FURG, Brazil, for providing references and ideas in the early phases of the research. Dr. Brian Anderson, Victoria University, for helping with some of the mathematics and for bouncing ideas about the physics of water motion in the shoreline. Prof. Andrew Chadwick, University of Plymouth, freely provided information about the BORESED Model he developed from gravel beach research in the United Kingdom.

I also thank Dr. Maree Hemmingsen and Dr. Martin Single for the many discussions regarding coastal research, the field trips and the advice that all had a hand in the formulation and development of the ideas in this thesis.

As any researcher and writer can attest, no such work would be possible with the support of friends and family. In particular I would like to pay special tribute to the incredible support of my parents Mary-Louise and Arthur Douglas Wethey. Also, Nicola and Terry Hockley for companionship, good meals and time out over the years that has preserved my sanity.

Last and most importantly, to my wife Michelle, words are not enough to describe my deep felt gratitude for her steadfast support of this project. Without her constant love and encouragement over the years, this work would never have been possible. Thank you.

CONTENTS

Abstract	iv
Acknowledgements	vi
Contents	viii
Figures and Tables	xii
List of Symbols	xix

Chapter 1.	The Research Problem	1
1.1	Purpose for research	1
1.2	Significance of Longshore Sediment Transport	2
1.3	Sediment Transport Systems	4
1.4	Mixed Sand and Gravel Beach Research	8
1.5	Morphodynamics of a Mixed Sand and Gravel Beach	10
1.6	Lake Shoreline Research	15
1.7	Oceanic and Lake Shoreline Differences	19
1.8	Conceptual Lakeshore Sediment Transport Model	24
1.9	Terms and Aims of Research	25

Chapter 2.	Lake Coleridge	27
2.1	Introduction	27
2.2	Geology and Topography	31
2.3	Climate and Catchment	36
	<i>Wind Measurements</i>	38
	<i>Water Balance</i>	46
2.4	Fieldsite	47
2.5	Summary	57

Chapter 3.	Fieldwork Programme	59
3.1	Fieldwork Programme Overview	59
3.2	Wave and Current Recording Instruments	63

	<i>InterOcean S4ADW</i>	63
	<i>WG-30 Capacitance Wave Gauge</i>	65
	<i>Marsh-McBirney Electromagnetic Current Meters</i>	67
3.3	Sediment Transport Measurement and Methods	68
	<i>Sediment Streamer Traps</i>	71
3.4	Summary	73
<hr/>		
Chapter 4.	Lake Waves	75
4.1	Introduction	75
4.2	Raw Data Analysis Methods	76
	<i>Wave Gauge Data</i>	76
	<i>InterOcean S4ADW Data</i>	79
	<i>Current Meter Data</i>	81
4.3	Comparison of Wave Gauge and S4 Pressure Sensor Data	82
4.4	Deep Water Wave Measurements	87
	<i>Wave Height</i>	88
	<i>Wave Period</i>	94
4.5	Comparison of Wave Height Statistics	99
4.6	Wave Length and Steepness	101
4.7	Waves in the Nearshore	105
	<i>Current Speeds</i>	105
	<i>Breaker Types</i>	106
	<i>Breaker Height and Depth</i>	112
	<i>Wave Direction and Refraction</i>	115
4.8	Summary	116
<hr/>		
Chapter 5.	Swash Zone Processes	119
5.1	Introduction	119
5.2	Swash Zone Research	120
5.3	Swash Zone Width and Run-up Length	121
	<i>Swash Length Equations</i>	128
5.4	Swash Zone Elevation and Run-up Height	131
	<i>Run-up Models</i>	139
5.5	Swash Zone Currents	145
	<i>Current Measurements</i>	148
<hr/>		
<hr/>		

	Swash Phase	158
	Swash Velocity Equations	161
5.6	Swash Zone Process-Response Model	168
5.7	Summary	170
<hr/>		
Chapter 6.	Longshore Sediment Transport	173
6.1	Introduction	173
6.2	NZ Studies of Longshore Transport in the Swash Zone	174
6.3	Overview of Sediment Transport Measurements	175
6.4	Grain Size Analysis	177
6.5	Calculating the Sediment Transport Rate	181
	<i>Hourly Transport Rate</i>	181
	<i>Volumetric Transport Rate</i>	182
	<i>Total Integrated Longshore Transport Rate</i>	183
6.6	Nature of Sediment Transport in a Lakeshore Beach	189
	<i>Role of Wave Height</i>	191
	<i>Role of Wave Period, Length and Steepness</i>	194
	<i>Role of Wave Direction</i>	197
	<i>Role of Swash Velocity</i>	200
	<i>Role of Swash Zone Slope and Width</i>	202
	<i>Role of Grain Size</i>	205
6.7	New Longshore Sediment Transport Equation	210
	<i>Practical Application of LEXSED Formula</i>	216
6.8	Bagnold Longshore Transport Derivation	220
6.9	Summary	221
<hr/>		
Chapter 7.	Sediment Transport Models	225
7.1	Introduction	225
7.2	Historical Development of Longshore Transport Equations	226
7.3	Development of the Inman and Bagnold Formula	228
7.4	Testing the Inman and Bagnold Formula	234
7.5	Variation of K with Environmental Parameters	237
	<i>Variation of K with Grain Size</i>	238
	<i>Variation of K with Iribarren Parameter</i>	243
7.6	Inman and Bagnold Formula Variations	249
<hr/>		

	<i>Brampton & Motyka Variation</i>	249
	<i>Chadwick Variation</i>	251
7.7	Stream Power Approaches to Sediment Transport Modelling	252
	<i>Bailard Equation</i>	252
	<i>Morfett Equation</i>	257
	<i>BORESED Model</i>	260
7.8	Dimensional Analysis Models of Longshore Transport	264
	<i>Kamphuis Equations</i>	265
	<i>Delft Equations</i>	270
	<i>LEXSED Formula</i>	274
7.9	Summary and Discussion	276
<hr/>		
Chapter 8.	Conclusion	285
8.1	Thesis Aims Revisited	285
8.2	Summary of Major Findings	289
	<i>Lake Waves</i>	289
	<i>Swash Zone Processes</i>	291
	<i>Longshore Sediment Transport</i>	294
	<i>Longshore Sediment Transport Models</i>	297
8.3	Suggestions for Future Research	300
<hr/>		
	Appendices	303
1	Summary Wind Data	303
2	(A) Wave Gauge Raw Data Printout	304
	(B) Current Meter Raw Data Printout	305
3	(A) Grain Size Percentile Calculation	306
	(B) Grain Size And Sorting Nomenclature	307
4	(A) Solid Density Calculation	308
	(B) Sediment Porosity and Volume Calculation	309
5	Hourly Wave Summary Statistics	311
6	Hourly Swash Zone Summary Statistics	325
7	Field Data Summary Statistics by Site	339
	References	343

FIGURES AND TABLES

Chapter 1	The Research Problem	
Figure 1.1	Lake Coleridge/Whakamatau area map	3
Figure 1.2	Schematic of wave orbital motions	5
Figure 1.3	Plan form of sediment transport process in littoral zone	6
Figure 1.4	Sediment transport modes	7
Figure 1.5	Mixed sand and gravel beach profile	11
Figure 1.6	Sandy beach profile	13
Figure 1.7	Idealised lake beach profile	23
Figure 1.8	Conceptual model of a lacustrine beach	25

Chapter 2	Lake Coleridge	
Figure 2.1	Lake Coleridge area map	29
Figure 2.2	Geology map of the Lake Coleridge area	32
Figure 2.3	Aerial photograph of Lake Coleridge	33
Figure 2.4	View of the southern end of Lake Coleridge	34
Figure 2.5	View of the northern end of Lake Coleridge	34
Figure 2.6	Length to width relationship of 20 largest South Island Lakes	35
Figure 2.7	Weather station on southern corner of Cottons Lagoon	39
Figure 2.8	Wind roses for all locations around Lake Coleridge	40
Figure 2.9	Scatter plot of wind speed against wind direction	41
Figure 2.10	Percentage wind directions for all Lake Coleridge wind data	42
Figure 2.11	Percentage wind strength for all Lake Coleridge wind data	43
Figure 2.12	Wind roses for selected Canterbury locations	44
Figure 2.13	(A) Monthly frequency of winds > 29 Kph	45
	(B) Monthly frequency of winds < 29 Kph	45
Figure 2.14	Plan-view fieldwork location	48
Figure 2.15	Survey profiles from site C010	50
Figure 2.16	View looking northwest from site C010	51
Figure 2.17	Survey profiles from site C040	51
Figure 2.18	View looking southwest from site C040	52
Figure 2.19	Aerial geomorphic map of fieldsite	53
Figure 2.20	Cottons Lagoon	56

Table 2.1	Dimensions of the 20 largest South Island lakes	36
Table 2.2	Shoreline orientation of sample sites	47
<hr/>		
Chapter 3	Fieldwork Programme	
Figure 3.1	Field equipment array	61
Figure 3.2	S4ADW showing mooring set-up	63
Figure 3.3	Wave staff deployed in action	66
Figure 3.4	Swash zone current meter	68
Figure 3.5	Sediment trap deployed in swash zone	72
<hr/>		
Chapter 4	Lake Waves	
Figure 4.1	A 30 s sample of a wave record	78
Figure 4.2	Correlation of H_s from the wave gauge against the S4	84
Figure 4.3	Correlation of T_z from wave gauge and T_s from S4	84
Figure 4.4	Wave heights frequency distributions from wave gauge	89
Figure 4.5	Wave height percentage exceedence curves	91
Figure 4.6	Regression of wind speed against H_{rms}	93
Figure 4.7	(A) Wind and wave trace in southeast conditions	94
	(B) Wind and wave trace in Gusty northwest conditions	94
Figure 4.8	Wave period percentage exceedence curves	95
Figure 4.9	Comparison of spectral band width and wind direction	96
Figure 4.10	Correlation of T_z and H_s	97
Figure 4.11	Correlation of spectral band width and peak spectral period	98
Figure 4.12	Linear regression of H_s and wave length calculated with T_z	102
Figure 4.13	Regression of H_s and wave steepness	104
Figure 4.14	Graphical output of breaker types measured in Lake Coleridge	109
Figure 4.15	Breaker types estimated from Lake Dunstan	110
Figure 4.16	Main breaker types observed in Lake Coleridge	112
Figure 4.17	Percentage exceedence curves for breaker heights	113
Figure 4.18	Frequency distribution of breaker depths	114
Figure 4.19	(A) Frequency distribution of deep water wave directions	116
	(B) Frequency distribution of shallow water wave directions	116
Figure 4.20	Breaker angles measured with the swash zone current meter	116

Table 4.1	Wave parameters calculated with S4 and wave gauge data	81
Table 4.2	Correlations of H_0 and T_z from wave gauge and pressure data	85
Table 4.3	Wave gauge wave height summary statistics	89
Table 4.4	Recalculated H_s values from the wave gauge and S4	91
Table 4.5	Regression statistics for wind speed versus H_{rms}	93
Table 4.6	Wave period summary statistics from wave gauge and S4	95
Table 4.7	Statistical ratios between different wave height parameters	101
Table 4.8	Wave steepness values measured in New Zealand lakes	103
Table 4.9	Phase velocity and wave orbital speeds	106
Table 4.10	Threshold limits for breaker criteria equations	108
Table 4.11	Summary statistics for the breaker criteria equations	108

Chapter 5	Swash Zone Processes	
Figure 5.1	Frequency distribution of the measured swash zone widths	122
Figure 5.2	Linear regression of wave height and swash zone width	124
Figure 5.3	Time series of swash slope and wave height	126
Figure 5.4	Regression between beach slope and swash zone width	127
Figure 5.5	Correlation between the measured and estimated X_{sw}	129
Figure 5.6	(A) curves for X_{sw} with varying slope	131
	(B) Estimate curves for X_{sw} with varying wave height	131
Figure 5.7	Correlation of critical S_{wl} with measured values	131
Figure 5.8	Method for calculating run-up	132
Figure 5.9	Frequency distribution of run-up heights	133
Figure 5.10	Regression of wave height and run-up	134
Figure 5.11	View along fieldsite foreshore showing scarps	135
Figure 5.12	View of along a low ridge in the shoreline	136
Figure 5.13	Regression of run-up with swash zone slope	138
Figure 5.14	Comparison of relative run-up to beach slope	138
Figure 5.15	Average relative run-up ratios (R/H)	139
Figure 5.16	Correlations of measured and calculated run-up	143
Figure 5.17	Correlation of Equation 5.11 and measured run-up	145
Figure 5.18	Measured run-up compared to tested equations	145
Figure 5.19	(A) Frequency distributions for mean swash velocity	149
	(B) Frequency distributions for max swash velocity	149
Figure 5.20	Relative difference between swash backswash velocity	150

Figure 5.21	Correlation between mean swash and backswash velocities	151
Figure 5.22	(A) Frequency distribution for the mean swash velocities	151
	(B) Frequency distribution for the mean backswash velocities	151
Figure 5.23	(A) Regression of wave height and swash velocity	153
	(B) Regression of wave period and swash velocity	153
	(C) Regression of swash zone slope and swash velocity	153
	(D) Regression of wave steepness and swash velocity	153
Figure 5.24	Difference of swash and backswash velocity against slope	154
Figure 5.25	Difference of swash and backswash velocity against H_{rms}	155
Figure 5.26	Regression of wave energy against mean relative swash velocity	156
Figure 5.26	Plot of mean swash velocity against the swash angle	157
Figure 5.27	Relationship between mean swash velocity and swash phase	160
Figure 5.28	Correlation of max swash velocities and Equation 5.14	162
Figure 5.29	Correlation of mean swash velocity and Equation 5.15	164
Figure 5.30	Estimate curves of Equation 5.15 swash velocity	164
Figure 5.31	Comparison of measured and estimated swash velocities	166
Figure 5.32	Correlation of swash velocities and Equation 5.16a	167
Figure 5.33	Estimate curves of Equation 5.16 mean swash velocity	167
Figure 5.34	Process-Response model of swash zone development	169
Table 5.1	Regression of X_{sw} and four environmental parameters	123
Table 5.2	Correlations of run-up and five environmental parameters	134
Table 5.3	Results of calculations from run-up equations	143
Table 5.4	Summary of swash zone velocity from coarse grained beaches	148
Table 5.5	Swash Zone flow velocity statistics	149
Table 5.6	Difference of swash and backswash at slope intervals	154
Table 5.7	Summary statistics of swash velocity equations	166
<hr/>		
Chapter 6	Longshore Sediment Transport	
Figure 6.1	Mean grain size distribution	179
Figure 6.2	(A) Distribution of D_{10} percentile grain sizes	179
	(B) Distribution of D_{90} percentile sizes grain sizes	179
Figure 6.3	Sorting of trapped sediment data	180
Figure 6.4	Typical modal classes in transit in the swash zone	181
Figure 6.5	Typical trap variation over a 10 min period	182
Figure 6.6	Swash zone transport flux distribution curve	185
<hr/>		

Figure 6.7	Total integrated transport rate calculation curve	186
Figure 6.8	Correlation of new integrated rate equations	189
Figure 6.9	Time series of sediment transport and wave height	192
Figure 6.10	(A) Regression of wave height and transport for all sites	193
	(B) Regression of wave height and transport (excl. C013)	193
Figure 6.11	Regression of wave height and transport rate at C010	194
Figure 6.12	Time series of longshore transport and wave period	195
Figure 6.13	(A) Regression of wave period and transport for all sites	196
	(B) Regression of wave period and transport (excl. C013)	196
Figure 6.14	Relative longshore sediment transport by wave direction	199
Figure 6.15	(A) Regression of swash velocity and transport for all sites	201
	(B) Regression of swash velocity and transport (excl. C013)	201
Figure 6.16	(A) Regression of slope and longshore transport for all sites	203
	(B) Regression of slope and longshore transport (excl. C013)	203
Figure 6.17	Relative and actual transport rate curves by swash slope	204
Figure 6.18	Forces acting on sediment grains in a fluid flow	206
Figure 6.19	Grain size threshold curve for the coarse sediment	206
Figure 6.20	(A) Scatter plot of swash velocity and D_{10} grain size	208
	(B) Scatter plot of D_{10} grain size and sediment transport rate	208
Figure 6.21	(A) Measured transport vs. LEXSED rates for all sites	213
	(B) Measured transport vs. LEXSED rates (excl. C013)	213
Figure 6.22	Forecast curves for new transport equation	215
Figure 6.23	Extended forecast curves using new transport equation	215
Figure 6.24	Evolution of barrier foreland	219
Figure 6.25	Correlation of Equation 6.11 against measured transport	220
Table 6.1	Summary statistics of longshore transport	188
Table 6.2	Variation in longshore transport rates by site	190
Table 6.3	Correlations of transport rate and environmental parameters	191
Table 6.4	Correlations between transport and H_{rms} by site	192
Table 6.5	Correlations between transport and period by site	195
Table 6.6	Correlations between transport and wave steepness by site	197
Table 6.7	Correlations between transport and breaker angles by site	198
Table 6.8	Correlations between transport and swash velocity by site	201
Table 6.9	Correlations between transport and slope by site	203
Table 6.10	Correlations between transport Iribarren number by site	205

Table 6.11	Correlations between transport and grain size by site	207
Table 6.12	Correlations of measured and new equation transport rates	213
Table 6.13	Statistics for measured and new equation transport rates	215
<hr/>		
Chapter 7	Sediment Transport Models	
Figure 7.1	Correlation of wave power (P_I) and ITR (I_I), in Komar (1976)	231
Figure 7.2	(A) Regression between LWP and ITR transport rate	235
	(B) Regression between LWP $\sin\alpha_b$ and ITR	235
Figure 7.3	(A) Regression between LWP and ITR with mod. I & B eqtn.	236
	(B) Regression between LWP and ITR with Equation 7.12	236
Figure 7.4	Variation in K with grain size, in Swart (1976)	239
Figure 7.5	Variation in K with grain size, in Bruno (1980)	240
Figure 7.6	Plot of K versus grain size, between beach types	241
Figure 7.7	Plot of D_{50} grain size versus K for Lake Coleridge data	241
Figure 7.8	Iribarren No. versus K , in Kamphuis and Readshaw (1978)	244
Figure 7.9	Wave steepness versus K , in Özhan (1982)	245
Figure 7.10	Breaker Iribarren versus K for Lake Coleridge data	247
Figure 7.11	K versus numerical K , in Bailard (1984)	255
Figure 7.12	Regression of Bailard stream power numerical K model	256
Figure 7.13	Correlation between Equation 7.25a and transport rate	259
Figure 7.14	BORESED estimates versus field data, in Chadwick (1991b)	261
Figure 7.15	BORESED versus transport rate from Lake Coleridge	263
Figure 7.16	Kamphuis model versus field data, in Kamphuis (1991)	267
Figure 7.17	Scale effects of laboratory and field data, in Kamphuis (1991)	268
Figure 7.18	(A) Kamphuis (1986) eqtn. versus Coleridge transport rate	269
	(B) Kamphuis (1991) eqtn. versus Coleridge transport rate	269
Figure 7.19	Delft model (Equation 7.34) versus Coleridge transport rate	271
Figure 7.20	(A) Correlation of Equation 7.35 with Coleridge transport rate	274
	(B) Correlation of Equation 7.36 with Coleridge transport rate	274
Figure 7.21	LEXSED versus measured transport rates	276
Figure 7.22	Summary of extreme value estimates from tested equations	283
Table 7.1	K values derived from studies on sand and gravel beaches	232
Table 7.2	Summary statistics of results from K I & B equations	246
Table 7.3	Correlations between LWP and ITR for K I & B equations	246

Table 7.4	Transport rates from Mod. I & B Eqtns. 7.19 & 7.20	252
Table 7.5	Summary statistics for results from BORESED model	264
Table 7.6	Summary statistics of results from Kamphuis equations	270
Table 7.7	Summary statistics of transport rates from Eqtns. 7.34-7.36	274
Table 7.8	Summary statistics of transport rates from LEXSED	276
Table 7.9	Summary data of tested longshore transport equations	278

LIST OF SYMBOLS

a	Sediment porosity parameter = $(1-n)$ (also a')
C	Wave celerity/velocity ($m\ s^{-1}$); calibration coefficient or constant
C_f	Drag coefficient (also C_d)
C_n	Wave group velocity ($m\ s^{-1}$) (also C_g)
C_o	Deep water wave velocity ($m\ s^{-1}$)
C_s	Shallow water wave velocity ($m\ s^{-1}$)
D	Grain size (m or mm); fetch duration (<i>min</i> or <i>hr</i>)
D_{50}	Median sediment size (<i>m</i> or <i>mm</i>)
D_{90}	Mean grain size at 90 th percentile of size distribution curve (<i>m</i> or <i>mm</i>)
D_{10}	Mean grain size at 10 th percentile of size distribution curve (<i>m</i> or <i>mm</i>)
D_d	Wave energy dissipation rate ($W\ m^{-2}$)
d	Water depth (<i>m</i>)
d_b	Breaker depth (<i>m</i>)
E	Total wave energy density (Nm^2)
e	Sediment porosity parameter or void ratio = $(1-n)$; exponent ≈ 2.71828
F	Fetch length (<i>km</i>)
f	Wave frequency = $(1/T)$
g	Gravitational acceleration ($9.81\ m\ s^{-2}$)
H	Wave height (<i>m</i>)
H_b	Breaker wave height (<i>m</i>)
H_{max}	Maximum wave height (<i>m</i>)
H_o	Deep water wave height (<i>m</i>)
H_{rms}	Root mean square wave height (<i>m</i>)
H_s	Significant wave height = $H_{1/3}$ (<i>m</i>)
$H_{1/10}$	Mean height of largest 1/10 waves (<i>m</i>)
h	Water depth (<i>m</i>)
I_l	Immersed weight sediment transport ($N\ s^{-1}$) (also I_{ls}) (N = Newtons)
i_t	Instantaneous sediment transport rate vector ($N\ s^{-1}$)
i_θ	Time averaged immersed weight transport rate vector ($N\ s^{-1}$)
K	Dimensionless coefficient also known as the ‘coastal constant’
K'	Dimensionless coefficient requiring calibration
K_Q	Dimensionless coefficient requiring calibration
k	Wave number = $(2\pi/L)$; empirical calibration coefficient
L	Wave length (<i>m</i>)
L_o	Deep water wave length (<i>m</i>)
L_s	Shallow water wave length (<i>m</i>)

M_s	Sediment mass (kg)
M_{50}	Median mass of one unit at 50 th percentile on mass distribution curve
m	Ratio of breaker depth to distance of breaker from shoreline
n	Wave-group to wave phase velocity ratio; void ratio
N_z	Number of zero-crossings in upward direction through mwl
P	Porosity (dimensionless)
P	Wave energy flux ($N\ s^{-1}$) (N = Newtons)
P_l	Longshore component of wave energy flux ($N\ s^{-1}$; $W\ m^{-1}$) (also P_{ls})
P_o	Threshold wave power ($N\ s^{-1}$)
P_+	Virtual wave power ($kg\ s^{-3}$)
Q	Longshore sediment transport rate ($m^3\ s^{-1} / hr^{-1} / yr^{-1}$) (also Q_l or Q_{ls})
Q_{Ax}	Transport volume of area below sediment trap ($m^3\ hr^{-1}$)
Q_{Ay}	Transport volume of area above sediment trap ($m^3\ hr^{-1}$)
Q_{Am}	Transport volume of area occupied by sediment trap ($m^3\ hr^{-1}$)
Q_m	Measured sediment transport volume (m^3)
R	Run-up height/elevation (m)
$R_{2\%}$	2 percent run-up exceedence (m)
S	Beach slope (deg or $\tan\ \beta$)
Sw_l	Swash length (m) (also l)
T	Wave period (s)
T_c	Wave crest period (s)
T_{cr}	Critical wave period (s)
T_p	Peak spectral wave period (s)
T_s	Significant wave period = $T_{1/3}$ (s)
T_z	Zero-crossing wave period (s)
T_w	Width of sediment trap (m)
t	Time; swash period (s)
$\tan\beta$	Beach gradient (rad)
u_m	Wave orbital velocity (ms^{-1})
u_{mb}	Wave orbital velocity at break point ($m\ s^{-1}$)
u_o	Wave orbital velocity at sea bed ($m\ s^{-1}$)
u_t	Instantaneous near-bottom velocity vector ($m\ s^{-1}$)
u_θ	Current vector ($m\ s^{-1}$)
u_+	Dissipation velocity ($m\ s^{-1}$)
u_{+cr}	Critical dissipation velocity ($m\ s^{-1}$)
\bar{V}	Mean wind speed ($m\ s^{-1}$)
V_s	Volume of sediment sample (m^3)
v_{sw}	Maximum swash velocity
\bar{v}_{sw}	Mean swash velocity
W	Sediment transport function (m)
w_s	Sediment fall velocity ($m\ s^{-1}$)

X_{sw}	Width of swash zone (m)
α	Wave angle (rad) (sometimes beach slope)
α_b	Breaker angle (rad)
β	Beach slope (foreshore/nearshore) (deg)
ε	Spectral band width parameter; surf scaling parameter
ε_b	Bedload efficiency factor
ε_s	Suspended load efficiency factor
ϕ	Dimensionless grain size measure; friction angle of sediment (deg)
γ	Wave height to water depth ratio; Mass of immersed sediment without pore spaces i.e. $(\rho_s - \rho)ga$ (Nm^2)
γ_b	Breaker height to breaker water depth ratio (aka breaker criterion/index)
η	Water surface elevation (m)
μ	Fluid viscosity ($Ns\ m^{-2}$)
π	pi = (3.14)
ρ	Density of sea/fresh water ($kg\ m^{-3}$)
ρ_s	Sediment density ($kg\ m^{-3}$)
σ	Wave radian frequency = $(2\pi/T)$ (s); sediment sorting (mm or ϕ)
τ	Fluid shear stress (Nm^{-2})
ω	Energy dissipation rate ($Nm^{-1}\ s^{-1}$)
ξ	Iribarren number (dimensionless)
ξ_b	Breaker Iribarren number (dimensionless)
ξ_o	Deep water Iribarren number (dimensionless)

Subscripts

b	<i>denotes breaker or breaker zone</i>
cr	<i>denotes critical values</i>
d	<i>denotes deep water</i>
o	<i>denotes deep water</i>
s	<i>denotes shallow water or; significant values</i>
sw	<i>denotes swash zone</i>
v	<i>denotes beach toe</i>

CHAPTER 1.

THE RESEARCH PROBLEM

"When Coleridge tried to define beauty, he returned always to one deep thought: beauty he said, is 'unity in variety'. Science is nothing else than the search to discover unity in the wild variety of nature."

L. Lederman (1993)

1.1 Purpose for Research

This thesis examines the nature of longshore sediment transport processes in a mixed sand and gravel lake shoreline, Lake Coleridge/Whakamatau, New Zealand (Figure 1.1). It focuses on relationships between the wave environment, the swash zone and the resulting sediment transport. There are three reasons why this investigation is relevant. Firstly, a great deal of coastal research over the past one hundred years has been conducted on sand beaches. Comparatively little research has been conducted on gravel beaches, and even less on mixed sand and gravel beaches. Although there are general principles that can be applied to these beach types, they exhibit significant differences in their morphodynamic responses to environmental conditions and in their process environments. Therefore, there is a need from a scientific perspective to gain a deeper understanding of how mixed sand and gravel beaches operate.

Secondly, we require a greater understanding of the processes of longshore sediment transport on mixed sand and gravel beaches. Many of these shorelines are eroding in New Zealand for reasons that are not always clearly understood. However, it is recognised that longshore transport is the single most important process that moves sediment into and out of a beach system and that there are distinct differences between the way this happens on a sand beach and on a mixed sand and gravel beach. There are more than just scientific justifications to researching this problem; it is also important from a coastal management perspective.

Thirdly, the bulk of the international coastal literature refers to oceanic beaches. As with mixed sand and gravel beaches, comparatively little is known about lakeshore systems. This is surprising considering that many towns are built near eroding lake shorelines. In New Zealand many lake beaches composed of mixed sand and gravel have erosion problems that threaten private property and public amenities. Although there are similarities between lakeshores and the open coast, there are differences in their process regimes. It is essential to have an accurate understanding of lakeshore beach systems if they are to be managed correctly.

In the coastal environment sediment transport is caused by a number of processes, operating in different directions, timescales and modes. Some of these processes are more relevant to mixed sand and gravel beaches and others to sandy beaches. It is important at the outset to understand and identify which of these is more applicable to the current study. This chapter aims to place the study into a research context, in terms of both the literature and the fieldwork. It highlights some of the differences between mixed sand and gravel and sandy beaches because, the process and morphology differences between these beach types dictates the approaches that must be taken in the research. There are also important differences between lacustrine and oceanic beaches and it is important to clarify these because there are some limitations in applying a study from a lacustrine to an oceanic setting.

1.2 Significance of Longshore Sediment Transport

Longshore sediment transport is one of the most widely studied nearshore processes. It is the single most important process that moves materials through a beach system and it occurs almost universally in beaches around the world. It is the process responsible for the development and stability of a beach. The net removal of sediments from a shoreline by these currents may result in long-term retreat of the coast, whilst a net influx may result in progradation. Although longshore sediment transport is a natural process, it is frequently disturbed by human activities. Coastal structures such as piers, ports and sea defences can modify sediment transfers along a coast by causing excess sedimentation on the ‘updrift’ side and erosion problems on the ‘downdrift’ side. For these reasons, it is an important processes to study and understand properly. Over the past sixty years a substantial amount of work has been directed toward this goal. Recent reviews of the subject are given by Komar (1998), Schoonees and Theron (1993) and Fredsøe (1993). Much of this work has involved the study of oceanic sandy coastlines and there is a good deal known about longshore transport in these systems. This is partly because a large amount of coastal development has taken place in these environments. But other shoreline types, such as mixed sand and gravel or lakeshores, are becoming equally heavily developed and require a more in-depth understanding. In a review of the international longshore sediment transport database, Schoonees and Theron (1993) noted that virtually no data had been collected from beaches with grain sizes between 0.6 and 15 mm. While it is recognised that there are differences in the way longshore transport processes operate in these environments, they have received little attention in the literature. This thesis is a response to this lack of knowledge.

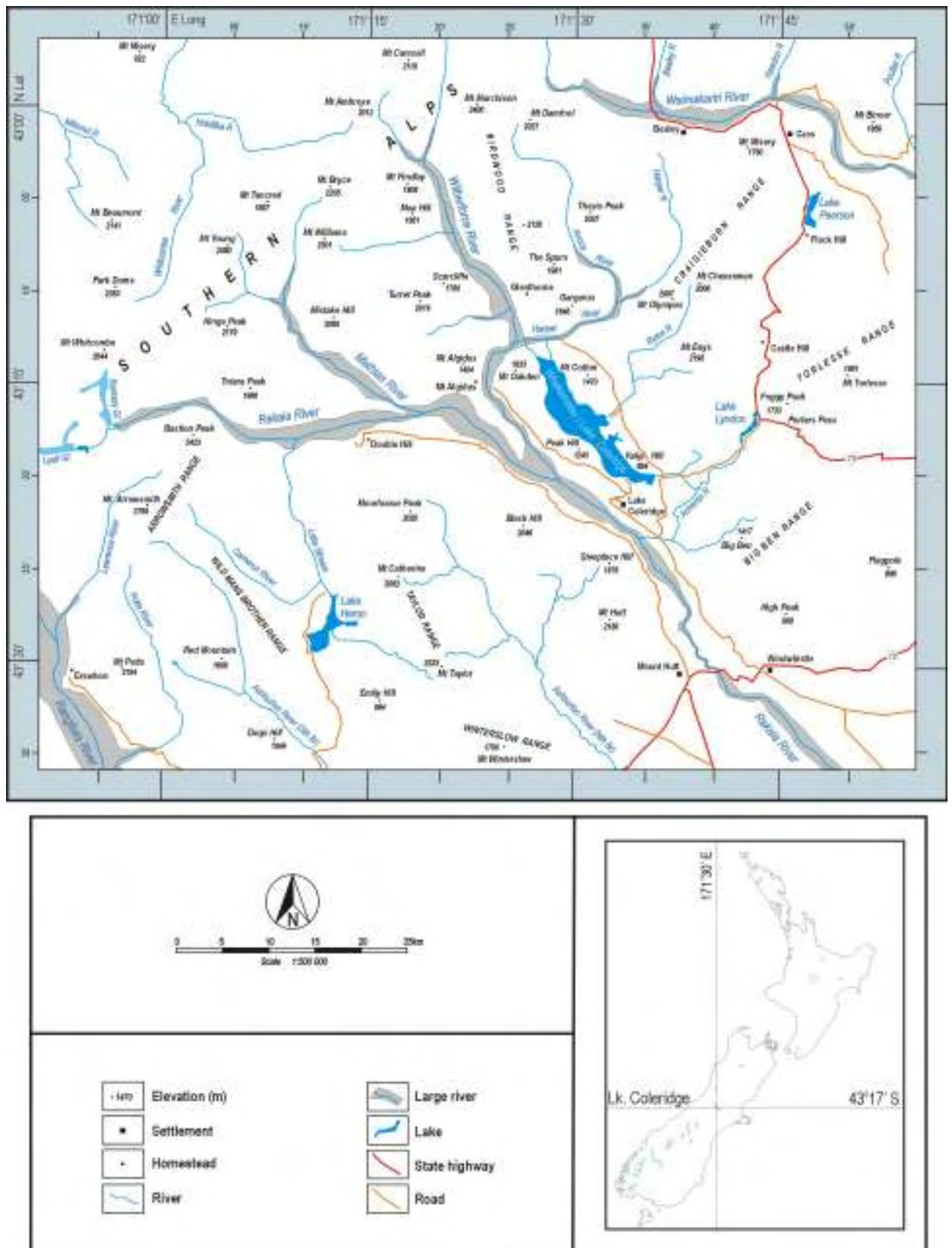


Figure 1.1 Lake Coleridge/Whakamata area map showing surrounding terrain, catchments and river systems. Lake Coleridge is a moderately sized alpine lake of glacial origin situated in the foothills of the Southern Alps, 110 km north-west of Christchurch in the mid-Canterbury high country of the South Island.

1.3 Sediment Transport Systems

When wind blows over water it exerts a stress on the surface, transferring some of its energy into the water and forming waves. These are the waves that people most commonly associate with the sea and are known generically as gravity waves. They are generated by the wind and are restored back to flat water by the forces of gravity. As these waves travel through the water, orbital motions are set up within the wave (Masselink & Hughes, 2003). In wave process terms, water that is deeper than half a wave length is defined as ‘deep water’ because wave action has negligible effects on the seabed (Figure 1.2). Likewise, the seabed exerts no influence on the wave form. When waves move into water approximately equal to half the wave length they begin to undergo a series of shoaling transformations. Here the water is defined as being of ‘intermediate depth’. The orbital motions in the wave now extend to the sea floor and become hindered by its presence, causing the wave to increase in height and become steeper. At this point sediment can be disturbed on the sea floor. As the wave advances into increasingly shallow water, the velocity of these movements intensifies to the point where they can initiate sediment transport (Huntley & Bowen, 1975). Here the water motions are oscillatory in nature and transport occurs in either an onshore or offshore direction. This process is commonly termed mass sediment transport. When the wave progresses into water that is $1/20^{\text{th}}$ of the wave length it is defined as ‘shallow water’. At this stage the water flow at the seabed becomes progressively hindered by friction, whilst water motion at the top of the wave continues to move relatively faster. It is this velocity differential that causes the wave to break creating a zone of high turbulence that is a major area of sediment entrainment and transport (Mizuguchi, 1980).

There are two main current systems that can develop in the nearshore forward of the breaking wave depending on the beach morphology and the angle at which waves approach the coast (Komar, 1998). The first, which occurs along gently sloping shorelines, is a cell circulation system that forms when waves approach a beach with their crests more-or-less parallel to the shoreline (shore-normal) (Figure 1.3a). In the surf zone there is a steady onshore mass transport of water forward of the breaking wave. To balance this onshore flow, a system of currents develop that channel the water back offshore. The currents are commonly known as rips and there can be a series of these spaced at regular intervals along a coastline (Short, 1985). The cell circulation systems have the ability to recycle a great deal of sediment onshore and offshore. The second main current system that can form forward of the breaking wave is a longshore current (Guza et al., 1986). Longshore currents can develop along most shoreline types, unlike the cell circulation system just described, but they manifest themselves in different ways depending on

the shoreline morphology. Conventionally, it is thought that when waves break at an oblique angle part of the water motion is directed forward to the shore and the rest is directed alongshore, the proportion depending on the incident wave angle. The longshore directed component can form a substantial current that flows parallel to the shoreline between the breakers and the beach (Figure 1.3b). These currents are capable of transporting large quantities of sediments out of the beach system (Komar, 1998).

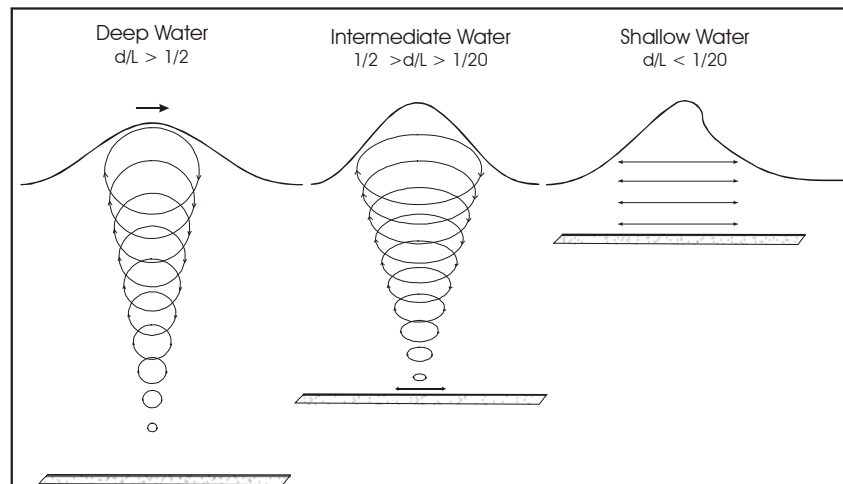


Figure 1.2 Schematic showing the array of water orbital motions under a wave. In deep water the motions approximate closed circular orbits. As the wave advances into intermediate water the motions become more elliptic as the wave ‘feels the bottom’. In shallow water the motions become a series of horizontal oscillatory movements capable of transporting sediment.

Any remaining energy after the process of wave breaking, propagates toward the beach as a bore and expels itself on the foreshore as swash, where another set of currents develop (Figure 1.3). Swash motion is asymmetrical consisting of an onshore phase with decelerating flow velocities known as the swash and an offshore phase characterised by accelerating flow velocities known as backswash (Masselink & Hughes, 2003). The swash ‘uprush’ is generally more turbulent and stronger than the backswash, which is generally calmer, flowing downslope under the influence of gravity. In this respect, the swash and backswash can be seen as two separate, yet related flow fields (Kirk, 1970). These currents entrain material and transport it in different ways depending on the wave conditions. When waves are shore-normal, sediment transport is generally on/off shore under the oscillatory flow. When the waves approach at an oblique, angle the asymmetry of the swash flow entrains the sediments in a longshore direction in a roughly zigzag fashion. The nature of these currents is highly controlled by the foreshore

slope and sediment composition. For reasons that will be explained below, swash zone transport is more important on steep beaches. Due to the critical role that it has in controlling the sediment budget of a steep, coarse grained beach, this study will be looking specifically at longshore sediment transport in the swash zone.

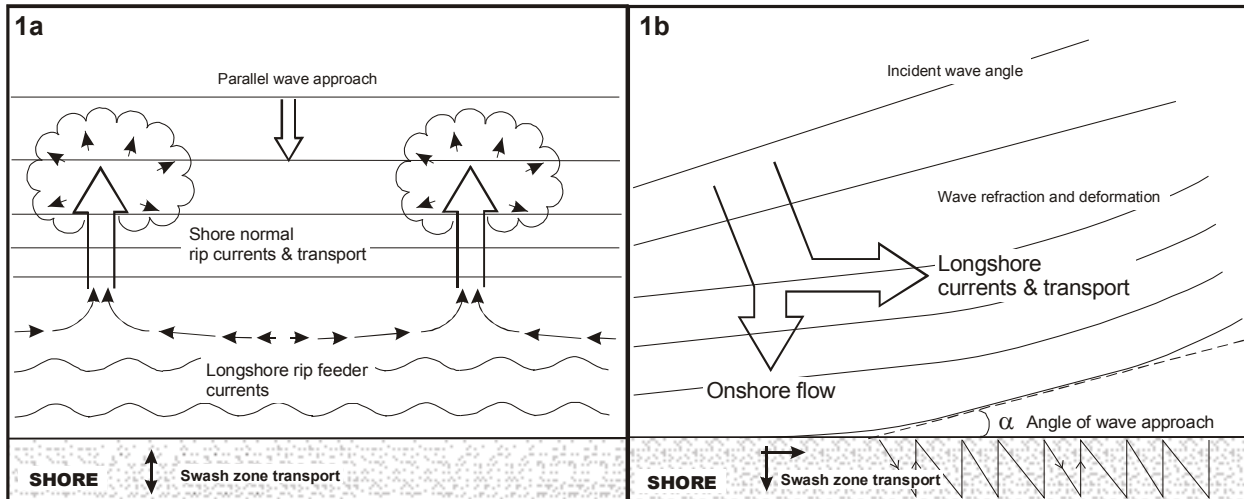


Figure 1.3 The two main types of current systems that can develop in the nearshore zone forward of the breaking waves. The first is a cell circulation system that develops when waves approach shore-normal. The second is a longshore current that forms when waves approach a shoreline at an oblique angle. A great deal of sediment can be transported in these currents. Sediment is also transported in the swash zone, the direction depending on the angle of wave approach. These two models can be viewed as end members of a continuous spectrum, as there are a number of different configurations that can occur in-between phasing from one extreme to the other.

The movement of sediments in a beach can be expressed as either gross or net transport rates. The sum of all the movements in a longshore or cross-shore direction is known as the gross sediment transport rate (Komar, 1998). It is useful to know the gross littoral rate when examining the long-term stability of a beach. The net longshore or cross-shore transport rate quantifies the sediment movement in a single direction. It is useful to know net rates in identifying which wave conditions are responsible for causing the most, or the least, sediment transport. This study will be concentrating on measuring the short-term net transport rate. The purpose of this is to quantify the amount of sediment transported during a certain event in order to identify the conditions responsible for causing erosion.

Once the sediment is in motion it can be broadly described as moving in one of two modes; bedload transport or suspended transport (Figure 1.4). There are no precise definitions of these

two terms, but they are based on the observation that two different mechanisms operate to transport sediment (Fredsoe & Deigaard, 1991). Bedload transport occurs when grains are in continual or frequent contact with the bed. Particles move by creeping, sliding or rolling along the bed, or by a processes known as saltation. Saltating particles will momentarily leave the bed and collide with other grains, setting them into motion and thereby continuing the process. It is common to see saltating particles at the advancing bore in the swash zone. Suspended transport occurs when particles leave the bed due to fluid turbulence and are predominantly transported in the water column. The settling velocities of these particles will differ depending on their size. The finest particles, those in the fine silt and clay size ranges, will remain in suspension for long periods of time and are often referred to as washload (Figure 1.4). The material that makes up the washload is not normally present in the bed because it is easily suspended by any fluid motion. As such, it is not considered part of the beach forming material and is not usually included in sediment transport measurements (Fredsoe & Deigaard, 1991). Particles in the sand size range will settle out of suspension more readily enabling them to become part of the beach forming sediment.

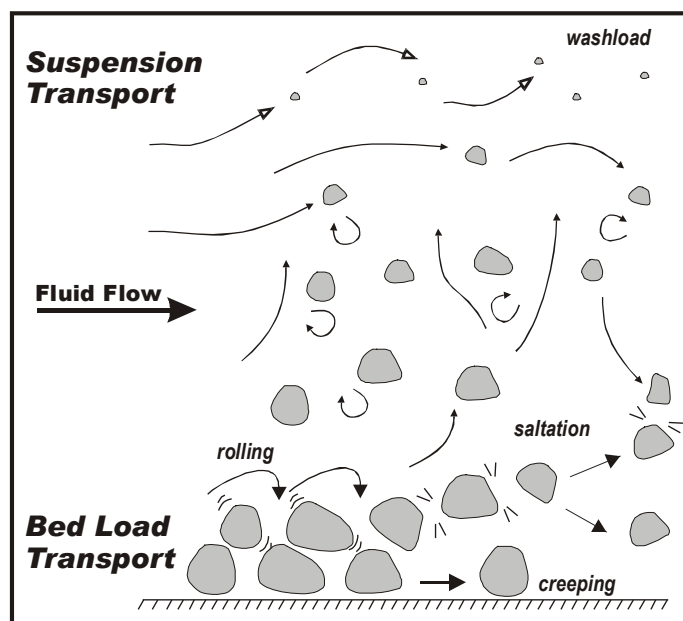


Figure 1.4 Sediment transport occurs predominantly by two modes. Bedload transport occurs at the sediment-fluid interface, whilst suspension transport occurs when grains are held aloft in the flow through turbulence.

Whether a particle is transported in suspension or by bedload is largely a function of the fluid velocity and the size, shape and density of the grain. Fine particles have low critical threshold velocities and are more readily set into motion. Coarser particles are more resistant to moving and may require considerable flow velocities to entrain. It is not uncommon to have a part of the load moving in suspension and a part moving at the bed. There is some debate as to which mechanism is more important in transporting sand (Komar, 1998), but it is generally accepted that gravel is transported as bedload, sands are transported through a combination of both bedload and suspension depending on the wave conditions, and the finest fraction is transported by washload. In mixed sand and gravel beaches both these mechanisms play a role but as will be discussed below, it is bedload transport that dominates.

1.4 Mixed Sand and Gravel Beach Research

Most coastal research has been directed toward understanding the processes and morphology of sandy beaches and a great deal of literature has come out of those countries where this is the predominant beach type, particularly the United States and Australia. To a much lesser extent there has also been some investigation of pure gravel beaches, notably in mid-latitude countries such as the United Kingdom, Canada and Ireland. However, between these two beach types there exists another lesser known beach type known as a mixed sand and gravel beach. A mixed sand and gravel beach is, as the name suggests, a beach composed from a homogenous mix of both sand and gravel in roughly equal proportions. In this way they are distinct from either pure sand or gravel beaches. They also differ in important ways from beaches that contain sand and gravel in different parts of the profile (i.e. non-homogenous). Most commonly this takes the form of a gravel high tide or storm ridge, perched on a sand base at the back of the profile (e.g. Chesil Beach, England). In this situation the beach presents two different systems; a sandy, dissipative low tide beach and a steep, reflective gravel beach at high tide (Jennings & Shulmeister, 2002). Although mixed sand and gravel beaches are rare on a global scale, in New Zealand they are a common feature of the coastline. For example, there is an almost continuous stretch of these beaches from Banks Peninsula to Oamaru on the North Otago coast. Similar examples are found on the North Canterbury, Marlborough and Hawke's Bay coastlines. They also occur on many lake shorelines, particularly the glacial lakes of the South Island, for example, Lakes Coleridge, Hawea and Tekapo.

Many of these mixed sand and gravel shorelines are actively eroding. The shoreline between Oamaru and Timaru has a net long-term retreat rate of 0.6 m yr^{-1} . North of Timaru, in the Canterbury Bight the net long-term erosion rate is even greater at up to 1.0 m yr^{-1} . This erosion is threatening property (e.g. Ashburton River Mouth), public amenities (e.g. Oamaru) and in some cases whole industrial estates (e.g. Washdyke, Timaru) (Flatman, 1997). In contrast to this there are areas of strong progradation on the same coastline. South Beach, Timaru experienced $6 \times 10^6 \text{ m}^3$ or 80 ha of accumulation between 1879 and 1963 and it is still gaining $60,000 \text{ m}^3 \text{ yr}^{-1}$ (Kirk, 1992a). Whilst Kaitorete Barrier which fronts Lake Ellesmere/Te Waihora, has prograded strongly at its northern end, it is eroding at its southern end (Hemmingsen, 1997). In all of these situations it is recognised that longshore sediment transport plays an important role in the causes of erosion. At Timaru the construction of the Harbour has effectively blocked the northward transport of sediments, resulting in strong progradation at South Beach and consequently severe erosion at Washdyke which is to the Port's north and updrift side (Kirk, 1992a). Despite the acknowledgment of the role that longshore sediment transport has in these problems, processes of sediment transport are poorly understood in mixed sand and gravel beaches.

The morphology and sedimentary petrology of mixed sand and gravel beaches is better understood than the processes operating in them. They were recognised as being morphologically different from other beach types as early as the 1920s, but apart from significant early works by Marshall (1929) and Speight (1930; 1950), most of the mixed sand and gravel beach literature dates from 1965 onwards. Much of this work has been devoted to describing morphology and sedimentary characteristics; Jennings and Shulmeister (2002), Hall (1995), Single (1992), Pickrill (1977), McLean (1967; 1969; 1970), McLean and Kirk (1969), Kirk (1967); to investigating nearshore current processes and swash zone dynamics, Delgado (1990), Neale (1987), Hewson (1977), Kirk (1975; 1970); to calculating sediment budgets, Flatman (1997), Gibb and Adams (1982), Kirk and Hewson (1978); and to constructing the Holocene histories of these beaches, Schulmeister and Kirk (1993), Armon (1974).

Whilst a few studies have briefly explored some issues related to longshore sediment transport, (Kirk, 1970; Hastie, 1983; Neale 1987; MacBeth, 1988; Worthington, 1989; Dawe, 2000), no single investigation has focused purely on the process. Some authors have attempted to quantify bulk sediment transport movements, usually in terms of annual rates. Hewson (1977) studied the morphology and sediments of the coastline between Oamaru and Timaru and calculated the sediment budget of the coastline. This involved determining the longshore

sediment transport direction and an annual average rate of movement. Hewson calculated that the net northward drift of material on this coast is $259,127 \text{ m}^3 \text{ yr}^{-1}$. Neale (1987) conducted a similar study to Hewson ten years later on the same stretch of coastline and calculated that the average net northward rate of transport was $51,288 \text{ m}^3 \text{ yr}^{-1}$. The conflicting results that have been obtained for longshore sediment transport rates have led to difficulties in accurately calculating sediment budgets for mixed sand and gravel beaches. In trying to calculate the sediment budget for the beaches of the South Canterbury Bight, Flatman (1997) found that there was an unexplained loss of sediment from the system. It has been suggested that this is potentially related to processes of abrasion and longshore sediment transport. In mixed sand and gravel beaches there is very little knowledge about rates of transport and its relationship to key wave properties such as height, period, angle and frequency of approach. Due to the limited understanding surrounding sediment transport in these beaches and the associated erosion problems facing many small communities, it is the aim of this investigation to examine and quantify the process of sediment transport in mixed sand and gravel beaches.

1.5 Morphodynamics of a Mixed Sand and Gravel Beach

Inman and Bagnold (1963) noted that there were differences in the process regimes between coarse-grained and fine-grained beaches. A typical oceanic mixed sand-gravel beach (Figure 1.5) averages 100-200 m in width, although can be as narrow as 20m or less if it is eroding. Average elevations above mean sea level are 4-6 m, but Kirk (1980) noted that they may get as high as 14m. In contrast, sandy beaches are a lot flatter and wider (Figure 1.6). Although there is a lot of variation, sand beach profiles can be up to 500-600 m across, with slope angles typically below 5° . These morphological differences, which are largely due to sediment composition, have important implications for the nearshore process environment. The two profile types dissipate wave energy differently, creating distinct nearshore current and sediment transport systems (Huntley and Bowen, 1975). Essentially, the sediment composition controls the depth of water across the profile and determines whether a beach is reflective or dissipative in nature. It will be recalled from Section 1.3 that the water depth exerts a controlling influence on wave shoaling, refraction and breaking.

Wave breaking is an important process of energy dissipation. Where a wave breaks has a significant impact on how much energy is directly available to do work on the shoreline. Essentially, the width and depth of the nearshore zone will control the distance over which

energy dissipation processes occur. Energy losses are greatest over wide, low sloping nearshore zones where waves break some distance from the shore. On steep gradient beaches where deep water extends closer to shore, wave energy losses due to shoaling are considerably less and the energy involved in wave breaking is expended over a much shorter distance. Consequently, there is less alteration of the deep water wave in the nearshore and waves are able to approach much closer to the foreshore before breaking (Van Wellen *et al.*, 2000). This has prompted some authors to refer to sand beach profiles as ‘dissipative’ and gravel beaches as ‘reflective’ in reference to the way in which wave energy is dispelled (Wright *et al.*, 1979).

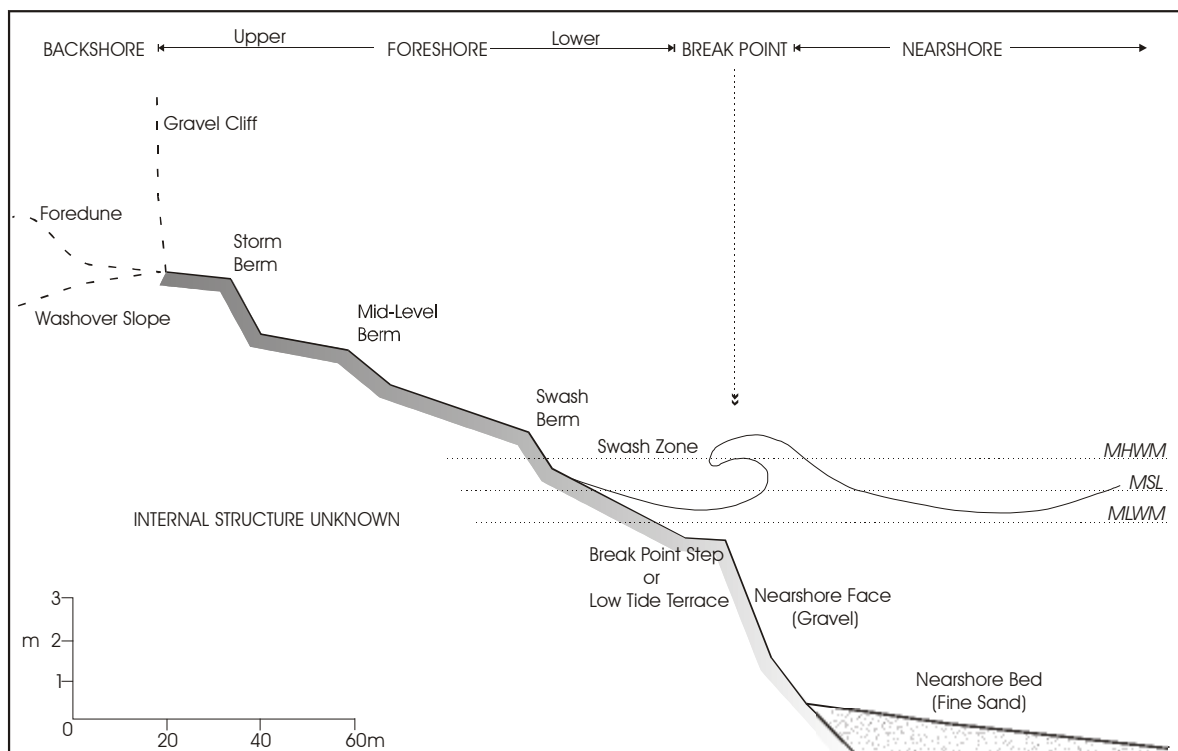


Figure 1.5 Typical morphology of a mixed sand and gravel beach profile. MHWM = mean high water mark; MSL = mean sea level; MLWM = mean low water mark. (Modified From: Kirk, 1980)

Mixed sand and gravel beaches have a steep ($5-12^\circ$) and often extensive foreshore, that extends from the upper storm berm to the low tide step (Figure 1.5). It is the zone that experiences the greatest morphological change (Kirk, 1980). The steep gradient of these beaches allows waves to advance very close to the shore before breaking. This usually occurs as a single line of plunging breakers at the base of the low tide or break point step. Waves breaking at all stages of the tidal cycle in average conditions ($<1.0\text{m}$) are confined to this narrow zone, hence it

tends to be very turbulent. The breaking wave then translates directly into swash. The swash is shorter and has much higher velocities when compared to sandy beaches. The backwash tends to be weaker as it rapidly percolates through the gravels causing the foreshore to be swash dominated (Kirk, 1980). The turbulence of the swash zone has the tendency to throw any fine material into suspension and transport it offshore, thus the lower foreshore is frequently characterised by coarse sediment. Most of the sediment transport that occurs on a mixed sand and gravel beach takes place in the lower foreshore. In fact, most of the active beach deposit is above the waterline. Accordingly, swash zone sediment transport is of greater significance than on sand beaches. This prompted Kirk (1980: 193) to describe the foreshore as the 'engine room' of a mixed sand and gravel beach.

Another consequence of the steep profile is that waves approaching the coast at an oblique angle do not undergo the same refraction processes as they do across a wide gently sloping nearshore (van Wellen *et al.*, 2000a). Wave refraction has the tendency to align waves shore-normal. As explained earlier, in this situation sediment transport in the swash zone occurs mainly in an on-offshore direction (Figure 1.3). This means that waves often break on a coarse grained shoreline at considerably greater angles than might be expected on a sandy beach. Wave angle is particularly important on coarse grained beaches, because oblique waves initiate longshore transport of materials in the swash zone. Kirk (1980) also noted that because of the reflective nature of the nearshore face, return circulation of water in the backwash occurs through the base of the breaker. Cell circulation systems (Figure 1.3a) and the associated nearshore morphology that this produces (e.g. bars and troughs) do not occur as they do on sandy beaches.

Below the water line immediately seaward of the break-point step is a steep gravel scarp termed the nearshore face or step (Kirk, 1980). The face is a continuous feature running alongshore. It abruptly gives way at its base to a gently sloping shelf composed of silts and sands too fine to remain in the turbulent foreshore. This fine material is derived from rivers and beach gravel attrition. Kirk (1980: 194) noted that it is often difficult to pinpoint on a beach the seaward limit of the nearshore where deep to intermediate water wave processes give way to shallow water wave processes. However on mixed sand and gravel beaches this dividing line is clearly defined in most conditions at the base of the nearshore face.

The sediments of the beach and inner shelf not only differ texturally, but they are also subject to separate transport systems. On mixed sand and gravel beaches, particles may move through the foreshore and into the nearshore, but they are not easily transported back. In other words it is

a one way system; materials lost offshore are usually lost permanently. Moreover, from investigations carried out by Tierney and Kirk (1978) and Kirk and Tierney (1985), it was shown that the fine sand of the inner shelf moves quite independently of the sediments on the shore. Hastie (1983; 1985) investigated the nearshore sediment transport processes of the mixed sand and gravel Timaru coastline, and supported Tierney and Kirk's ideas. Hastie found two independent littoral transport systems operating in the beach system. Coarser sediments were confined to the nearshore face and foreshore and were transported in bedload by swash action. Fine sand and silt was confined to the seabed and transported in suspension.

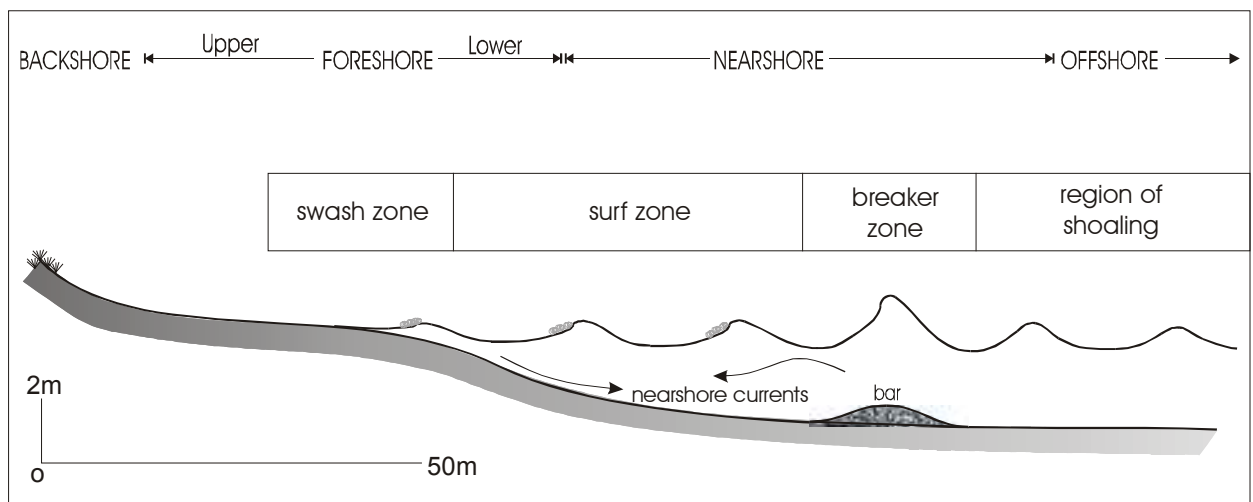


Figure 1.6 Typical morphology of a sandy beach profile.

On sandy beaches the morphodynamics are quite different. Wright *et al.* (1979) described broad sandy beaches as dissipative, exhibiting concave nearshore profiles and wide flat surf zones characterised by multiple lines of breakers up to 350 m offshore. In this way, much of the wave energy is dissipated through turbulence before it reaches the shore. Consequently, swash velocities are lower and have less capacity to transport sediment. In sand beaches the swash zone plays a lesser role to the movement of sediments in the nearshore. The nearshore topography is typically complex with one or more bar and trough systems. In Section 1.3 it was mentioned that cell circulation systems can form in the nearshore zone that are capable of moving significant quantities of sediment in both an on-offshore direction and a longshore direction (Figure 1.3). Short (1979) presented a morphodynamic model that describes the re-circulation of sediments between the nearshore and foreshore of sandy beaches. Based on the ideas of Bascom (1954), Short demonstrated that during storm episodes material is eroded from the foreshore and

deposited in the nearshore as a bar (Figure 1.6). This has the effect of creating a wider flatter profile causing waves to break further offshore, thereby reducing the erosive wave energy reaching the beach. During calm periods this bar is slowly eroded with the material being deposited back in the foreshore. Effectively the beach profile steepens and waves are able to break closer to the shore. The model was further developed by Wright and Short (1983) who concluded that sandy beaches are in dynamic equilibrium between two profiles: One that may be the product of accretion (reflective state) and another of erosion (dissipative state); although these morphodynamic states can exist for reasons other than erosion or accretion.

A problem faced when investigating mixed sand and gravel beaches is having to rely on models developed from the study of sandy beaches. In many cases the models, which are often offered as universal, are found to have limited applicability. The above comparison highlights some important distinctions between mixed sand and gravel and sandy beaches. It offers some explanation as to why models developed for sandy beaches are not always relevant to their mixed sand and gravel counterparts. It is recognised that hydrodynamic interactions with mixed sediments are more complicated than those found to occur in either pure sands or gravels (Kirk, 1980; McLean, 1970; Zenkovich, 1967). Yet, longshore transport is potentially less complex on mixed sand and gravel beaches than it is on sandy shores.

On sand beaches it is generally believed that transport occurs by breaking waves entraining the sediment, where it is then transported by nearshore currents (Komar, 1988; Kraus & Dean, 1987). Modelling the processes responsible for this has been difficult because variation in current velocities across the whole nearshore breaker zone is overwhelmingly complex. Such complexity is not an issue on mixed sand and gravel shorelines because there is only one line of breakers and sediment transport is initiated purely by an oblique wave approach angle (Figure 1.3b). Waves break directly onto the foreshore and sediment transport of beach forming material happens only in the swash zone and not in the nearshore (Kirk, 1980). The break-point step provides a clear demarcation between the nearshore and foreshore, a line that can be hard to define on other beach types. Waves break at this point in all but the severest conditions, simplifying the longshore sediment transport processes. Essentially, longshore sediment transport is only dependent on wave approach angle and wave power. Most of the morphological changes occur in the foreshore, not in the nearshore as on sandy beaches, making them more accessible to study.

1.6 Lake Shoreline Research

Whilst there is a limited amount of research that has been directed toward mixed sand and gravel beaches, even less is understood about lake shorelines, both overseas and in New Zealand. This study is aimed at understanding the processes of longshore sediment transport in the littoral zone of a mixed sand and gravel beach. However, because it has been conducted on a lake beach, it will primarily provide insights into the process environment of a lacustrine mixed sand and gravel beach. Consequently, it is important to recognise some of the differences and similarities with their open coast counterparts.

New Zealand has a large number of natural lakes for its size. There are 770 lakes over 0.5 km² and of these 268 (35%) are of glacial origin. The vast majority are under 5 km² in size, but 53 are over 5 km² and 15 are over 50 km² in size (Irwin, 1975). The lakes of this country are a significant economic, cultural and recreational resource. In pre-European times, the lakes were important mahinga kai (food gathering places) for Maori, particularly for the highly prized tuna (eel). This made lakes popular places to settle and numerous lakes around the country had pa sites located on their shores (e.g. Rotorua, Taupo, Ellesmere/Te Waihora). This popularity for settlement continued after the arrival of European settlers. There are now many towns and settlements adjacent to lakeshores and they face many of the same management problems associated with oceanic coasts. For example, a number of mixed sand and gravel lakeshores in New Zealand face erosion hazards. The beaches fronting the Hawea and Lake Te Anau townships are eroding into public amenities and require rock armouring and regular maintenance to prevent further losses. Shore erosion around Lake Pukaki has, on numerous occasions, damaged the highway and continues to threaten its existence. Queenstown, on the shores of Lake Wakatipu, has had its lower central business district inundated on several occasions over the past ten years due to high lake levels, most notably in mid-November 1999. New Zealand lakes are also economically important for tourism. Many travel packages involve tours of the southern lakes on the basis of their scenic and heritage values. Wanaka and Queenstown sustain large tourist industries on the shores of Lakes Wanaka and Wakatipu. In the North Island, Lake Taupo supports a large trout fishing industry, whilst Rotorua and its surrounding lakes with their geothermal attractions see some of the highest visitor numbers in New Zealand.

Many of these lakes have added management issues associated with their use for hydroelectric power generation and as water reservoirs for irrigation and flood control schemes. In New Zealand over 30 lakes are utilized for hydroelectric power generation supplying 78% of the country's electricity needs (Irwin, 1975; James, *et al.*, 2002). Hydro-lakes have their water levels artificially controlled, usually resulting in an increase of their natural operating range. The effects of this are varied, but it is common for shorelines to experience slumping and retreat (e.g. Pukaki), modification of the nearshore profile resulting in the permanent loss of material from the system and alteration of the sedimentary composition of the beach. Biologically, shoreline vegetation is often drowned (e.g. Monowai), exacerbating shoreline retreat, macrophyte weed beds can be destroyed, impacting on littoral zone biota and disrupting aquatic habitats for feeding and reproduction (Kirk and Henriques, 1986). The increasingly extensive use of lakes in this country has demanded better management for conservation and economic reasons. With the passing of the Resource Management Act (1991), any adverse environmental impacts caused by human agency, now have to be legally addressed.

Despite their prevalence and wide usage the lakes of this country had by the mid-1960s received only sporadic attention in the literature. One of the earliest scientific accounts was by Lucas (1904), who made bathymetric soundings and biological collections of a number of lakes around the country including Wakatipu and Taupo. Biological and taxonomic studies set the tone of research for the next sixty years. For example; Armstrong (1935) with a biological study of Lake Taupo; Percival (1937) who identified a new zooplankton species in Lake Ellesmere; and Flint (1938) who made a study of the phytoplankton of Lake Sarah. Professor Edward Percival stimulated a lot of the early research into the freshwater ecology of New Zealand lakes (Jolly and Brown, 1975). After 1965 a systematic survey of the larger lakes was begun by the New Zealand Oceanographic Institute (NZOI), in part driven by their increasing use for hydro-electric power generation. This involved detailed bathymetry surveys, sediment sampling and measurements of water clarity and temperature profiles (Irwin, 1972). In 1975 "*New Zealand Lakes*" was published, edited by V.H. Jolly and J.M. Brown. The book brought together for the first time a wide range of studies, both published and unpublished, conducted on New Zealand lakes. It was evident that limnological studies had up to that time, been concerned chiefly with the freshwater ecology and chemistry, biology, fisheries and formative geology of the lakes (Gage, 1959). A notable omission was the complete lack of any work concerning the geomorphology and processes of lake shorelines.

The first study of the geomorphology of lake shorelines was undertaken by Pickrill (1976) on Lakes Manapouri and Te Anau. Pickrill investigated lakeshore evolution by examining shoreline profiles and correlating them to measured wave and sediment variables. The study was in part motivated by the need to have a sound management plan for the operation of the two lakes for the Manapouri hydro-electric scheme. Twenty-two years later Allan (1998) completed a study of the shoreline development of Lake Dunstan, an artificially created hydro-lake. Allan examined the development of beaches around the lake as it was filled, making quantitative measurements of waves, sediments and changes in shoreline morphology. Building on the work of Pickrill, Allan refined and developed more exact lakeshore evolution models.

In between these two major studies there has been a growing body of literature that includes published peer reviewed articles, conference proceedings, unpublished Masterate and Doctoral theses and internal scientific and consultancy reports. According to Allan (1998) the literature can be broadly divided into three areas. The first concerns the morphodynamics of lakeshore beaches, with a particular focus on shoreline evolution and stability (Pickrill, 1978; 1985; Bunting, 1977; Kirk and Henriques, 1986; Macbeth, 1988; Spence, 1996; Allan, 1991; 1998; Kirk *et al.*, 2000; Kuru, 2004). The second area concerns the limnology of lake systems including studies of sedimentation (Irwin, 1978; Pickrill and Irwin, 1983), water turbidity and clarity (Hicks, 1996) and internal temperature structures (Irwin and Pickrill, 1982). The third main area is involved with lakeshore management (Mark and Johnson, 1985; James, *et al.*, 2002). A big proportion of this literature is in the form of unpublished reports that by and large concern the management of water levels of the big hydro-lakes. These reports also cover aspects of shoreline stability and morphodynamics: For example, Lake Taupo (Hicks *et al.*, 2000; Kirk and Single, 2000), Lake Waikaremoana (Taylor, 2001), Lake Te Anau (Kirk, 1985; Dawe and Hemmingsen, 2001), Lake Pukaki (Kirk, 1988; Bunting *et al.*, 2003), Lake Manapouri (Kirk and Single, 1988; Single, 2002), Lake Monowai (Kirk, 1992b; Dawe and Single, 2001), Lake Coleridge (Henderson, 1994; Kirk and Allen, 1995) to name just a few. To this can be added a fourth area that continues in the freshwater ecology tradition and biological studies that began some one hundred years ago.

Allan (1998) pointed out that in this body of literature there is relatively little detailed research concerning lakeshore processes. Apart from the work of Pickrill (1976; 1978; 1985) and Allan (1998) mentioned above, the only other studies that have involved some examination of lakeshore processes have been carried out by Allan (1991), who looked at how beaches respond to storm waves at Lake Pukaki and Macbeth (1988), who examined the beaches of Lake

Coleridge with respect to the wind/wave climate of the lake. Most recently, Allan and Kirk (2000) assessed lake wave development and characteristics from Lake Dunstan and Kirk *et al.*, (2000) looked at processes of shoreline erosion in Lake Hawea with special regard to wave run-up in the swash zone. In particular, there has been only one study of longshore sediment transport in a lacustrine environment; Worthington (1989) made some measurements of gravel transport on some Lake Coleridge beaches. Some longshore sediment transport measurements were also made by Pickrill (1976) in his study of Lakes Manapouri and Te Anau. Both these studies will be discussed in greater detail in later chapters. Commenting on this state of affairs, Allan (1998: 25) concluded that:

“Greater effort is therefore required by lacustrine investigators to provide quantitative measurements of waves, currents and sediment transport for the lakes of New Zealand as opposed to utilising theoretical approaches.”

In fact, this situation is not unique to New Zealand. An examination of overseas studies reveals that they too fall into the four broad areas identified above, a fact also noted by other lakeshore researcher's (Allan, 1998; Macbeth, 1988; Pickrill, 1985). By far the most studied lakes in the world are the Great Lakes of North America. A great deal of research has been published concerning these lakes, especially in the past fifty years. Since the early 1950s there has been a sustained period of rising water levels and shore erosion coupled with increasing development and pollution around the shores of these lakes (Cobb, 1987; Larsen, 1985). Consequently, much of the research has been driven by pollution and erosion management concerns (Meadows *et al.*, 1997; Angel, 1995; Davidson-Arnott, 1989; Hands, 1980; Thomas, 1973). Comparatively little work has been concerned with lakeshore processes, including longshore sediment transport. Most of the process work has cantered around shoreline development and beach responses to varying water level and wave conditions (Wood *et al.*, 1994; Lorang, 1993; Reid *et al.*, 1988; Coakley and Cho, 1972; Norrman, 1964). These studies in particular often acknowledge the importance of sediment transport processes, but tend to focus on cross-shore sediment transfers, nearshore currents and the response of the beach profile to these exchanges (Sheng *et al.*, 1989; Davidson-Arnott, 1986; Coakley and Skafel, 1982; Meadows, 1977; Sutton *et al.*, 1970). Other studies have concentrated on lakebed sedimentation and suspension transport processes (James *et al.*, 1997; Kumagai, 1988; Gilbert, 1975) and wind-wave development in low energy environments (Jin and Ji, 2001; Meadows and Wood, 1997; Smith, 1991). Therefore, this study will provide a significant amount of new information regarding longshore transport processes of a low energy lacustrine beach.

1.7 Oceanic and Lake Shoreline Differences

There are many similarities between lakeshore (lacustrine) beaches and those of the open coast. Both have shorelines composed of a wide range of materials, from unconsolidated sands and gravels through to hard rock shorelines. Both have wave activity that acts upon these shorelines, reshaping them through sediment transport processes to produce a variety of beach morphologies. Consequently, coastal geomorphologists who have studied lakeshores have observed that many of the findings relating to open coast processes are equally as applicable to lakes (Pickrill, 1978). However, there are differences between the two environments and these need to be acknowledged when extrapolating findings from a lacustrine to an ocean setting.

The major difference between lakes and oceans is their size. While this may seem obvious, it has critical implications for the processes that can develop and operate in the two environments. Most importantly, it affects wave development. The magnitude (H) and frequency (T) of a wave is a function of four factors, expressed in the relation:

$$H, T \approx f(FD\bar{U})d \quad 1.1$$

The first factor is the distance of water over which the wind blows, known as the fetch (F). This governs how much water the wind has to transfer energy into. The second is the duration (D) that the wind blows, which governs the amount of time that the wind has to generate waves. Third is the mean velocity (\bar{U}) of the wind, which determines how much energy is available for wave formation (CERC, 1984). Lastly, water depth (d) can be an important wave limiting factor in a shallow lake. These factors control the degree to which a wave can develop, specifically its height, period and length. Wave energy is proportional to the square of the wave height, in other words, the bigger the wave, the greater the energy it contains. It is this wave energy that does work on the shoreline, setting up water movements that transport sediment.

When waves begin to form they are coupled directly to the wind. If the wind stops blowing, the energy transfer from the wind to the water ceases and the waves stop forming. These waves are commonly known as 'sea' or wind waves and usually have periods less than 6 s with heights on average 0.5-1.0 m. However, if the wind blows for a sufficient length of time over a large expanse of water the waves will de-couple from the wind and travel away from the generation area under their own momentum. These are known as swell waves and typically have periods ranging from 6-16 seconds with heights averaging 1.0-2.0 m (Masselink & Hughes, 2003). The ratio between the height and length of a wave is known as the wave steepness. Short period waves tend to be steeper and more erosional in nature, whilst long period waves, more

commonly associated with ocean swell, tend to be flatter and more constructional in nature (Huntley and Bowen, 1975). Consequently, the size of a body of water will limit the type of wave that can form, producing differences in the wave regimes between lakes and oceans. In the open fetch ocean environment, waves of a range of magnitude and type are able to form, constrained only by the duration and velocity of the wind. In restricted fetch environments, such as sheltered inland waters and small lakes, swell waves are unable to develop. Here, the waves are frequently constrained by the fetch, producing small, short-period, lower energy waves, that are characteristically steeper and more erosive in nature (Pickrill, 1976). In addition, there may be extended periods of no wave activity. During these calm periods shoreline changes will be minimal. Thus, lake beaches that often have a limited sediment supply, can present significant erosion hazards (Kirk & Henriques, 1986).

An open coast beach can have multiple wave systems breaking across the nearshore at the same time. This can come about when swell waves, that may have been generated some days previous, approach a coastline where locally formed sea waves are also breaking. These wave systems may be from the same direction or opposite directions, producing amplification or interference between the two wave trains and altering nearshore current and sediment transport processes (Woodroffe, 2002; Kana, 1978). In a restricted fetch environment where swell waves do not form, waves can only approach the shoreline from one direction at a time, as they are controlled by the wind, simplifying the nearshore process environment. In fact, lake beaches often have a limited number of wave approach directions. Topography can exert a powerful constraining influence on the wind by channelling the flow down valley axes (Sturman *et al.*, 1985). This is particularly significant for narrow alpine lakes where a beach may receive waves from only one or two directions, limiting the beach forming and transport processes. Commonly, these lakes display two beach types that are end members of a continuous spectrum. The first is a beach that is aligned shore-normal to the prevailing wind-wave regime, termed a swash-aligned beach. On this beach sediment transfers occur in a predominantly on-offshore direction (Pickrill, 1976). These beaches are commonly found at the two ends of a lake or where a geological feature such as a spur headland runs perpendicular into the lake allowing a beach to form into the face of the prevailing conditions. The second is a beach that is aligned parallel to the prevailing wind-wave regime, termed a drift-aligned beach (Kirk & Henriques, 1986). These beaches are commonly found along the axial shores of a lake. On these beaches sediment transport occurs dominantly in the longshore direction, initiated by an oblique wave approach.

Another significant distinction between lakes and oceans is that lakes are tideless. The small scale of lakes compared the oceans means that the gravitational influence of the sun and moon are incapable of inducing water motions in the form of tides. But lakes are not without water level fluctuations. Although not as regular and predictable as tides, lakes do undergo seasonal and annual variations in their water levels. The water level in a lake is a balance between the inflow and outflow of water by rivers, precipitation and evaporation. A period of hot dry weather will cause a lake to loose water, whilst a prolonged period of wet weather will cause a lake to gain water (Brinkmann, 1985). This natural variation is known as the operating range. The fluctuation of water at a shore enables waves to act on different parts of the beach profile. In a oceanic setting, this fluctuation is a constant and regular cycle increasing or decreasing water depth over a beach profile. Sediment transport occurs over the full range of the profile throughout the tidal cycle. The difference in a lake is that the water level may be sustained at the same height on a profile for a period of days, weeks or even months. When lake levels are very low, waves may erode the lowest part of the profile that in an oceanic setting would never be exposed. When lake levels are very high, waves may access the backshore area of the profile that in an oceanic setting would normally be beyond reach of the water (Pickrill, 1976). The irregularity of these events means that lake shores have greater difficulty in developing an equilibrium with the environment and in fact, may never adjust to the conditions. For this reason, lake shores often present increased inundation and erosion hazards (Kirk and Henriques, 1986). Furthermore, variations in slope angle and sediment composition across a profile mean that sediment transport processes will alter depending on the part of the profile that is exposed to wave activity.

Shorter term water level fluctuations also occur in lakes. Just as wind and wave set-up can cause a localised elevation of water level in the shore of on oceanic beach, so too can this occur in lakes. However, in some lakes there is an added twist to this process. When the wind blows for an extended period of time over a lake surface, water levels can become slightly elevated at the windward end of the lake. When the stress exerted by the wind eases, the water seeks to become level due to the influence of gravity. In the process a pronounced wave may travel across the lake reflecting off the opposite shore and repeating the process until the it runs out of energy. This phenomenon is known as a seiche. The magnitude of water level oscillations caused by a seiche depends on the basin geometry and local wind fields (Csanady, 1978). Whilst a seiche does not have enough velocity to initiate sediment transport in the shoreline, they are responsible for causing water circulations that may contain a suspended sediment load (Green, 1975). Lake Wakatipu has a well known seiche, that behaves as close to a tide as can be found on a lake.

The preceding paragraphs have discussed the chief differences between lakes and oceans, highlighting the critical difference that scale effects exert on the process regimes of the two environments. While this applies to all lakes in general, a careful distinction was made between restricted and unrestricted fetch environments. In particular, restricted fetch environments were identified as sheltered inland waters such as harbours or bays and small lakes. It is important here to recognise that some lakes are so large that the fetch distances are more-or-less unrestricted. A good example of this is the Great Lakes of North America. Lake Superior, the largest of the five lakes is 563 km long, 257 km wide and with a surface area of 82 814 km² is the largest expanse of fresh water in the world. The large size of these lakes means that the wave and nearshore processes have more in common with oceanic coasts (Pickrill, 1985). Fetch lengths facing the prevailing winds are hundreds of kilometres long, allowing swell to develop. Wave heights commonly exceed one metre high and can be up to six metres. Many of the shores are gently sloping sandy beaches that exhibit the nearshore current circulation systems and transport processes seen on oceanic sandy coasts.

By contrast, the glacial lakes of the South Island are much lower energy environments. Fetch lengths are short and this usually restricts waves to under one metre in height. The shores are characteristically steep (7-8°) and more reflective in nature. A typical South Island glacial lakeshore has a wide range of sediments that are exposed to a low energy wind-wave regime (Kirk & Henriques, 1986). Pickrill (1976) noted that there are differences between the processes and morphology of sandy and gravel shores, just as there are between fine and coarse grained beaches of the open coast. The same is true of other glacial lakes. In a comprehensive survey of Lake Vättern, a 1905 km² glacial lake in Sweden, Norrman (1964) found a range of shoreline types and associated morphologies. Norrman observed that there are differences in the processes and responses of the various beach types. Lorang *et al.* (1993), in a study of Flathead Lake, Montana, a glacial lake similar to those of the South Island, found that coarse grained beaches are reflective in nature and fine grained beaches are dissipative. Coarse grained lakeshore beaches display processes more in common with mixed sand and gravel beaches of the open coast because waves approach very close to the shore before breaking. Waves break directly into the swash zone where the bulk of the sediment transport occurs. Longshore transport occurs in this zone, initiated by an oblique wave approach (Pickrill, 1976). Finer grained lakeshore beaches commonly display a ridge and runnel morphology. Sediment transport occurs across the nearshore and exchanges readily take place between the foreshore and nearshore (Lorang *et al.*, 1993).

After carefully examining the lakeshore profiles of Lakes Manapouri and Te Anau, Pickrill (1976; 1978) concluded that the beaches composed of unconsolidated sediments tended to develop a distinct three-part morphology in response to local wave, water level and sedimentary conditions, similar to a continental shelf (Figure 1.7). The foreshore is moderately steep ($7-8^{\circ}$) and occurs between mean water level and the upper limit of the active beach deposit. Immediately below water level is the more gently sloping ($5-6^{\circ}$) nearshore shelf. At the edge of the shelf, the slope steepens rapidly into the offshore face in which the sediment sits at its sub-aqueous angle of repose. Pickrill went on to show that there is a strong correlation between the fetch length and the width of the nearshore shelf. In general, shorelines that have long fetches and are exposed to high wave energies tend to develop wider, flatter shelves.

Pickrill's studies suggested that while longshore sediment transport played a role in the development of these profiles, on-offshore transfers were far more significant in the process. This assertion was challenged by Allan (1998) in his study of the shoreline development of Lake Dunstan. Allan argued that Pickrill's model was overly simplistic, ignoring antecedent conditions and downplaying the role that sediment characteristics, supply and transport have in exerting a control on beach development. Allan showed that in lakes, a range of beach profiles can develop in response to their orientation to the wind/wave regime, their sediment composition and the consequent sediment transport processes that will operate as a result of these conditions. Both these studies acknowledged the role that sediment transport has in altering the morphology of the profile, but neither directly examined the process. This thesis will address the need to examine in greater detail the process of longshore sediment transport in lacustrine environments.

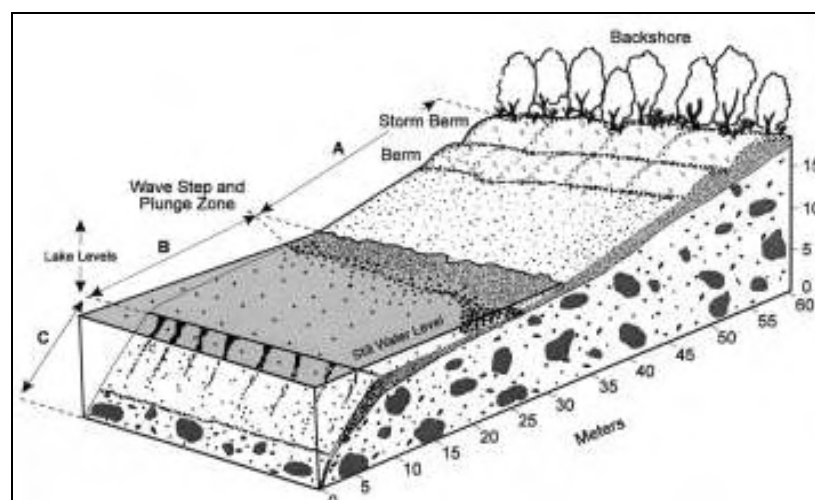


Figure 1.7 Idealised lake beach profile combining a three part morphology termed; the foreshore (A); the nearshore shelf (B) and; the offshore face (C). (From Allan, 1998: 10).

1.8 Conceptual Lakeshore Sediment Transport Model

The discussion of the previous sections has highlighted some of the many environmental variables important in the process of longshore sediment transport. Understanding the relationships between the environmental parameters can be complex, as many of them are interrelated. One way of organising and understanding the way in which numerous variables interrelate, is with a conceptual model. The utility of a conceptual framework for coastal studies was demonstrated by Krumbein (1963) with his well known process-response beach model. In recognition of the differences between an open-coast beach and a lakeshore beach, a process-response model has been developed for this study that highlights the important environmental conditions influencing longshore sediment transport in a mixed sand and gravel lakeshore (Figure 1.8). The structural flow of the model has been derived from the conceptual model developed by McLean and Kirk (1969), that illustrates the links between sediment sources and beach processes in shaping beach morphology and petrology. McLean and Kirk's ideas were influenced by Folk and Ward's (1957) 'source area hypothesis', put forward in their study of the sediment characteristics of a large bar in the Brazos River, Texas.

The level of dependency increases downward through the model. At the top of the model, the first order controls are independent of beach process. At the bottom, the third order controls are dependant on all the structural controls and the processes above them. The geology and topography of a costal or lacustrine environment has an influence upon and provides the physical setting in which the sedimentary and morphological and characteristics of a beach develop. Sediment transport occurs at the interface between the hydrodynamic and morphodynamic boundary. It is part of the process by which energy, in the form of waves and currents, is transmuted and dissipated. As part of these energy transfers, sediment transport reshapes the nearshore and foreshore of a beach profile. These morphodynamic changes have a strong feedback mechanism, altering the wave form and expression of wave energy dissipation. In turn, this alters the sediment transport process and the interplay between the process-response variables continues in a dynamic equilibrium. The model will be referred to in relevant sections throughout the thesis.

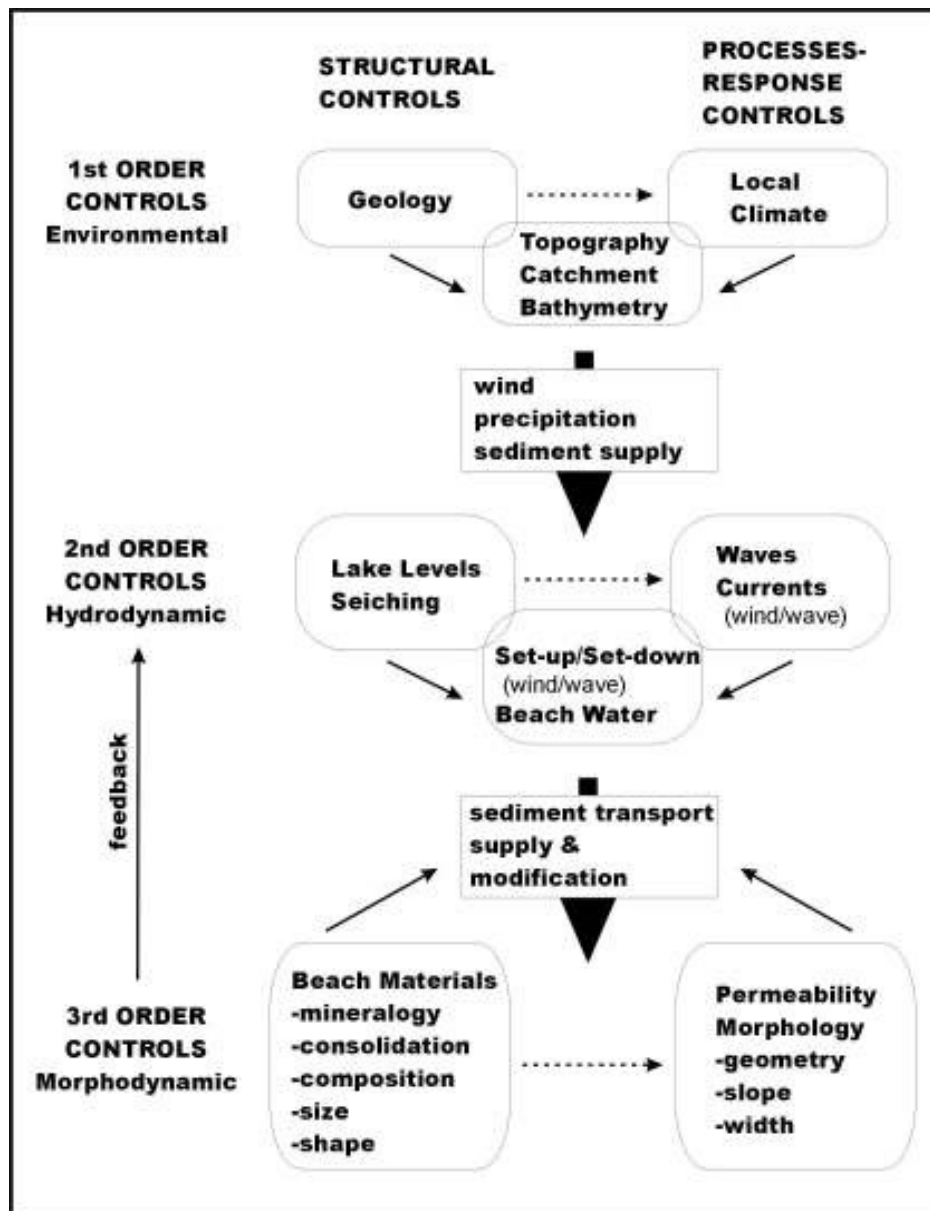


Figure 1.8 Conceptual model of a lacustrine beach, relating environmental, hydrodynamic and morphodynamic controls to illustrate their levels of dependency. Structural controls appear on the left hand side of the model. These controls do not cause a response, rather they exert an influence and constrain the manifestation of the process-response controls (indicated by dotted line).

1.9 Terms and Aims of Research

The differences between sand and mixed sand and gravel beaches have important research implications. In a mixed sand and gravel beach the dominant beach building sediments are confined to the foreshore where they are worked in the swash zone. Consequently, this is where longshore sediment transport investigations must focus. While this much is recognised about mixed sand and gravel beaches, there have been almost no measurements of longshore sediment transport rates and only a few studies have examined the hydrodynamic processes of the swash

zone. Much of the theory regarding mixed sand and gravel beaches pertains to findings from the open coast, because this study has been conducted on a lake shoreline it will provide important new insights into a lakeshore beach. Thus, the primary aim of this study is:

1. *Investigate the processes of longshore sediment transport in a mixed sand and gravel lakeshore beach.*

In doing so, the hydrodynamic processes of the swash zone will be examined, especially as they pertain to sediment transport. Thus, the secondary aim of this research is:

2. *Examine the swash zone processes of a mixed sand and gravel beach relevant to sediment transport.*

The main energy input at the shoreline arrives in the form of waves. On a mixed sand and gravel beach these are primarily incident gravity waves. High frequency lake waves have different characteristics to long period ocean waves and have received little attention in the literature. In sediment transport studies it is critical to have an accurate understanding of the wave characteristics and nature of wave breaking. It is this wave energy that sets up current motions that entrain and transport sediment along the shore. Thus the third aim of this thesis is to:

3. *Describe the nature of lake waves and the characteristics of wave breaking and energy dissipation that leads to the initiation of longshore sediment transport.*

From this research a sediment transport model will be developed that can be used to accurately estimate rates of longshore sediment transport to within an order of magnitude. Thus, the fourth aim is:

4. *Develop a first order model that can reasonably estimate longshore sediment transport rates for a mixed sand and gravel lacustrine beach.*

In the process, previously developed longshore sediment transport models will be tested for their effectiveness for use in mixed sand and gravel environments. Thus, the fifth aim is:

5. *Assess the effectiveness of commonly used longshore sediment transport models for use in mixed sand and gravel beaches.*

CHAPTER 2.

LAKE COLERIDGE

*“I’ve witnessed all the winds that blow, from Land’s End to Barbadoes-
Typhoons, pamperos, hurricanes eke terrible tornadoes.
All these but gentle zephyrs are, which pleasantly go by ye,
To the howling, bellowing, horrid gusts which sweep down the Rakaia”.*
M. Stoddart (1852)

2.1 Introduction

This chapter introduces the fieldsite and the Lake Coleridge environment in which it is situated. It is important to have an understanding of the local environment, as this influences many of the processes that operate on the lakeshore. With reference to Figure 1.7 in Chapter One, this will involve an examination of the local climate, geology and geomorphology of Lake Coleridge. These are the first order controls that influence lake shore development and associated beach processes, in particular longshore sediment transport. The chapter finishes by introducing the fieldsite and by providing a description of the locations where the field experiments and data collection have taken place.

Lake Coleridge is a moderately sized glacial lake situated on the eastern side of the Southern Alps in the mid-Canterbury high country (Figure 2.1). There are 475 lakes in the South Island and 56% or 268 of these are of glacial origin. Comparatively little is known about the shoreline processes of these lakes and in fact, of glacial lakes worldwide. This is surprising considering their ecological and economic significance. Many of the lakes have settlements on their shores and in all places there are management issues surrounding their development in terms of providing housing, public utilities, transport infrastructure and recreational amenities. Many of these lakes have been developed for hydroelectricity schemes, including Lake Coleridge and the environmental issues that this has raised has consistently required coastal management expertise. Frequently however, experts have very little direct information concerning the process and geomorphological environment of these lakes. There is little data concerning the wind and wave regimes, the processes of sediment transport and shoreline development of many of these lakes. This lack of information has at times led to misinformed decision making, resulting in serious problems that have required expert advice to manage (Kirk, 1988). Allan (1998) has commented that there is a real lack of detailed information that describes lakeshore processes in New Zealand.

Lake shorelines lend themselves to studying complex processes of sediment transport because they generally have simpler, lower energy wave environments than their open coast counterparts. The discussion in Chapter One highlighted the major differences and similarities between ocean and lake beaches. An important issue with the studies that have attempted to quantify transport rates on oceanic mixed sand and gravel beaches has been a lack of reliable wave data. In many studies there has been limited knowledge of the wind and wave climate. Part of this problem stems from a lack of suitable instrumentation by which to measure the nearshore process environment. Because the swash zones of mixed sand and gravel beaches are such high energy environments, most data collection instruments cannot withstand the forces subjected to them in this zone. This has limited the quality of data that can be collected. As such, researchers have had to rely on medium and long term data gained from beach surveying and aerial photo analysis by which to quantify transport rates. The lower energies experienced in a lake environment overcomes many of these problems. This not only makes them safer places to conduct research, it also means less wear and tear on equipment.

Lake Coleridge is an ideal place to study longshore sediment transport for a number of reasons. The Lake is 18 km long and 3.5 km wide at its maximum and contains around 45 km of shoreline (Figure 2.1). MacBeth (1988) made a morphological study of the beaches around Lake Coleridge and found that they were generally narrow, steep and composed of coarse sediments. In this respect, he commented that they are similar to the mixed sand and gravel beaches of the east coast of the South Island. The Lake is orientated northwest-southeast and subsequently, is exposed to strong north-westerly winds that blow down the Wilberforce valley and from southerly winds that blow up the Rakaia Valley. These winds can generate waves of up to 1.5 m high (MacBeth, 1988). Thus, it is small enough to be considered a low energy wave environment, but big enough to experience appreciably large waves that will provide useable results and give the study wider application. The orientation of the Lake to the prevailing wind ensures that many parts of the shoreline experience an oblique wave approach, and as a result, longshore sediment transport. This makes Lake Coleridge a good natural laboratory for examining the processes of long shore sediment transport in the high energy swash zone.

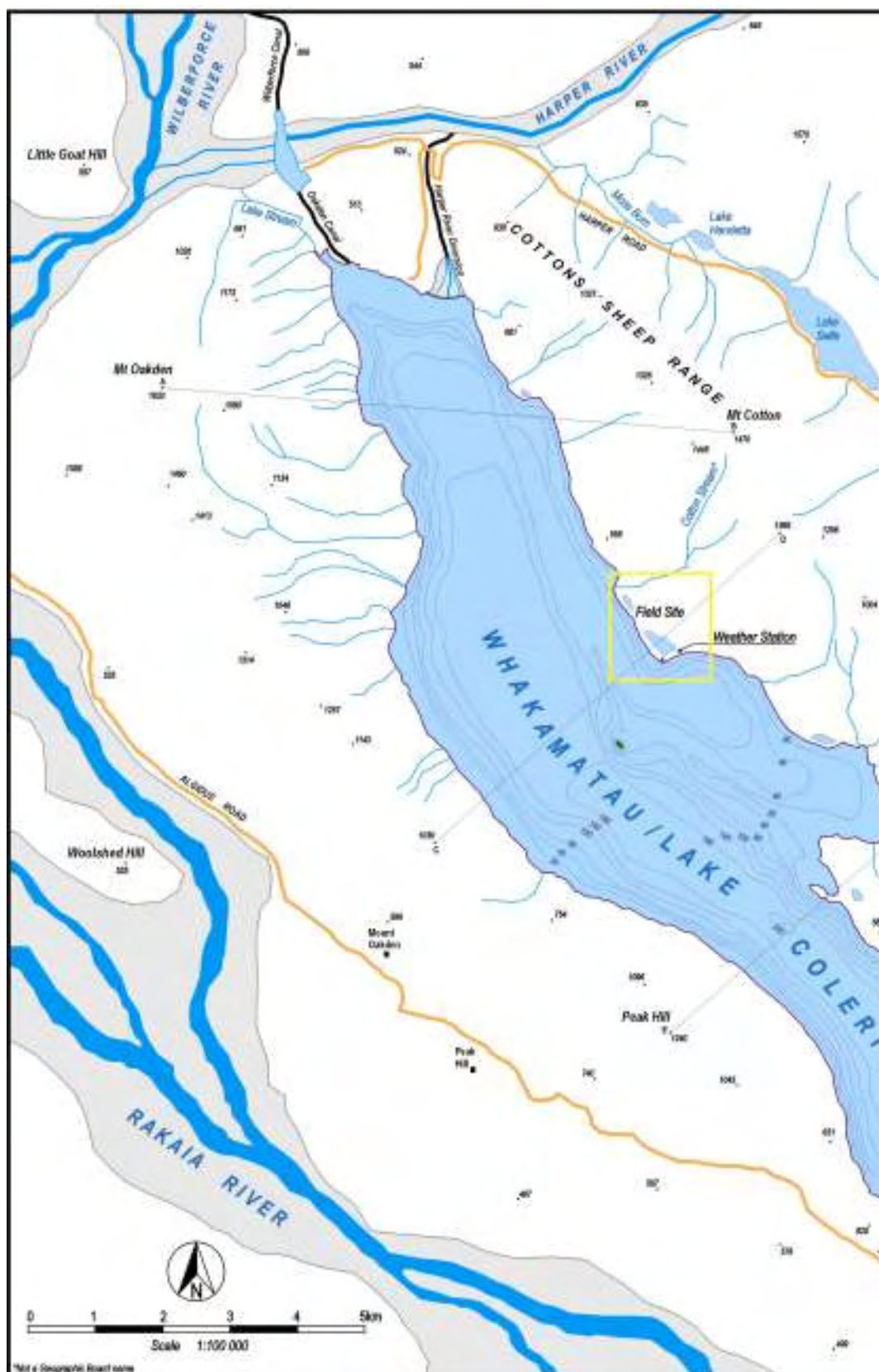
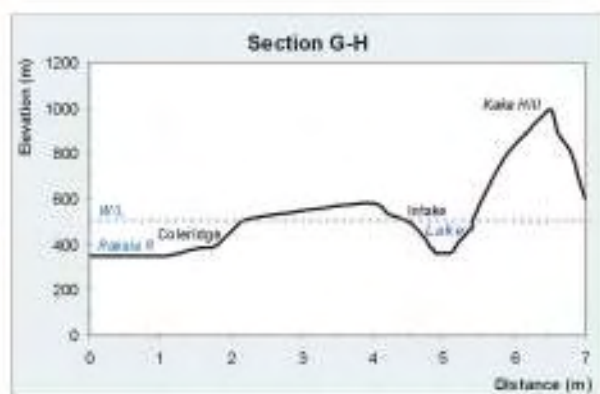
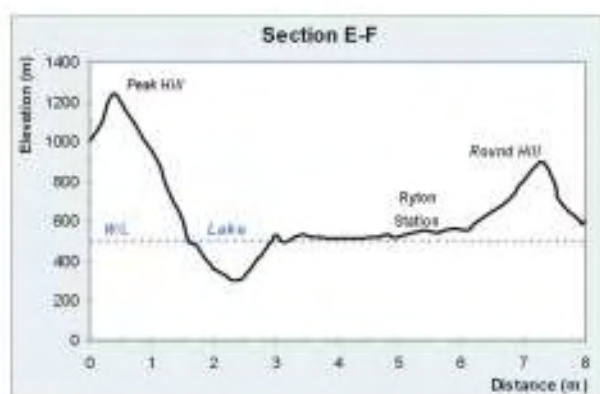
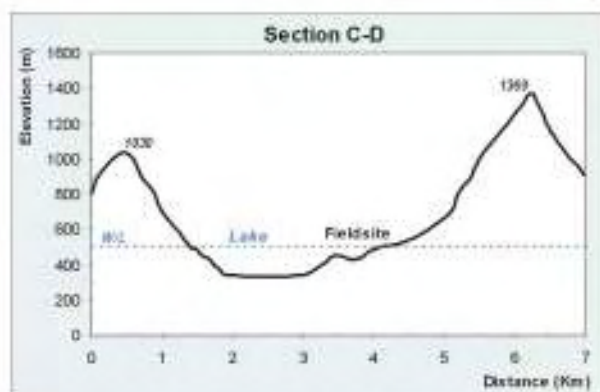
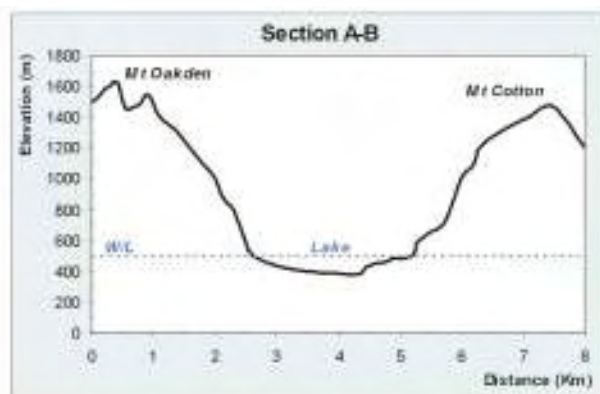
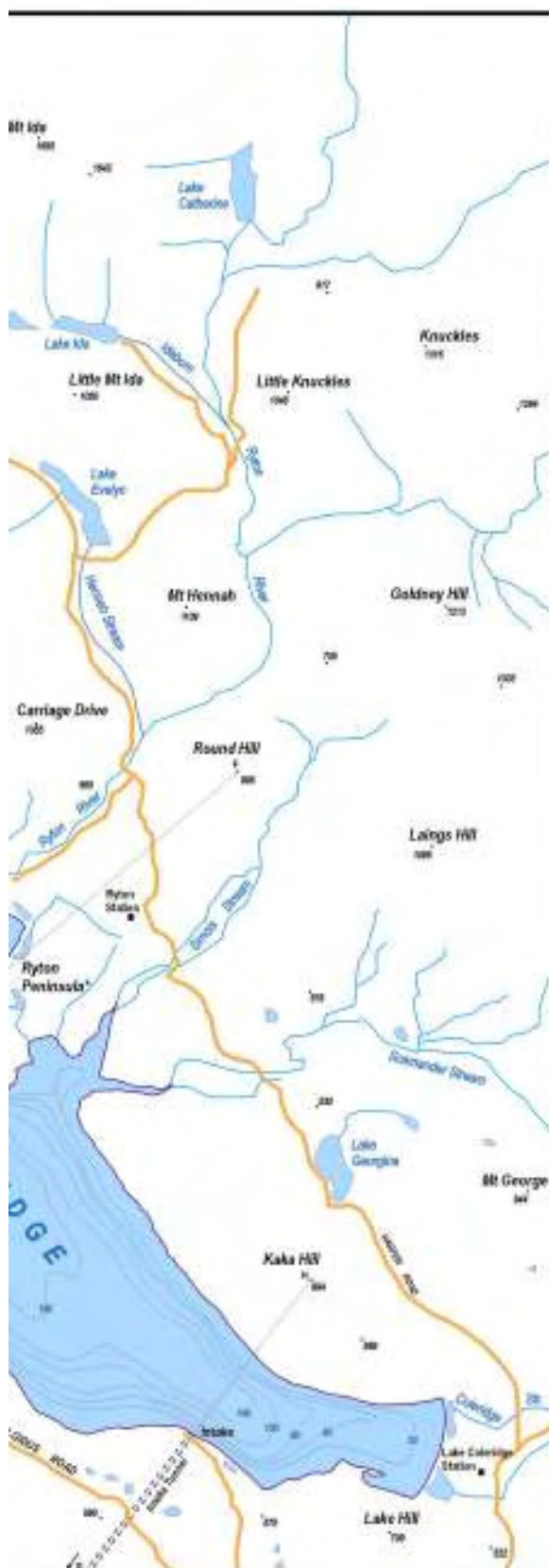


Figure 2.1 Lake Coleridge Map showing major geomorphic features, fieldsite location and cross-sections.

Continued next page...



2.2 Geology and Topography

Lake Coleridge lies in an area of complex glaciated terrain and this glacial activity is reflected in the geomorphology and sediments of the lakeshore (Figure 2.2). The Lake has formed in a deep depression excavated by a large glacier that occupied the Wilberforce Valley during the Late Pleistocene from around 110,000-14,000 B.P. This is illustrated by the cross-sections in Figure 2.1. Soons (1963; 1964) and Soons and Gullentops (1973) recorded 10 ice advances and retreats in the Late Pleistocene alone. It is thought that the Lake Coleridge basin was formed by the last of these advances in the Otiran Glacial Stage (24,000-14,000 B.P.) (Gage, 1975). This huge mass of ice furrowed deeply into the basement rocks of the area which are part of the Torlesse Supergroup and consist of steeply dipping and intensely folded greywacke and argillite units of Upper Triassic to Jurassic age (230-144 mya) (Figure. 2.2). These rocks have been divided into two units of overlapping age based on localized fossil evidence (Gregg, 1964). The older unit, laid down in the Triassic (248-213 mya) is known as the Balfour Series and is the dominant Series of the Lake Coleridge area. In the lower Harper River valley, there is a limestone and sandstone deposit of Tertiary age laid down in the Oligocene epoch (38-24 mya). This is part of the Landon Series, a large limestone sequence associated with the Castle Hill limestones to the northeast of Lake Coleridge.

The remainder of the geology of the area is encompassed by the Hawera Series. This Series is composed almost entirely of greywacke and argillite river gravels and glacial tills derived from the Torlesse Group. Around Lake Coleridge, the Hawera Series contains sediments of Late Pleistocene to Holocene age. The oldest of these is the Burnham Formation, attributed to glacial outwash aggradation of the Blackwater Glacial Advance (*ca.* 22,300-20,000 B.P.) (Gregg, 1964; Suggate, 1965). The second main formation around the Lake is the St. Bernard Formation, associated with the till and gravel of the Poulter Glacial Advance. This was the last major Otiran Stage Glacial Advance of the area, reaching a maximum at the southern end of the Lake around 14,000 years B.P. (Suggate, 1965). Following the retreat of the glacier, massive fluvio-glacial gravel aggradation occurred in the valleys. These are the Post-Glacial or Holocene deposits that cover the valley floors, surround the lake margins and form river fans. In the last glacial retreat the south-eastern end of Lake Coleridge was dammed by terminal moraines and fluvio-glacial outwash deposits. Suggate *et al.* (1978) examined the moraines in this area and dated the Lake to be no older than 13,000 years.

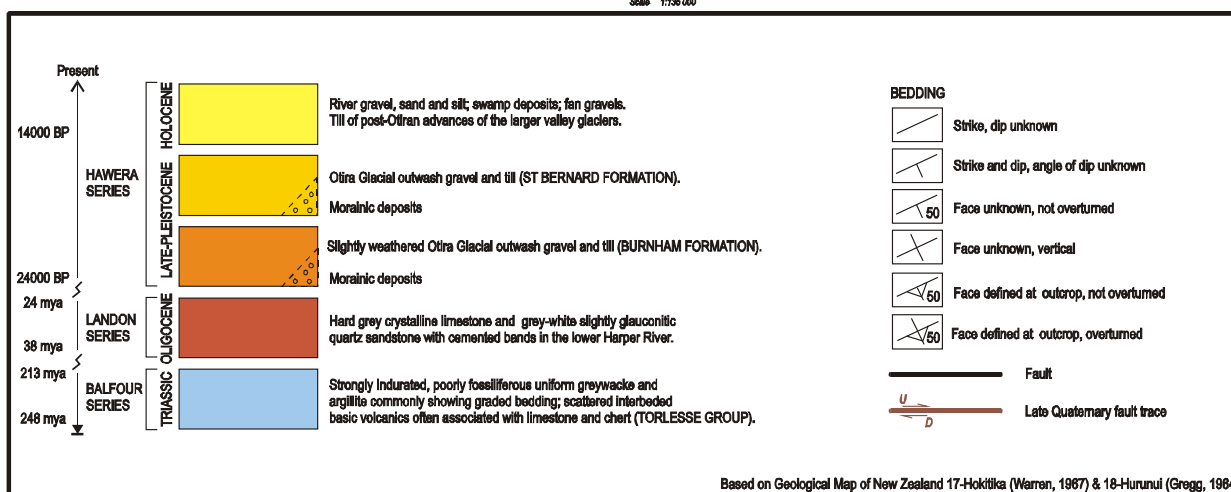
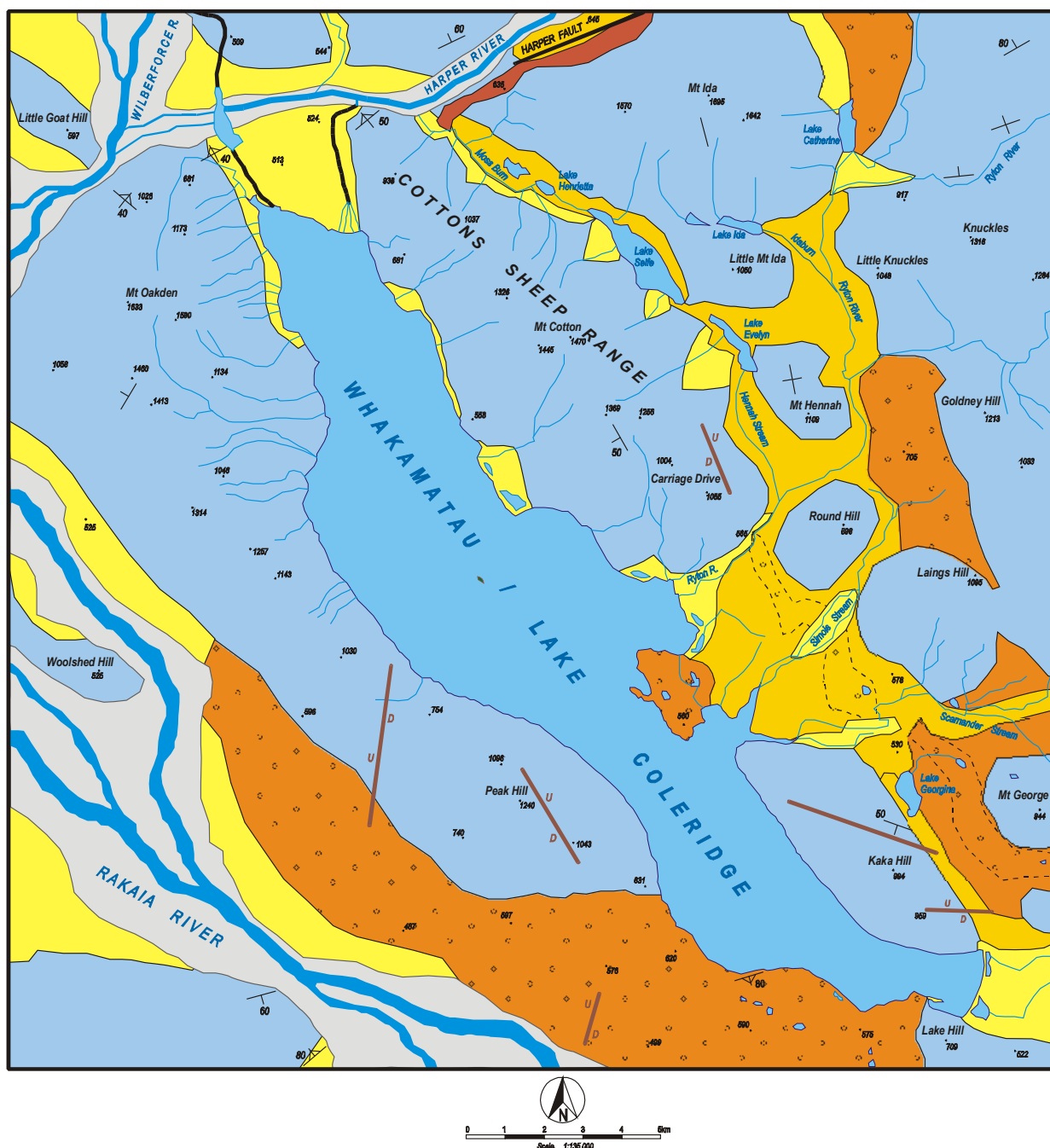


Figure 2.2 Geology map of the Lake Coleridge area. The majority of the catchment is composed of greywacke, making it the predominate lithology of the shoreline and its clastic sediments.

Lake Coleridge is a true fiord-type inter-montane alpine lake. Situated at 510 m above sea level, it is only 17 km from the main divide and almost completely surrounded by mountains (Figure 2.3). Almost half (48%) of the catchment is classified as steep, having slopes of between 26° - 35° (Livingston *et al.*, 1986). On its true left lies the Sheep Cotton Range, rising to 1470 m and Kaka Hill (994m), that drops sheer into the water. On its true right, it is tightly constrained by the Mount Oakden massif (1633 m) and Peak Hill (1240 m) range, that also descend directly into the lake. There are two areas of lower topography around the Lake; first, around the Ryton River delta and Peninsula where the terrain has been levelled by river and glacial action; and second, the terminal moraine deposits that have dammed the lake (Figure 2.4). However, the only true break in relief occurs at the northern end of the Lake where it opens into the Wilberforce River valley (Figure 2.5).

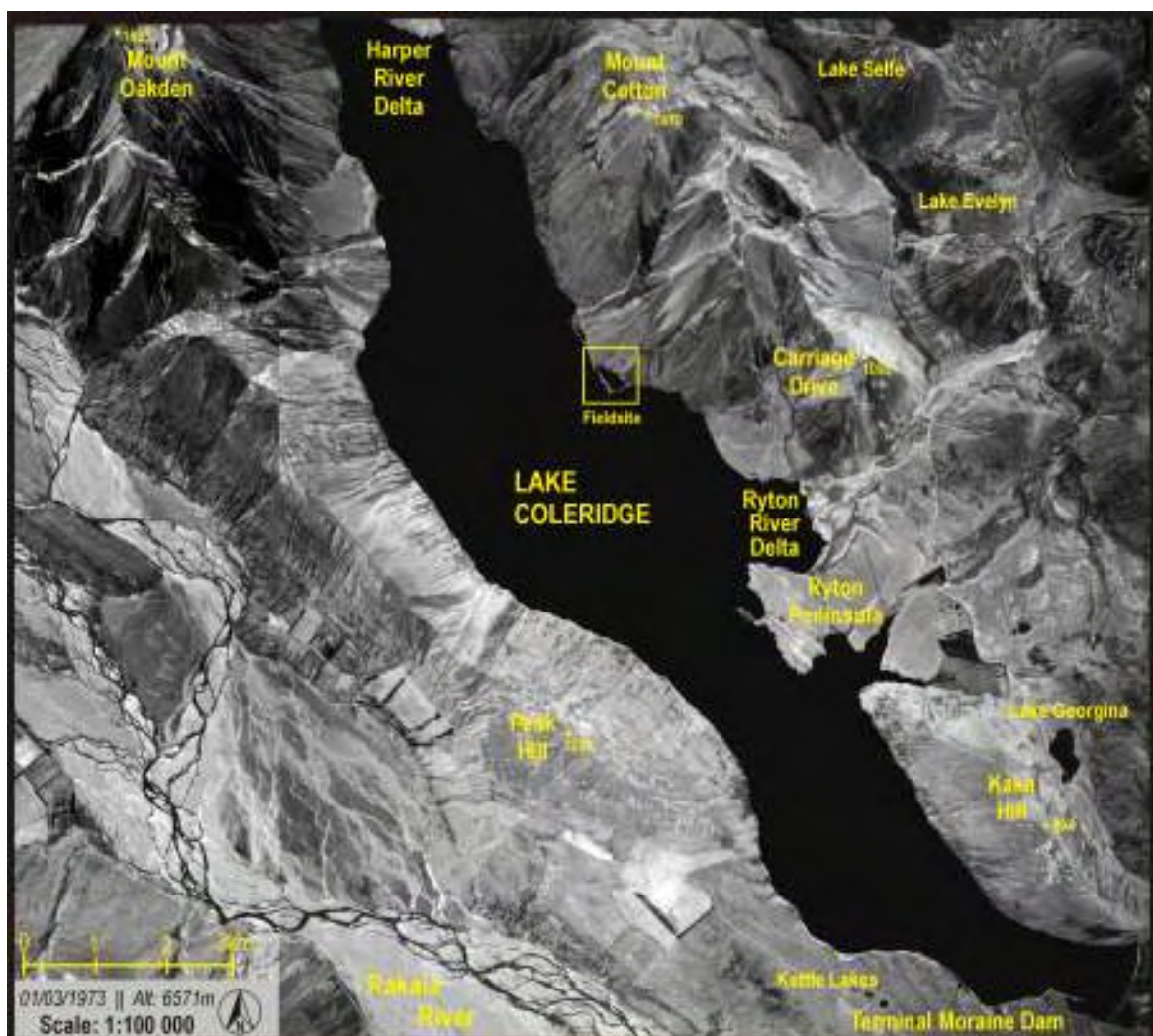


Figure 2.3 Aerial photograph of Lake Coleridge highlighting major geographical features mentioned in the text. The photograph reveals how tightly constrained the Lake is by the surrounding mountains. The only breaks in relief occur at the southern end of the Lake; around the Ryton Peninsula and delta complex and; the northern shore where the Harper River and Wilberforce canal enter the Lake. Spot heights are in metres above sea level.

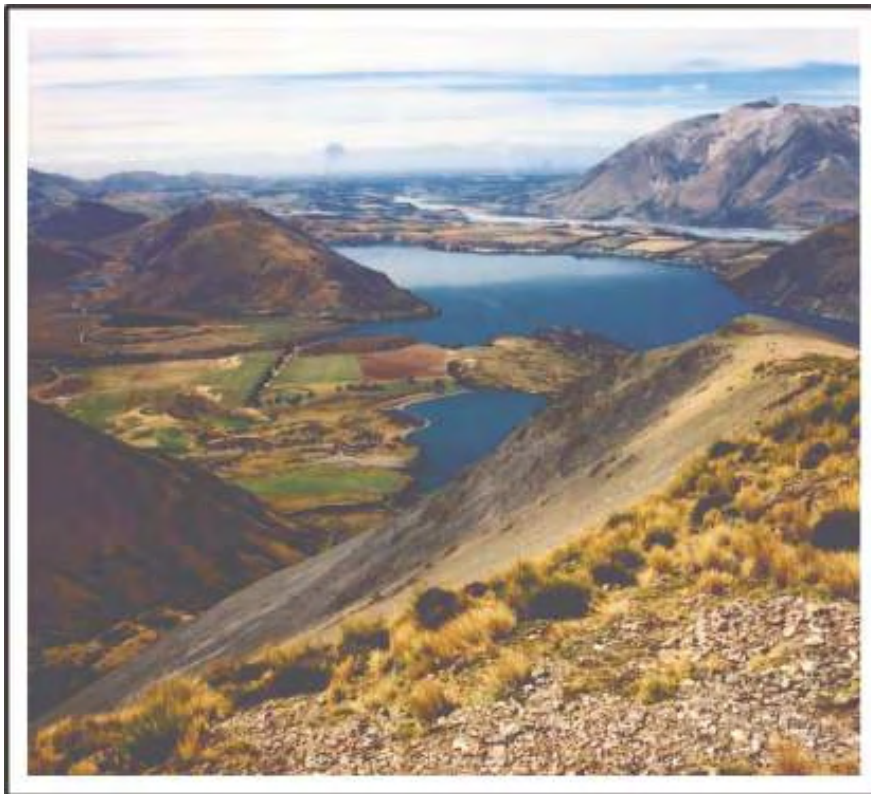


Figure 2.4 View of the southern end of Lake Coleridge from the Sheep Cotton Range showing the two areas of lower terrain. In the middle of the image, the glacially modified Ryton Peninsula can be seen jutting into the Lake, below which lies the Ryton River delta. The mountain in the top right hand side of the image is Steepface Hill (1876 m) at the northern end of the Mount Hutt Range. Immediately below this, the Rakaia River can be seen flowing between the foot of Steepface Hill and the terminal moraines that have dammed the Lake, preventing it draining into the Rakaia Valley.



Figure 2.5 View of the northern end of Lake Coleridge from the slopes of Mount Cotton. The Harper River delta is clearly visible in the north-eastern corner, behind which are a series of irrigated fields and the Wilberforce River flowing from right to left above its junction with the Rakaia. The lower slopes of Mount Oakden can be seen in the background. Note the large and steep alluvial outwash fan at the far left, similar to the outwash fan that backs the fieldsite area. Opposite this is another barrier foreland feature, very similar in form and structure to the foreland on which the fieldsite is located.

Pleistocene glaciations have been one of the most important lake generating mechanisms in New Zealand and around the world (Hutchinson, 1957). Glacial lakes comprise 61% of the total number of lacustrine environments in the South Island. By contrast, there are no glacial lakes in the North Island (Lowe & Green, 1987). Lakes occupying glacially over-deepened basins all bear distinctive features in common, that affect the morphology and process environment of the beaches (Sly, 1978). In general there is a strong positive correlation between the length of a lake and its maximum width. Glacial lakes are typically long, narrow and deep, reflecting the morphometry of the glacier that formerly shaped the valley. Lake Coleridge is 18 km long and 3.5 km wide at its maximum, tapering to 1km wide at its southern end and 1.5 km at its northern end. This gives it an area of 33 km² with around 45 km of shoreline, making it the twelfth largest natural lake in the South Island (Table 2.1). It is also deep, averaging 99 m and dropping to over 200 m at a point roughly in the middle of the Lake. The bathymetry reveals that that lake has a single deep trench with an area of relative shallows north of the Ryton Peninsula (Figure 2.1). Examination of Table 2.1 and Figure 2.6 reveals that in relation to the other major South Island lakes that occupy glacially over-deepened valleys, Lake Coleridge is moderate in size. Therefore, one can be confident that the results obtained from a field study at Lake Coleridge will be applicable to other glacial lakes.

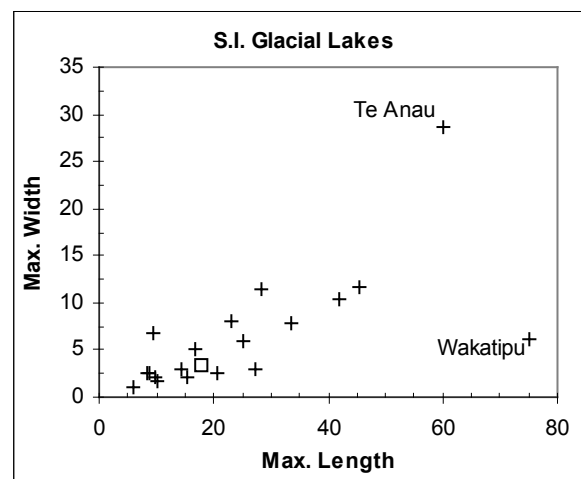


Figure 2.6 Plot showing relationships between length and width of the 20 largest South Island glacial Lakes. Lake Coleridge is indicated by the square marker, revealing that it is average in size. Wakatipu is inordinately long and narrow, whilst Te Anau has a number of arms leading into the Lake at right angles making it wide in places.

Table 2.1 Dimensions of the 20 largest (>5 km²) glacial lakes in the South Island, ranked in order of size. The depths of Lakes Poteriteri and Hakapoua are unknown. Data from Irwin (1975).

No.	Lake	Area (Km ²)	Length	Width	Depth
1	Te Anau	347.5	60.0	28.6	417
2	Wakatipu	289.2	75.2	6.2	380
3	Wanaka	180.1	45.5	11.6	311
4	Manapouri	143.3	28.3	11.5	444
5	Hawea	137.6	41.9	10.4	384
6	Pukaki	98.9	22.9	8.0	70
7	Tekapo	86.8	25.2	5.9	120
8	Hauroko	68.3	33.7	7.8	462
9	Ohau	53.9	16.8	5.1	129
10	Poteriteri	42.5	27.2	3.0	?
11	Brunner	36.1	9.4	6.8	109
12	Coleridge	32.9	17.8	3.5	200
13	Monowai	32.5	20.6	2.5	161
14	McKerrow	18.3	15.3	2.2	121
15	Rotoroa	21.4	14.4	2.9	145
16	Sumner	11.8	9.8	2.1	135
17	Kaniere	13.3	8.6	2.6	197
18	North Mavora	10.8	10.2	1.7	77
19	Rotoiti	9.2	8.5	2.6	82
20	Hakapoua	5.0	5.9	1.0	?

2.3 Climate and Catchment

The terrain in which Lake Coleridge resides exerts a powerful influence on the daily weather and local climate of the Lake and in turn, its lacustrine processes. Wind is directly responsible for wave generation and longshore transport, particularly on lake shores. Thus, it is important to have an understanding of the local wind climate. Wind data is also used for wave hindcasting and provides useful approximations for future wind events. New Zealand lies in a zone in which the prevailing winds are from the southwest to northwest. The Southern Alps exert a strong orographic influence on this westerly air stream by topographically channelling and accelerating the winds down its valleys. Lake Coleridge is ideally situated to receive these winds as it is orientated northwest-southeast and is directly open at its northern end to the strong winds that blow down the Wilberforce Valley. As discussed in Chapter One, waves on lakes are a function of the fetch length and wind velocity. Although the axial length of the Lake is only 18km, its steep sided slopes channel the wind for its entire length. These winds can generate waves of up to 1.5 m from the north (MacBeth, 1988) and up to 0.7 m from the south (James *et al.*, 1995), ensuring that many parts of the shoreline experience longshore sediment transport.

There are no meteorological stations permanently located at Lake Coleridge, so previous workers have either had to install their own, or rely on records from nearby locations. In fact, daily weather records from meteorological stations in close proximity to lakes in New Zealand are not common (Pickrill, 1976; Allan, 1998; Dawe & Hemmingsen, 2001). An extensive search was made of the digitally stored weather database at NIWA, of Metrological Service reports and other relevant publications in order to uncover any weather data that had been collected from Lake Coleridge. From this search, four data sets were identified. In the mid-1970s, wind data was collected by the Ministry of Works on a Lambrechts anemometer at the head of the Lake for the Wilberforce Diversion project. Both wind speed and direction were measured, derived from a single measurement taken on the hour. It was not stated exactly where the instrument was installed, apart from a general reference to it being at the Coleridge Diversion. Much of this data was subsequently lost and all that remains is a record from May 1977 to February 1978, covering a period of 231 days. This data has been collated and is summarised in Figure 2.7. Macbeth (1988) in his geomorphological study of Lake Coleridge beaches, obtained five years of wind speed and direction data collected by the New Zealand Metrological Service from the Lake Coleridge village. It covered the period from January 1983 to December 1987 and was measured with a Munro anemometer at three hourly intervals. Some assumptions had to be made in applying this data to Lake Coleridge because the Rakaia Valley, in which the village is situated, is orientated around 30° further west than Lake Coleridge, causing differences in the prevailing wind directions between the two valley systems. Although the data highlighted some general trends, MacBeth expressed reservations about some of the details. In particular, the data appeared to show an excessive number of calms, ranging from 28% of the time in January to 64% of the time in July. Macbeth (1988: 125) commented that this was contrary to his and other workers experience of the conditions at the Lake. Further examination of the data set reveals that there are very few readings of wind speed below 5 knots (*ca.* 10 kph). This has been found to be a particular problem with Munro wind data collection systems (Sturman, 1985). MacBeth (1988: 125) went on to say:

“Fortunately, this is of little importance for the purposes of this study since the waves generated by weak winds contain so little energy as to be insignificant in achieving much work (ie. sediment transport) in the beach system.”

However, it will be revealed in later chapters, light winds (< 10 kph) are more significant in causing sediment transport than may intuitively be expected, so any weather data used in this type of study must provide accurate measurements of light conditions.

Also collected from the Lake Coleridge Village, is a daily observation of wind speed and direction at 9am from the power station. However, it is felt that these readings do not provide an accurate enough representation of the daily weather conditions to be useful. Moreover, Sturman (1985) found that, similar to the problems with the Munro anemometer, visual observations of wind conditions are often inaccurate in light conditions. In a study by NIWA (Hicks, 1995) of the water clarity of Lake Coleridge, it was decided that there was too much uncertainty in extrapolating the weather data collected from Lake Coleridge Village. Consequently, a weather station was installed on Ryton Peninsula in 1993 and operated until January 1996. It was situated approximately 10 m above mean lake level at Lat. 43°18'0" Long. 171°31'6". The location was sheltered from the northeast by a rise but was exposed to the prevailing winds. This data was correlated with the wind data collected from the village and no significant correlation was found (Hicks, 1995). Unfortunately most of this data was subsequently lost. One year's data was salvaged covering the period from January 1995 to January 1996 that had a 50 day break in the record over the months of May-June. This data is presented in Figure 2.8. The wind direction is a vector average over the hour, whilst the wind speed is a singular burst sample taken on the hour.

Wind Measurements

Considering the critical relationship between wind and wave generation on lakes, a decision was made to install a weather station at the field site in order to collect wind data. On the 2nd of November 2001 a weather station was installed on the southern corner of Cottons Lagoon (Lat. 43°16'24" Long. 171°29'28") (Figure 2.1 & 2.7). It was situated on the crest of the barrier, above the active beach deposit, at 4 m above mean lake level. This site was chosen for two main reasons. Firstly, it was chosen to make readings as close as possible to the water surface, in order to get accurate information about the winds responsible for producing the waves that effect sediment transport. Many studies rely on wave hindcasting from weather records, but often there is a level of uncertainty about the results due to the fact that the weather data has been recorded at a location that is remote from the wave generation area. This is especially true of alpine lake environments, as discussed above. Secondly, because the area is flat and juts into the Lake, it is exposed to winds from both axial directions without interference from surrounding topographical features.



Figure 2.7 The weather station deployed on the southern corner of Cottons Lagoon.

The weather station incorporated a Vector Instruments cup anemometer and wind vane, mounted on a 2 m pole and connected to a Campbell 21x data logger. Readings of wind speed and direction were logged every minute and then averaged on the hour every hour, to produce a single hourly reading of the mean wind speed and direction. This information was then stored to memory. When remote weather stations are installed, a decision has to be made between data accuracy and memory storage. It was decided that the collection of hourly means allowed a balance between providing accurate measurements of the climatic variables important in wave generation, whilst providing enough memory to store up to eight weeks of data. The station operated until the 23rd of September 2003, when it was struck by lightning, causing irreparable damage to the data logger. Unfortunately, 7 weeks data was erased from the memory. In spite of this, a consecutive 21 month data record was collected (Nov 2001-Aug 2003), covering the fieldwork phase of the research programme. The 2002 portion of this data series is summarised in Figure 2.8.

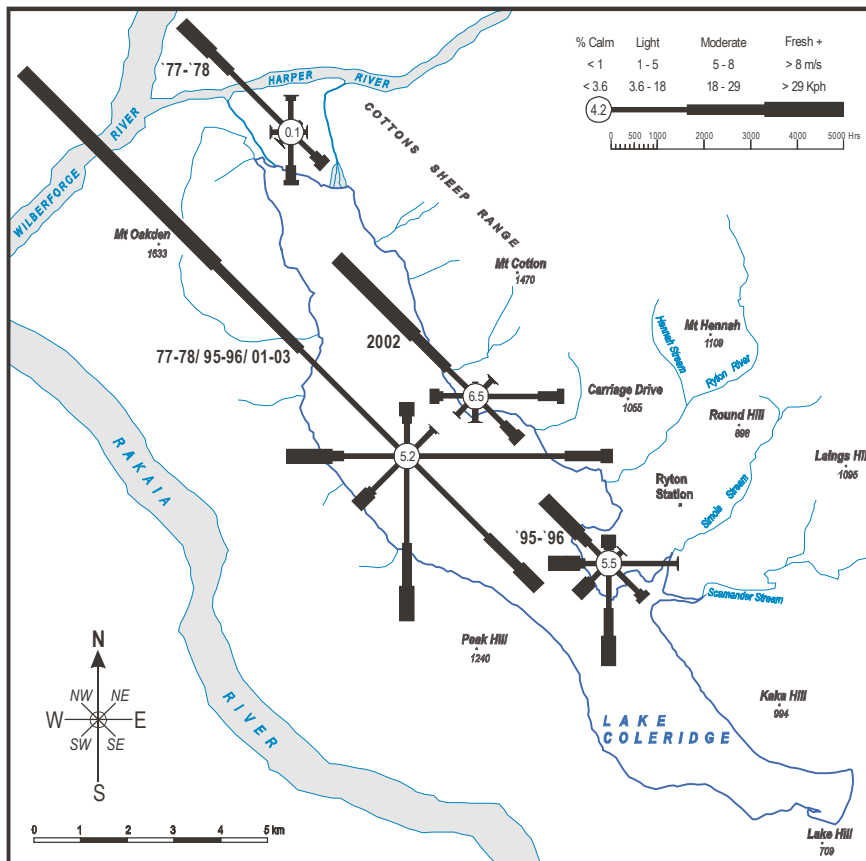


Figure 2.8 Wind roses for all locations around Lake Coleridge where wind data has been collected. The rose for the years '77-'78 contains eight months data; the rose for '95-'96 contains 11 months data; and the rose for 2002 contains a consecutive 12 months of data. The central rose is a collation of all available hourly data for the Lake.

The winds that a location receives are highly localised, especially in mountainous terrain and this is reflected in the wind roses for Lake Coleridge. Examination of Figure 2.8 reveals differences around the Lake in wind direction frequencies and strengths, highlighting the degree to which surrounding topography exerts an influence on the wind. At the head of the Lake there is a strong mode from the northwest wind that is channelled down the Wilberforce Valley and from the south-southeast winds that are channelled up the Lake. There is very little wind recorded from both east and west directions. Winds from these two directions are blocked by Mount Oakden to the west-southwest, and by Cottons Sheep Range to the east-northeast (Figure 2.3 & 2.5). By contrast, on Ryton Peninsula only 12 km to the southeast, the valley opens up a little and winds from the east and west feature more prominently in the record. At the field site, on Cottons Lagoon, the wind pattern differs again. Here the wind regime is strikingly bimodal (Figure 2.9). The dominant mode is from the northwest (45%), ranging from 290-320°, a direction from where the wind is also strongest. The second mode is more diffuse, ranging

through east-southeast from 60-120° (34%). Winds from this direction are more moderate and result from two weather conditions. One is under a southerly or south-easterly airflow and the other is a valley wind that occurs during the day, generated under anti-cyclonic conditions. The valley wind tends to blow more from the east, coming in at times from the low ground behind Ryton Peninsula (Figure 2.3 & 2.4). On the opposite side of the Lake, Peak Hill effectively blocks the southerly, a wind that is far more prevalent on Ryton Peninsula.

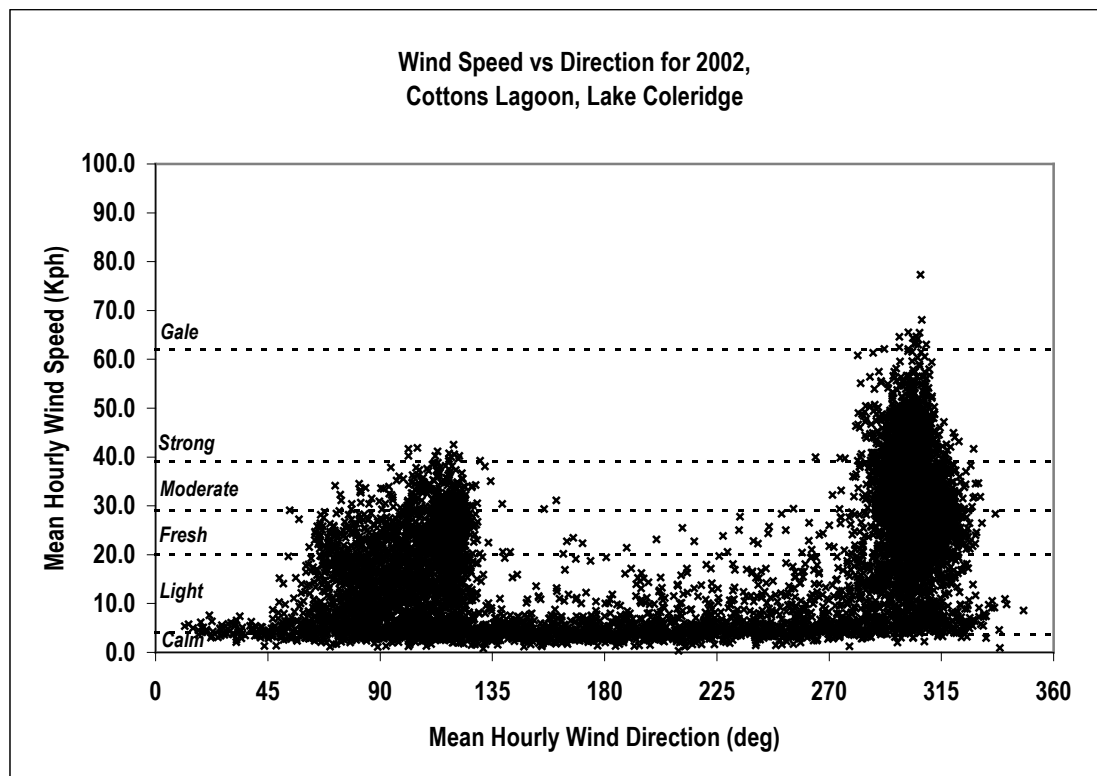


Figure 2.9 A scatter graph of wind speed against wind direction. Two clear modes emerge from the data. One at around 300° and the second at around 90°, with a diffuse scattering of light winds in between the two modes.

The wind pattern at these sites is a reflection of the synoptic weather patterns and the topography of the surrounding mountains; highlighting how important it is to carefully examine the local conditions before applying any assumptions derived from nearby locations. This has critical implications for wave development and wave hindcast modelling, because it indicates that the waves a site receives can be extremely site specific. Importantly, wind data collected from another location and used to hindcast wave conditions may be unreliable. A careful

examination of the surrounding topography is clearly needed when interpreting the wind and wave conditions for a lakeshore environment.

Despite the localised differences in winds, there is a general pattern of wind that characterises the Lake Coleridge environment. The central rose of Figure. 2.7 is a collation of all hourly wind data available for Lake Coleridge; 29,034 hours in total. The wind regime at the Lake is tri-modal (Figure 2.10). The dominant mode is from the northwest, where wind blows for 41% of the time. Winds from this direction are also the strongest. The second mode is more variable in nature, ranging east-southeast, from which it blows 21% of the time. As discussed above, winds from this quarter are generally light to moderate valley winds. A southeast weather pattern generates a wind that is similar in character to a light valley wind. The third mode is from the south and occurs for about 19% of the time. This southerly is generally stronger, but less consistent than the valley wind.

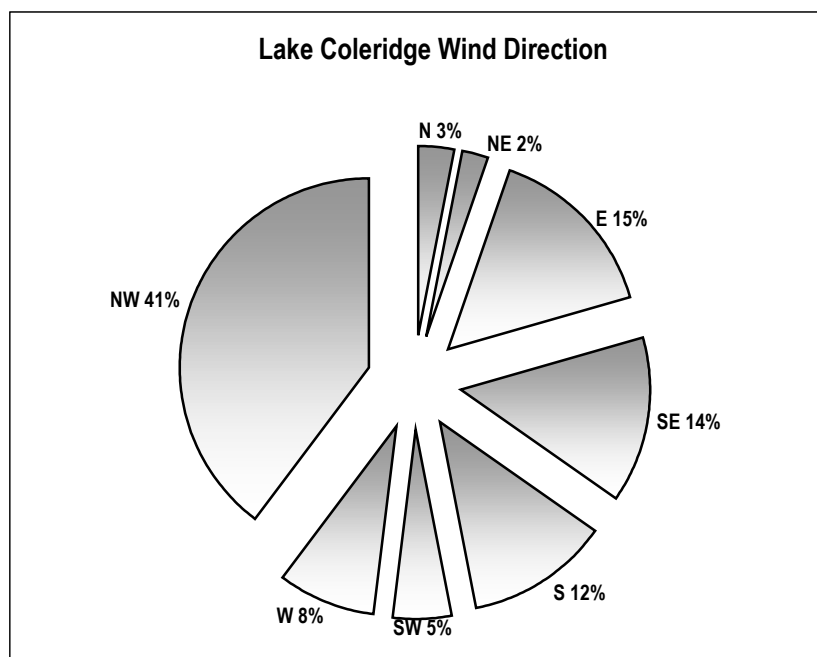


Figure 2.10 Percentage wind directions for all Lake Coleridge wind data.

A curious feature of Lake Coleridge is that there is a greater prevalence of the north-westerly at the northern end of the Lake and conversely, a greater prevalence of the southerly at the southern end of the Lake. While this may seem to be an artifice of the data, it was observed that wind events took a number of hours to ‘fill in’ the length of the Lake. In fact, it is not uncommon to have a north-westerly blowing at the northern end of the Lake and a southerly blowing at the

southern end at the same time, as one wind system gives way to another. A gradation in the frequency of winds from the northern to the southern end of the Lake might be expected. This observation is born out in the data, with more southerlies recorded on Ryton Peninsula and more north-westerlies at Cottons Lagoon. This feature of the wind regime was also occurs in other alpine lakes of the South Island, and was noted to occur at Lake Pukaki by Allan (1991).

Another characteristic of the wind at Lake Coleridge is its strength (Figure 2.11). Calm conditions, classified as less than 3.6 kph (1 m s^{-1}), occur on average only 5.2% of the time. Light winds, that range from 3.6-18 kph ($1\text{-}5 \text{ m s}^{-1}$) are most common, occurring 43.5% of the time. Moderate winds, those that range from 18-29 kph ($5\text{-}8 \text{ m s}^{-1}$) and fresh winds, that range from 29-39 kph ($8\text{-}11 \text{ m s}^{-1}$), occur for almost equal amounts of time at around 20% each. Winds stronger than 39 kph (11 m s^{-1}), blow for a significant 12% of the time at Lake Coleridge; a reflection of the accelerating affect that topography has on wind.

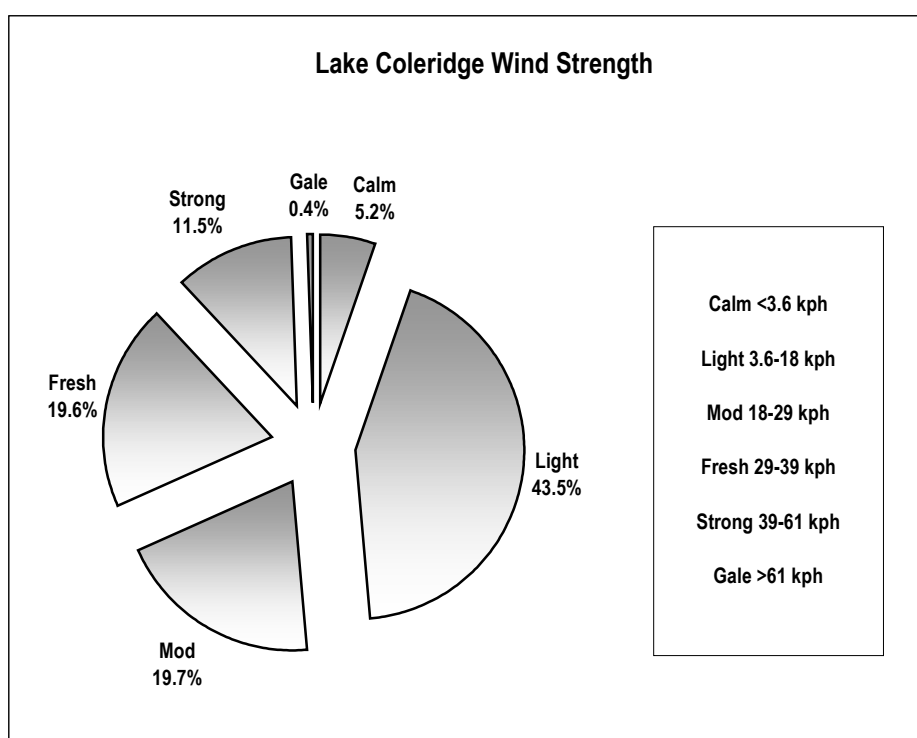


Figure 2.11 Percentage wind strength for all Lake Coleridge wind data.

Figure 2.12 presents wind roses from some of the weather stations in mid-Canterbury. Compared to Lake Coleridge, the winds observed in mid-Canterbury are lighter and occur more frequently from all directions. The difference at Methven and Lake Coleridge is striking, where the predominance of strong north-westerlies clearly point to the effects of the mountain environment. Another location where this occurs is Lyttelton Harbour, where the wind is channelled from the southwest and northeast through the harbour valley. The strength of the wind at Lake Coleridge will clearly be reflected in the wave regime and the process environment of the lakeshore beaches.

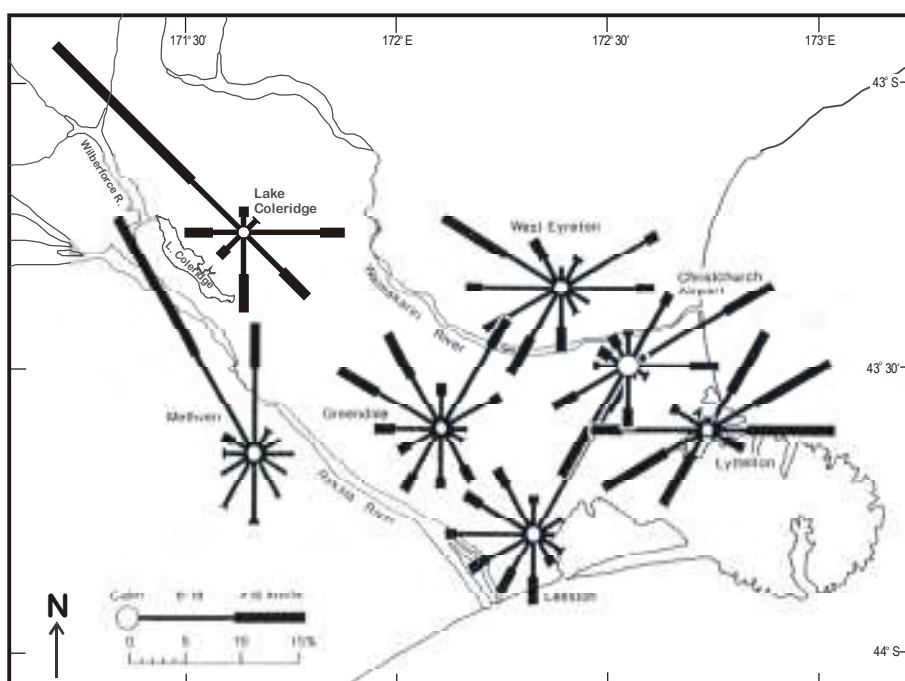


Figure 2.12 Wind roses for selected Canterbury locations. Modified from Ryan (1987: 18)

There is also a strong seasonal component to the wind at Lake Coleridge. The strongest winds occur in September and October, either side of the spring equinox (Figure 2.13a). During this time, the Lake experiences long periods of sustained north-westerlies, that frequently exceed gale force. The north-westerlies are punctured by blustery southerly events. These winds ease in November, where strong northwest events are interspersed amongst long settled periods. The wind picks up again around the summer solstice in late December and early January, before it settles into a summer pattern that consists mainly of diurnal lake breezes from the southeast, punctured by moderate to strong north-westerlies. A second windy period occurs around the autumn equinox in March, often continuing into early April, which is also dominated by north-

westerly events. After this, the wind settles down gradually through the months of May and June, with July being the calmest month on average, with the least north-westerlies (Figure 2.13b). The winter months have a high prevalence of south to southeast winds, but in general they tend to be a lot calmer. These seasonal patterns in the strength and direction of the wind at Lake Coleridge indicate that a seasonal variation in the rates of longshore sediment transport might be expected, with high rates in the spring and summer and lesser rates in the winter.

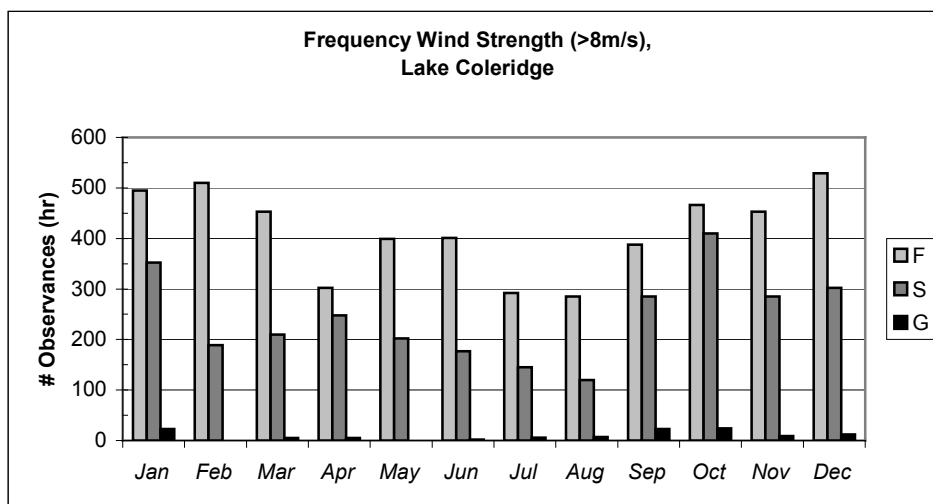


Figure 2.13a Monthly frequency of winds > 29 Kph (8 m s^{-1}). The occurrence of strong and gale force winds peaks around the spring equinox and summer solstice, with a smaller peak at the autumn equinox. F = fresh (29-39 Kph), S = strong (39-61 Kph), G = gale (> 61 Kph)

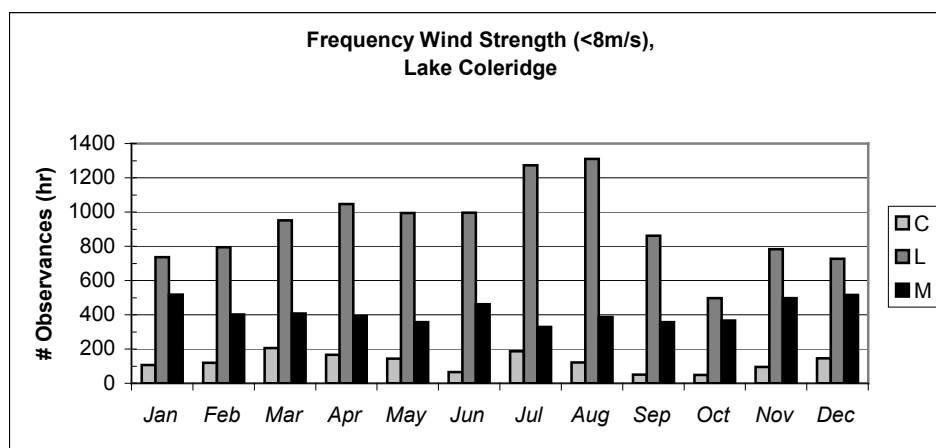


Figure 2.13b Monthly frequency of winds < 29 Kph (8 m s^{-1}). Calm and light winds occur throughout the year, but are most common through the winter months. C = calm (< 3.6 Kph), L = light (3.6-18 Kph), M = moderate (18-29 Kph).

From an examination of the wind data from Lake Coleridge, a bimodal wave climate would be expected, with waves from the northwest and from a range of angles from the south through east. We might expect to see on average, larger waves from the northwest and moderate sized waves from the south. The north-westerly is both stronger and more gusty than the south-easterly, which tends to build in strength and maintain a more constant flow. A seasonal aspect to the wave climate would also be expected with a greater number of large wave events in summer. A table with all the hourly wind direction and speed data available for Lake Coleridge can be found in Appendix 1. The wave regime of Lake Coleridge will be discussed in the following chapter.

Water Balance

Although the Lake is in close proximity to the Southern Alps and three major river systems, it receives very little rainfall and has a low natural water inflow. According to NIWA (2003), the mean annual rainfall averages between 750-1000 mm, which is some 500 mm lower than the surrounding area. Rainfall in the Wilberforce Valley, several kilometres northwest from the Lake, doubles to between 1500-2000 mm. The Lake lies in an area at the limits of both westerly and easterly rainfall. Most of the rain comes from southerly cold fronts. Unlike similar large glacial lakes in the South Island, Lake Coleridge is not fed and drained by a large braided river. At its southern end it is blocked by terminal moraines. At the northern end the lake has been blocked by fluvial aggradation from the Harper and Wilberforce Rivers. The Lake has a natural catchment of approximately 210 km² (Bowden, 1983). The main natural inflowing tributary, averaging 4 m³ s⁻¹, is the Ryton River, which drains the south-western slopes of the Craigieburn Range (Bowden, 1983). Curiously, the only natural outflow is the small Lake stream, at the northern end of the Lake, which used to flow into the Wilberforce River, but is now controlled for the purposes of hydroelectric power generation.

The potential for Lake Coleridge to supply water for a hydroelectric scheme was noted in the early 1900s. It was recognised that in order to support a hydroelectric scheme, water would have to be diverted into the Lake from other sources to boost the natural inflow. Two diversion canals were constructed at the northern end of the Lake, to bring in water from the Wilberforce and Harper Rivers. Combined with forest clearance, which has stripped the catchment, the natural inflow has increased six-fold, to about 28 m³ s⁻¹ (Macbeth, 1988). Although the natural water level range of the Lake was unknown, records of lake levels prior to the first diversion project in 1921, indicate that the Lake had a natural range of around 1.5 m. After 1922 the operating range

of the Lake increased gradually to reach a high of 5m through the 1950s. This led to a dramatic increase in shoreline erosion and following widespread concern, water levels were subsequently more tightly controlled (Bowden, 1983; Britten, 2000). The operating range of the Lake is now 3.8 m, ranging from a minimum 505.6 m above mean sea level (amsl), to a maximum 509.4 m amsl, with an average level of 508.0 m amsl. (John Dignan, Generation Manager, TrustPower, Lake Coleridge, 2001, *pers. com.*).

2.4 Fieldsite

Like most glacial lakes in the South Island, the most common shore type around Lake Coleridge is a lithified, hard rock shore. Notwithstanding this, and in spite of the low river inflows, there is no shortage of unconsolidated shore deposits around the Lake. The beaches of Lake Coleridge were studied in depth by Macbeth (1988) who classified them according to their morphology and the processes responsible for creating them. The field site (Figure 2.1 & 2.14) is located on what Macbeth (1988) described as a *cusped foreland*. It was chosen because it is an active beach, composed of unconsolidated mixed sands and gravels, that is exposed to the prevailing winds. In all, eight sites were used around the barrier foreland in the field programme, seven from the western side and one on the south-eastern side (Figure 2.14). These sites exhibited a range of environmental conditions, but the main difference was in shoreline orientation (Table 2.2). The south-eastern side has a straight linear beach, whereas the western beach exhibits considerable variation in shoreline orientation (Figure 2.14b). All sites were subject to waves from two main directions; the northwest and the southeast, that produced different wave conditions and approach angles. Further variations were measured at each individual site, where beach slopes and sediments varied from hour to hour.

Table 2.2 Sample site orientation in degrees, anticlockwise from north.

Site	CO14a	CO14b	CO10	CO11a	CO11b	CO13	CO40
Orientation	300	315	295 ±5	305 ±5	325 ±5	325 ±5	225

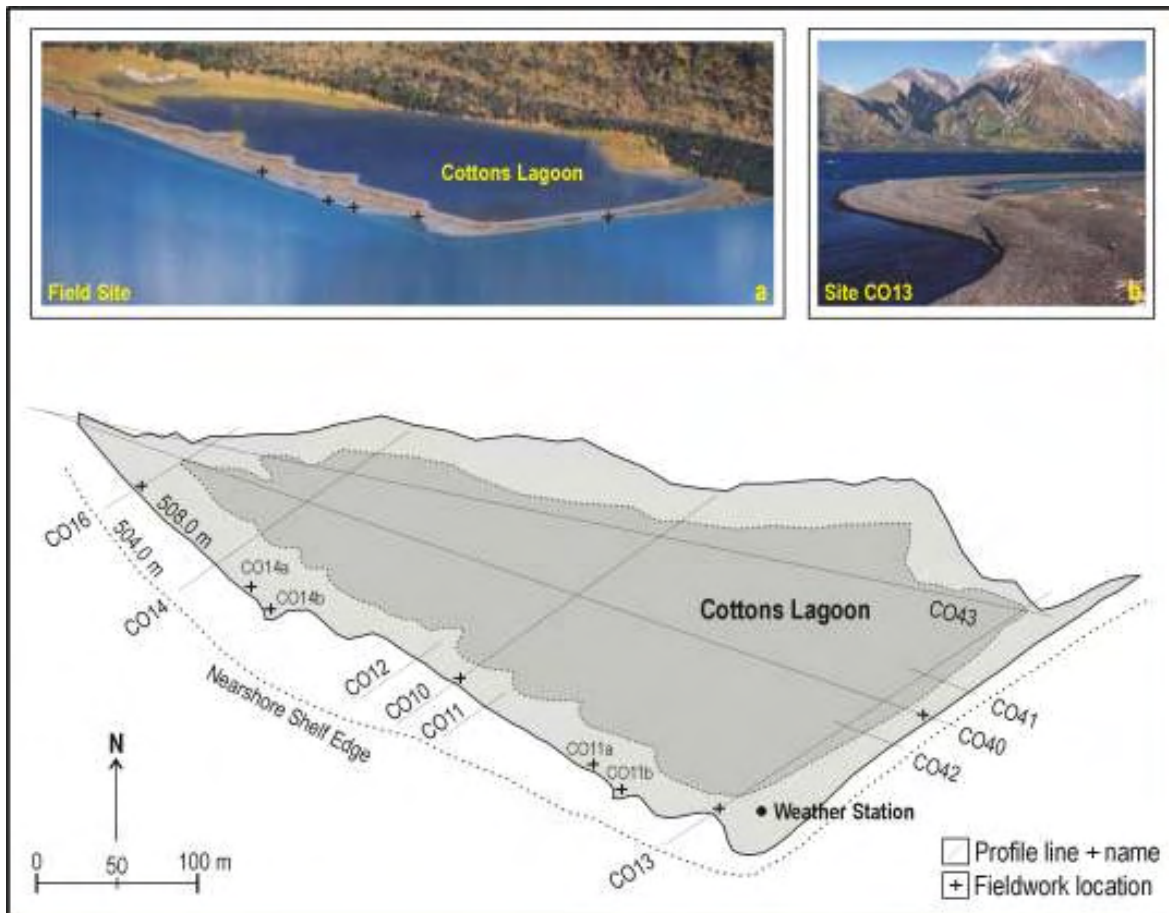


Figure 2.14 Plan view of the barrier foreland, showing survey lines and fieldwork locations.

Cusate forelands are depositional features in which the beach forms a roughly triangular shaped projection from the shore. Very little has been written about the formation of these unusual features, that are more commonly associated with alpine glacial lakes, than the open coast. They do not occur as universally as spits or barriers and this has perhaps contributed to their scant reference in the literature. Masselink and Hughes (2003) noted that the term has been somewhat misused in the coastal literature, in that it has been applied to features that are not strictly cusate forelands. It is generally accepted that they form where two dominant wave systems build a feature out from the shoreline from two opposing longshore current systems (Woodroffe, 2003; Komar, 1998). It is not surprising therefore that long narrow lakes with a bimodal wind directions provide ideal situations for the formation of these features. These features were noted by Norrman (1964) on Lake Vättern who suggested that they were built out by two wave energy maxima of oblique and contrary incidence to the coast. The use of the term *cusate* confuses their mode of formation, implying that they are built by processes similar to those that cause beach cusps. Because of the confusion surrounding the use of the term *cusate* foreland it is proposed here that they be termed *barrier forelands*. This recognises that they are a

salient feature of a shoreline that has been built by processes similar to those involved in forming barriers.

Macbeth identified five such features along the axial shores of Lake Coleridge. He noted that all except one were backed by scree or alluvial fan deposits and felt that the development of these features was related to an oversupply of sediment relative to the ability of waves to remove them. Thus, being unable to remove the excess sediment, it is the simply reshaped to form an equilibrium with the dominant wave approach angles. In the case of the field site, two opposing longshore current systems have built and co-joined two spits to form a barrier complex with an enclosed lagoon of Post-Glacial origin. The feature roughly resembles a right-angled triangle. The western side of the foreland measures 500 m, twice as long as the south-eastern side, which measures 250 m. The inner landward edge is slightly longer than the outer western edge, measuring 550 m in length. In total, the foreland and lagoon covers an area approximately 0.6 km² in extent, making the largest one at Lake Coleridge. It is not known exactly when the feature was formed. However, a carbon date taken from the bottom layers of a lagoon at the southern end of the Lake, would indicate that it had perhaps formed 5000-6000 years B.P. (Dr David Nobes, Department of Geology, University of Canterbury, 2003, *pers. com.*).

As discussed in Chapter One, lake beaches in particular, can assume an orientation that is either swash-aligned or drift-aligned. These two beach types are the end points in a system that has a range of intermediate forms. The orientation of Lake Coleridge, with its associated bimodal wind and wave regime, has produced a situation in which the beaches have, for the most part, attained either one of these two end points. It is important to recognise this alignment, because it governs the processes operating in a particular beach. It was this recognition that guided much of the work conducted by Pickrill (1976) on Lakes Te Anau and Manapouri and Allan (1998) on Lake Dunstan. The barrier foreland can be seen as having two separate beaches, the south-eastern one that is swash-aligned and the western one that is drift-aligned. As would be expected, the western drift-aligned beach exhibits a strong degree of longshore sediment transport.

According to Macbeth (1988), the foreland beaches of Lake Coleridge are typically steep (*ca.*10°) and narrow (*ca.*10 m). However, he characterised the whole Cottons Lagoon barrier foreland with only one profile, neglecting to survey the longer western side of the barrier. In this study, 10 profile lines were surveyed over a three year period to produce a more accurate description of the feature (Figure 2.14). The barrier foreland has an average profile more in line with Macbeth's (1988) description of a barrier beach, that is, widths of over 30 m and average

slopes of around 5° . Figures 2.15 & 2.17 present profile survey data from site CO10 on the western side of the barrier and site CO40 on the south-eastern side. The beach on the western side is *ca.* 50m wide with an average slope of 5° (Figure 2.16). On the southern-eastern side, the beach is *ca.* 30m wide with an average slope of 10° (Figure. 2.18). The beach on the southern side is both steeper and narrower, and deep water exists much closer to shore. In places there is a pronounced scarp at the back of the beach that probably formed when the Lake was held artificially high in the 1950s. On the western side there is an obvious and pronounced lag pavement in the offshore region. The lag pavement becomes more pronounced toward the northern end with a consequent reduction in beach width. The differences in profile width and slope between the two sides of the barrier are typical of the differences between a swash-aligned and drift-aligned beach.

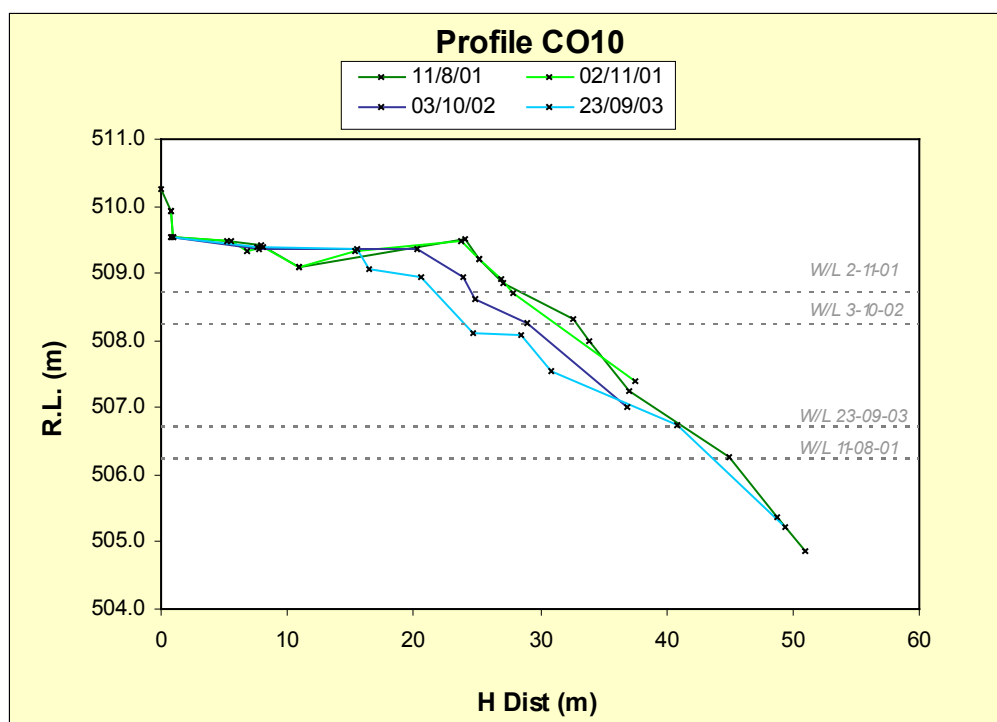


Figure. 2.15 Survey profiles from site CO10 on the western edge of the barrier foreland.

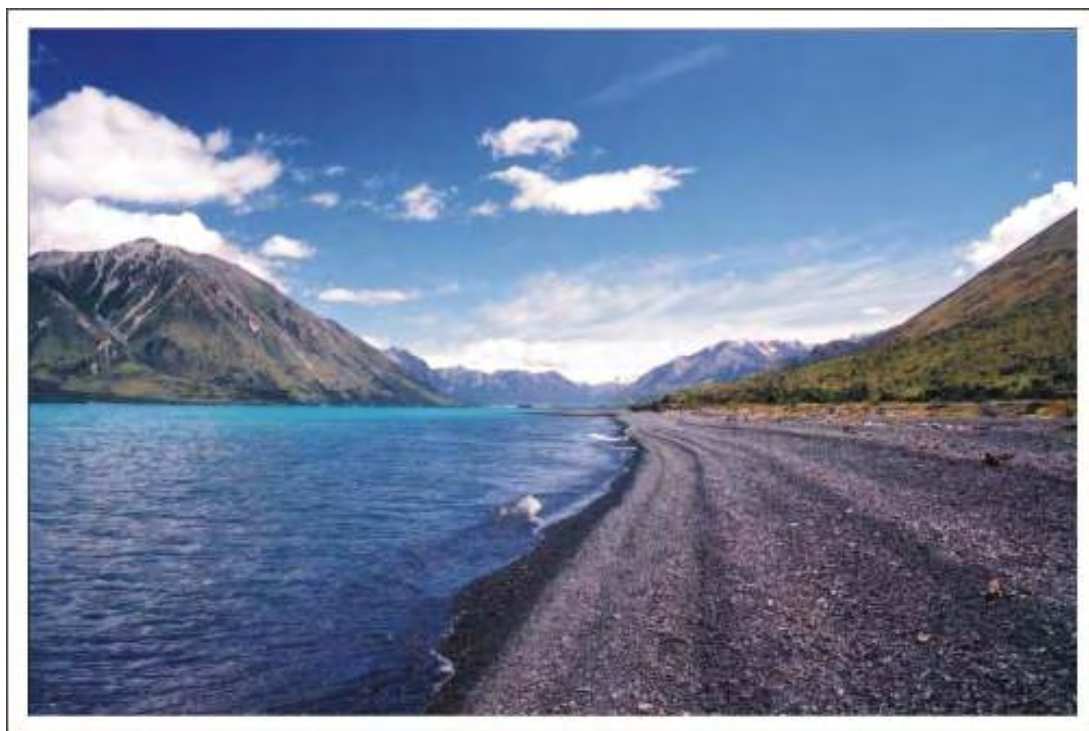


Figure 2.16 View looking northwest from site C010 in light southerly conditions. The water level is ca. 508.0 m amsl, giving about 30 m of foreshore. Mount Oakden appears on the left and Cottons Sheep Range on the right. Note the old scarp at the back of the beach, the small scale ridges in the foreshore and the colour of the water where the nearshore shelf terminates.

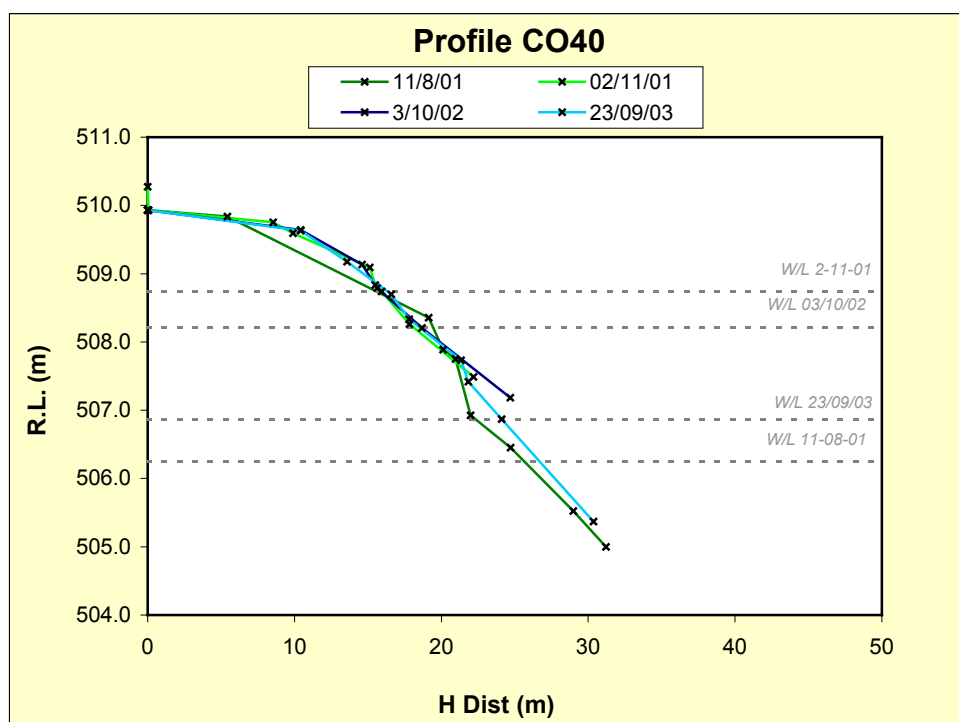


Figure. 2.17 Survey profiles from site C040 on the south-eastern side of the barrier foreland.



Figure 2.18 View looking southwest from site C040. The foreshore width is about 20 m at water level ca. 508.0 m amsl, making it much narrower and steeper than on the western side. The crest of the barrier (vegetated) is aligned 10° further east than the present swash-aligned beach, suggesting that longshore sediment transport rates were higher in the past. Note the many ridges in the foreshore that indicate previous water levels.

The sediments of the field site are a heterogeneous mix of coarse sands and fine gravels composed almost entirely of greywackes and argillites from the Torlesse Group. Small quantities of sandstone and jasper are also present in some places. The sediments are derived mainly from Cottons Stream, that drains from the Cottons Sheep Range and to a much lesser degree from a Post-Glacial, Holocene age cliff composed of glacial till (Figure 2.19). In the foreshore the mean size is 3.53 mm, but it ranges from 0.40-10 mm. The backshore is characterised in general by more moderately sorted coarse sands and granules. The sediments that lie in the average operating range of the lake are generally more poorly sorted. This zone is often characterised by a series of long, low gravel ridges composed of moderately sorted pebbles, with more poorly sorted mixed sands and gravels between the ridges. In the swash zone sediments are often better sorted and finer in nature. In the offshore zone, there is in most places, a wide lag pavement that runs to the edge of the nearshore self at around 503.0-504.0 m amsl, where the profile turns sharply and drops into deep water.

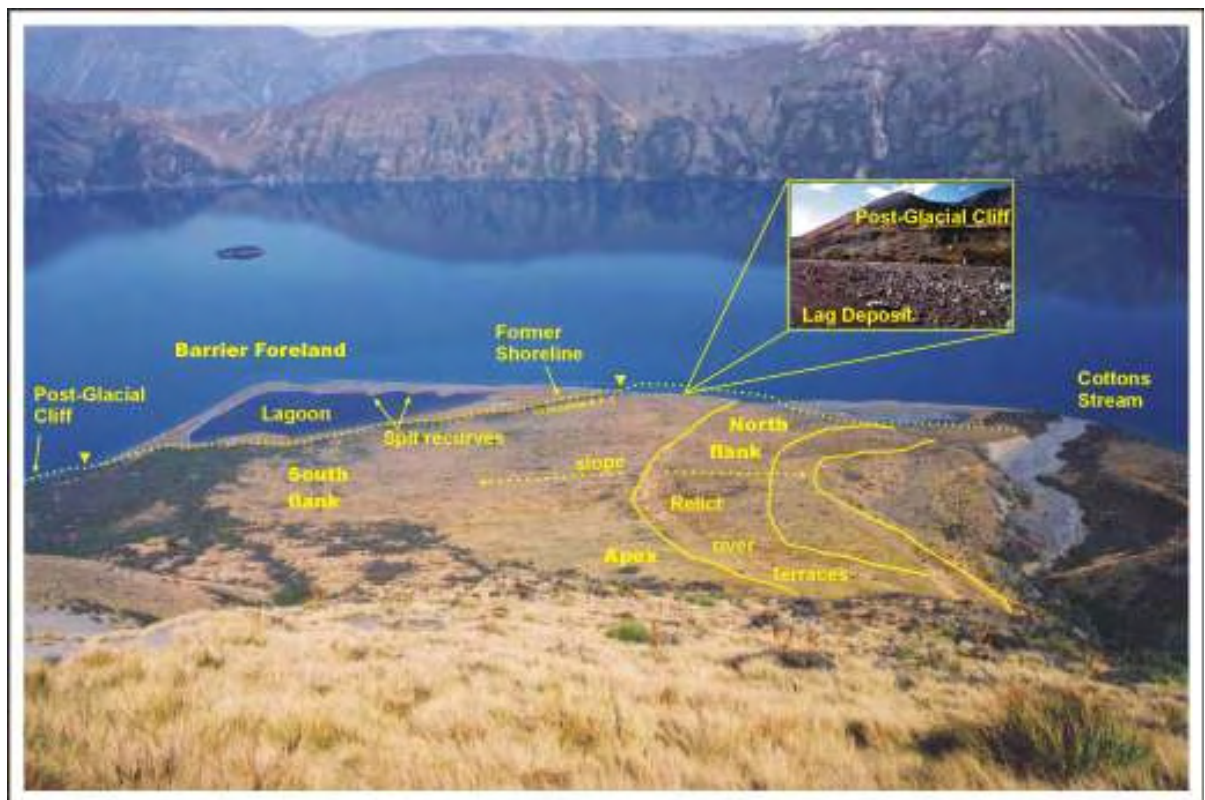


Figure 2.19 Aerial view over the barrier foreland and field site showing relevant geomorphic features. The foreland has built out on a shallow platform at the base of a large fan. The platform lies between two cliffs; one to the northwest, and the other to the southeast. Cottons Stream is now entrenched in the northern side of the fan. The nearshore shelf can be seen as a faint line under the water. Note the change in orientation of the former shoreline where it departs from the present shoreline at the proximal ends of the barrier (marked with triangles).

It is clear that the barrier has built out on top of a basement of some description, because the Lake here is very deep. It is widely accepted that barrier forelands, like barrier beaches, develop on a platform of some kind. Macbeth (1988) speculated that at Lake Coleridge, this surface is most likely to have been a lag pavement. As in other South Island glacial lakes, lag pavements form the most common unconsolidated shore deposit around Lake Coleridge. They form in limited wave energy environments where the finer fractions are able to be transported by wave activity, but the coarser fractions are not, and are thereby left in-situ to leave a coarse gravel and boulder ‘lag’ layer that effectively armours the beach (Kirk & Henriques, 1986). These surfaces usually have very low angles, less than 5° , indicating that they are erosional features.

The foreland has built at the base of a large cone shaped talus fan. This fan has built out with material derived from Cottons Sheep Range directly behind the lagoon (Figure 2.19). These fans are a common feature around the Lake and are built by a combination of colluvial and alluvial

processes (Gage, 1975). The sheer quantity of material in the feature compared to the size of the local streams indicates that it is unlikely to be a purely fluvial feature. There is a clear apex to the fan and there is no evidence to suggest that Cottons Stream has flowed over the southern flank. Instead, it has slowly cut into the fan surface working its way northward and away from the apex of the fan, as evidenced by a series of relict terraces. The stream has now entrenched itself in the northern limit of the flank. Smaller streams have worked the southern flank of the fan, leaving less prominent, yet still observable terraces. During the last Post-Glacial recession it was common for glacially over-steepened hillslopes to become destabilised (Gage, 1975). The area would have experienced a great deal of change at this time, with rapid fluvioglacial deposition, hillslope failure and down cutting of the gravel aggradation deposits by stream activity. It is not unreasonable to assume that the hillslope behind the lagoon probably failed repeatedly over a period of time to build up a large talus slope. Many South Island glacial lakes had higher water levels early in their formation (12,000-8,000 B.P.), at the start of the last Post-Glacial period. Around Lake Coleridge, moraine cliffs and truncated spurs indicate that lake levels were higher at some point in the recent past. As the Lake filled during this time, wave action would have cut into the base of this talus slope, shown as the relict shoreline in Figure 2.19. To the northwest and southeast of the present foreland, where the slope is steep, cliffs were formed. In between these two Post-Glacial cliffs was a large embayment where material from the base of the talus slope was redistributed to form a large shallow shelf lag pavement.

Long-term, the shorelines of the South Island glacial lakes have developed on a falling water level, as the ice retreated through the early Holocene, and the lake outlets developed (Kirk, 1988). The barrier foreland probably formed under such conditions, by the growth of two spits in the shallow waters of the lag pavement. Once a barrier begins to form, it generates its own self sustaining current system (Komar, 1998). The western spit would have been fed by sediments from Cottons Stream and the Post-Glacial cliff, transported alongshore through north-westerly wave action. Recurve features can be seen on the inside margin of this spit (Figure 2.14 & 2.19). In fact, there is evidence of more than one spit on this side of the barrier. About 50 m behind the ridge crest, there is low gravel ridge protruding above the bottom surface of the lagoon, that runs parallel with the present shoreline for about 150 m. This appears to be an earlier spit growth, that started developing perhaps when the water level was higher.

The south-eastern side of the barrier has formed by the longshore drift of material eroded from the edge of the fan under easterly and south-easterly wave action (Figure 2.19), forming a Post-Glacial cliff in the process. Measurements reveal that the crest of this barrier spit is aligned

10° further east than the present day beach, which as mentioned is swash-aligned to south-easterly wave conditions. This would suggest that in the past, under a higher water level, south-easterly waves have approached the shore at a slightly oblique angle, scoured material from the Post-Glacial cliff and initiated sediment transport in a westward direction. Now that the beach has achieved an equilibrium with the conditions it has become swash-aligned, and it is not growing at the rate that as it has in the past. Further support for this hypothesis can be found in the sediments of the beach. The Post-Glacial cliff from where the material for the southern spit has been derived contains small quantities of red jasper that effectively acts as a natural tracer. This jasper can be found all the way along the top ridge of the southern spit at a height of 511.0-512.0 m amsl. In the ridges of the present beach, average height 508.0 m amsl, the jasper only runs a third of the way along the beach. This would indicate that in the past, material moving in the longshore direction was able to build up the full length of the spit, whereas in present day conditions, it does not.

The western side of the barrier is longer and has a greater volume than the south-eastern side, having been supplied by more sediment due to the prevalence of the north-westerly. At some point around 5000-6000 years B.P. the two spits joined to form a continuous barrier and enclose a shallow lagoon (Figure 2.20). The base of the lagoon is covered by yellow-grey muds that thicken substantially toward the south-western corner of the lagoon. This mud is in part an accumulation of characteristically yellow wind blown loess, of the kind that frequently gets transported in the northwest winds that blow through the Wilberforce valley and pick up silt from the river bed. When the lagoon contains water, waves and currents generated by the northwest wind transport the material in suspension where they accumulate at the southern end of the lagoon. This is the deepest part of the lagoon and is where water remains for the longest periods of time. When full, the water depths here reach depths of 0.5 m. The barrier is most probably permeable or semi-permeable, as the water levels in the lagoon respond to changes in lake levels. The lagoon begins to empty when the water level in Lake Coleridge drops below the lowest point in the lagoon (508.0 m amsl), and fills gradually under a rising lake. There are no springs or streams that provide water for the lagoon and there is not enough rainfall to provide sufficient water to maintain its water level. Underneath the layer of mud is a thick series of wave worked gravel. The gravel is very similar to the sediments of the current beach. Toward the back of the lagoon, where the former shoreline is indicated on Figure 2.19, these gravels become increasingly angular and more poorly sorted, indicating that they have spent less time being reworked by wave activity. Significantly for the lakeshore management, the elevation of the old

shoreline lies between 509.0-509.2 m amsl, which is lower than the current maximum operating level of the Lake of 509.4 m amsl.



Figure 2.20 Cottons Lagoon. At no more than 0.5 m deep and covering an area of ca. 0.6 km², it forms an important wildlife habitat at Lake Coleridge. The base of the south-eastern ridge can be seen in the foreground. Under northwest wave action fine material is transported in suspension to the south-eastern end of the lagoon.

The feature is now largely in equilibrium with the wave environment and the lake operating regime. Analysis of the profiles over a three year period, indicates no significant long term erosion or progradation. At very low lake levels, a large lag pavement that marks the remnants of the Post-Glacial cliff, prevents the longshore transport of material from the northwest, and there is some reworking of material from the northern top of the foreland barrier. Material on the western side of the barrier is also transported northwest under south-easterly wave action, which balances somewhat the continual southward transport of material. On the southern side, a large lag pavement at the proximal end of the barrier severely restricts the transport of material along the shore at all lake levels. Winds from the easterly direction tend to be light, and the critical thresholds of the material in this lag are rarely exceeded. From measurements of longshore transport in this shoreline, it has been found that very little material moves along the shore. There are no streams eastward of the barrier to provide fresh sediment, and under normal operating conditions, waves are unable scour the base of the Post-Glacial cliff that originally

provided the material. The sediment on this side is characteristically better sorted, more platy, more rounded, and smaller in size than the materials on the western side of the barrier. This is all indicative of material that has experienced continual reworking by wave action in swash-aligned beach. Very little material is moved around the elbow of the barrier. Sediment here is deposited out of the swash current and a large, flat deposit of mixed sand and gravel characterises the area.

2.5 Summary

This chapter has discussed the broad scale features of the Lake Coleridge environment that affect the processes of longshore sediment transport. Lake Coleridge is a moderately sized alpine glacial lake situated on the eastern side of the Southern Alps. It is 18 km long and contains over 45 km of shoreline. A weather station was installed to take regular wind speed and direction measurements throughout the duration of the fieldwork programme. Almost two years of hourly data was recorded. It showed the wind regime of Lake Coleridge to be strongly bi-directional, with a mode from the northwest and the second from the southeast. The long axis of the lake is orientated northwest-southeast and is subject to strong turbulent winds that blow down the Wilberforce Valley and funnel along the length of the lake. Strong, but more consistent winds also blow from the south, which generate slightly different wave types. The orientation of the Lake to the prevailing wind ensures that many parts of the shoreline experience an oblique wave approach, and as a result, longshore sediment transport.

The wind at Lake Coleridge is persistent and strong. The weather station recorded times when strong to gale force north-westerlies blew consistently for periods of 2-3 days. Calm conditions were found to occur on average only 5.2% of the time. Light winds, that range from 3.6-18 kph are most common, occurring 44% of the time. However, winds in the range from 18-39 kph occur for an almost equal amount of time at around 39%. Winds stronger than 39 kph, blow for a significant 12% of the time at Lake Coleridge. It was shown that there is a strong seasonal component to the wind at Lake Coleridge. The strongest winds occur in September and October. During this time, the Lake experiences long periods of sustained north-westerlies, that frequently exceed gale force. A second windy period occurs around the autumn equinox in March, which is also dominated by north-westerly events. The calmest period occurs through the winter. The winter months have a high prevalence of south to southeast winds. These seasonal patterns in the strength and direction of the wind at Lake Coleridge indicate that a seasonal variation in the rates

of longshore sediment transport might be expected, with high rates in the spring and summer and lesser rates in the winter.

The shoreline contains many examples of coarse, unconsolidated, mixed sand and gravel beaches, similar in nature to those of the east coast of the South Island. The gravels derive from lateral glacial moraines eroded from the margins of the lake and from contemporary fluvial sources. The field site was located on a large barrier foreland complex, made up of two co-joined mixed sand and gravel barrier beaches. The beaches were originally two spits that grew out from the shoreline in response to large quantities of sediments being available for reworking by wave activity in the last Post-Glacial period. The field site presents a range of shoreline orientations to the wave conditions. The western side of the barrier has a drift aligned beach, in which sediments are regularly transported alongshore. This beach has a series of bays and cusps along its length in which waves approach at varying angles. The southern side of the barrier is swash aligned to the southerly winds and has a much stronger on-offshore component of sediment transport.

Lake Coleridge was shown to be a good natural laboratory for examining the processes of long shore sediment transport in the energy swash zone of a mixed sand and gravel beach. The high energy mixed sand and gravel beaches of the open coast present a formidable challenge to conducting research. The lower energy nature of a lake environment means that equipment can be safely deployed without being destroyed. This has allowed the collection of a high quality data set of a wide range environmental variables that can be analysed and correlated against rates of sediment transport. The next chapter will discuss the data collection methodology, provide an overview of the fieldwork programme and introduce the instruments used for the field measurements.

CHAPTER 3.

FIELDWORK PROGRAMME

*“The lake itself is most beautiful; the water so clear you can see
to an unfathomable depth... The mountains come steep to
the water’s edge, the rata trees fringe the side...
Only in one place (except the two ends of the lake)
can you ride on to the shore and shingle beach...”*
G.A.E Ross (1857)

3.1 Fieldwork Programme Overview

This chapter outlines the data collection methodology used in the fieldwork programme. It describes the instrumentation used for the data collection and the deployment procedure used in the field. The aim is to provide an integrated overview of the field-data collection and the array of instrumentation that was deployed in Lake Coleridge.

The field-data collection was designed to measure a range of environmental variables thought to be important in the process of longshore sediment transport, as illustrated in the process-response model in Chapter One (Figure 1.7). Careful planning was put into the design and execution of the fieldwork phase which spanned two years. Three fieldwork phases were conducted, covering the seasons of spring, summer and autumn. During the fieldwork season, deployments were planned for a duration of 5-7 days, after which time batteries needed recharging and data required uploading from the field laptop to a secure location for backup. An array of wave and current measuring devices was installed at a selected location in the field in order to measure a particular range of environmental variables. Measurements occurred hourly, for up to 13 consecutive hours. After a sufficient amount of data was collected at one site, the array was moved to another location thought to present a different range of environmental variables. In doing so, a range of data was collected from locations in which some environmental conditions remained the same or similar, whilst other environmental indicators varied. This allowed correlations between data sets in which some indicators were variable whilst others remained similar.

There are numerous techniques and devices available by which to measure waves and currents. In this study, four instruments were used to measure both waves and currents simultaneously in the offshore, nearshore and swash zone (Figure 3.1). The instruments were

chosen on the basis of their availability and suitability for use in a lakeshore mixed sand and gravel beach environment. In the offshore zone, an InterOcean S4ADW wave and current meter was installed to record wave height, period, direction and velocity. Also in the offshore area, to provide a comparison and backup to the S4, was a WG-30 capacitance wave gauge developed by the National Water Research Institute (NWRI), Canada and manufactured by Brancker Research. The wave gauge measured the total water surface variation and hence, the wave height and period. In the nearshore and swash zone were a pair of Marsh-McBirney model 512 electromagnetic current meters, measuring current directions and velocities. The wave gauge and Marsh-McBirney current meters were powered with a 12 V deep cycle marine battery, that provided sufficient power for the duration of a week long deployment.

The data produced by the wave gauge and current meters was streamed back in real-time to a shore-based Campbell Scientific CR23x data logger. The CR23x was programmed to execute a routine that took burst samples of this data for 18 minutes every hour. The wave gauge data was sampled at a rate of 10 Hz (0.1 s) and the two current meters at a rate of 2 Hz (0.5 s). With an internal non-volatile memory of 1.2 MB, the data logger was able to store up to 13 hrs of data. This yielded a large data set comprising 25 000 data points per hour of measurement. Five cumulative months of data were collected, including over 500 individual hours of high quality time series data.

The longshore sediment transport rates were investigated with the use of sediment traps that collected sediment whilst it was in motion during wind-wave events. Two sediment traps were placed in front of the current meters, one in the nearshore and the other in the swash zone, to collect sediment transported under wave and swash action. The traps were deployed for between 1 and 10 minutes depending on the conditions. This occurred concurrently with the wave measurements and yielded over 500 individual samples. In addition, the width and slope of the swash zone was measured hourly with an Abney level and staff. To backup the weather station measurements, hourly readings of wind speed and air temperature were made with a hand-held Kestrel 3000 digital wind meter.

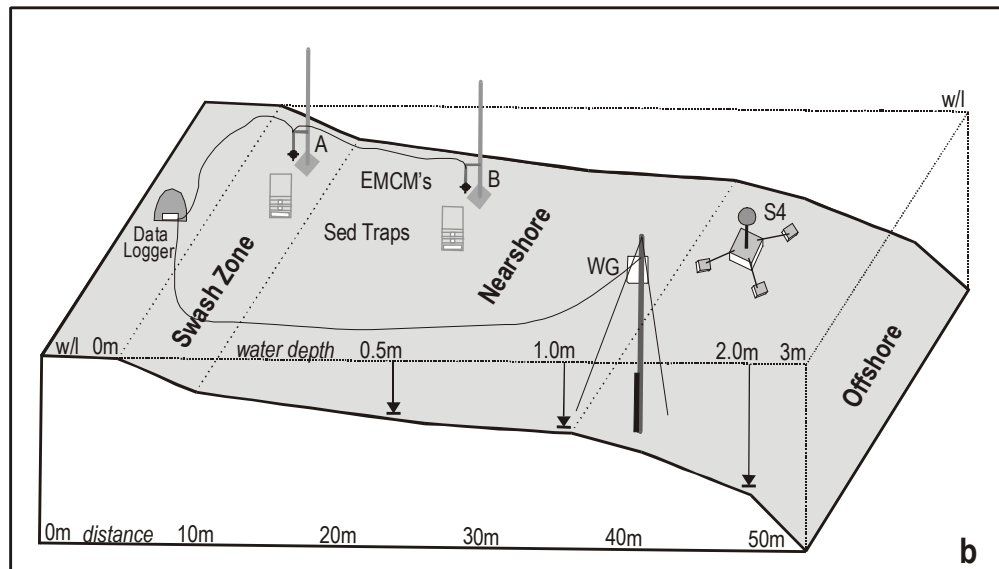
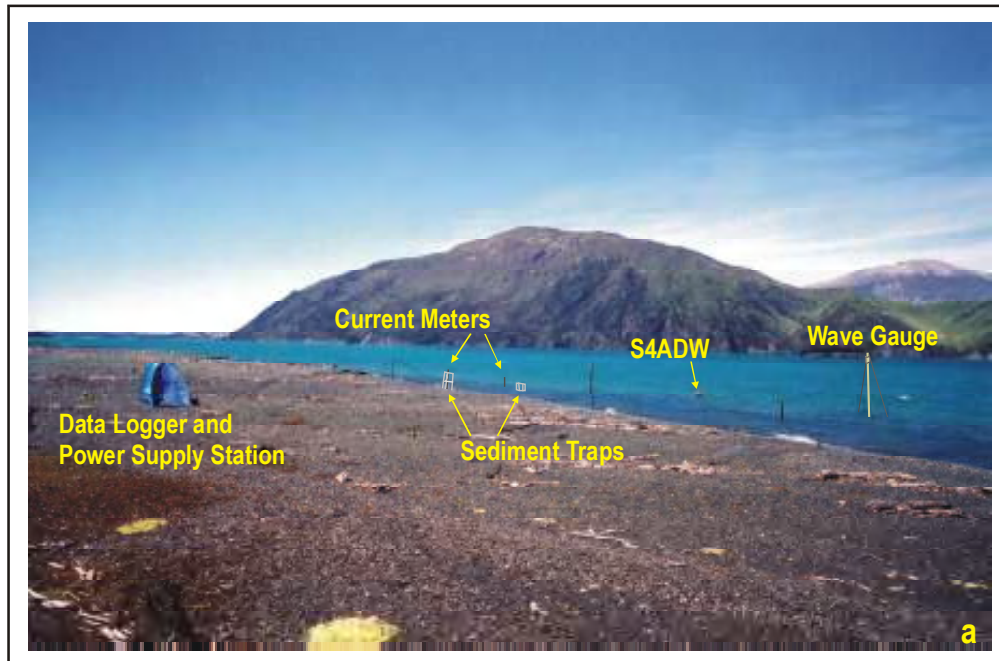


Figure 3.1. The field equipment array, as deployed on a typical day of data collection.

It was noted by Allan (1998) that there is no established methodology for making wave measurements in New Zealand lakes, including recommended sampling lengths. In the literature, the reported measurement lengths of wave records vary widely, from 10 min per hour through to a continuous time series. The choice of a recording length depends on the type of waves that are being measured and the particular part of the wave frequency spectrum required for analysis. If long period waves are being measured, a longer sampling length will be required to properly characterise the frequency spectrum. The wave data analysis standard produced by the Coastal Engineering Research Centre (Earle *et al.*, 1995), suggests that a 17 min sampling period per

hour will provide a sufficiently representative record of ocean wave conditions for most situations. Small lakes and restricted fetch environments are dominated by small frequency waves. Intuitively one might expect that a shorter sampling period would be sufficient to characterise the wave spectrum; 17 min being perhaps an unnecessarily long record for small period lake waves. However, because this remains an untested idea and because there are no standard record lengths for measuring lake waves, it was decided to take sample lengths of 18 min per hour. Although the standard for recording ocean waves is 17 min, using a prime number makes for difficult data manipulation. It was decided to increase the recording length by 1 min to provide a record that can easily be divided to investigate the potential development of a new standard for lake wave data collection.

Throughout the fieldwork programme every effort was made to install the wave gauge and S4 instruments in 'deep water', which in most conditions coincided to water depths of 1.0-1.5 m. This is significant for two reasons. Firstly, it ensures that Linear wave theory can be used to calculate the wave characteristics. Secondly, most transport equations require deep water wave parameters. Uncertainties often arise in longshore transport studies because wave data is frequently collected from instruments installed, due to physical or budgetary limitations, in intermediate or shallow water depths where waves have begun to shoal. Moreover, in sediment transport studies of wide dissipative beaches, transport normally occurs under heavily refracted and transformed waves. This requires the use of complex shoaling transformation models, such as Cnoidal wave theory or Boussinesq equations in order to approximate the wave and current fields (Ren *et al.*, 1997). As explained previously, this is not the case for coarse grained beaches, where deep water close to shore allows waves to approach very closely with little transformation. In low energy environments, such as Lake Coleridge, it is both physically possible and preferable to measure the deep water wave conditions, without having to extrapolate wave characteristics from shallow water wave equations.

3.2 Wave & Current Recording Instruments

InterOcean S4ADW

The S4ADW is a vector averaging instrument that has all its electronics and recording devices housed internally (Figure 3.2). It is powered by 6 alkaline D-sized batteries, that are also housed internally. With 20 MB of memory, there was sufficient memory to leave the S4 in the Lake for the duration of a weekly sampling programme. The wave characteristics are measured with a semiconductor strain gauge. The strain gauge is a pressure transducer device that measures variations in water pressure under the wave in order to derive wave height and period. It has a resolution of 4 mm and a precision of ± 10 mm (InterOcean, 1990). Current direction and velocities are obtained from four titanium electrodes located symmetrically around the centre of the external casing. The current direction serves as a de facto measurement of the wave direction as it effectively measures wave orbitals. The meters operate on the principle of Faraday's Law of Electromagnetic Induction. Water flowing through an electromagnetic field generates a voltage that is proportional to flow velocity past the sensor (InterOcean, 1990). It is an effective way to measure current velocities. On the S4 it produces readings with a resolution of 0.2 cm/s, accurate to within 2%, ± 1.0 cm/s (InterOcean, 1990).

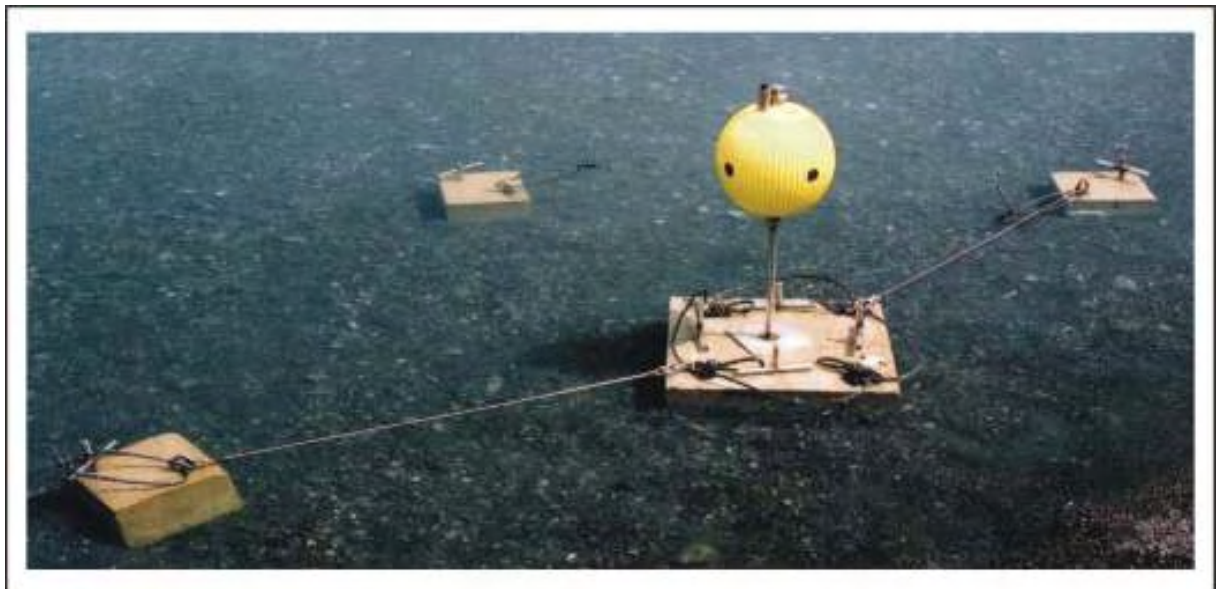


Figure 3.2 The S4ADW in shallow water showing the mooring block and anchor weights.

The S4 has two methods for measuring relative current direction. Onboard, it contains a fluxgate compass that measures current direction relative to magnetic north. This device is extremely sensitive to localised magnetic fluctuations that can be caused by metal objects or variations in the earth's magnetic field. If conditions prove unsuitable for using the fluxgate compass, direction can also be measured relative to the S4, as it contains an internal north and south pole. This enables the user to align the instrument physically to map grid or parallel to the shore, providing direction data to a point known to the user. Field testing showed the internal compass to be unreliable and it was decided not to rely on this feature. Rather, it was aligned relative to the shore, providing actual wave and current directions.

The S4 was programmed to record wave height and period, current direction and velocity for 18 minutes on the hour, every hour. Burst samples were taken at 2 Hz (0.5 s), the maximum sampling rate of the instrument, throughout the 18 min period. Two hertz is considered by many researchers to be too slow to accurately represent high frequency lake waves. Whilst the InterOcean S4 range of instruments have been widely used in oceanographic and coastal studies their use in low energy environments has not been widely reported. This is partly because of the inability of the older S4 models to sample at a faster rate, and partly due to the fact that low energy waves quickly attenuate under the wave form. It has long been recognised that pressure sensors do not easily resolve short-period waves, a feature that oceanographers have routinely taken advantage of to filter out high frequency 'noise' from a wave record (Draper, 1966). Consequently, there is some uncertainty surrounding the ability of pressure transducer devices to measure sufficient pressure variation under small magnitude, high frequency waves. In New Zealand there is only one other recorded instance of an S4 being used in a lake environment by Allan (1998) in his study of shoreline development at Lake Dunstan. Allan initially deployed the S4 in 3.0 m of water, but found that the wave attenuation was too great for any reliable measurements. It was subsequently moved into water of depths 0.8-1.2 m deep. Allan and Kirk (2000) recommended that instruments such as the S4 that use a pressure transducer, be calibrated against a capacitance wave gauge to increase confidence in the wave statistics; a practice that has been employed in the past to investigate the effectiveness of pressure transducers in the study of ocean waves (Bishop & Donelan, 1987; Esteva & Harris, 1970).

The S4 cannot distinguish between instrument movement and absolute movement. To ensure that it did not move under any circumstances, the S4 was bolted to a stainless steel shank and attached to a purpose built concrete mooring block measuring 0.5 x 0.5 x 0.2 m and weighing approximately 100 kg (Figure 3.2). Four 0.5 m stainless steel pegs were driven through pre-cast

holes in the block to firmly anchor it to the lake bed. In addition, three stainless steel wire stays were attached to the corners of the block and connected to three smaller 20kg concrete blocks that were in turn also pegged into the lake bed. To prevent the instrument from swivelling on the mooring, a square cove was pre-cast in the bottom of the block, into which a base plate of the same size was fitted and bolted onto the mooring shank. This was ensure accurate wave direction measurements. When deployed it sat 0.5m above the lake bed in water depths ranging from 1.5-2.0 m water depth, varying slightly throughout the week depending on lake levels. Because the instrument sat 0.5 m above the bed, this meant that the pressure sensor recorded waves 1.0-1.5 m below the water surface.

WG-30 Capacitance Wave Gauge

A wave gauge measures changes in capacitance along a length of electrically charged wire as it responds to variations in water level that occur due to wave approach (Figure 3.3). It is known as a surface piercing device because it protrudes some distance above the water line. They have been used widely in coastal research applications and have a proven and reliable track record (Scott, 2005; Foote & Horn, 1999; Ting & Kirby, 1995; Hall & Foster, 1990). It is a simple but precise instrument, measuring water level changes accurate to 0.4%, with a 2 ms response time. This makes them suitable for use in low energy wave environments because they provide a very accurate record of the water surface fluctuations and thus, of the wave form. The wave gauge was programmed to record for 18 min every hour, but at a faster sampling rate of 10 Hz or 0.1 s.

The wave gauge was made up of three components: A staff, the electronics housing and the capacitance wire (Figure 3.3). The staff was constructed from three hollow, anodised aluminium tubes of different diameters to produce a telescopic pole that extended to a height of 3.2 m. This enabled the staff to be collapsed for safe transportation and storage. An all weather housing was bolted to the top of the staff that contained the wave gauge electronics and into which the capacitance wire fed its signal. A power and data cable connected into the top of the box that carried DC current from a battery to run the gauge and fed data back to a shore based data logger. The capacitance wire ran out from underneath the housing and was attached to the bottom of the staff with a spring loaded lever. This held the wire taut in the water and away from the staff at an equal distance of 20 mm from top to bottom.



Figure 3.3 The Wave Staff. The white electronics housing can be seen at the top of the staff, above which the stays are connected to a three-way collar. The staff is connected by two struts to a waratah, that can just be seen sticking above water level.

To remain upright and vertical in the water, two struts were connected perpendicular to the middle of the staff that enabled the whole rigging to be attached to a 1.8m steel waratah driven into the lake bed. For further stability, three rope and wire stays were attached to the top of the rigging and connected to 20 kg concrete blocks (similar to those in Figure 3.2) that were hammered into the lake bed with 0.5 m long stainless steel pegs. The power and data cable was held aloft of the water level on a series of 1.8 m steel waratahs, leading to the shore based data logger. The whole set-up was deployed in 1.2 m water depth, varying by ± 0.10 m throughout a sampling week depending on lake levels. It proved to be a very reliable and durable piece of equipment, which when deployed with the above set-up, was capable of withstanding severe gale force winds and waves of up to 1.0 m high.

Marsh-McBirney Electromagnetic Current Meters

The Marsh-McBirney current meter is an extremely sensitive, yet durable device capable of withstanding the turbulent forces encountered in the nearshore and swash zone. The instrument consists of an electrically inert rubber polymer sphere that encases four equally spaced electrodes that are aligned around the horizontal axis. This sensor is attached to a stainless steel probe and power/data cable (Figure 3.4). It is an open channel current meter, in that the electrodes can detect current direction from any angle. Many sediment transport studies have used Marsh-McBirney current meters and they have been extensively tested in the field (Doering & Bowen, 1987; Aubrey & Trowbridge, 1985). They measure the water velocity by making use of Faraday's Law of Electromagnetic Induction. Faraday's Law states that; a conductor moving through a magnetic field produces a voltage (Kane & Sternheim, 1988). Because water is a conductor, it produces a voltage when moving through a magnetic field. The Marsh-McBirney current meter generates an electromagnetic field that extends up to 1.0 m around its sensor. When water flows through this field it produces a small electric current in the water. The magnitude of the current is directly proportional to the velocity of the water: The faster the water flow, the greater the voltage. The four velocity electrodes measure this voltage and store the values to memory. The water velocity is determined by a simple equation that converts the voltage into a current speed. The high sensitivity of these instruments mean that they do not read zero easily, even in still water. Before deployment, they require testing in still water in order to ascertain any off-set values that need to be applied to the raw data before processing. Off-set values were monitored throughout the duration of the field programme and were found to be reasonably constant at ± 0.01 .

The two current meters were each connected to an adjustable mounting on a stainless steel pole that was driven and pegged into the lake bed (Figure 3.4). The nearshore sensor was positioned in 0.50 m water and located 0.15 m above the lake bed. The second sensor was positioned in approximately the middle of the swash zone at 0.10 m above the bed and adjusted when required according to conditions. Ten centimetres is the minimum height above the bed that a sensor can be placed for measurements. To avoid any interference of the electromagnetic field, the meters were placed well away from all other electronic equipment. For the same reason, stainless steel was used to ensure that no residual magnetism in the metal interfered with the sensors. The current meters were connected to a shore based data logger that was programmed to sample at 2 Hz (0.5 s) for 18 min every hour. The analogue voltage signals were then converted into a digital format and stored to memory. The whole set-up was powered with a deep cycle 12 V marine battery.



Figure 3.4 Current meter (A) deployed in the swash zone showing a 3.5 s swash sequence. These conditions occurred during a strong northwest wind event generating mean wave heights of 0.25 m (0.40 m maximum) and mean wave periods of 1.8-2.0 s.

3.3 Sediment Transport Measurement and Methods

In an extensive review of field-data suitable for use in testing longshore sediment transport models, Schoonees and Theron (1993) identified a lack of data for grain sizes over 0.6 mm. Of the 42 data sets they reviewed, only two were concerned with coarse grained beaches. As mentioned previously, part of this stems from a lack of suitably robust instrumentation capable of withstanding and measuring the hydrodynamic forces that occur in the swash zone. Consequently, shoreline and beach profile changes have commonly been measured through aerial photograph analysis and beach profile surveying (Kirk 1975, Kirk, 1992a; Allan, 1998). Beach volume changes have often been measured at coastal structures such as groynes or jetties where accumulations and losses can be more easily quantified, especially if it is conducted in conjunction with dredging or sediment extraction (Kirk, 1992b). The advantage of this method is that it can encompass the full range of conditions including high energy storm events. However, whilst this gives an estimate of the total longshore sediment transport rate averaged over a period of months or years, the data is only an average long-term rate. It cannot resolve instantaneous or short-term rates in the order of hours (Schoonees & Theron, 1993).

In order to develop a model that can be used to calculate short-term sediment transport rates, it is necessary to measure sediment whilst it is in transit. Achieving this poses a particularly challenging set of problems and remains one of the more difficult environmental processes to quantify. In Chapter One it was explained that there are two modes of sediment transport; bedload and suspended load. While there is debate in the literature about which process dominates in sandy beaches, it is widely acknowledged that bedload transport dominates gravel beach transport. In mixed sand and gravel beaches, it was explained that there are two transport systems. One in the nearshore zone that is dominated by suspended transport of fine material. The second in the swash zone, dominated by bedload transport processes. Measuring sediment transported by either of these modes poses its own unique set of problems. Over the years a number of techniques have been developed for dealing with these problems, particularly on sand beaches, but for coarse grained beaches workers have largely relied on two techniques; traps and tracers. Sediment trapping and tracing techniques have been the two most widely used and replicable methods for quantifying short-term bedload transport rates, in both sand and gravel beaches.

Tracers are natural or artificial sediments tagged with fluorescent paint, magnetic or radioactive coatings and placed in the swash or surf zone where they can be tracked. The rate and spread of the dispersal pattern provides information about the transport rate over a period of hours or days. The general problems with determining a reliable transport rate with this method has been well documented (White, 1998; Komar, 1998; Kraus, 1987). But there are additional difficulties associated with using tracer methods in coarse grained beaches. In particular, there are uncertainties surrounding the degree to which a tracer is representative of the total integrated transport rate. Tracers of all types are rapidly buried in a gravel beach, especially in high energy conditions, leading to typically low recovery rates. Because of this, tracer runs are often restricted to low energy conditions. There has been some use made of electronically tagged (Workman *et al.*, 1994) and aluminium pebbles (Nicholls & Wright, 1991), that can be tracked with a radio transceiver or metal detector at depths of up to 0.8 m. But the high cost of production and time consuming recovery procedure mean that only a small number can be used at any one time. Moreover, these methods are only suitable for large grain sizes. In the heterogeneous sediment environment of a mixed sand and gravel beach, the whole range of sizes needs to be represented. A study by Van Wellen *et al.* (1998) indicated that transport rates derived from tracer studies in gravel beaches, over-estimated the actual rates. It was suggested that this was due to the temporal and spatial variability in the depth of sediment disturbance and the width of active beach. Both of these parameters need to be accurately known in order to

calculate sediment transport rates. The problem of calculating the depth of disturbance, which is much deeper and more variable in gravel beaches (Van Wellen *et al.*, 2000), has proved to be consistently difficult and unreliable. Very little work has been directed to this problem for New Zealand's mixed sand and gravel beaches on both the open coast and lakeshores.

In order to avoid the uncertainties surrounding the use of tracers, a decision was made to use sediment traps. A trap is a device that collects sediment whilst it is in motion and they offer a number of advantages over the use of tracers. A sediment trap provides an absolute measure of the transport rate from a point, at a time scale of seconds, minutes or hours (Kraus, 1987). This enables the movement of the sediment to be directly related to the wave and current conditions. Traps are capable of measuring sediment transport in both the bedload and suspended load phase. That is, they can quantify transport occurring both horizontally and vertically in the water column. Traps can also provide good information on the spatial variability of the transport rate. A number of traps can be deployed at the same time, providing a simultaneous measure of the distribution of the transport rate across the surf and swash zone (Wang *et al.*, 1998). Commenting on the use of traps Kraus (1987: 142) stated that:

“At the present time and for the immediate future, however, the refinement of traps appears to offer the most technically promising and economical avenue for obtaining point measurements of sediment transport rates to be used in quantitative engineering applications”.

There are some problems with using traps, but a lot of these relate to their use on high energy open coasts. Traps can be difficult to deploy in the unconsolidated sediments of a gravel beach and can become large structures that interfere with the hydrodynamics that govern sediment transport. In high energy conditions, a trap may fill very quickly and become impossible to retrieve, rendering the data unusable. There are also uncertainties about how representative one or two traps are of the total transport rate, considering that there are variations in transport across the nearshore and swash zone, especially as the water level fluctuates through the tidal cycle (Chadwick, 1989). In a comparison of traps versus tracers, Bray *et al.* (1996) found that trap volumes were several orders of magnitude less than volumes calculated from tracer methods. Bray concluded that it was preferable to use tracers in high energy environments, but that traps were reliable in low energy conditions. Lake Coleridge satisfies this criterion. Having a lower energy swash zone means that the traps do not have to be so cumbersome, minimizing its interference on the hydrodynamic processes. The trap can operate successfully without it being toppled over, scoured out or filled up, producing a more representative sediment transport rate.

Moreover, because lakes are not tidal, the position of the nearshore and swash zone does not change position across the beach face. Therefore, the trap can be placed in a set position, such as a swash zone, where the hydrodynamic conditions can remain known for the duration of the trapping.

Sediment Steamer Traps

Two streamer traps were designed and purpose built for use in a mixed sand and gravel lake beach environment (Figure 3.5). The streamer trap concept, that was first proposed and developed by Kirk (1970; 1973) was designed expressly to mitigate some of the common problems associated with traditional trap designs, namely bed scour and current flow interference. The design was based on a streamer trap, that was developed and used successfully by Kraus (1987) and Kraus and Dean (1987) for measuring sand transport. The traps were constructed from square tubular aluminium in the form of a frame measuring 1.0 m high x 0.4 m wide x 0.4 m deep. Onto the frame, a series of stainless steel trap mouths or apertures were mounted vertically at 60 mm increments. The bottom trap collected sediment transported in bedload, whilst those above collected sediment moving in suspension. The bedload trap measured 300 mm wide x 50 mm high and was capable of collecting up to 6 kg of sediment, before becoming ineffective. The suspended sediment trap apertures above this, measured 50 mm x 50 mm square, and were capable of collecting around 100-200 g of sediment.

A polyester mesh tube or streamer, from which the trap derives its name, was connected onto the rear side of every trap aperture. The streamers allow water to flow through freely, whilst collecting sediment when it is in motion. The trap bags were 0.5 m long and had a mesh size of 60 μm (0.06 mm) capable of trapping fractions as small as very fine sand (4 ϕ). This mesh size was chosen to ensure that the full range of sediment sizes present in the beach were trapped in the streamer, thereby avoiding sampling errors by material passing through the trap. The bag was connected onto the trap aperture with two heavy duty elastic ‘bungy’ cords and tied off at the end. This enabled the sediment to be removed quickly and easily into a storage bag, without the need for removing the whole trap aperture from the frame.

Throughout the sampling programme, one trap was placed in the swash zone and the second in the nearshore zone. The sampling was conducted according the method prescribed by Kraus (1987) with the mouth of the trap facing into the longshore current, aligned parallel to the beach. The swash zone trap was held to ensure that it did not point up or downslope minimising the

collection of any material moving in the cross-shore direction. The nearshore zone trap was held when required, but was able to stand on its own in most conditions. The traps were typically deployed for 5 min every hour, but ranged from 1-10 min depending on the conditions. In average conditions, this represented between 30 to 300 waves. This is a similar duration employed by Kraus (1987), Hay and Sheng (1992), Wang *et al.*, (1998) and Tonk and Masselink (2005). After this time, the sediment was removed from the streamers and bagged for laboratory analysis.



Figure 3.5 The sediment trap deployed in light to moderate south-easterly conditions. The bedload trap is under water. Above this is a suspended sediment trap. Connected to the back of the trap aperture is a polyester mesh tube, which traps the sediment whilst allowing the water through. The trap was designed to be as hydrodynamically transparent as possible, to avoid undue interference with the water flow.

3.4 Summary

This chapter has outlined the methodology and the procedures employed in the field to collect the raw environmental data that will be used to analyse the sediment transport and swash zone processes. A summary of the hourly raw data measurements making up the 493 hours of data, including wave statistics, currents, swash zone conditions, wind speed and direction can be found in Appendices 5 and 6. A number of instruments were used to collect a wide range of wave, current and sediment transport data. In the offshore area two instruments were installed to collect wave data. An InterOcean S4ADW wave and current meter was installed to record wave height, period, direction and velocity. To provide a comparison and backup to the S4, a WG-30 capacitance wave gauge measured the water surface variation, from which the wave height and period were derived. The instruments were installed in water depths of 1.0-1.5 m, that in most conditions corresponded to 'deep water'. The purpose of this was to measure waves before they were modified in the nearshore through shoaling and refraction processes. This ensured that Linear wave theory could more confidently be used to calculate the wave characteristics.

In the nearshore and swash zone, a pair of Marsh-McBirney electromagnetic current meters were installed to measure current directions and velocities. The wave and current meters were programmed to record for a duration of 18 minutes every hour. Sediment traps were placed in front of these two current meters, to collect material transported in the longshore direction under wave and current activity. The width and slope of the swash zone was measured hourly with an Abney level and staff. All measurements were made concurrently on an hourly basis through a wide variety of conditions to build a picture of the process environment of a lacustrine beach.

Sediment traps were used in favour of tracer methods so that accurate volumetric data sediment transport data could be collected. The relatively small size of a lacustrine beach means that total transport rates can be reasonably estimated from a trapping programme. Two traps were built, based a design known as a streamer trap. Streamer traps were designed specifically to minimise some of the problems that have been encountered with using traps in the field, such as bed scour and current interference. The trap employs a polyester mesh bag attached to a solid frame, that collects sediment in motion whilst allowing water to flow through the trap with minimal interference. The traps were designed to collect material transported in both bedload and suspended load.

The following chapter will describe the methods used to analyse the raw wave and current data that was collected in the field programme. Results of the deep water wave analysis will be presented and discussed, before moving into an examination of the nearshore wave transformations.

CHAPTER 4.

LAKE WAVES

“...the water motion in the breaker zone and the longshore sand transport mechanisms make one feel that it would be by unbelievable luck if the breaker type did not have an effect on the quantity of longshore sand transport.”

E. Özhan (1982)

4.1 Introduction

In the Chapter One, a process-response model was developed to illustrate the linkages between the important environment parameters controlling sediment transport. The importance of waves in this process was examined with particular reference to coarse grained beaches. There have been relatively few studies of lakeshore wave processes, despite the high level of human development around many lakes, both in New Zealand and overseas. Allan (1998) noted that, with regard to the New Zealand situation there are very limited data sets of lake wave measurements. Clearly, an understanding of the role of waves, their generation, magnitudes, periods and the way in which they shoal and break in the nearshore zone and swash zone is critical for a deeper insight into the sediment transport process operating in these environments. The important role that lake waves play in shaping lakeshore beaches and in controlling sediment transport was recognised by Pickrill (1976: 114) who emphasised that:

“The way in which wave energy is distributed around lake shorelines and dissipated on the beach face, controls the type of beach produced, the geometry, the morphology and the sediment distribution pattern both normal and parallel to the shoreline.”

This chapter presents results of the wave measurements made from Lake Coleridge. As described in the last chapter, wave data were collected with two instruments, the InterOcean S4 and the WG-30 wave gauge, sampling at different rates. It has been found that there are differences in the results that are produced by these two instruments and some of these are explored in this chapter. The methods employed to analyse the data are outlined and the wave environment of Lake Coleridge is examined with respect to those aspects most relevant to sediment transport processes. One outcome of this is that, it will provide more information about the nature of the waves that occur in New Zealand lakes. Following the deep water wave analysis, some results from the current measurements are presented. The nature of the nearshore wave transformations are discussed and a number of equations for estimating breaker conditions are examined for their usefulness in New Zealand lakes.

4.2 Raw Data Analysis Methods

Wave Gauge Data

The two most commonly used techniques for calculating wave height and period statistics are the zero-crossing and spectral analysis methods. Spectral analysis examines the variance in a wave record by plotting the spectral energy against the wave frequency or amplitude. Wave statistics are derived by identifying energy maxima in the spectrum that relate to certain wave heights and periods. The zero-crossing method analyses the record on a wave by wave basis to identify minima and maxima in the sample or means of the whole record. Subsets of this record are used to calculate statistics such as the significant wave height or period. Both approaches produce equally valid, but slightly different results (U.S. Army Corps of Engineers, 1992). For large data sets, the spectral analysis method requires specialized software, as it involves complex and time consuming calculations. The zero-crossing method uses equations that are more readily manipulated in a spreadsheet format. Consequently, a routine was written in Visual Basic that executed in Microsoft Excel to calculate the wave statistics with the zero-crossing method. The spreadsheet was modified for the present data set from a macro developed by (Allan, 1998). Data were processed in hourly subsets resulting in a tabulation of hourly wave height and period readings.

It will be recalled that the wave gauge measures the continuous total water surface elevation. Burst samples were taken of this record at 0.1 s intervals, for 18 min every hour. Analysis of this data proceeded in a number of steps. The datalogger stores information in a comma separated value (csv) form, that requires extracting and converting into usable data sets. This took place in the field with a laptop installed with Campbell Scientific datalogger support software, PC208W v3.01. The support software extracted the raw data as a single file that required separating into wave and current components. This was also achieved with the datalogger support software. Data were extracted from this single file in hourly blocks and converted into a format that could be manipulated in spreadsheet form. The hourly blocks were made up of 18 minutes of recordings comprising 10,800 data points that included time signature information (Appendix 2a).

The raw water-level data from the wave gauge then required detrending, to remove any long period water level variations not related to wind-wave activity, such as wave set-up, seiche or lake level changes. The method used followed that outlined by Earle et al. (1995), that employs standard linear regression techniques. The raw data were first demeaned by subtracting the mean

value for the record, from each individual value. This normalised the data set, producing a series of positive and negative values fluctuating about zero (still water level) that represented the wave crests and troughs. The demeaned values were then regressed against the time values to calculate a linear regression equation of the form ($y = ax \pm b$). This function was used to detrend the data set to produce the raw wave values (H_i) with the equation:

$$H_i = D - (an) \pm b \quad (4.1)$$

Where D is the demeaned value, n is the n^{th} value in the data set, and a and b are the coefficients from the linear regression. In this way, the wave crests and troughs were measured in reference to a non-fluctuating still water level, thereby filtering out any long period effects. The wave height data measured by the wave gauge are representative of the actual water surface elevations and no further conversion of the data is required (Allan, 1998). This contrasts with the data obtained by the S4, that requires further correction after detrending to account for the effects of wave attenuation.

The adjusted data were then analysed using the zero-crossing method presented in Tucker (1963) and Draper (1966) and further developed by Earle *et al.* (1995). The raw wave heights were derived by measuring the distances from the crest to trough from the mean water level, whenever a wave passes through zero (Figure 4.1). The aim is to measure the gravity waves ($T > 1$ s), whilst omitting the extremely high frequency wind-stress ripples that form on the surface of the water (Figure 4.1). Five wave height parameters were calculated from this raw data; the mean wave height (\bar{H}), the significant wave height (H_s), the root mean square wave height (H_{rms}), the highest one-tenth wave height ($H_{1/10}$) and the maximum wave height (H_{max}). The mean wave height is simply an average of all the wave crests in the record. The highest of all the crests is denoted as the maximum. The significant wave height is the mean of the highest one-third of all the waves in the record and is a widely used parameter. Whilst it has physical meaning, H_s is a statistically arbitrary value. Its use derives from the idea that large waves are more significant in energy terms than small waves. It has been shown that the parameter roughly corresponds to a visual estimate of the wave conditions (Komar, 1998). Similarly, the $H_{1/10}$ is the mean of the highest 10% of the waves in the record. The root mean square wave height (H_{rms}) is a form of standard deviation of the wave record, and provides the correct estimate of the wave energy (Komar, 1998). First developed by Longuet-Higgins (1952), it is defined as the sum of all the zero-crossing wave heights squared, multiplied by the zero-crossing frequency:

$$H_{\text{rms}} = \sqrt{\frac{1}{N_z} \sum_{n=1}^N H_n^2} \quad (\text{m}) \quad (4.2)$$

Where N_z is the number of zero-crossings in an upward direction through mean water level and H_n is the n^{th} wave. Komar (1998) noted that the H_{rms} parameter should preferably be used over the significant wave height in modelling work, because it is a mathematically more meaningful parameter.

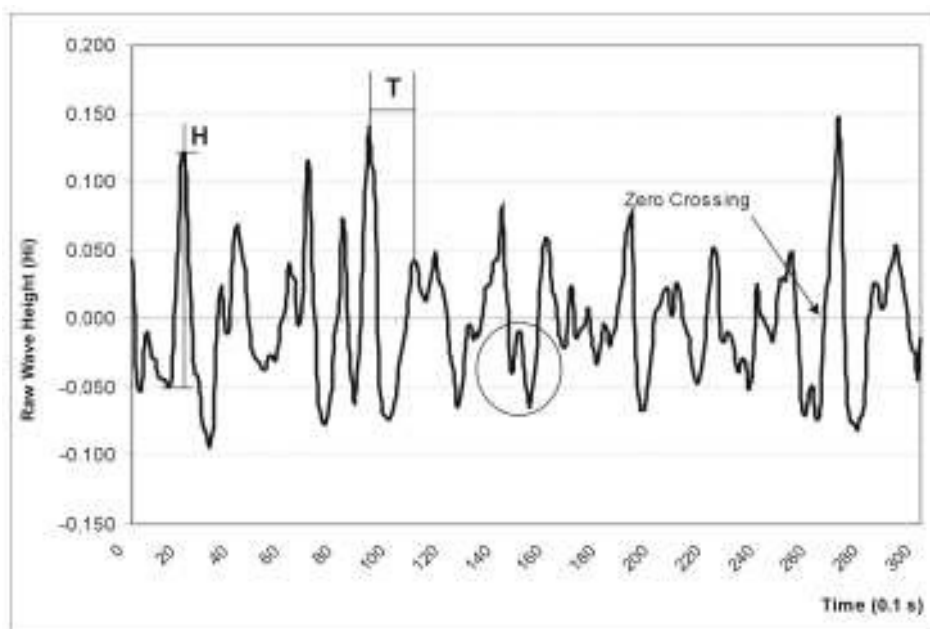


Figure 4.1 A 30 s wave record sample, collected at 1200 hrs on 14/12/01 from site C010. The first three seconds of this record are presented in Appendix 2a. The wave heights are calculated by measuring the distance from the crest to trough whenever the record crosses up through zero. Non-zero crossing, high frequency fluctuations, indicated in the circle, are not included in the calculations, effectively smoothing the data set. NB: y-axis data dimensionless.

Two wave period parameters were calculated with the zero-crossing method; the wave crest period (T_c) and the zero-crossing period (T_z). The zero-crossing period is calculated by dividing the duration of the record in seconds, with the number of zero-crossings (N_z). Like the root mean square wave height, T_z has both physical and mathematical significance and is the preferred parameter for modelling work (Draper, 1966). The zero-crossing period was the preferred parameter for Pickrill (1967) in the study of Lakes Te Anau and Manapouri, and Allan (1998) in the study of Lake Dunstan. Consequently, T_z is the also the preferred wave period statistic used in this study. It was found to consistently produce better results in modelling and correlation work. The crest period is the mean period for all the wave crests in the record. Tucker (1963) defined a wave crest as a point where the water level is momentarily stationary, with limbs falling to either side. Therefore it is possible that some crests may occur below mean water level.

This is illustrated by a small crest in the circle of Figure 4.1. The crest period is calculated by dividing the duration of the record in seconds with the number of wave crests (N_c). Once the zero-crossing and crest periods were known, the spectral band width parameter (ε) was able to be calculated:

$$\varepsilon = \sqrt{1 - \left(\frac{T_z}{T_c}\right)^2} \quad (4.3)$$

This ratio provides a measure of the width of the wave spectrum and is also a statistically significant parameter (Draper, 1966). If a wide range of frequencies is present, the short period waves will propagate on top of waves of longer period. This results in more wave crests than zero-crossings, as seen in Figure 4.1. In this situation, the spectral band width parameter will approach one. If a narrow band of frequencies is present, the number of wave crests will more closely equal the number of zero-crossings, and ε will approach zero (Draper, 1966). Storm wave spectrums typically display high spectral band width values, whilst swell wave spectrums have values closer to zero.

InterOcean S4ADW Data

The data collected with the S4 required downloading onto a laptop where analysis proceeded with a software programme called WAVE. The programme was written by InterOcean specifically for use with the S4 and the software is unable to convert data from other sources, such as the wave gauge. WAVE employs the Fast Fourier Transform (FFT) method of spectral analysis, developed by Cooley and Tukey (1967) and Harris (1974), to describe the wave characteristics. A standard FFT algorithm is used to calculate the Fourier coefficients of the pressure time series, as described in Trageser and Elwany, (1990). Before detailed analysis of the data sets can begin in WAVE, it is scanned for erroneous data points which, provided they occur in isolation, are patched by interpolation. The data is then detrended to remove any low frequency water level fluctuations, such as seiche activity. Following this a correction is applied to compensate for the effects of wave attenuation. Finally, a decision must be made on whether or not to apply a cosine taper window. Statistically, when the record length is small, it is desirable to weight the middle part of the record more heavily than the tails. The procedure involves multiplying the time series by a function that is dependent on the size of the taper window and the length of the record. This has the effect of smoothing out any discontinuities in the record by values lying outside the measurement range, particularly at the high frequency end (Trageser & Elwany, 1990). There is debate in the literature about the appropriateness of modifying data sets by employing such techniques (e.g. Harris, 1978; Taylor & Trageser, 1990),

but InterOcean recommend a taper window of 20%. In the analysis of the S4 data sets collected in Lake Dunstan, Allan (1998) experimented with the use of taper windows, but found that it made little difference to the final results. It was decided that the record lengths were of sufficient length to not require modification. The findings in this study support those of Allan (1998), and a decision was made not to apply a taper window to the data set.

Related to the statistical weighting of the data, there is provision in the WAVE software to apply a frequency cut-off limit to the tails of the spectral distribution. Lake waves are typically at high frequency end of the gravity wave spectrum. The typical distribution of an ocean wave data set is dominated by waves with 6-10 s periods. At the ends of the distribution there may be waves periods as long as 14-16 s or as short as 2-3 s. These short period high frequency waves, that are usually generated by local winds, sometimes occur on top of a longer period ocean swell and it may be desirable to exclude them from the analysis, as they may be an unimportant part of the energy balance. InterOcean (1990) recommend a cut off of 0.3 Hz (3.3 s) to avoid high frequency contamination of the wave spectrum. However, Allan (1998) commented that what is considered noise in oceanic environments is actually high frequency waves, characteristic of small lake environments. In lakes, these high frequency waves form the dominant part of the spectrum and it is necessary to include them in the analysis. Allan found that by increasing the cut-off frequency to 0.6 Hz (1.7 s), more representative wave heights could be obtained with the data from Lake Dunstan. In the present study, there was found to be a significant spectral peak at around 0.7 Hz, and so the cut-off frequency was increased slightly to 0.8 Hz (1.3 s). This reflects differences in the spectral characteristics between Lakes Coleridge and Dunstan and highlights the importance of examining raw data before applying filters or modifiers that may not be suitable for every location. Once the initial parameters are defined, the wave characteristics are calculated. A graphical time series and tabular summary of the results is generated, listing four wave height measures and five wave period statistics. In addition, the wave direction in degrees, the wave velocity and a parameter known as the spectral band width is also calculated.

A summary of the parameters calculated from both the S4 and wave gauge is given in Table 4.1. While definitions for most of these parameters were given in the wave gauge section, there are three wave period measures that were not calculated with the zero-crossing method; the peak spectral period, the significant wave period and the maximum wave period. The most important of these is the peak spectral period (T_p). This parameter is the period of maximum energy density in the frequency spectrum. The significant wave period is, like the significant wave height, the mean of the longest one-third of all the wave periods in the record.

Table 4.1 List of all the wave parameters calculated with the raw S4 and wave gauge data.

Wave Parameter	S4ADW	Wave Gauge
Mean Wave Height (\overline{H}) (m)	Yes	Yes
Significant Wave Height (H_s) (m)	Yes	Yes
Root Mean Square Wave Height (H_{rms}) (m)	Yes	Yes
Highest One-Tenth Wave Height ($H_{1/10}$) (m)	No	Yes
Maximum Wave Height (H_{max}) (m)	Yes	Yes
Significant Wave Period (T_s) (s)	Yes	No
Zero-Crossing Wave Period (T_z) (s)	Yes	Yes
Crest Wave Period (T_c) (s)	Yes	Yes
Peak Spectral Wave Period (T_p) (s)	Yes	No
Maximum Wave Period (T_{max}) (s)	Yes	No
Spectral Band Width (ϵ)	Yes	Yes
Wave Direction (α) (deg)	Yes	No
Wave Velocity (u) (m s ⁻¹)	Yes	No

Current Meter Data

The data from the Marsh-McBirney current meters were also processed in spreadsheet form and a routine was written that executed in Excel for the data analysis. After extraction from the data logger, it was divided into hourly blocks and converted into Microsoft Excel format. The hourly blocks were made up of 18 minutes of recordings, comprising 2160 data points for each of the current meters. An example of the raw data can be seen in Appendix 2b. The only pre-processing of the data required was the addition or subtraction of an off-set value, as discussed in the previous chapter, that typically ranged in the order of ± 0.01 . Once off-set values were applied to the raw data, current velocities and directions could be calculated for the nearshore and swash zone. The current velocity is given as the square root of the sum of the two axis values squared.

$$\sqrt{(Ax^2 + Ay^2)} \quad (\text{m s}^{-1}) \quad (4.4)$$

Where Ax and Ay are the raw data values from the two axes on the A current meter. These values were then analysed to produce a range of summary statistics calculated in minute and hourly time lengths. The raw current direction is calculated by taking the arctangent of the x-axis divided by the y-axis and multiplying by the ratio, 180 divided by pi:

$$\left(a \tan \frac{Ax}{Ay} \right) \times \left(\frac{180}{\pi} \right) \quad (4.5)$$

Once these calculations had been performed, it was possible to separate the data into on-shore and off-shore components of the flow.

When the raw data was processed and any spurious or corrupted records removed, 493 hours of concurrent time series data from the S4, wave gauge and Marsh-McBirney current meters was available for modelling. Post-processing, regression and correlation analysis of all the data sets from the S4, wave gauge and current meters was performed in Microsoft Excel and two statistical software packages; SPSS v11.0 for Windows and StatistiXL v1.5 for MS Excel. A summary of all the hourly wave data collected with the S4 and the wave gauge is presented in Appendix 5.

4.3 Comparison of Wave Gauge and S4 Pressure Sensor Data

It was noted by the U.S. Army Corps of Engineers (1992), that both the spectral analysis and zero-crossing approaches produce equally valid, but slightly different results. This contrasts with the findings of Harris (1970), who compared the results of four different techniques that each calculated a different wave height and period parameter. Two wave records were examined, composed of data obtained from two surface wave gauges and two pressure sensors. Harris found a high degree of correlation between the wave height measures, with a mean r value of 0.941, ranging from 0.868 to 0.987. The correlations for the wave periods were more variable, with r values ranging from as low as 0.131 to as high as 0.951, producing estimates that varied by as much as 10 s. It was noted that the correlations were better for higher waves, and thus by inference, longer periods. Harris concluded that it makes little difference what method is used to calculate wave height, as the results are nearly all the same. The same confidence could not be put in the wave period estimates, and Harris suggested that when comparing different wave period methods, it may be necessary to omit the low amplitude, high frequency waves from the analysis to produce more satisfactory results. However, as Allan (1998) noted, this would not be satisfactory when analysing lake waves, as they are most high frequency.

In order to increase confidence in the wave data measured by the two different instruments in Lake Dunstan, Allan (1998) and Allan and Kirk (2000) correlated the significant wave heights derived from the S4 with those from the wave gauge. A high degree of correlation was found between the two parameters, with a Pearson r value of 0.99. It was felt that this verified Harris's claim that it makes little difference what method is used to calculate wave height. However, Harris (1970) was examining *different* wave height parameters (e.g. H_s , H_{rms}), calculated with different *equations*. Allan (1998) compared the *same* wave height parameters (i.e. H_s), calculated with different *methods*; spectral analysis and zero-crossing. This would in part account for the

higher correlation coefficient. Allan also suggested that there may be differences due to the records coming from different wave environments, i.e. an ocean and a lake. When the wave period parameters from the S4 and wave gauge were compared, a high correlation was found with the zero-crossing periods ($r = 0.96$), which is not unexpected considering that they were calculated with the same method. Allan was surprised to find a high correlation ($r = 0.97$) between the significant wave period from the S4 and the wave-crossing period from the wave gauge. It was suggested quite rightly, that this was probably due to the narrow range of frequencies measured from the lake environment. However, a close examination of the data presented in Harris (1970) reveals that the correlation between these parameters was found to be 0.867. Whilst slightly less than that found by Allan, this was the second highest correlation for the period values calculated by Harris.

These contrasting conclusions make it worthwhile comparing some of the results from the two methods with data from Lake Coleridge. Figure 4.2 shows the correlation of the significant wave height measured from the wave gauge against that measured from the S4. The Pearson r coefficient is 0.86 and the t statistic is 38.06, indicating that the correlation is strong. This is less than the r value found by Allan (1998). It can be seen that the calculated wave heights are very similar in range. The mean height from the wave gauge is 0.17 m and 0.14 m from the S4. On average, measured H_s was slightly lower from the S4, and is probably due to wave attenuation. The data are reasonably scattered around the best-fit line throughout the range of wave heights, but tend to be slightly better correlated at lower heights. The reason for this not entirely clear, but is partly due to the spectral band width (ε) widening as the wave energy increases. This effect was also noted by Pickrill (1976), who found that the wave conditions became more variable at higher energies. When the *root mean square* wave height from the wave gauge was correlated with the *significant* wave height from the S4, it was found to be slightly better, with $r = 0.90$ and a t statistic of 46.75. This is also slightly less than that found by Harris (1970).

Figure 4.3 shows the correlation of the *zero-crossing* period from the wave gauge against the *significant* wave period from the S4. The Pearson r coefficient is 0.82 and the t statistic is 31.55, indicating another strong correlation. The correlation of the zero-crossing period from the wave gauge against the zero-crossing period from S4 produced a very similar result, with $r = 0.81$ and $t = 31.06$. Again, these correlations are not as strong as those found by Allan (1998), but in the range found by Harris (1970). Interestingly, the average zero-crossing period from the wave gauge was on average 30% less than that from the S4. This is the opposite of that found for the significant wave height. It is a reflection of the different sampling rates between the two

instruments. The wave gauge, sampling at a faster rate, was able to measure higher frequency waves than the S4, leading to a slight difference in the wave periods. A summary of the correlations between all the variables across the studies is presented in Table 4.2.

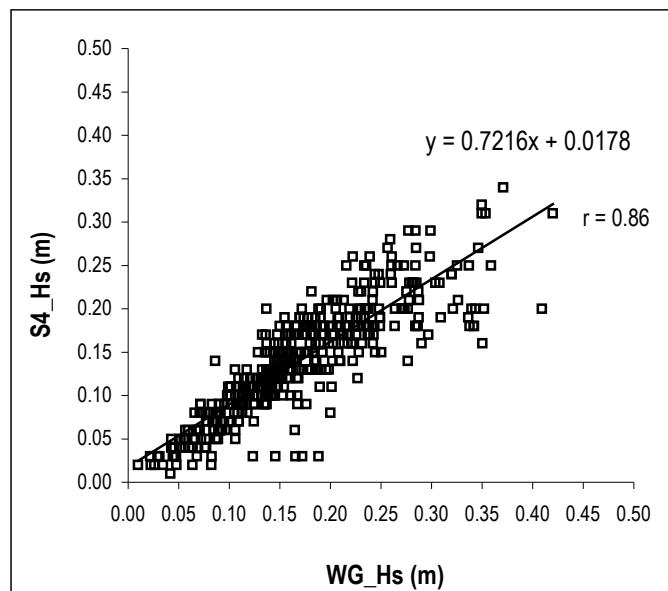


Figure 4.2 Correlation of significant wave heights (H_s) from the wave gauge against the S4. $n = 493$.

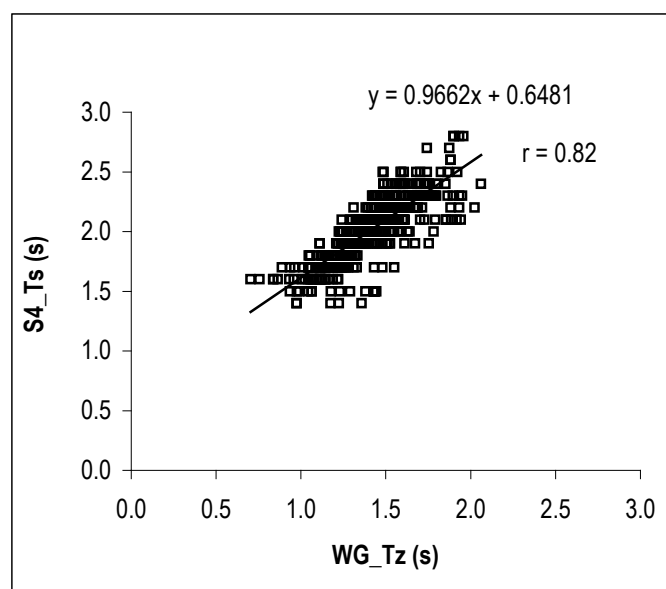


Figure 4.3 Correlation of zero-crossing (T_z) period from the wave gauge against the *significant* wave period (T_s) from the S4. The correlation of the zero-crossing periods from the two instruments was almost identical. $n = 493$.

Table 4.2 Comparison of the r coefficients from correlations of selected wave parameters calculated from wave gauge and pressure sensor data. WG=wave gauge; PS = pressure sensor (S4 in the case of Allan's and the present study).

	WG_Hs vs PS_Hs	WG_Hrms vs PS_Hrms	WG_Hs vs PS_Hrms	WG_Tz vs PS_Tz	WG_Tz vs PS_Ts
Harris (1970)	---	---	0.97	---	0.867
Allan (1998)	0.99	---	---	0.96	0.97
Dawe (present)	0.86	0.88	0.90	0.81	0.82

The differences between Allan's (1998) study and the present one are due to a range of factors, but the most important of these are probably the wave attenuation effects on the S4 and the faster sampling rate of the wave gauge. Allan found that in water depths of 0.85-1.40 m, the amount of wave attenuation ranged widely from 8% to 68% for waves in the order of 0.15 m with periods of 1.8-2.0 s. Allan & Kirk (2000), found that some of the S4 wave heights statistics were as much 40% less than those calculated from the wave gauge data. The most likely explanation offered for this was that, there were times when the S4 was operating in water slightly too deep to resolve the wave conditions. It was noted that this highlighted the importance of locating pressure sensors in very shallow water to obtain reliable measurements of high frequency lake waves. Linear wave theory shows that attenuation beneath the wave becomes more pronounced as the wave period decreases (Komar, 1998).

For the Lake Coleridge data, the significant wave height calculated from the S4 was on average 30% less than the significant wave height calculated from the wave gauge data. It is possible that some of this is due to the S4 being in water too deep to characterise the wave spectrum. In Chapter Three, it was explained that every effort was made to deploy to S4 in 'deep water', defined as depths over half the wave length ($d > 0.5L$). In Lake Coleridge, the calculated wave lengths ranged from 0.77-6.63 m, with an average of 3.26 m. This justified the positioning of the S4 in water depths of 1.5-2.0 m, because for much of the time, this was deep water as defined by the inequality ($d > 0.5L$). Denny (1988) stated that a pressure sensor must be located in sufficiently shallow water to detect the shortest period wave of interest. In Lake Coleridge, this would mean deploying the S4 in as little as 0.5 m of water, i.e. the nearshore zone. The deployment procedure for the S4 is time consuming and it was not practical or even possible to redeploy every time the conditions changed. For recording consistency, an average depth was chosen for the duration of a sampling period.

Allan and Kirk (2000) also expressed reservations about the ability of a sensor sampling at 2 Hz to accurately represent a high frequency lake wave spectrum. It was noted that as the wave energy conditions increased, there was a progressive shift in the peak frequency from 0.5 Hz (2.0 s) toward the shorter end of the spectrum at 0.65 Hz (1.5 s). In these conditions, it was felt there was a possibility that some of the data may be truncated from the spectrum. Indeed, in the present study there was a small but significant spectral peak identified at 0.7-0.8 Hz (1.3-1.4 s) in the S4 data. The wave gauge at Lake Coleridge was sampled at 10 Hz (0.1 s) to avoid this problem. Furthermore, Allan (1998) truncated the spectral analysis at 0.6 Hz when using WAVE to analyse the S4 data. This reflects differences in the energy spectrum between Lakes Coleridge and Dunstan, which would lead to differences in results, but it is possible that some high frequency data was truncated from the analysis. Allan (1998) also omitted waves below 0.10 m from the analysis, because it was felt that they were not an important part of energy balance. In Lake Coleridge, waves below 0.10 m were found to cause a significant amount of sediment transport in the swash zone, and were included in all analyses.

Allan and Kirk (2000) suggested that some of the variations between the S4 and wave gauge found in their study, may be due to a lack of data. In total, there were 110 eighteen minute sample records from the S4 and 53 eighteen minute sample records from the wave gauge. The present study has used 493 eighteen minute records to compare results from the S4 and wave gauge, and variations between the two instruments are still evident. These findings raise a number of important issues about using pressure sensors in lake environments. Despite the fact that the correlations between the wave parameters measured with the different instruments are strong, it is the variation in the magnitudes that causes concern. In a comparison between pressure sensors and wave gauges Esteva and Harris (1970) also found that, whilst there were good correlations between the two instruments, the wave gauge produced larger readings in the energy containing part of the spectrum. In this study, the wave gauge data provided consistently better correlations and between transport rates and wave conditions and was the preferred data set to work from. The S4 is perhaps not the most suitable instrument to measure lake waves. A small bottom mounted pressure sensor may be one solution to this problem, as it can more easily be shifted in response to the conditions. However, a capacitance wave gauge sampling at a fast rate provides the best method for measuring the water surface fluctuations in a low energy wave environment. A specifically designed study is required to properly examine the differences between capacitance wave gauges and pressure sensors in low energy wave environments. The observation of the U.S. Army Corps of Engineers (1992), that both the spectral analysis and zero-crossing approaches produce valid, but slightly different results is probably a fairly good

assessment. In conclusion, whilst the different methods produce similar results, in a low energy environment these differences are significant enough to warrant caution when using different methods to analyse wave records for scientific or management purposes.

4.4 Deep Water Wave Measurements

The discussion in Chapter One highlighted the important role that waves play in controlling the geomorphology and processes of a lake shore beach. With respect to the lakes of New Zealand, Allan and Kirk (2000) stated that:

“Given their importance, it is surprising to note that there is a dearth of information about the characteristics of waves that form on the inland waters of New Zealand, their distribution about lake shores, seasonal variability, and wave statistics (heights and periods.)”

Allan and Kirk (2000) was the first published study on the nature of lake waves in New Zealand. Most studies of New Zealand lakes have relied on visual observations or wave hindcasting to provide estimates of the wave conditions (Pickrill, 1976; Macbeth, 1988; Kirk, 1988; Worthington, 1989; Allan, 1991). Aside from a few consultancy reports that deal with a specific management issue, there are only two previous studies, both Doctoral theses, that have made quantitative measurements of lake waves; Pickrill (1976) and Allan (1998). In his study of Lakes Manapouri and Te Anau, Pickrill made three months of visual observations, but supported these with 46 wave recordings taken from two sites at Lake Manapouri and five sites around Lake Te Anau. The measurements were taken with a handheld wave gauge immediately lakeward of the breaker zone. Pickrill did not record the water depth or the length of time each record was sampled. The wave gauge was connected to an analogue chart recorder taking a continuous trace of the water level. The trace was digitised at 0.3 s (3.3 Hz) intervals and analysed by a computer programme to produce seven summary statistics. Any trace with waves below 0.05 m was not digitised and was omitted from the analysis. Allan (1998) took wave measurements from four locations around Lake Dunstan, Central Otago, with an S4 wave and current meter and capacitance wave gauge. In all, 251 eighteen minute sample records were made, 198 from the S4 and 53 from the wave gauge. Of the S4 data, 111 eighteen minute records that represented a range of storm events were selected for analysis. The remaining 87 records (44%) were of waves below 0.10 m and were omitted from the analysis.

During the field deployment at Lake Coleridge, over 1000 eighteen minute samples were recorded with the S4 and 575 eighteen minute samples were made with the wave gauge. The recordings were made in a wide range of conditions from four locations around the barrier foreland fieldsite. 493 hours of these recordings overlap, during which time measurements were made concurrently with the Marsh-McBirney current meters, the S4, the wave gauge and the two sediment traps, representing the bulk of the fieldwork programme. Similarly, these hours formed the main data set used in the analysis and modelling work. The remaining half of the recordings from the S4 were made during the hours of darkness and in extremely light conditions when the wave gauge was not operational. Eighty-two hours of wave measurements were made with the wave gauge, in conjunction with the current meters and two sediment traps, during an experiment that measured the distribution of the sediment transport rate across the swash zone. During this time, the S4 was not deployed.

Wave Height

The summary statistics of the wave height data from the wave gauge are presented in Table 4.3. The significant wave height (H_s) ranged from 0.01 to 0.42 m with a mean of 0.17 m. This compares favourably with visual observations made by Worthington (1989) over a 3 month period from the southern end of Lake Coleridge, who found mean significant wave heights ranged from 0.20 to 0.37 m. The mean maximum wave height was 0.35 m, and the maximum recorded wave height was 0.84 m, that occurred during a northwest wind event on 11/12/02. The maximum observed wave by Worthington was 1.20 m. In contrast, the mean wave height for all the data is only 0.08 m. Although it is not a commonly used statistic, it shows that the waves experienced at Lake Coleridge are generally of small amplitude. The wave height values are all moderately positively skewed and platykurtic, indicating that the height data are well represented across the size range, but that there is a tail of large wave heights. This is illustrated in Figure 4.4, that shows the frequency distributions for four wave statistics. This type of skewed distribution is commonly seen in wave data sets and is known as a Rayleigh distribution (Longuet-Higgins, 1992; Komar, 1998).

Table 4.3 Summary statistics of the wave height parameters measured with the wave gauge, $n = 493$. Mean data from the studies of Pickrill (1976) and Allan (1998) are included for comparison.

	H_{\max}	$H_{1/10}$	H_s	H_{rms}	H_{av}
Mean	0.35	0.22	0.17	0.20	0.08
Median	0.34	0.21	0.16	0.19	0.08
Mode	0.19	0.12	0.09	0.09	0.05
Minimum	0.03	0.02	0.01	0.01	0.01
Maximum	0.84	0.53	0.42	0.51	0.18
Skewness	0.55	0.48	0.51	0.52	0.37
Kurtosis	0.14	0.08	0.13	0.12	-0.04
Variance	0.02	0.01	0.01	0.01	0.001
Std. Deviation	0.15	0.09	0.07	0.09	0.03
Pickrill (1976) n = 47, 3.3 Hz	0.24	---	0.16	0.12	---
Allan (1998) n = 53, 2 Hz	0.49	0.34	0.27	0.16	0.16

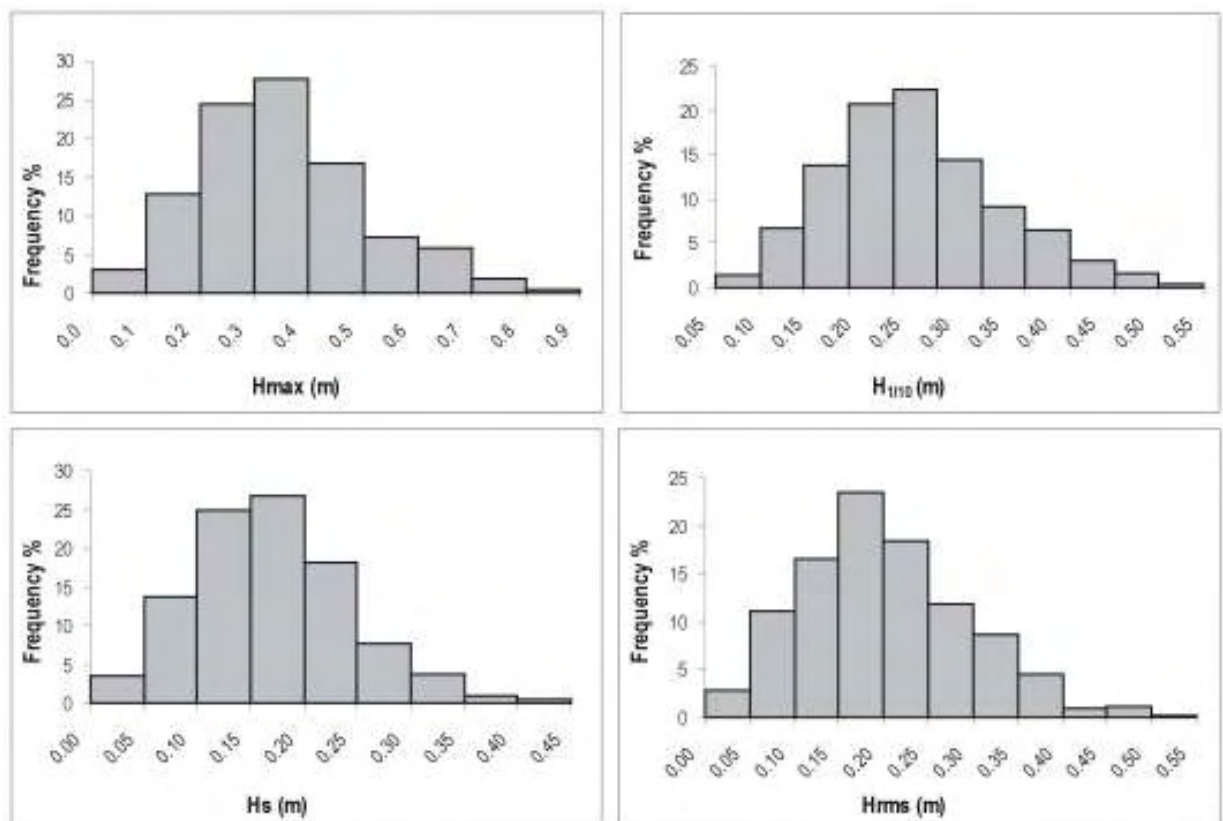


Figure 4.4 Frequency distribution graphs for four wave height statistics calculated from the wave gauge data showing a characteristic Rayleigh distribution. $n = 493$.

Table 4.3 also presents the mean wave height statistics calculated from the wave gauge data of both Pickrill (1976) and Allan (1998). The waves measured at Lake Coleridge are in the same range as those measured from other South Island glacial lakes. The mean H_s measured by Allan from Lake Dunstan was 0.27 m. This is higher than that recorded by Pickrill at Lakes Manapouri and Te Anau, and in the present study from Lake Coleridge. As discussed previously, Allan (1998) only included data above 0.10 m and restricted his measurements to storm events. However, he indicated that waves below 0.10 m accounted for a considerable 43.7% of the data collected with the S4. Figure 4.5 presents the exceedence curves for four of the wave height parameters measured with the wave gauge from Lake Coleridge. It shows that 50% of the significant wave heights were over 0.16 m, whilst only 5% of heights were above 0.30 m. Interestingly, significant wave heights below 0.10 m account for only 17% of the data, with only 3.4% of measured waves below 0.05 m. When the S4 data are analysed, this increases to 24% of waves below 0.10 m, and 6.5 % below 0.05 m. This is considerably less than Lake Dunstan, and is a reflection of the windy nature of the Lake Coleridge environment. It also indicates differences between the abilities of a wave gauge and a pressure sensor to accurately measure lacustrine waves. Of the maximum wave heights, 50% of the data are above 0.34 m and 15% is above 0.50 m and 2% of waves are above 0.75 m.

With respect to Lakes Manapouri and Te Anau, drawing comparisons with Pickrill's data is more problematic due to the limited data set and differences in methodology. Measurements were made with a hand-held wave gauge and as Pickrill (1976, p.123) stated, were taken "whenever suitable conditions prevailed." A hand-held wave gauge cannot detect the difference between water movement and movement of the wave gauge. This requires the operator to remain absolutely still, thereby restricting measurements to light and moderate conditions. Furthermore, Pickrill noted that there was a high prevalence of waves below 0.05 m in the record, but did not include them in the analysis. Notwithstanding this, the data from Lakes Manapouri and Te Anau show a similar trend to Lake Coleridge, with 50% of the significant wave heights above 0.15 m and 6% above 0.30 m. In an attempt to standardise these data sets, the Lake Coleridge data were recalculated without waves below 0.05 m and 0.10 m (Table 4.4). The results show only modest increases in the significant wave height in the order of 0.01 – 0.02 m.

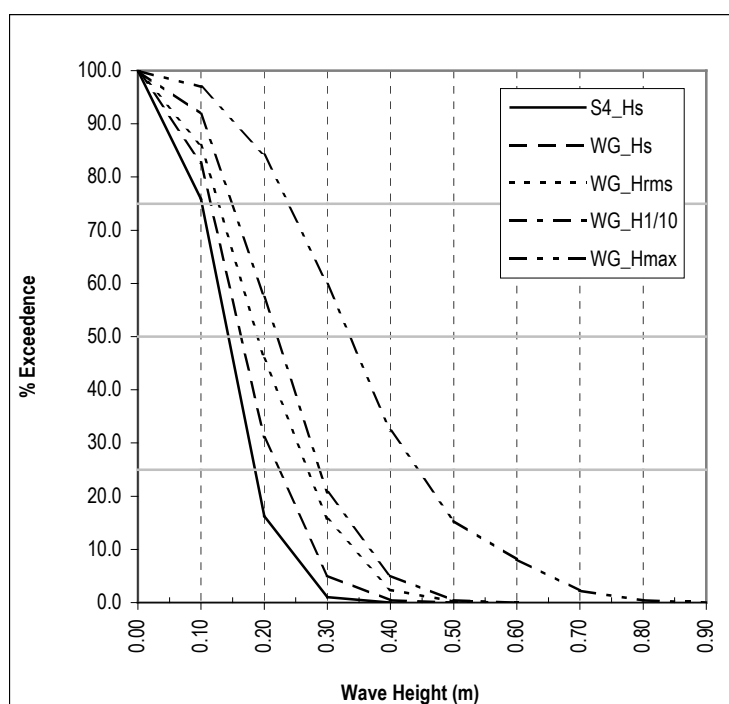


Figure 4.5 Percentage exceedence curves for four wave height statistics calculated from the wave gauge (WG) and S4 data.

Table 4.4 Significant wave height values from the wave gauge and S4 recalculated, omitting data below 0.05 m and 0.10 m, for comparison with data from three South Island lakes, Manapouri, Te Anau and Dunstan.

Hs	WG_all	S4_all	Pickrill (1976)	WG_>0.05	S4_>0.05	Allan (1998)	WG_>0.10	S4_>0.10
mean	0.17	0.14	0.16	0.17	0.15	0.27	0.19	0.17
min	0.01	0.01	0.05	0.05	0.05	0.11	0.10	0.10
max	0.42	0.34	0.35	0.42	0.34	0.53	0.42	0.34
Std. Dev.	0.07	0.06	0.07	0.07	0.06	0.11	0.06	0.05
Variance	0.005	0.004	0.050	0.005	0.003	0.012	0.004	0.002

Although the wave heights at Lake Coleridge are moderate in size, they are of the same order of magnitude to those found in other New Zealand lakes. More importantly, it is their regular and frequent occurrence that causes them to have a significant impact on the shoreline. This is reflected in the number of shoreline features around the Lake built by longshore transport processes. In Chapter two, Figure 2.11, it was noted that calm conditions ($< 1 \text{ m s}^{-1}$) occur for only 5.2% of the time. The remaining 94.8% of the time, waves are forming, propagating across the water and acting on the shoreline. It will be shown in Chapter Five that the small amplitude waves play an important role in longshore sediment transport. This challenges previous assumptions that low amplitude waves are an insignificant part of a lacustrine wave energy budget.

Wave height was found to be strongly linked to wind strength. Figure 4.6 is a regression between the wind speed collected from the weather station and the H_{rms} wave height calculated with data from the wave gauge. The relationship is not linear, rather wave height increases exponentially with increasing wind strength ($r^2 = 0.72$). The relationship displays a general linear increase in wave height up to wind speeds of around 10 m s^{-1} . Above this, small increases in wind speed result in significant increases in wave height. It is felt that this is not a statistical artefact, but that it reflects a physically meaningful process of wave development. At low wind speeds, the waves are of small amplitude and do not present a large surface area to the wind. As the wind speed increases and the waves continue to grow, they present an increasingly large surface for wind pressure to gain a ‘purchase’ on the water, in much the same way as a sail. The data suggests that there is a threshold when waves are approximately 0.20 m in height, after which small increases in wind speed rapidly build the wave. The equation for the regression can be used to reasonably estimate wave height from the wind speed:

$$H = 0.0451e^{0.1632\bar{V}} \quad (\text{m}) \quad (4.6)$$

Where \bar{V} is the mean wind speed in units of m s^{-1} . Using this equation, wave heights of 1.0 m might be expected to occur with sustained wind speeds of around 19.0 m s^{-1} (gale force) and 2.0 meter waves might be expected to occur at wind speeds over 23.3 m s^{-1} (severe gale force). At the field sites, waves appeared to become fetch limited in gale force conditions.

There is general variability across the full range of conditions. Some of the variation is caused by differences in the wave heights measured from different locations around the fieldsite. For example, site CO13 was in a slightly sheltered embayment and experienced slightly smaller waves than more exposed sites, such as CO10. However, when the data is sorted on the basis of wind direction, the variability become apparent (Table 4.5). In Chapter Two it was shown that wind regime for Lake Coleridge is strongly bimodal with prevailing winds from the northwest and southeast. The mean H_{rms} wave height from the northwest is 0.23 m, but only 0.13 m from the southeast, despite the fact that the fetch distances are 3.5 km longer from this direction. The north-westerly is stronger and more gusty, producing a more mixed wave state and a lower correlation with H_{rms} ($r^2 = 0.61$). The winds from the east and southeast are more consistent and stable, producing more even wave conditions and consequently, a better correlation with the wave height ($r^2 = 0.81$). This difference is illustrated in Figure 4.7 which presents two typical wind and wave traces for the prevailing conditions at Lake Coleridge. The data are over three consecutive days when the wind was blowing from the southeast and the northwest. In southeast conditions it can be seen that the wind builds gradually through the day and eases in the evenings, to produce a diurnal variation in wave activity (Figure 4.7a). In contrast, the northwest

does not have any diurnal variation and produces gusts and lulls in the record from hour to hour (Figure 4.7b). These differences cause variations in the rates and duration of longshore sediment transport and has produced shoreline features around Lake Coleridge that are dominated by the northwest. A striking feature of the waves revealed in Figure 4.7, is how quickly they grow in height with increases in wind strength. There is almost no lag time in the wave growth, revealing how closely linked the waves are to the wind. In an ocean or very large lake, waves can become decoupled from the wind and propagate under their own energy in the form of swell. This process does not occur in a small lake environment and is one of the most significant process differences between the two environments.

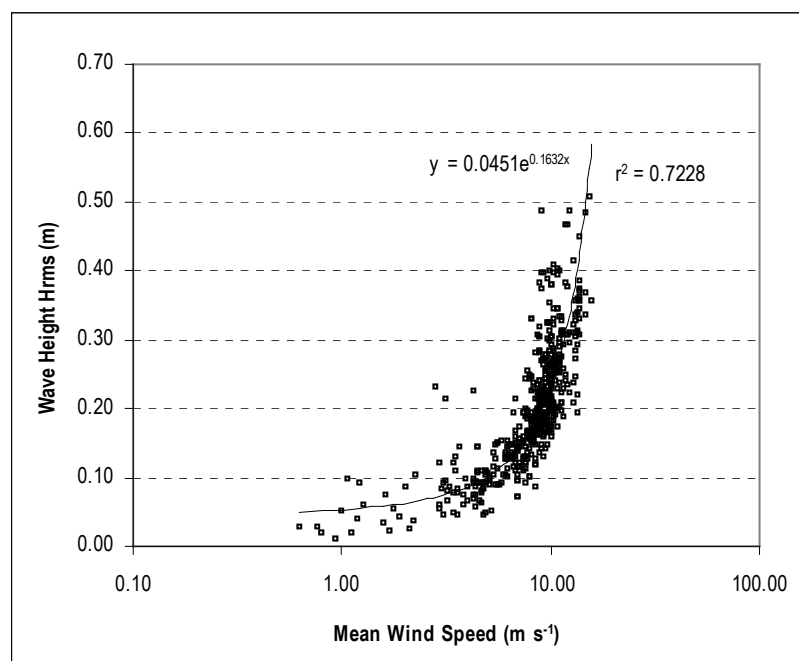


Figure 4.6 Regression of wind speed against the root mean square wave height from the wave gauge, showing a strong positive exponential correlation. $2.5 \text{ m s}^{-1} = 9 \text{ kph}$. $n = 493$.

Table 4.5 Regression statistics for wind speed versus root mean square wave height.

	Hrms	r^2	r	Std. Error	F stat.	Prob.
All	0.20	0.72	0.84	0.04	918.36	< 0.0001
Southeast	0.14	0.81	0.90	0.03	606.46	< 0.0001
Northwest	0.23	0.61	0.78	0.05	388.63	< 0.0001

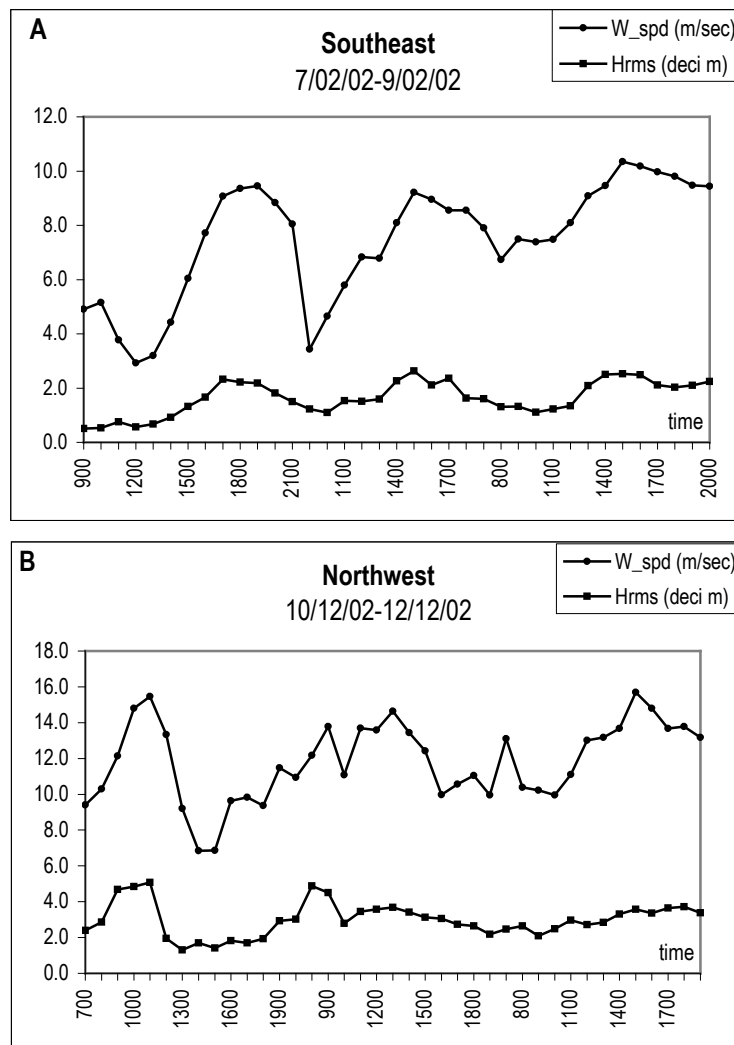


Figure 4.7 Wind and wave traces of three consecutive days of measurements $n = 39$. There is little lag time between the onset of wind and corresponding wave growth. Winds from the southeast commonly produce a diurnal pattern of wave activity (A). Gusty northwest conditions produce a mixed wave spectrum (B).

Wave Period

The wave period summary statistics are presented in Table 4.6 and the exceedence curves in Figure 4.8. Only the zero-crossing and crest period were calculated from the wave gauge data. Overall the data shows that there was a narrow band of wave periods measured at Lake Coleridge, with means ranging from 1.43 to 2.33 s. The S4 data produced slightly longer wave periods than the wave gauge. When the zero-crossing periods are compared, the mean S4 value is 0.55 s longer. However, the range in the respective data sets is exactly the same at 1.3 s. The mean minimums ranged from 1.3 to 1.4 s whilst the maximums ranged from 2.7 to 3.7 s. All the data sets are strongly negatively skewed, indicating the presence of many short period waves in

the spectrum. The data is also strongly platykurtic, indicating that an equitable number of wave periods were recorded in each size class. When compared to the measurements of Pickrill (1976) and Allan (1998), Lake Coleridge has similar wave periods to those found in other South Island lakes. The S4 data period statistics are very similar to those from Lake Dunstan. The fetch distances at Lake Coleridge are shorter than those at Lake Dunstan and this is reflected in the slightly shorter wave periods.

Table 4.6 Summary statistics of the wave period parameters measured with the S4 and wave gauge, $n = 493$. Mean data from the studies of Pickrill (1976) and Allan (1998) are included for comparison.

	WG_Tz	WG_Tc	WG_ε	S4_Tp	S4_Ts	S4_Tz	S4_Tc	S4_ε
Mean	1.43	0.75	0.84	2.33	2.03	1.98	1.77	0.42
Median	1.44	0.75	0.85	2.40	2.00	2.00	1.80	0.43
Mode	1.68	0.73	0.78	2.60	2.10	2.10	1.80	0.46
Minimum	0.70	0.42	0.47	1.30	1.40	1.40	1.30	0.21
Maximum	2.06	1.07	0.93	3.70	2.80	2.70	2.20	0.62
Skewness	-0.05	0.32	-2.92	-0.13	-0.05	-0.10	-0.22	-0.35
Kurtosis	-0.12	0.81	14.69	-0.18	-0.39	-0.28	-0.19	-0.45
Variance	0.05	0.01	0.00	0.25	0.07	0.06	0.03	0.01
Std. Deviation	0.23	0.09	0.05	0.50	0.27	0.25	0.18	0.08
Pickrill (1976) n = 47, 3.3 Hz	1.91	1.69	0.43	---	---	---	---	---
Allan (1998) n = 163, 2 Hz	---	---	---	2.46	2.54	2.18	2.00	0.34

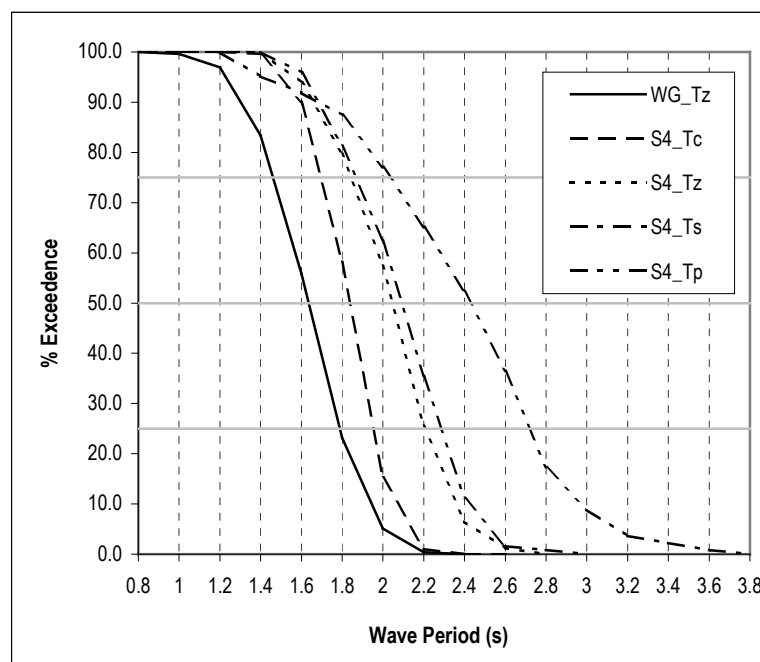


Figure 4.8 Percentage exceedence curves for four wave period statistics calculated from the S4 and wave gauge (WG) data.

A prominent feature of the Lake Coleridge wave gauge data is the high spectral band width value and associated small crest period. The mean is 0.84 with a range of 0.47 to 0.93, but 95% of the values lie between 0.75 and 0.90, creating a severely leptokurtic distribution. The spectral band width provides an indication of how spread the wave periods are across the frequency spectrum. Values closer to one indicate a mixed wave state that has a wide range of periods, more associated with stormy conditions. Values closer to zero indicate a more narrow banded spectrum, associated with more steady wind conditions. The parameter is a ratio between the zero-crossing and the crest wave period, calculated relative to the data set. Thus, when there are more crests in the record than zero-crossings, it indicates a mixed wave state and the spectral band width parameter will approach one. The mean crest period calculated from the wave gauge data was 0.75 s, almost half the mean zero-crossing period (1.43 s). That is, there are twice as many crests as zero-crossings in the record, indicating that the Lake commonly experiences stormy wave conditions. The geomorphology of the area exerts a strong influence on the wind, that is channelled and accelerated through the Lake Coleridge basin creating a gusty wind environment. When the spectral band width is sorted on the basis of wind direction, it shows that the highest values are associated with conditions from the northwest (Figure 4.9). This supports the observation that there are differences in the wave spectra from the two prevailing directions. Thus, there will be differences in the impacts that the waves from the northwest and southeast have on the shoreline.

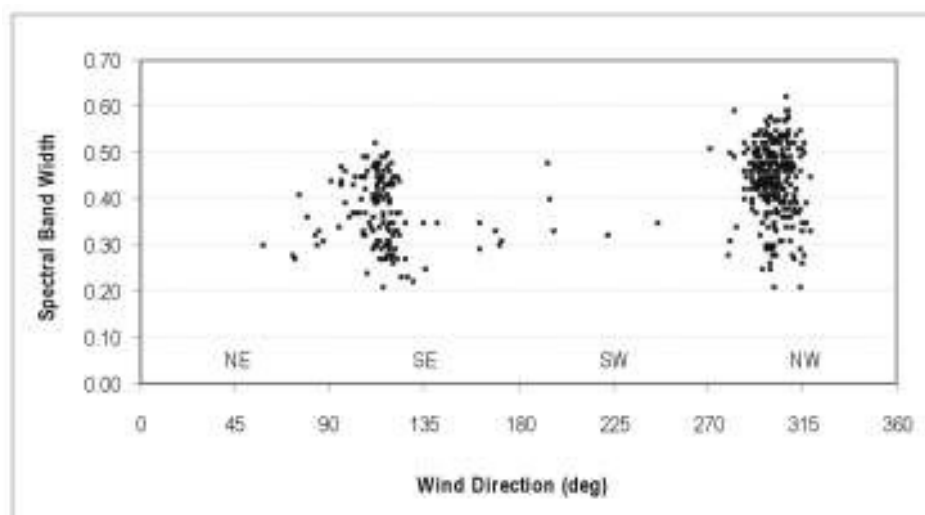


Figure 4.9 Comparison of spectral band width and wind direction. Northwest conditions produce higher spectral band width values, an indication of the stormy nature of these waves.

By contrast, the mean spectral band width measured with the S4 was 0.42, with a range of 0.21 to 0.62. This compares similarly with the mean from Lake Dunstan at 0.34. Again, this is a reflection of the different sampling methodologies and speeds between the two instruments. The wave gauge detects every fluctuation and crest in the water surface leading to a higher crest period. A pressure sensor does not detect these small surface changes, effectively smoothing out the data. This smoothing effect is accentuated by the slower sampling speed of 2 Hz. Figure 4.10. is a correlation between the zero-crossing wave period and significant wave height for the wave gauge and S4. A strong correlation is evident for both instruments with Pearson r coefficients of 0.91 for the wave gauge and 0.83 for the S4, and a t -test statistic of 47.40 and 34.30 respectively. It highlights the differences between the two instruments and indicates that there is less variability in the data measured with the wave gauge. This is consistent with the findings of Allan (1998), who found strong correlations between increases in wave period and height, but that the pressure sensor data was offset by 0.5 s to the right.

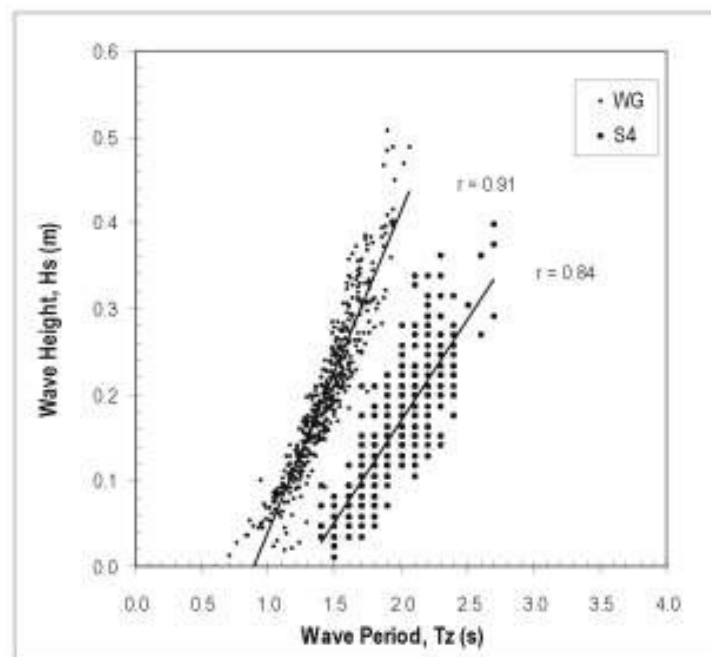


Figure 4.10 Correlation between zero-crossing wave period and significant wave height for the two instruments. The strong relationship is consistent with findings from other South Island lakes.

Increases in wave period are also strongly correlated with increases in the spectral band width (Figure 4.11). This suggests that in a small lake environment, larger waves are almost always associated with stormy conditions. Pickrill (1976) suggested that because lakes typically

experience a narrow range of high frequency, low amplitude waves, the spectral band width values should be closer to zero than one. Pickrill felt that lakes should experience waves more in common with swell than storm waves. This idea was broadly supported by Allan (1998), whose data from Lake Dunstan appeared to confirm the idea. However, the findings from Lake Coleridge show that in lakes, the wave groups are often highly mixed and present conditions more broadly similar to storm waves. This is because the waves in a small lake are directly linked to the wind, which can be variable and gusty, generating waves with a range of periods. Further, Allan (1998) noted that hindcasting models often struggle to estimate wave heights in these fetch restricted alpine environments, because the wind is accelerated down valleys in ways that the models cannot take into account. When spectral energy graphs of swell are compared to those from the wave generation area, they show that the areas where waves are generated typically display a wide range of periods (Komar, 1998), as is commonly known as ‘sea’. As the waves travel away from the generation area, there is a sorting process whereby waves of similar period group together producing a narrow spectrum of swell. This sorting process does not have a chance to occur in a small lake environment, and the wave spectrum remains in a mixed ‘sea’ state. The wave gauge sampling at 10 Hz has been able to finely resolve the full range of water surface fluctuations to a degree that has not been possible in previous studies of New Zealand lakes. This has produced a good representation of the wave conditions, showing them to be more complex than previously thought for small alpine lakes.

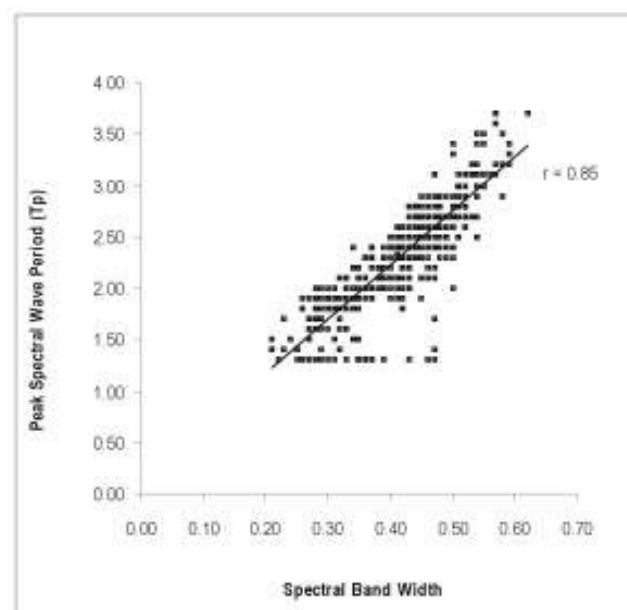


Figure 4.11 Correlation between spectral band width and peak spectral wave period showing that higher wave periods are associated more stormy conditions.

4.5 Comparison of Wave Height Statistics

Often in coastal management applications there is the need to make estimates of the potential wave conditions under a range of scenarios. In New Zealand, resource managers frequently have to make estimates of wave heights and run-up based on a few historical storm events or a limited understanding of the local wind patterns. Wave hindcasting may produce values for the significant wave height, but often there is the need to know the maximum or root mean square wave height for planning or modelling purposes. Longuet-Higgins (1952), produced a range of ratios between the various wave height parameters, based on theoretical considerations, that could be used to make estimates of wave height based on the knowledge of only one parameter (Table 4.7). These ratios were subsequently tested against field data and found to broadly agree with empirical observations. Allan and Kirk (2000) compared the findings from Lake Dunstan with the theoretical values from Longuet-Higgins (1952). They also presented wave data from Hastie (1985), that was associated with research into the nearshore sediment transport processes of a mixed sand and gravel shoreline. They found a good agreement for two of the four values for their wave gauge data, but found the H_{rms}/H_s ratio was lower than average. The H_{max} ratio was higher than average but just within range of the theoretical values. In contrast, the H_{rms}/H_s calculated from the work of Pickrill is lower than average and probably relates to the fact that his sampling was restricted to moderate conditions.

Table 4.7 presents the data from Allan & Kirk (2000) and extends the work with ratios calculated from the present study, including data from both the wave gauge and the S4. There was found to be a general agreement for the $(H_{1/10}/H_s)$ ratio, but the H_{max} and H_{rms} ratios from the wave gauge data are both higher than the theoretical values and the values found by other workers. The H_{max} ratio from the S4 is within range and this is a reflection of lower wave height recordings from the instrument. The (\bar{H}/H_s) ratio is variable, with the wave gauge data producing a slightly lower value and the S4 data a somewhat higher value. Curiously, the H_{rms} wave height is slightly higher than the H_s wave height. In studies of the relationships between the height variables of ocean waves, H_{rms} is usually found to be in the order of 30% lower than H_s (i.e. $H_{\text{rms}} \approx 0.71H_s$) (Komar, 1998). In this case, H_{rms} was found to be in the order of 15% more than H_s (i.e. $H_{\text{rms}} \approx 1.17H_s$). By contrast, Allan and Kirk (2000) found the H_{rms} value to be lower than H_s by a little over one half ($H_{\text{rms}} \approx 0.58H_s$).

The reason for these differences is not entirely clear, but it is probably due to a range of factors including differences in the spectral characteristics between lakes and oceans, and differences in the methodologies and sampling rates between the various studies. Preliminary resampling of the raw wave gauge data at 2 Hz indicates that H_{rms} wave height is around 40% lower when calculated with the slower data set, producing a (H_{rms}/H_s) ratio similar to that found by Allan and Kirk (2000). It will be recalled from Equation 4.2, that the H_{rms} wave height is calculated by summing all the wave heights in the record and multiplying this by the zero up-crossing frequency ($1/N_z$). The number of data points in an 18 min record sampled at 2 Hz is 2160. This increases to 10800 data points when sampling is at 10 Hz, a five-fold increase. When two records are examined from the same time period, one sampled at 10 Hz and the other at 2 Hz, it reveals that, whilst the sum of the wave heights increases by a factor of roughly five at the higher sampling speed, the number of zero up-crossings do not increase at the same rate. This has produced greater H_{rms} wave heights with the 10 Hz data.

Another possible reason for the diverging results is that the theoretical ratios derived by Longuet-Higgins (1952), were for a narrow banded spectrum that was not mixed with waves of different periods. To date, the data that has been used to test the theoretical ratios has been oceanic wave data. It has been shown that the Lake Coleridge data is frequently mixed with a range of spectral frequencies, but over a very narrow range of 1 – 3 s periods. Clearly, further research is required in this area to see if there are differences in the ratios that appear due to different sampling rates and wave spectrums. Nevertheless, it is possible to draw a few conclusions from these comparisons. The most useful parameters from this list are arguably the H_{max} and $H_{1/10}$ ratios. In management situations it is often the largest waves that need to be taken into account and having a simple equality such as this proves extremely useful. Fortunately, these ratios appear to provide the most reliable estimates. The $H_{1/10}$ ratio from this study agrees with both theory and empirical studies from ocean and lake waves. The H_{max} ratio appears to be higher for lake waves than for ocean waves. Data from the present study data and from Allan (1998) suggests that the maximum wave heights that might reasonably be expected to occur in lakes, is close to twice the significant wave height.

Table 4.7 Statistical ratios between different wave height parameters.

	H_{\max}/H_s	H_{10}/H_s	H_{rms}/H_s	\overline{H}/H_s
Longuet-Higgins (1952) theoretical values for a narrow spectrum	1.53-1.85	1.27	0.71	0.63
Pickrill (1976), wave gauge Lakes Manapouri & Te Anau, n = 46	1.45	---	---	---
Hastie (1985), pressure sensor Timaru, mixed sand and gravel coastline n = 3728. 10 min sample @ 2 hr	1.56	1.22	0.70	0.62
Allan & Kirk (2000), wave gauge Lake Dunstan. n = 53. 18 min sample @ 1 hr	1.84	1.27	0.58	0.61
Dawe (present study), wave gauge Lake Coleridge. n = 493. 18 min sample @ 1 hr	2.07	1.33	1.17	0.51
Dawe (present study), pressure sensor Lake Coleridge. n = 493. 18 min sample @ 1 hr	1.63	---	---	0.80

4.6 Wave Length and Steepness

The deep water wave length can be approximated with the following equation derived from linear wave theory:

$$L_o = \frac{gT^2}{2\pi} \quad (4.7)$$

Where T is the deep water wave period. The wave lengths were calculated using the zero-crossing period with data from both the wave gauge and the S4. Figure 4.12 is a linear regression between the significant wave height and wave length. Similar to the relationship between the wave period and height, it shows a strong positive correlation. Again, the wave gauge data shows less variability than the S4 data. Mean wave lengths were 3.26 m, with a range of 0.77 to 6.63 m from the wave gauge data, and 6.21 m with a range of 3.06 to 11.37 m from the S4 data. It suggests that the depth of water in which waves can affect the bottom is comparatively close to shore. The depth at which sediment can be disturbed by wave activity is approximately equal to half the wave length, but net sediment transport does not generally occur until depths at least one quarter the wave length. Using the wave gauge data, this would be in water as shallow as 0.20 m and at most 1.65 m.

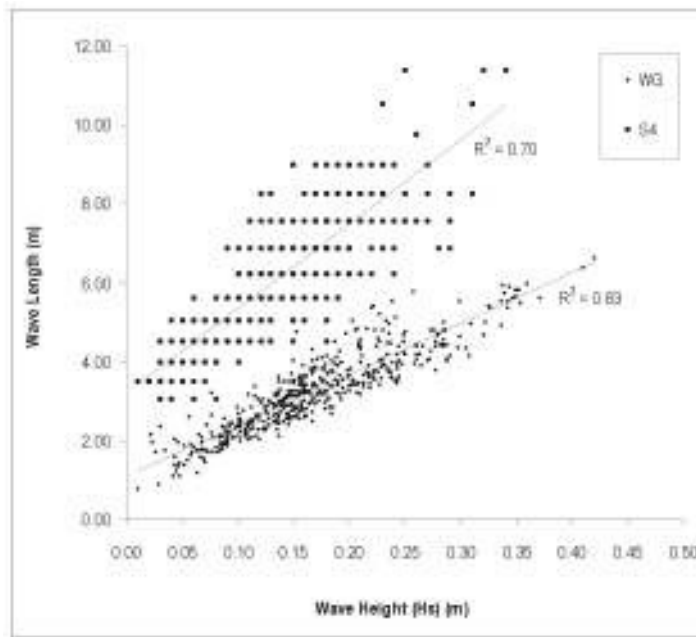


Figure 4.12 Linear regression between significant wave height and wave length calculated using the zero-crossing period.

The wave steepness is a ratio between the height and length of a wave (H/L) and provides information on the type of impact that a wave can have on a shoreline or coastal structure (Guedes Soares *et al.*, 2004). It has long been recognised that waves with a low height to length ratio, such as swell waves, tend to be depositional in nature by transporting sediment onshore and causing a beach to accrete. In contrast, steep waves tend to scour the foreshore and are more erosive in nature (Kraus *et al.*, 1991). These are the type of waves commonly associated with storm conditions. It has been noted by Pickrill (1978), Kirk & Henriques (1986) and Kirk (1988), that in general lake waves are typically steep and erosive. Table 4.8 presents a comparison of wave steepness values from Pickrill (1976), Allan (1998) and the present study, where H is the deep water significant wave height (H_s) and the wave length is calculated using the zero-crossing period (T_z). Allan calculated wave steepness ratios of 0.011 to 0.077 with a mean value of 0.036 for Lake Dunstan, using wave gauge and pressure sensor data sampling at 2 Hz (0.5 s). Pickrill found very similar results from Lakes Manapouri and Te Anau using a wave gauge and sampling at 3.3 Hz (3.0 s). Wave steepness values for Lake Coleridge were calculated by Worthington (1989) from visual estimates of wave height and length and were found to range from 0.01 to 0.08. For the present study, steepness values were calculated using the wave gauge data, that was sampled at 10 Hz (0.1 s). Values ranged from 0.010 to 0.074 with an average of 0.051. The mean value from Lake Coleridge is probably higher due to the faster sampling rate of the wave gauge

detecting more high frequency waves. The average wave steepness value calculated with the data from the S4 is 0.022, owing to the lower wave heights and longer periods measured with the instrument. This is more in line with the findings of Allan and Pickrill and again highlights differences between water surface and a water pressure records. Notably, regardless of the differences in sampling rates and methodologies, the wave steepness range remains the same across all the studies mentioned above, with an upper limit of around 0.077.

Table 4.8 Comparison of wave steepness values for quantitative wave data collected from New Zealand lakes. In all three studies, the steepness was calculated as a ratio of the significant wave height over the zero-crossing wave period.

Wave Steepness (H/L)	Min	Max	Mean
Pickrill (1976) (WG, 3.3 Hz)	0.012	0.077	0.031
Allan (1998) (WG + S4, 2 Hz)	0.011	0.077	0.036
Dawe (present study) (WG, 10 Hz)	0.010	0.074	0.051

Analysis of ocean wave records reveals that the average steepness of wind-driven storm waves is 0.025 (Holman, 1986; Guedes Soares *et al.*, 2004). Clearly, lake waves are capable of obtaining far greater steepness than ocean wind-waves and is probably related to the limited range of short wave periods that develop in restricted fetch environments. These extreme steepness values make an interesting comparison to ocean waves. Stansell *et al.*, (2003) found a clear relationship between increasing wave steepness and wave height for ocean wind-waves. Figure 4.13 shows the relationship between the root mean square wave height and wave steepness for Lake Coleridge. It reveals a strong positive logarithmic relationship with increasing wave height ($r^2 = 0.78$). Wave steepness values increase rapidly up to 0.045 at wave heights of around 0.10 m, after which, every 0.10 m increase in wave height (up to 0.5 m) corresponds approximately to a further 0.010 increase in wave steepness. The theoretical limiting wave steepness for deep water waves has been well established as being, $H_o/L_o = 0.142$ (Komar, 1998). Using the equation for the line, this limiting steepness would not be reached until wave heights achieved 10.0 m, an obvious impossibility in a small lake environment. In reality, limiting deep water wave steepness is found to be considerably less. Kirk (1970) noted that for short period waves the limiting steepness is around 0.076. The data for South Island lakes presented in Table 4.8 for deep water significant wave heights appear to support this limit. However, it is important to recognise that deep water wave steepness values vary slightly depending on the wave

parameters used in the calculation. For example, the maximum wave steepness calculated from the deep water root mean square wave height in Figure 4.13 is 0.090. The bulk of the values are below 0.076, but there are a few points above this threshold that correspond to the largest waves in the record.

Compared to ocean waves, the height that lake waves develop in relation to their lengths and periods appears to be out of proportion. This observation provides some insight into the mechanisms of wave development. It will be recalled from Figure 4.6, that lake waves develop height very quickly in relation to wind strength. It can now be seen that this rapid growth in height is also coupled with an equally rapid increase in wave steepness (Figure 4.13). This suggests that in wave generation, the height of the wave develops more quickly than the period. Following the initial wind energy input, the waves begin to propagate across the water and develop a periodicity with time and distance.

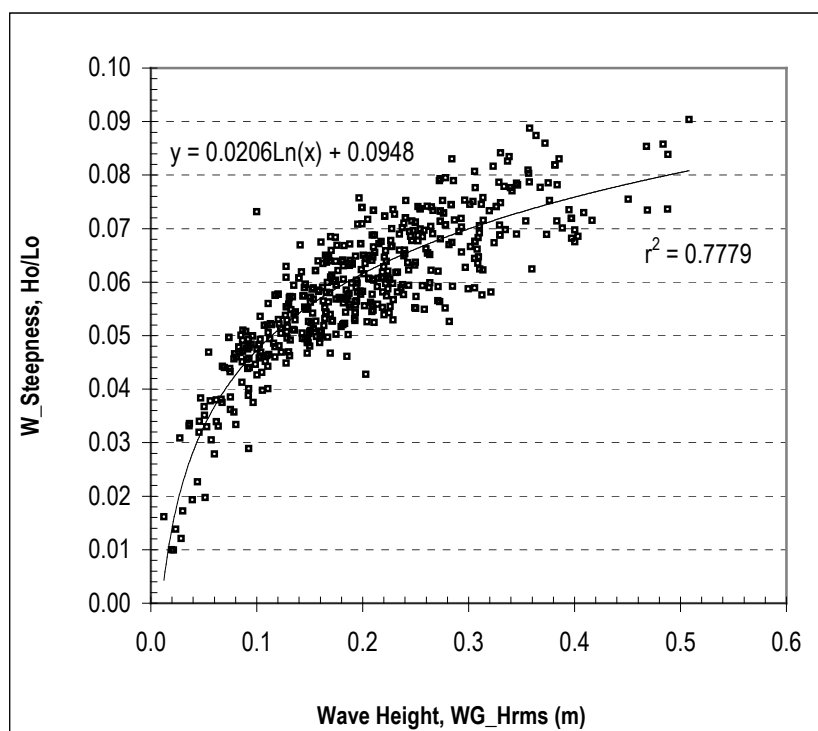


Figure 4.13 Regression of significant wave height against wave steepness showing a positive logarithmic relationship.

4.7 Waves In the Nearshore

Current Speeds

The characteristics of the deep water wave influence the changes that a wave experiences as it enters the nearshore zone. As a wave begins to shoal, the wave length shortens and the height increases, causing the wave to steepen and eventually break. Throughout this process, linear wave theory predicts that the wave period remains the same. To achieve this, the wave velocity must decelerate in order to satisfy the law of conservation of energy. Wave celerity or phase velocity in deep water (C_o) is derived from linear wave theory with the equation:

$$C_o = \frac{gT}{2\pi} \quad (4.8)$$

The shallow water approximation (C_s) is given as:

$$C_s = \sqrt{gh} \quad (4.9)$$

Where h is the depth of water defined as shallow relative to the wave length or at a some incremental point. Using these equations, the deep water wave velocities over the field programme range from 1.10 to 3.22 m s⁻¹, with a mean of 2.23 m s⁻¹. The shallow water velocities range from 0.62 to 1.80 m s⁻¹, with a mean of 1.25 m s⁻¹. When calculated as a ratio, this is a reduction in wave speed of just under one half the deep water value ($C_s / C_o = 0.56$).

Field studies have revealed differences between the theoretical predictions of phase velocity and actual measured rates (Thornton & Guza, 1982). Although the calculated velocities introduced above are approximated from the wave period, they cannot be entirely validated because surface measurements of wave velocity were not made. However, measurements were made of currents beneath the surface with the S4 in deep water and a Marsh-McBirney current meter in the nearshore zone. In effect, this provided measurements of the horizontal orbital velocity (u). Both sensors were positioned at approximately one third the distance above the bed relative to the water depth (*i.e.* $d = h/0.3$). The mean velocities recorded by the S4 ranged from 0.03 to 1.37 m s⁻¹ with a mean of 0.30 m s⁻¹. On average this worked out to be 10 times less than the calculated wave phase velocity. The current speeds measured in the nearshore zone ranged from 0.01 to 0.64 m s⁻¹ with a mean of 0.15 m s⁻¹. Again, this works out to be some 10 times less on average than the estimated phase velocities at the surface. A summary of all the calculations is presented in Table 4.9. As discussed previously, it can be demonstrated with linear wave theory that there is an attenuation of the orbital velocity with distance beneath the water surface and that this effect is more pronounced in short period waves. These findings imply that the wave attenuation effects are severe in a small lake environment. The theoretical predications show a decrease in

wave phase velocity of approximately one half as the waves travel into shallow water. The ratio difference between the measured deep water orbital velocities and the nearshore orbital velocities is just under one half ($u_s/u_o = 0.58$), almost identical to the phase velocity difference. This mirrors the theoretical predications that show that the wave velocity must slow down in order to satisfy conservation of energy laws. It is felt that linear wave theory provides good approximations of the wave conditions in a small lake environment, but that it presents a significant area of further research.

Table 4.9 Summary and comparison of wave phase velocity estimates calculated from linear wave theory and measured orbital velocities from the S4 in deep water and Marsh-McBirney current meter from the nearshore zone.

	<i>Deep Water</i>		<i>Shallow Water</i>	
m s⁻¹	$C_o = \frac{gT}{2\pi}$	S4 (u_o)	$C_s = \sqrt{gh}$	Current Meter (u_s)
Mean	2.23	0.30	1.25	0.15
Min	1.10	0.03	0.62	0.01
Max	3.22	1.37	1.80	0.64

Breaker Types

Wave breaking is dependant on wave steepness and nearshore bathymetry. The relationship between these factors produces different breaker types. In a carefully controlled laboratory study, Galvin (1968) identified four breaker types and defined them as spilling, plunging, collapsing, or surging. Galvin found that the four breaker types can reasonably be characterised by a dimensionless ratio that takes into account both the wave steepness and the beach slope:

$$\frac{H_o}{L_o S^2} \quad (4.8)$$

Where H_o and L_o are the deepwater wave height and length respectively and S is the nearshore slope, given as $\tan \beta$ (β = angle of slope in degrees). Galvin also developed a shallow water version of the equation that takes into account the effects of gravity and the wave period and uses the breaker height instead of the deep water wave height:

$$\frac{H_b}{gT^2 S} \quad (4.9)$$

Where H_b is the breaker height, usually taken as the significant breaker height and T is the deep water wave period. As the output value for the two equations increases, the breaker type changes from surging toward spilling. In general it has been observed that spilling breakers occur most

commonly when waves with high steepness break on a gently sloping beach. Plunging breakers tend to be less steep than the spilling form and are more associated with swell conditions. They are most common on beaches with high slope angles. This helps explain why plunging breakers are the most commonly occurring wave types on the steep mixed sand and gravel beaches of the New Zealand coastline.

A widely used breaking criteria equation is the surf similarity or Iribarren number (ξ). First proposed by Iribarren (1938) for use in coastal engineering applications, it is a dimensionless ratio between the bottom slope and the wave steepness. It was reintroduced by Battjes (1974) who provided a rigorous physical interpretation of the parameter and demonstrated that it also provides information about the breaker type. In addition, Battjes presented a shallow water equivalent known as the breaker Iribarren (ξ_b), derived by replacing the deep water wave height with the breaker wave height (H_b):

$$\xi_o = \frac{\tan \beta}{(H_o / L_o)^{0.5}} \quad (4.10a)$$

$$\xi_b = \frac{\tan \beta}{(H_b / L_o)^{0.5}} \quad (4.10b)$$

In this scheme, as the Iribarren number increases, the breaker type changes from a spilling toward a plunging and then surging wave. Finally, Guza and Bowen (1975) and Guza and Inman (1975) modified Galvin's shallow water equation (4.9) to produce the surf scaling parameter (ε):

$$\varepsilon = \frac{H_o 2\pi}{gTS^2} \quad (4.11)$$

The inclusion of the term 2π , effectively introduces a form of radian frequency ($2\pi/T$) into the formula. As the surf scaling parameter increases, the breakers change from surging toward spilling. Table 4.10 summarises the breaker classification limits from Equations 4.8 to 4.11. The relationships in Equations 4.8-4.11 have been tested against extensive laboratory data sets, but the application of these schemes to natural beaches has been problematic. Field studies have shown that it is difficult to identify any single breaker type occurring at a given time. Rather, it is more common to see a range of breaker forms merging from one type to another. In fact, whilst much laboratory work has gone into the development and verification of these equations, it was noted by Komar (1998) that this has not been matched by field testing of them on natural beaches.

Table 4.10 Threshold limits for five commonly used breaker criteria equations (Equations 4.8-4.11).

	$H_o/(L_o S^2)$ (Eq. 4.9)	$H_b/(gST^2)$ (Eq. 4.10)	ξ_o (Eq. 4.10a)	ξ_b (Eq. 4.10b)	ϵ (Eq. 4.11)
Surging	< 0.09	< 0.003	> 3.3	> 2.0	< 2.5
Plunging	0.09-4.8	0.003-0.068	3.3-0.5	2.0-0.4	2.5-33
Spilling	> 4.8	> 0.068	< 0.5	< 0.4	> 33

In order to provide insights into the nature of breaking lake waves and in an effort to redress the lack of field testing of the breaker criteria equations, the data from Lake Coleridge was tested against the five equations discussed above. A graphical output of the results from the calculations is presented in Figure 4.14, showing data from both the wave gauge and S4. The significant wave height was used in the deep water equations and the breaker wave heights were calculated using Equation 4.12. Summary statistics can be seen in Table 4.11. There appears to be no established standard for defining which part of the beach profile the slope angles are derived from for use in the various equations. For the purposes of this study, the average slope of the nearshore zone was used in the deep water equations (Figure 4.14a, c & d). This value was a reasonably consistent 5° at all sites. For the shallow water versions (Figure 4.14b & e), this value was substituted for the average slope at the base of the swash zone (8°). In most conditions, it was observed that the swash zone formed immediately landward of the breaking wave. Thus, this angle provides the closest measurement of the slope angle under the breaking wave.

Table 4.11 Summary statistics for the breaker criteria equations presented graphically in Figure 4.14, for the wave gauge and the S4. S and P denote spilling and plunging respectively.

Wave Gauge	$H_o/(L_o S^2)$	$H_b/(gST^2)$	ξ_o	ξ_b	ϵ
Min	2.36	0.03	0.32	0.36	1.16
Max	17.32	0.17	0.87	0.81	17.13
Mean	11.83 (S)	0.12 (S)	0.40 (S)	0.43 (P)	9.61 (P)
Median	11.68	0.12	0.39	0.43	9.41
Mode	10.88	0.12	0.41	0.44	6.80
Std. Dev.	2.43	0.02	0.06	0.05	2.92
Variance	5.93	0.000	0.003	0.00	8.56

S4	$H_o/(L_o S^2)$	$H_b/(gST^2)$	ξ_o	ξ_b	ϵ
Min	0.67	0.01	0.43	0.46	0.56
Max	9.87	0.11	1.16	1.34	11.61
Mean	5.11 (P)	0.06 (P)	0.62 (P)	0.61 (P)	5.77 (P)
Median	5.21	0.06	0.59	0.59	5.89
Mode	6.13	0.07	0.54	0.55	7.21
Std. Dev.	1.54	0.02	0.12	0.10	2.07
Variance	2.36	0.000	0.02	0.01	4.28

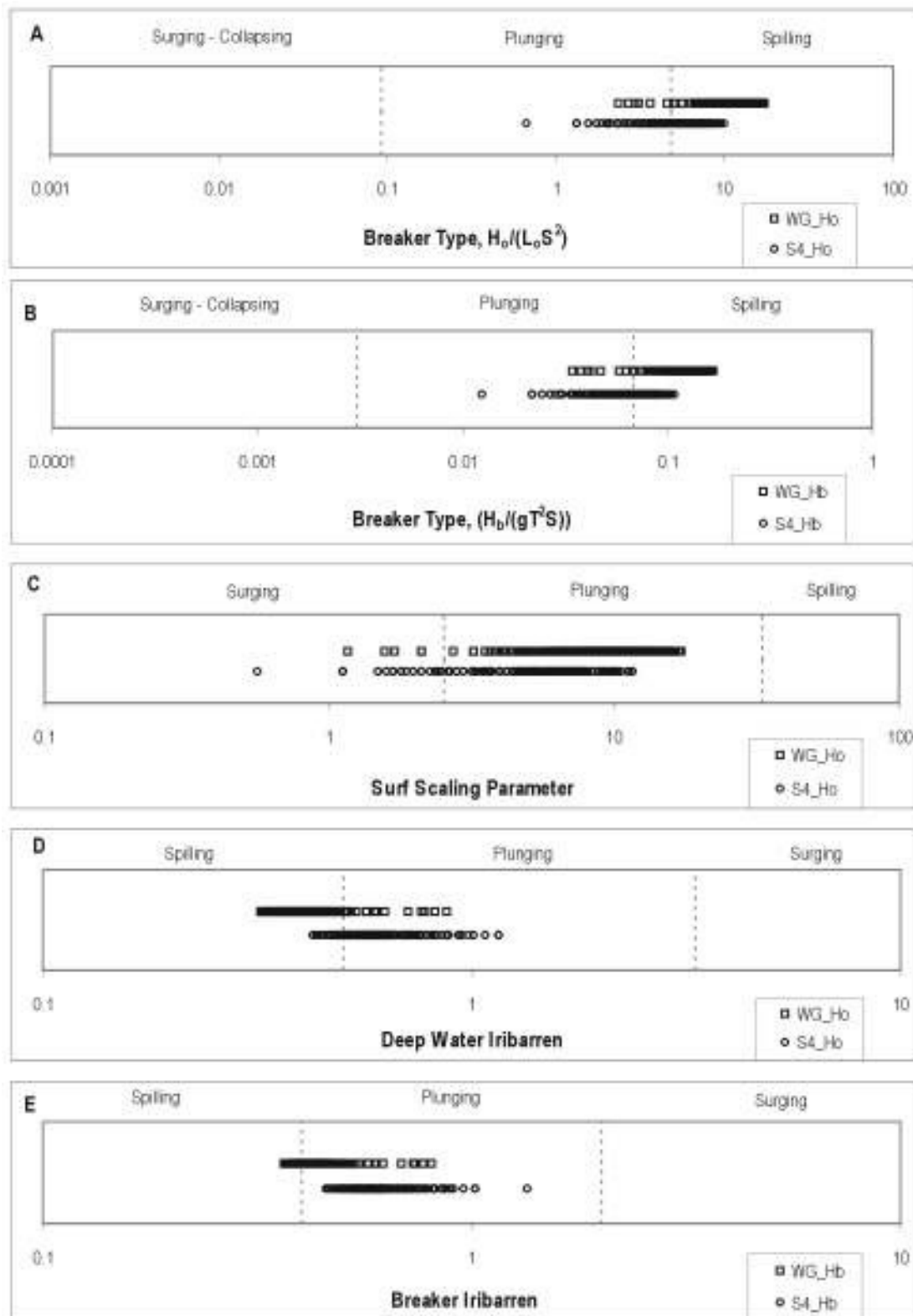


Figure 4.14 Graphical output of the results from the breaker criteria equations. From field observations, the breaker Iribarren statistics (E) derived from the wave gauge data appear to provide the closest indication of the conditions.

Visual observations of breaking waves from Lake Coleridge indicated that spilling and plunging breakers were the most commonly occurring types (Figure 4.16). At times, waves would appear as a transition between these types in a form of spilling-plunger. This transition type breaker was also observed in Lake Coleridge by Worthington (1989). The breaker type calculations confirm the visual observations. There is a reasonably equal proportion of plunging and spilling breaker types across the full range of conditions. The surging or collapsing type breaker was rarely observed in Lake Coleridge and this is supported by four of the five equations. There is a broad degree of agreement between all of the equations, especially between the deep water equation of Galvin (1968) (Figure 4.14a) and the Iribarren equation of Battjes (1974) (Figure 4.14d). The results of the surf scaling calculations (Equation 4.11) suggested that most waves were of the plunging to surging type and that spilling waves rarely occurred. This does not match observation. The data from the S4 suggest that plunging waves are more common than spilling waves. In contrast, the data from the wave gauge indicated a greater incidence of spilling breakers. This is because the wave gauge sampling at 10 Hz measured greater wave heights and steepness's than the S4, thereby increasing the value of the ratios. The wave gauge is probably a more accurate representation of the water conditions. Allan (1988) used Equation 4.9 to calculate the breaker types measured at Lake Dunstan with data sampled at 2 Hz and found that plunging breakers were the most commonly occurring type (Figure 4.15). However, Allan commented that spilling breakers were frequently observed.

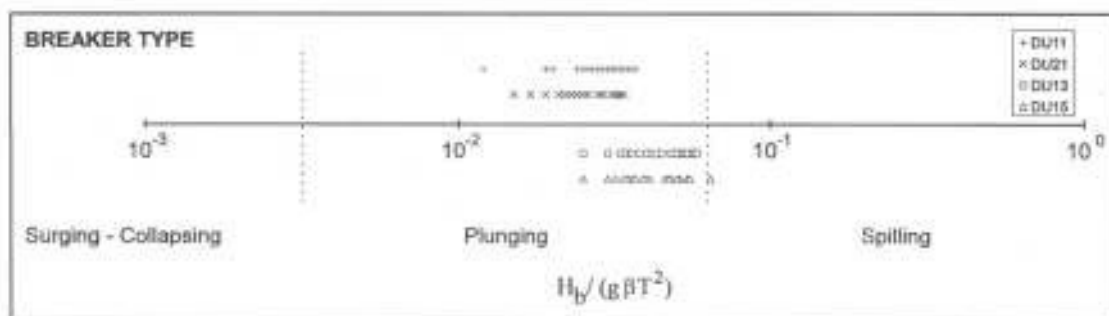


Figure 4.15 Breaker types estimated from Lake Dunstan using Equation 4.9. The data was collected by wave gauge and S4 sampling at 2 Hz. $n = 164$. (From: Allan, 1998: 172).

It is felt that the Iribarren parameters provide the best indication of the breaker types that occurred in Lake Coleridge. There was little difference in the results between the deep and shallow water equations of Galvin (1968). It was found that these equations had a low sensitivity to changes in slope. Observations from Lake Coleridge suggest that low amplitude waves are sensitive to small, localised changes in beach slope and the transition from deep to shallow water conditions is both spatially and temporally rapid. Galvin's equations were not able to properly respond to these changes. The deep water Iribarren number indicates that waves measured by the wave gauge would spill upon breaking owing to their steepness (Figure 4.14d). However, the shallow water Iribarren values show a higher incidence of plunging waves (Figure 4.14e). It is felt that this illustrates the changes that small amplitude lake waves undergo as they travel from deep water into shallow water, before they shoal and break. In deep water the generally high steepness values of the waves suggest that they will be of the spilling variety. As the waves approach the shoreline, there is often a rapid increase in beach slope, which induces the waves to plunge. This accounts for the higher number of plunging waves calculated with the shallow water Iribarren number when compared to the deep water values.

There is a correlation between wave height and breaker type, in that, spilling breakers are more commonly associated with high energy conditions (Figure 4.16b). The reason for this is twofold. First, spilling waves are the steepest of the breaker types. Figures 4.12 and 4.13 illustrated that as waves grow in height, there is an associated increase in wave length and steepness. This promotes the development of a spilling breaker. Secondly, the increase in wave height encourages waves to break in deeper water where the slope angles are lower, leading to a more spilling type wave. This is not to say that plunging waves do not occur in high energy conditions. In contrast, it has been observed that at low wave heights, breakers tend to be of the plunging form. At low wave heights waves are able to progress very close to the water line before breaking. This is also the point of maximum beach slope and induces the wave to plunge (Figure 4.16a). Low amplitude waves generally have a low steepness and this coupled with their ability to enter very shallow water means that in light conditions, waves are often of the plunging type. This fact is of great significance as it has implications for sediment transport. Kirk (1970) noted that on a mixed sand and gravel beach, the water in a plunging breaker is accelerated to great velocities as the lip curls over and is translated into swash. This highly turbulent process enables large quantities of sediment to be entrained in the swash zone. The implications of this will be explored in greater detail in the following chapter. Suffice to say, small plunging breakers are capable of entraining more sediment than might intuitively be expected for low amplitude waves.



Figure 4.16 The main breaker types witnessed in Lake Coleridge, plunging (a) and spilling (b). Plunging breakers were most the commonly observed breaker type and occurred in all conditions. Spilling breakers were generally associated with high energy conditions.

Breaker Height and Depth

There was no quantitative measurement of breaker heights in the field programme at Lake Coleridge. Consequently, the breaker heights in Equation 4.9 and 4.10b were calculated with a semi-empirical equation developed by Komar and Gaughan (1972):

$$H_b = 0.39g^{0.2}(TH_o^2)^{0.4} \quad (4.12)$$

This formula was derived from linear wave theory and was tested against both laboratory and field data. It has been found to show good agreement with natural waves. Breaker heights were

calculated using the significant wave height from both the wave gauge and S4. The exceedence curves can be seen in Figure 4.17. The equation appears to provide reasonable estimates of the breaker height when compared to field observations. Mean breaker heights from the wave gauge were 0.37 m with a maximum of 0.87 m. Interestingly, despite the differences between the wave gauge and S4, the mean breaker height calculated with the S4 data was 0.36 m, with a maximum 0.82 m.

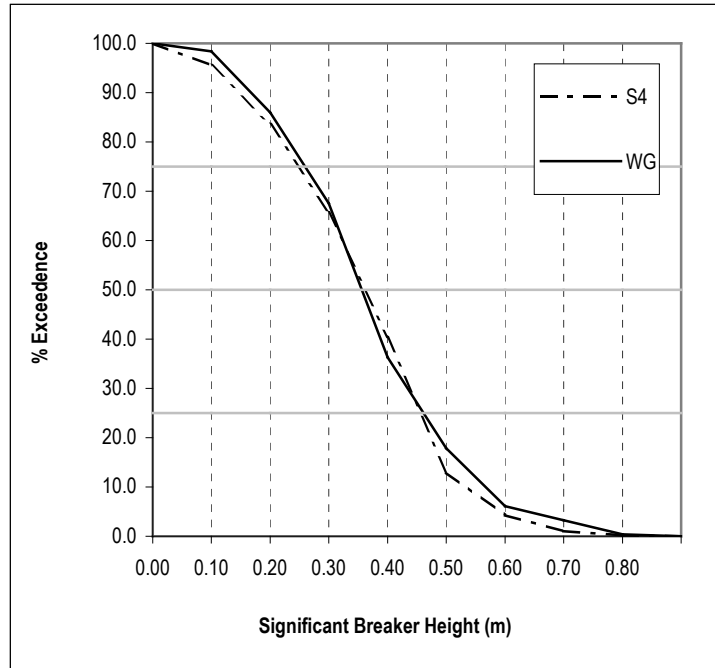


Figure 4.17 Percentage exceedence curves for breaker heights derived with Equation 4.12. The results provide good estimates of breaker conditions in the field.

Once the breaker height is known, it is then possible to calculate the depth of water at the break point with the critical breaking ratio, $\gamma_b = H_b/h_b$. A widely used theoretical value for the ratio of 0.78 was derived from solitary wave theory by Munk (1949), but empirical values were found to range from 0.73-1.03. With subsequent work showing a reliance of wave breaking on the wave steepness and beach slope, an empirical derivation based on a large data set was presented by Kaminsky and Kraus (1993) that used the deep water Iribarren number:

$$\gamma_b = 1.20\xi_o^{0.27} \quad (4.13)$$

The mean values for the ratio from the Lake Coleridge data were found to be 0.93 for the wave gauge and 1.05 for the S4. Rearranging Equation 4.13 and using the breaker height from

Equation 4.12, yields breaking depths ranging from 0.03 to 0.79 m with a mean of 0.34 m for the wave gauge and similar values for the S4 data, 0.04 to 0.82 m with a mean of 0.37 m. This indicates that that waves break in water depths approximately equal to the wave height. Whilst no quantitative measurements of the breaking depth were made, the water depth at the various instruments in the field was monitored daily. The depth of the nearshore Marsh-McBirney current meter was maintained in 0.5 m of water, which on average was 5-6 from the shore. In most conditions, waves broke landward of this sensor. Figure 4.18 shows the frequency distribution of breaking depths from the wave gauge data. It can be seen that 88% of the waves broke in water depths less than 0.5 m and 54% broke in depths less than the mean value of 0.34 m. This is another indication of how close to shore waves in these systems are able to approach before breaking. In high energy conditions waves were observed breaking immediately lakeward of the sensor, in water depths of 0.6-0.7 m. These observations agree closely with the derived estimates, suggesting that with good quality data these two equations (4.12 & 4.13) may be used in a small lake environment. Part of this utility stems from the fact that low amplitude laboratory wave data was used in the development of the equations.

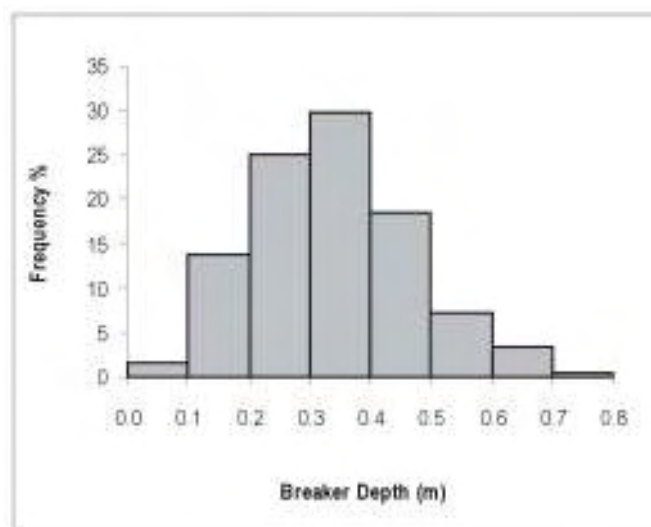


Figure 4.18 Frequency distribution of breaker depths calculating using Equations 4.12 and 4.13.

Wave Direction and Refraction

When waves approach a shoreline at an oblique angle and ‘feel’ the bottom of the lake or seabed, they begin to refract in response to the bathymetry. As the leading edge of a wave enters shallow water, it slows down, whilst the trailing edge remains relatively faster in deeper water. In this way, waves are refracted into a shoreline and the deep water wave angles lessen. This process can efficiently cause wave crests to approach parallel to a shoreline. As discussed in Chapter One, obliquely angled waves initiate longshore transport of sediment. On an open coast beach this process may begin a considerable distance from the shoreline, especially on gently sloping sandy beaches. Thus, rates of longshore sediment transport may be reduced in locations where there is strong wave refraction. Wave modification on a mixed sand and gravel beach is less pronounced, due to the presence of deep water close to shore (Kirk, 1980). On a lake shoreline this effect is more pronounced because low amplitude waves do not ‘feel’ the bottom until close to the beach toe. Figure 4.19 presents the wave directions measured by the S4 in deep water (A) and the those measured by the current meter in the nearshore area (B). In general it can be seen that the wave angles are very oblique and approach the shoreline at very high angles. This is a reflection of the topographic channelling of the wind down the long axis of Lake Coleridge, as discussed in Chapter Two. As the wind speed and wave height increase, the wave angles generally became more oblique to the shoreline. The most acute angles, those under 20° , were usually associated with low amplitude waves in light conditions.

Essentially, the beaches along the axial shores of the Lake experience waves with crests almost at right angles to the shoreline. It can be seen that some 18% of waves recorded by the S4 were between 80° - 90° . Eighty percent of wave directions measured by both instruments are over 40° . Only a small degree of wave refraction occurs from deep water to shallow water. The average deep water wave direction measured by the S4 was 60° . Whilst the mean angle measured by the nearshore current meter was a mere five degrees less, at 55° . The most significant change occurs in the wave angles between 80° - 90° . By the nearshore, less than 0.5% of waves were at angles over 80° . This can be seen by the increase in the number of waves between 60° - 70° in the nearshore; 33%, up from the 16% measured in deep water. This accounts for the 18% of waves measured from directions over 80° in deep water. In general, there is a slight shift to the left (toward more acute angles) in the distributions from deep water to shallow water. The wave refraction continues to the point of breaking. The onshore water flow directions measured by the current meter in the swash zone are presented in Figure 4.20. These measurements are a de facto measure of the breaker angle. It can be seen that there is further slight shift in the directions to

the left. The average breaker angle was 50° , a further 5° less than the mean wave angle measured in the nearshore.

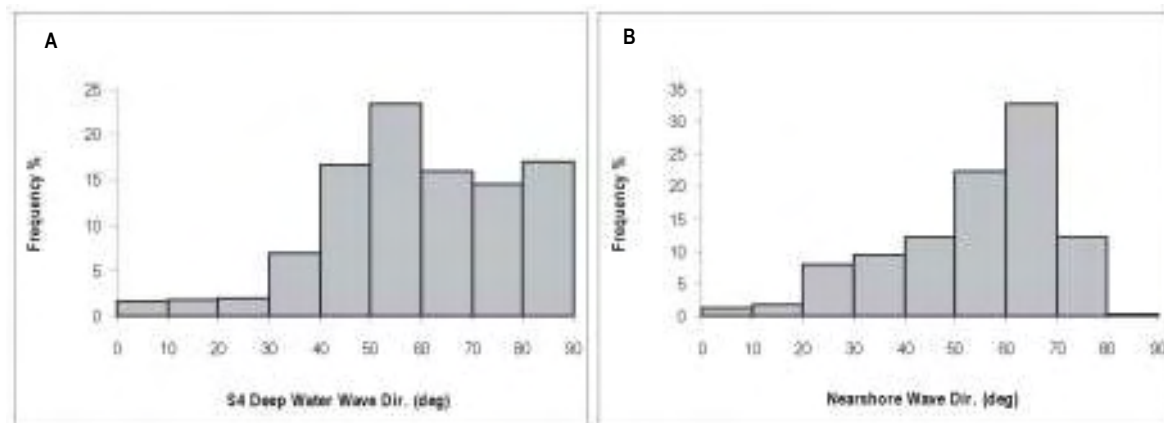


Figure 4.19 Wave directions measured with the S4 in deep water (A) and the nearshore current meter (B).

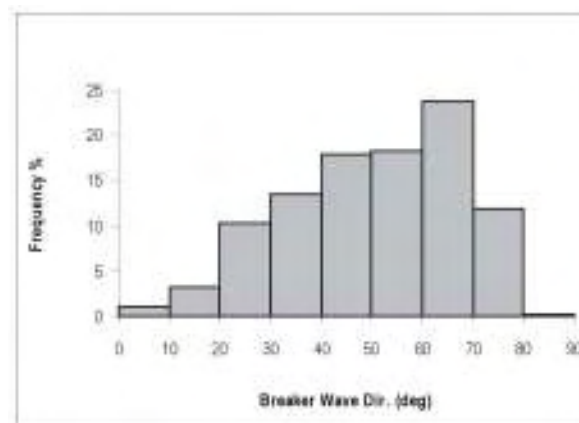


Figure 4.20 Breaker angles measured with the swash zone current meter.

4.8 Summary

This chapter has presented the results and provided a discussion and analysis of the deep water wave measurements from Lake Coleridge. Previous workers have had to rely on visual observations and apply a knowledge of oceanic wave characteristics to lacustrine studies. In only one previous study, Allan (1998), has any significant wave data been collected and analysed from a New Zealand lake. This study represents the single largest collection of high quality wave data for a New Zealand alpine lake and important insights have been made into lake wave processes. It is hoped the findings presented here will further an understanding of New Zealand's alpine lakes. Wave data was collected with two instruments, a bottom mounted pressure sensor sampling at 0.5s and a capacitance wave gauge sampling at 0.1s. The measurement of lake

waves at a 0.1 s sampling rate in New Zealand has not previously been reported in the literature and some points of difference were found between the results produced by the two instruments. Overall there was good correlation between the data measured with the respective instruments. However, there were differences in the magnitude between the data sets that caused concern. It was argued that these differences were due to two main factors. The first of these owes to the rapid attenuation of wave energy that occurs under high frequency lake waves. This limits the pressure fluctuations able to be detected by the S4. The second factor was due to the difference in sampling rates. It was demonstrated that the wave gauge detected a wider spectral range of high frequency waves than the S4.

The raw wave data was analysed with two commonly used methods for calculating wave height and period statistics. The S4 data were analysed with a custom software package employing the spectral analysis method, whilst the wave gauge data were analysed using the zero-crossing method in spreadsheet format. The Marsh-McBirney current meter data were also processed in spreadsheet format. In total, 493 hours of concurrent time series data from the S4, wave gauge and Marsh-McBirney current meters was available for modelling. The root mean square wave heights averaged 0.20 and ranged up to 0.51 m. Maximum wave heights averaged 0.35 m and ranged up to 0.84 m. All the wave height data sets were positively skewed, indicating the presence of extreme waves in the tail of the distribution. Although the wave heights at Lake Coleridge are moderate in size, they are of the same order of magnitude to those found in other New Zealand lakes. Fetch distances for the fieldsite ranged from 3.0 to 9.0 km. Wave height was found to be strongly linked to wind and responded rapidly to increasing wind strength in an exponential fashion.

Wave period was slower to respond to the wind, requiring time and distance for the wave length to develop. Overall, the data showed there was a narrow band of wave periods measured in Lake Coleridge, with means ranging from 1.43 to 2.33 s. All wave period distributions were negatively skewed, indicating the presence of many short period waves in the frequency spectrum. The wave spectrum was found to be more mixed and complicated than had previously been assumed for lake environments. Some authors have argued that because the range of wave periods experienced in lake is narrow, the wave spectrum should attain characteristics seen in ocean swell waves. However, the spectral band widths were found high (mean 0.84), indicating the presence of a wide range of periods relative to the mean, *i.e.* the data set was platykurtic. Mean wave lengths were 3.26 m, but ranged from 0.77 to 6.63 m. Using Linear wave theory, this suggested that the depth of water in which waves can affect the bottom is as shallow as 0.20 m

and at most 1.65 m. The waves were characteristically steep and it was shown that in a lake environment waves are capable of obtaining far greater steepness than ocean wind-waves. This suggested that lake waves are typically erosive in nature.

The deep water wave velocities were calculated with Linear wave theory and ranged over the field programme from 1.10 to 3.22 m s⁻¹, with a mean of 2.23 m s⁻¹. The shallow water velocities ranged from 0.62 to 1.80 m s⁻¹, with a mean of 1.25 m s⁻¹. When calculated as a ratio, this is a reduction in wave speed of just under one half the deep water value ($C_s / C_o = 0.56$). Deep water and nearshore current velocities were measured by the S4 and a Marsh-McBirney current meter. Both instruments were positioned in water approximately one third the distance above the bed relative to the water depth. The mean velocities recorded by the S4 ranged from 0.03 to 1.37 m s⁻¹ with a mean of 0.30 m s⁻¹. On average this was *ca.* 10 times less than the calculated wave phase velocity. The current speeds measured in the nearshore zone ranged from 0.01 to 0.64 m s⁻¹ with a mean of 0.15 m s⁻¹. This is also *ca.* 10 times less on average than the estimated phase velocities at the surface. The ratio difference between the measured deep water orbital velocities and the nearshore orbital velocities was just under one half ($u_s / u_o = 0.58$), almost identical to the predicted phase velocity difference. It was argued that this mirrors the theoretical predications indicating that wave velocity must slow in shallow water in order to satisfy conservation of energy laws. It was concluded that Linear Wave Theory provides good approximations of the wave conditions in a small lake environment. The findings also imply that wave attenuation effects are severe in a small lake environment.

Waves were found to progress very close to shore before breaking, typically in water less than 0.5 m deep. The two main breaker types observed in Lake Coleridge were spilling and plunging. This was confirmed by numerically with five breaker criteria equations. Due to the steep nature of lake waves, the deep water equations indicated a roughly equal number of spilling and plunging waves. However, the rapid increases in beach slope often caused the waves to plunge at the beach toe, leading to a greater proportion of plunging waves at the shoreline. Finally, it was shown that the deep water wave angles are generally very oblique to the shoreline and that wave refraction by waves entering shallow water is only in the order of 10%.

Upon wave breaking, the water is translated into swash and a new set of processes take over, requiring different models to understand the current flow properties. The swash zone characteristics will be examined in the next chapter.

CHAPTER 5.

SWASH ZONE PROCESSES

*“Who shut in the sea with doors, When it burst forth, When I said,
‘This far you may come, but no further, Here your proud waves must stop!’”*

Job 38:8,11

5.1 Introduction

When a wave reaches a limiting depth of water, it over-steepens and breaks under the influence of gravity. In a beach that has a wide, low sloping nearshore this process happens some distance from the beach face and the wave is dissipated as a series of bores across the surf zone. In this situation, the surf zone is the area of greatest energy saturation (Raubenheimer & Guza, 1996). It has been seen that in a low energy lake environment, small amplitude waves are able to approach very close to the shoreline before breaking. In Lake Coleridge wave breaking usually occurs within 5.0 m of the shoreline in water depths of less than 0.5 m. Compared to a wide dissipative beach, the wave energy is concentrated over a very narrow range at the point of breaking and the area immediately landward of this, which in most conditions is usually the swash zone.

The swash zone can be defined as an area of foreshore which experiences intermittent exposure to the atmosphere for short periods of time, from seconds to minutes, due to wave run-up (swash) and run-down (backswash) around the mean water level, excluding wind and/or wave set-up effects (Elfrink & Baldock, 2002; Holman, 1986). On low sloped beaches it can be difficult to identify the swash zone because there is a constant fluctuation between the inner surf zone and the swash zone in response to varying wave conditions. In fact, it was noted by Elfrink and Baldock (2002) that some of the research ascribed to the swash zone, in fact relates to the inner surf zone. However, it will be recalled from Chapter One that on a steep beach this area is generally spatially well defined. In the mixed sand and gravel beaches of the New Zealand coastline, the surf-swash zone boundary is characterised by a single breaker that translates directly into swash at the break-point step. The same process occurs in the low energy mixed sand and gravel beaches around Lake Coleridge. Thus, the swash zone determines the landward and lakeward boundary of the area most affected by wave action. A quantitative understanding of swash zone dynamics is essential for understanding sediment transport in a mixed sand and gravel beach.

This chapter examines the nature of the swash zone in Lake Coleridge. In particular, it looks at those aspects of the swash zone pertinent to sediment transport. Characteristics of swash zone development, swash length, run-up and swash zone currents will be discussed. A series of equations developed in this study will be introduced that provide good estimates of the run-up, swash zone width and swash current velocity. A new swash zone/foreshore process-response model is presented that illustrates the morphodynamic response of the swash zone to wave and swash activity. Throughout the analysis, the wave information collected with the wave gauge was found to provide consistently better correlations with the measured environmental data than the S4. Throughout this chapter, unless otherwise stated, the wave gauge data will be used in the regression analyses and calculations.

5.2 Swash Zone Research

The transformation of deep water waves through shoaling and translation into swash is a complex process. This complexity, coupled with the difficulty of making accurate measurements in the highly turbulent swash, has meant that research into swash zone processes has often been overlooked. However, because it forms the land-water interface, it is vital to understand the relationships between the swash zone and the foreshore and nearshore for an overall understanding of how a beach operates. It is an area of high sediment mobility where processes of erosion and accretion, run-up and overtopping all have an impact on the stability of the shoreline (Elfrink & Baldock, 2002; Holland & Puleo, 2001).

In recent years there has been a growing recognition of the need to understand the hydrodynamic and sediment transport processes that occur in this part of a beach (Butt & Russell, 2000; Elfrink & Baldock, 2002). Three main areas of investigation may be identified from the literature. The first concerns the modelling and estimation of wave run-up (Hughes, 2003; Raubenheimer & Guza, 1996; Holman, 1986). This has grown out of investigations into run-up and overtopping of engineered coastal structures (Waal & van der Meer, 1992; van der Meer & Stam, 1992). The second area is concerned with swash hydrodynamics, primarily concentrating on flow kinematics in the cross-shore direction (Erikson *et al.*, 2005; Baldock & Holmes, 1997; Holland *et al.*, 1995). An important area of this research has been in characterising the behaviour of water flow within the bore as it propagates up the beach face (Hughes, 1992). The third major research focus has been sediment transport processes, both bedload and suspended transport (Masselink & Hughes, 1998; Hughes *et al.*, 1997; Horn &

Mason, 1994). In particular, research has focussed on modelling the processes responsible for cross-shore sediment transport (Lorang, 2002; Katori *et al.*, 2001, Blewett *et al.*, 2000). There has been very little work into longshore transfers of water or sediment in the swash zone. Much of this work has taken place in laboratory wave flumes, but it has been found that there are processes that occur in natural beaches important in driving swash oscillations that are not easily replicated in the laboratory, such as edge waves.

It is now recognised that there are two distinct, yet not necessarily independent, processes responsible for controlling swash motion. Low frequency infra-gravity water motions, such as non-breaking standing waves and broken short wave bores that reform through the inner surf zone and collapse at the shoreline (Erikson *et al.*, 2005). Clearly this categorisation overlooks the situation in steep beaches, which as described previously, have a swash zone that is characterised by a single breaker in normal conditions, that translates directly into swash at the break point step. The swash in these beaches is driven primarily by the breaking incident wave (Butt & Russell, 2000; Kirk, 1970). This is not to say that the internal swash flow kinematics are any less complex, only there are less complicated interactions between the forcing mechanisms and the swash flow because it results from fewer environmental variables. Little research has been conducted into the swash zone of gravel beaches, largely due to the difficulties of making any measurements from this severely turbulent area. The most significant swash zone research on New Zealand's mixed sand and gravel beaches was conducted by Kirk (1970; 1975) from the beaches of Kaikoura. To the knowledge of the author there have been no quantitative studies of the swash zone conducted on New Zealand's lake shore beaches.

5.3 Swash Zone Width and Run-up Length

As noted above, there are several reasons for studying swash zone processes in mixed sand and gravel beaches. These factors apply equally to lake shore beaches, without the need to factor in corrections due to tidal translation. The swash zone boundary is clearly defined, making measurements of swash lengths and run-up heights accurate. In this way high quality correlations can be made with other measured environmental parameters. Furthermore, it is not necessary to model the complex interactions resulting from nearshore infra-gravity wave energy or reformed short wave bores. Infra-gravity wave motion was not detected during the course of the field measurements. The forcing mechanisms are simpler, relying solely on the breaking incident wave.

Throughout the field programme the width of the swash zone was measured hourly to an accuracy of 0.10 m. The width was measured with a rigid staff from the base of the breaking wave up to the mean maximum horizontal swash excursion limit, i.e. the area that experienced regular wetting from swash activity. The average was taken over a one minute period during which time there were typically around 30 swash advances. From observations it was estimated that this limit was reached by approximately 5-10% of the swash and that it was exceeded by 1-2% of all swash motions. In effect, this is a measure of the 2% exceedence limit or the critical swash length. In addition, the average slope of the swash zone was measured with an Abney Level to within 0.5° . The angle was taken by placing the level on a 1.5 m straight edge measuring staff that was laid horizontally in the middle of the swash zone. In this way localised variations were smoothed over and an average representative value for the slope was derived. Swash zone widths ranged from 0.05 m to 6.00 m, with a mean of 2.00 m (Figure 5.1). It can be seen from Figure 5.1 that the data are positively skewed (0.51) and platykurtic (-0.38) with a tail of swash widths above 4.0 m. The slope angles ranged from 3.0 to 20.0° , averaging 8.0° . A summary of the hourly swash widths and slope angles is presented in Appendix 6.

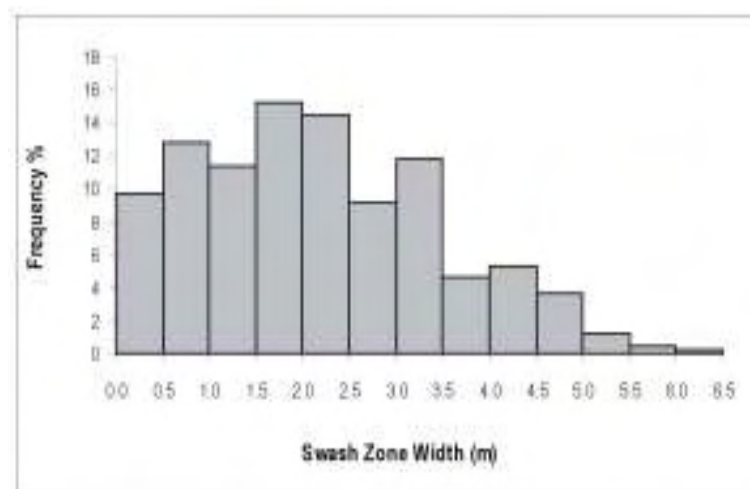


Figure 5.1 Frequency distribution of the measured swash zone widths showing a positively skewed distribution.

A multiple regression analysis was conducted against the swash width data. The correlation matrix can be seen in Table 5.1. Wave height was found to be responsible for the greatest variability, indicating that it exerts a primary control on the width of the swash zone. There is a strong positive relationship ($r = 0.91$) between increasing wave height and a widening of the swash zone (Figure 5.2). The strength of this relationship explains the skewness seen in Figure

5.1. Essentially it is a reflection of the distribution of wave heights. It will be recalled from the wave height distribution graphs (Figure 4.4) that there was a tail of high waves causing a positively skewed distribution. The waves in this tail were responsible for widest measured swash zones. The second important control was the slope of the swash zone ($r = -0.86$), which exhibits a negative relationship. This indicates that when the swash zone is wide, it attains a low gradient, whilst a narrow swash zone will generally be steep sloped. The wave period is closely related to the wave height and consequently the swash zone widens in response to increasing period ($r = 0.80$). The wave steepness was also included in the regression. The strength of the H_o/L_o correlation ($r = 0.85$), is a reflection of the wave height and period, but it indicates that the swash zone widens in conjunction with steepening waves. These correlations compare similarly with measurements from other mixed sand and gravel beaches. From careful measurements of the swash zone in the beaches at Kaikoura, Kirk (1975: Fig. 2) found a strong positive relationship between swash length and breaker height ($r = 0.82$). Worthington (1989) made measurements of swash widths from three beaches at the southern end of Lake Coleridge and compared the results to visual observations of the significant wave height. Worthington found a positive correlation at all sites with coefficients ranging from $r = 0.69$ to 0.91 and an average of $r = 0.77$.

Table 5.1 Regression coefficients of swash zone width (X_{sw}) against four other environmental parameters. The strongest correlation is found with H_{rms} .

X_{sw}	H_{rms}	β	T_z	H_o/L_o
r	0.91	-0.86	0.80	0.85
r^2_s	0.83	0.74	0.64	0.72
Std. Error	0.10	0.08	0.04	0.06
Prob.	< 0.0001	< 0.0001	< 0.0001	< 0.0001

It will be noticed that Figure 5.2 is a log-log plot and employs a logarithmic scale on both the ordinate and abscissa axes. When the residuals of the linear regression were plotted, the data exhibited heteroscedasticity, characterised by a fan shaped pattern in the residual scatter plot. It is a characteristic often displayed by positively skewed distributions. In other words, the variance in the data sets is multiplicative rather than additive and a linear model does not properly describe the data (Wild & Seber, 2000). This is indicative of the way in which small increases in wave energy often have measurably large impacts on the shoreline. In this situation it is valid to apply a logarithmic transformation to the data to try and achieve homoscedasticity, thereby

allowing a linear regression to be conducted (Zar, 1984). When the data were log-transformed the plotted residuals displayed a random pattern, indicating that the data were homoscedastic, and a linear regression was possible.

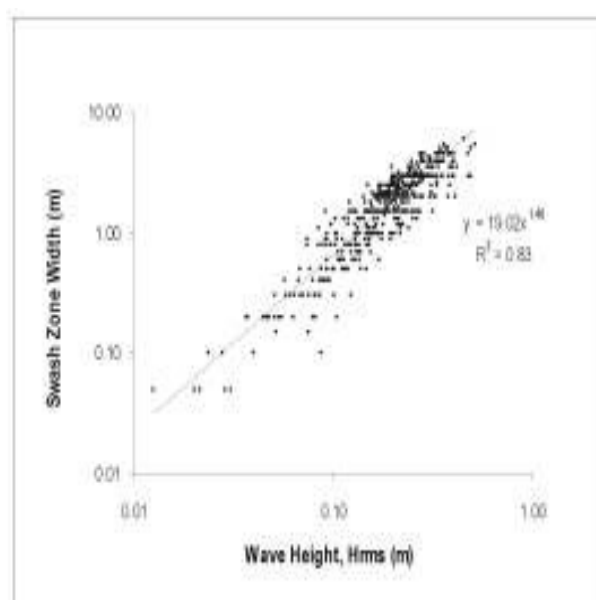


Figure 5.2 Linear regression between wave height and the width of the swash zone. $r = 0.91$, Std. Error = 0.10, $F = 2416$.

The regression analysis provides important insights into the nature of lakeshore swash zones. A notable difference between an open coast beach and a sheltered inland or lakeshore beach is that, in an open coast situation there is almost always wave energy being dissipated through wave breaking. There is always a discernable width to the surf or swash zone, even in light conditions. This is not the case on a low energy or lake shoreline where there may be sustained periods of little or no wave activity. As such, there is a time zero ($t = 0$) prior to the onset of wave activity when various environmental parameters also have a zero value such as; wave period and height, nearshore and swash zone current velocity, swash zone width, run-up height and length. The only exception to this is the beach slope at the water line, which often sits at angles approaching the repose of the sediment. In the beaches at the fieldsite this was around 20° . At the onset of wave activity the foreshore begins to develop a new equilibrium with the conditions, a process that may take a number of hours depending of the strength of the conditions. When the wave activity drops or ceases, a new equilibrium must be found. These changes in equilibrium stage are not as dramatic in higher energy open coast situations and this

creates differences in the relationships between certain environmental parameters, such as beach slope.

The relationship between the wave height and beach slope is illustrated in Figure 5.3, which shows a time series of four consecutive days of concurrent swash slope and wave height measurements. The wave height is shown for comparison and is not to scale. A very clear pattern can be seen between increasing wave height and decreasing beach slope. On the 6th of March, light to moderate south-easterly conditions prevailed, with mean wave heights of up to 0.16 m. At the start of the day the beach slope at the waters edge was inclined steeply at 20.0° and the wave heights were below 0.05 m. Throughout the day there was a gradual decrease in the beach slope as the wave conditions increased. Overnight, the wave activity ceased and the beach slope steepened back to 20.0°. On the 7th of March there was a change to a strong north-westerly, producing mean wave heights of up to 0.26 m. The slope quickly graded down in response to this activity. It was noted that sediment mobility and transport rates were high during these phases of swash zone development. In an overnight lull the beach steepened to 10°, but quickly scoured when the wave activity picked up again on the 8th of March. In the evening the wind eased and there was southwest change. Initially the wind was light and the beach slope was recorded at 13°, but throughout the day the wind strengthened and the wave height increased to 0.22 m, grading the swash zone back down to around 5-6°.

A cyclic process of foreshore steepening and flattening in mixed sand and gravel beaches was also reported by Kirk (1980). The mixed sand and gravel beaches of the open coast have foreshore slopes that range on average between 5 and 12°, very similar to that found in Lake Coleridge during periods of wave activity. In high energy conditions the foreshore flattens and a steep scour face often forms at the landward limit of the swash zone in response to erosive wave activity. Slopes in this face may exceed 20° (Dawe, 1997), similar to the slope angles in Lake Coleridge under zero wave conditions. When conditions ease, the foreshore tends to steepen in response to more depositional conditions. The mixed sand and gravel beaches in the lake and oceanic environments respond alike to the wave conditions, except on different time scales. In a lake environment the swash responds to short term energetic wind-wave conditions, that may occur on a diurnal basis. In the ocean setting, because there is rarely a period of complete calm, the equilibrium state of the beaches are different and they respond to longer term cycles of storm or steep wave conditions. This process is akin the erosion/accretion or storm/swell profile changes that occur in the nearshore and foreshore of a sandy beach, as discussed in Chapter One.

The difference being, that sediments are not transferred between the nearshore and foreshore, instead they remain in the foreshore where they are reworked by cross-shore and longshore sediment transport processes.

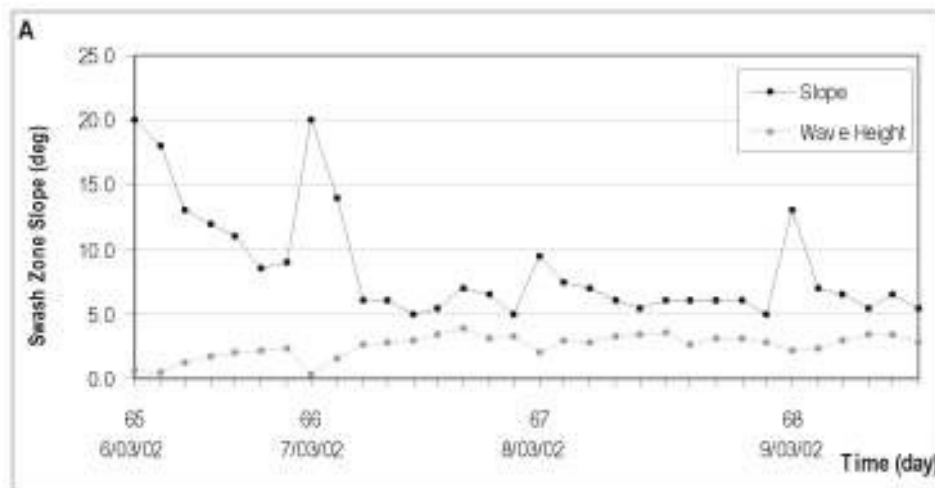


Figure 5.3 Time series of swash slope and wave height over four consecutive days of measurements. A clear pattern emerges between increasing wave height and decreasing beach slope. **NB:** The wave height is not to scale and has been exaggerated by a factor of 15 for the comparison.

This physical process of swash zone development helps explain the strong negative relationship between the swash length and the slope angle (Figure 5.4). When the slope is correlated against the relative swash width (X_{sw}/H_{rms}), a dimensionless swash width to wave height ratio, the relationship remains. However, there is some variability in the relationship. It can be seen that variability increases below slope angles of 10° , with swash zone widths ranging from 1.0 to 6.0 m. Much of this is due to the inconsistent nature of the wind, which causes the wave conditions to fluctuate from hour to hour. It was observed that the swash zone scoured down quickly in response to wave activity, but that it took longer for the beach slope to recover after the conditions eased. In other words, there is a lag in the response time between a drop off in the wave activity and an increase in the beach slope. Often there are lulls in the wave activity and a series of small waves may break onto a swash zone that had been heavily scoured in the previous hour. Thus the wave conditions are less than the width and angle of the swash zone would otherwise suggest. During these conditions, longshore sediment transport rates in the swash zone declined. These short term antecedent conditions play an important role in the swash zone of a lakeshore beach from hour to hour. In contrast, this role would be insignificant on an

oceanic shoreline. Above 10° the variability decreases and swash zone widths range from 0.05 to 1.0 m. At these widths, wave heights are low and there is limited swash zone development.

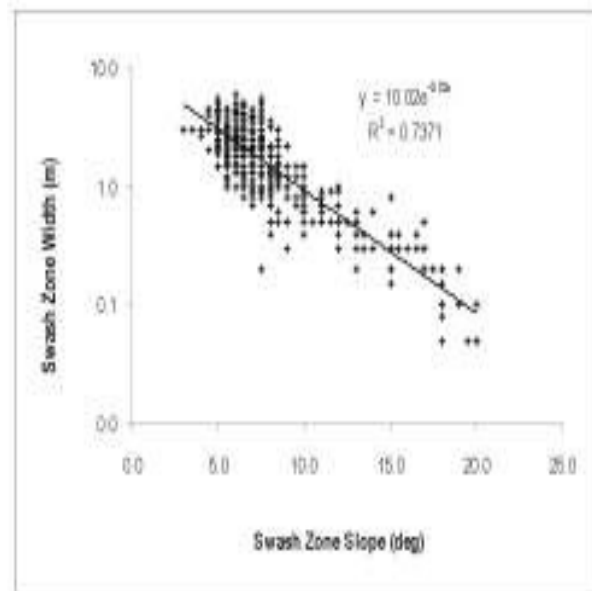


Figure 5.4 Regression between beach slope and swash zone width showing a negative exponential relationship. $r = -0.86$, Std. Error = 0.18, $F = 1614$.

Another feature of the swash zone development that was observed during the field work was that it widened both lakeward and landward. At the initial onset of wave activity, the swash zone widened rapidly in a landward direction in direct response to the increasing wave height. This caused the beach water table to rise in response to wave set-up above mean water level and the lower swash zone quickly became saturated, reducing sediment porosity and increasing the landward run-up of swash. In the mixed sand and gravel beaches of the open coast, Kirk (1975; 1980) and Blewett *et al.* (2000) noted that the upper limit of the swash zone is an area of water infiltration, whilst the lower swash zone is an area of water exfiltration. This was certainly observed to be case in the mixed sand and gravel beaches at Lake Coleridge. Noticeably, as the waves continued to grow in height, the swash zone would begin to grow lakeward. The wave analysis provides some explanation for this behaviour. As the wave height increases, so too does the wave period and in turn the wave length. This causes the waves to break further offshore in deeper water. Since the wave also has a corresponding trough, the oscillation around mean water level increases and the swash zone grows lakeward to meet the base of the breaking wave at a break point step. As the swash zone developed, it steepened slightly at its lakeward and landward

limits, relative to the average slope across the middle. Slope angles at this lakeward limit of the swash zone were slightly steeper than the average slope angle, due to the breaker causing intense scouring from vertical water motions within the breaking wave. In this way the fully developed swash zone attains something of a three-part morphology; a symmetry reflected in the morphology of the nearshore. The nearshore is characteristically broad across the middle with a downward sloping face at the lakeward limit and an upward sloping landward margin as it merges into the foreshore as described in Chapter One (Figure 1.7). When the wave conditions ease, the reverse process occurs. Immediately, the swash excursion distances decline in direct response to lower wave heights. As the swash zone narrows it becomes restricted to the lower and steeper part of the swash zone. Waves begin to break closer to shore as the lengths decrease. Thus, the process of the swash slope steepening in declining wave conditions is partly due to the physical nature of the swash zone. When the wave activity ceases, the water level drops, the swash zone disappears and water oscillates on a steeply inclined and linear section of the foreshore, sometimes the breakpoint step.

In a series of laboratory wave tank experiments into beach responses to wave activity, Inman and Bagnold (1963) found that for coarse grained beaches, the width of the beach rarely exceeded the wave length. It was not clear whether or not this included the nearshore area. Nevertheless, in Lake Coleridge the average wave length was 3.26 m, 1.25 m longer than the average swash zone width (2.01 m). The maximum wave length was 6.63 m, whilst the maximum swash zone width developed to 6.00 m. The correlation of the swash zone width with the wave length was the same as the wave period ($r = 0.80$) and this may provide a useful rule of thumb for small lake beaches.

Swash Length Equations

A general expression was derived from the regression analysis that reasonably estimates the swash zone width or the mean maximum swash width. It is simply taken as the deep water root mean square wave height divided by the slope of the swash zone:

$$X_{sw} = \frac{H_{rms}}{\tan \beta} \quad (\text{m}) \quad (5.1a)$$

The beach slope is calculated in radians, a dimensionless ratio, rather than degrees. Therefore, the expression is dimensionally correct and has a unit value in metres. When used to estimate the maximum swash length, it accounts for the effects of wind and wave set-up. It would be acceptable to substitute H_{rms} for the significant wave height. The deep water wave height was

used in favour of the breaker height, because these values were numerically estimated using Equation 4.12. When breaker height is used in the equation it produces estimates in the order of twice the measured values. Similarly, incorporating the wave period or wave steepness produces values that overestimate the width. Figure 5.5 is a correlation between the measured swash zone width and the values estimated with Equation 5.1a. The correlation coefficients are given under the scatter plot and all the indicators show a good agreement between the measured and the predicted values. The equation provides estimates to the same order of magnitude with values in the range of 0.03 to 5.81 m and an average of 1.75. This is slightly under the measured values, but provides a close estimate. It may be recalled that the measured values ranged from 0.05 to 6.00 m. Importantly, it gives estimates in the same range, that is, the expression is capable of approximating the extreme values, both low and high. It may be desirable to include an empirically derived coefficient (k) to account for this difference. The equation would take the form:

$$X_{sw} = k \frac{H_{rms}}{\tan \beta} \quad (m) \quad (5.1b)$$

Analysing the residuals from the regression analysis between the measured swash widths and those estimated from the general expression (Equation 5.1a), produced a value for k of 1.17. It is expected that this value will vary, depending on local conditions, but it provides a useful first order estimate.

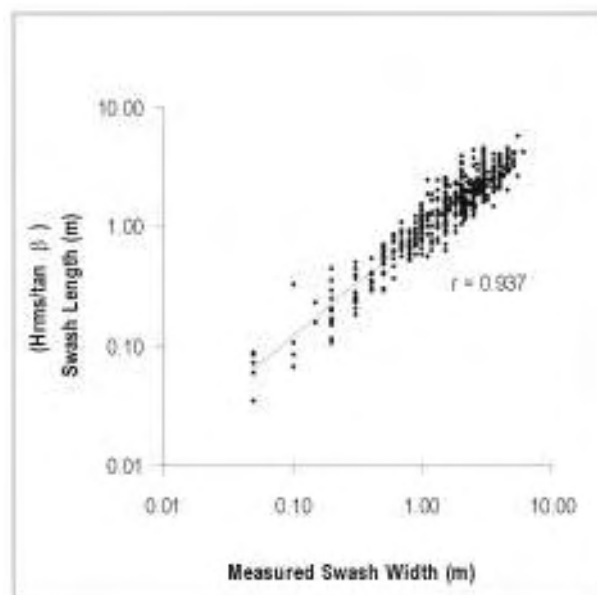


Figure 5.5 Correlation between the measured swash zone widths and the widths calculated with Equation 5.1a. $F = 3635$, Std. Error, 0.13, Sig. $P < 0.0001$.

A series of forecast curves were calculated using the general form of the equation (5.1a). These are presented in Figure 5.6. No swash zone angles below 3° were recorded, but the values at 2 degrees appear reasonable. At 1° the widths double due to the presence of one in the equation. Because slope angles this low are rarely encountered in the swash zone of a mixed sand and gravel beach it is not felt that this poses a serious limitation. Similarly, no wave heights over 1.0 m were recorded, but again the estimate curves for wave heights > 1.0 m appear reasonable. Presently it is suggested that the equation is applicable for conditions in the range of $\beta > 3.0^\circ$, $H < 1.0$ m. It can be seen that the swash width increases linearly with increasing wave height, but that it decreases in a curvilinear fashion with increasing slope angle.

One of the first equations for estimating the swash length was developed by Kemp (1958; in Kirk, 1975). It is an empirical expression that estimates the critical swash length (Sw_l):

$$Sw_l = \sqrt{\frac{1}{2} kgH_b} \quad (5.2)$$

Where H_b is the breaker height, g is gravitational acceleration and k is an empirical coefficient. The critical swash length is comparable to the swash zone width measurements taken from Lake Coleridge, which as discussed above were measured on the basis of the average maximum swash length. Using data from the mixed sand and gravel beaches at Kaikoura, Kirk (1970) calculated a value for k of 1.28, based on 33 samples. The field data from Lake Coleridge produced a value of $k = 1.33$, based on 493 points. Despite the significantly higher wave energy differences between the two beach environments, the values are remarkably similar. Inputting a value of 1.33 for k in Equation 5.2, the critical swash lengths were calculated from the Lake Coleridge data set. Figure 5.7 is a correlation between the empirically measured values and the estimated critical swash lengths. The correlation coefficient is 0.90, showing a strong relationship with the measured values. The estimates ranged from 0.43 to 2.39 m, with an average of 1.51 m. The mean value is approximately within range, but it was not good at estimating the extreme values. There is considerable spread in the swash lengths and Kemp's equation did not approximate this variation. The correlation gains strength from the breaker height that is derived from the deep water significant wave height and as shown above, the swash length is very closely related to this parameter. In Equation 5.1, the extreme values are well estimated with the inclusion of the swash slope parameters. Whilst the slope does not exert a primary control on the swash length it is a strong indicator of the conditions. This supports the findings of Kirk (1970; 1975) regarding the dominant role that the incident wave energy has in controlling the nature of the swash zone in steep mixed sand and gravel beaches.

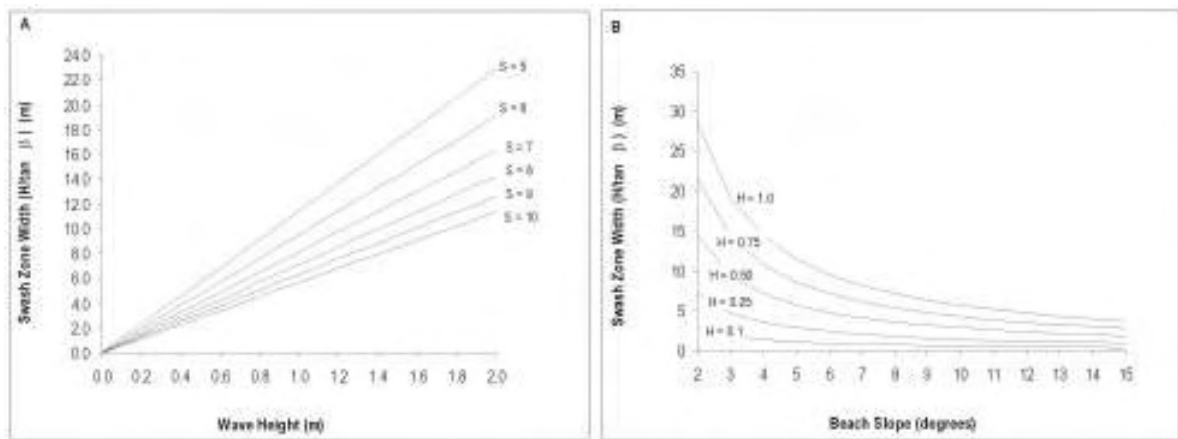


Figure 5.6 Forecast curves for swash zone width derived from Equation 5.1a. In Figure A, the curves are for varying slope angles given in degrees (S). In Figure B The curves are for differing wave heights (H).

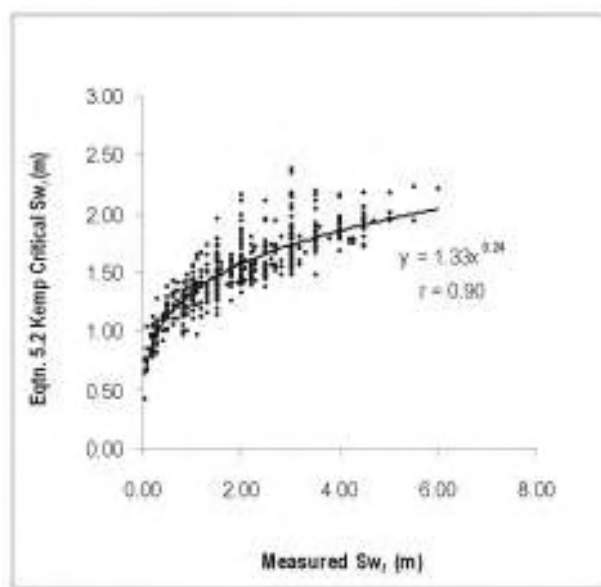


Figure 5.7 Correlation of critical swash lengths (Equation 5.2) with the measured values. $F = 2078$, Std. Error = 0.04, Sig. $P = < 0.0001$.

5.4 Swash Zone Elevation and Run-up Height

The vertical elevation attained by the swash above still water level is known as the run-up. Consideration of run-up is important because it governs the limit to which wave activity can act on a beach. During storm conditions this is especially important because the run-up limit will determine the limit of erosion and incidences of overtopping. In coastal management this will, in part, determine the design specifications of coastal protection works or minimum floor height restrictions for new buildings. Being able to accurately estimate maximum wave run-up limits can lead to more economically designed coastal structures. The high cost of building coastal

structures means that over engineering can lead to large cost over-runs if extreme conditions are not correctly assessed.

Once the width and slope of the swash zone are known, it is possible to calculate the run-up elevation and the height of the beach crest by rearranging the trigonometric ratio $\sin \theta = \frac{y}{r}$, where r is the radius of a circle, effectively the hypotenuse of a right-angled triangle, and y is the vertical axis (Figure 5.8). If waves are imagined to be travelling on the horizontal axis (x) from left to right, the radius can be viewed as the swash zone. The height above the x axis that the swash reaches can be calculated by rearranging the trigonometric ratio for the angle:

$$R_{2\%} = X_{sw} (\sin \beta) \quad (m) \quad (5.2)$$

Where $R_{2\%}$ is the elevation exceeded by 2% of all swash run-up events and X_{sw} is the width of the swash zone. The $R_{2\%}$ run-up is an important limit for coastal planning and engineering purposes and has long been used as a measure of the extreme run-up (Wassing, 1958; Holman, 1986). As discussed above, the width of the swash zone was measured to the average maximum run-up distance and from observation, it was estimated that 1-2% of swash run-up exceed this limit. Visual observations from Lake Coleridge indicated that this distance also provides a good indication of the height of the beach crest. The run-up heights ranged from 0.01 to 0.73 m, with a mean of 0.23 m (Figure 5.9). The majority of the run-up heights (76%) were between 0.10 and 0.40 m. The distribution is positively skewed (0.73), with a tail of extreme run-up events. This is a reflection of the skewed distribution of the swash lengths that were used in the run-up calculation. A summary of the hourly run-up heights can be found in Appendix 6.

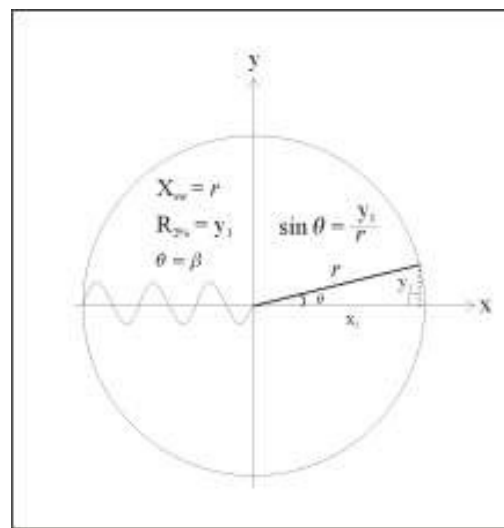


Figure 5.8 The run-up elevation can be calculated with the trigonometric ratio $\sin \theta = \frac{y}{r}$, where r is the swash zone width or critical swash length and y is equivalent to the run-up height.

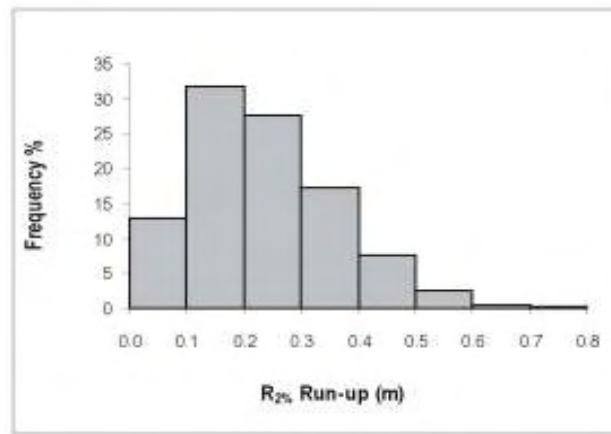


Figure 5.9 Frequency distribution of run-up heights. 76% of the values lie between 0.10-0.40 m. $n = 493$.

A multiple regression analysis was conducted against the run-up elevations using the wave height, period, swash zone slope, wave steepness, and breaker Iribarren. A correlation matrix from this regression is presented in Table 5.2. Like the swash length, the run-up is most strongly influenced by the wave height. The wave period also shows a positive correlation. The wave period increases with growing wave height and, thus, the run-up gains elevation in association with both these parameters. Consequently, there is a relationship with the wave steepness, that is, the run-up increases with greater wave steepness. The regression for the wave height can be seen in Figure 5.10. It shows a strong positive correlation ($r^2 = 0.77$) between increasing wave height and run-up elevation, emphasising again the direct role that wave height has in controlling swash zone conditions. The correlation was slightly weaker than that found for the swash length (Figure 5.2). This is similar to the findings of Kirk (1970; 1975), in a correlation between breaker height, swash length and run-up in the mixed sand and gravel beaches at Kaikoura. Kirk found that run-up heights also had a relationship to the wave period. Generally the shorter wave periods (7.5-8.5 s) produced higher run-up elevations than waves with longer periods (10 s). In Lake Coleridge the opposite was found to be the case. This is partly due to the wave steepness. The longest wave periods (e.g. 3.0 s) were associated with the largest storm waves and hence the steepest wave conditions. In an oceanic setting, waves with 7.0-8.0 s periods are usually associated with locally generated ‘sea’ waves that have a higher steepness than longer period swells. Therefore, some of the variation may be explained by the wave period.

Table 5.2 Regression coefficients of run-up elevation against five other environmental parameters. The strongest correlation is found with the root mean square wave height.

$R_2\%$	H_{rms}	β	T_z	H_o/L_o	ξ_b
r	0.88	-0.64	0.78	0.80	-0.71
r^2_s	0.77	0.41	0.61	0.64	0.50
Std. Error	0.11	0.11	0.05	0.07	0.03
Prob.	< 0.0001	< 0.0001	< 0.0001	< 0.0001	< 0.0001

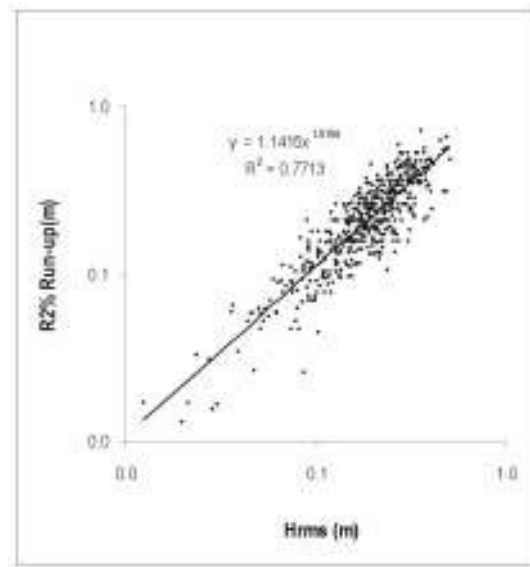


Figure 5.10 Regression between wave height and run-up. $r = 0.88$, Std. Error = 0.13, $F = 1655$.

Some of the scatter in the data is also due to beach morphology. A salient feature of mixed sand and gravel beaches is that their profiles are frequently non-linear, that is, the slope is interrupted with significant breaks caused by berms, scarps and beach ridges. On some occasions under a rising lake level, the swash run-up was limited for a time by a scarp formed previously at a higher lake level (Figure 5.11). This shortened the run-up elevation and swash length until the scarp was scoured lakeward and the sediment redistributed across the swash zone. This process was associated with sediment transport rates. Likewise, it was not uncommon to have a low ridge in the foreshore, with the beach sloping down either side of the feature (Figure 5.12). In high energy conditions under a rising lake level, swash was able to overtop such ridges, causing the swash lengths to be longer than average. In these situations the ridge was slowly pushed back landward until an equilibrium was attained in the foreshore with the lake level conditions. These features can remain in the foreshore for weeks until lake levels completely ‘roll-back’ or submerge the feature.



Figure 5.11 Scarps are often present in the foreshore of a mixed sand and gravel beach, such as found in Lake Coleridge. Under a rising lake level, the base of the scarp may become reactivated. In this situation, the swash is hindered for a time until the lake level either drops, or high waves erode the scarp landward to develop an equilibrium with the prevailing conditions. In the process, swash lengths and run-up heights will be lower than average. However, sediment transport rates increase as material from the scarp is eroded and redistributed across the swash zone.

It was noted by Lorang (2002: 90) that: “Estimating run-up elevation from offshore conditions is most reliable when wave breaking occurs close to the beach without a large intervening surf zone...” In a wide, dissipative, sandy shoreline, the swash zone is not directly connected to the breaking waves as it is on a mixed sand and gravel beach. Rather, there is a large intervening surf zone that Komar (1998) described as a ‘filter’ between the offshore deep water wave conditions and those occurring at the shoreline. Consequently, swash is not controlled by individually breaking waves. It is now understood that infragravity wave motions play an important role in swash run-up processes on dissipative beaches. Nevertheless, in a surprising result from a study into swash motions on sandy beaches, Guza and Thornton (1982) found that the significant run-up could be estimated by a simple relationship with the deep water wave height, $R_s = 0.7H$. In other words, the swash run-up gained an elevation in the order of 30% less than the wave height. By contrast, in the mixed sand and gravel beaches at Kaikoura, Kirk (1970; 1975) found that mean wave run-up attained elevations rarely less than the breaker wave height and frequently exceeded it by as much as 30% (*i.e.* $R = 1.3H$). In Lake Coleridge,

the average $R_{2\%}$ run-up elevations across the full range of environmental conditions is equivalent to:

$$R_{2\%} = 1.16H_{rms} \quad (5.3)$$

On average, run-up exceeds the deep water H_{rms} wave height by a factor of around 15%. It will be recalled the H_{rms} wave height was on average 17% higher than the significant wave height. When the mean R/H_s ratio is calculated, the coefficient in Equation 5.3 rises to 1.36. These coefficients are only mean values. There is considerable scatter across the range, in part due to the variation in beach slope.

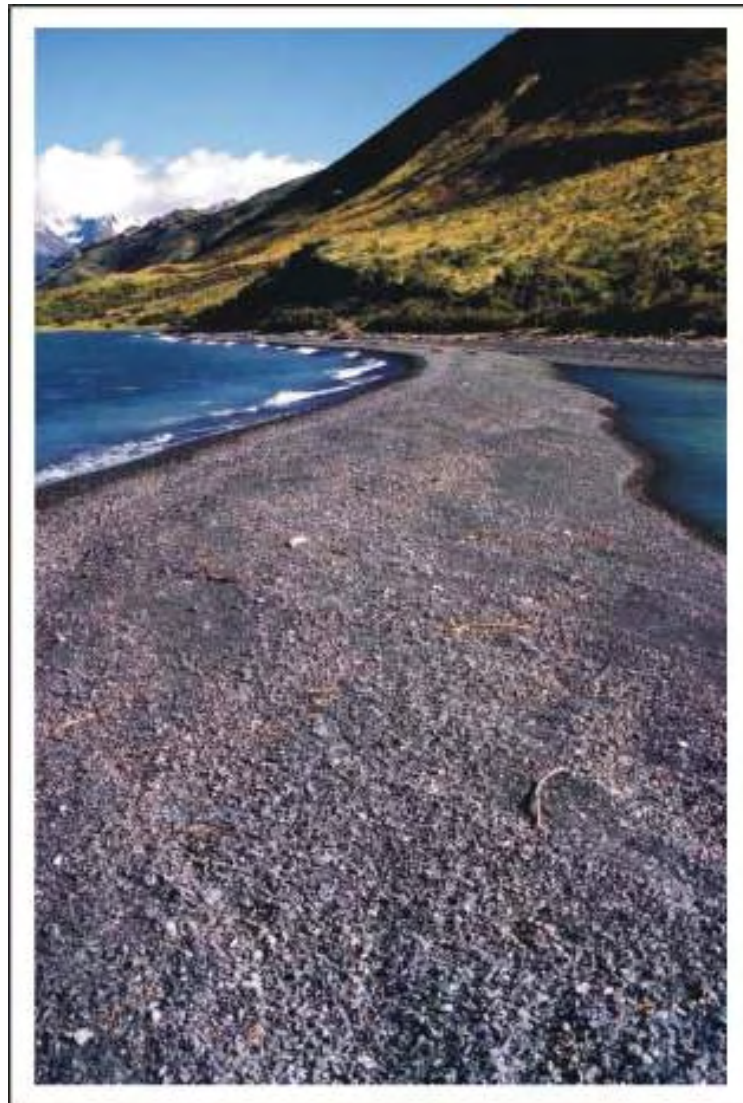


Figure 5.12 Occasionally low ridges formed in the Lake Coleridge fieldsite foreshore. When lake levels and wave conditions permit, the feature may be overtopped by swash. Evidence of recent overtopping at this site can be seen in the overwash lobes and runnels on the landward side of the barrier. This causes longer swash lengths than average as the water runs over the back of the ridge. Transport rates in the swash zone may be lower in this situation as backswash flows are inhibited. Note the water on the landward side that has permeated through the barrier in response to a rising lake level and has been added to by overwash.

It is generally accepted that run-up reaches higher elevations on steeper beaches than on lower sloped beaches (van der Meer & Stam, 1992). Intuitively, it might be expected that the beach slope would have an influence on run-up. However, there is debate in the literature about its significance (Komar, 1998). In this study it was found to be important. There was a general negative relationship between the swash zone slope and the run-up height ($r = -0.64$) (Table 5.2). That is, as the beach slope lowered, the run-up elevation increased. The correlation between the run-up heights and the breaker Iribarren number, which incorporates the beach slope and wave steepness is -0.71 . The Iribarren number is often incorporated into equations to estimate wave run-up. The lowest run-up elevations occurred when the swash zone was at its steepest (Figure 5.13). The highest run-up elevations occurred when swash zone slopes were between 6° and 8° . Again, this relates to the fact that there is a zero condition limit at which point there is no wave run-up. At this stage, the beach slope at the water line is steep. As the swash zone develops under wave activity, the run-up elevations increase due to increasing wave height and the slope is graded down. However, this process only continues to a point. At the lowest recorded slopes below 6° , the run-up elevations begin to reduce. Only a few slope angles below 5° were recorded, so it is difficult to draw any conclusions regarding run-up at these elevations.

When the run-up is calculated as a ratio with the wave height, a measure known as the relative run-up (R/H), a clearer pattern emerges (Figure 5.14). There is wide variability in the values, but there is a discernable increase in the extreme run-up elevations as the slope angle increases from 3° to 8° , after which the run-up declines. The decline at higher angles is possibly a function of beach porosity. It was observed that run-up was strongly affected by beach porosity at higher elevations on the foreshore. At the limit of swash run-up, the sediments are typically extremely porous and water quickly percolates in the beach, curtailing the swash flow. Therefore, run-up may increase with increasing beach slopes to a turning point, after which it declines due to both percolation and process feedback mechanisms (*i.e.* higher wave heights scour and lower the swash zone). Effectively the swash zone can be seen as having two equilibrium end states, during which time the foreshore is in balance with the conditions. At one end, the swash zone has limited development and the beach slope attains high slope angles ($> 10^\circ$) and at the other end the swash zone is fully developed with respect to wave activity and attains a slope angle of around 5° . When slope angles occur between these two end points, it is normally indicative of a change in the equilibrium stage as the foreshore responds to a change in conditions. Previous studies have also found a relationship between relative run-up and the wave period. No clear relationship was found in this study, with the strongest association found to be with the slope.

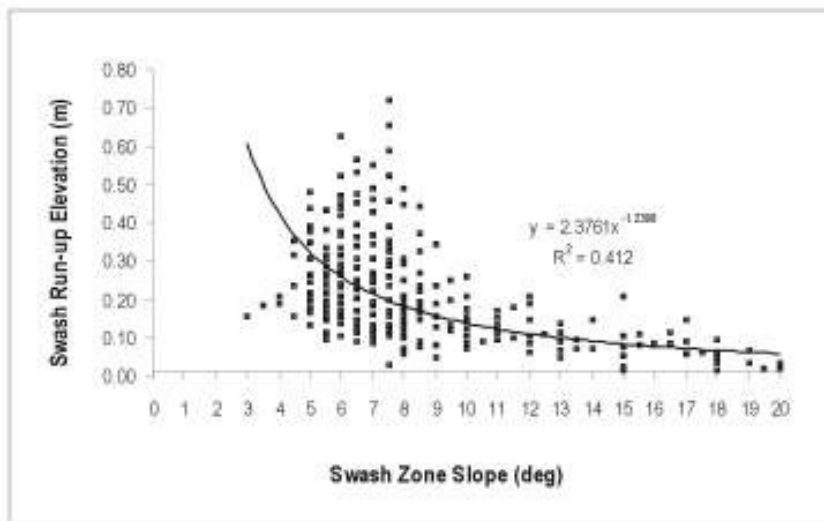


Figure 5.13 Regression of run-up with swash zone slope. $r = -0.64$, Std. Error = 0.21, $F = 344$.

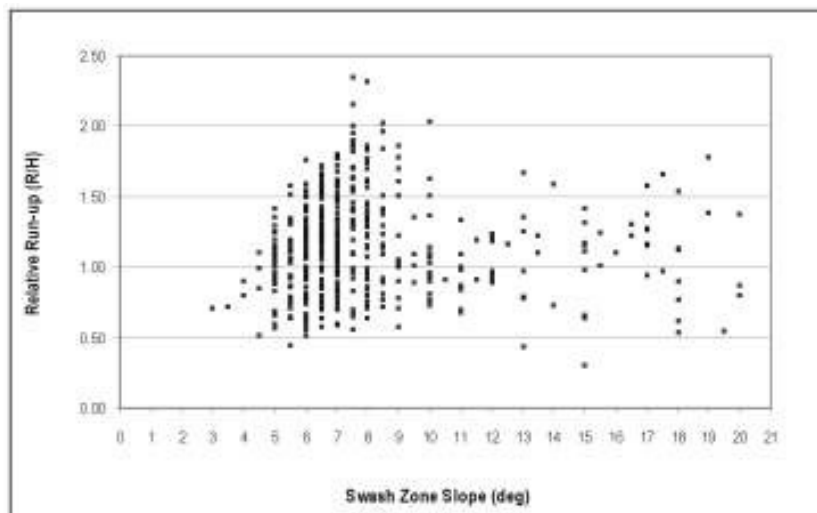


Figure 5.14 Comparison of relative run-up to beach slope. The highest run-up elevations occur at slopes between $7-8^\circ$.

Averaging the R/H ratios in each of the slope classes reveals some interesting figures. These are summarised in Figure 5.15. Below slopes of 5° , the elevation attained by the swash run-up was found to be on average 20% lower than the wave height. This is more in line with the findings from sandy beaches (Guza and Thornton, 1982). Slopes around 5° appear to form a threshold, around which run-up is proportional to wave height. Above 6° , run-up steadily increases with the slope to a maximum between 7° and 8° , as discussed above. On average, run-

up exceeds the wave height by 20% at slopes between 6° and 10° . Above 10° , the run-up heights generally reach elevations about 5-7% the wave height. Taking these ratios, Equation 5.3 can be rewritten to include the various empirically derived slope limits (S):

$$R_{2\%} = 0.8H_{\text{rms}} [S < 5^\circ] \quad (5.4a)$$

$$R_{2\%} = 1.2H_{\text{rms}} [5^\circ < S < 10^\circ] \quad (5.4b)$$

$$R_{2\%} = 1.05H_{\text{rms}} [S > 10^\circ] \quad (5.4c)$$

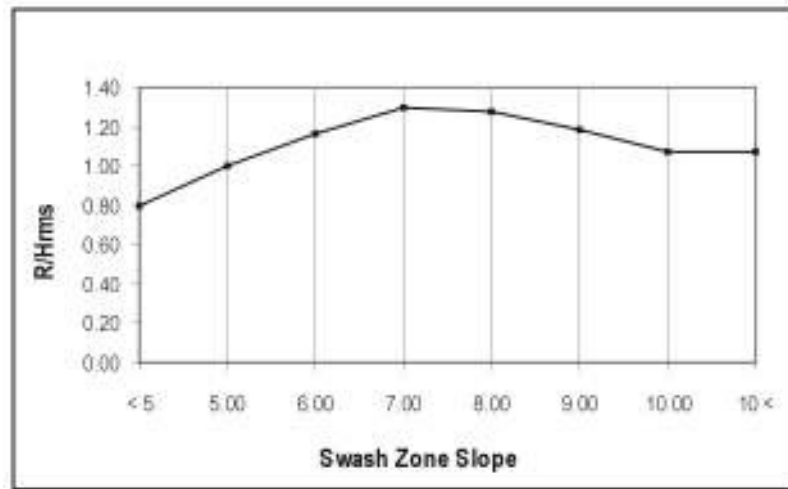


Figure 5.15 Average relative run-up ratios (R/H) ratios across the main swash zone slope classes measured in Lake Coleridge. Below slopes of 5° , run-up was found to be less than the wave height. Above 6° , run-up reached elevations that exceeded the wave height.

Run-up Models

Some of the earliest investigations of wave run-up were made by the Delft Hydraulics Laboratory, which started research into wave run-up of engineered coastal structures in 1936 (Wassing, 1958). Out of this work came one of the first numerical solutions to run-up, where a relationship was identified between the significant wave height (H_s) at the toe of the slope and the slope (S) of the structure:

$$\frac{R_{2\%}}{H_s} = 8 \tan \beta \quad (5.5)$$

Where $R_{2\%}$ refers to the vertical run-up elevation above still water level exceeded by two percent of the swash events, as discussed previously. It was developed for slopes no steeper than 16° and wave steepness values of around 0.05. In the United States, some of the earliest work was

conducted by Saville (1955; 1956; 1958) and Savage (1958). Like the research in the Netherlands, the focus of these investigations was in examining the vertical run-up that waves could reach on various types of coastal structures. The aim of this work was to identify the important environmental variables governing run-up. The work of Saville and Savage was incorporated into the Shore Protection Manual (1961) and was influential in setting the direction of run-up research for the next 30 years. In an examination of run-up on rock armouring coastal structures, Hunt (1959) continued this line of research and derived the empirical formula:

$$R = 2.3T\sqrt{H} \tan \beta \quad (5.6)$$

Where H and T are the wave height and period and $\tan \beta$ is the beach slope. Recognising the importance of beach slope and wave height in governing run-up, Battjes (1971) re-formatted the equation to include gravitational acceleration in order to make the expression dimensionally homogeneous. The equation took the form of:

$$R = CT\sqrt{gH} \tan \beta \quad (5.7)$$

Where C is an empirical coefficient. Using the data from Hunt (1959), Battjes calculated a coefficient of 0.4. Through further work with other data sets this increased to between 0.60-0.75 depending on the wave steepness. Battjes (1974) found that the run-up was closely related to the Iribarren number through the dimensionless relative run-up in the range $0.1 < \xi < 2.3$:

$$\frac{R}{H} = \xi \quad (5.8)$$

The Iribarren number was defined in Chapter Four (Equation 4.10). Battjes found the expression required an empirically derived correctional coefficient that varied from 0.4-1.0 depending on a range of environmental factors, including wave steepness and beach slope. Holman (1986) and van der Meer and Stam (1992) rearranged the work of Hunt (1959) and Battjes (1971; 1974) to produce a generalised relative run-up expression in the form of:

$$\frac{R_{2\%}}{H_s} = C\xi_o = \frac{C \tan \beta}{\sqrt{2\pi H_s / gT^2}} \quad (5.9)$$

Where C is an empirical coefficient, all other terms having been previously defined. The equation was developed to be valid in the case of plunging waves breaking onto moderate slopes. The value for C ranges widely depending on the slope from 0.4 to 2.86 (Battjes, 1974; Grüne, 1982; van der Meer and Stam, 1992). Kirk *et al.* (2000) rearranged this equation further to eliminate the need for the significant wave height on both sides of the equation to produce a non-relativistic, total run-up that incorporates wave set-up:

$$R_{2\%} = CS(H_o / L_o)^{1/2} = C(g / 2\pi)^{0.5} SH_s^{0.5} T \quad (m) \quad (5.10)$$

Kirk *et al.* (2000) used this equation to calculate extreme run-up events caused by storm waves on Lake Hawea, Central Otago. A value for C of 0.90 was used in the study, where it was noted that it partly accounts for such variables as grain size, frictional drag and porosity.

Employing the root mean square wave height, the zero-crossing wave period and the swash zone slope, run-up heights were estimated using Equations 5.3, 5.5, 5.7 and 5.10. The results are presented in Table 5.3 and Figure 5.16. The coefficient C in Equation 5.7 was calculated as being 0.91 for the field site beaches at Lake Coleridge. This is slightly higher than Battjes's suggested values and is a reflection of the direct role that wave height has in controlling run-up in a mixed sand and gravel beach. Regarding Equation 5.10, the coefficient C was calculated at an average of 2.97, which is also valid for Equation 5.9. Without this constant, the run-up elevations are approximately three times lower than estimated. This is at the extreme end of the range found in the literature and is again a reflection of the direct influence of the incident wave energy.

The simple wave height equality expression (Equation 5.3) performed the best of the four equations. It has the strongest correlation ($r = 0.88$) (Figure 5.16a) and estimated the minimum and mean values well, but it slightly under-estimated the extreme run-up heights (Table 5.3). Overall it estimated the range of values reasonably well, as illustrated by the small standard deviation value (0.11) and the even spread of values around the best fit line. The strength of the correlation derives directly from the wave height and illustrates the dominance of this parameter. It is purely empirically derived and at this stage is site specific. From research by Kirk (1970) it is apparent that run-up often exceeds wave height by up to 30% on coarse grained beaches. However, without further testing on other lakeshore mixed sand and gravel beaches, it is not known whether the coefficient applies equally to other locations.

The expression developed at the Delft Hydraulics Laboratory (Equation 5.5) for engineered slopes performed reasonably with a correlation to the measured data of $r = 0.73$ (Figure 5.16b). The mean values were estimated relatively well, but it did not estimate the extreme values in the range, over-estimating the minimums and under-estimating the maximums. The expressions derived by Battjes (1971) and Kirk *et al.* (2000), (Equations 5.7 & 5.10), performed modestly. They both have the same correlation coefficients ($r = 0.59$) because they employ the same configuration of environment variables, but the results they produce are slightly different (Figure 5.16c & d). Equation 5.7 estimates the mean values relatively well, but over-estimates the minimums and under-estimates the extreme run-ups. Equation 5.10 over-estimates both the

minimum and mean values, but performs the best of the four equations in estimating the extreme run-up values. There is considerable variation across the range of run-up values and Equations 5.5, 5.7 and 5.10 did not approximate this range well. This is reflected in the standard deviations, that are all lower than the empirical value (Table 5.3). In all the correlation scatter plots it can be seen that there is a weighting of data points below the best-fit line and considerable scatter above the line. Much of this scatter is a result of the over-estimation of the minimum values and derives from the variation in run-up heights due to slope. Equations 5.5, 5.7 and 5.10, all assume that run-up elevations increase in a linear fashion with increasing beach slope. However, this has not been found to be the case at Lake Coleridge. It will be recalled from Figure 5.13 that the relationship is non-linear and that run-up begins to decline above slope angles of 8° . The three equations do not recognise this change, highlighting important points of difference between the underlying assumptions in the models and the process-response regime of a mixed sand and gravel lakeshore beach.

Many of the run-up equations were developed for estimating run-up on impermeable linear slopes designed as coastal defence works in high energy open coast locations, such as dykes or seawalls. Some of these equations have subsequently been adapted for natural beaches. However, the equilibrium conditions in a lake are different to open coast beaches. In a lake, considerable change occurs in a shoreline composed of unconsolidated sediments at the onset of wave activity. It was noted above that the swash zone can be seen as having two equilibrium end states, in which the foreshore attains a balance with the conditions. At one end, the swash zone has limited development and the beach slope attains steep gradients. In these situations the wave energy is low and the equations over-estimate the run-up. The beach porosity plays an important role in this process. At the limit of swash, the porosity is high as the sediments lie at elevations above the beach water table. As discussed previously, this is an area of high water infiltration which quickly limits swash run-up. At increasing elevation in the foreshore above still water level, the sediments become increasingly porous because there is less water in the pore spaces between particles. Thus, the beach becomes drier at higher elevations. In moderate conditions before the swash zone fully develops, this high porosity causes lower run-up values than predicted by the models. Between slope angles of $6-8^{\circ}$ there is a general increase in run-up with elevation and the models performed best in this range.

Table 5.3 Results of calculations from run-up equations. Measured run-up is included for comparison.

metres	R _{2%}	Eqtn. 5.3	Eqtn. 5.5	Eqtn. 5.7	Eqtn. 5.10
Min	0.01	0.01	0.04	0.07	0.09
Max	0.72	0.59	0.51	0.51	0.66
Mean	0.23	0.23	0.20	0.23	0.30
Std. Dev.	0.13	0.11	0.07	0.07	0.09

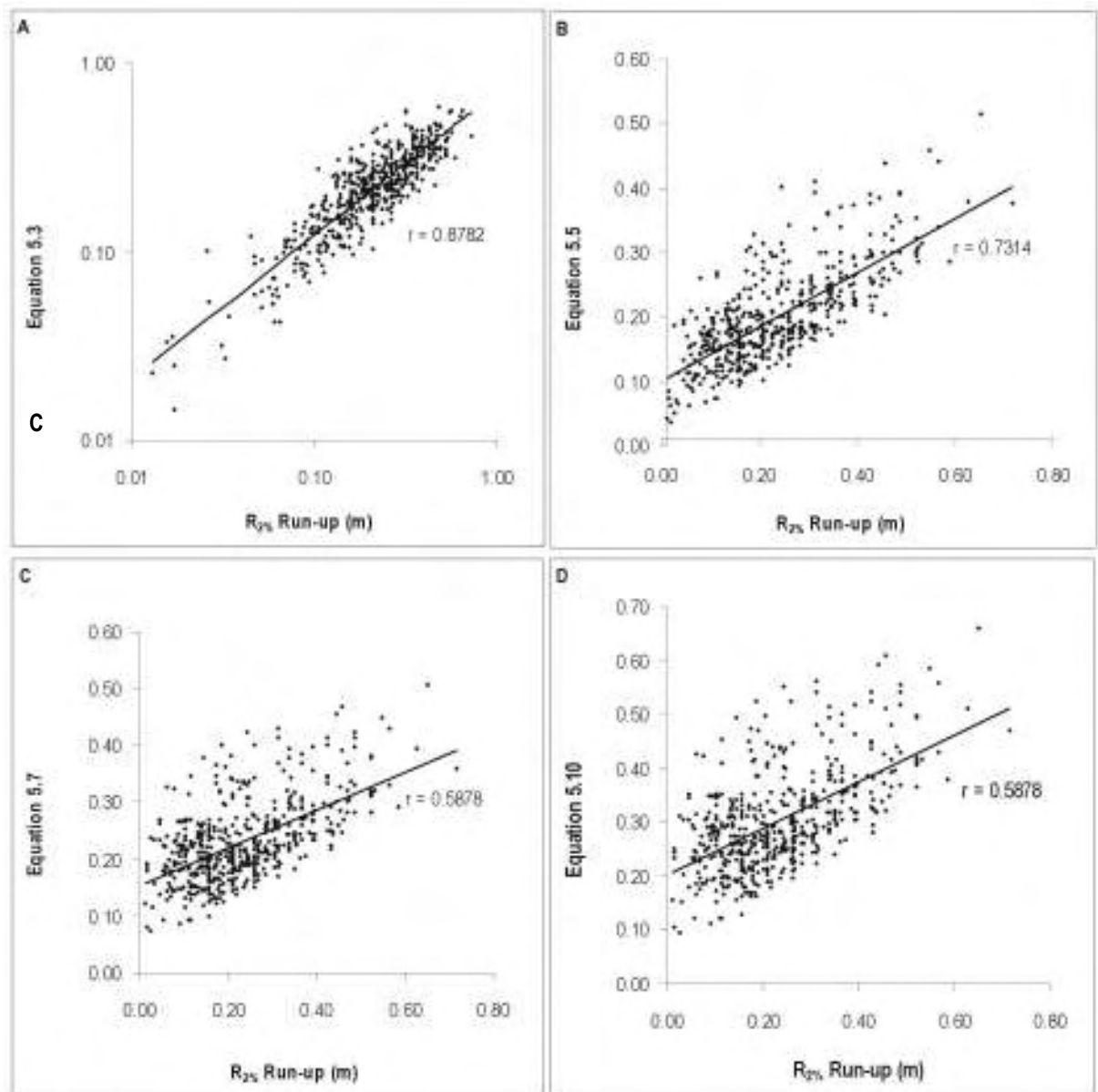


Figure 5.16 Linear correlations between measured $R_{2\%}$ run-up and estimated run-up from four equations. (A) $F = 1655$, Sig. $P < 0.0001$. (B) $F = 564$, Sig. $P < 0.0001$. (C) $F = 259$, Sig. $P < 0.0001$. (D) $F = 259$, Sig. $P < 0.0001$. The simple wave height equality expression (A) exhibited a logarithmic relationship and was transformed for linear a correlation. The three other equations exhibited a linear additive relationship.

Recognising these differences, Equation 5.7 was rearranged to account for the negative relationship between run-up and beach slope:

$$R_{2\%} = CT \frac{(gH_{rms})^{0.5}}{\tan \beta} \quad (m) \quad (5.11)$$

Where C is again an empirically derived coefficient, calculated to be 0.014 for the Lake Coleridge data set. By dividing with the swash slope, a ratio is formed between the wave height term and $\tan \beta$, in the same fashion as the critical swash length equation (5.1a). The correlation with the measured run-up is immediately improved ($r = 0.82$) (Figure 5.17). The estimated run-up values range from 0.01 to 0.68 m, with a standard deviation of 0.13. This is very similar to the measured range and the equation responds well across the array of slope conditions. Importantly, it provides a good indication of the extreme run-up elevations which can cause considerable erosion in storm conditions. The equation includes the three main variables involved in controlling run-up. Therefore it has a more general applicability than the wave height equality expression (Equation 5.3). Further research is required to quantify the effects of porosity and other variables which are incorporated into the expression through the C coefficient. Professor Paul Komar, Oregon State University (*pers. com.*, 2006) noted that by substituting 0.014 for C into Equation 5.11 it can be rearranged to provide:

$$\frac{R_{2\%}}{H_{rms}} = \frac{0.014g^{0.5}T}{H^{0.5} \tan \beta} \approx 1.16 \quad (5.12)$$

It may be recalled that the value 1.16 is the coefficient from Equation 5.3. Effectively there is a level of conformity between Equations 5.3 and 5.11. Whilst Equation 5.3 provides the best predictive formula for run-up elevation, Equation 5.11 acknowledges that other environmental variables play a role in controlling run-up. Figure 5.18 presents a summary and comparison between the measured run-up statistics and the estimated values calculated with the equations discussed above.

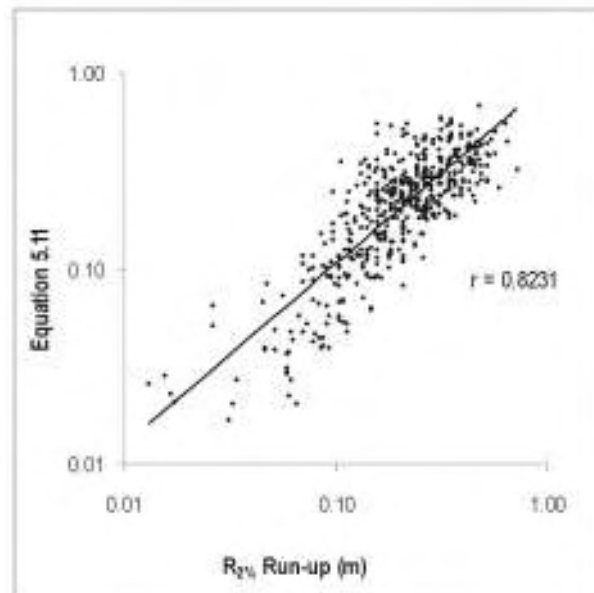


Figure 5.17 Correlation between equation 5.11 and the measured run-up heights. $F = 1031$, Sig. $P < 0.0001$.

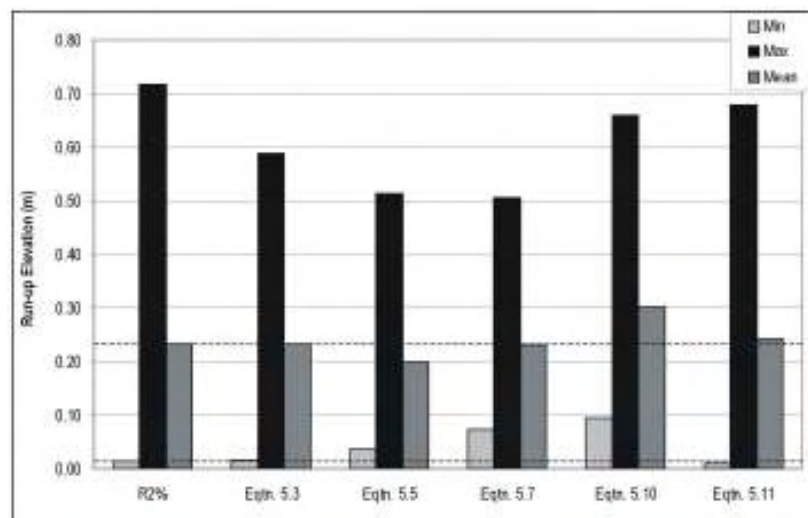


Figure 5.18 Comparison between output values from all the run-up equations developed and tested with the measured run-up heights (at far left). Equation 5.3 has the best correlation with the measured data, but equation 5.11 has better general applicability.

5.5 Swash Zone Currents

As a wave collapses there is a rapid conversion of potential energy into kinetic energy. On a steep beach much of the current flow is forced downward in a vertical direction, before translating horizontally into an advancing swash lens. During this process, sediment is entrained in the swash flow. Erosion and accretion in the foreshore of a mixed sand and gravel beach is the direct result of sediment transport processes in the swash zone. The previous sections have

discussed the processes of swash zone development in response to wave activity and the run-up and excursion lengths that swash is able to attain on the foreshore. These important quantities determine the spatial extent through which sediment is transported. One of the most critical hydrodynamic parameters that affects sediment transport is the shear stress at the water-sediment boundary (Ahrens & Hands, 1998). Shear stress is difficult to measure empirically, but a closely related parameter frequently used as a de facto is the water flow velocity (Hughes *et al.*, 1997). Many studies have investigated currents of the nearshore zone and flow properties of the breaking wave, but there are relatively few studies of the flow dynamics of the swash zone, especially in natural coarse grained beaches. In recent years there have been a few studies from the United Kingdom that have investigated the swash properties of steep gravel beaches by measuring depth of flow or pressure variations in individual swash and backswash lenses (Blewett *et al.*, 2001; 2000). There have also been some investigations of swash hydrodynamics of steep beaches in the laboratory (Baldock & Holmes, 1997). Unfortunately many of these investigations provide scant information with regards to velocity measurements.

In a study of the swash zone hydrodynamics of a steep beach near Sydney, Australia, Hughes *et al.* (1997) made concurrent measurements of sediment transport and flow velocities with an array of capacitance wire gauges, ducted impeller flow metres and sediment traps. The focus of the study was to investigate the sediment transport capacity of individual swash lenses. Measurements took place in the swash zone of a moderate to coarse sandy beach with a foreshore slope of 7.0° , that was fronted by a gently sloping low tide terrace. Wave heights averaged 0.5 m for the duration of the study. Instantaneous maximum velocities of over 5.0 m s^{-1} were recorded and time averaged velocities were in the range of 0.36 to 2.48 m s^{-1} . Hughes *et al.* (1997) expressed surprise at these high velocities and were compelled to verify them in a subsequent study. Shanehsaz-zadeh *et al.* (2001) recorded velocities as high as 2.0 m s^{-1} in the swash zone of a composite sand and gravel beach when incident waves were only in the order of 0.20-0.40 m. Kirk measured velocities across the swash zone of a mixed sand and gravel beach with a purpose built, force-plate dynamometer (1971; 1973). Breaker heights were visually estimated at 0.30-2.40 m. Average swash velocities of between $0.50\text{-}2.50 \text{ m s}^{-1}$ were recorded, with an overall mean of 1.68 m s^{-1} . Kirk noted that it was possible there were much higher maximum instantaneous speeds, but the dynamometer had an upper recording limit of 3.0 m s^{-1} . Novak (1972) presented research from a sediment transport study conducted on a steep cobble beach. Swash velocities were estimated with a series of painted rods, spaced at equal distances across the foreshore. The swash front was timed as it passed each pole to derive a mean velocity.

Wave heights were estimated from visual observations and ranged from 0.15 to 0.60m. Despite the coarse nature of the beach, mean swash velocities were reported at 1.6-2.1 m s⁻¹.

Kirk (1970) also demonstrated that the incident waves had a direct control on the swash velocity. It has been noted that the swash flows in a steep beach attain much higher velocities than those from a low sloping dissipative beach. This is because wave energy is dissipated on a low sloping beach as a series of bores across the inner surf zone. On a steeper beach the wave energy is expended directly in the swash zone. Huntley and Bowen (1975) conducted research into the swash hydrodynamics of both gently sloping and steep beaches. They recorded horizontal onshore velocities in steep beaches of up to 0.48 m s⁻¹, with waves as low as 0.15 m. The mean velocity measured on the gently sloping beach was 0.26 m s⁻¹, with a maximum of 0.29 m s⁻¹. Concurrent measurements of swash velocity and sediment transport were made in a gently sloping sandy beach on the Pacific coast of Japan by Katori *et al.* (2001). Wave heights ranged from 0.49-0.74 m, but the average longshore component of swash velocity never exceeded 0.20 m s⁻¹.

A summary of the swash velocities from the investigations discussed above is presented in Table 5.4. The table also includes some backswash flow velocities, from those studies that made the measurements. It will be noted that the mean backswash velocities are all in the order of 15% less than the swash velocities. This asymmetrical flow pattern is a commonly recorded feature of the swash zone. In the mixed sand and gravel beaches on the east coast of New Zealand, Kirk (1975) reported that the swash velocity rapidly accelerated to maximum speed after wave breaking and remained high across 80-90% of the swash zone, declining only at the very limits of the swash zone. Then as the flow reversed there was a slower, but no less rapid acceleration back downslope under the influence of gravity. Kirk (1970) recognised that the swash and backswash were two closely related yet independent flows. It was argued that the independent aspects of the flow field derived from the subtle difference in the forcing mechanism between the swash (incident waves) and backswash (gravity). This difference leads to an asymmetry in the flow field because the breaking wave provides much higher energy at the start of the flow than the more sedate effects of gravity. Kirk found that this difference also led to an asymmetry in the time duration between the swash and backswash. The average swash duration was found to be 2.98 s and the average backswash duration 4.25 s. Masselink & Hughes (1998) reported a similar swash flow pattern in a sediment transport study on a coarse sandy beach in Western Australia. They found that as the leading edge of the swash lens advanced up the shore, flow rates increased almost instantaneously from zero to the maximum speed, followed by a more gradual

decrease back to zero as the water depth narrowed. When the flow reversed, the opposite process occurred and the backswash gradually accelerated to a maximum at the base of the swash zone. This led to slight differences in the average flow velocities between the two flow phases, but statistical analysis suggested that it was enough to be significant. However, they did report significant differences in the time duration between the two flows, with swash durations ranging from 1.5-2.5 s, and backswash durations varying from 2.5-5.5 s. This is a finding consistent with other studies (Elfrink & Baldock, 2002).

Table 5.4 Summary of some swash zone velocity measurements from coarse grained beaches.

Source	Sediment size (mm)	Slope angle (deg)	Wave height (m)	Swash (m s^{-1}) Backswash (m s^{-1})		
				min.	mean	max.
Novak (1972)	pebble/cobble 27.0-110.0	---	0.15-0.60	---	1.6	2.1
Kirk (1975)	sand/gravel 0.5-8.0	5.0-12.0	0.30-2.4	0.50 0.25	1.68 1.40	2.50 2.25
Huntley & Bowen (1975)	gravel ---	7.5	0.15-0.30	0.08 ---	0.31 ---	0.48 ---
Hughes <i>et al.</i> (1997)	coarse sand 0.30	7.0	0.50	0.36 ---	1.32 ---	2.48 ---
Masselink & Hughes (1998)	coarse sand 0.50	8.0	0.40-0.50	0.32 0.32	1.14 1.00	1.86 1.69
Shanehsaz-zadeh <i>et al.</i> (2001)	sand/gravel 6.0-40.0	5.7	0.20-0.40	0.05 0.05	0.40 0.30	2.0 2.0

Current Measurements

As discussed in Chapter Three, currents in the swash zone were measured with a Marsh-McBirney electro-magnetic current meter. The device was positioned 10 cm above the bed at a point approximately one third the width of the swash zone as measured from the base of the breaking wave or the lakeward limit of the swash zone. This was considered a sufficient distance from the breaker to allow the swash to gain momentum away from the breaking face of the wave, ensuring that measurements were made of the swash bore. It also ensured that there was sufficient depth of water to allow the current meter to make a measurement in the water flow. The sensor was moved whenever necessary in order to maintain this position and ensure continuity of measurement across the wide variety of conditions. The current velocities and directions were calculated as hourly averages in both the onshore (swash) and offshore

(backswash) directions and as a combined swash-backswash total for the swash zone. A summary of the hourly swash zone velocities can be found in Appendix 6.

The mean velocities in the swash zone ranged from 0.01 to 1.07 m s⁻¹, with an overall mean value of 0.29 m s⁻¹ (Table 5.5). The data are positively skewed (0.98) with a long tail of high velocities, but 99% of the values occur below 0.80 m s⁻¹ (Figure 5.19a). The data are moderately leptokurtic, indicating a clustering of the velocities around the mean value. On average the maximum swash velocities are 3.5 times greater than the mean flows, ranging from 0.03 to 2.48 m s⁻¹ and averaging 0.98 m s⁻¹ (Figure 5.19b). With a skewness value of 0.12, the data attain an almost Gaussian distribution, but it is slightly platykurtic. These values are comparable to swash velocities measured in coarse grained, open coast beaches in the same range of wave height conditions (Table 5.4). In examining the distributions of the swash and backswash velocities of the Kaikoura data, Kirk (1975: Fig. 5) found that the mean maximum distributions were slightly negatively skewed and attained an almost Gaussian distribution, similar to the maximum velocities measured in Lake Coleridge.

Table 5.5 Swash Zone flow velocity statistics.

m s ⁻¹	Mean Total	Max Total	Swash	Backswash
Min	0.01	0.03	0.01	0.01
Max	1.07	2.48	1.08	1.04
Mean	0.29	0.98	0.28	0.27
Std. Dev.	0.15	0.47	0.15	0.15
Skewness	0.98	0.12	1.11	1.13
Kurtosis	2.06	-0.25	2.93	2.61

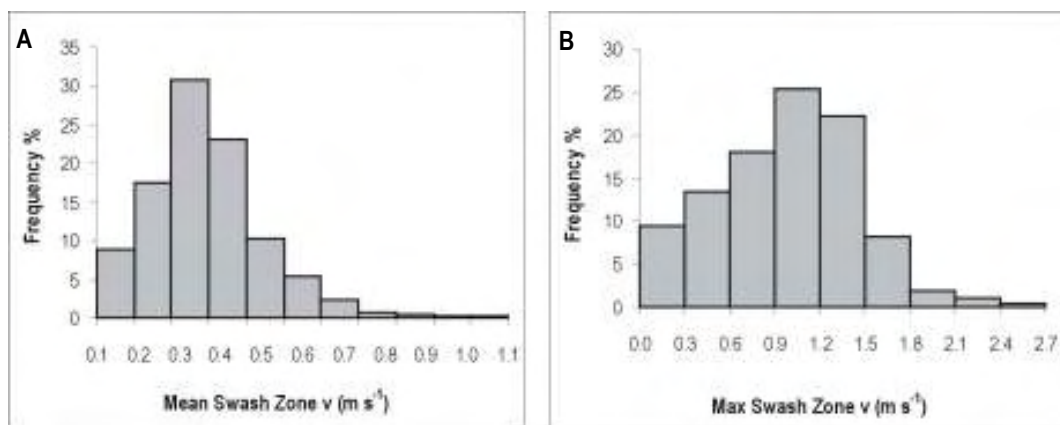


Figure 5.19 Frequency distributions for the mean and maximum hourly combined swash/backswash velocities. The mean swash distribution is positively skewed, whilst the maximum distribution is almost normally distributed. $n = 493$.

When the flow is separated into swash and backswash components, only slight velocity differences become apparent. In Table 5.5 it can be seen that the mean swash velocity is 0.28 m s^{-1} , whilst the mean backswash velocity is only 0.01 m s^{-1} less. This is similar to the findings of Masselink & Hughes (1998), who found no statistical difference between the velocity of the two flow phases. The mean maximum velocities are slightly higher in the swash, perhaps an indication of the high flow velocities forward of the breaking wave. When the data are analysed on a hourly basis, the small differences obscured by the averaging become more apparent. Figure 5.20 is a plot of the hourly difference between the swash and backswash against the mean flow velocity. Overall, there are more occasions when the swash flow has a higher average velocity than the backswash. When calculated as a percentage, the average swash velocity exceeds the backswash velocity 65% of the time. However, this difference is slight and 85% of the variation is less than 0.10 m s^{-1} . Noticeably, the swash dominates when the mean flow velocities are below 0.18 m s^{-1} . Backswash velocities generally only exceed swash velocities in higher energy conditions. The data suggests that there is a slight asymmetry in the flow pattern, but that it is a small difference. This is reinforced by Figure 5.21, which shows a very strong correlation between the swash and backswash ($r = 0.94$), indicating that the two flows are very closely related, but not identical. The distribution frequencies of the swash and backswash are presented in Figure 5.22. Both the distributions are strongly positively skewed and leptokurtic. These distributions provide clues about the influence of various environmental parameters on the swash and in turn, about the nature of the water flows in the swash zone.

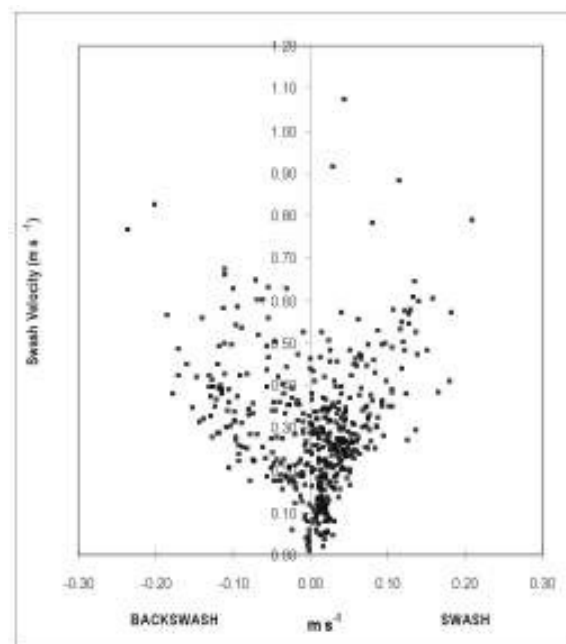


Figure 5.20 Scatter plot of the relative difference between the swash and backswash velocity plotted as a function of the mean swash velocity (y-axis). Each point represents the mean hourly difference. $n = 493$.

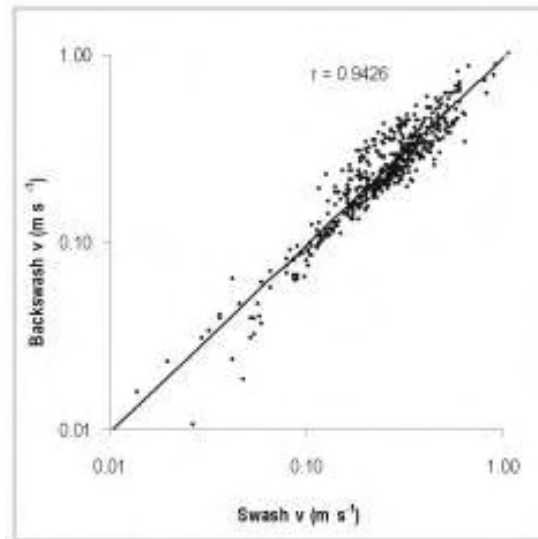


Figure 5.21 Correlation between the mean swash and backwash velocities indicating a very strong relationship. A small amount of variance exists between the two flows. Std. Error = 0.10, $F = 3914$, Sig. $P < 0.0001$.

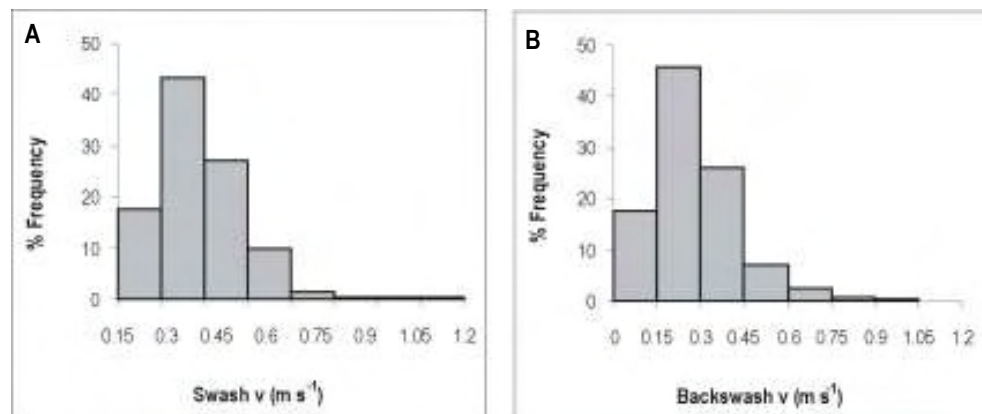


Figure 5.22 Frequency distributions for the mean hourly swash (A) and backwash (B) velocities. The scale on the both x-axes increases at increments of the standard deviation (0.15) of the distribution. Both the swash and backwash flows are positively skewed, but there is a strong leptokurtic element to the data, with a high percentage of values clustered around the mean. $n = 493$.

Due to the importance of swash velocity in controlling sediment transport, a multiple regression analysis was conducted against a range of environmental variables to identify those most responsible for causing variations in the swash flow. A summary of the four most important variables can be seen in Figure 5.23. The regression analysis reveals that the incident wave conditions have a strong influence on the swash flow ($r = 0.83$). As the wave height increases, there is a strong increase in the swash velocity. The strength of the relationship between the

incident wave energy and the swash velocity is mirrored in the skewed frequency distributions of the swash velocities (Figures 5.19 & 5.22). It will be recalled from Chapter Four that the wave height distributions were also positively skewed (0.50). The tail of high swash velocities in the distribution is caused by the largest waves in the wave height distribution. However, the wave height distributions were mesokurtic, whereas the swash velocity distributions are leptokurtic. Clearly other environmental variables are involved in influencing the swash, causing the variation in velocities to even out after wave breaking, as indicated by the high percentage of values clustered around the mean.

An examination of the wave steepness and swash zone slope distributions reveals that they are leptokurtic. The wave steepness distribution has a kurtosis value of 1.28 and swash zone slope a value of 3.34. Positive relationships were found with the wave period ($r = 0.72$) and the wave steepness ($r = 0.77$). As conditions intensify, more wave energy is supplied into the swash zone as the wave heights and wave periods become longer and the waves become steeper. The slope of the swash zone is also important. It displays a negative relationship, with a correlation coefficient of $r = -0.71$. As the wave energy increases, it begins to modify the foreshore by scouring down the swash zone slope. Thus, higher swash velocities are associated with lower slopes. Such a relationship was also found by Dolan and Ferm (1966) who studied foreshore response to variations in swash velocity. It was found that increasing wave height and swash velocity was associated with a flattening of the beach slope. Interestingly, the relationship strengthened as the wave energy declined. The correlation coefficient r , calculated for slope versus velocity, ranged from -0.65 in high energy conditions to -0.81 in low energy conditions. The general finding was that lower swash velocities were related to steeper profiles composed of coarse material where the run-up zone is relatively narrow. When the swash velocity is normalised to the wave height a similar pattern emerges, with the highest velocities at the lowest slope angles. As will be discussed further below, at slope angles between $6-10^\circ$, the swash velocities decline slightly due to turbulence in the swash zone.

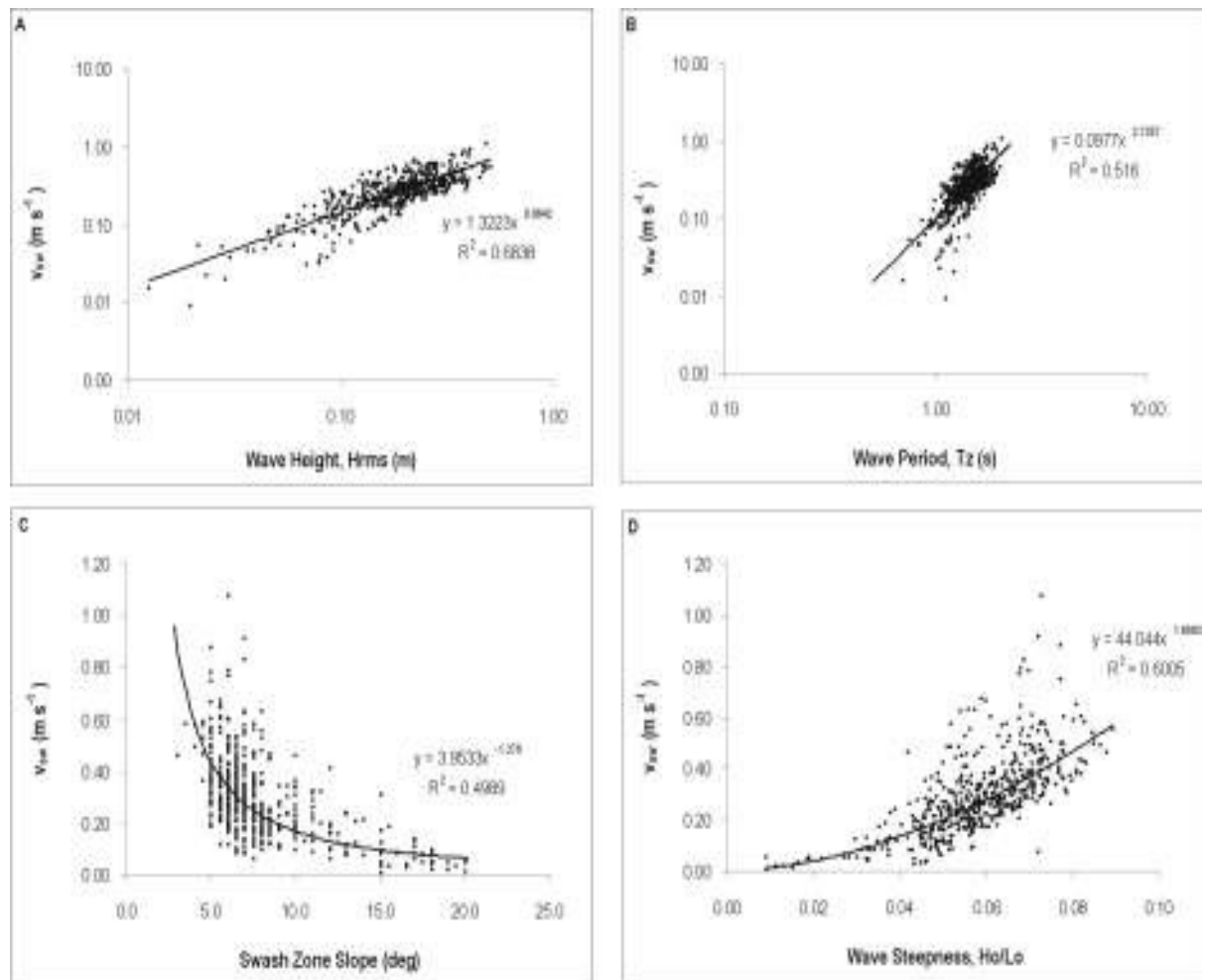


Figure 5.23 Linear Regressions of four environment parameters against the mean swash velocity. (A) Wave height: $r = 0.83$, Std. Err. = 0.16, $F = 1061$. (B) Wave Period: $r = 0.72$, Std. Err. = 0.19, $F = 526$. (C) Swash Zone Slope: $r = 0.71$, Std. Err. = 0.20, $F = 489$. (D) Wave Steepness: $r = 0.77$, Std. Err. = 0.18, $F = 738$.

The relationship with the slope is particularly interesting. It was noted above that there was only a small difference between the mean swash and backswash velocities and that this asymmetry was more apparent in low energy conditions. When the swash and backswash velocities are plotted against the slope angles, one reason for the asymmetry becomes apparent. In Figure 5.24 it can be seen that the swash flow dominates at slope angles over 10.0° . As discussed in the Section 5.3, at the onset of wave activity the foreshore is often steep and the beach water table is low, creating a highly porous foreshore. As the swash runs up the slope it is quickly absorbed into the sediments and the return backswash flow is much reduced. Table 5.6 lists the differences between the two flow directions through the range of slope angles. It will be noted that there is marked reduction in the swash velocity with increasing slope angle, as indicated by the regression analysis (Figure 5.23c). At slope angles up to 5° , the swash velocity is higher than the backswash flow. It was often observed that when the swash zone had been scoured down, the run-up would swirl around the upper swash zone before turning downslope.

The low slope angle does not provide the gravitational impetus to accelerate the reverse flow rapidly. Thus, the incoming incident wave energy is able to translate into swash without a great deal of interference with the backswash. This leads to high average velocities in the swash zone at low slope angles due directly to the wave height. At slope angles between $6\text{--}10^\circ$, the swash velocities decline slightly due to turbulence in the swash zone.

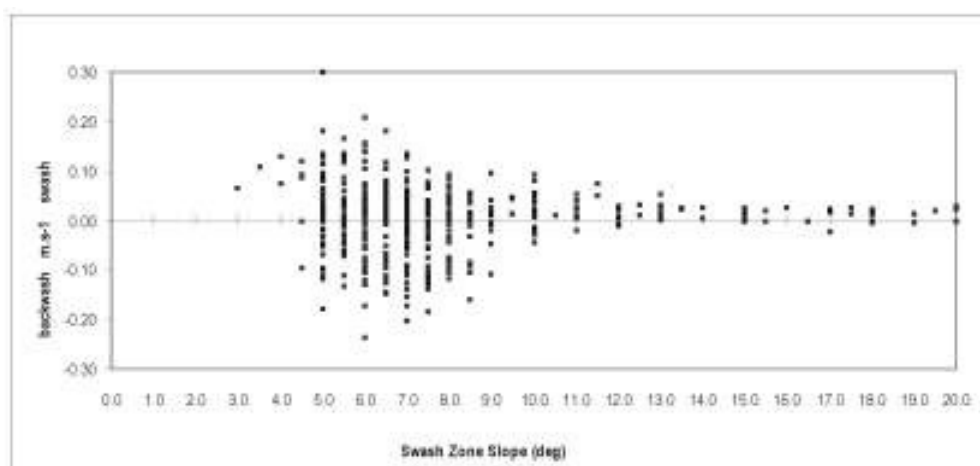


Figure 5.24 Scatter plot of the relative difference between the swash and backswash velocity plotted as a function of the swash zone slope. Each point represents the mean hourly difference. At higher slope angles, the swash flow dominates. When slope angles drop below 10° , the asymmetry between swash and backswash disappears. $n = 493$.

Table 5.6 List of the mean differences between the swash and backswash in the different slope classes.

Slope (deg)	mean swash m s^{-1}	mean backswash m s^{-1}	difference m s^{-1}
< 5	0.434	0.369	0.06
5.00	0.371	0.352	0.02
6.00	0.323	0.313	0.01
7.00	0.290	0.303	-0.01
8.00	0.250	0.251	0.00
9.00	0.194	0.184	0.01
> 10	0.152	0.135	0.02

At slopes between 6° and 10° the relative differences between the swash and backswash become negligible, but overall the velocities decline with increasing slope. As the wave energy increases, the foreshore slope is scoured down and the swash zone begins to develop an equilibrium with the conditions. In these transitional phases there is often a great deal of water in the swash zone, causing it to become turbulent and saturated. Kirk (1970; 1975) observed that in

these conditions backwash may dominate the flow field because, the large quantities of water being pitched forward from the breaking wave are unable to percolate into the foreshore. Therefore, the water remains on the surface of the swash zone and under the influence of gravity, recycles back downslope creating a strong flow of water that interferes with the incoming swash. Effectively, the backwash has the opportunity to develop without being reduced by environment variables such as porosity acting to soak up the swash energy. At the same time the incoming swash flow is reduced by interference from the backwash. Thus, the relative difference between the two phases is reduced and at the same time the average swash/backwash velocities decline due to turbulence. In Table 5.6, it can be seen that at slope angles of 7° , the average backwash velocity was higher than the swash velocity. Above 10° the mean swash/backwash velocities decline further and the relative difference between the two flows again becomes pronounced. The swash becomes slightly faster than the backwash and the flows become more asymmetric. High slope angles are usually associated with lower energy conditions and higher sediment porosity, causing a reduction in the backwash flow and the average velocity rates. This is illustrated in Figure 5.25 that shows a plot of the difference between the mean hourly swash and backwash against the wave height. Swash dominates the backwash when wave heights are below 0.10 m, but above 0.10 m the differences even out.

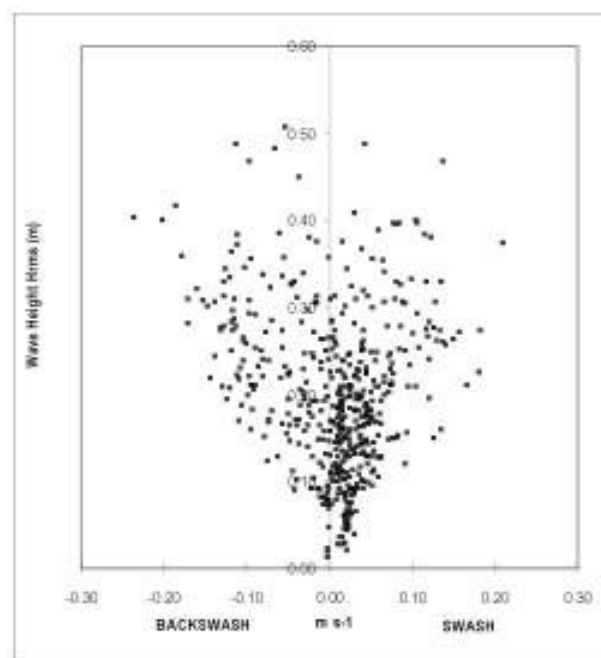


Figure 5.25 Scatter plot of the relative difference between the swash and backwash velocity plotted as a function of the wave height (y-axis). Each point represents the mean hourly difference. At wave heights below 0.10 m the swash flows are slightly faster than the backwash flows. Above 0.10m the differences even out. $n = 493$.

Kirk (1975) found a pronounced negative relationship between increasing wave energy and declining swash velocity. It was demonstrated that only a percentage of the wave energy was translated into swash and that this percentage declined with increasing wave height. In low energy conditions it was found that up to 60% of the wave energy becomes swash. As the wave energy increased this dropped to as low as 20%. Effectively the conversion of the breaker into swash becomes less efficient at higher wave energies due to high turbulence in the swash zone and there is a corresponding drop in the swash velocity. Figure 5.26 shows the wave energy correlated against the relative swash velocity. It can be seen that there is an upward trending relationship between the two variables in the same manner as the wave height regression. The relationship is not as strong as with the wave height because it is a relative velocity. It indicates that other variables, such as the beach slope described above, are also significant in the swash velocity equation. This is the opposite of the relationship found by Kirk (1975: Fig. 7) and again highlights the equilibrium differences between open coast and sheltered lake beaches. In a lake wave conditions can have a zero state. Thus, at the onset of wave activity there is a strong link between increasing wave height and swash velocity. As the foreshore responds to this activity it becomes scoured down. This transition stage can be turbulent and can effect swash velocities in the same manner described above. Once the waves reach a maximum, the swash zone attains a gentle slope and develops an equilibrium with the conditions.

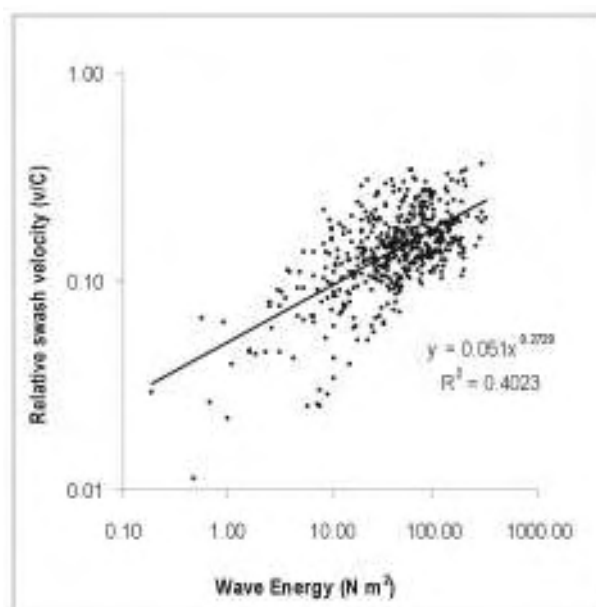


Figure 5.26 Regression of wave energy against mean relative swash velocity (v/C), where C is the Airy wave celerity. Swash velocity generally increases with the wave energy, despite the swash zone becoming more chaotic in these conditions.

A possible explanation for the lack of any significant difference between the relative swash and backswash velocities when the swash zone is developed, may be due to the ability of deep water waves in a lake to approach very close to shore with little modification. In Chapter Two, the wind regime of Lake Coleridge was identified as being bi-directional between the northwest and southeast. The field site was located on the long axial shore of the lake, allowing waves to approach the shoreline at very oblique angles. Figure 5.26 is a plot showing the mean swash velocity against the swash angles. It can be seen that a wide range of angles were measured, from 5° to 80° . It shows a wide scatter in the swash velocities across the full range of angles, but there is an observable increase in the upper range of velocities as the wave angle increases. This is because the highest energy wave conditions occurred when the winds were blowing down the long axis of the lake, parallel to the shoreline. In these conditions it was often observed that the swash did not reduce to zero velocity at the top of the flow, but maintained some momentum before flowing back downslope. There was a strong longshore directed component of the swash current due to high wave angles that experienced little refraction and modification across the nearshore zone. This was also observed by Worthington (1989) in Lake Coleridge, who noted that as the wave angle increased, the shape of the swash lens was skewed in a longshore direction. Swash is often thought to flow on an angle upslope, and in a straight line downslope to form a zigzag pattern. In Lake Coleridge it was more often observed flowing in a parabolic curve across the swash zone. As the wave angle increased, the curve became flatter and more longshore in direction. Therefore, the backswash flow often retained a component of momentum from the swash as it arced in a low parabolic curve across the shore. This generated high flow velocities in the longshore direction in both the swash and backswash. This may explain the strong relationship between the two flows seen in Figure 5.21 and the similarity in the velocities across a wide range of conditions.

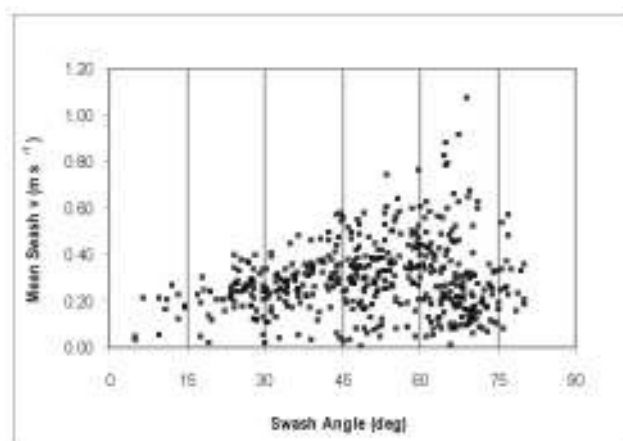


Figure 5.26 Plot of the mean swash velocity against the swash angle.

Swash Phase

Knowing the relationship between wave height and wave period is important for understanding how a shoreline responds to variations in deep water wave conditions. Relationships between the wave height, period and beach slope have been formalised in expressions such as the wave steepness and breaker criteria such as the Iribarren number. Kemp (1960; 1963) and Kemp and Plinston (1968) investigated the relationships between the surf and swash zone in coarse grained beaches that involved work in both the laboratory and the field. Kemp found that the difference between the incident wave period and the swash period was critical for controlling the hydrodynamic conditions in the swash zone and the morphological response of the foreshore. Kemp referred to this as the ‘phase difference’ and showed that it could determine whether a beach would erode or accrete. If the period of the swash run-up and run-down is equal to the wave period, the conditions are ‘in phase’ and the swash is able to drain off the foreshore before the arrival of another wave. In these conditions, it was demonstrated that the swash could attain maximum velocities without interference with other swash bores, leading to lower turbulence and deposition in the swash zone. By contrast, when the swash period is longer than the wave period, the swash zone is ‘out of phase’ with the wave conditions. In this situation the swash cannot drain off the foreshore before the following wave arrives and the two bores collide causing high turbulence and enhanced erosion of the foreshore. Kemp formalised this concept with an expression to derive the swash period:

$$t = \frac{2l}{(kgH_b)^{0.5}} \quad (5.13)$$

Where l is the swash length, g is acceleration due to gravity, H_b is the breaker height and k is an empirically derived coefficient that as discussed previously, was calculated at 1.33 for the Lake Coleridge data set. Kirk (1975) determined a value for k of 1.28 from swash zone measurements in the mixed sand and gravel beaches at Kaikoura. The phase is then taken as the ratio between swash period and the incident wave period (t/T). When conditions are in phase, the ratio is $t/T < 0.6$ and conditions are conducive to deposition. Intermediate conditions occur between $0.6 < t/T < 1.0$. High phase or erosive conditions occur with ratios $t/T > 1.0$.

Observations made throughout the field programme indicated that the conditions in the swash zone were almost always out of phase. There were only two conditions in which the swash was observed to be in phase. When waves of very low amplitude broke onto a steep foreshore that rapidly absorbed swash through percolation, or when the swash zone was fully developed and wave conditions were diminishing at the end of a wind-wave event. In this situation the swash

zone was still saturated, but under declining wave activity there was less turbulence in the swash zone and swash was able to run-up the shore with less hindrance. Throughout the discussion in this chapter it has been shown that these two conditions represent that the equilibrium end points in the stages that the swash zone progresses through as it develops in response to wave activity.

Using Kemp's equation for the swash period, an average value of 1.74 s was calculated for the Lake Coleridge data set. This figure produces an average phase ratio of 1.22. That is, the swash period was on average 22% longer than the wave period and conditions were out of phase. Observations suggested that the swash period was longer than this and it is felt that Equation 5.13 under-estimated the conditions in Lake Coleridge. A crude estimate of the swash period can be calculated by using the measured swash zone widths and velocities. Taking a distance of two thirds the width of the swash zone and assuming that one third of the swash excursions exceeded this limit, a significant swash length can be derived for each hour. Multiplying this length by two and dividing it by the measured swash velocity, an estimate of the swash period can be derived:

$$t = \frac{2(0.66X_{sw})}{v_{sw}} \quad (5.14)$$

Where X_{sw} is the measured width of the swash zone and v_{sw} is the maximum swash velocity. The swash period estimates range from 1.0 s to 6.0 s, with an average of 2.67 s. This produces an average phase ratio of 1.86, that appears reasonable when compared to observations. This indicates that the swash period was on average 86% longer than the wave period and that conditions were typically out of phase.

Figure 5.27 is a plot of the phase conditions calculated with Equation 5.14 against the mean swash velocity. It indicates that conditions were almost entirely transitional (0.6-1.0) or out of phase (> 1.0). There is a enormous scatter across the range, but there is a general indication that the highest swash velocities were associated with lower conditions of phase. The highest swash velocities were recorded when the swash zone slopes were at the their lowest, broadly confirming the visual observations discussed above. The other situation in which low phase conditions were observed was when the wave heights were low and the foreshore slopes were steep. Again, there is a wide scatter of values, but it can be seen that there is a small cluster of data points at low phase when the swash velocities are low.

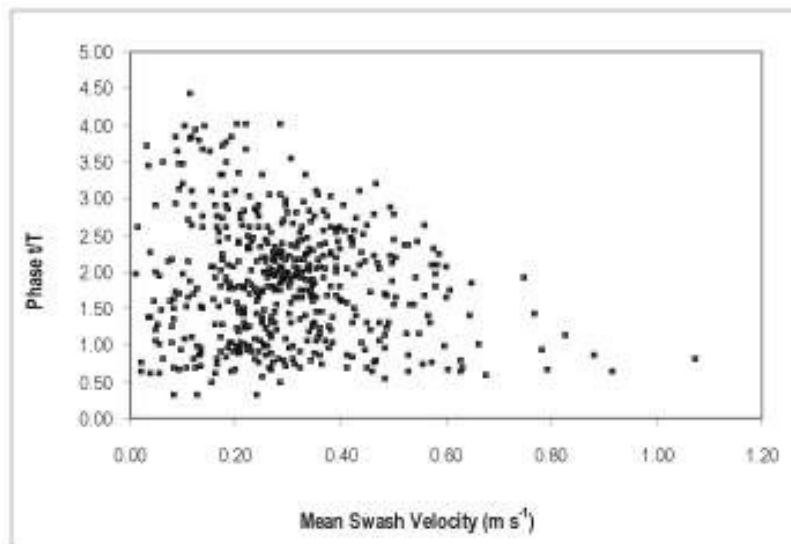


Figure 5.27 Relationship between mean swash velocity and swash phase. Conditions were rarely in phase, but there is a general trend of higher swash velocities at lower phase ratios.

The swash period in Lake Coleridge was almost always out of phase with the wave period, indicating that in the swash zone, conditions were most commonly erosional. This is because there is such a small range wave periods in a small lake environment, that break continually at the shore every 1-3 s creating a continual series of colliding swash bores that frequently do not clear the foreshore before the arrival of another wave. In fact, it was noted by Kirk (1975) that ‘in phase’ conditions were rarely observed in natural beaches. In Lake Coleridge, worsening phase conditions did not appear to greatly increase the turbulence of the swash zone, indicating that other environmental variables (H_s , T_z , S , Ho/Lo) are more important than the phase in controlling the swash velocity. Whilst the idea of the phase difference is a useful concept in theory, it is a difficult parameter to quantify. There is a great deal of variability in incident wave energy and conditions may move in and out of phase for short periods of time throughout the duration of a wind-wave event. Swash zone conditions are primarily controlled by the wave height and using this to define the processes and geomorphologic responses is both more certain and practical. Phase differences may produce short term variations in the transport rate over individual swash events, but over a period of hours these variations will be masked by the average conditions. Further research in this area would require detailed measurements of individual swash bores coupled with measurements of sediment transport and breaker conditions. Kirk (1975) made similar conclusions after testing the model against field data collected from the open coast mixed sand and gravel beaches at Kaikoura, but noted that it warranted further investigation.

Swash Velocity Equations

An equation to estimate the swash zone velocity would prove extremely useful for mixed sand and gravel beach applications. Linear wave theory is often extended into depth limited conditions where the general phase velocity expression reduces to:

$$C_s = \sqrt{gh} \quad (\text{m s}^{-1}) \quad (5.15)$$

Where C_s is the shallow water phase velocity, g is gravitational acceleration and h is the water depth at the point of interest. The velocity becomes dependent purely on the depth of water and the acceleration due to gravity. In the last chapter good agreement was found between the Linear approximations of wave celerity and the measured speeds. In a swash zone there is a component of kinetic energy from wave breaking that provides an extra energy input that needs to be taken into account. Depth measurements across the swash zone were not made in this study, but the water depth at the base of the swash zone is equivalent to the breaker wave height. Substituting this value into the equation it may be assumed that this provides an estimate of the maximum velocity after wave breaking. This approach was taken by Lorang (2000), in estimating the maximum velocity of the swash bore immediately after breaking on a boulder beach. Using the breaker height derived from Equation 4.12, the equation takes the form:

$$v_{sw} = \sqrt{gH_b} \quad (\text{m s}^{-1}) \quad (5.16)$$

The equation produces values that range from 0.52 to 2.93 m s⁻¹, with an average of 1.58 m s⁻¹. By comparison, the maximum swash velocities measured in the swash zone, range from 0.03 to 2.48 m s⁻¹, with an average of 0.98 m s⁻¹. The measured velocities are slightly lower, as might be expected, because they were sampled at a distance approximately one third the width of the swash zone in front of the breaking wave. As discussed previously, only a percentage of the wave energy is converted into swash flow. Kirk (1975) showed that, depending on the conditions, this conversion diverged widely from 20-60%. Analysing the residuals between the hourly measurements and the estimated values, reveals that on average the velocity reduction from the breaking wave to the point of measurement is in the order of 50%. When the residuals between the mean swash velocities and the values from Equation 5.16 are analysed, this reduction increases to around 85%. A correlation between the measured maximum swash velocities and Equation 5.16 (using the H_b wave height as the water depth) can be seen in Figure 5.28. There is a strong relationship with the measured values, illustrating the controlling influence of the wave height on the swash velocity.

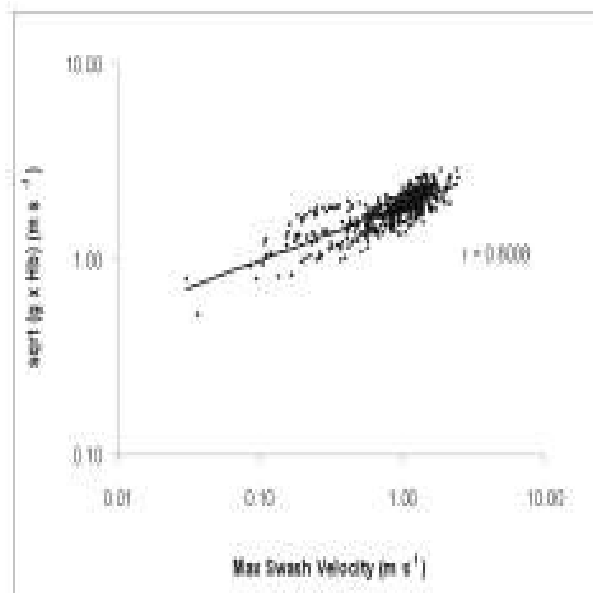


Figure 5.28 Correlation between maximum swash zone velocities and Equation 5.16, using H_b as the water depth. $F = 877$, Std. Error = 0.06, Sig. $P < 0.0001$.

Wave energy is proportional to the square of the wave height, so as wave amplitude declines, there is rapid decrease in the available energy for forward swash momentum. Novak (1972) suggested that low amplitude waves expended more of this energy on internal turbulence than in forward motion, because the swash is of such small volume and depth. Other factors inherent to coarse grained beaches, such as sediment roughness and porosity, serve to further reduce swash velocity. Clearly, a great deal of energy is dissipated through wave breaking and further reduced by turbulence in the swash zone.

In the discussion of the preceding section it was demonstrated that only a portion of the wave energy is converted into swash energy and that other factors such as sediment porosity and beach slope act to absorb some energy. Recognising this Kemp (1960) developed an equation that estimates the phase difference at a given point from the breaking wave. It is a derivation of the Linear celerity equation that includes a coefficient to take account of energy dissipation after wave breaking:

$$C_x = \sqrt{kgH_b \left(1 - \frac{x}{l}\right)} \quad (\text{m s}^{-1}) \quad (5.17)$$

Where k is the empirical coefficient from Equation (5.13) calculated as 1.33, H_b is the breaker height, l is the swash length and x is the distance landward from the breaker to the point of interest. Taking this distance to be the location of the Marsh-McBirney current meter, the

equation can be used to calculate the maximum measured velocities in the swash zone. The calculated values range from 0.35 to 1.94 , with an average of 1.23 m s⁻¹, which is higher than measured range, but within the same magnitude. The equation has the same correlation coefficient as Equation 5.16, as seen in Figure 5.28.

Taking into consideration the analysis and discussion of the previous sections it is clear that the wave height is the most important environmental parameter providing energy for generating swash currents in the foreshore. The wave period is also important, as it characterises aspects of the wave such as steepness. Using these two parameters to form a ratio of wave height over period produces an expression that gives an indication of the wave speed. The square root of this ratio provides a close estimate of the mean horizontal velocity in the swash zone (\bar{v}_{sw}):

$$\bar{v}_{sw} = k \sqrt{\frac{H_{rms}}{T_z}} \quad \text{m s}^{-1} \quad (5.18)$$

The H_{rms} wave height is a de facto measure of the water depth at the base of the swash zone and provides better correlations with the data than the estimated breaker depth. The calibration coefficient k is 0.78 and has units of m^{1/2} s^{-1/2} in order to make the equation dimensionally correct. The equation produces values that range from 0.10 to 0.40 m s⁻¹, with an average of 0.28 m s⁻¹. This is a good estimate for over 90% of the measured range but does not predict the extreme values at either the high or low end. The measured swash means range from 0.01 to 1.07 m s⁻¹, with a mean of 0.29 m s⁻¹, but 98% of this range occurs below 0.60 m s⁻¹. Figure 5.29 is a regression between the measured and predicted values. It shows a strong correlation with the data. It recognises that as the energy conditions rise, the swash velocities will increase in response to the wave height. The wave shape or the steepness provides an indication of the energy conditions, and using the wave period recognises this. In Lake Coleridge, high energy conditions are associated with steep waves, thus as the ratio becomes larger, the velocities increase. Using the square root recognises that at the onset of wave activity, there is an initial rapid increase or jump in energy conditions from zero, after which the energy conditions increase at a lesser rate. This suits a lake environment very well in which many relationships with wave energy display a logarithmic relationship. This is reflected in the forecast curves, that can be seen in Figure 5.30. The forecast estimates appear reasonable, indicating that this expression may have wider application to other low energy, coarse grained beaches. The equation is valid for range of $T < 3.0$ s and $H_s < 1.0$ m.

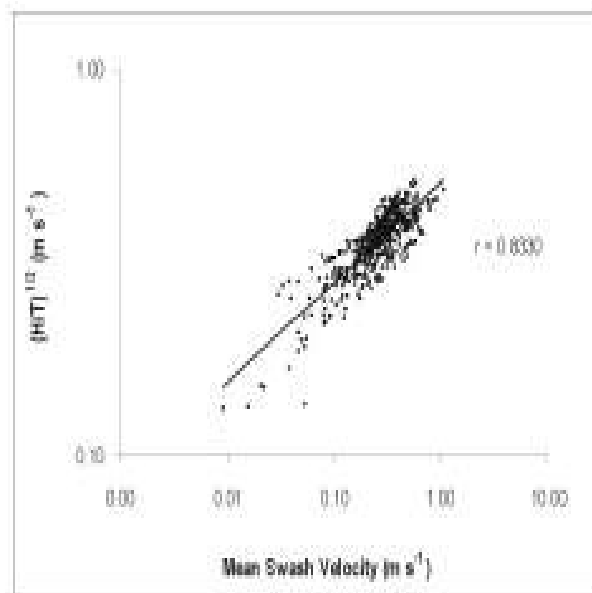


Figure 5.29 Correlation between mean swash velocity and Equation 5.18. $F = 1113$, Std. Error, 0.05, Sig. $P < 0.0001$.

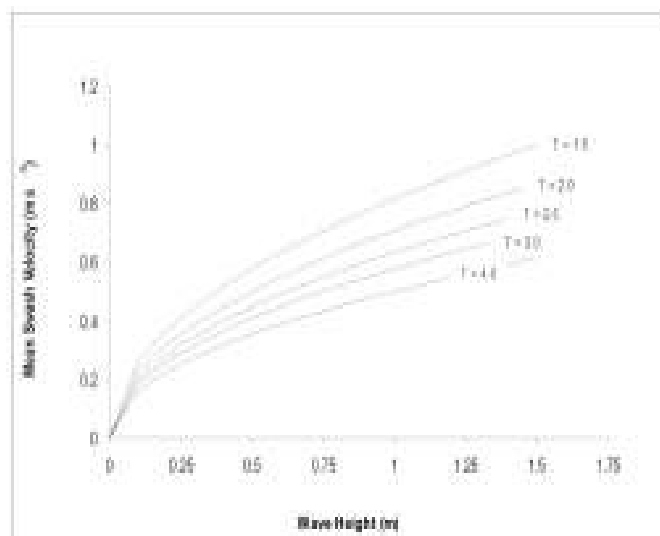


Figure 5.30 Forecast curves of mean swash velocity using Equation 5.18. The equation indicates that there is a logarithmic increase in swash velocity as the wave height increases. The equation also predicts higher velocities with shorter wave periods and steeper waves.

It was recognised that the beach slope also provided a good indication of the equilibrium conditions in the swash zone. Extreme high and low slopes are associated with equilibrium conditions, whilst intermediate slopes are an indication of transitional conditions. Figure 5.23c and Table 5.6 showed that as the beach slope increased, the swash velocity declined due to

turbulent swash conditions and greater porosity effects at higher slope angles. An expression that shows some promise in estimating the maximum velocities, takes Equation 5.18 as a ratio with the beach slope. This recognises the relationships discussed above and takes into account the effects of beach porosity at higher slope angles. This is also a de facto measure for the grain size or the frictional roughness of the beach, as coarse grained particles can attain steeper beach slope angles than finer particles. Two forms of the equation have been developed, one is the general expression, that provides the maximum velocities (v_{sw}) and the second is the mean expression (\bar{v}_{sw}) that requires an empirical coefficient:

$$v_{sw} = \sqrt{\frac{H_{rms}/T_z}{\tan \beta}} \quad (5.19a)$$

$$\bar{v}_{sw} = k \sqrt{\frac{H_{rms}/T_z}{\tan \beta}} \quad (\text{m s}^{-1}) \quad (5.19b)$$

The equations perform well across the range of conditions. A summary of the estimates is presented in Table 5.7, that also includes summary statistics for Equations 5.16-5.18. A graphical comparison of the maximum measured and estimated swash velocities is presented in Figure 5.31. It highlights the rapid dissipation of energy from the breaking wave into the swash zone. Equation 5.19a produces maximum velocities that range from 0.22 to 1.75, with a mean of 1.03. This compares favourably with the mean maximum swash velocity measured in Lake Coleridge of 0.98 m s^{-1} . Although it is not dimensionally correct, this can be rectified by multiplying the equation through by $1 \text{ m}^{1/2} \text{ s}^{-1/2}$. The equation does not estimate the extreme minimum ($< 0.20 \text{ m s}^{-1}$) or maximum ($> 1.80 \text{ m s}^{-1}$) recorded values, that account for 6% of the data in the tails of the distribution. Empirically measured data sets of the natural environment often contain outliers at the extreme ends of the distribution that are not easily predicted by mathematical models (Zar, 1984). The standard deviation of the measured maximums is 0.47 and the variance is 0.22, indicating considerable variability in the data. The k coefficient in Equation 5.19b was calculated from a residual analysis to be 0.27 and has units of $\text{m}^{1/2} \text{ s}^{-1/2}$ in order to make the equation dimensionally correct.. This modifies the general expression to take account for local limiting variations to produce an expression that gives a mean horizontal velocity in the swash zone. This indicates that the mean swash zone velocities are around 75% less than the maximum velocities in the breaking wave. Reassuringly, this is similar to the reduction calculated with the Linear wave celerity equation, which was in the order of 85%. Figure 5.32 shows the correlation between the measured and the predicted values ($r = 0.80$). The data values are evenly spread around the best-fit line, but some overestimation can be seen at the lowest end of the range. The forecast curves are presented in Figure 5.33. Again, the estimates appear reasonable and it is felt

that the expression warrants further testing. At this stage it is valid for low energy, coarse grained beaches in the range of $T < 3.0$ s and $H_s < 1.0$ m.

Table 5.7 Summary statistics from swash velocity equations compared with measured swash velocities.

m s ⁻¹	Measured Mean	Eqtn. 5.19b	Measured Maximum	Linear Max Eqtn. 5.16	Kemp Eqtn 5.17	Eqtn. 5.19a
Min	0.01	0.06	0.03	0.52	0.35	0.22
Max	1.07	0.47	2.48	2.93	1.94	1.75
Mean	0.29	0.28	0.98	1.85	1.23	1.03
Std. Dev.	0.15	0.08	0.47	0.26	0.26	0.29
Skewness	0.98	-0.43	0.12	0.12	-0.16	-0.43
Kurtosis	2.06	-0.10	-0.25	-0.24	0.02	-0.10
Variance	0.02	0.01	0.22	0.07	0.07	0.09

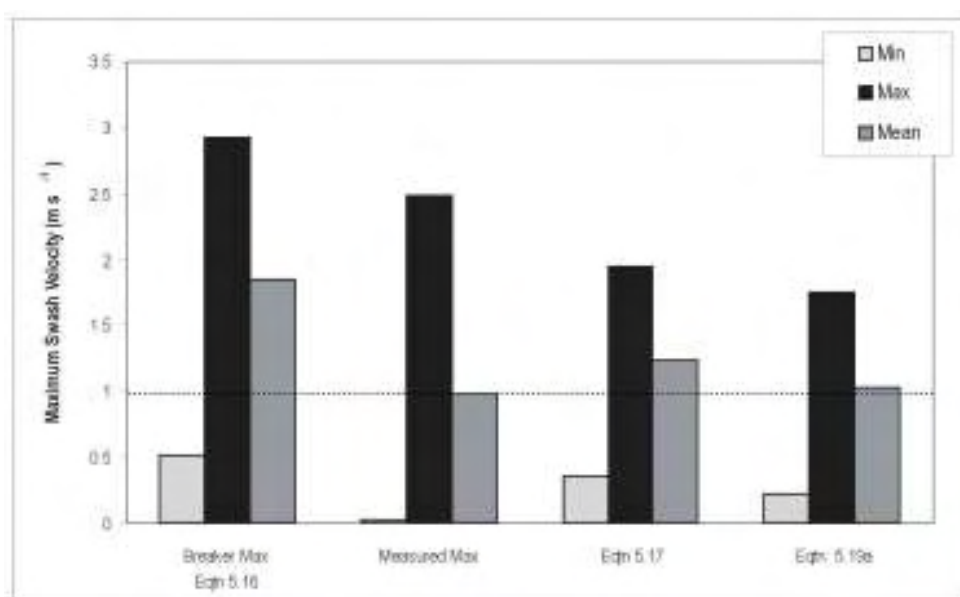


Figure 5.31 Comparison between maximum swash velocities measured in Lake Coleridge and the estimated values from three equations. Equation 5.16, on the left, is the maximum estimated velocity in the breaking wave. It can be seen that the velocity reduction from the breaking wave to the swash zone is rapid Equation 5.19a shows good agreement with the measured values.

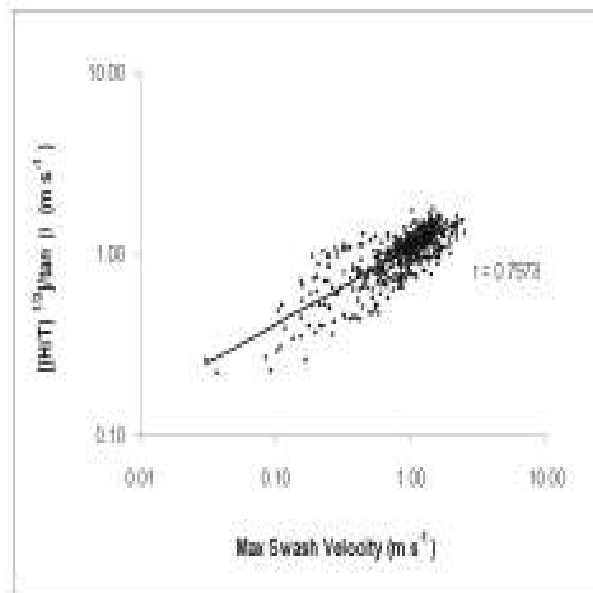


Figure 5.32 Correlation between maximum measured swash velocities and the velocities estimated by Equation 5.19a. $F = 856$, Std. Error = 0.09, Sig. $P < 0.0001$.

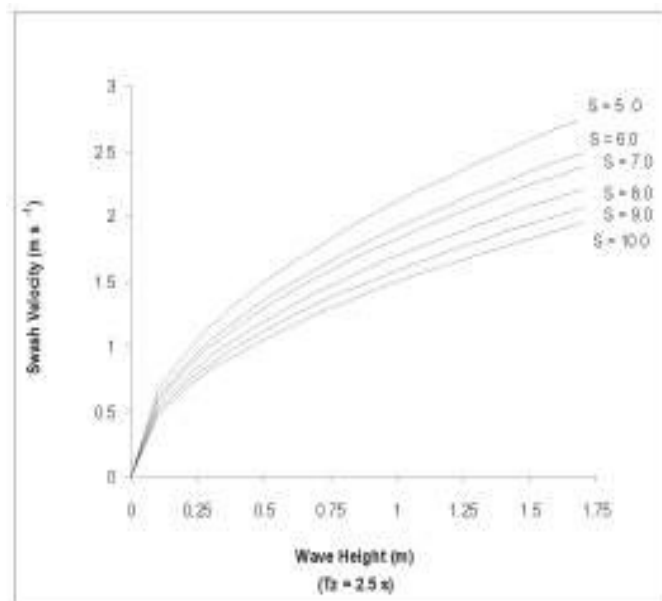


Figure 5.33 Forecast curves of mean swash velocity using Equation 5.19a. The equation indicates that there is a logarithmic increase in swash velocity as the wave height increases and slope angle decreases. The curves were calculated with a wave period of 2.5 s.

5.6 Swash Zone Process-Response Model

Drawing together the findings discussed in this chapter, a model has been developed to illustrate the morphodynamic development of the swash zone in response to wave activity (Figure 5.34). It shows the equilibrium stages the swash zone experiences with changing energy conditions. It is important to note that this is a short term dynamic equilibrium in which the foreshore slope forms a balance with the prevailing wave and swash forces. When $t = 0$ there is little or no wave activity. At this stage the foreshore is steep ($> 10^\circ$) and the swash zone is undeveloped. Low amplitude waves are quickly absorbed into the highly porous sediments and the swash may attain low phase with the wave period. This limits the run-up heights and the swash velocities remain low. At $t = 0.5$ the swash zone is transitional between zero stage and full development. In this stage, the foreshore responds rapidly to increasing wave energy conditions. Wave heights are in the order of 0.25-0.40 m. The swash zone widens landward and lakeward as it is scoured down. Sediment transport rates increase rapidly as the sediment is mobilised. Run-up elevations reach maximum height as the foreshore becomes saturated with water, whilst slopes remain moderate. Current velocities increase quickly but the swash becomes hindered in the turbulent conditions, that remains out of phase with the wave period. When $t = 1$ the swash zone develops an equilibrium with the conditions. At this stage it gains maximum widths of over 5.0 m and swash velocities are capable of reaching maximum speeds. The width that the swash zone attains in this stage depends on the wave heights, that are in the order of 0.50 m or greater. Run-up heights decrease, as the foreshore slope grades to below 5° .

Conditions in Lake Coleridge were most commonly found to be transitional. Importantly, the foreshore was always observed to enter a transitional phase when the wave energy conditions increased. However, the foreshore did not always develop a full end stage equilibrium as wind was often inconsistent. Thus, the foreshore was often seen to be in a state of flux with intermediate wave heights. When the conditions eased, the foreshore quickly reverted to the low energy equilibrium state. In the declining energy conditions after a storm event that had seen a fully developed swash zone, whether the swash zone entered the transitional stage, depended on how quickly the waves eased. If wave heights diminished but did not cease, the swash zone was observed to re-enter the transitional phase. If the wind completely ceased, the swash zone quickly attained a new equilibrium, with little transition, to the lower wave energy. With declining wave energy the transitional stage was often shorter in duration, as conditions tend to diminish quickly when wind speeds slacken. However, there were occasions when the swash zone fully developed from a zero state in as little as 2 hours. With respect to Kemps phase

model, the swash and wave period were found to be out of phase at all stages of swash zone development, but broadly it was observed that in phase conditions only occurred at times when the beach had developed an equilibrium with the conditions, *i.e.* at $t=0$ or $t=1$. This model has implications for lakeshore management because it indicates that the times of greatest shoreline change will occur in a stage of transition when erosion rates and run-up heights will be at their greatest.

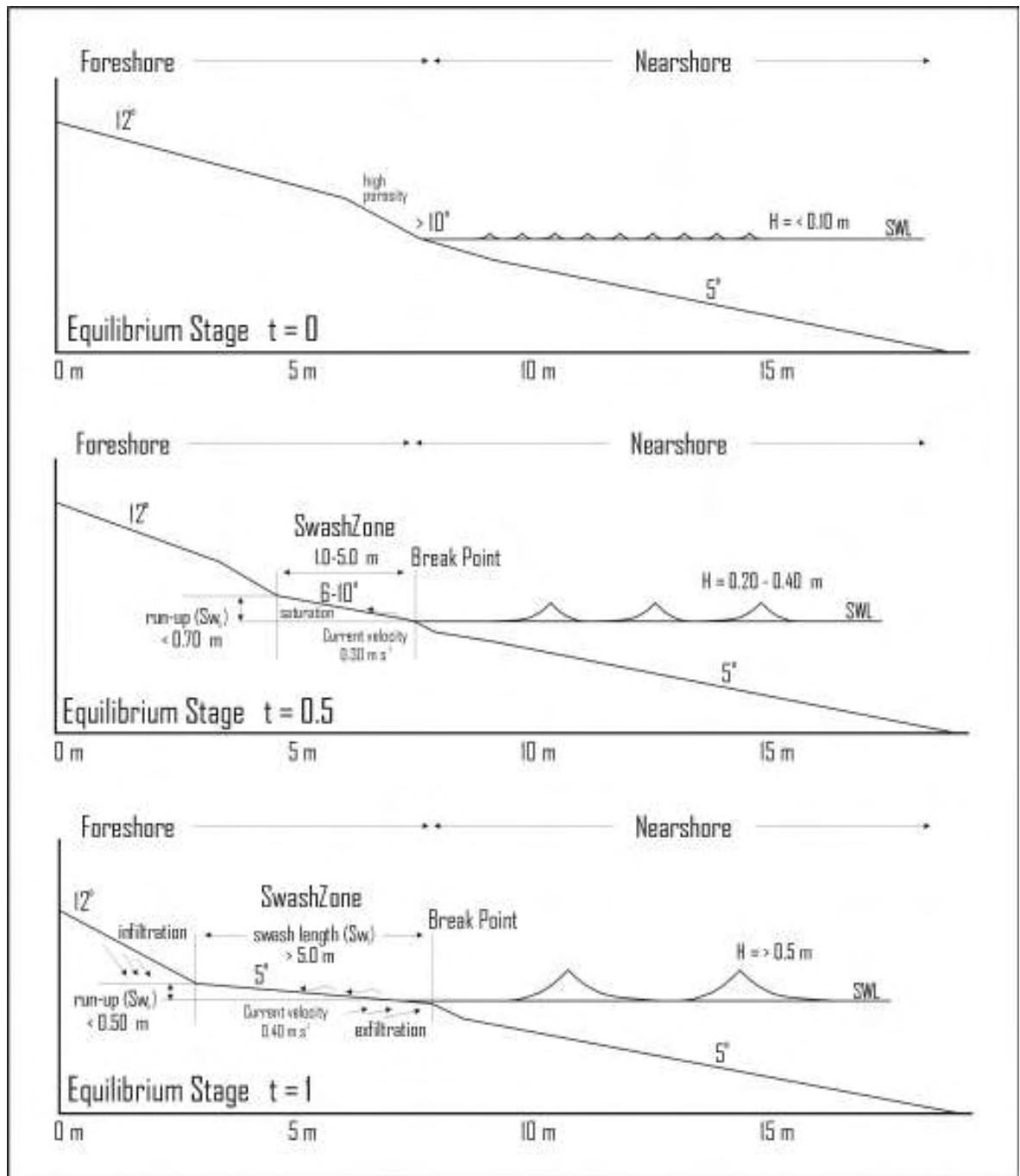


Figure 5.34 Morphodynamic process-response model of swash zone development. The swash zone exhibits three general stages, a zero state with little or no wave activity, a fully developed state at high wave energy and a transitional stage between the two end points.

5.7 Summary

This chapter has presented results and discussion of the first in-depth investigation into swash zone processes on a mixed sand and gravel lakeshore beach in New Zealand. The swash zone is effectively the ‘cutting edge’ between a body of water that experiences wave activity and the terrestrial environment. It is an especially important element of a mixed sand and gravel beach because it is the area that dissipates wave energy. As the swash zone absorbs this wave energy, sediment is entrained and processes of erosion and accretion determine whether the beach will retreat landward or prograde outward. Despite the importance of the swash zone in coarse grained beaches, it was noted that until recently it has largely been overlooked by research. Part of the reason for this stems from the difficulty of making measurements from the highly turbulent area forward of the breaking wave. Recent advances in scientific instrumentation have opened up new possibilities for research in coastal applications, but the swash zone remains a punishing environment for equipment. This has limited the quality of the data that can be collected from the swash zone. Many of these difficulties were overcome in the present by conducting the research on a lakeshore. Four new equations were presented that may be used to estimate the swash zone width, run-up elevation and mean and maximum swash velocity. A new swash zone morphodynamic model was developed that links foreshore response to these processes.

Wave energy governs many of the processes that occur in the foreshore. It was demonstrated in this chapter that it determines the width, the swash length, the run-up elevation and the current velocities that occur in the swash zone. It was found that the mixed sand and gravel beaches in Lake Coleridge display many similar process characteristics to their open coast counterparts. Some of the findings by Kirk (1970) regarding the swash zone of an oceanic mixed sand and gravel beach, were valid for the relatively lower energy lakeshore environment. Thus, findings from the present study may have wider applicability oceanic mixed sand and gravel beaches.

Many studies from open coast beaches are limited in their application to light or moderate energy conditions. Although Lake Coleridge is a low energy wave environment, the measurements cover the full range of conditions. Foreshore response to changing energy levels has been recorded from the smallest waves through to gale force northwest storm waves. This has offered insights into the equilibrium adjustments that a foreshore makes to varying conditions. There are times in a lakeshore or a sheltered beach environment when the energy conditions are very low or zero. This is not a condition that is frequently experienced in an open

coast beach. In low or zero wave energy conditions, the swash zone is undeveloped and the foreshore sediments often sit near the angle of repose. At the onset of wave activity, the foreshore quickly responds to the energy input and the swash zone begins a transitional phase as it develops a new equilibrium. A new lakeshore process-response model was presented, based on field observations and measurements from the swash zone, that formalises the equilibrium stages that a foreshore progresses through in response to wave activity.

The swash zone widened landward in response to increased wave height and lakeward in response to the wave length, as waves broke in deeper water. The swash zone ranged in width from 0.05 m to 6.0 m. It was found that the width of the swash zone was largely determined by the wave height. The slope of the swash zone was found to be an important secondary control on the width. An equation was developed, using these two variables, that estimates well the width of the swash zone under the full range of conditions experienced in Lake Coleridge. It was shown that at high slope angles the wave conditions are usually light. As the wave energy increases, the swash zone begins to be scoured by swash activity and the beach slope grades down. Thus, in a lake there is a negative relationship between beach slope and swash width.

The run-up heights were able to be calculated with the swash zone width and slope angle. Run-up elevations ranged from 0.01 m to 0.73 m and were found to be strongly related to the wave height and the beach slope. In general there was a negative relationship with the beach slope, in that the run-up increased as beach slopes became lower. A number of run-up equations were tested against the Lake Coleridge data set. The simplest expressions were found to perform better than more complicated equations, that took into account a wider range of environment variables. A common problem with the equations was over-estimating the run-up when slope angles were above 8° . An underlying assumption in these models is that run-up increases with increasing beach slope. In Lake Coleridge, highest run-up elevations were found to occur at intermediate slope angles of between $6-8^{\circ}$. Above 8° , run-up declined in response to beach porosity and lower wave energy conditions. An expression was developed that took account of this difference by making the run-up expression a ratio with the beach slope.

Swash velocities were surprisingly high for a small lake environment. Data was presented from other studies of coarse grained beaches from the open coast. The swash velocities in Lake Coleridge were comparable to beaches of the open coast in low energy conditions. In Lake Coleridge the mean velocities in the swash zone ranged from 0.01 to 1.07 m s^{-1} , with an overall mean value of 0.29 m s^{-1} . The maximum hourly velocities were much greater, averaging 0.98 m

s^{-1} , with a maximum recorded value of 2.48 m s^{-1} . Swash velocities were found to increase as the swash gradient became lower, with maximum velocities at beach slopes of 5° . At these gradients, the swash flow was dominant over the backwash flow. At slopes between 6° and 10° , swash velocities were found to be hindered by turbulence, but the relative differences between the swash and backwash flows were negligible. At slope angles above 10° there is a slight asymmetry to the swash/backwash flow velocities due to beach porosity. Run-up was found to be absorbed into the beach and the backwash flows became reduced. There is a strong link between increasing wave height and swash velocity. Velocities at the point of wave breaking were able to be estimated using the Linear shallow water approximation, in which the water depth was substituted with the breaker height. This produced estimates that ranged from 0.52 to 2.93 m s^{-1} . After breaking, these velocities quickly reduced through dissipation by approximately one half. The mean velocities were found to be in the order 70% less than the maximums. An expression was developed for estimating the mean horizontal velocity in the swash zone taken as, the square root of a ratio between the wave height and the wave period. A second expression was developed for estimating the maximum velocity in the swash zone, that divided the mean equation by the beach slope to account for increasing velocities at lower beach slopes. The resulting values showed strong correlations to the measured swash velocities. Moreover, the expressions have good predictive capability, estimating the extreme values across the full range of conditions measured in Lake Coleridge.

The following chapter introduces results from the sediment transport measurements made in the swash zone and builds on the findings presented in this chapter.

CHAPTER 6.

LONGSHORE SEDIMENT TRANSPORT

“...no claim to a reliable understanding of a natural process can be accepted until it can be explained in terms of basic natural principles...”.
D.L. Inman and R.A. Bagnold (1963: 529)

6.1 Introduction

In Chapter One it was explained that longshore sediment transport is a process that occurs when obliquely angled waves break at a shoreline and entrain sediment in a net direction along the shore. In a mixed sand and gravel beach, because there is no onshore transfer of sediment from the nearshore zone, it is the main process that brings fresh sediment into a beach system. Likewise, it is also the main process that removes sediment, causing a beach to erode. In the last chapter, the importance of the swash zone in a lakeshore mixed sand and gravel beach was established. The swash zone determines the landward and lakeward boundary of the area where sediment transport takes place. Despite the importance of longshore sediment transport to these beach types, very few studies have attempted to make any quantitative measurements of longshore sediment transport. Part of this arises from the difficulty of working in these beaches. This thesis is in part a response to this lack of knowledge about the swash zone transport processes in coarse grained beaches.

This chapter presents the results and a discussion of the sediment transport measurements made in Lake Coleridge. This is the first major study of longshore sediment transport processes on a mixed sand and gravel lakeshore beach in New Zealand. It has required the development of new analytical techniques to calculate sediment trap volumes and to estimate total longshore transport volumes in the swash zone. These new methods are outlined along with the procedures used in the sediments analysis. Important findings regarding the distribution of the longshore sediment transport flux across the swash are presented. Discussion then moves into an analysis of the key environment variables responsible for causing sediment transport. Based on these findings, a first order expression for estimating transport rates in low energy coarse grained beach is presented and a sediment transport budget of the fieldsite beaches is prepared based on calculations with the new expression. As noted in the last chapter, all the wave data used in the analysis is from the wave gauge, unless otherwise stated.

6.2 New Zealand Studies of Longshore Transport in the Swash Zone

Commonly, sediment transport rates are estimated by calculating the volume changes derived from profile surveys. Using this method, one of the few studies of longshore sediment transport was made by Neale (1987), in the mixed sand and gravel beaches of South Canterbury. Through examining a 10 year sequence of beach profile data, Neale determined that long-term fluctuations in the beach volume, causing net growth and retreat of the shoreline, were caused by 'slugs' of material intermittently injected into the foreshore from extreme events such as river floods. Potential rates of longshore sediment transport were estimated by Kirk (1992a) for the mixed sand and gravel beach south of Timaru, by calibrating a one-line shoreline response model using historical shoreline progradation rates. The model estimated net annual accumulation rates in the order of $40,000\text{--}70,000\text{ m}^3\text{ yr}^{-1}$ and mean instantaneous rates in the order of $0.020\text{--}0.025\text{ m s}^{-1}$.

In New Zealand, quantitative measurements of longshore sediment transport in lakeshore mixed sand and gravel beaches have been reported in only two studies. Pickrill (1976) made the first investigation of sediment movements in a New Zealand lake. Pickrill conducted some tracer experiments with natural sediments in 10 beaches on Lakes Te Anau and Manapouri. The in-situ material was first removed, measured, coated with fluorescent dye and placed back in the foreshore. Movement of the sediment was tracked over a period of hours or days, depending on the conditions. The results were mapped onto a plan of the beach to identify the dispersal patterns of different sized material. Experiments were conducted in five sandy beaches, one gravel beach, two lag pavement beaches and two sheltered gravel beaches. Pickrill was interested in the spatial distribution of sediment transport in the nearshore and foreshore of the different beach types. A similar approach was used by Worthington (1989) in four experiments at Lake Coleridge. Worthington tracked some pebble and cobble movements in a gravel beach, a pocket gravel beach, a lag pavement, and a mixed sand and gravel beach. Sediment was removed from the foreshore, measured with callipers and painted with different colours that identified different size grades. The material was placed in a line perpendicular to the foreshore and tracked over period of days. Results were mapped onto a plan view of the beach where rates and directions of movement of individual particles could be analysed. Results from the present study confirm some of Pickrill's and Worthington's findings and will be discussed later in the chapter.

Most studies of sediment transport in the swash zone have focussed on the cross-shore movements. For example, Kirk (1970) made measurements of the transport in the swash and backwash. Kirk's work has been the only study of this kind conducted on an oceanic mixed

sand and gravel beach in New Zealand. Horn and Mason (1994) investigated the relative proportions of bedload and suspended transport in the swash zone on four low sloping sandy beaches around the U.K. Two studies mentioned in the last chapter, Hughes *et al.* (1997) and Hughes and Masselink (1998), investigated sediment transport in individual swash lenses on two coarse grained sandy beaches. In a review of cross-shore sediment transport studies conducted in the swash zone of natural beaches, Butt and Russell (2000: 255) concluded that, "...very few data exist so far". A situation that can be said to apply equally to studies of longshore sediment transport in the swash zone.

6.3 Overview of Sediment Transport Measurements

As discussed in Chapter three, two sediment traps were used in the field studies. One was placed in the foreshore for between 0.5-10 min depending on the strength of the conditions. Most commonly, the trap was in place for 5 min in moderate conditions and 1 min in heavy conditions. On a few occasions the quantity of material moving in the swash zone was so great that 30 seconds was all that was required before the trap reached full capacity (*ca.* 6.0 kg). The weight of material collected ranged from as little as 100 g to as much as 5.5 kg. All the material was retained in the field and placed into bags for laboratory analysis.

Throughout the field study, material moved almost entirely in bedload. Hughes *et al.* (1997), found that in the swash zone, high shear stress values often cause the sediment to move in a sheet flow, whereby the whole bed becomes fluidised and moves in a layer several millimetres thick. This was observed a number of times in high energy conditions, when the swash zone contained large quantities of coarse sand. It has been suggested that the convention of separating the transport into bedload and suspended load is of little use in the swash zone and that it is more convenient to consider the total load under transport (Bailard, 1981; Butt & Russell, 2000). This is certainly the case in the mixed sand and gravel beaches at Lake Coleridge. Unlike the current systems in the nearshore of a sandy beach that may transport sediment for considerable distances, material does not move far in suspension in the swash zone. This is especially true in a small lakeshore swash zone. Any suspended material was quickly dropped as the flow decelerated at the limit of the swash zone. The sediment trap methodology was outlined in Chapter Three. It will be recalled that two trap openings were positioned above the bedload trap to collect any material in suspension. In most conditions these traps collected only trace amounts of sediment. This material was of such low volume that it was not considered to be a significant

part of the transport budget. In high energy conditions, it was not uncommon to have 10-50 g of pebbles and coarse sand in these traps that was flung into the opening whilst in saltation. As the material was moving in the longshore direction, a decision was made to include all this material in the trapped sampled, in effect making it a total longshore rate.

As discussed previously, a trap was also used in the nearshore. It was placed for 10-20 min at a time, at a point behind the breaking wave. It was not always physically possible to take measurements from this area, as it was necessary to hold the trap in high energy conditions. Nevertheless, it was deployed in a range of wave heights up to 0.50 m. The measured longshore transport rates were consistently nil in all but the severest conditions. Trace amounts of fine material was found in the trap in high energy conditions. This largely confirms previous observations that longshore sediment transport takes place forward of the breaking wave and in the swash zone. Further support for this comes from observations of the base plate of the current meter prop that sat flat on the nearshore bed. In sediment transport studies of estuarine environments, rates of deposition are commonly measured with a plate that is placed on the bed and left for a set period of time to accumulate sediment. The base plate of the nearshore current sensor acted in the same fashion, providing an indication of sediment movement. No significant accumulation was ever found on this plate. At times, small amounts of fine material and coarse sand was found, but at no stage was it completely covered with sediment. Similarly, neither was the plate ever found to have been scoured. By contrast, the base plate of the swash zone current meter was regularly scoured or covered by sediment. This indicates that even cross-shore movements of sediment are limited in this area.

In a series of laboratory wave tank experiments, Inman and Bagnold (1963) showed that steep crested waves with a short wave length did not cause a net movement of sediment in the nearshore area behind the breaker. Rather, they merely caused a to-and-fro motion of the sediment. These are the type of waves that were characteristically measured in Lake Coleridge. Underwater observations from the nearshore confirm the assessment of Inman and Bagnold. The velocities measured by the current meter at this point were typically low. As discussed in Chapter Five, the time averaged mean current velocity for the nearshore was 0.15 m s^{-1} . The nearshore sediments were characteristically coarse grained. Clearly the current velocity was not enough to entrain these sediments. Furthermore, on the lag pavements in Lake Coleridge, Worthington (1989) found that the coarser material often moved farther than the finer material, because the small grains became trapped in the interstices of the larger particles. This may partly explain why so little sand movement was detected in the nearshore at Lake Coleridge. In

contrast, on the sandy lakeshore beaches at Lakes Manapouri and Te Anau, Pickrill (1976) reported sand movement in all directions in the nearshore zone.

In general, the nature of longshore sediment transport in Lake Coleridge is very similar to that found in Lakes Te Anau and Manapouri. In the tracer experiments conducted by Pickrill (1976), it was found in the coarse grained beaches, that material moved alongshore in a narrow band approximately 3.0 m wide straddling the mean water level. On average, material was reported to have moved some 2.0-2.5 m landward of the mean water level and 0.5-1.0 m lakeward. Pickrill observed that this movement occurred only under the breaking wave and in the swash zone. This is very similar to the pattern in Lake Coleridge. It will be recalled from Chapter Five that the average width of the swash zone was 2.0-3.0 m and that it widened both landward and lakeward in response to wave activity. During periods of heightened wave activity, sediment is transported in this area in a longshore direction when waves approach oblique to the shoreline. The same pattern was found by Worthington (1989) in three beaches at the southern end of Lake Coleridge.

6.4 Grain Size Analysis

The trapped sediment was subjected to a grain size analysis in the sediments laboratory at the Department of Geography, University of Canterbury. The analysis proceeded using standard sieving methodology, as outlined in Lewis & McConchie (1994). Over 500 individual samples were dried, weighed and sieved at quarter phi intervals for 15.0 min in a Ro-tap sieve shaker. Sieve sizes ranged from 0.05 mm (4.25 ϕ , fine sand) to 11.0 mm (-3.5 ϕ , small pebbles), covering the full size range of most of the trapped samples. Pan fractions were negligible. Material too large for sieving (> 11 mm) was measured across the B-axis with a grain sizing template (a sheet of aluminium with square sieve holes cut at set phi sizes through which individual particles are passed). The raw data were calculated as a percentage of the total sample weight and then added to form a cumulative percent weight. It was hoped that a detailed grain size analysis would reveal differences in the entrainment thresholds of various grain sizes.

The raw grain size data were analysed with the method of moments, developed by Krumbein (1936) and outlined in Lewis and McConchie (1994). This produced the grain size statistics of the sample. The first moment is the mean grain size, the second moment is the standard deviation or the sorting of the sample. Both moments have dimensional unit values in millimetres or phi.

The third and fourth moments are dimensionless parameters providing the skewness and kurtosis of the distribution. The mean grain size can obscure the true nature of a sediment sample that has a large range of grain sizes from sand to gravel. It is often desirable to know the grain size at a particular point in the distribution curve, such as the 25th or 75th percentile grain size. In the sediment transport literature, the three most commonly used percentile measures are the median grain size (D_{50}) and the 10th (D_{10}) and 90th (D_{90}) percentile grain sizes. The D_{10} is the coarsest fraction (i.e. 90% of the distribution is smaller) and the D_{90} is the finest fraction. Commonly these statistics are derived from the plotted distribution curves of the raw cumulative sieve data. However, this process is time consuming and impractical for the analysis of large data sets. A simple mathematical method was developed to make the process easier, and is presented in (Appendix 3a). The grain size classifications and related statistical nomenclature can be seen in Appendix 3b. A modal analysis was also performed to identify different modes in the gravel or sand size fraction that may have been moving independently in the foreshore. The method followed that of Brotherhood and Griffiths (1947) and Curray (1960). The calculations were performed in Microsoft Excel spreadsheet.

The sediments collected in transit were a heterogeneous mix of coarse sands and fine gravels. A frequency distribution of the hourly mean grain size of the trapped sediments is presented in Figure 6.1. On the whole the material was coarse in nature. The mean grain size for all the sediment collected in the trap was 3.54 mm (-1.82 ϕ , granules). There were small quantities of fine sand (0.125-0.25 mm, 2-3 ϕ) and medium sand (0.25-0.50 mm, 1-2 ϕ) in a number of samples, the minimum size collected was in the order of 0.15 mm. However, the sand was more commonly coarse (0.50-1.0 mm, 0-1 ϕ) and very coarse (1.0-2.0 mm, 0 to -1 ϕ). At the threshold between sands and gravels, granule sized particles (2.0-4.0 mm, -1 to -2 ϕ) featured very strongly in the sediments collected in the trap. The mean grain distribution is positively skewed (0.81). It can be seen that a number samples had a mean grain size in the very small (4.0-8.0 mm, -2 to -3 ϕ) and small pebble range (8.0-16.0 mm, -3 to -4 ϕ). The largest material collected in motion was in the medium pebble range (16.0-32.0 mm, -4 to -5 ϕ). The mixed, coarse nature of the material is reflected in the 10th and 90th percentile sizes (Figure 6.2). There are only a few samples (2.5%) that have the coarsest fraction in the sand range (Figure 6.2a). These samples were pure sand. Most of the samples had their coarsest fraction in the pebble range. When the finest fractions are examined (Figure 6.2b), it can be seen that 87% of the samples contained a sand fraction. This also indicates that some 13% of the samples were almost pure gravel.

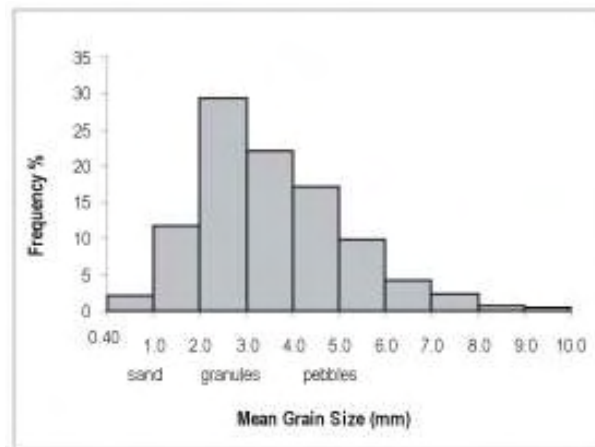


Figure 6.1 Mean grain size distribution. The material was generally coarse in nature. The most common grain size was in the granule range. $n = 493$.

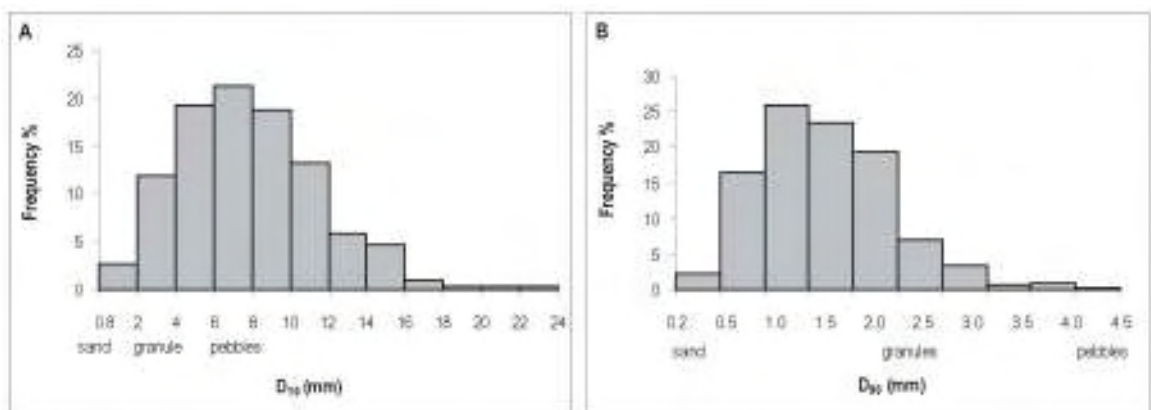


Figure 6.2 Distribution of coarse and fine percentile grain sizes D_{10} and D_{90} . $n = 493$.

These distributions are reflected in the sorting of the sediments (Figure 6.3a). Overall, 45% of the samples were poorly sorted (0.25-0.49) and a further 45% were moderately sorted (0.50-0.59). The remaining 10% were moderately well (0.60-0.69) to well sorted (0.70-0.79). These were the pure sands and gravels highlighted in the 10th and 90th percentile distributions. The mean sorting value was 0.55 (*i.e.* moderately sorted). This is interesting because the foreshore sediments at the fieldsite were generally found to be poorly sorted. Twenty four samples were taken across the survey profiles to characterise the general nature of the fieldsite sediments. The sorting values ranged from 0.17-0.53, with a mean value of 0.34. There were no moderately well or well sorted samples. This indicates that there is a general tendency for the sediments to become graded or sorted during transport.

Nevertheless, it must be emphasised that this is only a general tendency. There is no firm correlation between increasing wave energy and sorting between samples collected in the trap. It merely indicates that during transit, sediment tends to be slightly better sorted. There are a number of reasons for this. At times, some size sorting was observed across the swash zone. A coarse lag sometimes developed at the lakeward end of the swash zone, under the breaking wave, where sand had been scoured out through turbulence. This sand was transported forward and through the main section of the swash zone, causing a general size grading from coarse to fine across the swash zone. This material was collected in the trap, producing a well sorted sand sample. Likewise, there were occasions in easing conditions when the wave height dropped, leaving some of this sand stranded above the limit of swash. Renewed wave activity would mobilise the gravel fraction, causing a well sorted gravel mode to be transported alongshore. This interplay between the water level and the foreshore sediments was a regular occurrence. Essentially, as the water levels rise or drop, different deposits are reactivated, sometimes sand or gravel, often a mixture of the two. Thus, the sorting was dependent on the supply as much as any winnowing process. Frequently, these two modes were transported together. Figure 6.4 is a typical modal analysis distribution from material collected in the trap. It shows a secondary pebble mode being transported in the dominant coarse sand/granule mode.

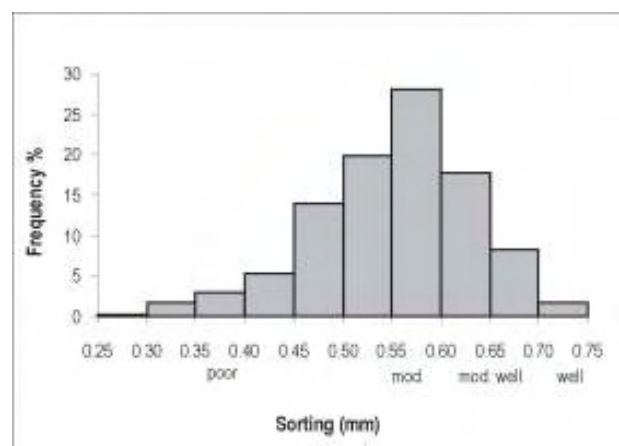


Figure 6.3 Sorting of trapped sediment data. The sediments were generally moderately sorted during transport. n = 493.

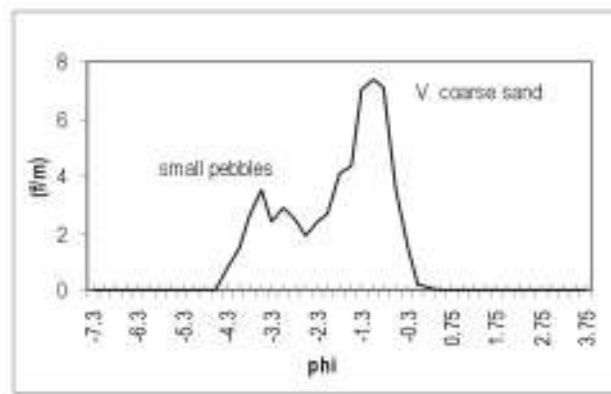


Figure 6.4 Typical modal classes in transit in the swash zone. 13/02/02, C010, 1500 hrs.

6.5 Calculating the Sediment Transport Rate

Hourly Transport Rate

With the weighed trapped sediment, it was then possible to estimate the hourly rates of sediment transport in a 0.3 m wide strip in the swash zone, this being the width of the trap. To achieve this, the trapped weight of material was multiplied by a factor that was a function of the trapping time and the number of minutes in one hour, $f = 60/t$, where t is the trapping time. For example, if the trapped sediment was collected over a 5 min period, the weight was multiplied by 12 to create a time averaged hourly transport rate (kg hr^{-1}). Hourly trapped rates ranged from 0.02 to $214.88 \text{ kg hr}^{-1}$ with an overall average of $26.68 \text{ kg hr}^{-1} \pm 10\%$. This requires the assumption that the transport rate remains reasonably steady over a period of 60 min. In sediment transport studies, wave conditions and transport rates are often assumed to remain constant over a period of hours or days. However, it has been noted that the longshore sediment transport flux in a swash zone can be highly variable (Chadwick, 1989). To allay uncertainty and satisfy the assumption that it is possible to multiply this weight out by a factor, a series of experiments were conducted with two sediment traps in the swash zone. Material was collected in sequential one minute and five minute periods in low and high energy conditions. A trap was first placed to collect sediment for one minute, then removed and another placed in the same position for the next minute and so on for 10 minutes. The material was weighed in the field and the process was repeated at 5 min intervals for 50 min. The amount of variability depended on the conditions, increasing as the wave energy increased, but on average the difference from one sample to the next was in the order of $\pm 10\%$. For example a 1.0 kilogram sample in one minute, may be measured at 0.9 kg the next and at 1.0 kg again the following minute (Figure 6.5). This is

due to natural variability in the wave trains and swash bores. Such variability is inherent in studies of this nature and must be accepted as a natural uncertainty. It is felt that $\pm 10\%$ is acceptable, considering the number of environment parameters that affect or influence sediment transport.

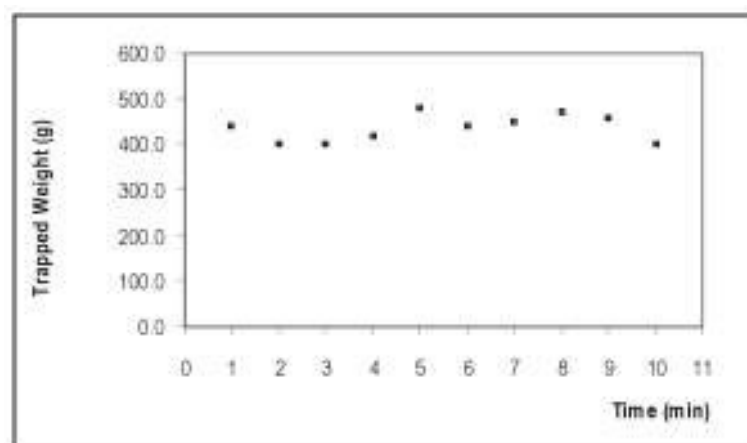


Figure 6.5 Typical trap variation over a 10 min period. Average minute to minute variation ranges from 2.2 to 12.5% and averages 7.3%.

Volumetric Transport Rate

To calculate the volumetric sediment transport rate, the volume of each sediment sample collected in the trap had to be known. With over 500 samples to measure, individual volume measurements would have been impractical and imprecise. No expression was found that could easily calculate sediment volumes. Thus, a numerical method was developed to efficiently and accurately estimate the volume of a sediment sample with a known weight. To achieve this, a knowledge of the mass, solid density and porosity of the sediment is required. Porosity is the amount of pore space in a packed sediment sample that can be occupied by air or water. The solid density is the mass of the sediment without these pore spaces.

The density calculation followed the method outlined in Lewis and McConchie (1994), that involves weighing a sample of the dry sediment in air and then measuring its displacement in a known volume of water (Appendix 4a). An average density value was calculated from a series of tests using samples taken from the trapped sediments. The fieldsite beaches are composed predominantly of greywacke (95%), a semi-metamorphosed sandstone and the closely related lithological unit, argillite (4%). The remaining 1% fraction is a coarse, well-indurated sandstone, which is essentially the un-metamorphosed remnants of the parent rock. The specific gravity of the fieldsite sediments is 2.85, giving it a density of 2850 kg m^{-3} . The specific gravity of quartz,

the commonly used measure for beach sediments, is 2.65 or 2650 kg m⁻³. This means that more wave energy is required to overcome the mass of greywacke to initiate transport than pure quartz.

Once a density measure is made, it then becomes possible to calculate the porosity and volume of the sediment. The porosity can be seen as the ratio difference between the mass of a sediment sample and the mass of an equal volume of the sediment without any pore spaces, *i.e.* the solid density mass. The expression is a dimensionless ratio calculated as a percentage:

$$P = \frac{M_s}{(V_s \times \rho_s)} \times 100 \quad (6.1)$$

Where P is the porosity, M_s is the mass of the dry sample in kilograms, V_s is the measured volume of the dry sample in cubic metres and ρ_s is the density of the sediment in kilograms per cubic metre (kg m⁻³). A working example with more details is provided in Appendix 4b. The denominator term is the mass of an equal volume the sediment without pore spaces. The Porosity values were calculated with samples typically collected in the sediment trap, composed of different grain size admixtures, ranging from the finest to coarsest fractions. This was identify whether or not different compositions of sediment had different porosities. Surprisingly, no significant variation was found. The average porosity value for the Lake Coleridge sediment is 0.615, which despite the coarse nature of the material, is almost identical to the general porosity value of 0.60 for sand. In percentage terms this implies that 38.5% of the sediment volume is pore space and 61.5% is solid sediment. The volume of a sediment sample collected in the trap can then be calculated by rearranging the porosity equation:

$$V_s = \frac{(M_s / P) \times 100}{\rho_s} \quad (\text{m}^3) \quad (6.2)$$

It is a ratio between the weight of the sample and the solid density of the sediment, in units of cubic meters. With this equation the volume of each sample collected in the sediment trap was calculated and an hourly cubic metre rate of sediment transport was derived. Hourly transport rates through the trap ranged from 1.14×10^{-5} to $1.23 \times 10^{-1} \text{ m}^3$ which covers a full 5 orders of magnitude. The average rate was $1.52 \times 10^{-2} \text{ m}^3 \text{ hr}^{-1} \pm 10\%$.

Total Integrated Longshore Transport Rate

A difficulty in sediment transport studies is knowing how a transport rate derived from trap or tracer data relates to the wider beach system or can be extrapolated to produce a total transport rate. Often a transport rate is given as cubic metres per metre of beach (m³ m⁻¹) and it is left to

the discretion of the practitioner to apply this to a particular beach system. Some studies have been conducted to determine the distribution of transport across the nearshore and through the surf zone, but to the authors knowledge, no studies have been published concerning the longshore sediment transport distribution in the swash zone of a gravel or mixed sand and gravel beach. It is important to correlate environment parameters with the total transport rate rather than the trapped rate. The volume of material moving through a 0.3 m strip in the swash zone may not be significantly different for example, if the swash zone is 3.0 or 4.0 m wide, when clearly the potential rate will be higher through a wider swash zone. One solution would be to multiply this rate by the width of the swash zone. However, this assumes that the transport rate is equal across the entire width. Swash velocities decelerate at the limit of up-rush and the water depth reduces to zero. Consequently, the transport rate will decline at the extremities of the swash zone. Longshore transport rates under the breaker might also be expected to differ from the trapped data, due to high turbulence around this zone and the vertically accelerated water flow. Moreover, it would require the assumption that every swash has a run-up length equal to the width of the swash zone, when this is simply not the case. In an investigation of transport models using data from the gravel beach at Shoreham, on the south English coast, Chadwick (1989) assumed that the transport rate was at a maximum near the breaker and declined in a linear fashion forward of the breaking wave to a zero point at the limit of swash. However, Kirk (1975) found that the velocities remained uniformly high across the swash zone, only tapering off at the limits.

To provide some information concerning this problem, a small study was conducted to determine the distribution of the longshore sediment transport flux across the swash zone. Over a five day period, two sediment traps were placed simultaneously in the swash zone at hourly intervals. The traps were positioned at different distances from the base of the breaking wave to build a series of measurements at set intervals across the swash zone. For example, one trap may have been placed at 0.5 m and the other at 1.5 m. These positions were calculated as a percentage of the width of the swash zone. In this way, measurements were taken at a variety of intervals across the swash zone (0-90%), relative to its width. Measurements were all made in moderate to high energy conditions to minimise variations due to wave height. Consistent northwest conditions prevailed through the study with wave heights ranging from 0.20-0.45 m, with a mean 0.35 m. Over 75% of the wave heights occurred between 0.25-0.40 m. The mean width of the swash zone was 3.75 m, with a range of 2.0-5.0 m. The material was weighed in the field and hourly rates of transport were calculated through different positions in the swash zone. This yielded 120 data points for analysis. The swash zone was divided into 10% slices and the

average transport rates were calculated for each section. The results were plotted and a time averaged swash zone transport distribution curve was produced (Figure 6.6).

In Figure 6.6 can be seen that there is a rapid increase in the transport rate in front of the breaking wave. Based on measurements from the nearshore, sediment transport immediately lakeward of the breaker is assumed to be zero, as indicated at the 0% lakeward limit. Immediately landward of the breaker, the transport rate increases rapidly from zero, to a maximum at around 20%. This is an area of high turbulence and the current vectors have a strong vertical component in the collapsing wave. Once the water flow translates horizontally into swash, the flow becomes more organised and the sediment transport rate increases uniformly. The rate remains high across the middle of the swash zone. A lot of swash activity occurs in this area where both swash and backswash carry high sediment loads. It is also an area that receives a lot of swash of short lengths. After the 50% width, the rate begins to decline. Unintentionally, there were fewer measurements around the middle mark and the decline here may appear sharper than reality. Nevertheless, at around the 70% width, the decline plateaus and remains steady until the very limit of the swash zone. Measurements were made at the 90-95% width and transport was assumed to be zero at 100%. The upper 30% of the swash zone intermittently receives swash and the overall transport rate declines in this area. It must be stressed that this is not the distribution that might be expected under an individual swash lens. This is the time averaged hourly longshore sediment transport flux through the swash zone.

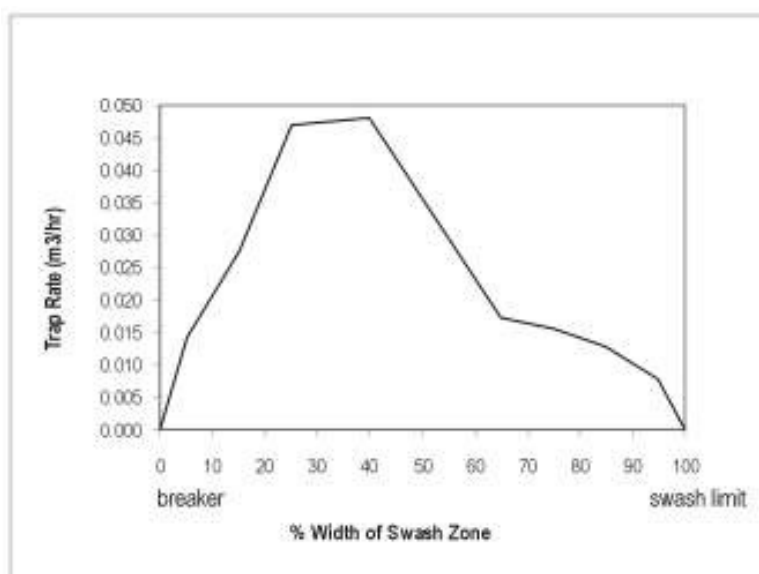


Figure 6.6 Swash zone transport flux distribution curve. Transport rates increase rapidly after wave breaking, remain high across the middle of the swash zone then decline at the swash limit.

Using standard numerical integration techniques, the area under this curve was calculated. The swash zone lends itself to using a definite integral equation to calculate the transport rate because it has clearly defined boundaries. Once it is known how the transport rates vary through the swash zone, it is possible to estimate a total integrated longshore transport rate. This requires a volume measurement from a known position in the swash zone that can be related to a section of the distribution curve, preferably the maximum point of transport. Throughout the field programme the swash zone sediment trap was positioned at around the 30% width mark. Effectively, this is in the area of maximum transport. The total average hourly transport through the swash zone can be defined as:

$$Q_l = \int_0^{X_{sw}} (Q_{Ax} + Q_{Ay} + Q_{Am}) dx \quad (\text{m}^3 \text{ hr}^{-1}) \quad (6.3)$$

Where Q_l is the volumetric longshore transport rate, 0 and X_{sw} are the limits of the swash zone, Q_{Ax} is the transport volume of the area below the trap, Q_{Ay} is the transport volume of the area above the trap, Q_{Am} is the measured transport volume of the area occupied by the trap and dx is the constant of integration, which reduces to unity in a definite integral calculation (Figure 6.7).

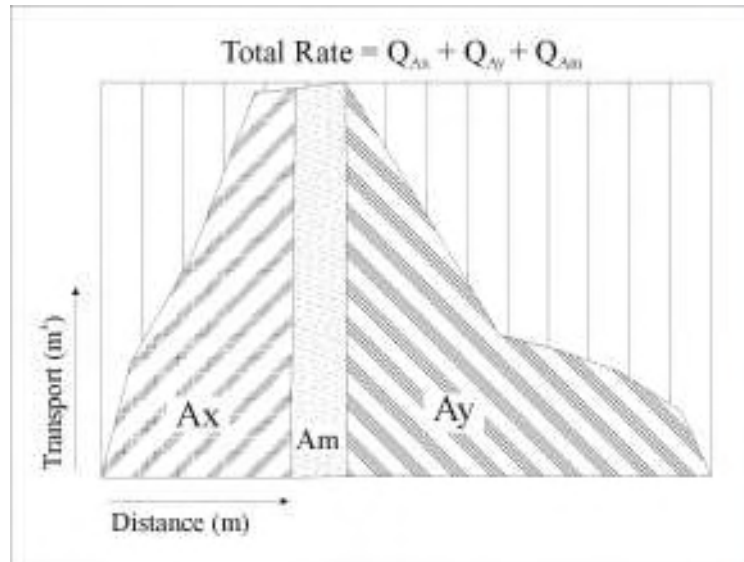


Figure 6.7 The total integrated longshore transport rate in the swash zone can be estimated by calculating the area under the mean distribution curve and then adding the measured transport rate (Q_{Am}), to the rates from the areas above and below the trap (Q_{Ax} & Q_{Ay}). The transport rate in Ax and Ay are derived from a knowledge of the measured rate.

Expanding these terms, an equation was written to calculate the total integrated longshore sediment transport rate.

$$X_{sw} > T_w \quad Q_l = \left[\frac{(X_{sw} \cdot Ax)}{T_w} \cdot Q_m \right] + \left[\frac{X_{sw} - (X_{sw} \cdot Ax + T_w)}{T_w} \cdot Q_m \right] + Q_m \quad (6.4a)$$

$$X_{sw} < T_w \quad Q_l = Q_m \quad (\text{m}^3 \text{ hr}^{-1}) \quad (6.4b)$$

Where X_{sw} is the width of the swash zone, A_x is the area below the trap, T_w is the width of the trap and Q_m is the measured transport volume in cubic metres. The first term calculates the width and volumetric transport rate of the swash zone below the trap. The second term calculates the area and transport volume above the trap. The last term is the measured volumetric rate. The three terms are added to produce a total integrated rate. The equation works by dividing the swash zone into a number of divisions equal to the width of the trap and multiplying these by a reduced transport rate equal to the area under the curve. Equation 6.4a is valid when the swash zone is wider than the sediment trap. If the swash zone is less than the trap width, the trap obviously collects the total material in transit and Equation 6.4b applies.

Using this equation, the total longshore transport rates through the swash zone were calculated for each hour of measurement. The sediment transport was measured in a wide variety of conditions and the volumetric rates reflect this, covering a full five orders of magnitude. The total transport rates range from a minimum of $1.10 \times 10^{-5} \text{ m}^3 \text{ hr}^{-1}$ to a maximum of $1.15 \text{ m}^3 \text{ hr}^{-1}$. The mean rate was $7.36 \times 10^{-2} \text{ m}^3 \text{ hr}^{-1}$. To the authors knowledge, no measurements of this kind have been made for a lacustrine beach in New Zealand. Similarly, no quantitative measurements of longshore sediment transport rates have been made from the swash zone of the oceanic mixed sand and gravel beaches. Based on the accumulation rates at South Beach, Timaru, a mixed sand and gravel shoreline, Tierney (1977) estimated the net annual transport rate to be $60,000 \text{ m}^3 \text{ y}^{-1}$. When calculated as an hourly rate, this is $6.84 \text{ m}^3 \text{ hr}^{-1}$. Clearly this is a very generalised figure, but it indicates that transport rates in a mixed sand and gravel lakeshore are considerably less than the open coast. Sediment transport rates from the gravel beaches in the United Kingdom are commonly expressed in the literature as a net annual accumulation rate, due to the difficulty of making measurements in these beaches (Van Wellen *et al.*, 2000a). Chadwick (1989) conducted some trap measurements on Shoreham Beach, West Sussex, over a five day period. Longshore transport rates were measured in the order of 1.0×10^{-2} , with wave heights ranging from 0.23-0.32 m. Chadwick faced some difficulties in measuring an accurate rate because of tidal translation across the shore and acknowledged that the rates were provisional. Nevertheless,

when compared to Lake Coleridge these rates are of the same order of magnitude for the wave conditions. Summary statistics for the transport rates are presented in Table 6.1. The first column is the raw sediment mass derived from the trapped data, converted into an hourly rate. The second column is this hourly mass converted into a volumetric rate. The last column is the total integrated longshore sediment transport rate. It was argued previously that the variation in transport would be more strongly highlighted by examining the total rate as opposed to the trapped rate. It can be seen that the variance in the data increases from the trapped volume to the total volume. The rates are all positively skewed, indicating the occurrence of a small number of high transport rates in the distribution. The distributions are also leptokurtic, especially the total rate. This shows that many of the values lie within the same order of magnitude as the mean. A summary of the hourly raw trap data and total rates can be found in Appendix 6.

Table 6.1 Summary statistics of the longshore sediment transport rates measured in the swash zone at Lake Coleridge. The first column is the raw mass of material in transit through the 0.3 m wide trap position. The second column is the volume of this raw mass. The last column is the total integrated rate.

	kg/0.3 m hr ⁻¹	m ³ /0.3 m hr ⁻¹	m ³ hr ⁻¹
Min	0.02	0.000011	0.000011
Max	214.88	0.1226	1.1538
Mean	26.68	0.0152	0.0736
Median	15.54	0.0089	0.0274
Std. Dev.	33.54	0.0191	0.1298
Variance	1124.87	0.0004	0.0168
Skewness	2.48	2.48	3.92
Kurtosis	7.95	7.95	20.56

After calculating the transport rates with Equation 6.4, a simplified approximation was developed that produces an almost identical value:

$$Q_l = 0.5 \left[Q_m \left(\frac{X_{sw}}{T_w} - 1 \right) \right] + Q_m \quad (\text{m}^3 \text{ hr}^{-1}) \quad (6.5)$$

The expression indicates that the total transport rate is equal to half the maximum rate when averaged across the swash zone. The equation works in the same way as Equation 6.4a by dividing the swash zone into a number of sections equal to the width of the trap. One of these sections is the measured rate, and is subtracted from the term. The sections are multiplied by the measured rate and then reduced by a factor of one half. The measured rate is added to produce the total integrated rate. The equation requires Q_m to be the maximum rate. A correlation

between the two equations can be seen in Figure 6.8. It shows an almost perfect correlation ($r = 0.9988$). Thus if the maximum longshore sediment transport rate is known, this equation may be confidently used to calculate the total rate.

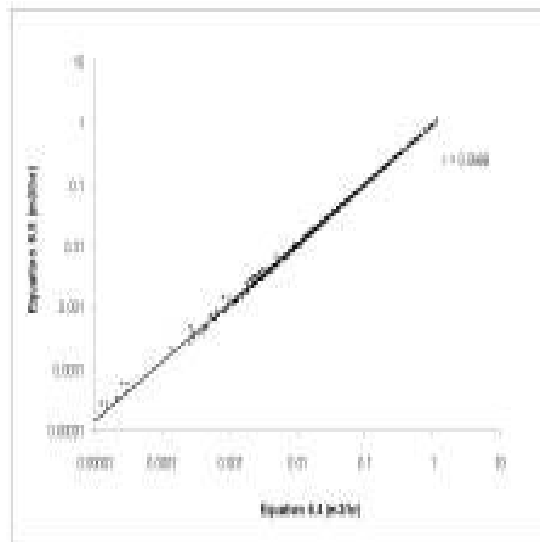


Figure 6.8 Linear correlation between Equation 6.4 and the approximation of Equation 6.5.

6.6 Nature of Longshore Sediment Transport in a Lakeshore Beach

Sediment transport results from the complex interaction between many different variables. As outlined in Chapter Two, a number of locations were chosen around the fieldsite in an effort to measure variations in the transport rate due to differences in beach morphology (Figure 2.14). The main difference was in shoreline orientation, that varied by as much as 30° . The transport rates measured at the different sites are presented in Table 6.2. Site CO10 was located in the middle of the long western side of the barrier foreland and had an orientation of $295^{\circ} \pm 5$. It is an exposed, straight drift-aligned, linear beach, open to wind and waves from every direction, except the northeast. Approximately half the field programme was conducted at this site, yielding 42% of the data set used in this study. Measurements took place here in light to moderate conditions with waves from the southeast (60%) and northwest (40%). Site CO14a was located at the northern end of this beach and has a similar morphology to CO10, with an orientation of 300° . There is a wider, more developed lag pavement in the nearshore at this site. Site CO14b was slightly angled and had a shoreline orientation some $10\text{--}15^{\circ}$ more to the north.

Only a few measurements were taken here (16 hrs) before a rise in the lake level straightened the shoreline orientation. Insufficient variation was found between these two locations and they will subsequently be treated together, where they account for 10% of the data set. Measurements were made at CO14 in moderate to strong southerly and north-west conditions. Sites CO11a and CO11b were several hundred metres to the south of CO10, at the end of the linear beach. Site CO11a had an orientation of around $305^{\circ} \pm 5$, whilst CO11b was aligned around $325^{\circ} \pm 5$. Aside from this difference, both were broadly similar to CO10. The strongest conditions experienced during the fieldwork occurred at these two sites, during which strong to gale force north-westerlies prevailed. Site CO13 was located in a small sheltered embayment on the south-western corner of the barrier foreland and had an orientation of $325^{\circ} \pm 5$. Moderate north-westerlies prevailed during measurements at this location. The longshore sediment transport rate on the southern side of the barrier at site CO40 was found to be nil. In northwest conditions there was no wave activity on this side of the barrier. In southerly conditions waves crests approached normal to the shoreline and the transport was predominantly cross-shore in the swash zone. In the final analysis, the differences between the sites were subtle. Considerable variability in the wave and swash zone conditions was measured, leading to variations in the transport rate, but it was similarly large at each site. The main difference coming from variations in incident wave energy. Summary statistics for variations in a number of parameters measured at each site are presented in Appendix 7.

Table 6.2 Variation in transport rates by site in cubic metres per hour. The last row indicates the number of hours of data that each site contributed to the data set, with the relative percentage in the brackets.

LST (m ³ /hr)	CO10	CO14a & b	CO11a	CO11b	CO13
Min	0.000011	0.002212	0.001287	0.000832	0.000034
Max	0.490	0.433	0.944	1.154	0.058
Mean	0.053	0.069	0.189	0.131	0.010
n	208 (42%)	49 (10%)	57 (12%)	76 (16%)	103 (20%)

Multiple regression analysis was conducted between the environmental variables measured in the field and the total longshore sediment transport rate. The correlations were consistently stronger with the total rate as opposed to simply the trapped weight of material. This is because the total rate is a more accurate description of the longshore transport conditions. Table 6.3 presents the Pearson *r* correlation coefficients for the regression analysis between the longshore sediment transport rates and the measured environment variables. The correlations were reasonably consistent from site to site. The one exception was CO13 that showed slightly lower

correlations with the measured parameters. The reasons for this will be explored further in the following discussion, but on the whole, sites CO10, 11a & b and 14a & b, can be viewed as exposed high energy beaches, which together accounts for 80% of the data set. Site CO13 had characteristics similar to a sheltered pocket beach that experienced modified wave energy, as seen by the considerably lower transport rates. It can be seen the wave height and steepness and the swash velocity are the most important controlling variables. Other swash zone conditions including the width and run-up height and slope were also found to be important. Less important was the wave direction and the grain size. The following discussion will explore these differences in greater detail.

Table 6.3 Pearson r correlation coefficients for the most important environment parameters influencing longshore sediment transport.

LST (m ³ /hr)	H _{rms}	T _z	H _o /L _o	W_dir α	V _{sw}	X _{sw}	R _{2%}	tan β	D ₅₀
All	0.78	0.66	0.78	0.28	0.75	0.68	0.66	-0.54	0.25
Excl. CO13	0.88	0.79	0.80	0.26	0.77	0.81	0.81	-0.63	0.32

Wave Height

Wave height is the most widely used variable incorporated into longshore sediment transport equations (Schoonees & Theron, 1995). The dominant controlling influence of wave height in a lakeshore beach was demonstrated in the last chapter and its role in sediment transport was signalled in the previous section. Table 6.4 shows a breakdown of the correlations between longshore transport and the wave height by site. The correlation with the wave height differs slightly from site to site as might be expected, due to natural variability. At all sites it can be seen that the longshore transport rate increases with the wave height. At the high energy sites, 79-84% of the sediment transport rate can be explained by variations in the wave height ($r^2 = 0.79-0.84$). The strong controlling influence that wave height has over longshore sediment transport is illustrated in Figure 6.9. It shows a time series of three consecutive days of measurements at site CO10 during light to moderate southeast conditions with waves ranging from 0.05-0.26 m. The transport rate tracks up and down in direct relation to the changing wave conditions, with no lag time. Two clear spikes appear in the time series. These are indicative of times when the swash zone was fully saturated and the sediments become fluidised, leading to a dramatic increase in the quantity of material able to be transported. This most often, but not always, happened with

finer material. In the example shown, the first spike occurred with a mean grain size of 4.12 mm (-2.04 ϕ , very small pebbles). The second spike occurred when the swash zone had a mean grain size of 2.21 mm (-1.14 ϕ , granules), whilst in the preceding hour the mean size was 4.62 mm and proceeding hour it was 5.95 mm.

Table 6.4 Correlation coefficients, including the standard error of the estimate, for the regressions between longshore sediment transport and H_{rms} wave height by site. NB: First row contains mean wave heights, not correlation coefficients.

	CO10	CO14a&b	CO11a	CO11b	CO13	All	excl. CO13
Mean H_{rms}	0.16	0.27	0.23	0.26	0.20	0.20	0.20
r	0.90	0.87	0.92	0.89	0.71	0.78	0.88
r^2	0.81	0.75	0.84	0.79	0.50	0.61	0.77
Std. Err.	0.38	0.28	0.29	0.32	0.39	0.51	0.39
n	208	49	57	76	103	493	390

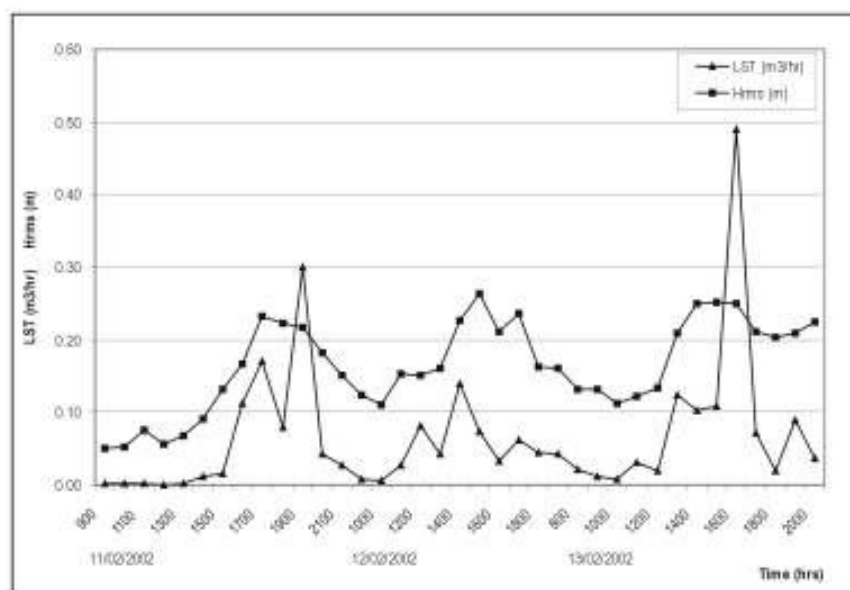


Figure 6.9 Time series of longshore sediment transport and wave height over three consecutive days of measurements at site CO10, illustrating the strong interconnected relationship. At times under increasing wave activity the swash zone became fluidised and the transport rate increased dramatically, as indicated by the spikes. These measurements occurred under light to moderate southeast conditions.

The correlation with the wave height at site CO13 is somewhat less, where 71% of the longshore sediment transport can be explained by the wave height. CO13 was a sheltered site that had the characteristics of a pocket beach. These small beaches are not an uncommon feature around lakeshores. The site can be seen in Figure 2.14b as the embayment on the corner of the barrier foreland. It experienced a degree of wave refraction and modification in the nearshore and this led to smaller breaking waves than the measured deep water wave heights indicated. In hindsight it may have been preferable to install the wave gauge in the shallow water inside the embayment. An experiment with the data was conducted to see if the correlation was indeed explained by the wave height. When the attenuated S4 wave height data was substituted for the wave gauge data, the correlation improved to $r^2 = 0.73$. Whilst it would not be correct to use this data in any analysis, it provides an indication of the reason why the correlation is considerably less for this site. Figure 6.10 shows the graphical representation of the regression analysis. The low longshore sediment transport rates at site CO13 can be seen in the cluster below the best-fit line in 6.10 (A). By contrast, the correlation with the CO13 data excluded shows an obvious improvement 6.10 (B).

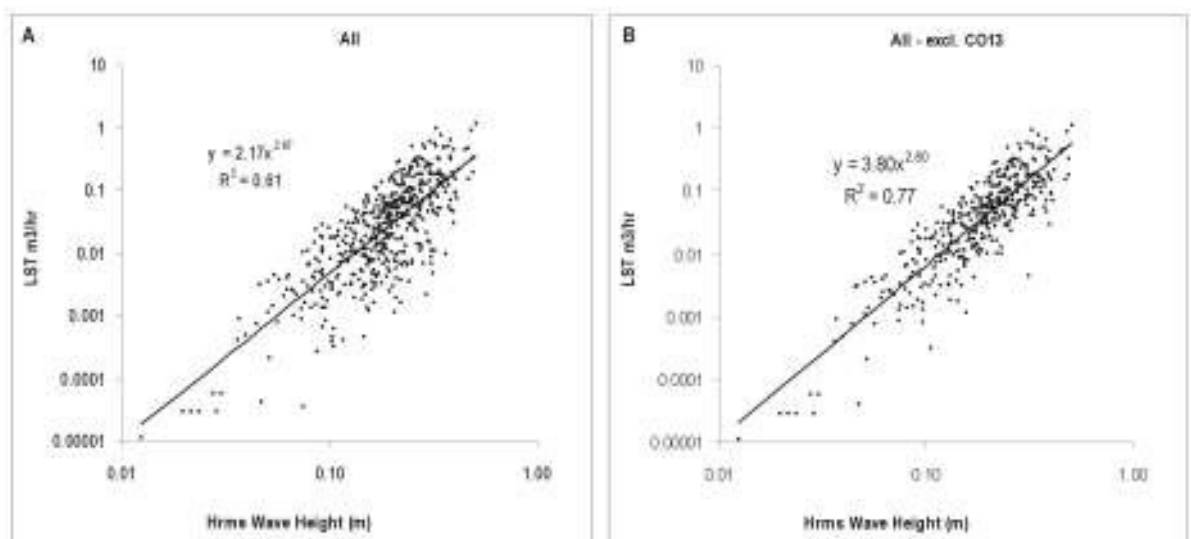


Figure 6.10 Linear regressions of the wave height against longshore sediment transport at all sites (A) and excluding site CO13 (B).

Masselink and Hughes (1998) found a strong relationship between sediment transport and the swash velocity cubed. In the present study, this cubic relationship was found to exist with the wave height. It will be noted that the equation for the regressions is a power relationship (Figure 6.10). That is, the longshore transport rate is equal to a coefficient multiplied by the wave height

raised to a power. In this case, a power close to three (*i.e.* a cubic relationship.). In fact, in the correlations for the individual sites listed in Table 6.4, the regression equations indicate that the transport is related to the wave height cubed. This is illustrated in Figure 6.11. Again this demonstrates the exponential nature of wave energy and the power growth relationships that result from increases in wave height.

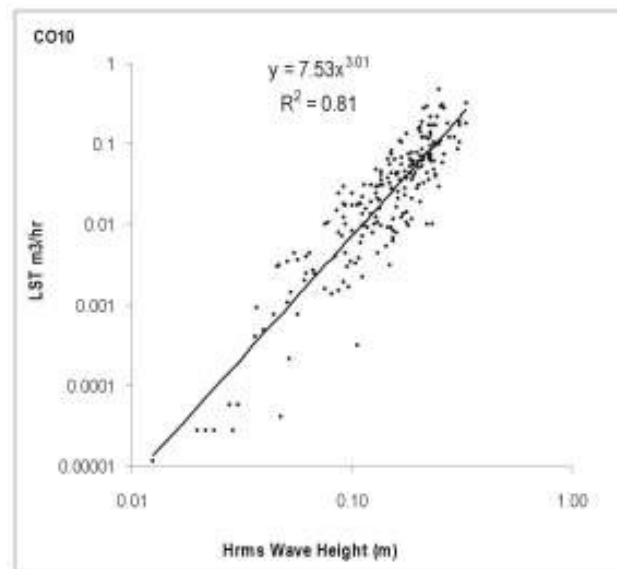


Figure 6.11 Linear Regression of wave height against longshore sediment transport rate at site CO10. The regression equation indicates that the sediment transport is equal to a coefficient multiplied by the wave height cubed. The strong correlation is characteristic of the relationship found at other sites.

Wave Period, Length and Steepness

In a purely physical sense, the sheer mass of water contained within a wave increases as it becomes longer. This provides more water and hence the energy that it contains, for effecting sediment transport. This is one reason why waves generated in unrestricted fetch environments, such as the open ocean, are significantly more powerful than the high frequency waves typically generated in a lake. Thus, the longer the wave period, the greater the sediment transport potential. For this reason, wave period is commonly incorporated into longshore sediment transport models because there is usually found to be a correlation with the sediment transport rate (Van Wellen *et al.*, 2000a; Kamphuis, 1991). Table 6.5 presents the coefficients for the

regression analysis between the measured longshore transport rates at each site and the zero-crossing wave period. In general it shows that there is a strong relationship between increasing wave period and longshore transport. This is illustrated in Figure 6.12, a time series of four consecutive days of measurements showing the changes in sediment transport with wave period. It can be seen that small changes in the wave period have a large impact on the transport rate, as indicated by the large spike near the end of the recording period. The relationship weakens slightly, but holds when the period is correlated against the relative longshore transport (Q/H).

Table 6.5 Correlation coefficients by site for the regressions between longshore sediment transport and wave zero-crossing period (T_z).

	CO10	CO14a&b	CO11a	CO11b	CO13	All	excl. CO13
Mean T_z	1.32	1.61	1.44	1.51	1.49	1.43	1.41
r	0.76	0.86	0.91	0.88	0.72	0.66	0.79
r^2	0.58	0.73	0.82	0.77	0.52	0.44	0.62
Std. Err.	0.55	0.29	0.31	0.34	0.38	0.61	0.5
n	208	49	57	76	103	493	390

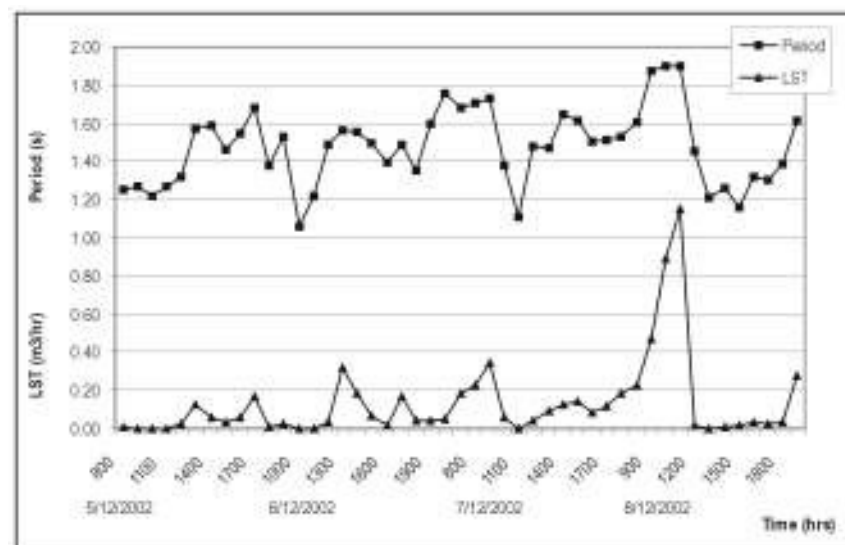


Figure 6.12 Time series of longshore sediment transport and wave period over four consecutive days of measurements at site CO11b, during moderate to strong northwest conditions. Small changes in the wave period result in large changes in the transport rate.

Nevertheless, there is considerable variability in the relationship with the wave period. The sites with the highest transport rates (CO14, CO11a & b) show the strongest relationships, where it accounted for between 73-82% of the variation in transport. Rates were measured at these locations during strong northwest conditions. At sites CO10 and CO13, the correlations are lower, indicating that wave period accounted for between 52-58% of variation in the transport

rate. Other environmental variables aside, the main difference at these two sites is in the wave activity. The correlations appear to be lower in lighter and more variable conditions. At site CO10 measurements were taken during light to moderate southeast and northwest conditions. The mean wave period was shorter (Table 6.5) and the wave height lower (Table 6.4). In Chapter Four it was shown that the wave period increases in relation to the wave height, but that it develops more slowly in response to strengthening wind activity. Analysis reveals little difference between the waves from the southeast and the northwest at site CO10. Rather it appears to be more related to the strength of the conditions. This effect can also be seen at site CO13, in which measurements were made during moderate northwest conditions. Part of the lower correlation at this site also relates to the reasons outlined in the last section, in that there was a degree of wave modification in shallow water at this site, that was not recorded by either the wave gauge or the S4. Taking this into consideration, Figure 6.13 presents the graphical linear regressions for all the sites (A) and excluding CO13 (B). The low transport rates at CO13 can again be seen below the best-fit line in 6.13a. The steep slope of the line indicates the relatively small range in wave period values found at Lake Coleridge. Importantly, it suggests that small changes in wave period have a large impact on the transport rate.

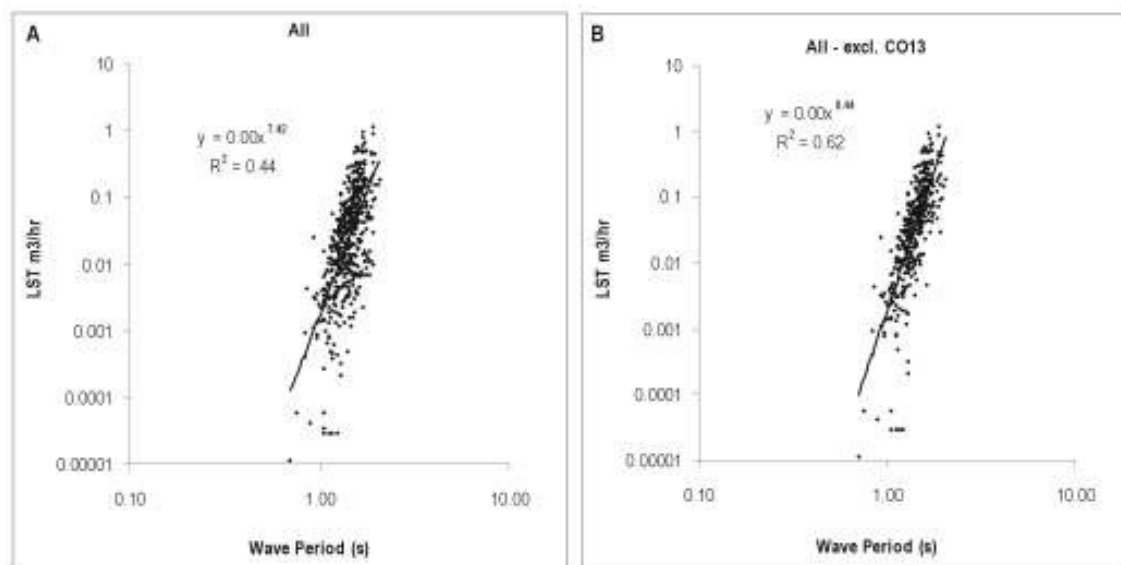


Figure 6.13 Linear regressions of the wave period against longshore sediment transport at all sites (A) and excluding site CO13 (B).

The above findings suggest that a variable that involves both the wave height and period might better account for the variations. Table 6.6 shows the correlations with the wave steepness, a ratio between the wave height and length. Deep water wave length is derived directly from the wave period and as a consequence displays the same correlations. In general, there is a strong correlation between increasing wave steepness and sediment transport. The correlation with the steepness improves over the wave period at site CO10 and as a whole with the entire data. Whilst the individual correlations don't improve at the other sites, the steepness does provide more clues concerning variations in the transport rate. The two sites with the highest transport rates CO11a & b, both experienced the steepest waves. As discussed above, even though the wave period lengthens with increasing wave activity, the height develops more rapidly and hence the ratio increases. Site CO10 and CO13 had the least steep waves and the lowest transport rates. This fits the accepted notion that steeper waves tend to be more erosive in nature leading to increased scouring of the foreshore. Pickrill (1976) commented that applying the concept of wave steepness to a lake environment is meaningless because all the waves are steep. Whilst this may be true, there are clearly degrees of steepness within lake waves. This relative steepness is reflected in the variations in transport rates at Lake Coleridge.

Table 6.6 Correlation coefficients by site for the regressions between longshore sediment transport and wave steepness. There is a clear increase in the transport rate as the wave steepness increases.

	CO10	CO14a&b	CO11a	CO11b	CO13	All	excl. CO13
Mean H_o/L_o	0.055	0.062	0.068	0.071	0.054	0.059	0.060
r	0.83	0.76	0.83	0.79	0.68	0.78	0.80
r²	0.69	0.57	0.68	0.63	0.47	0.61	0.65
Std. Err.	0.48	0.37	0.41	0.43	0.40	0.51	0.48
n	208	49	57	76	103	493	390
Mean LS T	0.053	0.069	0.189	0.131	0.010	0.074	0.090

Wave Direction

It is generally accepted that obliquely angled waves initiate longshore sediment transport along a shoreline with the transport rate increasing with an increase in the wave angle. When the waves approach parallel to the shoreline, it is thought that longshore sediment transport reduces to zero. This has largely been found to be the case at Lake Coleridge. At site CO40 on the south side of the fieldsite, longshore sediment transport rates were close to zero when southeast wave crests approached parallel to the shoreline. It was noted that material transported across the

swash zone was thrown both left and right shoreward of the breaking wave through saltation. Pickrill (1976) found that material moved in both directions on the foreshore during shore normal wave approach, but that the distances travelled were low. Similar variable dispersal patterns were found by Worthington (1989) in Lake Coleridge during tracer experiments. When wave angles increased above a few degrees, longshore sediment transport was initiated.

Deep water wave directions were measured from 0 to 80° in Lake Coleridge, but despite the large variation in the wave approach, the variation with the wave direction was not as significant as expected. This is a surprising result because on oceanic beaches, longshore transport rates have a strong relationship with the wave approach angles. The correlation coefficients for the regression analysis are presented in Table 6.7. The regression was conducted against the breaker swash angle, in order to most closely measure the angle of water flow initiating transport in the swash zone. There is a general correlation between increasing breaker angle and transport rate, but it is weak to moderate correlation. Again, the sites that experienced the highest transport rates (CO 11a & b, CO14) showed the best correlations with the wave direction, with 22-30% of the variation explained by breaker angle. When the wind strength increased, the wave angles became more oblique to the shoreline. In light and variable conditions, the correlation weakened, as seen at sites CO10 and CO13. The most significantly different site was CO13, which relates to the sheltered nature of this site.

Table 6.7 Correlation coefficients by site for the regressions between longshore sediment transport and the breaker angles ($\sin \alpha_b$).

	CO10	CO14a&b	CO11a	CO11b	CO13	All	excl. CO13
$\sin \alpha_b$	57	56	44	42	46	51	52
r	0.25	0.47	0.46	0.55	0.10	0.28	0.26
r^2	0.06	0.22	0.21	0.30	0.01	0.08	0.07
Std. Err.	0.83	0.5	0.65	0.59	0.55	0.79	0.78
n	208	49	57	76	103	493	390

In Table 6.7 it is noted that the correlation is made with the sine of the wave angle. Wave direction in degrees is usually converted to non-dimensional radians and then multiplied by a trigonometric function to represent that part of the wave energy directed alongshore. The three most commonly used wave direction parameters are; $\sin \alpha$, $\sin \cos \alpha$, and $\sin^2 \alpha$ (Komar & Inman, 1970; Longuet-Higgins, 1972; Van Wellen *et al.*, 2000a). The longshore transport rate was most strongly correlated with the $\sin \alpha$ parameter. Some workers have found that the

transport rates increase with breaker angle up to 45° , after which the transport rate declines (Bailard, 1984; Kamphuis, 1991). In these situations the $\sin^2 \alpha$ parameter is often used. This was not found to be the case in this study. Transport rates do appear to increase with wave direction up to 30° , but above this, the transport rates become evenly scattered in relation to wave direction. This is illustrated in Figure 6.14, that shows the relative transport rate against the breaker angle. The relative transport rate was taken as the wave steepness divided by the transport rate, in an effort to normalise the effect of wave height and period. Although not strictly a non-dimensional comparison, it illustrates the trend. Most of the waves approached the shoreline at very oblique angles between 40° and 70° . The bi-directional wind regime limited the waves to two directions, southeast and northwest. In fully developed conditions, these waves travelled with crests more or less at right angles to the beaches along the axial shoreline of the Lake. Thus, the fieldsite is a transport aligned beach. Whilst there was variation within these directions, it appeared to have a limited effect on sediment transport.

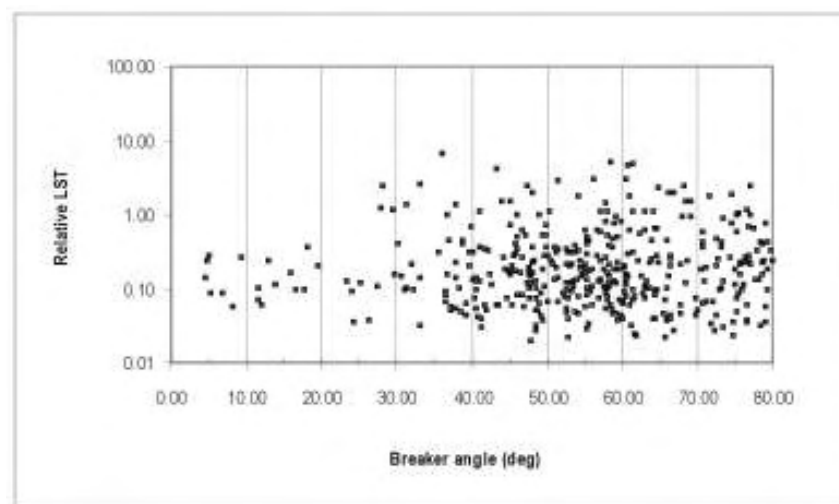


Figure 6.14 Relative longshore sediment transport by wave direction. The rate generally declines at lower wave angles, but above 30° there is much scatter in the data. The small cluster around zero is from a few measurements made during shore normal wave conditions.

Much of the variation seen in Figure 6.14 was due to shoreline orientation. The S4 and the current meters were always aligned at right angles to the shoreline in order to measure the wave angle relative to the shoreline. However, the water flow direction in the waves was not greatly altered by simply breaking on a shoreline with a slightly different orientation. In Table 6.7 it can be seen that the mean wave angles varied by only 13° , despite efforts to measure differences of

up to 30° . Even though the shorelines had slightly different orientations and the waves appeared visually to be breaking at slightly different angles, the internal water flow kinematics was not radically different. The nearshore bathymetry did not sufficiently refract the deep water waves. As discussed in Chapter Four, the wave refraction across the nearshore was limited and breaker angles were only in the order of 10% less than the deep water angles. These small differences were less important than other key environmental parameters such as wave height and period. This is a new and surprising result. Field studies of longshore sediment transport on oceanic beaches indicate a stronger reliance on the wave direction (Schoonees & Theron, 1994). It may be that on coarse grained beaches the degree of the wave angle is less important than has been found for sandy beaches. In other words, the degree of the wave angle may control whether or not sediment is placed in a longshore motion, but that it does not control the magnitude, which is dictated by factors such as the wave height and period.

Swash Velocity

The importance of the swash zone currents in controlling foreshore response was highlighted in the last chapter. The swash velocity is frequently used as de facto measure of the shear stress exerted on the bed sediments (Masselink & Hughes, 1998). When the shear stress exceeds a critical threshold, sediment is entrained and transport is initiated. Despite this, it is not often incorporated into sediment transport equations. Part of this stems from the lack of research concerning swash hydrodynamics and from the difficulty in accurately estimating the swash current velocities. The mean swash velocity was found to be an important factor influencing sediment transport in the beaches at Lake Coleridge. The correlations can be seen in Table 6.8. There is a strong relationship at all sites between sediment transport and swash velocity ($r = 0.62-0.82$), particularly at the exposed sites, where it accounts for up to 67% of the variation in transport rates. The relationship at CO13 is again weaker than that found at the other sites. Figure 6.15 shows the regression between longshore sediment transport and mean swash velocity, with and without site CO13 included. The reason for this becomes clearer when the swash zone currents are separated into swash and backswash components.

Table 6.8 Correlation coefficients by site for the regressions between longshore sediment transport and mean swash velocity. Also included is the maximum and swash/backswash velocities. It can be seen that the difference between the swash and backswash at site CO13 is significantly greater. This has contributed to a lower transport rate at this site. NB: first row are velocities, not correlation coefficients.

	CO10	CO14a&b	CO11a	CO11b	CO13	All	excl. CO13
Mean V_{sw}	0.27	0.37	0.39	0.33	0.23	0.29	0.31
r	0.80	0.77	0.74	0.82	0.62	0.75	0.77
r^2	0.64	0.59	0.54	0.67	0.38	0.56	0.60
Std. Err.	0.51	0.36	0.49	0.41	0.43	0.54	0.51
n	208	49	57	76	103	493	390
max V	0.87	1.23	1.14	1.19	0.87	0.98	1.02
Fwdsw_ V	0.28	0.37	0.33	0.31	0.30	0.28	0.30
Bcksw_ V	0.25	0.35	0.29	0.34	0.23	0.27	0.29
diff	0.03	0.02	0.04	-0.03	0.07	0.01	0.01
Mean LS T	0.053	0.069	0.189	0.131	0.010	0.074	0.090

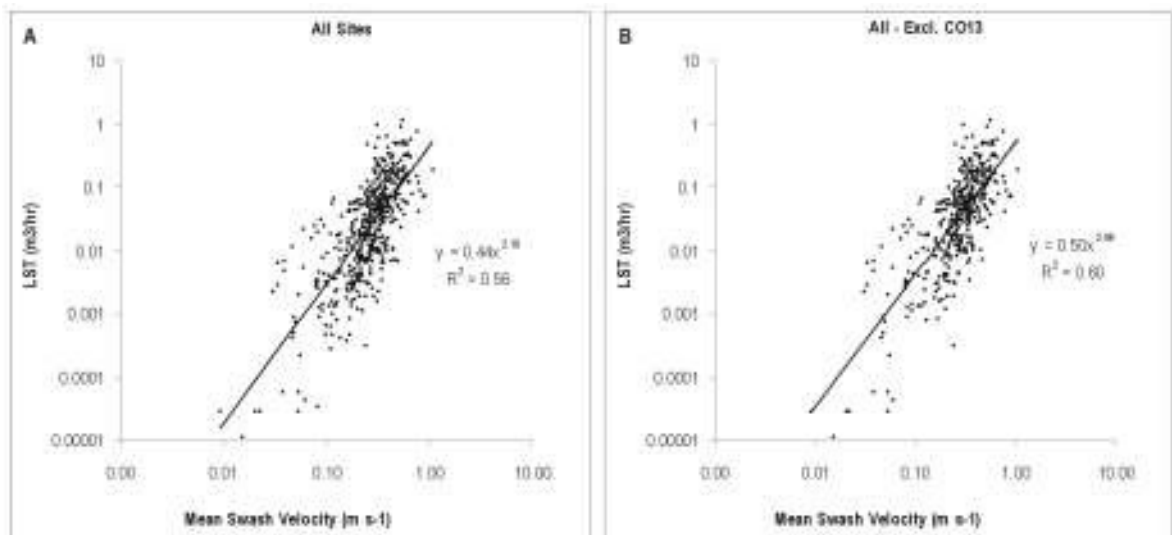


Figure 6.15 Linear regressions of the mean swash velocity against longshore sediment transport at all sites (A) and excluding site CO13 (B). The low transport rates due to a lower mean swash zone current velocity at site CO13 can be seen in the cluster of values beneath the best-fit line in figure A.

Table 6.8 also provides a summary of the swash, backswash and maximum velocities recorded at each site. The magnitude of these values is reflected in the mean swash zone velocity and they follow the same trend of producing higher rates of transport with increasing magnitude. The correlations with these values are very similar to the mean swash zone velocity coefficients shown in the table. In the swash velocity discussion in Chapter Five, it was shown that there was a weak asymmetry in the flows between the swash and backswash. In general the swash was

stronger than the backwash, however at times the backwash component became slightly more dominant. This can be seen at site CO11b. On the whole this asymmetry was too subtle to have an impact on the transport rates. The sediment transport was predominantly controlled by the magnitude of the velocity. The exception to this can be seen at site CO13. Measurements were made at this site under a rising lake level. Due to foreshore morphology, a stranded beach crest was reactivated. The beach sloped downward behind the crest and overtopping swash was absorbed into the sediments. This stranded material in transport near the upper swash zone and severely restricted longshore sediment transport.

Essentially, the reason for the lower backwash velocity and hence the longshore transport rate, is because of overtopping. This supports observations that gravel barrier features are pushed landward under erosive wave activity (Kirk, 1992). It suggests that longshore sediment transport rates are lower when these features are being overtopped, with some material being rolled over the back of the barrier and remaining in the system, rather than being lost to longshore transport. By contrast, the highest transport rates that occurred at site CO11a can also be partly attributed to foreshore morphology. Under a rising lake level an old scarp feature at the back of the swash zone was reactivated during one week of measurements. This caused increased sediment availability in the swash zone as the base of the scarp was scoured by swash activity during strong northwest wave conditions.

Swash Zone Slope and Width

Again the relationship with slope proves interesting and complex. Overall, the highest total transport rates are associated with the lowest slopes, declining consistently as the slope increases. The relationship weakens slightly, but holds when the swash slope is correlated against the relative longshore transport (Q/H). This is well illustrated in Figure 6.16. The highest transport rates are associated with swash zone gradients below $0.10 (6^\circ)$. The lowest slopes are associated with the highest swash velocities and widest swash zones. As the slope increases, the swash zone narrows and the swash velocity and wave energy decline. In Table 6.9 it can be seen that the lowest swash gradients are associated with the highest transport rates. Whilst this is the general trend, the correlations with the slope show that there is considerable variability in the relationship. The variability increases as the swash slopes become lower. Sites CO10 and CO14, that exhibited the steepest slopes, also displayed the strongest correlations ($r = -0.64$ & -0.74). As the swash zone widens there is greater variability in the swash flow. Sites CO11a & b and CO13 have correlations ranging from $r = -0.37$ to -0.53 . The correlation at site CO13 is the

weakest. As discussed in Chapter Five, there are often occasions after a wind-wave event during which time the wave heights and swash velocities are declining, when the swash zone is wider than would normally be exhibited. In other words, there is a lag time for the swash zone to steepen up after a storm event. During this period transport rates are lower than the width of the swash zone would indicate.

Table 6.9 Correlation coefficients by site for the regressions between longshore sediment transport and swash zone slope. NB: first row values are mean gradients, not correlation coefficients.

	CO10	CO14a&b	CO11a	CO11b	CO13	All	excl. CO13
$\tan \beta$	0.16	0.15	0.10	0.12	0.13	0.14	0.14
r	-0.64	-0.74	-0.53	-0.42	-0.37	-0.54	-0.63
r^2	0.41	0.54	0.28	0.18	0.14	0.30	0.40
Std. Err.	0.66	0.38	0.62	0.64	0.51	0.69	0.63
n	208	49	57	76	103	493	390
Mean LS T	0.053	0.069	0.189	0.131	0.010	0.074	0.090

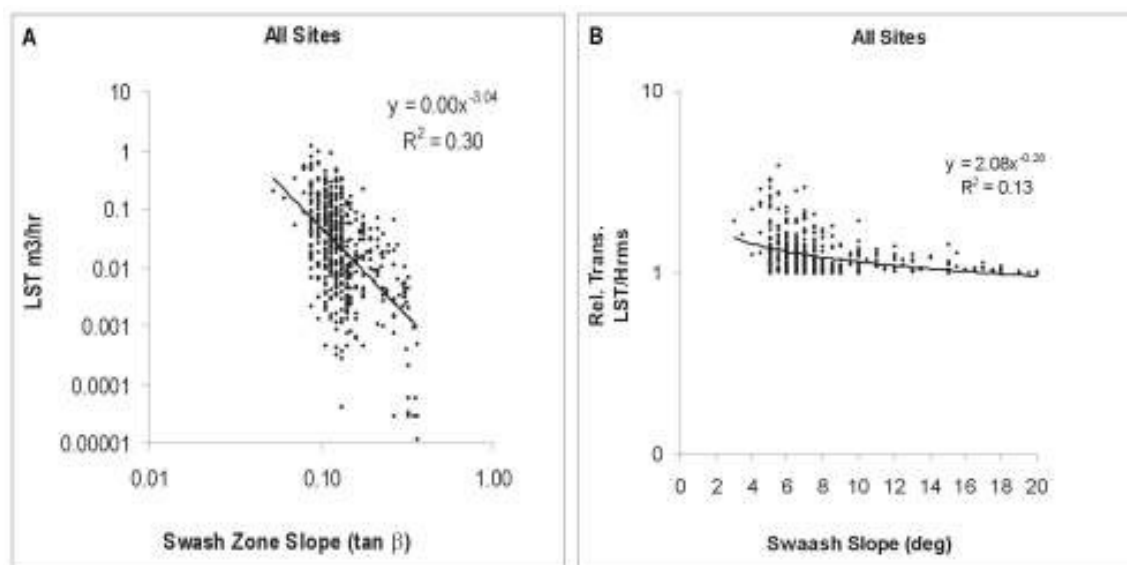


Figure 6.16 Linear regressions of the swash zone slope against longshore sediment transport at all sites (A) and relative transport (B). There is a gradual decline in the transport rate as the foreshore gradient increases.

When the transport rate is normalised by the width of the swash zone to create a relative transport rate, an interesting pattern emerges (Figure 6.17). In very low and zero energy conditions the transport rate is low. As the wave energy increases there is an immediate jump in the transport rate that increases steadily to a point when the slopes reach 10° . It will be recalled from the process-response model presented in Figure 5.34, that this slope angle occurs at the

threshold between low and moderate wave energy conditions. Slope angles between $6-9^{\circ}$ occurred during increasing wave energy as the slope become lowered through scouring. Below slope angles of 10° , the relative transport rate declines to a low point at around 7° . This is the average gradient of the swash during wave energy transition conditions. When the foreshore develops an equilibrium or adjusts to high energy conditions, the relative transport rate begins to increase again. This occurs typically at slope angles of around 5° . When the foreshore is in equilibrium with the conditions, the swash and wave energy is used most efficiently to transport sediment. During transition conditions, the energy is dissipated through turbulence, leaving less available for longshore sediment transport. Observations suggest that the onshore transport component remains high as material is redistributed about the foreshore, but the longshore directed component is lower.

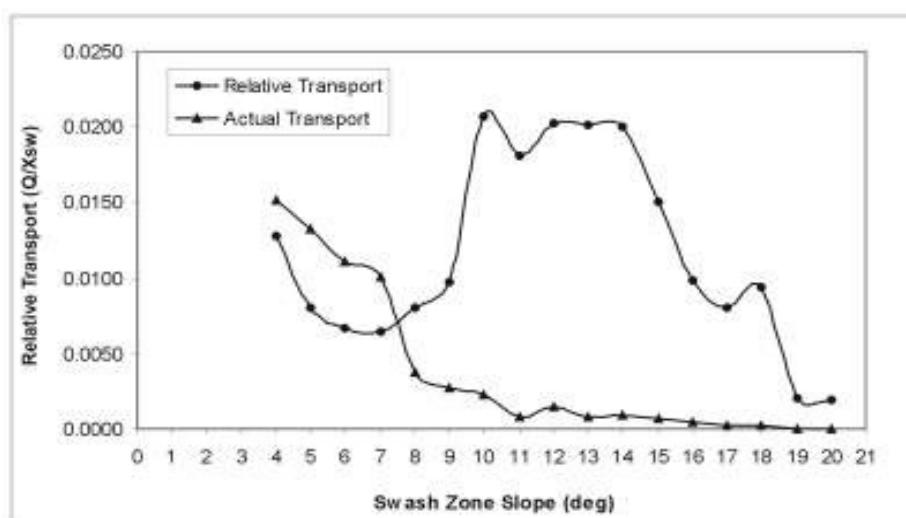


Figure 6.17 The relative and actual transport rate curves by swash slope. It can be seen that the actual quantity of material transported declines as the swash slope increases. However, the relative transport rate shows that the highest transport rates are associated with the equilibrium slopes at 5° and 10° . Above 15° , transport rates decline due to low energy. At the transition slopes between 5° and 10° , turbulence in the swash zone lowers the potential transport rate, even though wave energy conditions may be high.

The relationship between the wave steepness and the beach slope is expressed by the Iribarren number (Battjes, 1974). Based on the preceding discussion, it might be expected that there be a relationship between the breaker type and sediment transport. Table 6.10 presents the correlation coefficients for the regressions at each site. Excluding site CO13, there is a strong negative relationship with the Iribarren number. It will be recalled that there were both spilling and plunging wave recorded in Lake Coleridge. The threshold between spilling and plunging is 0.40.

At sites CO11a & b, where the transport rates were highest, the mean Iribarren number is on this threshold. It indicates that spilling waves have greater potential for transporting sediment than more plunging waves. The two sites with the highest Iribarren numbers, CO10 and CO13, also had the lowest transport rates. During transition conditions, that were frequently experienced at these two locations, plunging wave were most common. As a wave breaks through plunging, a lot of the energy is consumed in the breaking process and the efficiency of the resulting swash current declines.

Table 6.10 Correlation coefficients by site for the regressions between longshore sediment transport and the shallow water Iribarren number. NB: first row values are mean Iribarren numbers, not correlation coefficients.

	CO10	CO14a&b	CO11a	CO11b	CO13	All	excl. CO13
Mean ξ_b	0.45	0.42	0.40	0.40	0.44	0.43	0.43
r	-0.74	-0.65	-0.65	-0.55	-0.32	-0.68	-0.71
r^2	0.55	0.43	0.43	0.30	0.10	0.46	0.51
Std. Err.	0.57	0.43	0.55	0.59	0.52	0.60	0.57
n	208	49	57	76	103	493	390
Mean LS T	0.053	0.069	0.189	0.131	0.010	0.074	0.090

Grain Size

A great deal of research has been conducted into the relationships between grain size and rates of sediment transport. A grain of sediment at rest is held in place by the effects of gravity. When water flows over a bed of sediments, a new set of forces on the grain act to entrain the sediment in the fluid flow, working against the force of gravity. A lift force due to the Bernoulli effect and a drag force due to the fluid velocity acts on each individual grain exposed to the fluid flow (Figure 6.18). Much work has focussed on defining the critical thresholds at which sediment grains are entrained in the fluid flow (Leeder, 1982). A task that has proved extremely difficult because of the large numbers of variables involved. Commonly, critical threshold conditions for the initiation of sediment transport have been determined experimentally and empirically from field studies. This usually results in the generation of a curve that plots the grain size against the threshold shear stress or fluid flow (Figure 6.19). In the case of mixed sediments, the situation is further complicated by the fact that different grain sizes have different critical thresholds. In some tracer studies at Lake Coleridge, Worthington (1989) generally found that the finer material moved farther than the coarse material on a mixed sand and gravel beach. However, on a lag pavement, Worthington found the movement of the finer material was frequently impeded by the largest fraction. This ‘bed roughness’ is an important concept in sediment transport as

uniform beds have been found to encourage higher rates of sediment transport than non-uniform beds (Kleinhans & Rijn, 2002). Thus in mixed beds, it is possible to have finer fractions becoming entrained, whilst the coarser fraction remains immobile. Generally it has been found that the mean size of the material moving in the bedload fraction becomes coarser as the flow velocity or shear stress increases (Komar, 1996), as seen in Figure 6.19. Therefore, it might be expected that as the wave energy and swash velocity increases, the mean and maximum grain size entrained in the swash zone will become larger.

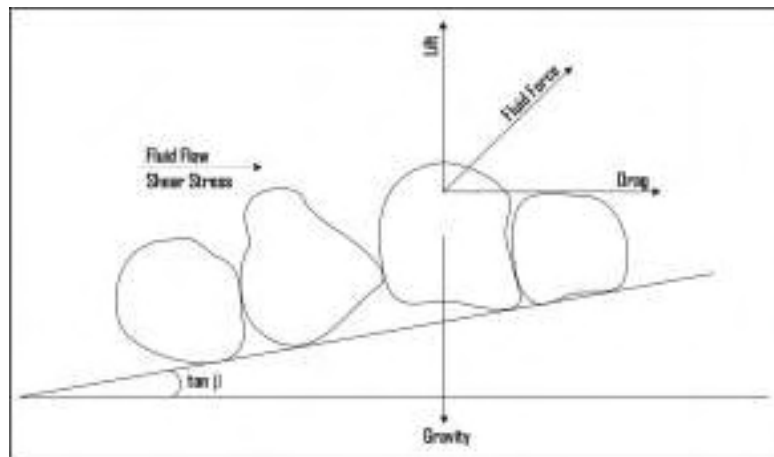


Figure 6.18 Forces acting on sediment grains in a fluid flow. (After: Leeder, 1982: 68).

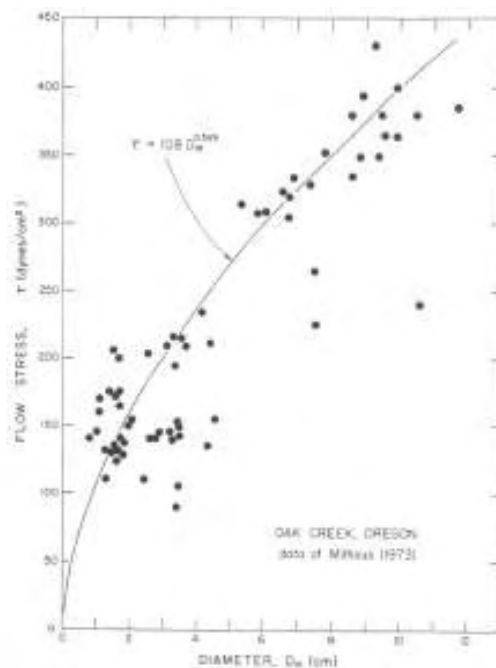


Figure 6.19 Grain size threshold curve for the coarsest bedload sediments sampled from the bed of a stream at various flow velocities. (From: Komar, 1996: 147).

Surprisingly, despite the wide range of grain sizes present in the foreshore at Lake Coleridge, very low correlations were found between the swash velocity, transport rate and grain size. Table 6.11 presents results of the regression analysis between the mean swash velocity and median grain size (D_{50}). In general it can be seen that very low correlations exist between the two variables. When the data set is examined as a whole, the correlation $r = 0.25$, but a mere 0.06% of the variation can be explained by sediment size. When the regression was conducted with the coarsest fraction in the samples (D_{10}), the correlations were unchanged. Figure 6.20a is a scatter plot of the maximum swash velocities against D_{10} grain size. It can be seen that few current speeds were measured below 0.10 m s^{-1} , and that above this velocity, every grain size in the measured range is entrained. Figure 6.20b shows the correlation between the coarsest fraction and the transport rate. Clearly, the size of the material has had very little influence on the transport rates measured in Lake Coleridge. The strongest correlations were found at sites CO10 and CO13, ($r = 0.48$ and 0.36 respectively), where 10-20% of variation in the transport rate can be explained by the grain size. There are a few cases when sand sized material was collected during low velocities, as seen in Figure 6.20. These occurred in very low energy conditions and have provided some of the correlation. At the other sites the correlation was more or less zero.

Table 6.11 Correlation coefficients by site for the regressions between longshore sediment transport and the mean grain size.

	CO10	CO14a&b	CO11a	CO11b	CO13	All	excl. CO13
D_{50}	3.28	3.61	3.82	3.64	4.08	3.60	3.47
r	0.48	-0.11	0.01	0.07	0.36	0.25	0.32
r^2	0.23	0.01	0.00	0.01	0.13	0.06	0.10
Std. Err.	0.75	0.56	0.73	0.71	0.51	0.79	0.77
n	208	49	57	76	103	493	390

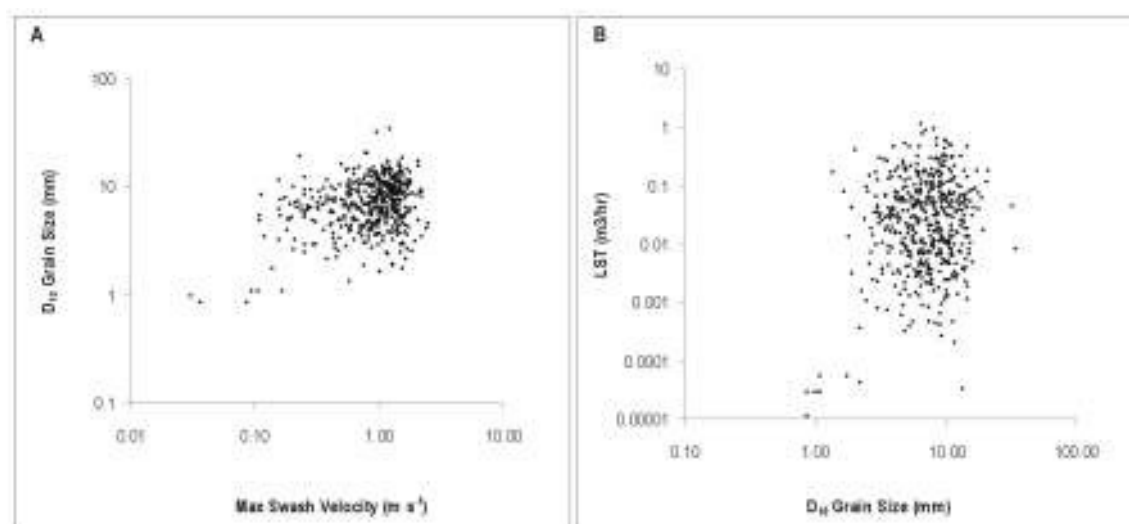


Figure 6.20 Scatter plots of the mean swash velocity and D_{10} grain size (A), and the D_{10} grain size and sediment transport rate (B). Poor correlations indicate the low influence of grain size in the sediment transport process of a mixed sand and gravel beach.

There are three main reasons why the correlations are poor. The correlation difference between the sites provides a clue to the first and main reason. Site CO10 and CO13 experienced the lightest conditions and the lowest average swash velocities. Measurements were made at the other sites during the strongest conditions. Thus, relative to the measurements made at each site, a weak relationship with grain size was found at the sites that experienced a greater range in wave activity. This suggests that overall, the wave activity was too energetic to detect small scale variations in the transport rate due to sediment size. The energy input and range of materials present in the foreshore is such that, the critical thresholds are almost always being exceeded. Even in low energy conditions, swash velocities have been sufficient to exceed critical entrainment thresholds for a wide size range. On only two occasions were the maximum swash velocities recorded below 0.10 m s^{-1} . The mean maximum swash velocity was 0.98 m s^{-1} and the maximum was 2.48 m s^{-1} . Clearly, there is enough energy supplied by the breaking wave to entrain all the grain sizes present in the swash zone, i.e. $0.125\text{--}32.0 \text{ mm}$ (3.0 to -5.0ϕ , fine sand to large pebbles).

In the swash zone of the mixed sand and gravel beaches at Kaikoura, Kirk (1970) found the same process occurred. Under the breaking wave, all the bed sediments were entrained and transported across the swash zone, regardless of size. The very high energies and turbulence that occurs in this area does not discriminate between small variations in grain size. Kirk found that the net transport rates in the swash zone were more important than the individual rates that

occurred in single swash lenses. There is no question that the sediment transport rate increases with increasing flow velocity, as illustrated above. However, in some respects sediment transport in the high energy swash zone has been found to be more of a stochastic process. That is, there is always sediment in motion, it is simply the magnitude of the rate that varies. This finding reinforces the dominant role of wave activity in controlling sediment transport. When the transport is normalised by the wave height to neutralise this effect, the poor correlations with grain size remain.

Thus, the second reason for the poor correlations is related to the range of grain sizes. Ninety percent of the mean grain sizes were between 1.0-6.0 mm, and 85% of the coarse fraction (D_{10}) was 2.0-16.0 mm in diameter. The conditions regularly experienced in Lake Coleridge mean that this is not a wide enough range to detect differential transport rates. Had the beach materials contained sizes into the cobble range, a stronger correlation may have been found. In light of this, the third reason relates to the data collection and measurement procedures. Collecting sediment for up to 5 or 10 minutes averages out swash to swash variations of the sediment size in motion. Clearly, the effects of grain size are not significant enough for variations to be detected at the scale measured in the present study. It is possible that there were variations in the sediment sizes being transported by individual swash lenses, depending on the velocity, but the field set-up was not designed to make these small scale measurements. To determine this, experiments would require an analysis of individual swash events with concurrent sediment transport and velocity measurements. It is not necessary to know such fine details when calculating the bulk sediment transport.

On a final note, it is also probable that the size fractions moved at different rates. Kirk (1970) noted that whilst the whole swash zone was mobilised, there were differences in the distances that size fractions were moved. However, this study was not designed to measure sediment velocity. Traps measure the discharge rate, not the distances travelled by an individual grain. One problem with conducting studies of this type in a natural beach, is that it relies on and assumes that all the size range is available for transport. From observations in the field, it was noted that at times, the sediments in the swash zone were unimodal, consisting of one main size fraction. It will be recalled that the some of the samples collected in the trap were well sorted, pure sands or gravels. Thus, there were times when the swash current may well have been sufficiently powerful to entrain gravel sized sediment, but that it was simply not available for transporting.

Pickrill (1976: 305) hypothesised that “waves of low amplitude may be as ineffective in moving coarse material as zero energy conditions”. This study has shown that even relatively coarse material can move in low energy conditions and that a wide range of sizes is easily transported by low amplitude lake waves. A fact that was later acknowledged by Pickrill when examining the movement of tracer material placed in the foreshore of sheltered beach located in the Hope Arm of Lake Manapouri, that was found to be moved by waves generated over fetch distances as short as 340 m. Pickrill (1976: 311) commented that “coarse material is entirely mobile even in extremely low energy environments”.

6.7 New Longshore Sediment Transport Equation (LEXSED Formula)

The discussion of the previous section highlighted what were found to be the most important environmental parameters controlling longshore sediment transport in a lakeshore beach. Inman and Bagnold (1963: 529) commented that: “...no claim to a reliable understanding of a natural process can be accepted until it can be explained in terms of basic natural principles...”. Working from a first principles basis, it was demonstrated that sediment transport is most controlled by the forcing functions or the wave energy. Wave height was the most dominant controlling variable and displayed a very strong correlation with the sediment transport rate at all sites. The wave period and the mean swash velocity were also found to be significant, as were expressions that incorporate two or more of these parameters, in particular, the wave steepness and Iribarren number. Aspects of foreshore morphology, such as slope and grain size were shown to have a far more variable influence on the sediment transport rate and proved to play a secondary role in the process.

Based on these relationships, an expression has been developed that displays an excellent correlation with the measured transport data. The trapped sediment data was effectively a bulk averaged rate, that smoothed the uncertainties and high variability that occurs in individual swash lenses. Thus, this expression is intrinsically a rate that takes account of the many small cumulative effects that occur in the swash zone and influence sediment transport. The core of the equation is the root mean square wave height cubed, divided by the deep water wave length. It will be recalled that the regression analysis between the wave height and longshore sediment transport rate indicated a relationship with the cube of the wave height. In effect, this term is a form of wave steepness. This energy is dissipated through breaking in the swash zone and in the

process exerts a shear stress on the foreshore sediments. Thus, the expression is multiplied by the mean swash velocity (\bar{v}_{sw}), as this provides the closest estimate of the shear stress and takes accounts for the wave dissipation after breaking. The swash also takes account of the swash zone width, as the highest velocities are associated with the widest swash zones and the greatest transport rates. Thus, the longshore sediment transport rate (Q_l) is proportional to:

$$Q_l \propto \left(\frac{H_{rms}^3}{(gT^2/2\pi)} \right) \cdot \bar{v}_{sw} \quad (6.6)$$

It is a dimensionally correct expression that produces values in units of cubic metres per second ($m^3 s^{-1}$). In effect, it is the instantaneous longshore sediment transport rate. The hourly rate can be calculated by multiplying this through by the number of seconds in an hour (3600). The length of the sediment trap was 0.5 m. Thus, this is the transport rate through a 0.5 m wide cross-section of the beach. It is customary to define shoreline changes in lineal metre increments. It would be acceptable to define the spatial limits of the this equation as $m^3 s^{-1}$ per lineal meter of beach. An important issue that arises in all studies concerning longshore sediment transport is the question of averaging scales both temporally and spatially. Spatially, authors frequently fail to identify exactly what part of the beach a longshore transport model refers to, whether it be the foreshore, the breaker zone or some average of the whole system. In this case the formula applies to very clear defined spatial and temporal limits.

The equation provides excellent correlations with the measured data, but requires a calibration coefficient (k) to produce values of the correct magnitude. This constant takes account of variables such as the beach porosity, that has been found to play an important role in the swash zone by absorbing wave energy, but was not explicitly measured. A final term included in the equation is the sine of the breaker angle (α_b). The longshore transport of material occurs when waves break at an oblique angle to the shore. Although there was a only a moderate correlation between increasing sediment transport and breaker angle, there was a general increase up to 30° . This parameter provided the best correlations with the data over other wave angle terms and pending further research is included to produce a general expression that can be used at other locations. Thus, the total integrated longshore sediment transport rate in the swash zone is presented as the Low Energy Mixed Sediment transport or LEXSED formula:

$$Q_l = k \left(\frac{H_{rms}^3}{L_o} \right) \cdot \bar{v}_{sw} \cdot \sin \alpha_b \quad (\text{m}^3 \text{ s}^{-1}) \quad (6.7)$$

Through residual analysis, k is found to have a value of 0.02. The root mean square wave height has consistently provided the best correlations with measured environmental variables and is used here in favour of other wave height parameters. However, it would be acceptable to use the significant wave height. The breaker height was not measured in the field and it was decided not to use a derivative form of the wave height. The deep water wave parameters, height, period and length have also provided consistently good correlations with the measured data, as opposed to the shallow water equivalents. As has been demonstrated, wave modification in the nearshore has been minimal, due to the presence of deep water close to shore and low amplitude waves. This has meant that the deep water variables have in general been able to be successfully used for modelling purposes. The one exception perhaps, has been site CO13, where some wave modification that was unmeasured, provided lower correlations between the longshore sediment transport rates and the wave variables. Nevertheless, Equation 6.7 deals with this variability reasonably well, in part because it takes into account the currents responsible for transporting the sediments in the swash zone. The sediment grain size proved too unreliable a variable to incorporate into the equation due to the poor relationship found with the transport rate. At this stage, no grain size parameter is incorporated into the equation.

Figure 6.21 shows the correlation between the measured and estimated longshore sediment transport rates, produced by Equation 6.7. A strong correlation can be seen across the full range of measured conditions. The data points are evenly scattered around the best-fit line. Figure 6.21a presents the correlation against all the data and 6.21b excludes the data from site CO13. Encouragingly, the correlation coefficient only improves by 0.02 by excluding this site. This indicates that the equation is suitably robust and capable of dealing with sites that may have conditions that differ slightly from the those that were used in the development of the expression. Table 6.12 shows the correlation coefficients by site for Equation 6.7. It can be seen that the equation performs well at site CO13, providing a correlation of $r = 74$. There is close agreement at the other sites, with the correlation coefficients ranging from $r = 0.84$ - 0.90 .

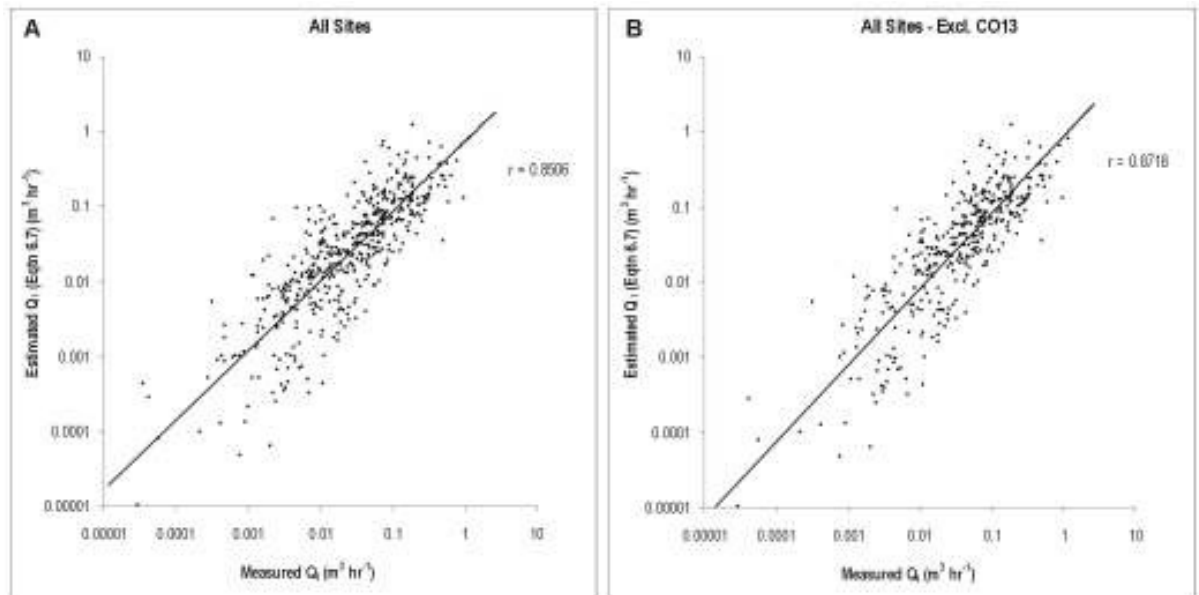


Figure 6.21 Correlations between the measured longshore sediment transport rate and the rate estimated by LEXSED (Equation 6.7). The correlation for all the sites is shown in (A), whilst (B) the correlation excluding data from site CO13 is shown in (B). Despite the previous problems with this site, the correlation remains strong when it is included in the analysis. Std. Error = 0.47. $F = 1285$ Prob. < 0.0001.

Table 6.12 Correlation coefficients by site for Equation 6.7 against the measured transport rates.

Site	r	Std. Error	Prob.
CO10	0.88	0.46	< 0.0001
CO14	0.84	0.54	< 0.0001
CO11a	0.90	0.29	< 0.0001
CO11b	0.88	0.28	< 0.0001
CO13	0.74	0.38	< 0.0001

The expression provides good estimates of the total integrated longshore sediment transport rate in the swash zone. Table 6.13 shows the summary statistics for the measured and estimated hourly rates. The measured rates range from 0.000011 to 1.154 m³ hr⁻¹, with a mean of 0.074 m³ hr⁻¹. The estimated rates range from 0.000002 to 1.265 m³ hr⁻¹, with a mean of 0.073 m³ hr⁻¹. Significantly, the range in the data is very similar. The standard deviation and variance measures are almost identical. This is also reflected in the skewness and kurtosis values, that are both similar. Clearly the equation is capable of picking up the extreme highs and lows in the transport rate. This is important because in storm conditions large amounts of material can be moved in a relatively short period of time, causing shoreline retreat, overtopping and inundation. From a planning and management perspective it is critical to have knowledge of the potential damage that can be caused by a storm event. From a scientific perspective the high energy nature of the

coastal environment means that most of the research has been restricted to low energy conditions. Thus, many relationships are found to break down in storm conditions. In a review of field data for sediment transport data collected in natural beaches, Schoonees and Theron (1993: 21) identified a clear lack of data for high energy storm conditions, they concluded that:

“A serious consequence of this lack of data is that longshore transport formulae are calibrated almost exclusively against data for mild conditions while, in the case of an average annual longshore transport budget, a few storms usually contribute by far the most to the total sediment transport. In other words, the most important predications for which the formulae are used, are for conditions outside their calibration range.”

A strength of the new equation is that it derives from a very wide range of environmental conditions, from light air to strong gale force northwest winds, from gentle to steep gradient foreshores, from acute to oblique wave angle approaches and from coarse sand to large pebble sized sediment. The equation has been found to perform well across all these conditions.

Developing an equation of this type not only requires that the special case for Lake Coleridge be defined, but that it has wider applicability to similar situations. In this case, other coarse grained beaches in low energy environments, such as the glacial lakes of the South Island. Figure 6.22 shows two forecast curves for wave heights up to 1.0 m. The forecasts appear reasonable and fit within the range measured at Lake Coleridge. As waves become steeper the transport rate increases, in the same manner found in the field. Presently, the equation is applicable to coarse grained beaches with a mean grain size over 1.0 mm and wave heights under 1.0 m. However, the general principles of this expression will apply to the mixed sand and gravel beaches of the open New Zealand coastline, as the two beaches studied in Lake Coleridge are essentially very similar to their open coast counterparts. In the interest of science, forecast curves were calculated for the range of waves that are experienced in the mixed sand and gravel beaches of the open coast. Using a wave approach angle of 10° and the same k coefficient of 0.02, the hourly cubic meter rates were calculated. A value for 2.5 m s^{-1} was used for the swash velocity, based on the findings of Kirk (1970). Again, the estimates appear within the range that might be expected to occur in a natural mixed sand and gravel beach. The curves indicate that steep, plunging storm waves are capable of moving large quantities of sediment. Whilst the long, low swell, tends to be more depositional in nature.

Table 6.13 Summary statistics for the measured and estimated longshore sediment transport rates

LST ($\text{m}^3 \text{hr}^{-1}$)	Measured	Estimated
Min	0.000011	0.000002
Max	1.154	1.265
Mean	0.074	0.073
Std. Dev.	0.130	0.125
Variance	0.017	0.016
Skewness	3.924	4.190
Kurtosis	20.560	25.041

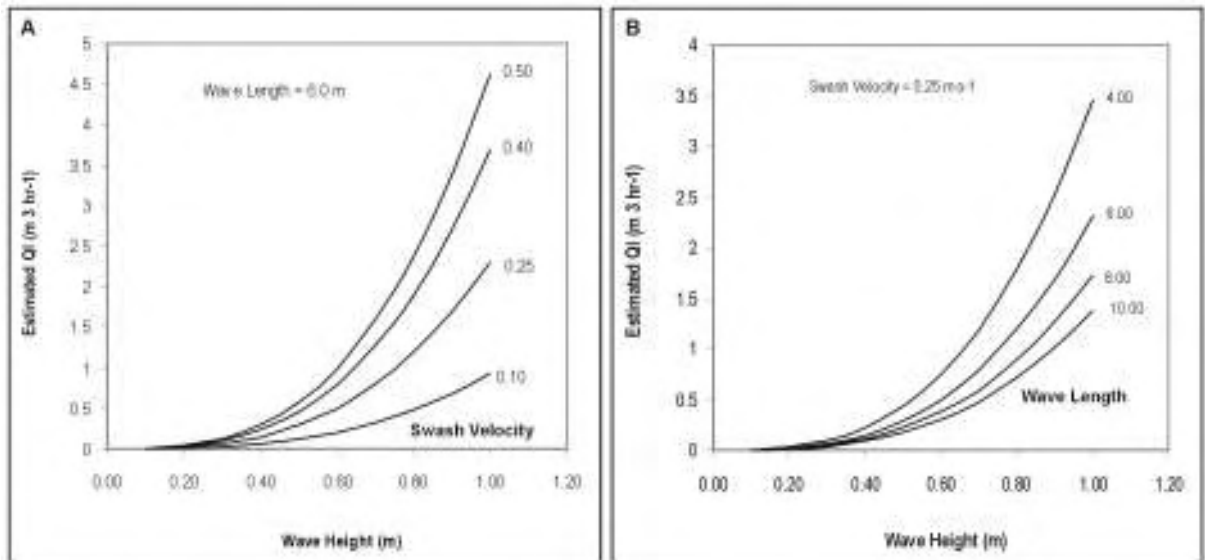


Figure 6.22 Forecast curves for Equation 6.7. (A) shows a variable wave height and swash velocity. (B) shows a variable wave height and wave length. It can be seen that sediment transport increases in an exponential fashion with increases in the wave energy.

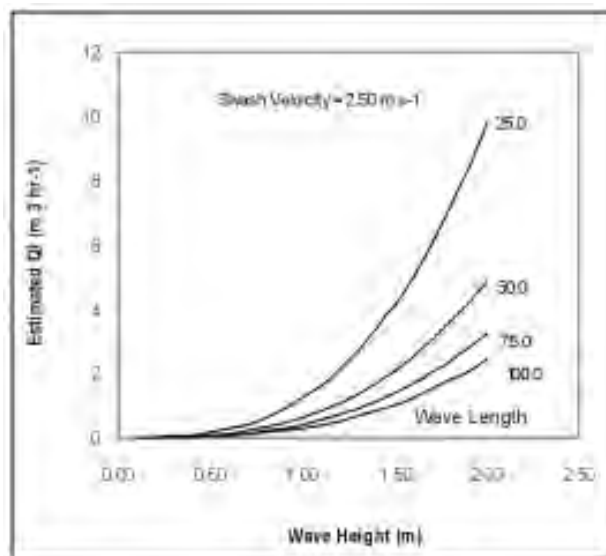


Figure 6.23 Extended forecast curves using Equation 6.7 using wave variables commonly found in unrestricted open coast locations. Wave approach angle = 10.0° .

Practical Application of LEXSED Formula

Using Equation 6.7, it is possible to estimate the annual longshore sediment transport rates of the barrier foreland to a high degree of accuracy. All that is required is a knowledge of the wave height, period and angle of approach. There are a number of models available for wave hindcasting purposes. In a restricted fetch environment, the NARFET model has been found by Allan (1998) and Allan and Kirk (2000) to provide reasonable wave hindcasting estimates. One criticism of the model is that it assumes uniform surrounding topography. Allan (1998) commented that often in mountainous terrain, the wind is accelerated down valleys, causing highly localised variations in wind strength influence wave generation. Allan found that NARFET did not take these topographic effects into account. An initial assessment using NARFET with the Lake Coleridge data produced mixed results, in part due to the severe topographic forcing of the wind down the Wilberforce Valley.

In the present case, another approach is to use the empirically derived regression equation between the wave height and wind speed data measured in the field. It was discussed in Chapter Four that a strong relationship was found between the measured wave heights and the wind speed recorded by the weather station ($r = 0.85$). An expression was presented (Equation 4.6) that was derived from a regression analysis between the two variables, that has a regression coefficient of ($r^2 = 0.72$):

$$H_{rms} = 0.0451e^{0.1632\bar{V}} \quad (6.8)$$

Where \bar{V} is the mean hourly wind speed. By solving the equation, the resulting values show excellent agreement with the measured wave heights. An even stronger relationship exists between the wave height and wave period ($r = 0.92$), also discussed in Chapter Four. The wave period can be estimated with the regression equation ($r^2 = 0.85$):

$$T_z = 2.29H^{0.28} \quad (6.9)$$

Finally, formulas for calculating the swash velocity were presented in Chapter Five. The expression used here is Equation 5.16, that estimates the mean swash zone current velocity with the wave height and period.

$$\bar{v}_{sw} = \sqrt{\frac{H_{rms}}{T_z}} \quad (6.10)$$

Thus, hourly wave height and period statistics can be calculated using the hourly wind speed data. Deriving the wave length from the values produced by Equation 6.9, and substituting these three equations into the LEXSED Formula (Equation 6.7), the hourly longshore sediment

transport rate was calculated for an entire year using the 2002 wind data set. The wind direction was used to provide information on the wave direction. In this way both the gross and net annual longshore sediment transport rates were calculated for the western and south-eastern side of the barrier foreland.

The annual gross longshore sediment transport rate for 2002 through a 1 m cross-section of the beach on the western side of the barrier is estimated to be $818.5 \text{ m}^3 \text{ yr}^{-1}$. The mean hourly rate is $0.093 \text{ m}^3 \text{ hr}^{-1}$, which compares favourably to the mean empirically measured rate of $0.074 \text{ m}^3 \text{ hr}^{-1}$. Using the wind direction as an indication of the wave approach angles, the net rate is calculated to be $755.1 \text{ m}^3 \text{ yr}^{-1}$ from the north and $63.4 \text{ m}^3 \text{ yr}^{-1}$ from the south, producing a total net southward movement of material in the order of $691.7 \text{ m}^3 \text{ yr}^{-1}$. The dominant northwest wind-wave direction produces a strong net transport rate from north to south. By way of comparison, it will be recalled that the net longshore sediment transport rate for South Beach, a mixed sand and gravel beach on the Timaru coastline, is estimated to be $60,000 \text{ m}^3 \text{ yr}^{-1}$. The net annual longshore sediment transport rate at Shoreham Beach, West Sussex, in the United Kingdom is in the order of $15,000 \text{ m}^3 \text{ yr}^{-1}$ (Van Wellen *et al.*, 2000a).

Using the profile survey data to estimate the volume of material in the barrier foreland, it is possible to calculate an average annual lineal growth rate and estimate the amount of time taken for the barrier foreland complex to develop. The current volume of the 500 m long western side of the barrier is *ca.* $62,500 \text{ m}^3$. Bearing in mind that the gross annual rate was estimated to be in the order of $800 \text{ m}^3 \text{ yr}^{-1}$, this indicates that around 1.3% of the total volume of the beach system is transported through the foreshore annually. The 250 m long south-eastern side has a volume of *ca.* $18,750 \text{ m}^3$. The beach has a maximum depth of around 5.0 m from the barrier crest to the lakeward limit of the beach deposit. This is equivalent to the water-level operating range of the Lake in the 1950s. Prior to the development of the Lake for hydro-electric power, the natural operating regime was in the order of 1.5-2.0 m. The present study has quantitatively established that sediment transport in a mixed sand and gravel beach, is confined to the area landward of the breaking wave. Thus, the water-level range controls the depth or height to which sediment is transported elevation wise on the beach. Taking into consideration extreme high water levels, it would be fair to assume that the beach prior to human intervention was in the order of 2.5 m deep. This allows for the beach crest to lie above the average highest water level events and effectively enclose the lagoon in its present configuration.

Recalculating the volumes with this assumption, suggests the western side of the barrier was built with 31,250 m³ of material and the south-eastern side built with 9375 m³. Using this to calculate an average annual lineal beach growth rate, it is possible that the western side of the barrier grew at a rate of *ca.* 10.0 m per annum and the south-eastern side at a rate of *ca.* 1.5 m per annum. It will be recalled that the top ridge on the south-east side of the barrier is aligned some 10° further north from the present day shoreline, suggesting that wave crests from the southeast approached the shoreline at a slight angle, initiating a longshore transport of material. Once the spit joined with the western arm, the beach aligned into the prevailing conditions and stabilised. The western side of the barrier has become drift-aligned and material is presently being deposited around the elbow of the feature to form a broad flat beach deposit. Thus, over time, the volume of the barrier has slowly increased. Fresh material is supplied to the beach from Cottons Stream, to the north of the barrier, when lake levels are high enough to form a continuous beach from the stream mouth and across a large lag pavement to the barrier. At other times, material is scavenged from the northern end of the beach. The profile here is about 40 m wide. By the middle of the barrier the beach widens to 50 m and at the end of the beach the profile widens to 60 m. In effect, creating a reverse spit morphology, whereby the proximal end of the barrier spit becomes eroded and the material is deposited at the distal end. This is a unique feature of mixed sand and gravel spits, that later become barriers. The most notable example being Kaitorete Barrier, at the northern end of the South Canterbury Bight.

A plan form map of the beach evolution is presented in Figure 6.24. It shows a time line of the stages of development in the barrier foreland complex. Based on present transport rates, the western side of the barrier may have grown in as little as 50 years. The growth rate of the south-eastern side has been comparatively slower, taking some 150 years to meet up with the western arm. This is because this side does not experience longshore sediment transport from northwest generated waves. It will be recalled from Chapter Two, that the wind regime of Lake Coleridge is bi-directional, but that wind from the northwest is both stronger and more prevalent than wind from the southeast. The whole complex has developed on a lag pavement eroded from the base of a talus fan, also discussed in Chapter Two. Thus, the growth of the barrier has ultimately been controlled by the structural geomorphology of the site. This is the reason why the western side of the barrier did not keep growing into Lake Coleridge ahead of the south-eastern arm.

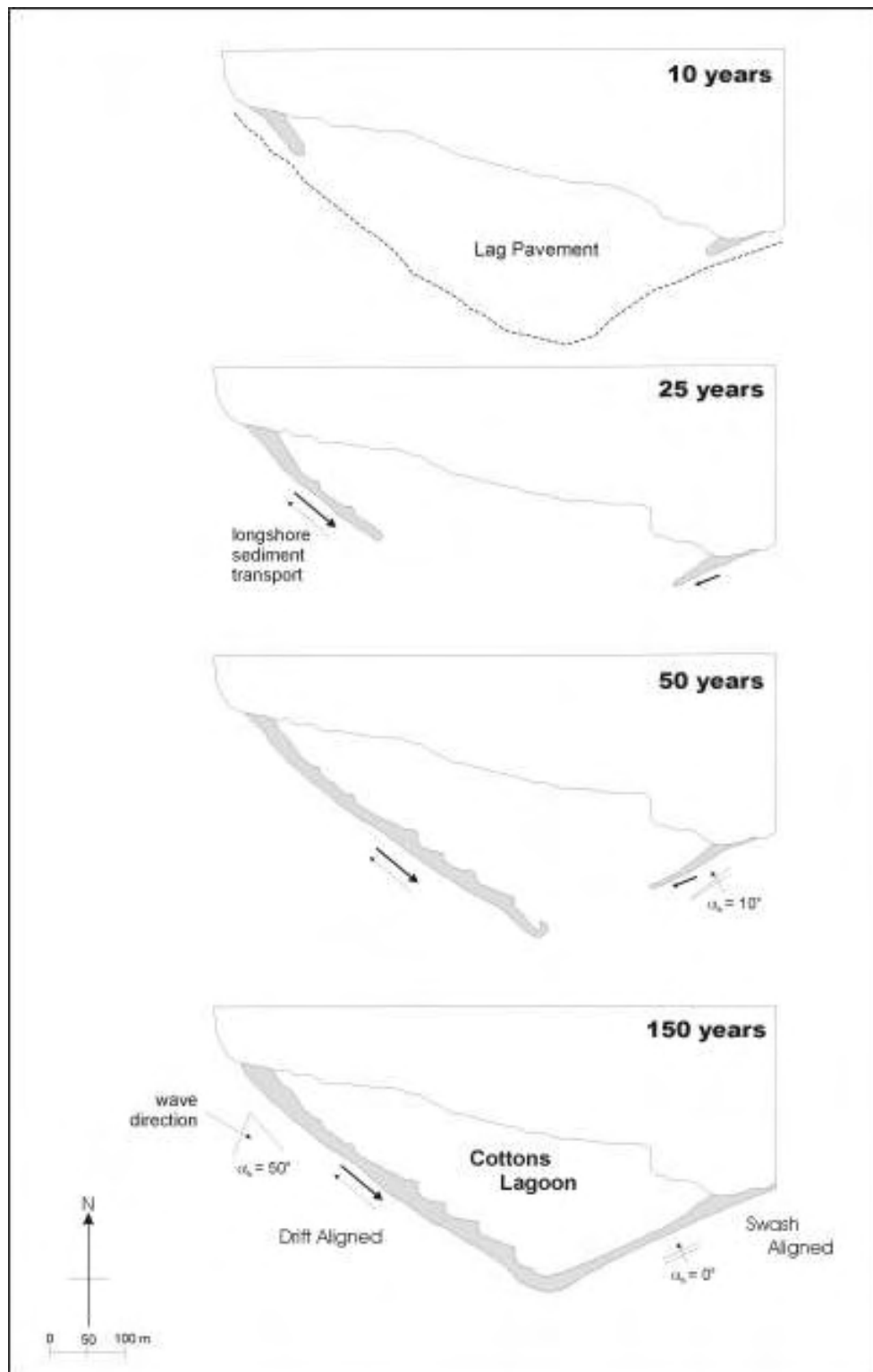


Figure 6.24 Plan form representation of the development of the barrier foreland complex on which the fieldsite was located. Using a combination of survey profile data, wind data collected by the weather station and Equation 6.7 for estimating the longshore sediment transport rates, an annual average growth rate for the barrier complex was calculated. The western side of the barrier has probably grown at around 10 m year, and taken 50 years to reach its present length. The south-eastern side has grown much slower, at around 1.5 m per year, taking around 150 years to reach its present length. It is not known exactly when this feature formed. Beach outline was based on aerial photographs.

6.8 Bagnold Longshore Transport Derivation

Professor Paul Komar, Oregon State University (*pers. com.*, 2006), suggests another approach could also prove useful. Komar (1998) used the transport model developed by Bagnold (1963; 1966) to show that, when applied to sandy beaches, Bagnold's transport formula is equivalent to: $Q_l = 0.088H_{rms}^2 v_l$, where v_l is the longshore current velocity. Applying Komar's derivation to the present study, the longshore current term (v_l) can be replaced by $v_{sw} \sin \alpha_b$, which is effectively the longshore component of the swash velocity. This yields an equation that has a fundamental process derivation based on Bagnold's approach to sediment transport:

$$Q_l = k(H_{rms}^2 \cdot v_{sw} \cdot \sin \alpha_b) \quad (\text{m}^3 \text{ s}^{-1}) \quad (6.11)$$

The equation performs soundly when correlated against the measured longshore sediment transport data (Figure 6.25). It incorporates the main elements involved in controlling longshore sediment transport. Using residual analysis against the Lake Coleridge data set k has a value of 0.0018. The Pearson correlation coefficient $r = 0.80$ and the regression coefficient $r^2 = 0.65$. This is slightly weaker than the LEXSED model as is probably due to the simpler formulation of Equation 6.11 that does not take into account factors such as the wave period and steepness. A similar equation that uses the wave energy is developed and discussed in the following chapter.

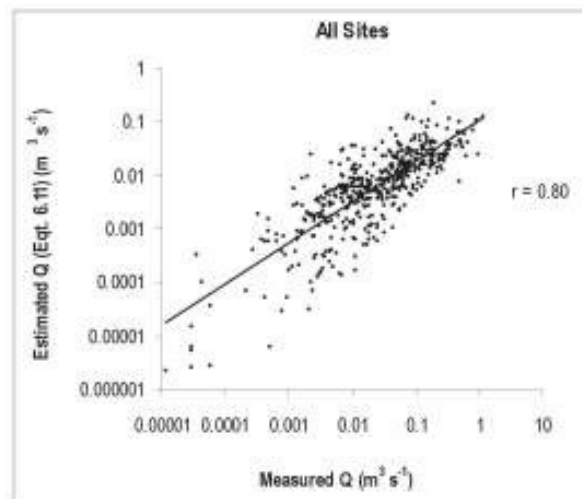


Figure 6.25 Correlation of Equation 6.11 against the measured longshore transport data.

6.9 Summary

This chapter has presented results from the sediment transport measurements made in Lake Coleridge. It was noted at the start of this chapter that this was the first major study of its kind conducted in a New Zealand mixed sand and gravel lakeshore beach. As such there have been no other studies by which to make firm comparisons. Sediment transport was measured by way of two traps, one located in the nearshore and the other in the swash zone. Very little material was found to be transported longshore in the nearshore area. The shear stress exerted by the waves crossing the nearshore is simply insufficient to entrain the coarse gravels than commonly characterise the nearshore bed. Longshore sediment transport was found to occur exclusively in the swash zone, landward of the breaking wave. Sediment was entrained at the base of the swash zone and transported up and along the foreshore in the swash and back downslope in the reverse flow. Some grains were thrown into the air by saltation in this process, but most of the material moved as bedload. Over 500 samples were collected in the field programme. The weight of material collected in the trap ranged from as little as 100 g though to 5.5 kg.

The sediments collected in transit were a heterogeneous mix of coarse sands and fine gravels. In general the material was relatively coarse in nature. The mean grain size for all the sediment collected in the trap was granule sized material, 3.54 mm in diameter. Small quantities of fine sand and medium sand appeared regularly in the trapped material in small quantities. However, the sand was more commonly coarse, in the range of 0.5-2.0 mm. There was a significant mode between 4.0-8.0 mm in the pebble size range, whilst the largest material collected in motion was 32.00 mm. Many of the samples were poorly to moderately sorted, but a significant number were found to be moderately well sorted. This contrasted with the generally poor sorting of the sediments in the foreshore. In the process of being transported, the sediments were sorted to a degree. This sorting frequently produced samples that were coarse skewed with a lag of larger material.

The trap data were converted into hourly rates of sediment transport by multiplying the trapped weight of material by a factor that was a function of the trapping time and the number of minutes in one hour. A series of experiments were conducted to satisfy the assumption required to make this calculation. Material was collected in sequential one minute and five minute periods in low and high energy conditions. The trapping variation was found to be consistent from one sampling to the next in the order of $\pm 10\%$. Hourly trapped rates ranged from 0.02 to 214.88 kg hr⁻¹ with an overall average of 26.68 kg hr⁻¹ $\pm 10\%$. These rates were then converted into a

volumetric rate. A numerical method was developed that accurately estimates the volume of a sediment sample of known weight, that uses the porosity and density of the sediment. The density was determined by measuring the sediment displacement in a known volume of water with samples typically collected in the trap. The mean density of the Lake Coleridge greywacke is 2850 kg m^{-3} . The porosity was calculated as the ratio between the mass of a sediment sample and its equivalent solid density mass. The average porosity value for the Lake Coleridge sediments was found to be 0.615. In other words, 38.5% of the sediment volume is pore space. The volume of each sample was calculated as the ratio between the weight of the sample collected in the trap and the solid density of the sediment, to produce an hourly cubic metre rate. Hourly transport rates through the trap ranged from 1.14×10^{-5} to $1.23 \times 10^{-1} \text{ m}^3$ which covers 5 orders of magnitude. The average rate was $1.52 \times 10^{-2} \text{ m}^3 \text{ hr}^{-1} \pm 10\%$ and most of the rates were within this order of magnitude.

The volumetric rates were used to calculate the total integrated longshore sediment transport rate in the swash zone. To achieve this, a study was conducted to determine the distribution of the longshore transport flux across the swash zone. Traps were placed at pre-set distance across the swash zone and variations in the transport rate at increasing distances landward of the breaker were measured. The transport rate was found to increase rapidly immediately forward of the breaker from zero to the maximum at around a distance 20% the width of the swash zone. The rate remains high across the middle of the swash zone. A lot of swash activity occurs in this area where both swash and backwash carry high sediment loads. It is also an area that receives a lot of swash of short lengths. After the 50% width, the rate begins to decline until around the 70% width, the rate plateaus and remains steady until the very limit of the swash zone, where it reduces to zero. With this data, a curve was developed that represented the longshore transport flux across the swash zone. Using numerical integration, the area under this curve was calculated and an equation written to estimate the transport rates above and below the trap in the swash zone. The measured transport from the trap was added to these estimates to produce a total integrated rate. The total transport rates ranged from a minimum of $1.10 \times 10^{-5} \text{ m}^3 \text{ hr}^{-1}$ to a maximum of $1.15 \text{ m}^3 \text{ hr}^{-1}$. The mean rate was $7.36 \times 10^{-2} \text{ m}^3 \text{ hr}^{-1}$. No previous measurements or calculations of this kind have been made for a New Zealand lakeshore beach.

Correlation and regression analysis was conducted between the environmental variables measured in the field and the total longshore sediment transport rate. The correlations were consistently stronger with the total rate as opposed to simply the trapped weight of material, validating the total integrated calculations. Sediment transport was found to result from the

complex interaction between a number of different variables. Measurements were taken from seven locations in the field, in a wide range of conditions. Importantly, measurements covered high energy storm events. In many coastal research projects, data collected from natural beaches is made during low energy conditions. The models derived from these studies are often found to have limited application and cannot be applied to storm events. The correlations were reasonably consistent from site to site. The one exception was site CO13 that experienced a degree of wave modification.

Sediment transport was found to be most strongly controlled by the wave height, period and mean swash velocity, *i.e.* the energy inputs or forcing functions. A strong correlation was also found with the wave steepness. The wave direction dictates if longshore sediment transport is to occur. When waves break at an oblique to the shore, transport is initiated. The rate generally increases with increasing angle up to around 30° . Above this the transport rates varied considerably in relation to the breaker angle. Surprisingly, despite the wide range in grain sizes present in the foreshore, very poor relationships were displayed between the grain size and transport rates. There was a very general increase in the grain size when transport was initiated. But once in motion, all the grain sizes were found to be moved in the swash zone. The high flow velocities under the breaking wave and in the swash zone exceed the entrainment thresholds for all the sediment sizes present in the beach. With regards to the beach slope, the highest transport rates were associated with the lowest beach slopes. This is largely because the swash zone is at its widest and the current velocities fastest, when the foreshore gradient is low. When the relative rates were examined, the highest transport rates were associated with slope angles at 5° and 10° . The lowest relative rates were associated with the transition slopes between 6° and 9° . This lends further support the process-response model of swash zone development, presented in Chapter Five. Thus the sediment transport rate was defined by a few key environmental variables; the wave height, wave length and swash velocity.

An expression was developed, termed LEXSED, that divides the cube of the wave height and the wave length, which together is a form of wave steepness, and multiplies this by the mean swash velocity and the wave approach angle. A calibration coefficient is included to produce values of correct magnitude. The formula produces values in cubic metres per second and is a total integrated rate for the whole swash zone. The values produced by the equation showed very good correlations to the empirical data, including site CO13. The expression provides good estimates of the total integrated longshore sediment transport rate in the swash zone. The measured rates range from 0.000011 to $1.154 \text{ m}^3 \text{ hr}^{-1}$, with a mean of $0.074 \text{ m}^3 \text{ hr}^{-1}$. The

estimated rates range from 0.000002 to $1.265 \text{ m}^3 \text{ hr}^{-1}$, with a mean of $0.073 \text{ m}^3 \text{ hr}^{-1}$. Considering the wide range of conditions that were measured in the field, it performs well in taking account of the variability found in natural beaches. Thus, the formulation shows some promise in being able to be applied to other lakeshore locations. Moreover, because it embodies underlying principles common to longshore sediment transport on all mixed sand and gravel beaches, it has potential in being adapted for use in oceanic applications.

Using the equation, the annual longshore sediment transport rates for the fieldsite beaches were calculated. Hourly wave height statistics for a whole year were derived from the wind data collected by the weather station. Gross annual transport rates on the western side of the barrier beach are *ca.* $800 \text{ m}^3 \text{ yr}^{-1}$. The net rates are *ca.* $740 \text{ m}^3 \text{ yr}^{-1}$ from the north and *ca.* $60 \text{ m}^3 \text{ yr}^{-1}$ from the south, a reflection of the dominance of the northwest wind. The hourly average rate for 2002 was found to be $0.093 \text{ m}^3 \text{ hr}^{-1}$, which compared favourably with the average hourly rate of $0.074 \text{ m}^3 \text{ hr}^{-1}$ measured in the field. Using the beach profile survey data to calculate the volume of material in the barrier foreland, an annual lineal growth rate was approximated and estimates were derived for the amount of time taken for the barrier foreland to develop. It was estimated that the western side of the barrier developed its full length in around 50 years, growing at 10 m per annum. The south-eastern side took longer to develop due to its orientation and sheltered aspect and took around 150 years to develop, growing at 1.5 m per annum.

This chapter has presented a discussion and analysis of the nature of longshore sediment transport in a lakeshore beach. The outcome of this has been the development of an equation that can be used to reasonably estimate rates of longshore sediment transport. The following chapter examines some widely used longshore sediment transport equations that have been developed from studies of open coast beaches and assesses their potential for estimating transport rates on both oceanic and lacustrine mixed sand and gravel beaches.

CHAPTER 7.

SEDIMENT TRANSPORT MODELS

*“As far as the laws of mathematics refer to reality,
they are not certain; and as far as they are certain,
they do not refer to reality.”*

Albert Einstein

7.1 Introduction

The modelling of sediment transport in the coastal zone has received a great deal of attention over the years and this has led to the development of a wide range of models based on different physical principles. The primary aim of much of the research has been to produce reliable models for understanding the process of sediment transport. Much of the early work was descriptive in nature, but by the early 20th century it was recognized by engineers that rates of longshore transport needed to be quantified in order to safely build in the coastal environment (Clarke, 1921; Matthews, 1934). It was apparent that the rate of sediment transport alongshore was dependent on the magnitudes of the various processes acting within the beach system. The goal was to develop models that could determine the littoral transport rate based on a knowledge of the wave and current processes responsible for sediment transport. These models have been developed for use in a variety of different settings and frequently they have been applied by authors to situations beyond that for which they were originally intended.

This chapter tests and evaluates a series of longshore sediment transport models in order to identify those that have potential application to mixed sand and gravel beaches. There are numerous sediment transport models to select from in the coastal engineering literature. The vast majority have been developed for calculating longshore sediment transport rates on sand beaches. Thus, many of the formulae contain parameters that take account of processes not found to occur in mixed sand and gravel beaches. Accordingly, only equations that have been developed for coarse grained beaches or generalised expressions that contain principles common to all beaches, were selected for testing. The chapter begins by charting the significant historical work that lead to the development of the most widely recognised and used littoral sediment transport equation; the Inman and Bagnold formula, also referred to in the literature as the CERC (Coastal Engineering Research Center) and SPM (Shore Protection Manual) formula. The Inman and Bagnold formula is discussed in depth, leading to an explanation of why it is suitable for use in mixed sand and gravel beaches and in particular, mixed sand and gravel lake shorelines. This is followed by a discussion of variations of the Inman and Bagnold formula and similar models

that have been applied to gravel beaches. Following this, some equations that have attempted to account for the shear stress exerted on the sediment by adapting principles from unidirectional stream power transport models are examined. Finally, a series of expressions that have been derived from a dimensional analysis between transport rates and environment parameters are reviewed. These equations have been developed from studies in laboratory wave flumes. The equations were solved using the hourly wave and current data from Lake Coleridge and the results correlated with the total integrated longshore sediment transport rates. The wave statistics measured by the wave gauge were used in all the calculations. This chapter presents a discussion and analysis of the results from this exercise.

7.2 Historical Development of Longshore Sediment Transport Equations

One of the pioneering attempts to give longshore transport a mathematical framework was made by Munch-Peterson (1938 *in* Beach Erosion Board, 1950). Munch-Peterson presented an equation that took into account what he intuitively thought were the most important variables involved in longshore sediment transport:

$$M = k(1/8 h^2 L) \cos \alpha \quad (7.1)$$

where ‘M’ is what Munch-Peterson referred to as the ‘material moving power’, k is a coefficient, h is the wave height, L is the wave length, (together the expression $(1/8 h^2 L)$ constitutes the wave energy), and α is the incident wave angle. The aim was to define the transporting ability of the waves as a function of the wave energy and crest angle. Munch-Peterson noted there was a concurrent increase in sediment transport with increasing wave angles and this has remained a critical parameter in longshore transport models. The concept of ‘material moving power’ is an important one as it formed the basis of what is now commonly referred to as the wave power or energy flux approach to longshore sediment transport modelling. Due to a lack of wave data, Munch-Peterson hindcast the wave statistics from wind information in order to calculate the volumetric transport rate. This is one of the first recorded instances of using wind data in this manner and it has remained a popular line of research to the present.

In a report published in 1947, the Scripps Institute of Oceanography also suggested that the work performed by waves in the nearshore zone might be a useful parameter for relating the littoral transport rate to wave action (Inman & Bagnold, 1963). Following this suggestion, the

United States Army Corps of Engineers (USACE) began making use of a littoral transport factor (Q) in studies of the southern Californian coastline in order to estimate the dominant direction and volume of sand transport from hindcast data (Handin & Ludwick, 1950). The Q factor was defined as:

$$Q = k(we) \sin 2 \alpha \quad (7.2)$$

where Q is the total annual sand transport, w is the wave work factor, e is the wave energy per unit length of wave crest, α is the wave angle, and k is a coefficient. It was acknowledged at the time that the equation had not been proved through field investigations, and so like the Munch-Peterson (1938) formula was a theoretical attempt to quantify the longshore transport process. Despite the fact the two formulas were conceived independently, they bear a striking similarity because they are based on the same concept. Both incorporate a term for calculating the wave energy and a term for calculating how much of this energy is expended in a longshore direction. Also of note in both equations is the k coefficient, which at the time was incorporated to account for any unknown or unquantified variables involved in the process. At the time of the Handin and Ludwick (1950) study, k was of unknown magnitude and thus it was assumed to be constant and equal to unity.

The first study that attempted to empirically correlate sediment transport rates with wave characteristics was made by Watts (1953) at Lake Worth, Florida. Watts related the wave energy to the volume of sand bypassing the south Lake Worth inlet. Grounded in linear wave theory, and building on the ideas of Munch-Peterson (1938), Handin and Ludwick (1950) and others from USACE, he proposed that the longshore transmission of wave energy be calculated with the following formula:

$$E_T = (41 T h_s^2 n \tanh (2\pi d_s/L_s)) t \sin \alpha \cos \alpha \quad (7.3)$$

where T is the wave period, h_s is the shallow water wave height, n is the wave energy reaching the shore, d_s is the shallow water wave depth, L_s is the shallow water wave length, t is the duration of the wave train under consideration, and α is the angle of the wave crest to the shore. The idea behind incorporating both the sine and cosine of the wave angle was to first calculate the longshore energy component at a point ($\sin \alpha$), and then to obtain the total energy component along the length of the wave crest ($\cos \alpha$). The introduction of the term ' E_T ' was the first serious attempt to quantify what has become regularly known as the 'longshore component of wave

power'. Watts then established that the volumetric sand transport rate was a linear function of 'E_T':

$$Q = 0.0011(E_T)^{0.9} \quad (7.4)$$

The success of the Lake Worth study spurred similar projects by USACE. Caldwell (1956) in his study at Anaheim Bay, California and Savage (1959) summarizing previous work, obtained similar relationships indicating that the volumetric longshore sediment transport rate was in some way proportional to the wave energy flux.

7.3 Development of the Inman and Bagnold Formula

In their seminal work, Inman and Bagnold (1963) stated that to be dimensionally correct the sediment transport rate should be expressed as an immersed weight rather than a volumetric rate, taking into account the buoyancy effect or excess density of the sediment when it is immersed in the transporting medium – water. This is best thought of when considering the density of water (1.0) compared to the density of a typical grain of sediment (2.65). In this case the grain has an excess density of 1.65 in water, compared to 2.65 if it was sitting on the dry beach. When this grain is transported it is subjected to a shearing stress that the laws of physics demand must be maintained in equilibrium by two equal and opposing forces. One being a downward acting or normal force due to gravity. The other is an upward acting or dispersive force that must necessarily be equal to the immersed weight or excess density of the grain in order to support the grain in transport against the normal stress. They proposed the following relationship:

$$I_l = (\rho_s - \rho)ga'S = K \times P_l \quad (\text{N s}^{-1}) \quad (7.5)$$

Where I_l is the immersed weight sediment transport rate including the sediment transported in bedload and suspended load, ρ_s and ρ are respectively the densities of fresh/sea water and the sediment and g is gravity. a' is a measure of the sediment porosity given as $(1-n)$, where n is the percentage of void space, usually around 0.40, giving a typical a value of 0.60. S is the volume of sediment transported by the longshore current gained from empirical equations such as (7.3). The term $(a'S)$ is the volume of purely the sediment alone without any pore spaces. The equation then states that I_l should be proportional to the longshore component of wave power (P_l) multiplied by a constant (K). The idea was to derive a transport rate without resorting to field

measurements of sand transport, similar to that conceptualised by Watts (1953) in equation (7.4). The term P_l is similar to Watt's E_T but was redefined as:

$$P_l = (ECn) \cdot \sin \alpha_b \cdot \cos \alpha_b \quad (\text{W m}^{-1}) \quad (7.6)$$

Where ECn is the wave energy flux, which can be thought of as the rate of movement of the energy available for dissipation and the transporting of sediment over the beach. E is the wave energy per unit surface area of the waves at the break point. The expression for wave energy is derived from linear wave theory and is given as, $\frac{1}{8} \rho g H^2$. The equation illustrates the exponential nature of wave energy, in that, small increases in wave height, result in large increase in wave energy. A fact that has been illustrated numerous times in the present study. Longuet-Higgins (1972) stated that, in deep water, linear wave theory is a surprisingly good approximation to reality and that the wave energy equation is accurate with errors of only a few percent. Cn is the wave group velocity, that is, the velocity at which the wave energy is propagated forward. As discussed in Chapter Five, in shallow water, linear wave theory defines this as the square root of the water depth multiplied by gravitational acceleration, \sqrt{gh} . α is the wave breaker angle relative to the shoreline and is usually taken as the breaker angle. K is the constant, a dimensionless coefficient independent of the unit system used to define I_l and P_l . As conceived by Munch-Peterson (1938), K was incorporated to account for some unquantified variable(s) acting to absorb a proportion of the longshore energy component. Inman and Bagnold, (1963: 547) defined K as:

“...the ratio of the rate of the work done in transporting the sediment to the total power available and can be considered as an efficiency coefficient.”

Regarding equation (7.5) Inman and Bagnold stated that it was purely empirical and that it failed to suggest what other factors may affect the value of the constant. They went on to make a rational derivation of K and in the process developed another equation that took into account the role of nearshore currents in the transport process. They calculated the K ratio to be 17% efficient (i.e. yielding a coefficient of 0.17), making the point that at threshold conditions it will be equal to zero. Thus, it should be expected that calculated K values will increase toward a maximum as transport conditions become fully developed.

The equation was further developed and tested through extensive fieldwork by Komar (1969) for his doctoral dissertation, as presented in Komar and Inman (1970), and has subsequently

been widely referred to as the SPM or CERC formula, as many workers involved in validating the model did so under the auspices of the Coastal Engineering Research Center, as published in the well known Shore Protection Manual. Professor Paul Komar, Oregon State University (*pers. com.*, 2006) objects to the equation being referred with either of these acronyms, as it implies that the model was developed by the Coastal Engineering Research Center, when in fact this is not the case. The equation shall be referred to here as the Inman and Bagnold formula as it was presented in a paper written by Inman and Bagnold (1963). The equation was presented simply as:

$$I_l = KP_l = K(ECn) \sin \alpha \cos \alpha \quad (7.8a)$$

Expanding the terms:

$$I_l = KP_l = K \left[\frac{1}{8} \rho g H_{br}^2 \right] \sqrt{g d_b} \sin \alpha_b \cos \alpha_b \quad (7.8b)$$

Where ρ is the density of water, g is the gravitational constant, H_{br} is the breaker wave height, d_b is the breaker water depth, and α_b is the breaker angle. Komar (1976) pointed out that there are two good reasons for relating P_l (longshore wave power) and I_l (immersed transport rate) as opposed to P_l and Q_l (volumetric rate). Firstly, I_l and P_l have equivalent units of work (Newtons per second, $N s^{-1}$ and Watts per metre, $W m^{-1}$) so that they can be related by a dimensionless coefficient (K). Secondly, the equation takes into consideration the density of the sediment being transported. Thus, it can be applied to beaches composed of sands, gravels or different mineralogies. Komar and Inman demonstrated empirically for the first time that the longshore sediment transport rate is directly proportional to the longshore component of the wave energy (Figure 7.1). The equation is meant to account for the total longshore sediment transport forward of the breaking wave moving by both bedload and suspension load. The volumetric rate can then be calculated by rearranging equation (7.5) yielding:

$$Q_l = \frac{I_l}{(\rho_s - \rho)g(1-n)} \quad (m^3 s^{-1}) \quad (7.9)$$

In the absence of any volumetric sediment transport data to calculate I_l in the above equation, it can be rearranged with equation (7.8) to give:

$$Q_l = \frac{K}{(\rho_s - \rho)g(1-n)} P_l \quad (m^3 s^{-1}) \quad (7.10)$$

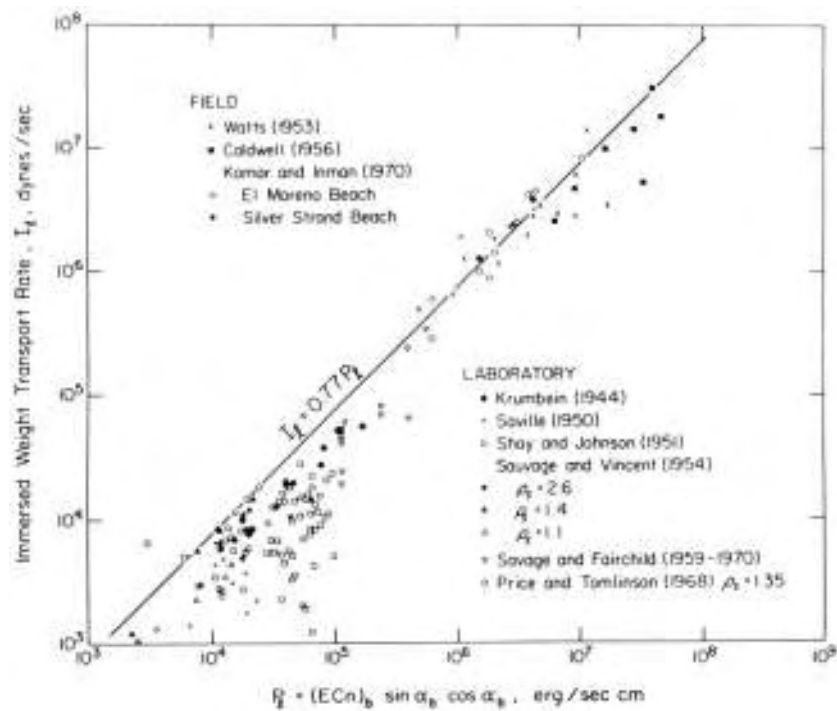


Figure 7.1 Plot presented in Komar (1976: 207) showing the relationship between the immersed weight longshore transport rate and the longshore component of wave energy, effectively validating the model. Note that the K value of 0.77 over-predicts the laboratory measurements.

A great number of studies over the years have attempted to further test the validity of this model (Galvin & Vitale, 1976; Bruno *et al.*, 1980; Dean *et al.*, 1987; Nicholls & Wright, 1991; Schoonees & Theron, 1994). One particular focus of the investigations has been determining values for the K coefficient. It is important to have an accurate assessment of K when using the Inman and Bagnold equation because employing a value that is too high or low will grossly over or under-predict the transport rate. Komar and Inman (1970) yielded an average value for K of 0.77, which became the design standard (later reduced to 0.70). It was hoped that K would be a constant defined through field studies. However, it soon became apparent that there is a lot of variability in K . A summary of some of the investigations that have yielded estimates of K are presented in Table 7.1. Komar (1988) calculated average K values from the Watts (1953) and Caldwell (1956) studies of 0.89 and 0.63 respectively. Other studies have produced values ranging from 0.013 (Wright, 1985) to 1.15 (Dean *et al.*, 1982).

In part due to the variations in K , many authors have criticised the Inman and Bagnold model as being too simplistic by not taking into account other process variables occurring in the nearshore zone (Longuet-Higgins, 1972; Greer & Madsen, 1978; Kamphuis *et al.*, 1986; Zyserman *et al.*, 1991). The model assumes that longshore transport is caused solely by waves

approaching the shore at an oblique angle and makes no account for potential wind or tidal currents. Although it is designed to provide a measure of the total longshore transport rate, it cannot calculate the on-off shore transport. It also takes no account of the grain size of the sediment being transported or its entrainment threshold, a criticism made particularly by gravel beach researchers. Another common criticism of the model related to this, is that it was developed for use on sandy beaches only and that due to the variability in K , it must be calibrated for every site. Zyserman *et al.* (1991), stated that the formula has limited applicability and that applying it to beaches outside of the range used to validate the model must be done with reservation. The model has also been found to under-predict transport rates at threshold conditions (Schoonees & Theron, 1994). But as discussed above, this should be no surprise considering that Inman and Bagnold (1963) stated that this was to be expected. Indeed, it has been found that despite the lack of an incipient motion criterion, the equation still estimates sediment transport rates reasonably accurately in fully developed conditions (Schoonees & Theron, 1994).

Table 7.1 K values derived from field data highlight considerable scatter in the coefficient. However, the data display the broad difference between sandy beaches (top half) and gravel beaches (bottom half). Compiled from Komar (1988) and Voulgaris (1999).

Study	Location	D_{50}	N	K
Watts (1953)	Lake Worth, Florida	0.40	4	0.89
Caldwell (1956)	Anaheim, California	0.40	6	0.63
Moore and Cole (1960)	Cape Thompson, Alaska	1.00	1	0.18
Komar & Inman (1970)	Silver Strand, California	0.18	4	0.77
Lee (1975)	Lake Michigan, US	? sand	8	0.42
Knoth & Nummedal (1977)	Bull Is, South Carolina	? sand	5	0.62
Inman <i>et al.</i> (1980)	Torrey Pines, California	0.20	2	0.69
Duane & James (1980)	Point Mugu, California	0.15	1	0.81
Bruno <i>et al.</i> (1981)	Channel Is. Harbor, California	0.20	7	0.87
Dean <i>et al.</i> (1982)	Santa Barbara, California	0.22	7	1.15
Dean <i>et al.</i> (1987)	Rudee Inlet, Canada	0.30	3	1.00
Nicholls (1982)	Hurst Pit, UK	22.0	1	0.023
Wright (1985)	Hengistbury Head, UK	32.0	6	0.013
Chadwick (1987)	Shoreham, UK	15.0	7	0.031
Bray (1990)	Chartmouth, UK	32.0	8	0.018
Kosyan <i>et al.</i> (1994)	Black Sea	? gravel	27	0.012
Bray <i>et al.</i> (1996)	Shoreham, UK	44.9	4	0.04
Voulgaris <i>et al.</i> (1999)	Whitstable, UK	22.5	2	0.015

Despite the criticisms, the Inman and Bagnold formula has been used extensively in coastal applications because it is easy to understand and use. All that is required is a knowledge of the wave height and angle of approach. This data can be derived from a number of sources and thus

it can be used in a wide variety of situations where data sets may be limited or nonexistent. Extensive field trials have produced site specific K values that produce reasonable first order estimates of transport in sandy beaches. In gravel beaches, the Inman and Bagnold formula and its variants have been moderately successful – much to the surprise of some researcher's (Chadwick, 1989; Van Wellen et al., 2000).

However, workers should neither be overly surprised nor critical of the fact that the Inman and Bagnold formula over simplifies processes in sandy beaches or that it is reasonably accurate on gravel beaches. As it was pointed out above, although Inman and Bagnold (1963) were attempting to create a model that could be used on sandy beaches, they stated explicitly that the equation was only a first order attempt and acknowledged that it required further work. Whilst it is true that the model has been largely validated on sandy beaches, Inman and Bagnold (1963: 550) were quite clear that it showed best results on steep coarse sand beaches with limited nearshore circulation systems, a fact overlooked by most authors. One reason the formula came to be associated with sandy beaches is due to work by Komar and Inman (1970), who validated the model through fieldwork on two sandy beaches with different average grain sizes; Silver Strand Beach, California ($D_{50} = 0.18\text{mm}$) and El Moreno Beach, Mexico ($D_{50} = 0.60\text{mm}$). They calculated the K coefficients to be 0.77 and 0.82 respectively and concluded that due to the negligible difference, K was not dependent on the grain diameter in the sand sizes. Because of this finding, it was assumed by many workers that it could be applied to sandy beaches everywhere. Over the years the model's first order status was forgotten and through repeated field trials it became assumed that the model was complete. However, the bulk of the data used by Komar to validate the model come from El Moreno, described as a steep, coarse grained beach some 30 m wide with a low energy wave environment. Komar and Inman (1970: 266) stated:

“Because of the steepness of the beach face, the breaking waves plunge and form an intensive swash zone with only a narrow surf zone”.

The model was essentially validated on a coarse sandy beach, morphodynamically similar to the type of beach that Inman and Bagnold (1963) stated it was most applicable. Thus, it should not be unexpected that there have been some problems applying it to sandy beaches and why it has been met with more success on coarse grained beaches. The type of beach that Inman and Bagnold (1963) envisaged it being most applicable to, is similar to the low energy coarse grained beaches found in many lakes both in New Zealand and overseas.

7.4 Testing the Inman and Bagnold Formula

To test Equation 7.8 with the Lake Coleridge data set, both the immersed weight transport rate (I_l) and the longshore wave power (P_l) were calculated. In this way, K can be derived. To convert the measured transport rates into the immersed transport rate, Equation 7.9 is rearranged to give:

$$I_l = (\rho_s - \rho)g(1-n)Q_l \quad (\text{N s}^{-1}) \quad (7.11)$$

It will be recalled that the density of the Lake Coleridge sediments (ρ_s) was determined as 2850 kg m^{-3} , whilst the density of fresh water (ρ) is 1000 kg m^{-3} . The porosity ($1-n$) was found to average 0.61. The sediment volume (Q_l) used was the instantaneous total integrated rate *i.e.* in cubic metres per second. For the Lake Coleridge data set, Equation 7.11 yielded values that range from 3.51×10^{-5} to 3.55 N s^{-1} and average 0.23 N s^{-1} . Again, this illustrates the very wide range in energy levels that were recorded in the field programme. These are comparable to measurements made in coarse gravel beaches by workers in the United Kingdom (Chadwick, 1989), during conditions with waves heights in the same range (0.30 m) as that measured in Lake Coleridge. However, these rates pale in comparison to those measured in large sandy beaches that can be up to 1000 N s^{-1} . The longshore wave power was calculated by substituting H_{rms} into Equation 4.12 to derive the breaker height, in this case the root mean square breaker height. This was used to calculate the breaker energy (E). Komar (1998: 392) stated that using the root mean square wave height “...corresponds to the correct assessment of the wave energy”. The wave celerity (Cn) was calculated using the breaker height as a de facto for the water depth, *i.e.* $\sqrt{gH_{br}}$, as discussed in Chapter Five (Equation 5.14a). Values for the longshore wave power range from 0.31 to 1840.21 W m^{-1} and average 256.00 W m^{-1} . This is comparable to values for wave power from the open coast in low energy conditions. The wave power is noticeably higher than the immersed transport rate. The large difference is partly a reflection of the amount of unmodified wave energy arriving at the shoreline and the relatively small area over which it is dissipated. Thus, the transport rate appears low compared to the input wave energy. On a wide sandy beach, the potential longshore transport rate is much higher, because wave energy dissipation through the nearshore zone entrains large volumes of sediment over a wide area.

Figure 7.2a presents the regression between the immersed transport rate and the longshore wave power. The wave power is on average some three orders of magnitude higher than the sediment transport rate. This is reflected in the K value of 0.00091. Some of the data points

below the best-fit line are from site CO13, but it indicates that more energy is dissipated in the process of breaking, than is available for transporting sediment. There is considerable scatter both above and below the best-fit line. The correlation between the two values is moderate, with correlation coefficients of $r^2 = 0.57$ and $r = 0.75$. Nevertheless, this is good relationship compared to that found by other workers. In a review of the CERC formula using a wide range of data sets, Schoonees and Theron (1994), found a mean $r^2 = 0.20$ and $r = 0.44$, for data sets with grain sizes ($D_{50} < 1.0$ mm). When only the highest quality data was used, the correlations increased to $r^2 = 0.41$ and $r = 0.64$.

Figure 7.2b shows the longshore wave power calculated without the cosine term. It can be seen that the correlation improves to $r^2 = 0.62$ and $r = 0.79$. Longuet-Higgins (1972) pointed out that multiplying the wave energy by both the sine and cosine of the wave approach angle does not produce the longshore component of the energy flux and is in fact incorrect. It was suggested that the cosine term be removed from the equation and that the wave energy need only be multiplied by the sine of the breaker angle to derive the longshore component. This observation is supported by the present study. It will be recalled that the best correlations with the sediment transport rate were found with the sine of the wave angle. With the cosine term omitted, value of K reduces to 0.00049. Introducing the cosine term, whilst reducing the magnitude of the wave power, only serves to weaken the correlation.

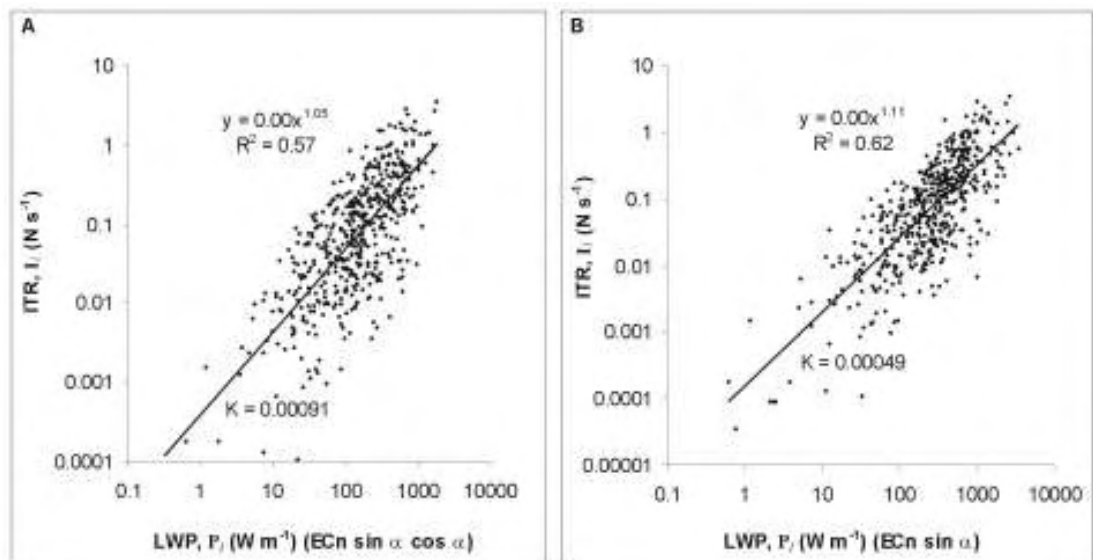


Figure 7.2 (A) Linear regression between longshore wave power and immersed sediment transport rate, $r = 0.75$, $F = 640$, Std. Error = 0.54, Prob. < 0.0001. (B) Regression with longshore wave power equation calculated without the cosine term, $r = 0.79$, $F = 799$, Std. Error = 0.51, Prob. < 0.0001. (ITR = immersed weight transport rate; LWP = longshore wave power).

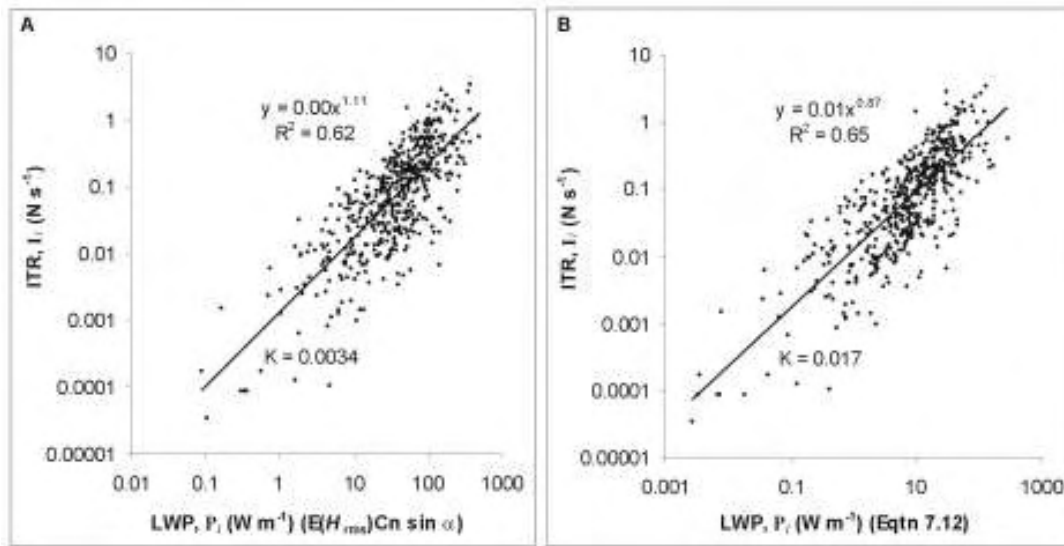


Figure 7.3 (A) Linear Regression between longshore wave power and immersed sediment transport rate with wave energy derived from deep water H_{rms} and omitting the cosine of the breaker angle, $r = 0.79$, $F = 800$, Std. Error = 0.51, Prob. < 0.0001. (B) Regression with longshore swash power calculated with Equation 7.12, $r = 0.81$, $F = 922$, Std. Error = 0.48, Prob. < 0.0001.

It has been found in this study that deep water waves approaching a coarse grained beach are not greatly modified before breaking at the shoreline. Thus, because the breaker height is a derived value and is perhaps higher than observations suggest, it would not be unreasonable to calculate the wave energy in terms of the deep water wave height. Figure 7.3a presents the results of calculating the longshore wave power with the deep water H_{rms} . It can be seen that whilst it does not improve the correlation, it does produce a longshore wave power that is an order of magnitude less, with a K value of 0.0034. Taking this idea one step further and substituting the mean swash current velocity for the wave celerity, produces a longshore swash power with good correlations to the transport rate ($r^2 = 0.65$, $r = 0.81$) (Figure 7.3b). Swash is the final dissipating process after wave breaking, containing the last energy available for transporting sediment. The mean swash velocity is the closest approximation to the shear stress exerted on the sediments. Thus it is not strictly physically correct to refer to Equation 7.12 as a longshore swash power. Nevertheless, Equation 7.8 may be redefined for mixed sand and gravel beaches by using the deep water H_{rms} to calculate the wave energy, substituting the wave celerity for the mean swash velocity and dropping the cosine of the breaker angle:

$$I_l = k \left[\frac{1}{8} \rho g H_{rms}^2 \right] \cdot \bar{v}_{sw} \cdot \sin \alpha_b \quad (\text{N s}^{-1}) \quad (7.12)$$

The k value in this equation increases by another order of magnitude to 0.017. This is very close to the k coefficient of the LEXSED formula (Equation 6.7), suggesting that a similar environmental variable or combination thereof, is acting to reduce the available wave energy for transporting sediment. The improved correlation and the reduction in the magnitude of the longshore wave power by using Equation 7.12 (Figure 7.3b) indicates that k is closely related to the processes of wave energy dissipation, as first suggested by Inman and Bagnold (1963). It will be noted that this formulation is not dissimilar to the Bagnold longshore sediment transport derivation presented in the last chapter (Equation 6.11).

This is the first time the K values in the Inman and Bagnold model have been accurately calibrated for mixed sand and gravel lakeshores in New Zealand. Previous authors have had to rely on educated guess work due to a lack of any empirical measurements. It highlights the need for the Inman and Bagnold model to require field verification, specifically in order to calibrate the K coefficient. Kamphuis and Readshaw (1978) concluded that the Inman and Bagnold model best applies to situations where the breaking waves are plunging or surging. With a properly defined K value, the expression shows some promise in being used on mixed sand and gravel beaches. One problem with using the longshore wave power, is that it is derived purely using the wave height. It has been shown in this study that the wave period is also important. Although waves may be seen as solitary at the point of breaking, and therefore divorced from the period and length, the period determines the wave length and the ratio of these two parameters defines the wave steepness. It has been shown in this study that the wave steepness is very important as it defines the shape of the wave, a shape that is maintained to the point of breaking and has an influence on sediment transport.

7.5 Variations of K with Environmental Parameters

Due to the variability in K , a lot of effort has focused on the environmental factors not taken into account by Equation 7.8, that might be affecting the parameter. K was always introduced to account for these, but it became apparent that it was not going to be a simple constant (Kamphuis & Readshaw, 1978; Bruno *et al.*, 1980). These investigations have led to variations of the Inman and Bagnold equation.

Variation of K with Grain Size

It is recognised that beaches composed of coarser materials experience lower rates of longshore transport because coarse grained sediments require more energy to transport. Thus, it is thought that K values should be lower on coarse grained beaches because the coefficient accounts for energy dissipation. Yet surprisingly, a size parameter has been commonly absent from many sediment transport models. Neglecting considerations of the grain size might be a big source of error in longshore transport calculations (Moutzouris, 1988). A number of authors have tested the connection between K and grain size in an effort to identify a possible correlation (Komar & Inman, 1970; Swart, 1976; Bruno *et al.*, 1980; Dean *et al.*, 1987; del Valle *et al.*, 1993, Voulgaris, *et al.*, 1999). One aim of these studies has been to produce a range of K values that can be applied to beaches with different grain sizes.

One of the first attempts to link K with grain size was made by Swart (1976) who developed a series of predictive equations for both longshore and on-offshore sediment transport. One aspect of the research was an examination of the Inman and Bagnold equation. Swart stated that it was a useful overall predictor in assessing the sediment budget of a beach. It was argued that, because lighter material should be transported more readily than heavier material under the same wave conditions, K will be a function of the grain size of the bed material. Re-evaluating the longshore sediment transport data base used to support the Inman and Bagnold equation, Swart presented a graph that showed a clear variation of K with grain size (Figure 7.4). This contradicted the findings of Komar and Inman (1970) who found no relationship between K and grain size, as discussed above. Swart then presented a solution for K that varies as a function of the median grain size. The formulation was limited to fine and medium sand beaches, but further work by Schoonees and Theron (1994) extended its application into coarse sand situations. When the Swart (1976) equation is substituted into equation (7.8) and (7.9) it takes the form:

$$Q_l = 0.166 \log_{10} \left(\frac{0.00146}{D_{50}} \right) P_l \quad (\text{m}^3 \text{s}^{-1}) \quad (7.13)$$

Where Q_l is the total volumetric longshore transport rate. This equation was tested by Schoonees and Theron (1994) against a large data set, with D_{50} ranging in size from 0.1-1.0 mm. It was found that even with the inclusion of a grain size parameter the equation gave variable results and in fact weakened the correlation slightly between the longshore wave power and the transport rates. When tested against the Lake Coleridge data set it produced volumes three to four orders of magnitude higher than the measured rates and produced a similarly small

weakening of the correlation with the transport rates ($r^2 = 0.56$, $r = 0.74$). Despite the efforts of Schoonees and Theron to apply the formulation to coarse grained beaches, it contains underlying principles derived from empirical studies on sandy beaches, that are not able to properly account for the sediment transport processes in the swash zone of a coarse grained beach.

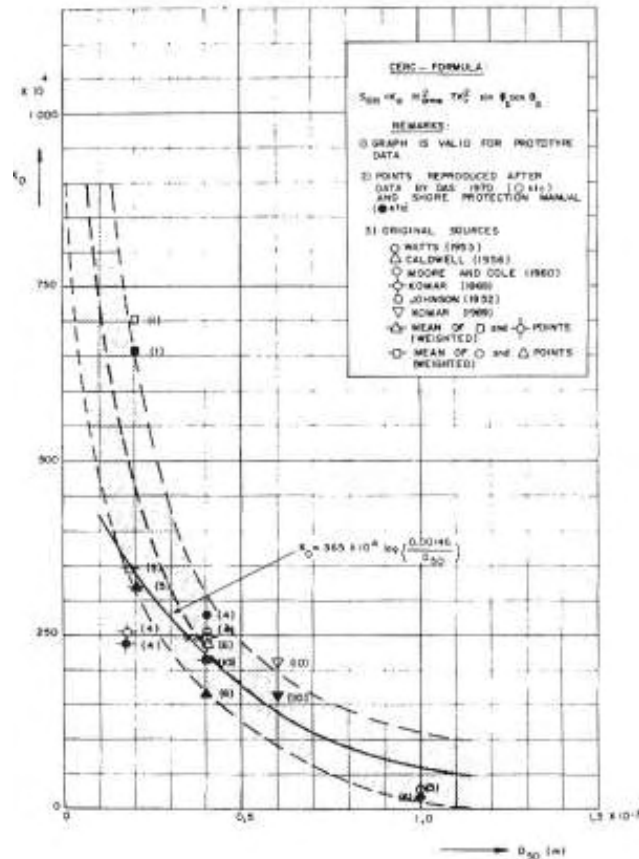


Figure 7.4 Graph presented in Swart (1976: 1130) showing a variation of K with grain size based on older data sets from; (Johnson, 1952; Watts, 1953; Caldwell, 1956; Moore & Cole, 1960; Komar, 1969).

The work of Swart (1976) was supported by Bruno *et al.* (1980) who presented a similar graph that showed a relationship in sandy beaches between grain size and the K coefficient (Figure 7.5). It was based on the results of previous studies, many of which are included in Table 7.1. The problem with this graph is that the relationship is produced solely by the value obtained by Moore and Cole (1960) that appears in the lower right hand side of the chart. This is the same point that appears in Figure 7.4. The quality of the data used to calculate this figure has been called into question by Komar (1988) who concluded that without this one point, the trend is random. Komar (1988) re-examined these old data sets and again found that there are no explicit variations in K for sand-sized sediments and that it is independent of grain size.

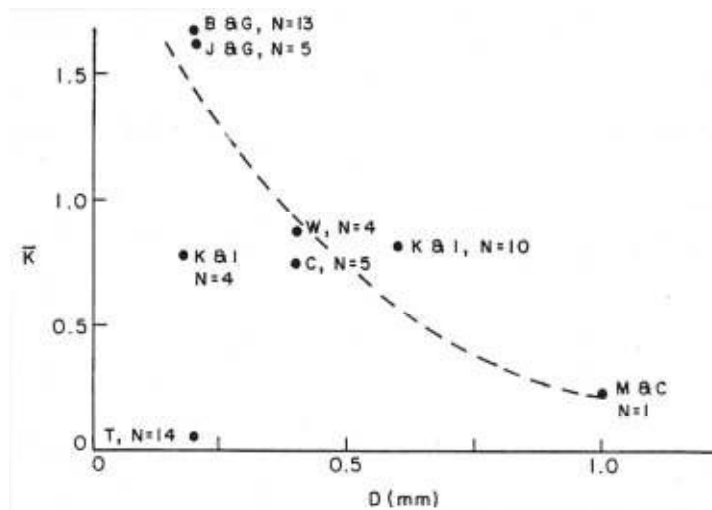


Figure 7.5 Plot of grain diameter versus K as presented in Bruno et al. (1980: 1460), showing the relationship between the two variables.

The debate over whether or not K is related to grain size has prompted some authors (Komar, 1988) to comment that investigations needed to include estimates from gravel beaches. When this occurred, the trend became more obvious. Nicholls and Wright (1991) conducted a study into sediment transport on gravel beaches by using aluminium pebble tracers. It was found that K values were 7-100 times lower than for those found on sandy beaches, similar to the findings in this study. Work on this issue in the United Kingdom was followed up by del Valle *et al.* (1993), who examined the longshore sediment transport of the Adra River Delta, Spain. Five zones with different grain size characteristics were identified along the Delta front ranging from 0.33-2.0 mm. Transport rates based on shoreline fluctuations from 30 years of aerial photographs were correlated to wave characteristics in order to calculate K values. It was found that the calculated K values from each zone decreased with increasing grain size. Despite some of the problems in using long term data in this manner, the general trend was confirmed by Voulgaris *et al.* (1999), who presented K values calculated from a number of gravel beach studies from the United Kingdom over a 17 year period. The studies of Nicholls and Wright (1991), del Valle *et al.* (1993) and Voulgaris *et al.* (1999) are some of the very few that have been concerned with calculating K values from gravel shorelines. The data from these studies, presented in Table 7.1, is plotted graphically in Figure 7.6, which also includes the mean value from the Lake Coleridge data set. Variation in K is evident for both beach types, suggesting that grain size is only one of the variables affecting K . It is apparent that K is considerably lower in coarse grained beaches. However, when K was correlated with grain size within the Lake Coleridge data set, no relationship was found between the two variables (Figure 7.7).

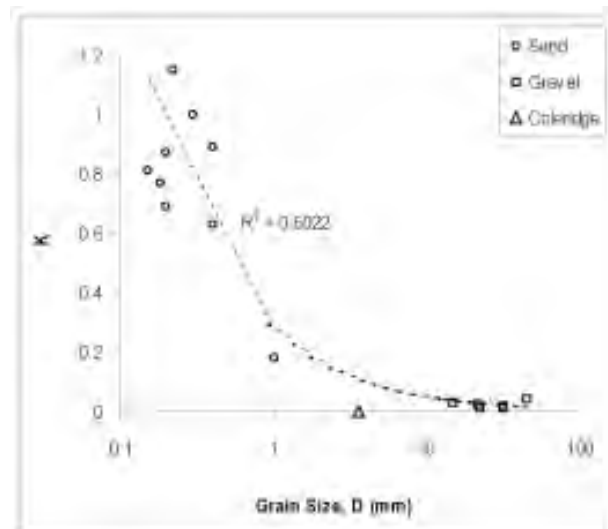


Figure 7.6 Plot showing broad difference in K between sand and gravel beaches using the data from Table 7.1 and the mean value for Lake Coleridge (0.00091). When plotted in highly averaged terms, there is a clear correlation between K and grain size.

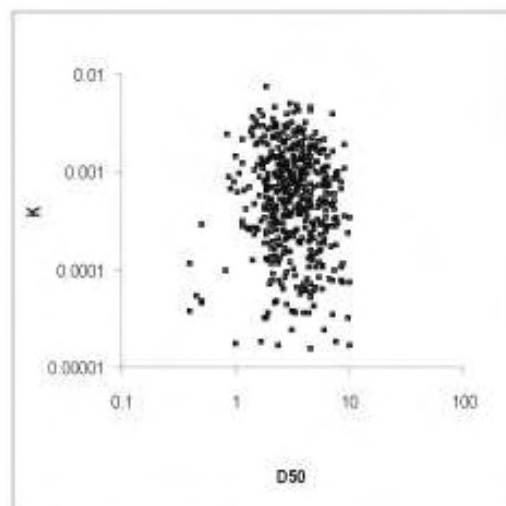


Figure 7.7 Scatter plot of D_{50} grain size versus K for the Lake Coleridge data set. There is no meaningful relationship between the two values.

The findings from this study highlight some interesting facts about variation in the K coefficient. The relationship with the grain size causes variations in K in two ways. Most simply, larger sized material requires more wave energy to transport, leading to lower K values. However, it is argued here that this effect is secondary to the structural role that coarse grained beaches exert on wave breaking. The morphology, particularly of the mixed sand and gravel

beaches of the east coast of New Zealand and of the glacial lakeshores, exerts an influence on wave breaking by allowing the deep water wave to approach the shoreline with little modification. The sharp rise in beach slope at the shoreline, induces wave breaking on a steep slope at the break point step, often resulting in a plunging wave at the base of foreshore. Thus, there is a very large input of kinetic wave energy concentrated in the breaker at the base of the swash zone. This produces a high longshore wave power value. Even at Lake Coleridge, the wave power values are comparable to lower energy open coast conditions. The physical dimensions of the swash zone and foreshore (width and steepness), dictate purely how much area containing sediment is available for transport. Thus, a short, steep swash zone presents a smaller area for wave dissipation and less potential volume of sediment to move, than a wide, dissipative surf zone. If 1.0 m waves break on these shores, the wave power component of Equation 7.8 will produce an equal value. However, the potential transport rate is higher in the wider surf zone because there is simply more sediment available for movement, and the ratio between the wave power and transport rate becomes smaller.

In a wide sandy dissipative beach there may be a nearshore zone and breaker zone 100-200 m wide that serves as an area for the development of longshore current and the transport of sediment. The sheer size of the surf zone and the quantity of material that can be moved in a wide dissipate beach far exceeds the physical limitations of the swash zone of a gravel beach. Thus, it is the ratio between the longshore wave power and the immersed weight sediment transport rate that causes lower K values for gravel and mixed sand and gravel beaches. Moreover, there is more depth in the water column in the nearshore to contain sediment in a suspended form. In the swash zone, transport occurs in a rapidly thinning flow of water, predominantly as bedload. Purely and relatively on a per metre basis, there is simply more capacity for sediment transport in a sandy beach. The corollary being, that K values are lower on coarse grained beaches because the ratio difference between input wave energy and output sediment transport is larger. Within a beach system there is little evidence to suggest that K is affected by grain size, supporting the claim of Komar (1988). Kamphuis (1991) concluded that the transport rate was more a function of the beach slope than the sediment grain size. However, when K values from different beach types are examined, it is clear there is a difference between gravel and sandy beach systems. In sand beaches K values are in the order of 0.50-1.0; in gravel beaches they are in the order of 0.01-0.04; in coarse grained, low energy shorelines of Lake Coleridge they are in the order of 0.001.

Variation of K with Iribarren Parameter

Owing to the complications in linking K to grain size, there have been attempts to correlate K to other related environmental factors including beach slope and wave steepness. In two laboratory studies of longshore sediment transport Kamphuis and Readshaw (1978) and Kamphuis and Sayao (1982) showed that there was a strong relationship between sediment transport, beach slope and wave steepness. Kamphuis and Readshaw incorporated the slope and wave steepness into a transport formula via the Iribarren number, a parameter that was discussed in Chapter Four. The Iribarren number has been tested over the years against an extensive data set including both field and laboratory measurements and can be derived from both Bore Theory and dimensional analysis (Arcilla, *et al.*, 1988). It illustrates the importance of the beach slope in controlling breaker conditions and helps explain why plunging breakers are the most commonly occurring types on steep mixed sand and gravel beaches.

When Kamphuis and Readshaw (1978) correlated the breaker Iribarren with K , they found that it was not a true constant, but rather that it increased with higher Iribarren numbers (Figure 7.8). From the straight line relationship in Figure 7.8 it was suggested that:

$$K = 0.7\xi_b \quad \text{for } 0.4 < \xi_b < 1.4 \quad (7.14)$$

They proposed that one of the reasons why Komar and Inman (1970) found good correlations between transport rates and the Inman and Bagnold model, was that the breaker and slope conditions between the two study beaches would have produced different Iribarren values. At El Moreno, the beach was steep and the waves were more plunging in nature, indicating high Iribarren values. At Silver Strand the beach was gently sloping and characterised by spilling breakers, therefore indicating low Iribarren values. Kamphuis and Readshaw (1978) implied that it was this variation in the Iribarren parameter that was instrumental in the correlation.

Kamphuis (1990) later found from laboratory studies, that in some instances the dependence on beach slope was stronger than the grain size. It was concluded that the sediment transport rate is closely related to energy dissipation in the breaker zone. The findings from this study support this notion. In Chapter Six it was shown that there was a very poor relationship between the grain size and the transport rate, a finding highlighted in the last section. The relationship with the beach slope, the wave steepness and the Iribarren number was much firmer. However, the relationship with the beach slope is opposite to that usually reported in the literature. It was found in this study that the transport rate increases with a lowering beach slope (*i.e.* negative),

because of the equilibrium relationship between wave energy and the development of the swash zone. Nevertheless, this supports the argument postulated in the last section, that the beach morphology and slope and way this influences wave breaking and dissipation, has a stronger influence on the K parameter than the grain size.

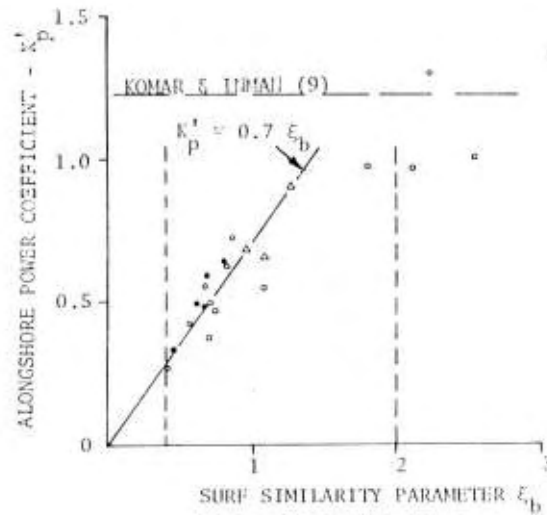


Figure 7.8 Plot presented in Kamphuis and Readshaw (1978: 1672) showing the relationship between K and the Iribarren number.

Further laboratory studies have also pointed to a relationship between sediment transport and the Iribarren number, but the results have been mixed. Vitale (1981) studied links between nearshore radiation stresses, the breaker energy flux and transport rates. In the process he also examined the role of the Iribarren parameter. The findings were comparable to Kamphuis and Readshaw's (1978) study, but he used the deep water Iribarren number instead, in an effort to mitigate the scaling effects that arise in using a laboratory wave tank. Similarly, Özhan (1982) examined the role of breaker type on longshore transport and also found that K increases with an increasing Iribarren number, but that the choice of slope measurement produced a lot a variability in the results. For example, there are up to three zones that may be associated with wave breaking and sediment transport in a beach system: firstly, the offshore slope leading to the outer breaker zone; secondly, the nearshore slope and surf zone, and; thirdly, the inner surf zone and foreshore slope characterized by wave bores and swash. Using the average offshore slope, Özhan was able to show that the deep water Iribarren was related to K by a least square relationship:

$$K = 1.26(\xi_o)^3 \quad \text{for } 0.4 < \xi_b < 1.2 \quad (7.15)$$

However, when the average nearshore and foreshore slopes were used in the Iribarren computation, the relationship with sediment transport became highly scattered. Instead, it was found that K had more reliance on simply the wave steepness with K values decreasing as the wave steepness increased. In this way, the highest transport rates occurred under collapsing breakers. Using data from his own study, Özhan showed that; $K = 0.007 (H_o/L_o)^{-1.0}$. When he incorporated the data from Vitale (1981), Kamphuis and Readshaw (1978), and from a well known study by Saville (1950), the least square equation became (Figure 7.9):

$$K = 0.015 (H_o/L_o)^{-0.82} \quad (7.16)$$

Finally, Bodge and Kraus (1991) examined data from a number of field and laboratory studies that looked at the links between breaker parameters and longshore transport. The laboratory data clearly showed that an increase in the Iribarren number resulted in an increase in K , but the field data was highly scattered. Nevertheless, they presented the relationship:

$$K = 0.37 \ln \zeta_b + 0.59 \quad (7.17)$$

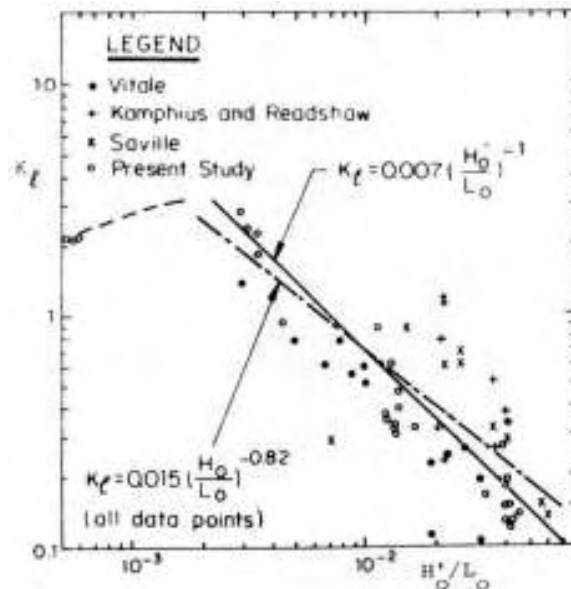


Figure 7.9 Plot presented in Özhan (1982: 271) showing the relationships between wave steepness and the K coefficient from three previous studies that examined the same relationship. The best fit lines are inverse power correlations and the equations are least square fits.

Most of the studies that have examined the relationship between the Iribarren number and transport rates have been based on sand-sized sediments. The relationships in gravel shorelines have not been fully explored. The K values in Equations 7.14-7.17 were calculated from the Lake Coleridge data set and included in the Inman and Bagnold formula (Equation 7.8), (i.e. KP_I). Table 7.2 presents the summary statistics of the transport rates estimated by the CERC formula with the inclusion of the K estimate equations. It can be seen that the rates are reduced by an order of magnitude from the raw wave power values of Equation 7.6. However, the transport rate is still over-estimated by all the equations. The results were regressed with the immersed weight transport rate and can be seen in Table 7.3. The table also includes the regression with the deep water wave steepness and the Iribarren number. It can be seen that there is a moderately strong relationship with the wave steepness, but the correlation is weaker against the Iribarren number. This is similar to the findings of Özhan (1982), seen in Figure 7.9, who also found a stronger relationship with the wave steepness over the Iribarren number. The relationship with the Iribarren number is negative due to the beach slope, but the relationship with the wave steepness is positive because higher transport rate were associated with steep peaked storm waves.

Table 7.2 Summary statistics for the results of using the equations highlighted in this section that employ the wave steepness and Iribarren number to define K . All of the formulations over-estimate the transport rate.

	Eqtn. 7.11 ITR (I_I)	Eqtn. 7.6 LWP (P_I)	Eqtn. 7.14 KP_I	Eqtn. 7.15 KP_I	Eqtn. 7.17 KP_I	Eqtn. 7.16 KP_I
Min	0.000035	0.30	0.16	0.18	0.15	0.14
Max	3.55	1840.21	490.84	91.76	428.78	209.83
Mean	0.23	256.00	73.09	16.82	65.90	35.18
Std. Dev.	0.40	281.93	77.48	16.34	68.85	34.85

Table 7.3 Correlation coefficients between the longshore wave power and immersed weight transport rate. The first column is the regression with the original equation, as seen in Figure 7.2a. The second two columns show the correlation with the deep water wave steepness and the breaker Iribarren. The last four columns use the K parameter defined by the equations presented in this section. All of the equations reduce the correlation with the transport rate slightly.

	CERC Eqtn 7.8	H_o/L_o	ξ_b	Eqtn 7.14 KP_I	Eqtn 7.15 KP_I	Eqtn 7.17 KP_I	Eqtn 7.16 KP_I
r	0.75	0.78	-0.68	0.74	0.69	0.74	0.75
r^2	0.57	0.61	0.46	0.55	0.47	0.54	0.56
Std. Error	0.54	0.51	0.6	0.55	0.60	0.55	0.56

Despite the relationships found between the beach slope, breaker type and the transport rate, when Equations 7.14, 7.15 & 7.17 are included into the Inman and Bagnold formula, the correlations with the Iribarren number weaken slightly (Table 7.3). Part of the reason for this, is the lack of variability in the Iribarren parameter for the Lake Coleridge data. Figure 7.10 shows the relationship between the breaker Iribarren and the K values derived from the regression between the immersed transport rate and the longshore wave power presented in Figure 7.2a. It can be seen that no correlation exists with the K parameters. A similar relationship is found when the wave steepness is correlated against K . Part of the reason the Iribarren number does not improve the correlation when included into the Inman and Bagnold model, is that it predicts an increase in the transport rate with an increase in the beach slope. This is the opposite of the findings in this study, that found an increase in the transport rate with a lowering of the foreshore slope. The relationship with the immersed transport rate when the wave steepness K value is included (Equation 7.16) remains unchanged. If the mean wave steepness value from Lake Coleridge (0.06) was plotted on Figure 7.9, it would lie in the bottom right corner and blow the line, roughly conforming to the relationship found in the other studies. Thus, whilst there may be differences in the K value due to the Iribarren number and wave steepness between beach types, within a beach system, the variation becomes far more inconsistent. This is similar to the findings regarding the grain size discussed above.

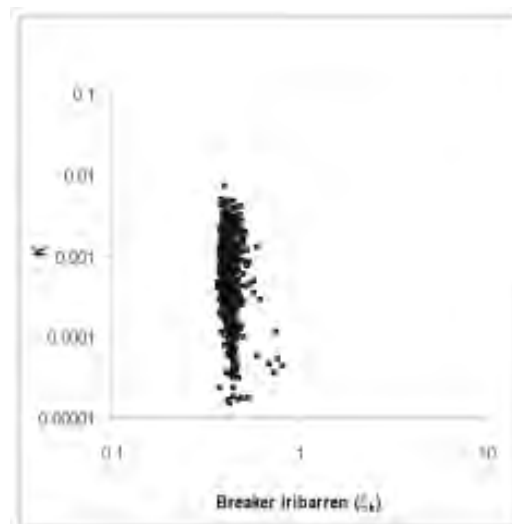


Figure 7.10 Relationship between Breaker Iribarren and K . Like the grain size, there is no correlation between the two parameters.

One of the problems in linking K to environmental variables such as grain size, foreshore slope and wave steepness, is that these controls are interrelated; grain size influences foreshore slope and porosity, which in turn influences wave steepness. It is a complex problem that does not provide easy solutions. Over two decades ago Dean *et al.* (1982) concluded that it was unknown whether variability in K was due to recording errors or to true variations in the coefficient. Schoonees and Theron (1993) reviewed the large number of longshore sediment transport studies that had been used to develop and verify the most widely used longshore transport models. They looked at field data only, neglecting laboratory studies due to uncertainties in the scaling effects. The aim was to examine the quality of the data and to determine if measurement techniques were contributing to discrepancies in the outcomes, particularly the Inman and Bagnold model. Another intention was to calibrate the Inman and Bagnold model with only the highest quality data in an effort to produce a reliable value for the K coefficient. They found that many methods have been used to measure both the sediment transport rates and wave characteristics over both long and short term periods. They also pointed to the paucity of data from beaches with coarse grain sizes, steep slopes and large breaker heights. Essentially, it was concluded that much of the data used in coastal transport modelling was of questionable quality and only a handful of studies could acceptably be used to calibrate littoral transport models. Regarding the K coefficient, Schoonees and Theron (1994) found that even using the highest quality data, there was still considerable scatter in the values. They went on to say that no reliable relationship had been established between K and grain size. Komar (1988:1250) concluded:

“It is apparent that K should depend on basic environmental parameters such as sediment grain sizes. Therefore, the absence of such trends must result from the quality of the data. This should come as no surprise in view of the various techniques that have been used to measure sand transport rates on beaches and to collect the data on waves and currents.”

Thus, in reply to Dean *et al.*'s (1982) question, it is accepted by many authors that a lot of variations in K are indeed due to differences in measurement and data quality. Presently, the uncertainty surrounding the K coefficient remains.

In this study it was hoped that by collecting high quality data on sediment transport rates, waves and currents in a beach that exhibited a range of sand and gravel size material, a reasonable investigation of variations in K could be accomplished without questions surrounding the quality of the data casting doubt onto the results. It has been found the relationship with K and grain size occurs on inter-beach scale, but variations within a beach system are non-existent. In the last chapter it was seen that when plunging waves break in the swash zone, the thresholds

of all the material in the swash zone were exceeded and all the sediment was placed in motion. It is fair to assume that breakers in the surf zone of a sandy beach produce a similar effect amongst sand sized sediments. The morphology exerts a control on the way in which waves interact with a beach system, and to a degree this is the influence that sediment size has on K . Coarse grained beaches produce steep foreshores and plunging waves, allowing waves of comparable size to entrain larger sediment than would possibly occur on a sandy beach. Thus, the variations are more related to the way in which energy is dissipated, rather than the size of the sediment. Despite this, the relationship between K and the Iribarren number and wave steepness was non-existent. On its own these two parameters show a correlation with the transport rate, but when included into the Inman and Bagnold model, they were not found to perform well against the coarse grained beaches in Lake Coleridge. It is felt that any substitute for the K coefficient will be need to be a simple integer, perhaps a value that derives from a classification of the particular beach system to which it is being applied. For example, 0.70 for sandy beaches, 0.10 for gravel beaches and 0.001 for lakeshore beaches.

The Inman and Bagnold model itself shows reasonable correlations with the transport rates in a coarse grained beach, but in general it was not found to perform any better than it for sandy beaches. The strength of the formula is its simplicity and flexibility. It was shown in this study, that it can be adapted to different beach types with a few modifications, to improve its performance. It is the magnitude estimates that causes the concern, hence the inclusion of the K coefficient. This is a theme common to all studies sediment transport in the natural environment where there are a multitude of variables and complex interactions that all play a part in influencing the movement of sediment. A degree of uncertainty may have to be accepted with the results of transport models and that the outcomes are best estimates only.

7.6 Inman and Bagnold Formula Variations

Brampton and Motyka Variation

As well as incorporating a parameter that accounts for the effects of grain size, some authors have included a term that accounts for the threshold of sediment movement. One of the first attempts to include a threshold term in the Inman and Bagnold equation was made by Brampton and Motyka (1984), who proposed the following relationship derived from empirical studies of gravel beach morphodynamics:

$$Q_l = \left[\frac{K}{\gamma} P_l \left[\frac{L}{D_{90}} \right]^\varepsilon \left[1 - \frac{8.1 D_{90}}{H} \right]^\beta \right] \quad (\text{m}^3 \text{s}^{-1}) \quad (7.18)$$

Where K is the dimensionless coefficient, $\gamma = (\rho_s - \rho)ga$ as in Equation 7.10, P_l is the longshore wave power, L is the wave length, H is the wave height, D_{90} is the 90th percentile grain size, and ε and β are constants that need to be evaluated from field measurements. The first term is the conversion factor between volumetric and immersed rates, the second term is a dimensionless particle size and the last term accounts for the threshold of sediment entrainment. Brampton and Motyka (1987) later simplified the equation by reducing the ε and β exponents to zero, effectively eliminating them from consideration. This was rationalised on the basis that breaking waves below 0.5 m were to be ignored when using the formula. However, this is an unusual decision considering that one might expect the threshold of entrainment to occur for many grain sizes with waves below 0.5 m. It has been found that apart from lower K values, this modification does not produce results on gravel beaches significantly different from the original Inman and Bagnold equation (Van Wellen *et al.*, 2000a).

Encouraged by the potential of Equation 7.18, Chadwick (1989) in a study of gravel beach transport models, proposed a similar simplification by reducing ε to 0 and β to 1 and omitting the dimensionless particle size term:

$$Q_l = \left[\frac{K}{\gamma} P_l \left[1 - \frac{8.1 D_{90}}{H} \right] \right] \quad (\text{m}^3 \text{s}^{-1}) \quad (7.19)$$

This variation was met with reasonable success by Chadwick and later by Van Wellen *et al.* (1998) who found it to be the most accurate in predicting long-term gravel transport rates for Shoreham Beach, West Sussex, England, when compared to six other equations. Chadwick calculated a K value of 0.07 when applying this equation to Shoreham field data, compared to a value of 0.05 for the original Inman and Bagnold equation.

Equation 7.19 was tested against the Lake Coleridge data set. The K coefficient was calculated to be 0.00099, which is marginally higher than the K derived the CERC expression of 0.00091. This is similar to the difference found by Chadwick (1989) and indicates that without the K coefficient, the transport volumes would be some 3–4 orders of magnitude higher than estimated. This is due to the longshore wave power term (P_l). When calibrated, the mean transport rates were well estimated by the equation, but it over estimated the extreme low and high values. Despite this, there is no improvement in the correlation to the transport rates ($r =$

0.74). In fact the inclusion of the grain size parameter caused a very slight reduction from the longshore wave power correlation seen in Figure 7.2a. This is similar to the effect on the correlation seen in Equation 7.13, and is in line with the findings discussed above, in that no relationship was found with the grain size.

Chadwick Variation

The data sets available to Chadwick (1989) at the time were insufficient to apply Equation 7.19 to short term data, so he developed another variation of Equation 7.8 that included a threshold term only. It was derived from a correlation of transport rates versus wave power measurements of Shoreham Beach and so it is empirically based:

$$Q = \frac{K}{\gamma} (P_l - P_o) \quad (\text{m}^3 \text{s}^{-1}) \quad (7.20)$$

Where P_l is again the longshore wave power and P_o is the threshold wave power. Chadwick derived a K value of 0.037 using this equation for the Shoreham data and was encouraged by its success in predicting longshore transport rates. In a later study by Van Wellen *et al.* (2000a) the equation was one of the most accurate in a group of 12 other formulas. However, because the equation contains no other environmental parameters it must be calibrated for each situation it is applied to and as such, its solutions are site specific. Chadwick (1989: 393) concluded his study by saying that: “...further progress in quantifying the longshore transport of coarse materials can be made from field studies.”.

The wave power threshold (P_o) in the Lake Coleridge data set was found to be so low, that its impact on the transport volumes calculated with Equation 7.20 was negligible. The reasons for this have been fully discussed in previous sections, but essentially relates to the fact that no grain size threshold was determined from this study. It was found that when waves break, even of the smallest magnitude (*i.e.* 0.05 m) in the swash zone of a mixed sand and gravel beach, sediment is placed into motion. K was found to be 0.00094. Without the inclusion of the grain size parameter, the correlation increased slightly from Equation 7.19 ($r = 0.75$). This is identical to the CERC correlation coefficient seen in Figure 7.2a and does not appear to offer any advantages over the original model when tested against the Lake Coleridge data set. Similar to Equation 7.19, the expression also under estimates the extreme high transport rates. Summary statistics for the transport rates estimated by the two equations, converted into $\text{m}^3 \text{hr}^{-1}$, can be seen in Table 7.4.

Table 7.4 Summary statistics for volume transport rates calculated with Equations 7.19 and 7.20. The rates have been converted in $\text{m}^3 \text{hr}^{-1}$. The mean rates are within range, but the extreme high values are not well estimated.

Q_i	LST ($\text{m}^3 \text{hr}^{-1}$)	Eqtn. 7.19	Eqtn. 7.20
Min	0.000011	0.000086	0.000049
Max	1.154	0.583	0.562
Mean	0.074	0.078	0.078
STD	0.130	0.088	0.086

7.7 Stream Power Based Approaches to Longshore Sediment Transport Modelling

Bailard Equation

The Inman and Bagnold formula and its variations outlined above, are all based foremost on a consideration of the total wave energy or wave power. In a broader sense, these equations fall under the general umbrella of energetics based approaches to modelling sediment transport. However, due to some of the problems with determining longshore sediment transport rates with the wave power approach, some authors have looked back to the first principles upon which it was based in an effort to develop a more physically realistic model. In a series of papers in the late 1970's and early 1980's Bailard and Inman (1979; 1981) and Bailard (1981; 1984) proposed a new sediment transport equation. Rather than being based on a consideration of the wave power, it was instead based on a consideration of the bed shear stress or stream power. The stream power is a measure of the energy transfer from the fluid phase to the solid phase. It was grounded in the physics of fluid hydraulics that was explored in depth in the foundational work of Bagnold (1963; 1966), that also led to the development of the CERC equation. Bagnold (1963) developed a model from studies of unidirectional sediment transport in streams, in which he established that the immersed weight bedload sediment transport rate is proportional to the rate of energy dissipation of the stream. He went on to develop an equation for use in the nearshore environment by substituting the flow parameters that represented stream flow, for ones that represented wave induced currents. In the surf zone, it was suggested that there is no net transport affected by wave induced oscillatory water movements, but that any current superimposed on this system will cause a net transport in the direction of the current. It was also suggested that the energy dissipation involved in this process acted to support the sediment in a

quantity equal to the immersed weight of the sediment. This conceptual model was expressed with the equation:

$$i_{\theta} = K' \omega \frac{u_{\theta}}{u_m} \quad (7.21)$$

Where i_{θ} is the time-averaged immersed weight transport rate per unit width in the θ direction, u_{θ} is a steady current in the θ direction, ω is the local time-averaged rate of energy dissipation, u_m is the wave orbital velocity and K' is a dimensionless constant. Almost all other energetics equations have been based upon this model, including the Inman and Bagnold formula.

However, there are limitations with the model. It has been found to over-simplify the transport process, ignore important environmental variables and relies too heavily on average rates rather than instantaneous rates (Inman & Bowen, 1963; Bailard & Inman, 1981). The model cannot deal with time-varying situations as this is not necessary in the case of unidirectional stream flow where the water and sediment motions are assumed to be steady and directed downslope. Bailard (1981) attempted to produce a generalised form of this model that could be applied to a wide range of nearshore conditions. The rather weighty equation that was developed represents the time-varying total load transport over a sloping bed, presented as:

$$\left\langle \vec{i}_t \right\rangle = \left[\rho c_f \frac{\varepsilon_B}{\tan \phi} \right] \left\langle \left| \vec{u}_t \right|^2 \right\rangle \vec{u}_t \left\langle - \frac{\tan \beta}{\tan \phi} \right\rangle \left\langle \left| \vec{u}_t \right|^3 \right\rangle \hat{i} + \left[\rho c_f \frac{\varepsilon_S}{w_s} \right] \left\langle \left| \vec{u}_t \right|^3 \right\rangle \vec{u}_t \left\langle - \frac{\varepsilon_S}{w_s} \tan \beta \right\rangle \left\langle \left| \vec{u}_t \right|^5 \right\rangle \hat{i} \quad (7.22)$$

Where \vec{i}_t is the instantaneous sediment transport rate vector, \vec{u}_t is the instantaneous near-bottom velocity vector, ρ is water density, c_f is a drag coefficient, ε_B and ε_S are respectively the bedload and suspended load efficiency factors, ϕ is the internal angle of sediment friction, $\tan \beta$ is the nearshore slope, w_s is the sediment fall velocity and \hat{i} is a downslope unit vector. Terms within the $\langle \rangle$ brackets indicate that they are time-averaged quantities. The model indicates that the transport rate consists of two components. The first, a velocity induced transport directed parallel to the current and the second, gravity induced transport directed downslope. The left hand side of the equation deals with bedload transport and the right hand side deals with the suspended load. The model assumes that the instantaneous sediment transport rate is directly proportional to the rate of energy dissipation in the surf zone. It attempts to deal with the unsteady oscillatory

currents of the nearshore in a variety of conditions and is able to estimate both the longshore and on-off shore sediment transport.

It is widely used as a sediment transport module in morphodynamic models (Mason, *et al.*, 1999). In a comparative study involving 10 transport equations, the model was found to be one of the most accurate (Schoonees & Theron, 1995). To date it has been mostly used in sand beach applications, because its basic assumptions apply primary to the surf zone. But there have been some recent attempts to apply it to gravel beaches in the United Kingdom (Soulsby, 1997; Mason *et al.*, 1999). In these studies it has performed moderately well in estimating the tidally-averaged longshore gravel transport, although it tends to provide over-estimations (Soulsby, 1997). Mason *et al.* (1999) found it to be less suited to predicting cross-shore transport. This is because the translation of the breaker forward in the swash zone is not well represented in the model, in which it is assumed that the wave and swash conditions are more symmetrical.

Due to the difficulty in obtaining measurements for a number of the variables in Equation 7.22 and in part due to its unwieldy nature, Bailard (1984) proposed a simplification of the model. The idea was to merge aspects of his stream power model with the wave power CERC model via the K coefficient. Bailard's rationale was to develop a sediment transport model that preserved the simplicity of the Inman and Bagnold formula, but in a way that extended its range of application. Simplifying assumptions were used in the model and then calibrated against field and laboratory measurements of longshore transport rates. Bailard proposed that K was a function of the breaker angle, the orbital velocity magnitude and the sediment fall velocity:

$$K = 0.05 + 2.6\sin^2 2\alpha_b + 0.007 u_{mb}/w_s \quad (7.23)$$

Where α_b is the breaker angle, u_{mb} is the orbital velocity at the break point and w_s is the sediment fall velocity. This is then substituted into the Inman and Bagnold formula (Equation 7.8). When correlated against field measurements of K values it was found to perform reasonably well (Figure 7.11). One advantage of the model is that it can be applied to a broader range of conditions, in particular to beaches composed of mixed grain sizes through the sediment fall velocity term. The model more accurately accounts for the suspended and bedload components of sediment transport. There are several limitations to the model as outlined by Bailard (1984), the most significant being that it simplifies the complex flow fields in the nearshore zone both vertically and cross-shore. Another limitation of the model is that it uses drag coefficient at the bed as a de facto for estimating the rate of energy dissipation, to which the rate of transport is

proportional, instead of making computations directly from the breaking wave at the surface. The assumption being that the boundary layer between the solid and liquid phase is the dominant factor controlling the sediment transport flux. However, as Bailard (1984: 1464-5) stated at the time, this was only conjecture. Finally, the model does not include a threshold term for sediment motion. It was argued that in field conditions, threshold effects were not significant. This has certainly been the finding of sediment transport in a natural beach in the present study.

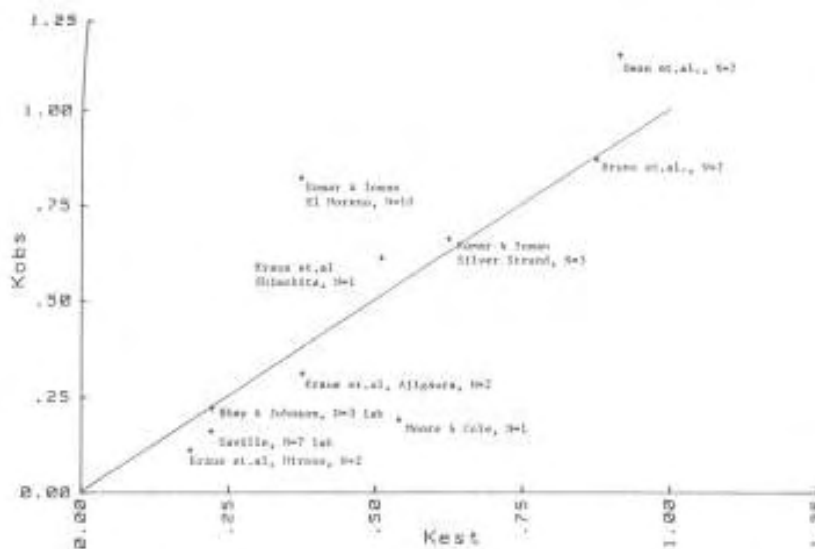


Figure 7.11 Plot presented in Bailard (1984: 1465) showing the comparison between the K coefficient calculated from field data (y-axis) and the predicted K from equation (7.22) (x-axis).

The generalised total load transport equation derived by Bailard (1981) (Equation 7.22) is overly complicated for the case of a lakeshore mixed sand and gravel beach, where nearshore velocity fields, near-bottom orbital velocity vectors and suspended transport are not a significant part of the transport process. Nevertheless, the principles behind the Bailard equation merit its testing in a lakeshore mixed sand and gravel beach. In particular, the way in which it accounts for transport that occurs due to a downslope velocity flow vector, much as might be expected in the swash zone of a steep, coarse grained foreshore. Equation 7.22, has been used to estimate transport rates in gravel beaches. In doing so the equation was found to over estimate the transport rate. It was suggested that this was a consequence of having no threshold term (Van Wellen *et al.*, 2000). However, it has been argued that this should not be a problem because the velocities in the highly turbulent breaker zone of a gravel beach exceed threshold conditions for the vast majority of the time. Because suspended transport is negligible in gravel beaches, Van

Wellen *et al.* (2000a) proposed that the right hand term in Equation 7.23 could be dropped when applying it to these situations. Even though this removes the influence of grain size, the modification was found to be slightly more accurate when applied to gravel beaches in the United Kingdom:

$$K = 0.05 + 2.6 \sin^2 2\alpha_b \quad (7.24)$$

Suspended sediment transport has not been found to be important in the swash zone of the beaches at Lake Coleridge. Thus, Equation 7.24 was tested against the data set. Figure 7.12 presents the correlation between the immersed transport rate and the longshore wave power including the K term from Equation 7.24. Despite the principles that the expression incorporates, it only displays a moderate relationship with the transport rate. The equation over-estimates the transport rates by three orders of magnitude. Values range from 0.13 to 4708.98 N s^{-1} , and average 546.21 N s^{-1} . The mean measured rate for Lake Coleridge is 0.23 N s^{-1} . Due to the high wave approach angles, the K values were too high, with a of mean 1.87. As has been shown for the Lake Coleridge data, K values are required to be in the order of 10^{-3} when using the CERC model. Essentially, the model has been developed for high energy open coast situations, with waves that have been acutely refracted across a nearshore zone. As mentioned above it has also been found to over-estimate transport rates in gravel beaches it has been tested on in the United Kingdom, such as Shoreham (Van Wellen *et al.*, 2000a).

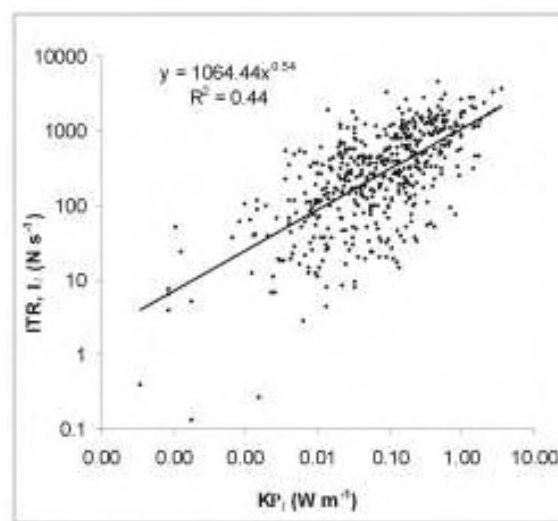


Figure 7.12 Linear regression between transport rate and KP_i , where P_i is calculated from equation 7.6 and Bailard numerical K from Equation 7.24, $r = 0.67$, $F = 394$, Std Error = 0.61.

Morfett Equation

Morfett (1988; 1989) took a similar approach to Bailard by developing a formula that was in part based on a stream power transport model proposed by McDowell (1989). Stream power has been recognised as one of the most powerful concepts used in the study of sediment transport in steady, uniform fluvial flows. It is best understood as being the shear velocity of the stream flow required to overcome the resistance of the bed and transporting sediment. As with Bailard's formula outlined above, the idea was influenced by the theories of Bagnold (1963; 1966). Bagnold (1980; 1986) further developed his idea in two papers in which he showed that there is a strong correlation between rates of bedload transport and excess stream power across the entire spectrum of grain sizes from silts to gravel. Excess stream power is the difference between total stream power and the amount of power that is just sufficient to initiate sediment transport. Bagnold (1986) showed that at constant stream power, the bedload transport rate actually decreased with increasing flow depth. McDowell (1989) generalised Bagnold's equations by replacing the flow depth with a bed friction and shear stress function, making them applicable to unsteady, turbulent flow conditions. McDowell called his function the 'virtual' stream power. It was found to be applicable to streams with grain sizes up to 300 mm across a range of stream flow conditions. It was also suggested that the equation might be suitable, with adjustment, for use in estuarine and coastal environments.

Morfett (1988) was encouraged by its potential application to the marine environment and so he made a derivation based on the idea that the longshore transport rate is a function of the rate of energy dissipation of the breaking wave. In this respect, the dissipation velocity was selected as the parameter for defining the virtual wave power. It was assumed that transport would occur when the dissipation velocity exceeded a critical threshold value:

$$Q_l = K_Q \frac{[P_+^{1.5} (\sin \alpha_b)^{0.75}]}{[g(\rho_s - \rho)D_{90}^2]} \quad (\text{m}^3 \text{ s}^{-1}) \quad (7.25a)$$

where:

$$P_+ = \rho(u_+^3 - u_{+cr}^3) \quad (\text{kg s}^{-3}) \quad (7.25b)$$

and:

$$u_+ = \left[\frac{D_d^{0.33}}{\rho} \right] \quad (\text{m s}^{-1}) \quad (7.25c)$$

The virtual wave power is denoted as P_+ and is calculated at the breaker. $\sin \alpha_b$ is the breaker angle and K_Q is a dimensionless coefficient that must be calibrated for each site, but has been

found to be in the order of 2.84×10^{-5} . The dissipation velocity is denoted by (u_+) . In the dissipation velocity equation there is a term for calculating the wave energy dissipation rate D_d . There are a number of equations over the years that have been derived to calculate this parameter. Morfett (1988; 1989; 1990) himself used several that increased in complexity with each paper, but here the equation that is most suited to a lake wave environment was selected. It is based on a dissipation model developed by Battjes and Janssen (1978):

$$D_d = \frac{(\rho g^{1.5} H^3)}{(4H^{0.5} L)} \quad (\text{W m}^{-2}) \quad (7.26)$$

The virtual wave power (P_+) expression demands that the critical dissipation velocity corresponding to the threshold of sediment movement also be calculated. Morfett (1990) derived an equation that calculated the critical dissipation velocity for waves breaking onto the foreshore and translating into swash. It was based on his earlier work and calibrated against a large field and laboratory data set from the United Kingdom.

$$H_{cr} = 1.5D_{50}(1 - [0.24 \log(1000D_{50})]\gamma^{-1})^{-1} \quad (7.27)$$

Where D_{50} is the median grain size and γ is the wave breaking criterion, given as a ratio of the breaker height over the breaker depth (H_b/h_b). This is then used in Equation 7.26 to calculate the critical dissipation rate. The model has been used with mixed success to calculate longshore sediment transport rates and model shoreline evolution of gravel beaches in the United Kingdom. In a one-line shoreline evolution experiment for two gravel beaches (Shoreham and Brighton) on the South English coastline, Morfett (1988) found that it did a good job in estimating measured rates for Shoreham, but that it performed poorly for Brighton Beach. In a later study, Van Wellen *et al.* (2000a) found that it was moderately accurate, but that it tended to under-estimate transport rates. Energy dissipation is an important process in the swash zone of a mixed sand and gravel beach. Thus, because the model was developed specifically for gravel beaches, it warrants testing with the Lake Coleridge data.

When Morfett's model was calculated, it broke down with the inclusion of the critical dissipation velocity term (u_{+cr}). Using Equation 7.27 to estimate the critical dissipation rate, values were produced that at times were higher than the dissipation velocity, leading to negative results. On the basis that critical thresholds for sediment entrainment have not been found to be important for swash zone transport, a decision was made to omit the term. Without the critical

velocity the model produces reasonable results. The K_Q coefficient was calculated to be 0.04, which is less than the large gravel beaches in the United Kingdom. The ratio between the virtual wave power and the dissipation velocity is lower in the low energy Lake Coleridge environment. The mean dissipation velocity is 0.011 m s^{-1} and the mean virtual wave power is 0.0015 kg s^{-3} . Without calibration, the raw mean transport volume produced by the equation is $5.42 \times 10^{-4} \text{ m}^3 \text{ s}^{-1}$. When calibrated, there is considerable scatter in the results. It over-estimates both the extreme high and low values. The standard deviation and variance of the distribution is twice as large as the distribution of the measured values. This was also found to be the case when it was applied to Brighton Beach (Morfett, 1988). Figure 7.13 shows the correlation between the transport rates and the measured values. There is a wide range in values above and below the best-fit line and the $r = 0.67$. This correlation is very similar to Bailard's derivation (Figure 7.12). It was thought the stream power models would perform well in the swash zone, because sediment is entrained in a flow similar to that of a stream. However, swash zone currents and flow direction have been found to be more complex than previously thought in this study. The model does not manage with an oscillating swash direction, that at times produces an asymmetrical flow. Moreover, some of the underlying assumptions in the models are not important in a mixed sand and gravel lake beach, such as the critical threshold and grain size terms.

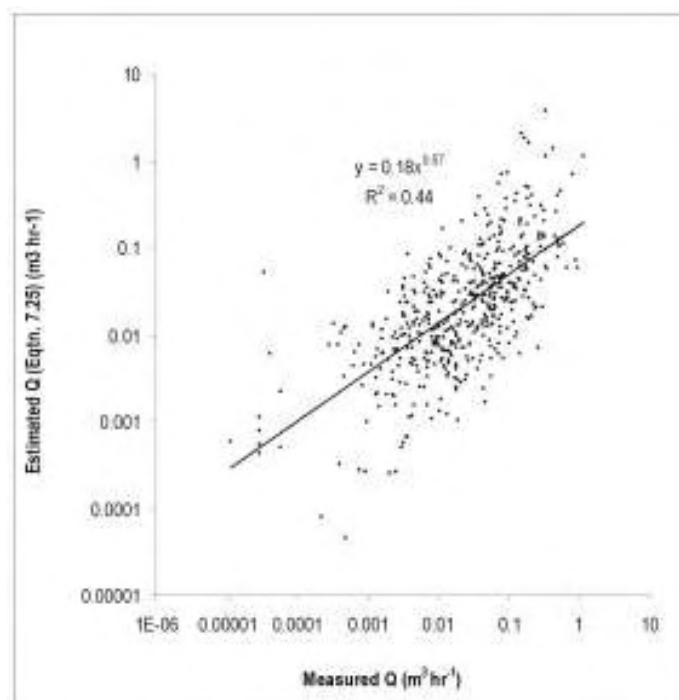


Figure 7.13 Correlation between Morfett's equation (7.25a) and the measured transport rate converted into $\text{m}^3 \text{ hr}^{-1}$. It shows a moderate correlation to the measured values. $r = 0.67$, $F = 390$, Std Error = 0.52. $K_Q = 0.04$.

BORESED Model

The work of Morfett outlined above, spurred further efforts by researchers in the United Kingdom into developing a longshore sediment transport model for use in gravel beaches. Chadwick (1991a; 1991b) developed a model that comprised a hydrodynamic module coupled with a bedload transport formula. Chadwick based his model on bore propagation theories in which the bore represents the progress of broken waves through the surf and swash zone. Bore models are based on shallow water wave equations where the bore is represented as a discontinuity and where mass and momentum are conserved. The equations are computationally intensive, requiring numerical integration with very small time and space lengths. This limits its application to providing instantaneous solutions only, rather than time averaged outputs. Bore theory was pioneered by Peregrine (1972) in which he presented the first depth integrated solutions to finite amplitude shallow water wave equations. Peregrine incorporated these equations into a mathematical model of a shore-normal propagating bore of uniform velocity flowing across a low sloping beach. Hibberd and Peregrine (1979) worked further to validate this model by providing numerical solutions to the proposed equations. Packwood (1983) extended the range of this model to incorporate bed friction, periodicity and beach porosity. Finally, Ryrie (1983) attempted to derive solutions from the work of Packwood to account for the flow regime in obliquely incident bores, separating the onshore and longshore components of the flow.

At the time, bore model theories were used mainly in engineering applications for determining run-up, overtopping and wave reflection on coastal defence structures (Kobayashi, *et al.*, 1987). However, Chadwick (1991a) felt that it had potential to be applied to gravel beaches because the translation of the breaker in the swash zone of a gravel beach approximates that of a bore. Thus, Chadwick developed the model to provide estimates of the instantaneous longshore transport of gravel in the swash zone. Five sets of equations were developed by Chadwick for calculating the hydrodynamic conditions of the bore flow. The bulk of the equations deal with the solution of the onshore and longshore motion, with the other sets dealing with calculating the shoreline and seaward boundary of the bore flow. For the sediment transport component of the model, Chadwick used the virtual stream power equations developed by McDowell (1989), as discussed above. The total longshore transport rate is determined by summing the instantaneous transport rates across the surf and swash zone through time. The model required that only one parameter, a friction coefficient, be calibrated against field data. This was done with long-term data from Shoreham Beach. The hope was that this parameter would not be site specific and thus, that the equation be universally applicable.

The model was then tested and checked against three data sets; two from a laboratory and one from the field (Figure 7.14). It was found that the longshore transport rate is approximately proportional to the wave height $(H-H_{cr})^{2.15}$, the wave period $(T-T_{cr})$ and the wave angle $(\sin \alpha_b)$, where H_{cr} and T_{cr} are the critical values for initiation of transport. This is similar to the CERC equation, except that Chadwick's model includes critical threshold terms. Additionally, it was found that the model shows a correlation with the grain size $(1/D_{50}^{0.5} - 1/D_{cr}^{0.5})$ and the beach slope $(\tan \beta^{1.14})$. With respect to the grain size, it was found that the transport rate declines with increasing grain size. Related to this, Chadwick found that as the beach slope increased so too did the transport rate. Chadwick argued that the steeper the beach, the smaller the distance over which energy is dissipated. This in turn leads to higher longshore velocity flows and thus increases the transport rate. Importantly, this means that at some low value of beach slope, the longshore transport will reduce to zero depending on the threshold conditions. Chadwick (1991b) concluded that the test results were sufficiently encouraging to warrant further testing of the model. But he cautioned that due to the small data sets with which he had tested the model, greater confidence in the model's predictive power could only be confirmed with further testing from other gravel beach sites.

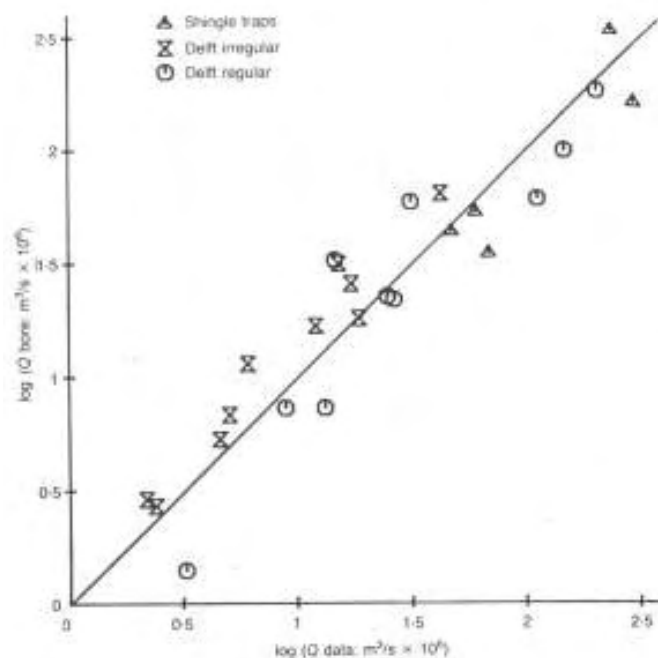


Figure 7.14 Plot presented in Chadwick (1991b: 752) showing the correlation between the BORESED model and field and laboratory data.

Due to the mathematical complexity of the model and due to the good correlations between the transport rate and the key variables wave height, period, angle, sediment size and beach slope, Chadwick (1991b) considered deriving an algebraic solution for the model. This was presented in Van Wellen, *et al.* (2000a):

$$Q = 1.34 \left[\frac{(1+e)}{(\rho_s - \rho)} \right] \left[H_{sb}^{2.49} T_z^{1.29} \tan \beta^{0.88} D_{50}^{-0.62} \sin 2\alpha_b^{1.81} \right] \quad (\text{m}^3 \text{ s}^{-1}) \quad (7.28)$$

Where H and T are the wave height and period, $\tan \beta$ is the beach slope, D_{50} is the median grain size and α is the wave angle. The first term accounts for the immersed density of the sediment where, ρ_s is the density of sediment and ρ density of water. Statistical analysis revealed that this algebraic expression did not differ significantly from the model. The preliminary results from testing this version of the model against field data from Shoreham Beach were promising. But the authors recommended that it be further tested against field data from sites other than those from which it was developed and calibrated. The equation highlights the importance of wave variables in controlling longshore sediment transport, but also shows that grain size and beach slope play a role. The equation contains an inherent threshold of motion term from the parent model. Owing to the complexity of the parent model, it has not been widely used. But Van Wellen *et al.* (2000a) expressed the hope that this simpler equation may be able to be universally applied to estimate gravel beach transport rates.

When tested against the Lake Coleridge data set the model produced results that were some two orders of magnitude higher than the measured volumetric rates. The equation produces mean rates of $3.37 \times 10^{-3} \text{ m}^3 \text{ s}^{-1}$, compared to the measured rates of $2.04 \times 10^{-5} \text{ m}^3 \text{ s}^{-1}$. Similar to the two previous stream power based models, there is a wide scatter in the estimated values that range from 3.77×10^{-6} to 4.43×10^{-2} . The equation requires further calibrating by a coefficient equal to 0.01. Figure 7.15 shows the correlation with the Lake Coleridge data. It provides slightly a better correlation than the two previously examined stream power energetics models ($r = 0.71$). This is a reflection of the fact that it was developed from empirically based gravel beach transport data. The higher energy nature of these open coast gravel beaches explains in part why the model over-estimates the transport rates. However, there is considerably more scatter about the best-fit line than the correlation presented by Chadwick (1991b) seen in Figure 7.14. In the field studies from which this equation was derived, the transport rate was found to increase with increasing beach slope. This is the opposite of that for the beaches at Lake Coleridge and helps explain some of the scatter in the data. This again highlights the need to be aware of the underlying

processes that have been taken into account in the formulation of a sediment transport model. It is important that these processes are in line with those that occur in the system to which a model is being applied.

It will be recalled that the Lake Coleridge data showed a stronger correlation with the sine of the breaker angle and the deep water wave height. Thus, the performance of BORESED is improved by substituting the breaker height for the root mean square wave height and taking the breaker angle as $\sin \alpha_b$, as opposed to $\sin 2\alpha_b$ ($r = 0.74$). The main advantage of this modification is that the magnitude of the estimates improves dramatically, but it still requires a calibration coefficient of 0.18. Summary statistics of these results can be seen in Table 7.5. On the whole the stream power based models examined in this section have not performed as well as the simpler waver power formulations embodied in the CERC model. This is a reflection of the dominant influence of the wave energy and wave height in controlling many aspects of the swash zone and sediment transport in a mixed sand and gravel lake beach. The next section will look at attempts to derive transport models from more controlled laboratory conditions.

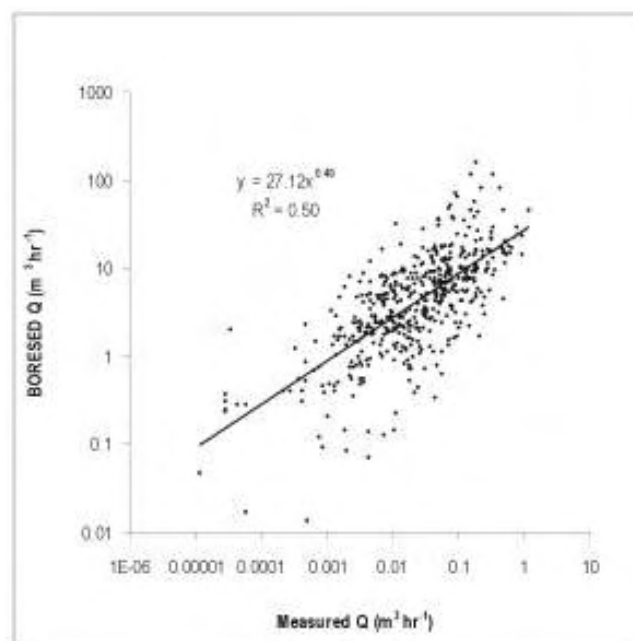


Figure 7.15 BORESED model correlated with measured transport volumes from Lake Coleridge. $r = 0.71$, $F = 489$, Std. Error = 0.41.

Table 7.5 Summary statistics for results from the BORESED model and the modified version. Measured transport rates are shown for comparison. It can be seen that BORESED overestimates by two orders of magnitude.

Q (m³ hr⁻¹)	LST	BORESED	Mod. BORESED
Min	0.0000114	0.0135677	0.000281
Max	1.15	159.77	12.15
Mean	0.07	8.54	0.59
Std. Dev.	0.13	14.36	1.08
Calibration	---	0.01	0.18

7.8 Dimensional Analysis Models of Longshore Sediment Transport

Due to the difficulties of developing and verifying models from empirical field studies, many authors turn to the controlled conditions of the laboratory in an effort to eliminate many of the uncertainties involved in field measurements. In the laboratory, key parameters involved in the transport process can be measured with accuracy. Frequently this begins with a deductive procedure in which the many variables thought to play a role in the transport process are included into a conceptual model. Some of these variables will be more important than others and in some contexts, some may be of negligible influence. A popular approach for organising these variables into a mathematical framework that has relevance for the ‘real’ world is to employ dimensional analysis. When a model is formulated as a collection of symbols, they need to be linked to the actual physical processes they represent. In other words, dimensional analysis attempts to anchor abstract mathematical concepts to the observable world. In particular, this is achieved by assigning the symbols with a system of units such as metres or seconds that can be measured from the real world, whether that be in the laboratory or in the field. One of the first such attempts at this was by Castanho (1970). Castanho’s study showed that grain size and shear stress play an important role in the transport process. Longshore sediment transport is a function of a combination of wave, fluid, sediment and beach-profile parameters. At the most fundamental level the process can be represented with the general functional expression presented by (Kamphuis, 1991):

$$Q = f \{H, T, \alpha, d, \rho, \mu, g, x, y, z, t, \rho_s, D, \beta\} \quad (7.29)$$

Where H , T and α are respectively the wave height, period and angle, d is the water depth, ρ is the fluid density, μ is the fluid viscosity, g is gravitational acceleration, x, y and z are space coordinates, t is time, ρ_s is the sediment density, D is the grain size and β is the beach slope.

Kamphuis Equations

Because of the large number of parameters in such an expression, many of which are interrelated, it is necessary to simplify the equation. Relating sediment transport to only wave or shear stress properties would over-simplify the process. Nevertheless, it is not possible to include every parameter involved in the process because many of the mechanisms are poorly understood or too complicated to represent mathematically (Kamphuis, 1986). Analysis proceeds by forming dimensionless ratios between the various parameters and exploring the mathematical relationships between the variables, rather than through considerations of the physical processes involved in the transport of material (Komar, 1998). For example, ratios may be formed between the wave height and wave length or the wave height and sediment size because they can be represented with the same dimensional units. In this way Kamphuis (1991) recast equation (7.29) to present a dimensionless sediment transport parameter (π_Q), where ϕ is a function:

$$\pi_Q = \phi \left[\frac{H}{gT^2}, \alpha, \frac{H}{d}, \frac{H(H/T)}{(\mu/\rho)}, \frac{x}{gT^2}, \frac{y}{gT^2}, \frac{z}{d}, \frac{t}{T}, \frac{\rho_s}{\rho}, \frac{H}{D}, m \right] \quad (7.30)$$

Kamphuis and co-workers (Kamphuis & Readshaw, 1978; Kamphuis & Sayao, 1982; Kamphuis *et al.*, 1986; Kamphuis, 1990; 1991) directed a considerable amount of research into using dimensional analysis methods to understand longshore sediment transport. From work conducted in a laboratory wave basin, Kamphuis and Readshaw (1978) were able to show that the longshore transport rate is dependant on the beach profile, the breaker type and the rate of energy dissipation. These interrelated quantities are expressed by the Iribarren number, which was discussed in Section 7.5. Kamphuis and Sayao (1982) confirmed this finding with further wave basin research and presented a formula that illustrated the dependence of the littoral transport rate on breaker height, period angle and beach slope. In this formula Kamphuis and Sayao also introduced a new term for the beach slope ($m = d_b/\lambda_b$) that is a ratio between the breaker depth and the distance of the breaker from the still-water shoreline. The intention was to create a beach profile term that reflected the slope conditions in the breaker zone, rather than using a crude average term for the entire nearshore profile. The Kamphuis and Sayao (1982) formula was developed for sandy beaches and showed good agreement with laboratory data, but it underestimated field measured transport rates. It was hypothesised at the time that this was due to the additional transport that occurs in suspension that was not taken into account by the model.

Following nine years of research, Kamphuis *et al.* (1986) presented an energetics type equation that calculated the mass transport rate:

$$Q = 1.28 \frac{(mH_{sb}^{3.5})}{D} \sin 2\alpha_b \quad (\text{kg s}^{-1}) \quad (7.31)$$

Where m is the beach slope term introduced by Kamphuis and Sayao (1982) as discussed above, H_{bs} is the significant breaker height, D is the mean grain size, and α_b is the breaker angle. In this model the transport rate increases with increasing beach slope, but there is some offset with an increase in grain size. The equation was tested against time-averaged long-term field data as well some short-term data derived from both trapping and tracer studies. It revealed that although there was no systematic difference between the method of data collection, the equation over-estimated the transport rate at low energy levels and under-estimated at higher energy levels. It was hoped that with the inclusion of grain size and beach slope, the model could be applied more universally to a wider range of beach types from which it was initially developed. Van Wellen *et al.* (1998) tested it against field data collected from Shoreham Beach, West Sussex, where it was found to over-predict measured transport rates by a factor of 1.5-2.0.

Following a series of irregular wave tests in a laboratory wave tank, Kamphuis (1990) developed a dimensionless expression that was a reduced form of Equation 7.30:

$$\frac{Q}{(\rho H_{sb}^3 / T_p)} = 0.0013 \left[\frac{H_{sb}}{L_o} \right]^{-1.25} m_b^{0.75} \left[\frac{H_{sb}}{D_{50}} \right] \sin^{0.6} (2\alpha_b) \quad (7.32)$$

With further data analysis, Kamphuis (1991) presented a dimensional form of this equation:

$$Q = 2.27 \left[H_{sb}^2 T_p^{1.5} m_b^{0.75} D_{50}^{-0.25} \sin^{0.6} (2\alpha_b) \right] \quad (\text{kg s}^{-1}) \quad (7.33)$$

This model includes the same variables of Equation 7.31, but with the addition of the peak spectral wave period (T_p). It also retains the unusual beach slope measure (m), which other authors have substituted with $\tan\beta$, the standard measure of beach slope (Schoonees & Theron, 1996). The model shows that the sediment transport is proportional to the square of the wave height, but unlike Equation 7.31, also has some sensitivity to the wave period. It also shows that sediment transport increases with steeper beach slopes, which is the opposite of that found in Lake Coleridge. However, this effect is somewhat mitigated with the increase in grain size. The

equation was based on an extensive laboratory data set and tested against a wide range of field data presented in the literature. Kamphuis (1991) claimed that it correctly predicted sediment transport over a large range of grain sizes. It is essentially a bulk sediment transport expression that relates the longshore wave thrust to the sediment transport rate. In this respect it is an energetics type equation, but one that has a different mathematical and experimental basis in its formation. Kamphuis found that it slightly over-estimated gravel transport and suggested that this was due to the extra absorption of wave energy through percolation, that is not experienced on sandy beaches (Figure 7.16). This has been confirmed by Van Wellen *et al.* (2000a), who found both Equations 7.31 and 7.33 to over-estimate transport on gravel beaches. In a review of 52 longshore sediment transport formulae, Schoonees and Theron (1996) found Kamphuis's (1991) formula (Equation 7.33) to be the most accurate. The equation's accuracy results from the inclusion of variables that are important in the longshore transport process across a wide range of beach types.

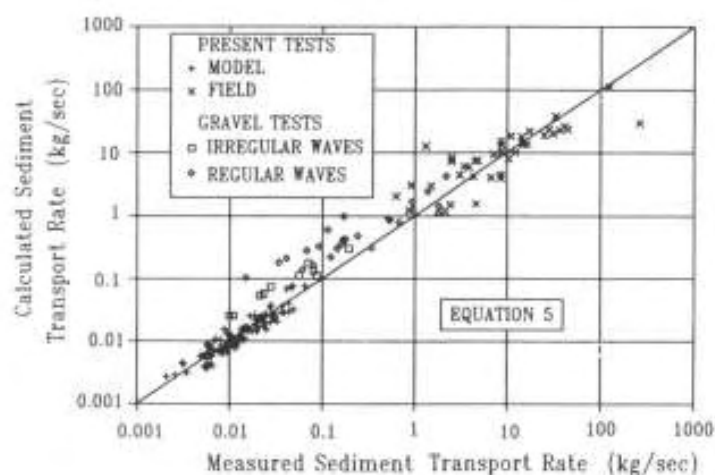


Figure 7.16 Graph presented in Kamphuis (1991: 635) showing the slight over-prediction on gravel transport with his model. The model was developed from laboratory wave tests using both regular and irregular waves. It was then checked against a wide range of field data.

One of the main problems in using laboratory derived models to calculate transport rates in the field, is that the effects of scale differences are poorly understood. Conditions in the laboratory can be carefully controlled and accounted for during measurements. In the field there are wave effects that cannot be easily replicated in laboratory wave basins, for example, infra-gravity wave motion. However, a lot of the complexities of an open coastal environment do not exist in a small lake environment. Small lake environments have neither swell waves, nor highly

developed nearshore current systems. As such, the effect that swell waves introduce into the transport process are eliminated. The waves that form in these situations are locally generated, similar to the waves that are formed in a laboratory wave basin. Kamphuis (1991) showed that although scale effects existed between his laboratory data and the field data, the correlations between the measured and the predicted rates were robust (Figure 7.17). Intuitively, one might expect the scale effects to be less than what is found to occur in swell dominated environments. The widespread testing that Kamphuis' formulae (Equations 7.31 & 7.33) have received in both sand and gravel beach environments, make it worthwhile testing them in the relatively small scale Lake Coleridge environment.

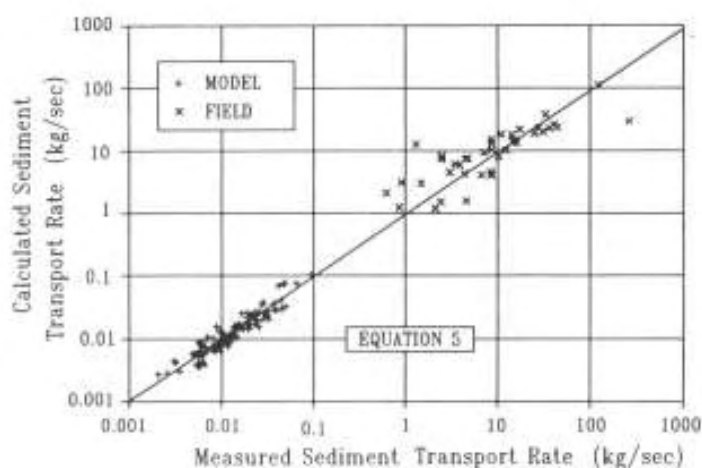


Figure 7.17 Scale effect of laboratory data when compared to field data in the correlation between measured and predicted rates using equation (7.33) as presented in Kamphuis (1991: 634).

The total kilogram per second rate was calculated from the raw trapped data with the same method introduced in Chapter Six, to enable correlation with the Kamphuis Equations, 7.31 and 7.33. Both formulations use the $\sin 2\alpha$ wave angle term, which for reasons already discussed, does not best model the situation in Lake Coleridge. Thus, it was substituted with the $\sin \alpha_b$ term. The results can be seen in Figure 7.18. The models are an improvement over the stream power models, but the data do not conform in the neat linear fashion seen above in Figures 7.16 and 7.17. Kamphuis's later expression (Equation 7.33) was found to perform more satisfactorily than Equation 7.31. There is a wide scatter in the values from Equation 7.31 that be seen in Figure 7.18a. This scatter decreases with Equation 7.33, which is reflected in the standard error of the estimates that reduce from 0.41 to 0.29, with the later model. The two models were both

found to over-estimate the transport rate. This is possibly due to the effect of porosity in absorbing wave energy, that Kamphuis mentioned was not accounted for in the equations and has been found to play an important role in this study. Table 7.6 shows a summary of the results, where it can be seen that both models over-estimate by two orders of magnitude.

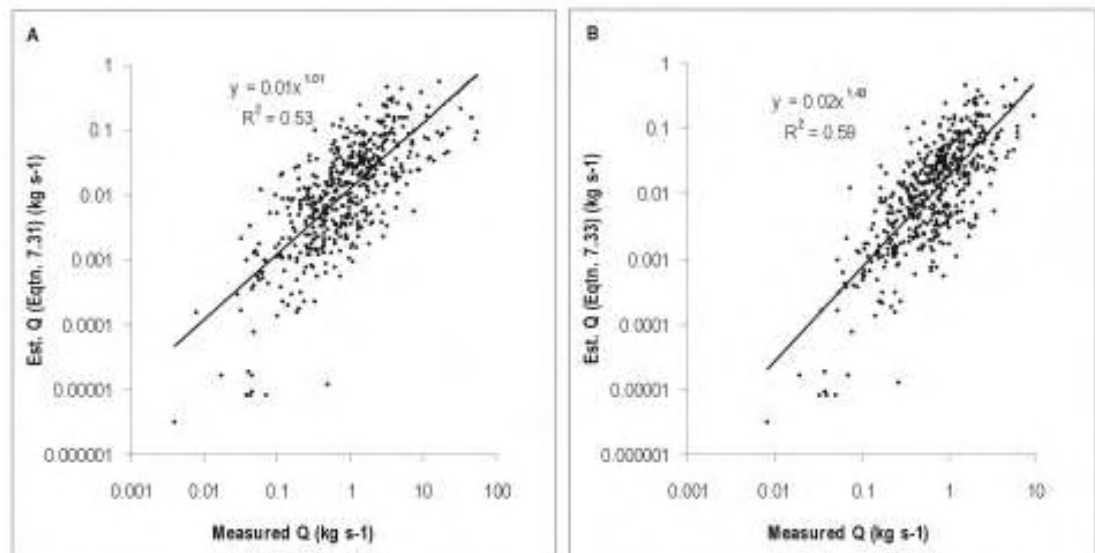


Figure 7.18 (A) Correlation of Equation 7.31 with measured transport rate in kg s^{-1} . $r = 0.76$, $F = 563$, Std Error = 0.41. (B) Correlation with Equation 7.33. $r = 0.77$, $F = 695$, Std Error = 0.29. Kamphuis's later equation (B) can be seen to provide better correlations with the measured rates.

Overall, Equation 7.33 is a superior formulation. Equation 7.31 grossly over-estimates the extreme values and has a comparatively high standard deviation. Calibration coefficients have been calculated for both equations, at 0.02 and 0.03 respectively and are shown in the table. These could be used when applying the equations to other coarse grained, low energy beaches. Figure 7.17 shows the scaling effect of measurements from the laboratory to the field. When compared to Figure 7.18b, note that the values measured in Lake Coleridge fall neatly between those recorded in the laboratory by Kamphuis and those measured in the field. Illustrating the point that lakes are good natural laboratories for studying coastal processes. One problem with these equations is that the results produce a mass transport rate in kilograms per second. To convert this to a volumetric rate requires a knowledge of the sediment density and porosity. Whilst the porosity of unconsolidated beach sediments is reasonably constant at 0.60, the density varies considerably. Unless otherwise known, this would require determining before any shoreline evolution modelling could proceed.

Table 7.6 Summary statistics of the results from Equations 7.31 and 7.33. Equation 7.33 provides stronger correlations and closer estimates to the measured results. Calibration coefficients for the equations are in the last row.

Q (kg s ⁻¹)	Measured	Eqtn. 7.31	Eqtn. 7.33
Min	0.000003	0.00384	0.00820
Max	0.56	53.20	9.52
Mean	0.04	2.10	1.02
Std. Dev.	0.06	4.88	1.07
Calibration	---	0.02	0.03

Delft Equations

The Delft Hydraulics Laboratory has conducted many investigations into longshore sediment transport. Sediment transport of coarse grained materials has been a particular focus of the research. Following a series of tests in the late 1970s and early 1980s van Hijum and Pilarczyk (1982) developed an equation derived from laboratory experiments of random irregular waves breaking onto a gravel beach. The equation was found to agree well with laboratory rates of gravel transport:

$$Q = 0.000712 (g D_{90}^2 T) W (W - 8.3) \left[\frac{\sin \alpha_v}{\tanh(k h_v)} \right] \quad (\text{m}^3 \text{s}^{-1}) \quad (7.34a)$$

where:

$$W = \frac{H_s (\cos \alpha_v)^{0.5}}{D_{90}} \quad (7.34b)$$

and:

$$k = \frac{2\pi}{L_o} \quad (7.34c)$$

Where H_s , L , and T are the usual wave parameters, g is the gravity constant, D_{90} is the 90th percentile grain size, α_b is the breaker angle at the beach toe, h_v is the water depth at the beach toe and k denotes the wave number. The model takes into account the grain size and includes a threshold term $W(W-8.3)$ for the initiation of transport, that occurs when, $H_s (\cos \alpha)^{0.5} > 8.3 D_{90}$. The equation involves a combination of both deep and shallow water wave parameters measured at the beach toe (subscript v).

When the equation was tested against the Lake Coleridge data set, it broke down when the significant wave height was used in the calculation of W (Equation 7.34b). It will be recalled that this also occurred with the virtual wave power model of Morfett (1988) (Equation 7.25) and can be explained for the same reasons. The equation incorporates a threshold ratio term from which a constant is subtracted. At times the ratio is smaller than the constant (-8.3), producing a mix of negative values that when multiplied through the equation generate negative transport rate. This is because wave and sediment transport measurements were recorded from extremely low energy conditions and the threshold coefficients in the equations exceeded the energy levels that have been found to initiate sediment. This challenges the underlying assumption of the model regarding threshold conditions, implying that sediment is entrained by lower current velocities than previously thought. The problem was rectified by using the significant breaker height. The water depth at the beach toe was not measured and was substituted with the significant breaker height. This is an acceptable assumption as waves most commonly broke close to, or at the base of the swash zone, which is in effect the beach toe. The wave angle at this point was taken as the onshore swash flow direction measured by the current meter. Figure 7.19 shows the correlation with the measured transport rates ($r = 0.71$). The equation does not perform as well as the Kamphuis equations. There is considerable scatter in the results across all energy conditions. The mean rate estimated by the equation is $4.63 \text{ m}^3 \text{ hr}^{-1}$, which is two orders of magnitude higher than the measured rate of $0.07 \text{ m}^3 \text{ hr}^{-1}$. It requires further calibrating by a coefficient equal to 0.015, in order to be applied to a low energy beach.

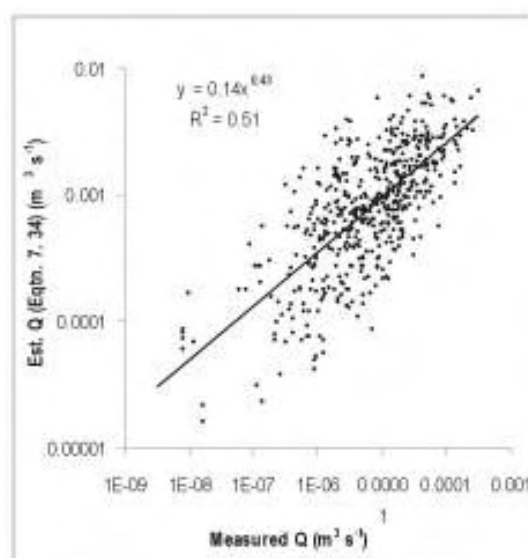


Figure 7.19 Correlation of the Delft model (Equation 7.34) with measured transport rate in $\text{m}^3 \text{ s}^{-1}$. $r = 0.71$, $F = 507$, Std Error = 0.35.

Some authors have criticised the model on the basis that it introduces unnecessary complications and makes the equation difficult to apply to other sites (Chadwick, 1989). Due to the difficulty of obtaining estimates from the beach toe Chadwick (1989) recast the Delft equation to use breaking wave conditions and dropping the wave angle ratio in favour of $\sin \alpha_b$:

$$Q_l = 0.0013(gD_{90}^2 T) \left[\frac{H_{sb}(\cos \alpha_b)^{0.5}}{D_{90}} \left[\frac{H_{sb}(\cos \alpha_b)^{0.5}}{D_{90}} - 8.3 \right] \sin \alpha_b \right] \quad (\text{m}^3 \text{ s}^{-1}) \quad (7.35)$$

Following a series of laboratory and field tests, van der Meer (1990) also recast the original Delft equation. This version requires the significant deep water wave conditions and like the Kamphuis equation (7.35) contains the peak spectral wave period (T_p):

$$Q = 0.0012(gD_{n50} T_p) \left[H_s (\cos \alpha_b)^{0.5} \left(\frac{H_s (\cos \alpha_b)^{0.5}}{D_{n50}} - 11 \right) \right] \sin \alpha_b \quad (\text{kg s}^{-1}) \quad (7.36a)$$

where:

$$D_{n50} = \left[\frac{M_{50}}{\rho_s} \right]^{1/3} \quad (7.36b)$$

van der Meer introduced a new grain size measure (D_{n50}) (Equation 7.36b). This parameter represents the median mass of a grain at the 50th percentile (M_{50}) of the mass distribution curve of the sediment being transported. Both these equations are quite similar to the original formula, differing only in slight variations of the threshold terms and the constants. Chadwick's (1989) variation uses breaker values and van der Meer's (1990) equation uses deep water values, whilst the original Delft formulation requires the use of both deep and shallow water parameters. When tested against measured field data, the original Delft equation and its derivatives have been found to over-estimate gravel transport rates by 2-5 times (Chadwick, 1989; van der Meer, 1990; Van Wellen *et al.*, 1998; Van Wellen *et al.*, 2000a). This may in part be due to the scaling effects associated with laboratory derived formulae. It may also be due to energy dissipation factors, such as porosity, that are not taken into account by the models as found in the Kamphuis (1991) equations.

Figure 7.20 shows the correlations for Equations 7.35 and 7.36 against the measured rates from Lake Coleridge. Summary statistics for the calculations can be seen in Table 7.7. Equation 7.35 produces very similar results to the original Delft formulation, but provides slightly better correlations, validating the modification of Chadwick (1989). Estimated transport rates range

from 0.020 to 31 m³ hr⁻¹, with an average of 4.63 m³ hr⁻¹. This is considerably higher than the actual rates, that averaged 0.07 m³ hr⁻¹. In order to produce results of the correct magnitude, a calibration coefficient of 0.016 was determined for this equation. No problems were experienced with the threshold term as the equation incorporates the wave breaker height. Similarly, this was not a problem with Equation 7.36, in which the significant wave height term was reintroduced by van der Meer (1990). The threshold calculated with the median sediment mass term, rather than the D_{90} grain size, generated a larger ratio from which to subtract the constant. The grain mass term, whilst an interesting concept, is a difficult parameter to properly determine. It was approximated by calculating the volume of a sphere based on the median B-axis diameter of the trapped sediment data and then calculating the mass of this sphere, via the sediment density. This was the only practical method, but it assumes a sphericity that did not truly exist in the sediments. It can be seen in Figure 7.20b that van der Meer's (1990) expression is a slight improvement over Chadwick's (1989) version. However, it under-estimates the transport rates and requires calibrating with a coefficient of 17. The mean rate estimated with Equation 7.36 is 7.19 kg hr⁻¹, compared to the measured rate of 129.0 kg hr⁻¹. This appears worse than Chadwick's (1989) equation (7.35), but is in fact lower. Equation 7.35 over-estimates the rates by a factor of 66. It is not known exactly why this equation should under-estimate the rates, but is probably for two reasons. The grain size mass term produces very small fractions compared to the standard grain size diameter and this reduces the magnitude significantly. Second, the threshold constant in this version was increased from -8.3 to -11. Thus, the model assumes a higher sediment entrainment threshold.

Equations 7.34 to 7.36 were developed specifically for use in natural gravel beaches. When applied to the gravel beaches in the United Kingdom, they have been found to over-estimate the rates in the order of 2-5 times. When applied to the Lake Coleridge data sets two of the models over-estimated the rates in the order of 60 times. This highlights the problems introduced by scaling effects when applying models developed from laboratory analysis. The third model under-estimated the rates by a factor of 17. This suggests that the threshold terms in the expressions may be more suitable for pure gravel and cobble beaches where the size of the sediment is known to hinder transport rates. Gravel beaches of the United Kingdom are often fronted by a low tide terrace composed of sand. At high tide this forms a shallow nearshore area that causes wave breaking and modification in a manner that does not occur in the mixed sand and gravel beaches in New Zealand. In the mixed sand and gravel beaches of the open coast and glacial lakes, waves commonly break at the base of the swash zone, generating current velocities of such magnitude that threshold terms become irrelevant. Thus, the threshold terms are not

necessary for estimating transport rates in a mixed sand and gravel beach. Nevertheless, these equations showed an improvement over the stream power models of the previous section.

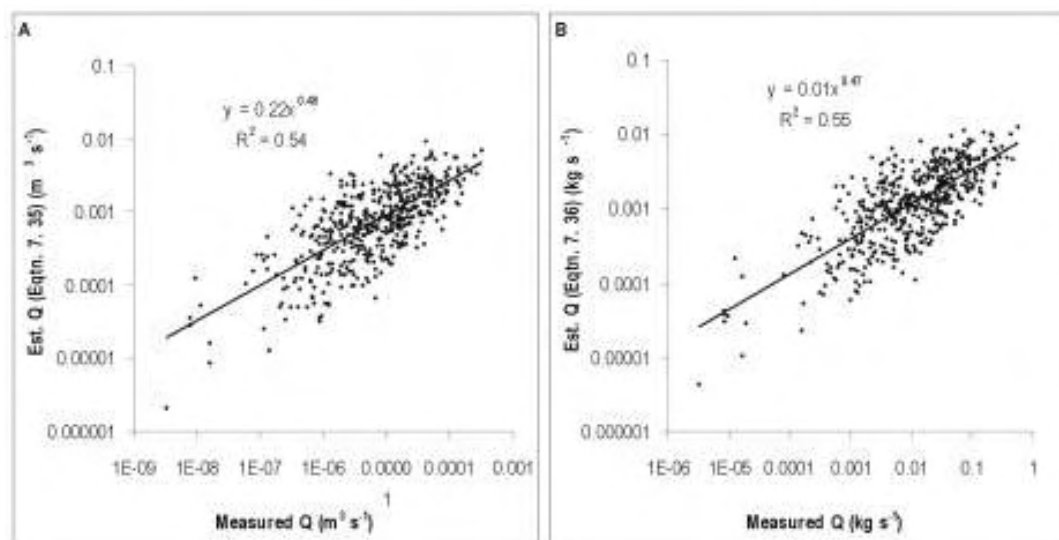


Figure 7.20 (A) Correlation of Equation 7.35 with measured transport rate in $\text{m}^3 \text{s}^{-1}$. $r = 0.73$, $F = 576$, Std Error = 0.36. (B) Correlation with Equation 7.36 in kg s^{-1} . $r = 0.74$, $F = 608$, Std Error = 0.35. The two models perform more satisfactorily than the original Delft model.

Table 7.7 Summary statistics for the estimated transport rates from Equations 7.34-7.36, converted into hourly rates. The columns headed LST are the empirically measured rates from Lake Coleridge. The three models all require calibrating to produce results of the correct magnitude for use on coarse grained lake beaches. The coefficients are presented in the last row.

Q	LST ($\text{m}^3 \text{hr}^{-1}$)	Eqtn 7.34 ($\text{m}^3 \text{hr}^{-1}$)	Eqtn. 7.35 ($\text{m}^3 \text{hr}^{-1}$)	LST (kg hr^{-1})	Eqtn. 7.36 (kg hr^{-1})
Min	0.000011	0.019750	0.007652	0.012	0.015
Max	1.15	31.19	32.42	2022.34	45.53
Mean	0.07	4.63	4.44	129.00	7.19
Std. Dev.	0.13	4.60	4.66	227.50	7.24
Calibration	---	0.015	0.016	---	17.0

LEXSED Formula

To recap, in the last Chapter a new sediment transport expression was developed, based on the analysis of an extensive data set of wave, current and sediment transport information collected in Lake Coleridge. The equation is given as the wave height cubed, divided by the wave length and multiplied by the mean swash velocity and the breaker angle. A coefficient (k) is also included

that requires calibrating, depending on the application. For Lake Coleridge it was determined to be 0.02 and it is reasonable to assume that this applies equally to other coarse grained lakeshore beaches. Presently its application is valid for conditions; $H < 1.0$ m, $D_{50} > 1.0$ mm. The equation is presented here again:

$$Q_l = k \left(\frac{H_{rms}^3}{L_o} \right) \cdot \bar{v}_{sw} \cdot \sin \alpha_b \quad (\text{m}^3 \text{ s}^{-1}) \quad (7.37)$$

The equation is deterministic, in that it is empirically derived from studying the statistical relationships between the main variables influencing sediment transport. It has been developed from a first principles basis and has units of $\text{m}^3 \text{ s}^{-1}$. With the inclusion of the swash velocity it validates the attempts, discussed above, in applying concepts of stream power to model longshore sediment transport in coarse grained beaches. It recognises that the dominant mode of sediment transport occurs in the swash zone, in a bore of flowing water. Effectively, the swash velocity acts as de facto measure for the shear stress exerted on the sediment at the bed. The equation shows good a correlation to the measured data $r = 0.85$ $r^2 = 0.72$, which are the strongest correlation and regression coefficients of all the models tested (Figure 7.21). The value of the k coefficient suggests that there are some effects that are not being taken into account by the model. These effects are possibly related to internal energy water kinematics

LEXSED performs robustly across the full range of wave energy conditions, accurately estimating both the highest and lowest extremes (Table 7.8). This is because the data set from which it was derived encompassed storm conditions. Most of the models reviewed above underestimated the extreme high rates. In an extensive review of the empirical field data base for longshore sediment transport studies, Schoonees and Theron (1993) identified a clear lack of measurements for high energy and storm conditions. Many of the models presented in the literature are only valid for low to moderate energy conditions and have been found to perform poorly when applied beyond these limits. It is extremely important that a sediment transport model is able to provide close estimates for these conditions, because storm waves are responsible for a large percentage of the long-term transport rate. In Chapter Six an annual sediment budget was presented for the fieldsite beaches, based on hourly wind speed data collected at the Lake. Hourly wave heights and transport rates were calculated for the year of 2002. It was found that storm waves over 0.60 m accounted for a mere 1% of the distribution, yet were responsible for an astonishing 10% of the total annual gross littoral transport rate. By contrast, waves under 0.10 m, that accounted for 17% of the distribution, were only responsible for 2% of the total annual rate.

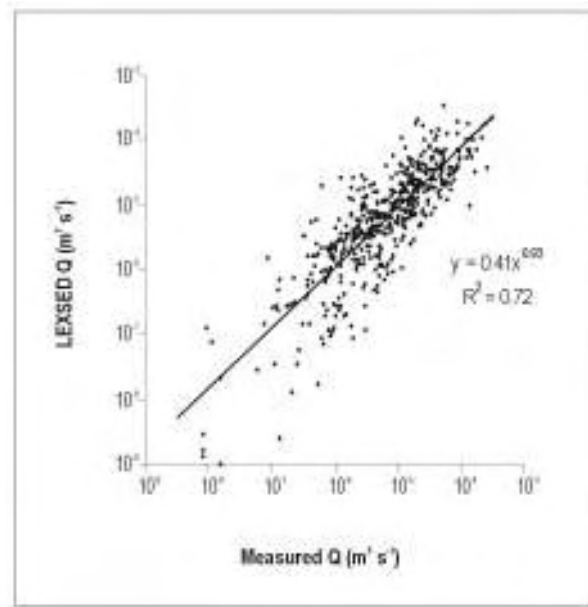


Figure 7.21 Correlation between the measured longshore sediment transport rate and the rate estimated by LEXSED model developed in the present study. $r = 0.85$, $F = 1285$, Std. Error = 0.47, Prob. < 0.0001.

Table 7.8 Summary statistics for the measured and estimated longshore sediment transport rates using the LEXSED formula. The model shows close agreement with the measured statistics, importantly with measures such as the variance and the skewness, indicating that it is able to estimate extreme high conditions.

LST (m ³ hr ⁻¹)	Measured	Estimated LEXSED
Min	0.000011	0.000002
Max	1.154	1.265
Mean	0.074	0.073
Std. Dev.	0.130	0.125
Variance	0.017	0.016
Skewness	3.924	4.190
Kurtosis	20.560	25.041

7.9 Summary and Discussion

Since 1950, a plethora of scientific papers have presented the development, testing and application of longshore sediment transport models. Some of these models have been derived from empirical field studies (Watts, 1953; Swart, 1976), others from laboratory studies (Kamphuis & Readshaw, 1978; Hijum & Pilarczyk, 1982), whilst some have been deduced directly from physical and mathematical principles (Bagnold, 1963; Bailard, 1981). The aim of

this chapter has been to identify and discuss longshore sediment transport equations that may have potential application to lakeshore and/or other low energy coarse grained beaches and in a broader sense, to the mixed sand and gravel beaches of the open coast. A summary of the equations that were tested and/or developed in this study, including the new expression presented in Chapter Six, are shown in Table 7.9. The models were identified on the basis of three main criteria. First, and perhaps most importantly, the equation had to have some regard for the processes operating in a coarse grained beach. Second, equations were chosen on the basis that they had either been modified or specifically developed for use in a gravel beach environment. Third, equations were chosen that appeared or were purported to be generalised expressions, that is, in some way universally applicable.

The equations are grouped on the basis of the physical principles on which they were derived and fall into three main categories; wave power, stream power and dimensional analysis. The models were discussed under these headings throughout the chapter. Within these headings, the equations are grouped according to their formulation. *I&B* refers to the Inman and Bagnold formula presented as Equation 7.8. *K I&B* stands for those expressions that sought to provide a numerical solution for *K* via a series of environmental parameters, such as grain size or beach slope. *MOD I&B*, is a modification of the Inman and Bagnold formula, that is distinctly different, yet still maintains a reliance on the longshore wave power. These models all fall under the wave power group, because they are based on a physical interpretation of the power or force of the wave energy. Dimensionally, they are expressed in terms of Watts per meter (W m^{-1}) or Newtons per second (N s^{-1}). The stream power models are based on the idea that shear stress at the bed is the most important determinant of sediment transport. These models were derived from a consideration of the physical processes that intuitively and observationally occur in unidirectional stream flows. These equations are normally expressed in terms of a cubic metre per second rate ($\text{m}^3 \text{s}^{-1}$). The dimensional analysis equations have been derived from empirical studies of sediment transport in both the laboratory and natural beaches. The equations are developed by correlating measured environmental variables with volumetric or mass transport rates, in order to identify the dominant controlling processes. The results can be expressed dimensionally in a number of ways, but most commonly it is in terms cubic metre per second ($\text{m}^3 \text{s}^{-1}$) and sometimes as kilogram per second (kg s^{-1}).

Table 7.9 The longshore sediment transport equations tested against measured transport rates from Lake Coleridge, showing correlation and calibration coefficients. Some of these models may be used to estimate rates of longshore sediment transport in appropriate situations. Further notes are supplied below.

Source	Equation #	<i>K</i>	<i>r</i>	<i>r</i> ²	Std. Err.	Calibration
Wave Power						
<i>I&B</i>						
1. Inman & Bagnold (1963)	7.8b	0.00091	0.75	0.57	0.54	N/A
2. Present Study	7.8b (sin α_b)	0.00049	0.79	0.62	0.51	N/A
<i>K I&B</i>						
3. Swart (1976)	7.13	0.39	0.75	0.56	0.40	---
4. Kamphuis & Readshaw (1978)	7.14	0.30	0.74	0.55	0.55	---
5. Özhan (1982)	7.15	0.09	0.69	0.48	0.60	---
6. Özhan (1982)	7.16	0.16	0.73	0.53	0.56	---
7. Bodge & Kraus (1991)	7.17	0.28	0.74	0.55	0.55	---
<i>MOD I&B</i>						
8. Brampton & Motyka (1984) & Chadwick (1989)	7.20	0.00094	0.75	0.56	0.41	N/A
9. Chadwick (1989)	7.19	0.00099	0.74	0.55	0.40	N/A
10. Present Study	7.12	0.017	0.81	0.65	0.48	N/A
Stream Power						
11. Bailard (1984) & Van Wellen <i>et al.</i> (2000a)	7.24	1.87	0.67	0.44	0.61	---
12. Morfett (1988)	7.25a	0.04	0.67	0.44	0.52	N/A
<i>BORESED</i>						
13. Chadwick (1991) & Van Wellen <i>et al.</i> (2000a)	7.28	---	0.71	0.50	0.41	0.01
Dimensional Analysis						
<i>KAM</i>						
14. Kamphuis <i>et al.</i> (1986)	7.31	---	0.76	0.58	0.41	0.02
15. Kamphuis (1991)	7.33	---	0.77	0.59	0.29	0.03
<i>DELFT</i>						
16. Hijum & Pilarczyk (1982)	7.34a	---	0.71	0.50	0.35	0.015
17. Chadwick (1989)	7.35	---	0.73	0.53	0.36	0.016
18. van der Meer (1990)	7.36	---	0.74	0.55	0.35	17.0
<i>LEXSED</i>						
19. Present Study	7.37	0.02	0.85	0.72	0.47	N/A

- 1.) *K* values are included for those models that specify this parameter.
- 2.) A calibration is included for some models where appropriate and can be used in the equation to calculate transport rates for beaches similar to those on which this study took place *i.e.* low energy, coarse grained.
- 3.) (N/A) indicates that the model is correctly calibrated with the *K* value specified and can be applied to low energy, coarse grained beaches.
- 4.) (---) indicates that it is not appropriate to further calibrate the model, because the equation is intended to produce a numerical solution for the *K* coefficient. In their present state these models are not correctly calibrated for use on low energy, coarse grained beaches.

Most models have been developed to calculate the transport rates of sandy beaches. This reduced the number of available equations markedly, because a lot of the process parameters in these equations are simply not relevant to the beach systems in this study. However, some of the models are based on broad principles that occur in any beach environment, even if they have been validated with data from sand beaches. One such model, is the Inman and Bagnold formula (Inman & Bagnold, 1963), which has been discussed in depth in this chapter. Although the model has been largely validated from empirical studies of sand transport, at its core the model is based on the sediment transport theories of Bagnold (1963; 1966). The model has been criticised for its simplicity, but it is this very simplicity that makes its application to mixed sand and gravel beaches viable. As was discussed in Section 7.3 it was originally conceived from a coarse grained prototype beach. The formula comprises a few key environmental variables, incorporated by terms for the wave energy, celerity and breaker angle and balanced with a calibration coefficient denoted K . The coefficient effectively accounts for an array of unquantified variables not included in the equation. This is one reason why the model has been applicable to a range of beach types. However, the coefficient is highly variable and this precludes the possibility of it being a constant.

The Inman and Bagnold model was found to perform moderately well when tested against the Lake Coleridge data set. In Table 7.9 it can be seen that the Pearson correlation coefficients are $r = 0.75$ and $r^2 = 0.57$. For a highly dynamic, natural beach system this is correlatively significant and indicates that when correctly calibrated, it can be used to estimate transport rates with a degree of confidence. Typical correlations from open coast sandy beaches have been found to be in the order of $r = 0.45$ $r^2 = 0.20$ (Schoonees & Theron, 1994). This validates the original limits of the model and suggests that the underlying theory behind the model is robust. The model has been criticised for being mathematically incorrect. Longuet-Higgins (1972) stated that the $\cos \alpha_b$ term should be removed from the equation on the basis that this did not provide a correct assessment of the longshore directed component of the wave power. Indeed, the predicative strength of the formula was improved by omitting the $\cos \alpha_b$ term, $r = 0.79$ $r^2 = 0.62$, as indicated by the second equation in Table 7.8.

Much research has been directed toward identifying the environmental factors responsible for variation in the K coefficient. The aim has been to provide a numerical solution for the parameter. Many authors have suggested that K is related to the grain size, the idea being that larger sediment requires greater force to move and thereby absorbs a greater amount of the wave energy. The beaches of the fieldsite exhibited a range in sediment sizes from fine sand to large

pebbles. The sediment collected in the traps was sieved at quarter phi intervals to assess whether there was any dependence of the transport rate on variations in the grain size. Rates were correlated against a range of grain size summary statistics including the D_{10} , D_{50} , D_{90} , the modal classes and the skewness. No such correlation was found. K had a correlation coefficient close to zero. It was found in this study that the swash velocities routinely exceeded the incipient motion thresholds of all the sediment sizes. Other attempts have been made to link K to the wave steepness, beach slope and the Iribarren number. Similarly, K was not found to present any relationship with these variables. Incorporating the numerical solutions for K into the Inman and Bagnold model (Equations 7.13-7.17) resulted in the mean rates being over-estimated by 2-3 orders of magnitude. Moreover, most of the equations presented weaker correlations with the immersed transport rate than the original Inman and Bagnold formula. It is recommended that these equations not be applied to low energy coarse grained beaches in their present format.

It was found that K is more related to the wave energy dissipation effects exerted by the beach morphology on the breaking wave. Sandy beaches have been found to have K values between 0.50-1.00, with a average around 0.70. Gravel beaches have almost all been found to have K values of between 0.04 to 0.01. In Lake Coleridge they range between 0.00050-0.001. The change in magnitude of the K values between these environments, is simply a reflection of the decreasing volumes of sediment transport that occur in these systems. Thus, whilst no difference in K can be identified within a beach system, variations appear between the main morphological types. In part, the beach morphology is controlled by the grain size. Thus, in effect it has a secondary role in the wave energy dissipation process. One possible solution to the problem of defining K , is to identify a mean value for use within certain limits. For example, 0.70 for sandy beaches, 0.1 for gravel beaches and 0.001 for low energy shorelines.

There have been a number of proposed variations of the Inman and Bagnold formula over the years, and some of these were discussed in Sections 7.4 and 7.5. The variants tested in this study incorporated a wave energy threshold term (Equations 7.19 & 7.20) developed for gravel beach applications by Brampton & Motyka (1984) and Chadwick (1989). The models both required that K be calibrated. The value of the coefficient was found to be similar to the original model (Table 7.9). No improvement in the predictive power of the model was found by these two variations, partly because no threshold limits were identified from the field studies. Sediment transport appeared to be stochastic in nature, in that all the sediment under the breaking wave was set into motion in all but zero energy conditions.

Out of the analysis of the Inman and Bagnold model and drawing on the findings from the present study a variation to the formula was proposed. The predicative capability of the formula was greatly improved by using the root mean square wave height in place of the breaker height, to calculate the wave energy term, and by substituting the wave celerity for the swash velocity, as presented in Equation 7.12. When tested against the transport rates from Lake Coleridge the correlation coefficients increased to $r = 0.81$ and $r^2 = 0.65$. Considering the similarity of open coast mixed sand and gravel beaches to those in this study, these results suggest that when calibrated, it would be suitable for open coast applications. The mean swash velocity could be calculated with Equation 5.14a, 5.16 or 5.17. Acknowledging the uncertainty that may surround these calculations when extended to open coast situations, it is suggested that at the very least, the cosine term be dropped when applying the Inman and Bagnold model to mixed sand and gravel beaches.

Following on from the Inman and Bagnold model, there have been similarly conceived energetics equations that have validity for coarse grained beaches. One of these is the Bailard (1981; 1984) formula, based on a consideration of stream power or bed shear stress, that was also derived from the fluid transport theories of Bagnold. The Bailard model took into account a wide range of environmental factors involved in the transport process, including a consideration of the grain size. The concept of using stream power to represent the transport process encouraged the development of a number of gravel transport models in the United Kingdom, some of which were tested in the present study (Morfett, 1988; Chadwick, 1991; Van Wellen *et al.*, 2000a). They are based on the idea that the bore flow in the swash zone is somewhat similar to the flow conditions of a stream. In general, these models performed the most poorly of all those tested against the Lake Coleridge data sets. They presented the lowest correlations and over-estimated the transport rates. All these models included wave energy threshold terms to account for the incipient motion of gravel in swash bore flow. However, these term were not found to be valid for the low energy beaches in this study. Moreover, because they were developed for pure gravel beaches of the open coast, they suffered scaling effects when applied to Lake Coleridge.

Due to the difficulties of obtaining reliable data from field studies by which to develop sediment transport models, some researchers have turned to the controlled conditions of the laboratory. This has resulted in the development of numerous equations. The equations tested in this study were those that were purported to be universally applicable (Kamphuis *et al.*, 1986; Kamphuis, 1991), or had been developed specifically for estimating rates of gravel transport,

such as those developed at the Delft Hydraulics Laboratory (Hijum & Pilarczyk, 1982). Laboratory derived equations are often found to over-estimate transport rates due to scaling effects inherited in the models from the small scale conditions of a wave flume being extended into the natural environment. Indeed, with one exception, all these models over-estimated the transport rates and required further calibration coefficient in the order of 10^{-2} . These terms are summarised in Table 7.9. Despite this, these models all performed reasonably well when tested against the Lake Coleridge data sets. The best performing model in this group was Equation 7.33, proposed by Kamphuis (1991). In general all the wave power expressions required calibrating with a coefficient in the order of 10^{-3} . Whilst the stream power and dimensional analysis equations, including the LEXSED formula and the Inman and Bagnold model variation (Equation 7.12) proposed here, all required calibrating with a coefficient in the order of 10^{-2} . This suggests that the dimensional analysis and stream power equations are all accounting for a degree of energy dissipation not taken into account by the wave power equations.

These findings indicate that identifying the cause and effects of wave energy dissipation on sediment transport rates, is an area of promising future research. Energy arriving in the form of waves at a shoreline is reduced to zero through a number of mechanisms. Defining the quantity of energy that is used to transport sediment is a challenging and complex task. Clearly, the calibration coefficients are acting as a de facto wave energy reduction factor. The internal water flow kinematics that lead to wave dissipation need to be more fully understood in order clarify this issue. Furthermore, the precise details of the energy transfer mechanism at the boundary layer between water and sediment needs to be fully understood. In all of the models, the transport rate is expressed in terms of an instantaneous per second rate, however, most measurements of sediment transport take place over a period of minutes, hours or even days. It is possible there is a degree of time-domain scaling occurring between the wave power and the resulting sediment transport.

Despite the different underlying theories of the equations, the range of variables incorporated into them and the methods used in their derivation the equations were all correlatively similar. showing correlation coefficients in the range $r = 0.67-0.77$ and $r^2 = 0.44-0.59$. The common variable in these expressions is the wave height, which is indisputably the dominant controlling environmental variable in a lakeshore beach. It also reflects the importance of obtaining high quality data to input into the equations. Schoonees and Theron (1993) found a wide range in the quality of data that has been used over the years to validate sediment transport models and demonstrated that the best correlations were always achieved with the highest quality data. The

high quality data set prepared in this study has validated, to a similar degree all of the tested models. Furthermore, it also validates the methods used to collect and analyse the empirical field data lends credibility to its continued use.

The significant difference between the models occurs in the magnitude of the estimates. Most of the equations over-estimated the rates and required further calibrating. With the calibration coefficients incorporated into the equations, the mean values are reasonably estimated, but the extreme high rates are mostly under-estimated. This limits their predicative application to moderate conditions and reflects the energy conditions from which they were developed. Figure 7.22 summarises in graphical form the results of the extreme estimates. The equations that produce a numerical value for K are not included, because if properly calibrated they would produce the same estimates as the Inman and Bagnold formula. Some of the equations were found to grossly over-estimate the extremes. It can be seen that the model that provides the closest estimate is the LEXSED formula developed in the present study. These findings demonstrate that due caution must be taken when applying sediment transport models to low energy beaches. The calibration coefficients determined from this study of the respective equations (Table 7.8), should serve to produce first order approximations if applied to low energy coarse grained shorelines.

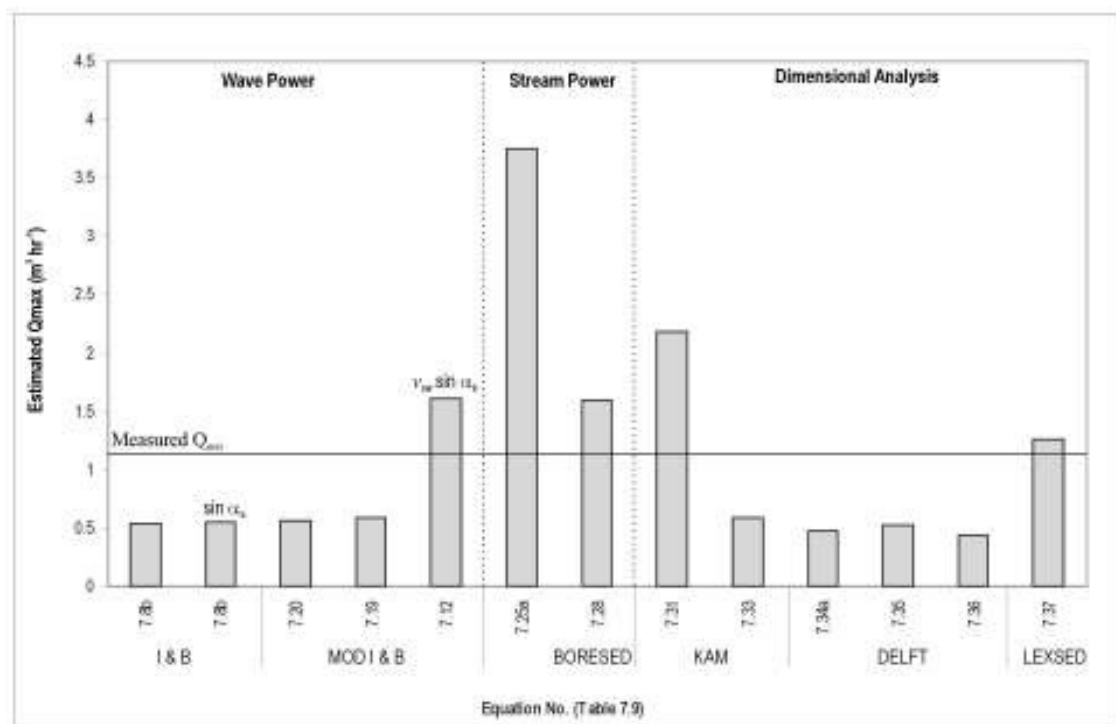


Figure 7.22 Summary of the extreme value estimates from the equations tested and developed in this study, excluding the K I&B expressions. It can be seen that most of the equations under-estimate the extreme values. The LEXSED formula provides the closest estimate.

Overall the LEXSED formula provides the best transport estimates and correlations with the measured data. The underlying physical principles on which it is based and the high quality empirical data that was used to validate it, indicate that it has potential wider application to other low energy coarse grained shorelines. Furthermore, it also has potential application to mixed sand and gravel beaches of the open coast, to which the beaches of the alpine glacial lakes bear many similarities. The modified Inman and Bagnold formulation presented in Equation 7.12 performs second best of all the equations and with calibration has good potential in being applied to the open coast mixed sand and gravel beaches. Further research is required in this area to validate the swash velocity equations presented in Chapter Five, that are required for Equation 7.12 and the LEXSED formula. Of the other models tested, Equation 7.33 produced by Kamphuis (1991) is the most accurate. A finding also made by other authors (Schoonees & Theron, 1996). It showed the third highest correlation with the measured data and of all the equations it has the lowest standard error. With calibration, the equation provides good mean estimates. The more generalised Kamphuis (1986) expression (Equation 7.31) also performed reasonably well and may be preferable in some situations, where less information is known about a beach and greater flexibility in an equation is desired. Finally, if only the barest information regarding wave heights can be obtained for a beach location, the Inman and Bagnold model will provide useful first order estimates of the transport rate when calibrated without the cosine term.

The combined effects of numerous interrelated variables, introduce complexities into the process of longshore sediment transport. This study has highlighted the importance of conducting empirical studies on natural beaches in order to understand the complex interactions between the processes responsible for causing sediment transport. The next and final chapter summarises the major findings of the study and offers some suggestions for further research.

CHAPTER 8.

CONCLUSION

8.1 Thesis Aims Revisited

This study has been a response to the lack of detailed knowledge concerning the processes of longshore sediment transport in mixed sand and gravel beaches. Due to the difficulty of conducting research on high energy open coast mixed sand and gravel beaches, the study took place in a lacustrine environment and thereby provided insights into the processes of a lakeshore beach. Therefore, it remains first and foremost a study of the processes in a low energy shoreline. Pickrill (1976) expressed the opinion that lakeshores are ideal places in which to study coastal processes because of their many similarities to open coast beaches. Pickrill went on to say that lake beaches have the same hydrodynamic characteristics of oceanic shorelines and studies conducted on them avoid the scaling problems inherent in laboratory studies. There is merit in this observation and it is an idea that influenced the locating of the field site on a lakeshore mixed sand and gravel beach.

The mixed sand and gravel beaches examined in the present study have much in common, in terms of both their processes and geomorphology, with those found on the open coast. The morphological similarities were explored in the introductory chapter. Structurally, they both exhibit a steep foreshore, a narrow swash zone and a gently sloping nearshore. Deep water in the nearshore area of the lacustrine and oceanic mixed sand and gravel beaches allows waves to progress close to shore with limited shoaling and refraction. From observations of open coast mixed sand and gravel beaches it has been noted that longshore currents become only weakly developed and that gravel is not transported longshore in this zone. The findings in Lake Coleridge confirm this observation. Longshore currents were insufficient to initiate the longshore sediment transport of all but silt sized material. At Lake Coleridge, waves commonly broke as a single line of breakers and translated directly into swash where transport was initiated in the swash zone. The longshore transport of material occurred primarily forward of the breaking wave in the swash zone. Kirk (1980) noted that this process is a defining characteristic of the mixed sand and gravel beaches of the open coast. Kirk (1970) also found that wave height is the dominant variable controlling many of the processes that occur in a mixed sand and gravel beach forward of the breaking wave, such as run-up and sediment transport. Of all the features in

common between the lacustrine and oceanic mixed sand and gravel beaches, it is the similarities of the swash zone that are of greatest importance. It is the swash zone that absorbs most of the wave energy and where all of the beach building sediments are transported in bedload. The relationships between wave height, run-up elevation, swash velocity and sediment transport will apply to the open coast swash zone. It is logical and reasonable to expect that many of the findings concerning the transport of sediment in the swash zone will be applicable to the oceanic mixed sand and gravel beaches. Whilst it is true that there are many similarities between oceanic and lacustrine beaches, it remains to be tested whether the models developed in this study will face scaling effects when applied to oceanic beaches. Scaling effects were found to occur when applying models developed from oceanic beaches to Lake Coleridge and it would be surprising if this did not occur in reverse. Nevertheless, the broad underlying principles established in this study regarding swash and sediment transport processes will apply to oceanic mixed sand and gravel beaches.

Although Lake Coleridge may be considered low energy when compared to oceanic beaches, it can by no means be considered low energy when compared to other lakes. It is exposed to strong northwest and southerly winds that become topographically channelled along the Lake, generating comparatively large waves for its size. Many studies of oceanic beaches are limited to making measurements during low to moderate energy conditions. The models that are derived from these studies suffer from the fact that they are only valid for a limited range of conditions. In effect, they suffer from energy level scaling. By studying shoreline processes in a lake, it was possible to make measurements that covered the full range of wave energy conditions. This avoided the problem of energy scaling and produced a series of equations that promise to be widely applicable within lake environments.

In one respect this thesis has been an exploration. It is the first attempt that has been made to quantify the process of longshore sediment transport in the swash zone of a mixed sand and gravel lake beach in New Zealand, effectively fulfilling the primary aim of the thesis which was to:

1. *Investigate the processes of longshore sediment transport in a mixed sand and gravel lakeshore beach.*

By concurrently measuring longshore sediment transport by the use of sediment traps and wave and current conditions, correlations were able to be made between variables such as wave height and period and the sediment transport rate. In this way the most important factors

influencing sediment transport on a mixed sand and gravel beach were identified. The wave height and swash velocity were found to be of particular significance. The research identified where in the beach longshore sediment transport takes place and where it does not occur. This has been an important finding because it clearly highlights differences in the process regime between mixed sand and gravel and sandy beaches. The conditions under which longshore transport occurs and the threshold conditions for lake environments were also determined, providing valuable information for lakeshore management. Further research will be required to assess the degree to which the findings apply to the open coast mixed sand and gravel beaches, but due to the similarities of the two beach environments, the results show promise in being applied to the open coast situation.

Studying the hydrodynamic processes in the swash zone of oceanic gravel beaches has proved difficult and consequently knowledge concerning this part of the beach has been limited. Previous studies of mixed sand and gravel beaches have indicated that longshore sediment transport occurs predominantly in the swash zone of these beach types. Kirk (1980) referred to the foreshore as the 'engine room' of a mixed sand and gravel beach. This study has demonstrated that swash is the 'engine', initiating sediment transport and driving foreshore response. Thus, the swash zone was the spatial focus of the research, fulfilling the secondary aim which was to:

2. *Examine the swash zone processes of a mixed sand and gravel beach relevant to sediment transport.*

The nature of the swash zone and its relationship with the energy inputs was examined in depth leading to the development of a process-response model of the swash zone of a lakeshore beach. Relationships were found between wave conditions, foreshore slope and run-up elevations and swash width. These were formalised in a series of equations that can be used to make estimates of run-up and swash width for a range of conditions. The run-up and swash width determine the area through which sediment is entrained and transported through a mixed sand and gravel beach. The rate at which this occurs is dependent on the swash velocity. The environmental variables controlling swash velocity and direction were examined and formalised by a series of equations that can be used to estimate the mean and maximum swash velocity.

Wave energy was found to be the dominant controlling force in a mixed sand and gravel lakeshore. It is expected that this will be the case for the open coast mixed sand and gravel

beaches. Lake waves have received little attention in the literature and for a research project of this nature it was critical to have a clear understanding of the nature of wave breaking and energy dissipation at the shoreline. Important findings were made about lake waves in the research, fulfilling the third aim of this thesis which was to:

3. Describe the nature of lake waves and the characteristics of wave breaking and energy dissipation that leads to the initiation of longshore sediment transport.

An array of electronic wave and current instruments, coupled with simultaneous measurements of the wind conditions allowed an examination of the conditions that lead to the formation, growth and decay of lake waves. The study highlighted the type of waves that are able to form in a small lake environment, where they break and the degree of refraction and modification that occurs as they shoal across the nearshore. The study was able to demonstrate the limited nearshore current development that occurs and together provide explanations for where the sediment is transported in the beach and why it is limited to the area forward of the breaking wave.

Wave, current and sediment transport measurements were made concurrently in the shoreline. Through analysing this data, a sediment transport model (LEXSED) was developed that can accurately estimate rates of longshore sediment transport in a low energy mixed sand and gravel beach, fulfilling the fourth aim which was to:

4. Develop a first order model that can reasonably estimate longshore sediment transport rates.

The formula incorporates the most important environment variables controlling longshore sediment transport. This is the first equation that has been developed specifically for the mixed sand and gravel beaches found in New Zealand. It applies specifically to lakeshore beaches, but it embodies principles that apply equally to the oceanic mixed sand and gravel beaches. The equation was tested by producing an annual sediment budget for the field site beaches, that was compared to measured rates. In doing so, a model was produced illustrating the historic geomorphic development of the barrier foreland on which the fieldsite was located.

In the development of the LEXSED formula, established longshore sediment transport models were examined for their suitability and effectiveness for application to mixed sand and gravel beaches, fulfilling the fifth aim which was to:

- 5. Assess the effectiveness of commonly used longshore sediment transport models for use in mixed sand and gravel beaches.*

An extensive search of the literature was undertaken to identify equations that incorporate principles of sediment transport that have some applicability to coarse grained beaches. Using the data collected from the field measurements, hourly sediment transport rates were calculated and compared with measured rates. The effectiveness of each equation was discussed and one relatively simple, but widely used model was found to outperform all the other equations tested. This has been the largest and most comprehensive testing of longshore sediment transport equations for use in New Zealand's mixed sand and gravel beaches.

8.2 Summary of Major Findings

A summary of the major findings from this study, as they pertain to the five main aims of the thesis, are outlined below.

Lake Waves

The wave measurements made in Lake Coleridge resulted in the collection of a large, high quality data set. Important new insights were made into lake wave processes in New Zealand's alpine lakes. Although the wave heights measured in Lake Coleridge were moderate in size, they are of the same order of magnitude to those found in other New Zealand lakes.

1. The root mean square wave heights averaged 0.20 m and ranged up to 0.51 m. Maximum wave heights averaged 0.35 m and ranged up to 0.84 m. All the wave height data sets were positively skewed, indicating the presence of tail of extreme high waves in the distribution.
2. By comparing the ratios between the different wave height statistics, the maximum wave heights that might reasonably be expected to occur in lakes, is approximately twice the significant wave height.
3. Wave height was found to be strongly linked to the wind and responded rapidly to increasing wind strength in an exponential fashion.

4. Wave period responded more slowly and requires time and distance for the wave length to develop. Overall the data showed that there was a narrow band of wave periods with means ranging from 1.43 to 2.33 s. All wave period distributions were negatively skewed, indicating the presence of many short period waves in the spectrum.
5. The wave spectrum was found to be more mixed and complicated than had previously been assumed for lake environments. Some authors have argued that because the range of wave periods experienced in lakes is narrow, the wave spectrum should attain characteristics seen in ocean swell waves. However, the spectral band width parameters, a value between 0 and 1, were found to be quite large, with 95% of the values between 0.75 and 0.90. The wave regime attained the characteristics of a storm wave spectrum.
6. Mean wave lengths were 3.26 m, but ranged from 0.77 to 6.63 m. Using Linear wave theory, this suggests that the depth of water in which waves can affect the bottom is as shallow as 0.20 m and at most 1.65 m.
7. The waves were characteristically steep and are capable of obtaining far greater steepness than oceanic wind-waves. Values ranged from 0.010 to 0.074, with an average of 0.051.
8. The deep water wave velocities were calculated with Linear wave theory and ranged over the field programme from 1.10 to 3.22 m s⁻¹, with a mean of 2.23 m s⁻¹. The shallow water velocities ranged from 0.62 to 1.80 m s⁻¹, with a mean of 1.25 m s⁻¹. When calculated as a ratio, this is a reduction in wave speed of just under one half the deep water value ($C_s / C_o = 0.56$).
9. The orbital velocities measured in deep water were 0.03 to 1.37 m s⁻¹ with a mean of 0.30 m s⁻¹. On average, this is 10 times less than the calculated wave phase velocity.
10. The orbital velocities measured in the nearshore zone ranged from 0.01 to 0.64 m s⁻¹ with a mean of 0.15 m s⁻¹. This is also 10 times less on average than the estimated phase velocities at the surface. This indicates that the wave attenuation effects are severe in a small lake environment.
11. The ratio difference between the measured deep water orbital velocities and the nearshore orbital velocities is just under one half ($u_s / u_o = 0.58$), almost identical to the predicted phase velocity difference.
12. Linear wave theory was found to provide good approximations of the wave conditions in a small lake environment.
13. Waves progressed very close to shore before breaking, typically in water less than 0.5 m deep.
14. The two main breaker types measured in Lake Coleridge were spilling and plunging.
15. Due to the steep nature of the lake waves, the deep water equations indicated a roughly equal number of spilling and plunging waves. However, the rapid increases in beach slope often

caused the waves to plunge immediately landward of the swash zone, leading to a greater proportion of plunging waves at the shoreline.

16. Deep water wave angles are were very oblique to the shoreline, averaging 50° , and were recorded between 0 to 90° .

17. Wave refraction from deep to shallow water only causes the wave angles to be altered in the order of 10%. Thus, breaker wave angles are similar to the deep water values.

Swash Zone Processes

The swash zone is an extremely important element of a mixed sand and gravel beach because it is an area that dissipates a large portion of the wave energy. As the swash zone absorbs this wave energy, sediment is entrained and processes of erosion and accretion determine whether the beach will retreat landward or prograde outward. In this study new equations were developed to estimate the swash zone width, run-up height, mean and maximum swash velocity. New findings were made concerning foreshore response to wave activity and a new model was developed that formalises the morphodynamic process.

1. There are times in a lakeshore or a sheltered beach environment when the energy conditions are very low or zero. This is not a condition that is frequently experienced in an open coast beach. In low or zero wave energy conditions, the swash zone is undeveloped and the foreshore sediments often sit near the angle of repose. At the onset of wave activity, the foreshore quickly responds to the energy input and the swash zone begins to develop a new equilibrium. A process-response model was developed (Figure 5.34) based on field observations and measurements, that formalises the morphodynamic responses of the swash zone to wave activity.

2. The beach slope provides a good indication of the equilibrium conditions in the swash zone. Extreme steep ($> 10^{\circ}$) and low slopes ($< 5^{\circ}$) are associated with equilibrium conditions, whilst intermediate slopes are an indication of transitional conditions ($6-9^{\circ}$). Steep slopes were associated with low energy wave conditions and low slopes were associated with high energy wave conditions.

3. The swash zone is largely determined by the wave height and ranged in width from 0.05 m to 6.0 m. The swash zone widened landward in response to increased wave height and lakeward in response the wave length, due to waves breaking in deeper water. The slope of the swash zone was found to be an important secondary control on the width.

4. At high slope angles the wave conditions are usually light. As the wave energy increases, the swash zone begins to be scoured by swash activity and the beach slope grades down. Thus, in a

lake there is a negative relationship between beach slope and swash width. An equation was developed, using the wave height and beach slope that provides close estimates of the swash zone width under a wide range of conditions. The value of k was determined to be 1.17:

$$X_{sw} = k \frac{H_{rms}}{\tan \beta} \quad (m) \text{ (Eqtn. 5.1b)}$$

5. The $R_{2\%}$ run-up heights were calculated with the swash zone width and slope angle by rearranging the trigonometric ratio $\sin \theta = \frac{y}{r}$:

$$R_{2\%} = X_{sw} (\sin \beta) \quad (m) \text{ (Eqtn. 5.2)}$$

Run-up elevations ranged from 0.01 m to 0.73 m and were strongly related to the wave height and the beach slope. On average, run-up exceeds the deep water H_{rms} wave height by a factor of around 16%, and can be approximated by:

$$R_{2\%} = 1.16 H_{rms} \quad (m) \text{ (Eqtn. 5.3)}$$

6. In general a negative relationship existed between the beach slope and the run-up, *i.e.* as the run-up increased, the beach slopes became lower. The highest run-up elevations were found to occur at intermediate slope angles of between 6° - 8° . Above 8° , the run-up declined in response to beach porosity and lower wave energy conditions.

7. A number of run-up equations were tested against the Lake Coleridge data set and found to perform moderately. A common problem was over-estimation when slope angles were over 8° . An underlying assumptions in the models is that the run-up increases with increasing beach slope.

8. A generalised run-up equation for lake environments was developed, that takes into account the negative relationship between beach slope and run-up, by rearranging a widely used equation. C is an empirical coefficient calculated to be 0.014:

$$R_{2\%} = CT \frac{(gH_{rms})^{0.5}}{\tan \beta} \quad (m) \text{ (Eqtn. 5.11)}$$

9. Swash velocities were high for a small lake environment. The swash velocities in Lake Coleridge were comparable to beaches of the open coast in low energy conditions. Mean velocities in the swash zone ranged from 0.01 to 1.07 m s⁻¹, with an overall mean value of 0.29 m s⁻¹.

10. The maximum hourly velocities were much greater, averaging 0.98 m s⁻¹, with a maximum recorded value of 2.48 m s⁻¹.

11. A direct negative correlation exists between declining swash velocities and increasing foreshore slope. Maximum velocities occurred at beach slopes of 5° .

12. At low gradients of 3 - 5° , the swash flow was dominant over the backwash flow.

13. At slopes between 6° and 10° , swash velocities were found to be hindered by turbulence, but the relative differences between the swash and backswash flows were negligible.

14. At slope angles above 10° there is a slight asymmetry to the swash/backswash flow velocities due to beach porosity. The run-up is absorbed into the beach and the backswash flow is reduced.

15. There is a strong link between increasing wave height and swash velocity. Reasonable estimates of the maximum swash velocity were able to be made by modifying the general phase velocity expression derived from Linear wave theory. The water depth term (h) is substituted for the breaker height (H_b). The expression provides good estimates of the average maximum velocity that ranged from 0.52 to 2.93 m s^{-1} , but was unable to estimate the extreme value statistics:

$$v_{sw} = \sqrt{gH_b} \quad (\text{m s}^{-1}) \text{ (Eqtn. 5.16)}$$

16. After wave breaking, these velocities quickly reduced through dissipation by approximately one half. The mean velocities were found to be in the order 70% less than the maximums. It was found that other environmental variables play a role in controlling swash velocities of a mixed sand and gravel beach. An equation was developed for estimating the mean velocity (\bar{v}_{sw}) in the swash zone that takes into account the effects of wave steepness. The H_{rms} wave height is a de facto measure of the water depth at the base of the swash zone and provides better correlations with the data than the estimated breaker depth. The calibration coefficient k is 0.78 and has units of $\text{m}^{1/2} \text{ s}^{-1/2}$ in order to make the equation dimensionally correct:

$$\bar{v}_{sw} = k \sqrt{\frac{H_{rms}}{T_z}} \quad \text{m s}^{-1} \text{ (Eqtn. 5.18)}$$

17. A variation of Equation 5.18 was developed that also takes into account the effects of foreshore slope, in particular, the limiting effects of increased porosity at higher elevations. Two forms of the equation were developed, one being the general expression, that provides the maximum velocities (v_{sw}) and the second being the mean expression (\bar{v}_{sw}) that requires an empirical coefficient (k), determined to be 0.27 . Although the expressions are not dimensionally correct, this can be corrected by multiplying them through by $1 \text{ m}^{1/2} \text{ s}^{-1/2}$. The equations perform well across a wide range of conditions and estimate the extreme high and low values well. The mean expression is able to estimate the extreme velocity values that Equation 5.18 cannot:

$$v_{sw} = \sqrt{\frac{H_{rms}/T_z}{\tan \beta}} \quad (\text{Eqtn. 5.19a})$$

$$\bar{v}_{sw} = k \sqrt{\frac{H_{rms}/T_z}{\tan \beta}} \quad (\text{m s}^{-1}) \text{ (Eqtn. 5.19b)}$$

Longshore Sediment Transport

This was the first major longshore sediment transport study of its kind undertaken on a mixed sand and gravel beach and on a lakeshore in New Zealand. Over 500 samples were collected in transit by the sediment traps during the field programme. The weight of material collected in the trap ranged from as little as 100g though to 5.5 kg. New methods analytical methods were developed to calculate sediment transport volumes and the total integrated transport rate for the swash zone. Sediment transport was found to result from the complex interaction between a number of different variables. The combined effects of numerous interrelated variables, introduce complexities into the process of longshore sediment transport. A new sediment transport equation was presented that takes into account the most important environment parameters controlling sediment transport in a mixed sand and gravel beach. The results from the expression showed excellent correlations to the measured data and it has the potential to be applied to other mixed sand and gravel beaches. This study highlighted the importance of conducting empirical studies on natural beaches in order to understand the complex interactions between the processes responsible for causing sediment transport.

1. Longshore sediment transport rates in the nearshore zone were found to be nil or close to nil in all conditions. The current velocities were too low to entrain sediments at the bed, that was characteristically coarse in nature.
2. Longshore sediment transport was found to occur exclusively in the swash zone, forward of the breaking wave. Sediment was entrained at the base of the swash zone under the breaking wave and transported up and along the shore in the swash flow. 99.9% of the material moved in bedload.
3. The sediments collected in transit were a heterogeneous mix of coarse sands and fine-large gravels. The mean grain size for all the sediment collected in the trap was granule material, 3.54 mm in diameter. Small quantities of fine sand and medium sand appeared regularly in the trapped material in small quantities. However, the sand was more commonly coarse, in the range of 0.5-2.0 mm. There was a significant mode between 4.0-8.0 mm in the pebble size range, whilst the largest material collected in motion was 32.00 mm.
4. Many of the samples were poorly to moderately sorted, but a significant number were found to be moderately well sorted. This contrasted with the generally poor sorting of the sediments in the foreshore. In the process of being transported, the sediments became better sorted. This sorting frequently produced samples that were coarse skewed with a lag of larger material.
5. Hourly trapped rates ranged from 0.02 to 214.88 kg hr⁻¹ with an overall average of 26.68 kg hr⁻¹ ±10%.

6. A numerical method was developed to convert the mass transport rate into a volumetric rate. The method accurately calculates the volume of a sediment sample of known weight with the porosity and density of the sediment.

$$V_s = \frac{(M_s / P) \times 100}{\rho_s} \quad (\text{m}^3) \text{ (Eqtn. 6.2)}$$

7. Hourly transport rates through the trap ranged from 1.14×10^{-5} to $1.23 \times 10^{-1} \text{ m}^3$, a full 5 orders of magnitude. The average rate was $1.52 \times 10^{-2} \text{ m}^3 \text{ hr}^{-1} \pm 10\%$ and most of the rates were within this order of magnitude.

8. From laboratory measurements, the mean density of the Lake Coleridge greywacke was calculated to be 2850 kg m^{-3} and the mean porosity was found to be 0.615:

9. Through field measurements, the longshore transport flux across the swash zone was found to vary with distance from the breaker. The transport rate was found to increase rapidly immediately forward of the breaker from zero to the maximum at around a distance 20% the width of the swash zone. The transport rate remains high across the middle of the swash zone. Much swash activity occurs in this area where both swash and backswash carry high sediment loads. After the 50% width, the rate begins to decline until around the 70% width, where the rate plateaus and remains steady until the very limit of the swash zone, where it reduces to zero.

10. Using numerical integration, the area under this curve was calculated and an equation written to estimate the transport rates above and below the trap in the swash zone. The total integrated average hourly transport through the swash zone can be calculated by:

$$X_{sw} > T_w \quad Q_l = \left[\frac{(X_{sw} \cdot Ax)}{T_w} \cdot Q_m \right] + \left[\frac{X_{sw} - (X_{sw} \cdot Ax + T_w)}{T_w} \cdot Q_m \right] + Q_m \quad (\text{m}^3 \text{ hr}^{-1}) \text{ (Eqtn. 6.4a)}$$

The total transport rates ranged from a minimum of $1.10 \times 10^{-5} \text{ m}^3 \text{ hr}^{-1}$ to a maximum of $1.15 \text{ m}^3 \text{ hr}^{-1}$. The mean rate was $7.36 \times 10^{-2} \text{ m}^3 \text{ hr}^{-1}$.

11. A simplified approximation to Equation 6.4a was developed that produces an almost identical value ($r = 0.9988$):

$$Q_l = 0.5 \left[Q_m \left(\frac{X_{sw}}{T_w} - 1 \right) \right] + Q_m \quad (\text{m}^3 \text{ hr}^{-1}) \text{ (Eqtn. 6.5)}$$

It requires that the sediment trap be located in the area of maximum sediment transport. This is a distance approximately 30-50% the width of the swash zone landward from the beach toe or breaking wave.

12. Sediment transport was found to be most strongly controlled by the wave height, period and mean swash velocity, *i.e.* the energy inputs or forcing functions. A strong correlation was also found with the wave steepness.

13. The wave direction dictates if longshore sediment transport is to occur. When waves break at an oblique angle to the shore, transport is initiated. The rate generally increases with increasing angle up to around 30° . Above this the transport rates varied considerably in relation to the breaker angle.

14. Despite the wide range in grain sizes present in the foreshore, very poor relationships were displayed between the grain size and transport rates. There was a very general increase in the grain size when transport was initiated. But once in motion, all the grain sizes were found to be moved in the swash zone. The high flow velocities under the breaking wave and in the swash zone exceed the entrainment thresholds for all the sediment sizes present in the beach.

15. The highest transport rates were associated with the lowest beach slopes. This is because the swash zone is at its widest and the current velocities fastest, when the foreshore gradient is low.

16. By filtering out the effects of the swash zone width, the relative transport rates were examined. The highest transport rates were associated with the equilibrium slope angles at 5° and 10° . The lowest relative rates were associated with the transition slopes between 6° and 9° . This finding lends further support the process-response model presented in Figure 5.34.

17. An expression was developed that divides the cube of the wave height and the wave length, which together is a form of wave steepness, and multiplies this by the mean swash velocity and the wave approach angle. A calibration coefficient, k , was included to produce values of correct magnitude. It was determined through residual analysis to be equivalent to 0.02. The formula produces values in cubic metres per second and is a total integrated rate for the whole swash zone. It was termed the Low Energy Mixed Sediment transport or LEXSED formula:

$$Q_l = k \left(\frac{H_{rms}^3}{L_o} \right) \cdot \bar{v}_{sw} \cdot \sin \alpha_b \quad (\text{m}^3 \text{ s}^{-1}) \text{ (Eqtn. 6.7)}$$

18. The expression performs well across a wide range of energy and morphological conditions and the estimates showed very good correlations to the empirical data ($r = 0.85$, Std. Error = 0.47. $F = 1285$ Prob. < 0.0001).

19. The measured rates range from 0.000011 to $1.154 \text{ m}^3 \text{ hr}^{-1}$, with a mean of $0.074 \text{ m}^3 \text{ hr}^{-1}$. The estimated rates using LEXSED range from 0.000002 to $1.265 \text{ m}^3 \text{ hr}^{-1}$, with a mean of $0.073 \text{ m}^3 \text{ hr}^{-1}$.

20. Presently, the equation is applicable to low energy, coarse grained beaches in the range $H < 1.0 \text{ m}$, $D_{50} > 1.0 \text{ mm}$ However, because it embodies underlying principles common to all mixed sand and gravel beaches, it has potential in being adapted for use in oceanic applications.

21. Using hourly wind speed and direction data from the weather station and the LEXSED formula to estimate longshore sediment transport rates, an annual sediment transport budget was

calculated for the fieldsite beach. Gross annual transport rates on the western side of the barrier beach were calculated to be in the order $800 \text{ m}^3 \text{ yr}^{-1}$. The net rates are *ca.* $740 \text{ m}^3 \text{ yr}^{-1}$ from the north and *ca.* $60 \text{ m}^3 \text{ yr}^{-1}$ from the south, a reflection of the dominance of the northwest generated wind-waves.

22. The hourly average transport rate for 2002 was found to be $0.093 \text{ m}^3 \text{ hr}^{-1}$, which compares favourably to the average hourly rate of $0.074 \text{ m}^3 \text{ hr}^{-1}$ measured in the field.

23. Using the beach profile survey data to calculate the volume of material in the barrier foreland, an annual lineal growth rate was approximated and estimates were derived for the amount of time taken for the barrier foreland to develop. It was estimated that the western side of the barrier developed its full length in around 50 years, growing at 10 m per annum. The south-eastern side took longer to develop due to its orientation and sheltered aspect and took around 150 years to develop, growing at 1.5 m per annum.

24. A derivation of Bagnold's (1963; 1966) transport model was presented that uses the longshore component of the swash velocity in place of the longshore current velocity. The equation performed well when tested against the measured transport rates. The calibration coefficient $k = 0.0018$. It incorporates all the main elements that control longshore sediment transport in the swash zone of a mixed sand and gravel beach:

$$Q_l = k(H_{rms}^2 \cdot v_{sw} \cdot \sin \alpha_b) \quad (\text{m}^3 \text{ s}^{-1}) \text{ (Eqtn. 6.11)}$$

Longshore Sediment Transport Models

Sixteen longshore sediment transport equations were evaluated by testing the calculated estimates against the measured Lake Coleridge data set. Sediment transport models were identified that had either been modified or specifically developed for coarse grained beaches or was a generalised sediment transport equation that contained variables common to all beaches. The LEXSED model developed in this study was found to perform the strongest of all the models tested.

1. The Inman and Bagnold model was identified as containing broad principles suitable for mixed sand and gravel beach application. It was found to perform moderately well when tested against the Lake Coleridge data set. Pearson correlation coefficients were found to be $r = 0.75$ and $r^2 = 0.57$. K was determined to be 0.00091.

2. The predictive power of the model was further improved when the $\cos \alpha_b$ term was omitted from the equation. The correlations with the transport rate improved, $r = 0.79$ $r^2 = 0.62$ and the K value dropped to 0.00049.

3. A mixed sand and gravel beach variation of the formula was proposed that takes into account the shear stress in the swash zone by substituting the wave celerity with the mean swash velocity. The breaker height is substituted with the root mean square wave height:

$$I_l = K \left[\frac{1}{8} \rho g H_{rms}^2 \right] \cdot \bar{v}_{sw} \cdot \sin \alpha_b \quad (\text{N s}^{-1}) \text{ (Eqtn. 7.12)}$$

The K value increases by an order of magnitude to 0.017. When tested against the Lake Coleridge data, the correlation was found to improve to $r = 0.81$ and $r^2 = 0.65$. This model performed second best in the evaluation. The similarity of open coast mixed sand and gravel beaches to those in this study, suggests that when calibrated, this equation will be suitable for open coast applications.

4. Much research has been directed toward identifying the environmental factors responsible for variation in the K coefficient. Many authors have attempted to correlate K to the grain size and beach slope and/or Iribarren number. No such correlation was found in this study between K and the grain size, the beach slope, the wave steepness or the Iribarren number.

5. Incorporating the numerical solutions for K into the Inman and Bagnold model (Equations 7.13-7.17) resulted in the mean rates being over-estimated by 2-3 orders of magnitude. Moreover, most of the equations presented weaker correlations with the immersed transport rate than the original Inman and Bagnold formula. It is recommended that these equations not be applied to low energy coarse grained beaches.

6. It was found that K is more closely related to the wave energy dissipation effects exerted by the beach morphology on the breaking wave. Sandy beaches have been found to have K values between 0.50-1.00, with a average around 0.70. Gravel beaches have almost all been found to have K values of between 0.04 to 0.01. In Lake Coleridge they range between 0.00050-0.001. The change in magnitude of the K values between these environments, is a reflection of the decreasing volumes of sediment transport that occur in these systems. Whilst no difference in K can be identified within a beach system, variations appear between the main morphological beach types. In part, the beach morphology is controlled by the grain size. Thus, in effect it has a secondary role in the wave energy dissipation process.

7. One possible solution to the problem of defining K , is to identify a mean value for use within certain limits. For example, 0.70 for sandy beaches, 0.1 for gravel beaches and 0.001 for low energy shorelines.

8. There have been a number of proposed variations of the Inman and Bagnold formula over the years. The variants tested in this study incorporated a wave energy threshold term developed for gravel beach applications (Equations 7.19 & 7.20). No improvement in the predictive power of the model was found by these two variations.

9. The stream power models performed the most poorly of all the equations tested (Equations 7.24-7.28). All these models included a wave energy threshold term to account for the incipient motion of gravel in swash bore flow. This term was not found to be valid for the low energy beaches in this study.
10. The dimensional analysis equations provided the most satisfactory results of all the equations. All these models over-estimated the transport rates and required further calibration coefficients in the order of 10^{-2} . However, they displayed the best correlations to the measured rates.
11. The best performing model in the dimensional analysis group was Equation 7.33, proposed by Kamphuis (1991) with correlations coefficients of $r = 0.77$ and $r^2 = 0.59$.
12. In general all the wave power expressions required calibrating with a coefficient in the order of 10^{-3} . Whilst the stream power and dimensional analysis equations, including the LEXSED formula and the Inman and Bagnold model variation (Equation 7.12) proposed here, all required calibrating with a coefficient in the order of 10^{-2} . This suggests that the dimensional analysis and stream power equations are all accounting for a degree of wave energy dissipation not taken into account by the wave power equations.
13. Despite the different underlying theories of the equations, the range of variables incorporated into them and the methods used in their derivation, the equations were all correlatively similar. Correlation coefficients were in the range, $r = 0.67$ - 0.77 and $r^2 = 0.44$ - 0.59 . The common variable in these expressions is the wave height. Wave height was found to be dominant controlling environmental variable in a lakeshore beach. The equations also performed well because the quality of the input data was high.
14. The significant difference between the models occurs in the magnitude of the transport estimates. Most of the equations over-estimated the rates and required further calibrating. With the calibration coefficients incorporated into the equations, the mean values are reasonably estimated, but the extreme high rates are mostly under-estimated. This limits their predicative application to moderate wave energy conditions.
15. Due to scaling effects, care must be taken when applying sediment transport models developed from oceanic beaches to low energy locations. The calibration coefficients determined from this study (Table 7.8), should serve to produce first order approximations if applied to low energy coarse grained shorelines.
16. Overall the LEXSED formula provides the best transport estimates and correlations with the measured data. The underlying physical principles on which it is based and the high quality empirical data from which it was developed, indicate that it has potential wider application to other low energy coarse grained shorelines. Examples of these occur not only in the glacial lakes

of the South Island, but also in locations such as Fiordland, the Marlborough Sounds and Abel Tasman National Park. Management issues surrounding the use of fast ferries through some of these sheltered water ways provide an ideal place to apply the run-up, swash zone velocity and transport equations developed in this thesis. Furthermore, it also has potential application to mixed sand and gravel beaches of the open coast, to which the beaches of the alpine glacial lakes bear many similarities.

8.3 Suggestions for Future Research

A greater understanding of the processes operating in oceanic and lacustrine mixed sand and gravel and beaches is required for coastal management and scientific purposes. This study has provided new insights into lake wave characteristics, foreshore response and sediment transport processes in a mixed sand and gravel lakeshore beach. However, there is still much to be learnt about these beach types and lakeshore processes in general. Much research potential exists in these areas for both students and experienced campaigners. It is customary to provide a few thoughts and suggestions for further research and a some potential projects are outlined here.

1. Further testing of the equations developed in this thesis to estimate swash zone velocity, width, run-up elevation and longshore sediment transport rates will prove extremely useful in validating and improving the predicative accuracy of the equations. Initially this work will best be conducted in the other large South Island glacial lakes. However, there is a pressing need to address the lack of knowledge regarding the oceanic mixed sand and gravel beaches. The potential application of the findings from this study to the oceanic mixed sand and gravel beaches needs to be ascertained. The task holds a sense of urgency in light of the serious net long-term erosion problems and management issues facing many of these beaches, for example Washdyke barrier, South Canterbury.

2. This study highlighted the process of wave dissipation for controlling the amount of energy available for sediment transport. Further study is required to investigate the dissipation effects of wave breaking and the process that act to absorb wave energy in the swash zone. Currently no sediment transport model is able to properly account for this effect. An area of potential research is to examine the effect of porosity on swash flow.

3. A surprising result in this study was the inability to find any clear relationship between the grain size and transport rates. The critical grain thresholds were regularly exceeded in the swash zone and this study did not have enough small scale resolution to detect minor variations in the transport capacity of individual swash bores. A careful study is needed into the effects that grain size has in the initiation of sediment transport. In particular, critical threshold velocities need to be defined for beds of mixed grain sizes. Such a study could examine the sediment transport rates of different sized material under individual swash lenses, correlated to concurrent measurements of the swash velocity. These studies might also use tracers. The use of tracers is fraught with difficulty in oceanic mixed sand and gravel beaches, but offers more promise in low energy lakeshores. Tracer technology has advanced considerably in recent years. The development of cheap electronic radio transceivers that can be inserted into individual grains offers the possibility of tracking the rates and travel distances of different sized material. These measurements could be made concurrently with wave and swash measurements in order to more fully explore the relationships between grain size and sediment transport rates.

4. A study is needed to validate or otherwise reject the use of pressure sensors to measure lake waves. A series of careful measurements could be made concurrently with a pressure sensor and wave gauge in incremental water depths to clearly and accurately assess the effects of wave attenuation on the pressure sensor. The study would be best conducted to cover a range of wave energy conditions. In the process, the study would shed new light on the attenuation of energy beneath lake waves and provide information about wave modification in response to increasingly shallow water. In this study the breaker heights were derived from an equation that was based on empirical field data from ocean beaches. There was uncertainty about the accuracy of the estimates from this equation. By measuring the changes in wave height and celerity across the nearshore, a precise examination could be made of the wave shoaling experienced by high frequency lake waves. Such a study could also examine use of linear wave theory to estimate breaker heights and phase velocities in the nearshore. studies conducted examining cross-shore variations in bore velocities and heights through the shoaling and breaking process.

5. More information is required regarding small-amplitude, high frequency lake waves and wind-wave hindcasting. A study is required to examine the relationship between wind and wave generation in alpine lakes, with the aim of validating or modifying a hindcasting model such as NARFET. The South Island glacial lakes are commonly orientated northwest-southeast and have strongly bi-directional wind regimes. It would be a good idea to locate a wave staff and weather

station at both ends of the lake, to measure the generation and growth of wave activity over distance. In particular, to look at the growth of wave period in relation to wave height.

6. A simple descriptive examination of the waves that are generated in the major lakes of the South Island would prove immediately useful for a variety of management issues. In particular with regards to the regulatory requirements to avoid, remedy or mitigate any adverse effects arising from the use of many of these lakes for hydro-electric power generation. Such a study would provide a wealth of data for other applications. For example, an examination of the differences between various wave height statistics (*e.g.* H_s , H_{rms} , H_{max}) with waves of different periods. The root mean square wave height is commonly derived from the significant wave height. It was found in this study that the conversion did not apply to lacustrine waves. A large lake wave data set could help clarify the use of conversion ratios for estimating wave height statistics from the significant wave height.

APPENDIX 1 SUMMARY WIND DATA

Hourly totals of wind speed and direction , by month, of all wind data measured at Lake Coleridge. Wind in m s⁻¹.

Date	N	NE	E	SE	S	SW	W	NW	< 1.0	1-5	5-8	8-11	11-17	> 17
May '77	43	3	7	61	31	5	9	197	0	213	73	63	7	0
Jun '77	139	1	6	76	36	9	10	386	2	443	140	75	3	0
Jul '77	160	7	7	38	198	25	17	292	0	638	88	17	1	0
Aug '77	83	9	6	84	135	7	29	390	1	527	130	71	14	0
Sep '77	63	5	18	96	155	2	26	160	0	328	130	60	7	0
Oct '77	6	0	0	11	10	3	4	290	0	118	73	87	46	0
Nov '77	6	0	1	28	52	4	6	337	0	123	122	125	64	0
Dec '77	3	2	9	122	58	2	38	485	1	261	204	188	65	0
Jan '78	2	4	3	116	109	3	20	309	0	256	128	135	47	0
Feb '78	11	1	3	123	80	1	9	233	0	171	131	128	31	0
Jan-95	58	4	44	57	223	62	106	190	24	170	112	182	240	16
Feb-95	47	11	85	56	226	26	68	153	46	267	127	177	55	0
Mar-95	26	8	135	135	193	44	70	133	43	366	140	129	62	4
Apr-95	35	17	120	60	114	60	111	203	31	272	88	130	194	5
May-95	14	3	75	22	41	18	25	54	12	144	26	37	33	0
Jul-95	15	25	263	89	129	49	77	97	64	439	58	82	100	1
Aug-95	14	9	207	91	142	78	93	110	58	426	85	115	53	7
Sep-95	13	6	121	124	204	53	87	112	35	335	113	101	123	13
Oct-95	41	8	61	45	143	104	157	185	21	181	96	136	286	24
Nov-95	22	8	75	76	262	55	104	118	30	311	129	134	112	4
Dec-95	23	7	57	89	217	58	90	203	50	274	135	153	122	10
Jan-96	18	1	93	60	88	117	125	173	40	198	70	135	220	12
Nov-01	0	15	134	185	25	23	42	260	42	214	203	156	68	1
Dec-01	0	10	140	151	23	25	59	336	36	239	222	203	44	0
Jan-02	1	23	228	168	35	26	35	228	50	275	220	166	33	0
Feb-02	1	21	216	153	17	21	47	196	40	244	154	178	56	0
Mar-02	1	18	123	100	35	24	59	384	46	222	121	224	130	1
Apr-02	2	32	200	128	49	57	56	196	79	414	135	67	25	0
May-02	1	21	103	60	43	43	90	383	62	301	137	171	73	0
Jun-02	6	19	83	36	25	31	57	463	26	311	167	136	80	0
Jul-02	2	43	194	72	59	42	75	257	77	437	116	85	27	2
Aug-02	2	31	154	78	47	47	83	302	63	357	172	99	53	0
Sep-02	0	13	49	25	21	35	103	474	16	198	114	227	155	10
Oct-02	0	16	96	80	23	23	56	450	27	199	197	243	78	0
Nov-02	2	9	189	131	28	21	46	294	24	259	165	163	105	4
Dec-02	0	9	110	182	22	14	43	364	60	214	159	173	136	2
Jan-03	2	14	172	192	26	21	34	283	33	292	186	147	79	7
Feb-03	1	23	123	151	32	24	34	284	34	284	121	155	78	0
Mar-03	4	32	206	194	49	31	43	185	116	364	146	100	18	0
Apr-03	2	33	220	120	35	38	39	233	56	360	170	105	29	0
May-03	2	28	139	80	39	44	69	343	69	337	121	128	89	0
Jun-03	0	13	90	40	23	33	76	445	37	243	154	190	94	2
Jul-03	5	35	128	88	45	29	60	354	46	397	155	125	18	3
77-'78	516	32	60	755	864	61	168	3079	4	3078	1219	949	285	0
95-'96	326	107	1336	904	1982	724	1113	1731	454	3383	1179	1511	1600	96
2001	0	25	274	336	48	48	101	596	78	453	425	359	112	1
2002	18	255	1745	1213	404	384	750	3991	570	3431	1857	1932	951	19
2003	16	178	1078	865	249	220	355	2127	391	2277	1053	950	405	12
Total	876	597	4493	4073	3547	1437	2487	11524	1497	12622	5733	5701	3353	128

APPENDIX 2 RAW DATA PRINTOUTS

Appendix 2a

A three second sample of the raw data from the wave gauge in spreadsheet format.

J Day	Hr/Min	Time	Raw Values
348	1200	0.0	-654.5
348	1200	0.1	-710
348	1200	0.2	-745
348	1200	0.3	-752
348	1200	0.4	-735
348	1200	0.5	-712
348	1200	0.6	-708
348	1200	0.7	-718
348	1200	0.8	-728
348	1200	0.9	-729
348	1200	1.0	-740
348	1200	1.1	-742
348	1200	1.2	-744
348	1200	1.3	-743
348	1200	1.4	-748
348	1200	1.5	-742
348	1200	1.6	-709
348	1200	1.7	-661.8
348	1200	1.8	-602.2
348	1200	1.9	-578.4
348	1200	2.0	-577.6
348	1200	2.1	-604
348	1200	2.2	-673
348	1200	2.3	-719
348	1200	2.4	-737
348	1200	2.5	-742
348	1200	2.6	-761
348	1200	2.7	-774
348	1200	2.8	-782
348	1200	2.9	-793

Appendix 2b

A 10 s sample of the raw data produced by the current meters in spreadsheet format. The sensor values output a signal on two axes (x & y). A and B refer to the two meters.

J Day	Hr/Min	Time	raw Ax	raw Ay	raw Bx	raw By
340	1000	0.0	-0.061	0.129	-0.057	-0.266
340	1000	0.5	-0.098	-0.013	-0.09	-0.267
340	1000	1.0	-0.077	0.018	-0.118	-0.278
340	1000	1.5	-0.111	0.087	-0.067	-0.273
340	1000	2.0	-0.134	0.053	-0.057	-0.271
340	1000	2.5	-0.115	0.075	-0.118	-0.271
340	1000	3.0	-0.157	0.043	-0.098	-0.267
340	1000	3.5	-0.123	0.105	-0.077	-0.251
340	1000	4.0	-0.121	0.019	-0.07	-0.156
340	1000	4.5	-0.128	-0.038	-0.105	-0.278
340	1000	5.0	-0.103	-0.011	-0.075	-0.283
340	1000	5.5	-0.094	0.07	-0.037	-0.254
340	1000	6.0	-0.08	0.028	-0.079	-0.28
340	1000	6.5	-0.091	0.063	-0.088	-0.265
340	1000	7.0	-0.087	0.005	-0.044	-0.275
340	1000	7.5	-0.098	-0.001	-0.062	-0.275
340	1000	8.0	-0.084	0.089	-0.105	-0.258
340	1000	8.5	-0.116	0.142	-0.112	-0.157
340	1000	9.0	-0.14	-0.021	-0.094	-0.236
340	1000	9.5	-0.128	0.123	-0.105	-0.283
340	1000	10.0	-0.11	0.105	-0.099	-0.271

APPENDIX 3

PERCENTILE CALCULATION & SIZE GRADES

Appendix 3a

Equation to locate n^{th} percentile of sediment grain size distribution

(After: Author)

Choose the two cumulative weight % values from the raw sieve data that lie either side of the n^{th} percentile of interest, then apply the equation:

$$n_{\%}(mm) = x_1 - \left(\frac{x_1 - y_1}{y_2 - x_2} \right) \times (n - x_2)$$

Where: x_1 = upper mm grain size that corresponds to the upper weight cum%

x_2 = upper weight cumulative %

y_1 = lower mm grain size that corresponds to the lower weight cum%

y_2 = lower weight cumulative %

$n = n^{\text{th}}$ percentile of interest (10^{th} in this case)

Using the data from the sediment sample in the table below:

$$D_{10} = 2.83 - \frac{(2.83 - 2.38)}{(12.0 - 9.5)} \times (10 - 9.5)$$

$$D_{10} = 2.75$$

Raw sieve data from trapped sediment collected at site CO14b
(03-04-02) at 0900 hrs.

Size (mm)	Size (ø)	Wt Ret (g)	Wt (%)	Wt (cu%)	D ₁₀
11.31	-3.50	1.60	0.3	0.3	2.75
9.51	-3.25	2.70	0.5	0.9	
8.00	-3.00	1.80	0.4	1.2	
6.73	-2.75	6.70	1.3	2.6	
5.66	-2.50	4.00	0.8	3.4	
4.76	-2.25	3.80	0.8	4.1	
4.00	-2.00	3.70	0.7	4.9	
3.36	-1.75	8.60	1.7	6.6	
x₁ = 2.83	-1.50	14.90	3.0	x₂ = 9.5	
y₁ = 2.38	-1.25	12.30	2.5	y₂ = 12.0	
2.00	-1.00	18.20	3.6	15.6	
1.68	-0.75	21.30	4.3	19.9	
1.41	-0.50	33.40	6.7	26.5	
1.19	-0.25	47.10	9.4	35.9	
1.00	0.00	55.10	11.0	46.9	
0.841	0.25	82.20	16.4	63.4	
0.707	0.50	75.80	15.1	78.5	
0.595	0.75	45.80	9.1	87.6	
0.500	1.00	48.70	9.7	97.3	
0.420	1.25	11.00	2.2	99.5	
0.354	1.50	2.10	0.4	100.0	

Appendix 3b

Grain size and sorting nomenclature

Grain Size		Nominal Classifications	
(mm)	(phi Ø)		
64-128	-6 to -7	small cobble	GRAVEL
32-64	-5 to -6	large pebble	
16-32	-4 to -5	medium pebble	
8-16	-3 to -4	small pebble	
8-4	-2 to -3	very small pebble	
2-4	-1 to -2	granules	
1.0-2.0	0 to -1	very coarse sand	SAND
0.50-1.0	1 to 0	coarse sand	
0.25-0.50	2 to 1	medium sand	
0.125-0.25	3 to 2	fine sand	

Based on classifications from Wentworth (1922) and Dawe (1997).

Sorting (σ)		Nominal Classification
(mm)	(phi Ø)	
> 0.80	< 0.35	very well sorted
0.70-0.80	0.50-0.35	well sorted
0.60-0.69	0.71-0.50	moderately well sorted
0.50-0.59	1.0-0.71	moderately sorted
0.25-0.49	2.0-1.0	poorly sorted
0.05-0.24	4.0-2.0	very poorly sorted
< 0.05	> 4.0	extremely poorly sorted

Based on classifications of Folk and Ward (1957) and Folk (1965).

Skewness	Nominal Classification
> +1.00	extremely coarse skewed
+0.30 to +1.00	strongly coarse skewed
+0.10 to +0.30	coarse skewed
-0.10 to +0.10	near symmetrical
-0.30 to -0.10	fine skewed
-1.00 to -0.30	strongly fine skewed
< -1.00	extremely fine skewed

Based on classifications of Folk and Ward (1957) and Folk (1965).

APPENDIX 4

DENSITY AND POROSITY CALCULATIONS

Appendix 4a

Procedure for the determination of the solid density (specific gravity) of a sediment sample
(After: Lewis, D.W. & McConchie, D. (1994), Analytical Sedimentology)

1. Dry 50-100 g of the sample and weigh to 0.1 g
2. Place the weighed sample into a bottle half filled with water. Insert a glass stopper and shake until the dispersion is complete. Almost fill the bottle with water and allow the sample to settle for several minutes.
3. Completely fill the bottle and insert the stopper. Dry the outside of the bottle and weigh it to 0.1 g.
4. Empty and wash the bottle and fill with water; insert stopper; dry bottle and weigh to 0.1 g
5. The solid density is calculated as follows:

$$\rho_s = \frac{(\rho_w \times M_s)}{(M_b + H_2O) + (M_s) - (M_b + H_2O_{(s)})}$$

Where: ρ_s = solid density ($kg\ m^{-3}$)

ρ_w = density of water at temperature of test ($1000\ kg\ m^{-3}$)

M_b = mass of bottle (kg)

M_s = mass of dry sample (kg)

H_2O = water

$H_2O_{(s)}$ = mass of water & sample (kg)

Density Calculation for Lake Coleridge greywacke collected by trap from the fieldsite.

Sample No.	P_w	M_s	$P_w \cdot M_s$	$M_b + H_2O$	$M_b + H_2O_{(s)}$	$(M_b + H_2O) + M_s - (M_b + H_2O_{(s)})$	P_s
1	1.00	271.00	271.00	929.40	1105.60	94.80	2.86
2	1.00	272.50	272.50	954.90	1130.60	96.80	2.82
3	1.00	294.40	294.40	933.00	1123.20	104.20	2.83
4	1.00	303.30	303.30	952.80	1150.10	113.00	2.86
5	1.00	205.20	205.20	949.80	1084.40	70.60	2.91
6	1.00	218.50	218.50	949.10	1091.10	76.50	2.86
Mean Solid Density							2.85

Appendix 4b

Procedure for the determination of porosity and volume of a sediment sample

(After: Author)

Total porosity is the percentage pore space of a sediment sample that can be occupied by air or water. It is calculated as a ratio between the bulk weight and the solid density of a known volume of sediment using the following procedure:

1. Place dry sample into a beaker/cylinder of known volume and weight
2. Weigh to 0.1g (minus the weight of the beaker)
3. Porosity is calculated as follows:

$$P = \frac{(M_s - M_c)}{(V_c \times \rho_s)} \times \frac{100}{1}$$

Rearranging to calculate Vol. x from a known weight:

$$V_s = \frac{(M_s / P) \times 100}{\rho_s}$$

Where: V_s = volume of sediment sample
 P = total porosity (%)
 M_s = dry mass of sample (kg)
 M_c = mass of cylinder (kg)
 V_c = volume of the cylinder (m^3) (in which measurements are made)
 ρ_s = Solid density ($kg\ m^{-3}$) (as calculated with above equation)

Porosity calculation for sediment samples collected by trap from the fieldsite at Lake Coleridge

Sample No.	V_c	P_s	$V_c * P_s$	M_s	P (%)
1 & 2	500.00	2.85	1425.00	879.10	61.69
3 & 4	500.00	2.85	1425.00	876.50	61.51
5 & 6	500.00	2.85	1425.00	873.50	61.30
					61.50
					38.50
					0.61

Mean Porosity
Mean % Pore space
 a'

Samples 1 & 2: D_{50} 1.11mm (V.coarse sand), 0800 hrs, CO11b, 11-12-02

Samples 3 & 4: D_{50} 3.73mm (Granules), 0900 hrs, CO11b, 11-12-02

Samples 5 & 6: D_{50} 5.53mm (V. small pebbles), 1800 hrs, CO11b, 11-12-02

List of Symbols used in Appendices 5 and 6

Hr	hour
H_{\max}	maximum wave height
$H_{1/10}$	highest 1/10 wave height
H_s	significant wave height
H_{rms}	root mean square wave height
\overline{H}	mean wave height
T_p	peak spectral wave period
T_z	zero-crossing wave period
T_s	significant wave period
T_c	crest wave period
ε	spectral band width
X_{sw}	swash zone width
Slp	slope
Dir	direction
Sw	swash
Bsw	backswash
$\overline{v_{\text{sw}}}$	mean swash velocity
v_{\max}	maximum swash velocity
$R_{2\%}$	highest 2% run-up
D_{90}	90 th percentile grain size (coarse)
D_{50}	median grain size
D_{10}	10 th percentile grain size (fine)
LST	longshore sediment transport
ITR	immersed weight sediment transport rate
kg/0.3m/hr	mass transport rate through trap
m ³ /0.3m/hr	volumetric transport rate through rate

APPENDIX 5

WAVE SUMMARY STATISTICS

Date	Hr	Site	WG_H _{MAX}	WG_H _{1/10}	WG_H _s	WG_H _{RMS}	WG_H̄	WG_T _z	WG_T _c	WG_ε
14/12/01	1200	CO10	0.25	0.18	0.14	0.15	0.07	1.34	0.74	0.83
14/12/01	1300	CO10	0.37	0.21	0.16	0.19	0.08	1.44	0.75	0.86
14/12/01	1400	CO10	0.40	0.23	0.18	0.22	0.09	1.51	0.76	0.86
14/12/01	1500	CO10	0.39	0.27	0.20	0.24	0.10	1.53	0.77	0.86
14/12/01	1600	CO10	0.41	0.27	0.20	0.24	0.10	1.47	0.78	0.85
14/12/01	1700	CO10	0.48	0.29	0.22	0.26	0.11	1.54	0.80	0.85
14/12/01	1800	CO10	0.40	0.25	0.19	0.22	0.09	1.49	0.76	0.86
14/12/01	1900	CO10	0.38	0.22	0.17	0.20	0.08	1.41	0.77	0.84
15/12/01	1000	CO10	0.30	0.19	0.14	0.15	0.07	1.32	0.80	0.79
15/12/01	1100	CO10	0.28	0.19	0.15	0.15	0.08	1.29	0.80	0.78
15/12/01	1200	CO10	0.34	0.20	0.15	0.17	0.08	1.34	0.77	0.82
15/12/01	1300	CO10	0.40	0.21	0.16	0.18	0.08	1.35	0.76	0.82
15/12/01	1400	CO10	0.30	0.20	0.15	0.16	0.08	1.28	0.73	0.82
15/12/01	1500	CO10	0.29	0.20	0.15	0.16	0.08	1.33	0.76	0.82
15/12/01	1600	CO10	0.34	0.20	0.17	0.19	0.09	1.39	0.79	0.82
15/12/01	1700	CO10	0.33	0.20	0.15	0.18	0.08	1.35	0.75	0.83
16/12/01	800	CO10	0.09	0.06	0.04	0.05	0.03	0.89	0.55	0.79
16/12/01	900	CO10	0.14	0.10	0.08	0.08	0.05	1.06	0.73	0.73
16/12/01	1000	CO10	0.21	0.13	0.10	0.11	0.05	1.27	0.71	0.83
16/12/01	1100	CO10	0.22	0.14	0.11	0.12	0.06	1.24	0.72	0.81
16/12/01	1200	CO10	0.21	0.13	0.10	0.11	0.05	1.23	0.71	0.82
16/12/01	1300	CO10	0.18	0.12	0.09	0.09	0.05	1.14	0.71	0.79
16/12/01	1400	CO10	0.16	0.12	0.09	0.10	0.05	1.23	0.71	0.82
16/12/01	1500	CO10	0.14	0.10	0.08	0.08	0.04	1.19	0.73	0.79
16/12/01	1600	CO10	0.23	0.12	0.09	0.10	0.05	1.11	0.71	0.77
17/12/01	1200	CO10	0.16	0.10	0.07	0.09	0.04	1.06	0.67	0.78
17/12/01	1300	CO10	0.22	0.16	0.12	0.14	0.06	1.31	0.68	0.86
17/12/01	1400	CO10	0.23	0.17	0.13	0.15	0.07	1.31	0.71	0.84
17/12/01	1500	CO10	0.26	0.19	0.14	0.17	0.07	1.38	0.71	0.86
17/12/01	1600	CO10	0.40	0.24	0.18	0.23	0.08	1.61	0.74	0.89
17/12/01	1700	CO10	0.42	0.28	0.21	0.27	0.09	1.75	0.73	0.91

Please note: This is an abridged digital version.

For more data please contact author: imdawe@paradise.net.nz

APPENDIX 6

SWASH ZONE SUMMARY STATISTICS

Date	Hr	Site	X_{sw} (m)	Sw Slp°	\bar{V}_{sw} m s ⁻¹	V_{max} m s ⁻¹	Sw_v m s ⁻¹	Bsw_v m s ⁻¹	R _{2%} (m)	Wave Dir°	LST Vol m ³ /0.3m/hr
14/12/01	1200	CO10	1.50	5.5	0.34	0.89	0.36	0.32	0.14	59.40	0.00213
14/12/01	1300	CO10	2.20	7.0	0.34	1.09	0.34	0.33	0.27	57.82	0.00500
14/12/01	1400	CO10	1.80	6.5	0.38	1.32	0.38	0.38	0.20	54.45	0.00296
14/12/01	1500	CO10	3.00	5.0	0.37	1.27	0.38	0.36	0.26	47.22	0.01729
14/12/01	1600	CO10	2.00	6.0	0.35	1.14	0.35	0.34	0.21	49.11	0.01044
14/12/01	1700	CO10	2.50	6.5	0.32	1.24	0.33	0.32	0.28	47.66	0.01278
14/12/01	1800	CO10	2.60	6.0	0.29	0.97	0.30	0.28	0.27	43.54	0.01536
14/12/01	1900	CO10	2.00	5.5	0.28	0.95	0.29	0.28	0.19	46.73	0.00824
15/12/01	1000	CO10	1.80	7.0	0.22	0.78	0.23	0.22	0.22	51.19	0.00238
15/12/01	1100	CO10	1.80	6.5	0.26	0.77	0.26	0.25	0.20	53.07	0.00341
15/12/01	1200	CO10	2.00	6.5	0.29	1.06	0.29	0.29	0.23	51.18	0.00364
15/12/01	1300	CO10	1.80	6.0	0.29	0.93	0.30	0.28	0.19	51.15	0.00280
15/12/01	1400	CO10	1.90	5.5	0.26	0.76	0.26	0.25	0.18	43.25	0.00985
15/12/01	1500	CO10	2.00	6.0	0.27	0.94	0.28	0.26	0.21	51.00	0.00657
15/12/01	1600	CO10	2.30	5.5	0.33	1.17	0.35	0.31	0.22	53.01	0.00944
15/12/01	1700	CO10	2.20	5.0	0.27	0.93	0.28	0.27	0.19	46.99	0.00352
16/12/01	800	CO10	0.20	7.5	0.06	0.37	0.06	0.06	0.03	49.65	0.00004
16/12/01	900	CO10	0.30	9.0	0.11	0.25	0.11	0.09	0.05	65.80	0.00136
16/12/01	1000	CO10	0.50	9.0	0.19	0.81	0.20	0.18	0.08	45.90	0.01006
16/12/01	1100	CO10	0.50	10.0	0.16	0.87	0.16	0.15	0.09	28.55	0.01181
16/12/01	1200	CO10	0.50	11.0	0.13	0.56	0.14	0.13	0.10	32.22	0.01392
16/12/01	1300	CO10	0.50	12.5	0.13	0.59	0.13	0.12	0.11	27.72	0.01308
16/12/01	1400	CO10	0.50	10.5	0.13	0.61	0.14	0.13	0.09	29.73	0.01323
16/12/01	1500	CO10	0.40	15.0	0.12	0.55	0.13	0.12	0.10	13.25	0.00936
16/12/01	1600	CO10	0.20	13.0	0.24	0.75	0.24	0.24	0.04	51.54	0.00325
17/12/01	1200	CO10	0.10	15.0	0.13	0.41	0.13	0.12	0.03	69.72	0.00149
17/12/01	1300	CO10	0.50	11.0	0.32	0.73	0.34	0.30	0.10	74.11	0.03537
17/12/01	1400	CO10	0.80	15.0	0.31	0.82	0.31	0.31	0.21	70.59	0.03509
17/12/01	1500	CO10	1.00	12.0	0.41	1.42	0.41	0.41	0.21	70.23	0.03172
17/12/01	1600	CO10	1.50	8.0	0.63	1.96	0.61	0.64	0.21	71.16	0.04237

Please note: This is an abridged digital version.

For more data please contact author: imdawe@paradise.net.nz

APPENDIX 7

SUMMARY STATISTICS BY SITE FOR MEASURED ENVIRONMENTAL PARAMETERS

Site locations can be seen in Figure 2.14 (p48).

Deep water root mean square wave height measured by wave gauge.

H_{rms}	CO10	CO14a&b	CO11a	CO11b	CO13
Min	0.01	0.07	0.07	0.07	0.07
Max	0.33	0.49	0.39	0.51	0.40
Mean	0.16	0.27	0.23	0.26	0.20
Median	0.15	0.27	0.22	0.26	0.19
Std. Dev.	0.07	0.12	0.08	0.09	0.07
Variance	0.00	0.01	0.01	0.01	0.00
Skewness	0.06	-0.23	0.14	0.36	0.43
Kurtosis	-0.51	-1.04	-0.96	0.23	-0.26

Deep water wave period measured by wave gauge.

T_z	CO10	CO14a&b	CO11a	CO11b	CO13
Min	0.70	1.01	0.97	0.97	1.04
Max	1.75	2.06	1.75	1.96	1.92
Mean	1.32	1.61	1.44	1.51	1.49
Median	1.34	1.60	1.46	1.51	1.48
Std. Dev.	0.20	0.28	0.20	0.20	0.21
Variance	0.04	0.08	0.04	0.04	0.04
Skewness	-0.31	-0.60	-0.20	-0.24	-0.02
Kurtosis	0.04	-0.27	-0.83	0.10	-0.48

Deep water wave length calculated with deep water wave period measured by wave gauge.

L_o	CO10	CO14a&b	CO11a	CO11b	CO13
Min	0.77	1.58	1.48	1.48	1.70
Max	4.80	6.63	4.80	5.97	5.76
Mean	2.80	4.14	3.30	3.60	3.52
Median	2.78	4.02	3.34	3.58	3.40
Std. Dev.	0.82	1.33	0.88	0.95	0.97
Variance	0.67	1.76	0.77	0.91	0.94
Skewness	0.12	-0.24	0.02	0.18	0.26
Kurtosis	-0.25	-0.63	-1.05	0.16	-0.48

Breaker wave direction measured by current meter.

$H_b \alpha$	CO10	CO14a&b	CO11a	CO11b	CO13
Min	4.79	32.87	11.92	6.49	14.54
Max	80.11	69.87	71.10	70.85	72.91
Mean	56.79	56.35	43.63	42.23	45.51
Median	61.27	58.78	43.85	41.21	47.51
Std. Dev.	17.06	9.19	11.15	15.01	17.69
Variance	291.06	84.48	124.42	225.21	312.81
Skewness	-1.06	-0.47	0.03	-0.11	0.07
Kurtosis	0.57	-0.64	0.69	-0.63	-1.48

Swash zone gradient.

$\tan \beta$	CO10	CO14a&b	CO11a	CO11b	CO13
Min	0.08	0.09	0.05	0.09	0.09
Max	0.36	0.32	0.18	0.17	0.32
Mean	0.16	0.15	0.10	0.12	0.13
Median	0.13	0.12	0.10	0.11	0.12
Std. Dev.	0.07	0.07	0.02	0.02	0.03
Variance	0.01	0.00	0.00	0.00	0.00
Skewness	1.26	1.33	1.33	0.32	3.55
Kurtosis	0.63	0.47	2.99	0.21	21.60

Swash zone width.

X_{sw}	CO10	CO14a&b	CO11a	CO11b	CO13
Min	0.05	0.20	0.80	0.90	0.15
Max	3.50	4.50	4.50	6.00	4.00
Mean	1.24	1.92	2.74	3.38	2.21
Median	1.10	2.00	2.60	3.50	2.20
Std. Dev.	0.83	1.20	1.11	1.22	0.83
Variance	0.69	1.43	1.23	1.48	0.70
Skewness	0.57	0.28	0.19	-0.24	-0.12
Kurtosis	-0.43	-0.95	-1.01	-0.68	-0.67

Mean measured swash velocity.

\bar{v}_{sw}	CO10	CO14a&b	CO11a	CO11b	CO13
Min	0.01	0.03	0.08	0.08	0.08
Max	0.67	1.07	0.75	0.58	0.49
Mean	0.27	0.37	0.39	0.33	0.23
Median	0.26	0.34	0.37	0.34	0.22
Std. Dev.	0.14	0.26	0.16	0.10	0.09
Variance	0.02	0.07	0.02	0.01	0.01
Skewness	0.52	0.80	0.08	-0.01	0.58
Kurtosis	0.07	0.23	-0.63	-0.04	0.04

Median grain size.

D_{50}	CO10	CO14a&b	CO11a	CO11b	CO13
Min	0.40	0.88	0.84	0.89	0.62
Max	9.10	10.14	9.08	8.37	10.12
Mean	3.28	3.61	3.82	3.64	4.08
Median	2.99	2.71	3.51	3.30	3.64
Std. Dev.	1.67	2.28	1.80	1.64	2.10
Variance	2.78	5.20	3.25	2.68	4.40
Skewness	0.86	1.21	0.90	0.81	1.07
Kurtosis	0.53	0.71	0.69	0.08	0.66

REFERENCES

A

- Ahrens, J.P. (1981), *Irregular Wave Run-up on Smooth Slopes*. Technical Aid No. 81-17, Coastal Engineering Research Center, Waterways Experiment Station, Vicksburg, Mississippi.
- Ahrens, J.P. & Hands, E.B. (1998), Velocity parameters for predicting cross-shore sediment movement. *Journal of Waterway, Port, Coastal and Ocean Engineering*, 24 (1), 16-20.
- Allan, J.C. (1991), *Storm-Induced Surf Zone Processes and Beach Profile Response at Lake Pukaki, South Island, New Zealand*. MSc. Thesis, Department of Geography, University of Canterbury, Christchurch, New Zealand, 214pp.
- Allan, J.C. (1998), *Shoreline Development at Lake Dunstan*. Ph.D. thesis. Department of Geography, University of Canterbury, Christchurch, New Zealand, 461pp.
- Allan, J.C. & Kirk, R.M. (2000), Wind wave characteristics at Lake Dunstan, South Island, New Zealand. *New Zealand Journal of Marine and Freshwater Research*, 34, 573-591.
- Angel, J.R. (1995), Large scale storm damage on the U.S. shores of the Great Lakes. *Journal of Great Lake Research*, 21 (3), 287-293.
- Arcilla, A.S., Vdaor, A. & Pous, J. (1988), Improved longshore sand transport evaluation. *Proceedings of the 21st International Conference on Coastal Engineering*. American Society of Civil Engineers, 1382-1395.
- Armon, J.W. (1974), Late Quaternary shorelines near Lake Ellesmere, Canterbury, New Zealand. *New Zealand Journal of Geology and Geophysics*, 17, 63-74.
- Armstrong, J.S. (1935), Notes on the biology of Lake Taupo. *Transactions and Proceedings of the Royal Society of New Zealand*, 65, 88-94.
- Aubrey, D.G. & Trowbridge, J.H. (1985), Kinematic and dynamic estimates from electromagnetic current meter data. *Journal of Geophysical Research*, 90 (C12), 9137-9146.

B

- Bailard, J.A. (1981), An energetics total load sediment transport model for a plane sloping beach. *Journal of Geophysical Research*, 86 (C11), 10 938-10 954.
- Bailard, J.A. (1984), A simplified model for longshore sediment transport. *Proceedings of the 19th International Conference on Coastal Engineering*. American Society of Civil Engineers, 1454-1469.
- Bailard, J.A. & Inman, D.L. (1979), A re-examination of Bagnold's granular-fluid model and bedload transport equation. *Journal of Geophysical Research*, 84 (C12), 7827-7833.

- Bailard, J.A. & Inman, D.L. (1981), An energetics bedload model for a plane sloping beach: Local transport. *Journal of Geophysical Research*, 86 (C3), 2035-2043.
- Baldock, T.E. & Holmes, P. (1997), Swash hydrodynamics on a steep beach. *Proceedings of the Conference of Coastal Dynamics*. American Society of Civil Engineers, 784-793.
- Baldock, T.E. & Holmes, P. (1999), Simulation and prediction of swash oscillations on a steep beach. *Coastal Engineering*, 36, 219-242.
- Bagnold, R.A. (1963), Mechanics of marine sedimentation. In Hill, M.N. (ed.), *The Sea: Ideas and Observations on Progress in the Study of the Sea*, Vol. 3. New York, Wiley-Interscience, pp507-582.
- Bagnold, R.A. (1966), *An Approach to the Sediment Transport Problem from General Physics*. U.S. Geological Survey Professional Paper, 422-I, 37pp.
- Bagnold, R.A. (1980), An empirical correlation of bedload transport rates in flumes and natural rivers. *Proceedings of the Royal Society of London*, A372, 453-473.
- Bagnold, R.A. (1986), Transport of solids by natural water flow: Evidence for a worldwide correlation. *Proceedings of the Royal Society of London*, A405, 369-374.
- Baldock, T.E. & Holmes, P. (1997), Swash hydrodynamics on a steep beach. *Coastal Dynamics '97: Proceedings of the Conference on Coastal Dynamics*. American Society of Civil Engineers, 784-793.
- Bascom, W.H. (1954), Characteristics of natural beaches. *Proceedings of the 4th International Conference on Coastal Engineering*. American Society of Civil Engineers, 163-180.
- Battjes, J.A. (1971), Run-up distributions of waves breaking on slopes. *Journal of Waterways, Harbors, and Coastal Engineering Division*. American Society of Civil Engineers, 97(WW1), 91-114.
- Battjes, J.A. (1974), Surf similarity. *Proceedings of the 14th International Conference on Coastal Engineering*. American Society of Civil Engineers, 466-480.
- Battjes, J.A. & Janssen, J.P.F.M. (1978), Energy loss and set-up due to breaking of random waves. *Proceedings of the 16th International Conference on Coastal Engineering*. American Society of Civil Engineers, 569-587.
- Beach Erosion Board, (1950), Munch-Peterson's littoral drift formula. *Bulletin of the U.S. Army Corps of Engineers*, 4, 1-31. [Redraft of speech given in 1938].
- Bishop, C.T. & Donelan, M.A. (1987), Measuring waves with pressure transducers. *Coastal Engineering*, 11 (4), 309-328.
- Blewett, J.C., Holmes, P. & Horn, D.P. (2000), Swash hydrodynamics on sand and shingle beaches. *Proceedings of the 27th International Conference on Coastal Engineering*. American Society of Civil Engineers, 597-609.
- Blewett, J.C., Holmes, P. & Horn, D.P. (2001), Field measurements of swash on gravel beaches. *Proceedings of the 4th Conference of Coastal Dynamics*. American Society of Civil Engineers, 828-837.

- Bodge, K.R. & Kraus, N.C. (1991), Critical examination of longshore transport rate magnitude. *Coastal Sediments '91*. American Society of Civil Engineers, 139-155.
- Brampton, A.H. & Motyka, J.K. (1984), Modelling the plan shape of gravel beaches. *POLYMODEL 7 Conference*. Sunderland Polytechnic, U.K., 219-233.
- Brampton, A.H. & Motyka, J.K. (1987), Recent examples of mathematical models of U.K. beaches. *Coastal Sediments '87*. American Society of Civil Engineers, 515-530.
- Bray, M.J., Workman, M.H., Smith, J. & Pope, D. (1996), Field measurements of shingle transport using electronic tracers. *Proceedings of the 31st MAFF Conference for River and Coastal Engineers*, 10.4.1-10.4.13.
- Brinkmann, W.A.R. (1985), Association between summer temperature and precipitation patterns over the Great Lakes region and water supplies to the Great Lakes. *Journal of Climatology*, 5, 161-173.
- Britten, R. (2000), *Lake Coleridge: The Power, the People, the Land*. Hazard Press, Christchurch, New Zealand, 382pp.
- Brotherhood, G.R. & Griffiths, J.C. (1947), Mathematical derivation of the unique frequency curve. *Journal of Sedimentary Petrology*, 17 (2), 77-82.
- Brown, D.A. (1975), *The Dynamics of Pebble Shape and Size Selection by Waves*. M.A. thesis, Department of Geography, University of Canterbury, Christchurch, New Zealand, 137pp.
- Bruno, R. O. & Gable, C.G. (1976), Longshore transport at a littoral barrier. *Proceedings of the 15th International Conference on Coastal Engineering*. American Society of Civil Engineers, 1203-1222.
- Bruno, R. O., Dean, R.G. & Gable, C.G. (1980), Littoral transport evaluations at a detached breakwater. *Proceedings of the 17th International Conference on Coastal Engineering*. American Society of Civil Engineers, 1453-1475.
- Bruno, R. O., Dean, R.G., Gable, C.G. & Walton, T.L. (1981), *Longshore Sand Transport Study at Channel Island Harbour, California*. U.S. Army Corps of Engineers, Coastal Engineer Resource Center Technical Paper No.81-82.
- Bunting, D.G. (1977), *Lake Pukaki Shoreline Stability: A Preliminary Engineering Geological Investigation*. MSc. thesis, Department of Geology, University of Canterbury, Christchurch, New Zealand, 153pp.
- Butt, T. & Russell, P. (2000), Hydrodynamics and cross-shore sediment transport in the swash-zone of natural beaches: A review. *Journal of Coastal Research*, 16 (2), 255-268.

C

- Caldwell, J.M. (1956), *Wave Action and Sand Movement Near Anaheim Bay, California*. U.S. Army Corps of Engineers, Beach Erosion Board Technical Memorandum No. 68, 21pp.

- Castanho, J. (1970), Influence of grain size on littoral drift. *Proceedings of the 12th International Conference on Coastal Engineering*. American Society of Civil Engineers, 891-898.
- Chadwick, A.J. (1989), Field measurements and numerical model verification of coastal shingle transport. In Palmer, M.H. (ed.), *Advances in Water Modeling and Measurement*. British Hydromechanics Research Association, The Fluid Engineering Centre, Cranfield, Bedford, pp381-402.
- Chadwick, A.J. (1991a), An unsteady flow bore model for sediment transport in broken waves. Part 1: The development of the numerical model. *Proceedings of the Institute of Civil Engineers*, Part 2 (91), 719-737.
- Chadwick, A.J. (1991b), An unsteady flow bore model for sediment transport in broken waves. Part 2: The properties, calibration and testing of the numerical model. *Proceedings of the Institute of Civil Engineers*, Part 2 (91), 739-753.
- Clarke, F.W. (1921), Timaru Harbour. Timaru Harbour Board Plan 271. *New Zealand Nautical Almanac 1936*.
- Coakley, J.P. & Cho, H.K. (1972), Shore erosion in western Lake Erie. *Proceedings of the 15th Conference of Great Lakes Research*, 344-360.
- Coakley, J.P. & Skafel, M.G. (1982), Suspended sediment discharge on a non-tidal coast. *Proceedings of the 18th International Conference on Coastal Engineering*. American Society of Civil Engineers, 1288-1304.
- Coastal Engineering Research Center (1984), *Shore Protection Manual*. 4th Edition. U.S. Army Engineer Waterways Experiment Station, Vicksburg, Mississippi, (2 Vols.).
- Cobb, C.E. Jr. (1987), The Great Lakes' troubled waters. *National Geographic*, 172 (1), 2-31.
- Cooley, J.W. & Tukey, J.W. (1967), The Fast Fourier Transform. *Institute of Electrical and Electronics Engineers, Spectrum*, 4, 63-70.
- Csanady, G.T. (1978), Water circulation and dispersal mechanisms. In Lerman, A (ed), *Lakes: Chemistry, Geology, Physics*. Springer-Verlag, New York, 21-64.
- Curry, J.R. (1960), Tracing sediment masses by grain size modes. *International Geological Congress*. Report of the 21st Session, Copenhagen, Denmark, 119-130.

D

- Dalrymple, R. A. (1992), Prediction of Storm/Normal Beach Profiles. *Journal of Waterways, Port, Coastal and Ocean Engineering*, American Society of Civil Engineers, 118 (2), 193-200.
- Damgaard, J.S. & Soulsby, R.L. (1996), Longshore bed-load transport. *Proceedings of the 25th International Conference on Coastal Engineering*. American Society of Civil Engineers, 3614-3627.
- Davidson-Arnott, R.G.D. (1986), Rates of erosion of till in the nearshore zone. *Earth Surface Processes and Landforms*, 11, 53-58.

- Davidson-Arnott, R.G.D. (1989), The effect of water level fluctuations on coastal erosion in the Great Lakes. *Ontario Geography*, 33, 23-39.
- Dawe, I.N. (1997), Sediment patterns on a mixed sand and gravel beach, Kaikoura, New Zealand. M.Sc. thesis, Department of Geography, University of Canterbury, Christchurch, New Zealand, 184pp.
- Dawe, I.N. (2000), Sediment patterns on a mixed sand and gravel beach, Kaikoura, New Zealand. *Journal of Coastal Research Special Issue 34*. (ICS 2000 Proceedings), 267-277.
- Dawe, I.N. & Hemmingsen, M. (1999), *Catamaran Wake from "Fiordland Express" on the Shoreline of Lake Te Anau*. Unpublished report to Fiordland Travel, Te Anau by Land and Water Studies International Ltd., 23pp.
- Dawe, I.N. & Single, M.B. (2001), *Lake Monowai Beach Profile Monitoring Network: An Assessment of Shoreline Change*. Unpublished report to TrustPower Ltd. by, Land and Water Studies International Ltd., 38pp.
- Dean, R.G., Berek, E.P., Gable, C.G. & Seymour, R.J. (1982), Longshore transport determined by an efficient trap. *Proceedings of the 18th International Conference on Coastal Engineering*. American Society of Civil Engineers, 954-968.
- Dean, R.G., Berek, E.P., Bodge, K.R. & Gable, C.G. (1987), NSTS measurements of total longshore transport. *Coastal Sediments '87*. American Society of Civil Engineers, 652-667.
- del Valle, R., Medina, R. & Losada, M.A. (1993), Dependence of coefficient *K* on grain size. *Journal of Waterway, Port, Coastal and Ocean Engineering*, 119 (5), 568-574.
- Denny, M.W. (1988), *Biology and Mechanics of the Wind-Swept Environment*. Princeton University Press, New Jersey, 329pp.
- Delgado, C. (1990), *A Field Study of Morphodynamics at North Bay Beach, Kaikoura*. M.Sc. thesis, Department of Geography, University of Canterbury, Christchurch, New Zealand, 108pp.
- Doering, J. C. & Bowen, A.J. (1987), Skewness in the nearshore zone: A comparison of estimates from Marsh-McBirney current meters and colocated pressure sensors. *Journal of Geophysical Research*, 92 (C12), 13173-13183.
- Dolan, R. & Ferm, J. (1966), Swash processes and beach characteristics. *The Professional Geographer*, 18 (4), 210-213.
- Dubois, R.N. (1973), Seasonal variations of a limnic beach. *Geological Society of America Bulletin*, 84, 1817-1824.
- Draper, L. (1966), The analysis and presentation of wave data: A plea for uniformity. *Proceedings of the 10th International Conference on Coastal Engineering*. American Society of Civil Engineers, 1-11.

E

- Earle, M.D., McGehee, D. & Tubman, M. (1995), *Field Wave Gaging Program: Wave Data Analysis Standard*. Misc. Paper CERC-95-1, U.S. Army Engineer Waterways Experiment Station, 33pp.
- Eaton, R.O. (1951), Littoral processes on sandy coasts. *Proceedings of the 1st International Conference on Coastal Engineering*. American Society of Civil Engineers, 140-154.
- Elfrink, B. & Baldock, T. (2002), Hydrodynamics and sediment transport in the swash zone: A review and perspectives. *Coastal Engineering*, 45, 149-167.
- Erickson, L., Larson, M. & Hanson, H (2005), Prediction of swash motion and run-up including the effects of swash interaction. *Coastal Engineering*, 52, 285-302.
- Esteva, D. & Harris, D.L. (1970), Comparison of pressure and staff wave gage records. *Proceedings of the 12th International Conference on Coastal Engineering*. American Society of Civil Engineers, 101-116.

F

- Flain, M. (1970), *Lake Coleridge Provisional Bathymetry*. 1:23 760. New Zealand Oceanographic Institute Chart, Lake Series.
- Flatman, M. R. (1997), *Cliff Erosion and Coastal Change, Mid-Canterbury*. M.Sc. thesis, Department of Geography, University of Canterbury, Christchurch, New Zealand, 176pp.
- Flint, E.A. (1938), A preliminary study of the phytoplankton in Lake Sarah (New Zealand). *Journal of Ecology*, 26, 353-358.
- Fredsøe, J. (1993), Modelling of non-cohesive sediment transport processes in the marine environment. *Coastal Engineering*, 21, 71-103.
- Fredsøe, J. & Deigaard, R. (1991), *Mechanics of Coastal Sediment Transport*. Advanced Series on Ocean Engineering – Vol. 3, World Scientific, Singapore, 369pp.
- Folk, R.L. (1965), *Petrology of Sedimentary Rocks*. Hemphills, Austin, Texas, 159pp.
- Folk, R.L. & Ward, W.C. (1957), Brazos River Bar: A study in the significance of grain size parameters. *Journal of Sedimentary Petrology*, 27 (1), 3-26.
- Foote, M. & Horn, D. (1999), Video measurement of swash zone hydrodynamics. *Geomorphology*, 29 (1), 59-76.

G

- Gage, M. (1959), On the origin of some lakes in Canterbury. *New Zealand Geographer*, 15, 69-75).
- Galvin, C. (1968), Breaker type classification on three laboratory beaches. *Journal of Geophysical Research*, 73 (12), 3651-3659.

- Galvin, C. (1972), A gross longshore transport rate formula. *Proceedings of the 13th International Conference on Coastal Engineering*. American Society of Civil Engineers, 953-970.
- Galvin, C. & Vitale, P. (1976), Longshore transport prediction – SPM 1973 equation. *Proceedings of the 15th International Conference on Coastal Engineering*. American Society of Civil Engineers, 1133-1148.
- Gibb, J.G. & Adams, J. (1982), A sediment budget for the east coast between Oamaru and Banks Peninsula, South Island, New Zealand. *New Zealand Journal of Geology and Geophysics*, 25, 355-352.
- Gilbert, R. (1975), Sedimentation in Lillooet Lake, British Colombia. *Canadian Journal of Earth Sciences*, 12, 1697-1711.
- Grant, U.S. (1943), Waves as a transporting agent. *American Journal of Science* 241, 117-123.
- Gregg, D.R. (1964), *Geological Map of New Zealand: Sheet 18, Hurunui (1st ed.)*. 1:250 000. Department of Scientific and Industrial Research, Wellington, New Zealand.
- Green, J.D. (1975), Heat Budgets. In Jolly & Brown (eds), *New Zealand Lakes*. Auckland University Press, Auckland, New Zealand, 106-109.
- Greer, M.N. & Madsen, O.S. (1978), Longshore sediment transport data: A review. *Proceedings of the 16th International Conference on Coastal Engineering*. American Society of Civil Engineers, 1563-1576.
- Grüne, J. (1982), Wave run-up caused by natural storm surge. *Proceedings of the 18th International Conference on Coastal Engineering*. American Society of Civil Engineers, 785-803.
- Guedes Soares, C., Cherneva, Z. & Antao, E.M. (2004), Steepness and asymmetry of the largest waves in storm sea states. *Ocean Engineering*, 31, 1147–1167.
- Guza, R.T. & Thornton, E.B. (1982), Swash oscillations on a natural beach. *Journal of Geophysical Research*, 87 (C1), 483-491.
- Guza, R.T., Thornton, E.B. & Christensen, N., (1986), Observations of steady longshore currents in the surf zone. *Journal of Physical Oceanography*, 16, 1959-1969.

H

- Handin, J.W. & Ludwick, J.C. (1950), *Accretion of Beach Sand Behind a Detached Breakwater*. U.S. Army Corps of Engineers, Beach Erosion Board Technical Memorandum No. 16, 13pp.
- Hands, E.B. (1980), *Prediction of Shore Retreat and Nearshore Profile Adjustments to Rising Water Levels on the Great Lakes*. Technical Paper No. 80-7, U.S. Army Engineer Waterways Experiment Station, 119pp.

- Hall, S. (1995), *Morphology and Morphodynamics of the Beaches of Northern Pegasus Bay*. M.Sc. thesis, Department of Geography, University of Canterbury, Christchurch, New Zealand, 158pp.
- Hall K. R. & Foster D. N. (1990), Internal and external pressure measurements in reshaped breakwaters. *Coastal Engineering*, 14 (3), 215-232.
- Harris, D.L. (1970), The analysis of wave records. *Proceedings of the 12th International Conference on Coastal Engineering*. American Society of Civil Engineers, 85-100.
- Harris, D.L. (1974), Finite spectrum analyses of wave records. *Proceedings of the International Symposium on Ocean Wave Measurement and Analysis*, 107-124.
- Harris, F.J. (1978), On the use of windows for harmonic analysis with discrete fourier transform. *Proceedings of the Institute of Electrical and Electronics Engineers*, 66, 51-83.
- Hastie, W.J. (1983), *Sediment Transport in the Nearshore Marine Environment, Timaru, New Zealand*. Ph.D. thesis, Department of Geography, University of Canterbury, Christchurch, New Zealand, 406pp.
- Hastie, W.J. (1985), Patterns of bedload transport in the nearshore marine environment, Timaru, New Zealand. *Preprints of the 1st Australasian Conference on Coastal and Ocean Engineering*.
- Hay, A.E. & Sheng, J. (1992), Vertical profiles of suspended sand concentration and size from multifrequency acoustic backscatter. *Journal of Geophysical Research*, 97, 15, 661-15,667.
- Henderson, R.D. (1994), *Analysis of Lake Level Fluctuations on Lake Coleridge*. Report to Electricity Corporation of New Zealand by, National Institute of Water and Atmospheric Research (report No. ELE903).
- Hemmingsen, M. (1997), *The coastal geomorphology of Te Waihora (Lake Ellesmere)*. MSc. thesis, Department of Geography, University of Canterbury, Christchurch, New Zealand, 206pp.
- Hewson, P.A. (1977), *Coastal Erosion and Beach Dynamics in South Canterbury - North Otago*. M.A. thesis, Department of Geography, University of Canterbury, Christchurch, New Zealand, 132pp.
- Horn, D.P. & Mason, T. (1994), Swash zone sediment transport modes. *Marine Geology*, 120, 309-325.
- Holman, R.A. (1986), Extreme value statistics for wave run-up on a natural beach. *Coastal Engineering*, 9, 527-544.
- Howell, G.L. (1988), Shallow water directional wave gages using short baseline pressure arrays. *Coastal Engineering*, 35 (1), 85-102.
- Hibberd, S. & Peregrine, D.H. (1979), Surf and run-up on a beach: A uniform bore. *Journal of Fluid Mechanics*, 95, 323-345.

- Hicks, D.M. (1995), *Assessment of Factors Affecting Turbidity in Lake Coleridge*. Unpublished report to Electricity Corporation of New Zealand, Dunedin and the Lake Coleridge Working Party, by National Institute of Water and Atmospheric Research (NIWA), Report No. ELE908-2, 32pp.
- Hicks, D.M., McKerchar, A.L. & O'Brian, R. (2000), *Lakeshore Geomorphic Processes, Lake Taupo*. Unpublished report to Mighty River Power, Hamilton, by National Institute of Water and Atmospheric Research (report No. MRP00504-1).
- Holland, K.T. & Puleo, J.A. (2001), Variable swash motions associated with foreshore profile change. *Journal Geophysical Research*, 106 (C3), 1613-1623.
- Hughes, M.G., Masselink, G. & Brander, R.W. (1997), Flow velocity and sediment transport in the swash zone of a steep beach. *Marine Geology*, 138, 91-103.
- Hughes, S.A. (2003), *Estimating Irregular Wave Runup on Smooth, Impermeable Slopes*. U.S. Army Corp of Engineers. Report CHETN-III-68, 11pp.
- Hunt, I.A. (1959), Design of seawalls and breakwaters. *Journal of the Waterways and Harbor Division*, ASCE, 85(WW3), 123-152.
- Huntley, D.A. & Bowen, A.J. (1975), Comparison of the hydrodynamics of steep and shallow beaches. In Hails & Carr (eds), *Nearshore Sediment Dynamics and Sedimentation*, Wiley, London, 69-109.
- I
- InterOcean (1990), *Surface Wave Characteristics From Pressure and Particle Kinematics Measurement*. InterOcean Systems Inc., San Diego, California, 17pp.
- Irwin, J. (1972), New Zealand lakes bathymetric surveys 1965-1970. *New Zealand Oceanographic Institute Records*, 1 (6), 107-126.
- Irwin, J. (1975), *Checklist of New Zealand Lakes*. New Zealand Oceanographic Institute, Memoir 74, 161pp.
- Irwin, J. (1978), Bottom sediments of Lake Tekapo compared with adjacent Lakes Pukaki and Ohau, South Island, New Zealand. *New Zealand Journal of Marine and Freshwater Research*, 12, 245-250.
- Inman, D.L. & Bagnold, R.A. (1963), Littoral Processes. In Hill, M.N. (ed.), *The Sea: Ideas and Observations on Progress in the Study of the Sea*, Vol. 3. New York, Wiley-Interscience, pp529-553.
- Inman, D.L. & Bowen, A.J. (1963), Flume experiments on sand transport by waves and currents. *Proceedings of the 8th International Conference on Coastal Engineering*. American Society of Civil Engineers, 137-150.
- J
- James, M., James, G., Hawes, I. & Hicks, M. (1995), *The Effects of Lake Level Changes on the Ecology of Lake Coleridge*. Unpublished report to Electricity Corporation of New

Zealand by National Institute of Water and Atmospheric Research (NIWA), Report No. ELE906.

James, R.T., Martin, J., Wool, T. & Wang, P.F. (1997), A sediment resuspension and water quality model of Lake Okeechobee. *American Water Resources Association*, 33 (3), 661-680.

James, M., Mark, A. & Single., M. (2002), *Lake Managers Handbook: Lake Level Management*. Ministry for the Environment, 87pp.

Jennings, R. & Shulmeister, J. (2002), A field based classification scheme for gravel beaches. *Marine Geology*, 186, 211-228.

Jin, K. & Ji, Z. (2001), Calibration and verification of a spectral wind-wave model for Lake Okeechobee. *Ocean Engineering*, 28, 571-584.

Jolly, V.H. & Brown, J.M.A. (1975) (eds), *New Zealand Lakes*. Auckland University Press, Auckland, New Zealand, 388pp.

K

Kamphuis, J.W. (1990), Littoral sediment transport rate. *Proceedings of the 22nd International Conference on Coastal Engineering*. American Society of Civil Engineers, 2402-2415.

Kamphuis, J.W. (1991), Alongshore sediment transport rate. *Journal of Waterway, Port, Coastal and Ocean Engineering*, 117 (6), 624-640.

Kamphuis, J.W. & Readshaw, J.S. (1978), A model study of alongshore sediment transport rate. *Proceedings of the 16th International Conference on Coastal Engineering*. American Society of Civil Engineers, 1656-1674.

Kamphuis, J.W. & Sayao, O.J. (1982), Model tests on littoral sand transport rate. *Proceedings of the 18th International Conference on Coastal Engineering*. American Society of Civil Engineers, 1305-1325.

Kamphuis, J.W., Davies, M.H., Nairn, R.B. & Sayao, O.J. (1986), Calculation of littoral sand transport rate. *Coastal Engineering*, 10, 1-21.

Kana, T.W. (1977), Suspended sediment transport at Price Inlet, South Carolina. *Coastal Sediments '77*. American Society of Civil Engineers, 366-382.

Kana, T.W. (1978), Surf zone measurements of suspended sediment. *Proceedings of the 16th International Conference on Coastal Engineering*. American Society of Civil Engineers, 1725-1743.

Kane, J.W. & Sternheim, M.M. (1988), *Physics*. 3rd Edition. John Wiley & Sons, 843pp.

Katori, S., Tanaka, K., Kubota. & Takezawa, M. (2001), Field measurements of on-offshore sediment transport rate in the swash zone. *Proceedings of the 4th International Conference on Coastal Dynamics*, American Society of Civil Engineers, 898-907.

- Kemp, P.H. (1960), The relationship between wave action and beach profile characteristics. *Proceedings of the 7th International Conference on Coastal Engineering*. American Society of Civil Engineers, 262-277.
- Kemp, P.H. & Plinston, D.T. (1968), Beaches produced by waves of low phase difference. *Journal of the Hydraulics Division*. American Society of Civil Engineers, 94 (HY5), 1183-1195.
- Kemp, P.H. (1963), A field study of wave action on natural beaches. *Proceedings of the 10th International Association of Hydraulic Research*, 1, 131-138.
- Kirk, R.M. (1967), *Beach Morphology and Sediments of the Canterbury Bight*. M.A. thesis, Department of Geography, University of Canterbury, Christchurch, New Zealand, 173pp.
- Kirk, R.M. (1970), *Swash Zone Processes: An Examination of Water Motion and the Relations Between Water Motion and Foreshore Responses on Some Mixed Sand and Shingle Beaches, Kaikoura, New Zealand*. Ph.D. thesis, Department of Geography, University of Canterbury, Christchurch, New Zealand, 378pp.
- Kirk, R.M. (1971), Instruments for investigating shore and nearshore processes. *New Zealand Journal of Marine and Freshwater Research*, 5 (2), 358-375.
- Kirk, R.M. (1973), *An Instrument System for Shore Process Studies*. British Geomorphology Research Group Technical Bulletin, No. 10, 23pp.
- Kirk, R.M. (1975), Aspects of surf and runup processes on mixed sand and gravel beaches. *Geografiska Annaler*, 57A (1-2), 117-133.
- Kirk, R.M. (1980), Mixed sand and gravel beaches: Morphology, processes and sediments. *Progress in Physical Geography*, 4 (2), 189-210.
- Kirk, R.M. (1984), *Enhancement of Coastal Protection by Beach Realignment, South Beach, Timaru*. Unpublished report to the engineer's department, Timaru Harbour Board.
- Kirk, R.M. (1985), *Foreshore Erosion and Shoreline Management: Te Anau Township*. Unpublished report to Electricity Corporation of New Zealand, The Guardians of Lakes Manapouri and Te Anau and Te Anau Community Council and Wallace County, 31pp.
- Kirk, R.M. (1988), *Processes of Shoreline Change and Their Management at Lake Pukaki*. Unpublished Report to Electricity Corporation of New Zealand, 233pp.
- Kirk, R.M. (1992a), Artificial beach growth for breakwater protection at the Port of Timaru, east coast, South Island, New Zealand. *Coastal Engineering*, 17, 227-251.
- Kirk, R.M. (1992b), *A Shoreline Stability Assessment and a Monitoring Network for Lake Monowai, Fiordland*. Unpublished report to The Guardians and Southland Electric Power Supply, Invercargill, 49pp.
- Kirk, R.M. & Allan, J.C. (1995), *Delta formation at the Harper Diversion, Lake Coleridge*. Unpublished report to the Lake Coleridge Working Party and Electricity Corporation of New Zealand, 19pp.

- Kirk, R.M. & Hewson, P.A. (1978), A coastal sediment budget for South Canterbury - North Otago. *Proceedings of the Conference on Erosion Control and Assessment in New Zealand*. New Zealand Association of Soil Conservators, 93-120.
- Kirk, R.M. & Henriques, P.R. (1986), Physical and Biological aspects of shoreline change: Lake Ohau, South Island, New Zealand. *Journal of Shoreline Management*, 2, 305-326.
- Kirk, R.M., Komar, P.D., Allan, J.C. & Stephenson, W.J. (1996), *Shoreline Erosion, Hawea Township, Lake Hawea, Central Otago*. Unpublished report to Contact Power Ltd, Clyde, by Land and Water Studies International Ltd., 44pp.
- Kirk, R.M., Komar, P.D., Allan, J.C. & Stephenson, W.J. (2000), Shoreline erosion on Lake Hawea, New Zealand caused by high lake levels and storm-wave runoff. *Journal of Coastal Research*, 16 (2), 346-356.
- Kirk, R.M. & Single, M.B. (1988), *Beach Changes on Lakes Manapouri and Te Anau, 1973-1988*. Unpublished report to Electricity Corporation of New Zealand and The Guardians of Lakes Manapouri and Te Anau, 37pp.
- Kirk, R.M. & Single, M.B. (2000), *Shoreline Management: Lake Taupo*. Unpublished report to Mighty River Power, Hamilton, by Land and Water Studies International Ltd.
- Kirk, R.M. & Tierney, B.W. (1985), Sedimentation and harbour development at the port of Timaru. *Preprints of the 1st Australasian Conference on Coastal and Ocean Engineering*, 393-400.
- Kobayashi, N., Otta, A.K. & Roy, I. (1987), Wave reflection and run-up on rough slopes. *Journal of Waterway, Port, Coastal and Ocean Engineering*, 113 (3), 282-298.
- Komar, P.D. (1976), *Beach Processes and Sedimentation*. Prentice-Hall, New Jersey, 429pp.
- Komar, P.D. (1978), Relative quantities of suspension versus bed-load on beaches. *Journal of Sedimentary Petrology*, 48 (3), 921-932.
- Komar, P.D. (1988), Environmental controls on littoral sand transport. *Proceedings of the 21st International Conference on Coastal Engineering*. American Society of Civil Engineers, 1238-1252.
- Komar, P.D. (1996), Entrainment of sediments from deposits of mixed grain sizes and densities. In Carling, P.A. & Dawson, M.R. (ed.'s), *Advances in Fluvial Dynamics and Stratigraphy*. John Wiley & Sons, pp127-181.
- Komar, P.D. (1998), *Beach Processes and Sedimentation 2nd Edition*. Prentice-Hall, New Jersey, 544pp.
- Komar, P.D. and Inman, D.L. (1970), Longshore Sand Transport on Beaches. *Journal of Geophysical Research*, 75 (30), 5914-5927.
- Kraus, N.C. (1987), Application of portable traps for obtaining point measurements of sediment transport rates in the surf zone. *Journal of Coastal Research*, 3 (2), 139-152.
- Kraus, N.C. & Dean, J.L. (1987), Longshore sediment transport rate distributions measured by trap. *Coastal Sediments '87*. American Society of Civil Engineers, 881-896.

- Kraus, N. C., Larson, M. & Kriebel, D. L. (1991), Evaluation of Beach Erosion and Accretion Predictors. *Proceedings of Conference on Coastal Sediments '91*, American Society of Civil Engineers, 572-587.
- Krumbein, W.C. (1936), Application of logarithmic moments to size frequency distribution of sediments. *Journal of Sedimentary Petrology*, 6 (1), 35-47.
- Krumbein, W.C. (1963), *A Geological Process-Response Model for Analysis of Beach Phenomena*. U.S. Army, Corps of Engineers, Beach Erosion Board Bulletin, 17.
- Kumagai, M. (1988), Predictive model for resuspension and deposition of bottom sediment in a lake. *Japanese Journal of Limnology*, 49 (3), 185-200.

L

- Larsen, C. (1985), *A Stratigraphic Study of Beach Features on the Southwestern Shore of Lake Michigan: New Evidence of Holocene Lake Level Fluctuations*. Environmental Geology Notes, No.112, Illinois State Geological Survey, 31pp.
- Lawrence, J., Chadwick, A.J. & Fleming, C. (2000), A phase-resolving model of sediment transport on coarse grained beaches. *Proceedings of the 27th International Conference on Coastal Engineering*. American Society of Civil Engineers, 624-636.
- Lawrence, J., Karunarathna, H., Chadwick, A.J. & Fleming, C. (2002), Cross-shore sediment transport on mixed coarse grain sized beaches: Modeling and measurements. *Proceedings of the 28th International Conference on Coastal Engineering*. American Society of Civil Engineers, 2565-2577.
- Lewis, D.W. & McConchie, D.M. (1994), *Practical Sedimentology*. 2nd Edition. Chapman & Hall, New York, 213pp.
- Leeder, M.R. (1982), *Sedimentology: Process and Product*. George Allen & Unwin, London, 344pp.
- Longuet-Higgins, M.S. (1952), On the statistical distribution of the height of sea waves. *Journal of Marine Research*, 11 (3), 245-266.
- Longuet-Higgins, M.S. (1972), Recent progress in the study of longshore currents. In Meyer, R.E. (ed.), *Waves on Beaches and Resulting Sediment Transport*. Academic Press, New York, pp203-248.
- Lorang, M.S., Stanford, J.A., Hauer, F.R. & Jourdonnais, J.H. (1993), Dissipative and reflective beaches in a large lake and the physical effects of lake level regulation. *Ocean and Coastal Management*, 19, 263-287.
- Lorang, M.S. (2000), Predicting threshold entrainment mass for a boulder beach. *Journal of Coastal Research*, 16 (2), 432-445.
- Lorang, M.S. (2002), Predicting the crest height of a gravel beach. *Geomorphology*, 48, 87-101.

Lucas, K. (1904), A bathymetrical survey of the lakes of New Zealand. *Geographical Journal*, 23, 645-760.

M

MacBeth, I.L. (1988), *Coastal Analogues? Beaches of Lake Coleridge*. M.Sc. thesis, Department of Geography, University of Canterbury, Christchurch, New Zealand, 172pp.

McDowell, D.M. (1989), A general formula for estimation of the rate of transport of non-cohesive bed-load. *Journal of Hydraulic Research*, 27 (3), 355-361.

McLean, R.F. (1967), Plan shape and orientation of beaches along the east coast, South Island. *New Zealand Geographer*, 23, 16-22.

McLean, R.F. (1969), the supply of gravel to New Zealand's greywacke beaches. *Coastal Research Notes* 2, 5-6.

McLean, R.F. (1970), Variations in grain size and sorting on two Kaikoura beaches. *New Zealand Journal of Marine and Freshwater Research*, 4 (2), 141-64.

McLean, R.F. & Kirk, R.M. (1969), Relationships between grain size, size-sorting, and foreshore slope on mixed sand-shingle beaches. *New Zealand Journal of Geology and Geophysics*, 12 (1), 138-155.

Mark, A.F. & Johnson, P.N. (1985), Ecologically derived guidelines for managing two New Zealand lakes. *Environmental Management*, 9, 34-42.

Marshall, P. (1929), Beach gravels and sand. *Transactions of the New Zealand Institute*, 60, 324-365.

Masselink, G. & Hughes, M.G. (1998), Field Investigation of sediment transport in the swash zone. *Continental Shelf Research*, 18, 1179-1199.

Masselink, G. & Hughes, M.G. (2003), *Coastal Processes and Geomorphology*. Arnold, London, U.K., 354pp.

Matthews, E.R. (1934), *Coastal Erosion and Protection*. In Komar, P.D. (1998), *Beach Processes and Sedimentation 2nd Edition*. Prentice-Hall, New Jersey, U.S., 544pp.

Mason, T., Voulgaris, G., Simmonds, D.J. & Collins, M.B. (1997), Hydrodynamics and sediment transport on composite (mixed sand/shingle) and sand beaches: A comparison. *Coastal Dynamics '97: Proceedings of the Conference on Coastal Dynamics*. American Society of Civil Engineers, 48-57.

Mason, T., Van Wellen, E. & Chadwick, A.J. (1999), Application of Bailard's energetics model for shingle sediment transport. *Coastal Sediments '99*. American Society of Civil Engineers, 907-921.

- Meadows, G.A. (1977), *A field Investigation of the Spatial and Temporal Structure of Longshore Currents*. PhD. thesis, Purdue University, 167pp.
- Meadows, G.A., Meadows, L.A., Wood, W.L., Hubertz, J.M. & Perlin, M. (1997), The relationship between Great Lakes water levels, wave energies and shoreline damage. *Bulletin of the American Meteorological Society*, 78 (4), 675-683.
- Mizuguchi, M. (1986), Experimental study on kinematics and dynamics of wave breaking. *Proceedings of the 20th International Conference on Coastal Engineering*. American Society of Civil Engineers, 589-603.
- Meadows, G.A., Wood, W.L. & Meadows, L.A. (1997), Wave climatology of the Great Lakes. *Shore and Beach*, 65 (2).
- Moore, G.W. & Cole, J.Y. (1960), Coastal processes in the vicinity of Cape Thompson, Alaska. In Kachadoorian, T. (ed.), *Geologic Investigations in Support of Project Chariot in the Vicinity of Cape Thompson, Northwestern Alaska- Preliminary Report*. U.S. Geological Survey Trace Elements Investigation Report 753, p 41-55.
- Morfett, J.C. (1988), Modelling shingle beach evolution. *Proceedings of the Symposium on Mathematical Modelling of Sediment Transport in the Coastal Zone*. IAHR, 148-155.
- Morfett, J.C. (1989), The development and calibration of an alongshore shingle transport formula. *Journal of Hydraulic Research*, 27 (5), 717-730.
- Morfett, J.C. (1990), A “virtual power” function for estimating the alongshore transport of sediment by waves. *Coastal Engineering*, 14, 439-456.
- Morfett, J.C. (1991), Numerical model of longshore transport of sand in surf zone. *Proceedings of the Institute of Civil Engineers*, Part 2 (91), 55-70.
- Moutzouris, C.I. (1988), Longshore sediment transport rate vs. cross-shore distribution of sediment grain sizes. *Proceedings of the 21st International Conference on Coastal Engineering*. American Society of Civil Engineers, 1959-1973.

N

- Neale, D. M. (1987), *Longshore Sediment Transport in a Mixed Sand and Gravel Foreshore, South Canterbury*. M.Sc. thesis, Department of Geography, University of Canterbury, Christchurch, New Zealand, 243pp.
- New Zealand Metrological Service, 1968 to 1986. *Metrological Observations for 1968 to 1986: Stations in New Zealand, Outlying Islands and Antarctica*. Ministry of Transport. Misc. Pub. 109.
- Nicholls, R.J. (1985), *The Stability of the Shingle Beaches in the Eastern Half of Christchurch Bay*. Ph.D. thesis, Department of Civil Engineering, University of Southampton, Southampton, U.K., 468pp.
- Nicholls, R.J. & Wright, P. (1991), Longshore transport of pebbles: Experimental estimates of *K*. *Coastal sediments '91*. American Society of Civil Engineers, 920-933.

Norrman, J.O. (1964), Lake Vättern: Investigations on shore and bottom morphology. *Geografiska Annaler*, 46 (1-2), 1-238.

Novak, I. (1972), Swash-zone competency of gravel-size sediment. *Marine Geology*, 13 (4), 335-345.

O

Özhan, E. (1982), Laboratory study of breaker type effect on longshore transport. In Sumer, B.M. & Müller, A. (ed.'s), *Mechanics of Sediment Transport*. Proceedings of Euromech 156. A.A. Balkema, Rotterdam, pp265-274.

P

Packard, W.P. (1947), Lake Coleridge catchment: A geographic survey of its problems. *New Zealand Geographer*, 3 (1), 19-40.

Packwood, A.R. (1983), The influence of beach porosity on wave uprush and backwash. *Coastal Engineering*, 7, 29-40.

Palmer, H.R. (1834), Observations on the motions of shingle beaches. *Royal Society of London Philosophical Transactions* 124 (1), 567-576.

Peregrine, D.H. (1972), Equations for water waves and the approximations behind them. In Meyer, M.H. (ed.), *Waves on Beaches and Resulting Sediment Transport*. Academic Press, New York, pp95-121.

Percival, E. (1937), New species of Copepoda from New Zealand lakes. *Records of the Canterbury Museum*, 4, 169-175.

Pickrill, R.A. (1976), *The Lacustrine Geomorphology of Lakes Manapouri and Te Anau*. Ph.D. thesis, Department of Geography, University of Canterbury, Christchurch, New Zealand, 402pp.

Pickrill, R.A. (1977), Coastal processes, beach morphology, and sediments along the north-east coast of the South Island, New Zealand. *New Zealand Journal of Geology and Geophysics*, 20, 1-16.

Pickrill, R.A. (1978), Beach and nearshore morphology of Lakes Manapouri and Te Anau, New Zealand: Natural modes of the continental shelf. *New Zealand Journal of Geology and Geophysics*, 21 (2), 229-242.

Pickrill, R.A. (1980), Beach and nearshore morphology and sedimentation in Fiordland, New Zealand: A comparison between fiords and glacial lakes. *New Zealand Journal of Geology and Geophysics*, 23, 469-480.

Pickrill, R.A. (1983), Wave-built shelves on some low-energy coasts. *Marine Geology*, 51, 193-216.

Pickrill, R.A. (1985), Beach changes on low energy lake shorelines, Lakes Manapouri and Te Anau, New Zealand. *Journal of Coastal Research*, 1 (4), 353-363.

Pickrill, R.A. & Irwin, J. (1983), Sedimentation in a deep glacier-fed lake – Lake Tekapo, New Zealand. *Sedimentology*, 30, 63-75.

R

- Raubenheimer, B. & Guza, R.T. (1996), Observations and predictions of run-up. *Journal of Geophysical Research*, 101, 25575-25587.
- Reid, J.R., Sandberg, B.S & Millsop, M.D. (1988), Bank recession processes, rates and prediction, Lake Sakakawea, North Dakota, U.S.A. *Geomorphology*, 1 (2), 161-189.
- Ren, X., Wang, K.H. & Jin, K.R. (1997), A Boussinesq model for simulating wave and current interaction. *Journal of Ocean Engineering*, 24 (4), 335-350.
- Ross, G.A.E. (1857), A description of Lake Coleridge. In Anderson, M. (1965), *The Good Logs of Algidus*. A.H. & A.W. Reed, Wellington, New Zealand, 199pp.
- Ryan, A.P. (1987), *The Climate and Weather of Canterbury*. New Zealand Meteorological Service, No.115 (vol.17), 66pp.
- Ryrie, S.C. (1983), Longshore motion generated on beaches by obliquely incident bores. *Journal of Fluid Mechanics*, 129, 193-212.

S

- Savage, R.P. (1959), *Laboratory Study of the Effect of Grains on the Rate of Littoral Transport*. U.S. Army Corps of Engineers, Beach Erosion Board Technical Memorandum No. 14.
- Saville, T. (1955), *Laboratory Data on Wave Run-up and Overtopping on Shore Structures*. Technical Memorandum No. 64. Beach Erosion Board, U.S. Army Corps of Engineers, 32pp.
- Saville, T. (1956), Wave run-up on shore structures. *Journal of the Waterways and Harbors Division*, 82 (WW2). American Society of Civil Engineers, 925-1 – 925-14.
- Saville, T. (1958), Wave run-up on composite slopes. *Proceedings of the 6th International Conference on Coastal Engineering*. American Society of Civil Engineers, 691-699.
- Schoonees, J.S. and Theron, A.K. (1993), Review of the field-data base for longshore sediment transport. *Coastal engineering*, 19, 1-25.
- Schoonees, J.S. and Theron, A.K. (1994), Accuracy and applicability of the SPM longshore transport formula. *Proceedings of the 24th International Conference on Coastal Engineering*. American Society of Civil Engineers, 2595-2609.
- Schoonees, J.S. and Theron, A.K. (1996), Improvement of the most accurate longshore transport formula. *Proceedings of the 25th International Conference on Coastal Engineering*. American Society of Civil Engineers, 3652-3665.
- Schulmeister, J. & Kirk, R.M. (1993), Evolution of a mixed sand and gravel barrier system in North Canterbury, New Zealand, during Holocene sea-level rise and still-stand. *Sedimentary Geology*, 87, 215-235.
- Scott, N. (2005), Estimating steep wave statistics using a wave gauge array. *Applied Ocean Research*, 27 (1), 23-38.

- Scripps Institute of Oceanography (1947), *A Statistical Study of Wave Conditions at Five Sea Localities Along the Californian Coast*. University of California Wave Report No. 68. LaJolla, California, 34pp.
- Shanehsaz-zadeh, A., Holmes, P. & Blewett, J. (2001), Swash-zone hydrodynamics on mild and steep beaches. *Proceedings of the 4th Conference of Coastal Dynamics*. American Society of Civil Engineers, 838-847.
- Sheng, Y.P., Cook, V., Peene, S., Eliason, D., Wang, P.F. & Scofield, S. (1989), A field and modeling study of fine sediment transport in shallow waters. *Estuarine and Coastal Modeling*, American Society of Civil Engineers, 113-122.
- Short, A.D. (1979), Wave power and beach stages: A global model. *Proceedings of the 16th International Conference on Coastal Engineering*, American Society of Civil Engineers, 1145-1162.
- Short, A.D. (1985), Rip current type, spacing and persistence, Narrabeen Beach, Australia. *Marine Geology*, 65, 47-71.
- Single, M.B. (1992), *High Energy Coastal Processes on Mixed Sand and Gravel Beaches*. Ph.D. thesis, Department of Geography, University of Canterbury, Christchurch, New Zealand, 220pp.
- Soulsby, R.L. (1997), *Dynamics of Marine Sands: A Manual for Practical Applications*. Thomas Telford Publications, London.
- Smith, J.M. (1991), *Wind-Wave Generation on Restricted Fetches*. Misc. Paper CERC-91-2, U.S. Army Engineer Waterways Experiment Station, 25pp.
- Speight, R. (1912), On a shingle spit in Lake Coleridge. *Transactions of the New Zealand Institute*, 45, 331-335.
- Speight, R. (1930), Lake Ellesmere Spit. *Transactions of the Royal Society of New Zealand*, 61 (1), 147-169.
- Speight, R. (1950), An eroded coastline. *Transactions of the Royal Society of New Zealand*, 78 (1), 3-13.
- Spence, C.M. (1996), *The Beach Morphology of a Volcanic Lake: Lake Rotorua*. M.A. thesis, Department of Geography, University of Canterbury, Christchurch, New Zealand, 134pp.
- Stansell, P., Wolfram J. & Zachary, S. (2003), Horizontal asymmetry and steepness distributions for wind-driven ocean. *Applied Ocean Research*, 25, 137-155.
- Stephen, W.J.M. (1974), *Wave Processes and Beach Responses on a Coarse Gravel Delta*. Ph.D. Thesis, Department of Geography, University of Canterbury, Christchurch, New Zealand, 395pp.
- Sturman, A.P., Fitzsimons, S.J. & Holland, L.M. (1985), Local winds in the Southern Alps, New Zealand. *Journal of Climatology*, 5, 145-160.

- Suggate, R.P. (1965), *Late Pleistocene Geology of the Northern Part of the South Island, New Zealand*. Department of Industrial and Scientific Research, Geological Survey Bulletin No. 77, 91pp.
- Sutton, R.G., Lewis, T.L. & Woodrow, D.L. (1970), Nearshore sediments in southern Lake Ontario, their dispersal patterns and economic potential. *Proceedings of the 13th Conference of Great Lakes Research*, 308-318.
- Swart, D.H. (1976), Predictive equations regarding coastal transport. *Proceedings of the 15th International Conference on Coastal Engineering*. American Society of Civil Engineers, 1113-1132.
- Swart, D.H. & Fleming, C.A. (1980), Longshore water and sediment movement. *Proceedings of the 17th International Conference on Coastal Engineering*. American Society of Civil Engineers, 1275-1294.
- T**
- Taylor, G. & Trageser, J.H. (1990), Directional wave and current measurements during Hurricane Hugo. *Proceedings of Marine Instrumentation '90*, 118-140.
- Thomas, R.L. (1973), The distribution of mercury in the sediments of Lake Huron. *Canadian Journal of Earth Sciences*, 10, 194-204.
- Tierney, B.W. (1977), Coastal changes around the Port of Timaru. *New Zealand Geographer*, 33 (2), 80-83.
- Tierney, B.W. & Kirk, R.M. (1978), Nearshore sediment movement around the Port of Timaru. *Proceedings of the 7th New Zealand Harbour Engineers Conference*. Harbours Association of New Zealand, 80-104.
- Ting, F.C.K. & Kirby, J.T. (1995), Dynamics of surf-zone turbulence in a strong plunging breaker. *Coastal Engineering*, 24 (3), 177-204.
- Tonk, A. & Masselink, G. (2005), Evaluation of longshore transport equations with OBS sensors, streamer traps, and fluorescent tracer. *Journal of Coastal Research*, 21 (5), 915-931.
- Trageser, J.H. & Elwany, H. (1990), The S4ADW: An integrated solution to directional wave measurements. *Proceedings of the 4th IEEE Working Conference on Current Measurement*, 1-15.
- Tucker, M.J. (1963), Analysis of records of sea waves. *Proceedings of the Institution of Civil Engineers*, 26, 305-316.

U

- United States Army Corps of Engineers (1992), *Coastal Littoral Transport*. U.S. Army Corps of Engineers, Engineer Manual EM 1110-2-1502, Washington DC, 143pp.

V

- Van der Meer, J.W. & Stam, C.M. (1992), Wave run-up on smooth and rock slopes of coastal structures. *Journal of Waterways, Port, Coast and Ocean Engineering*, 118 (5), 534-550.
- van Hijum, E. (1976), Equilibrium profiles and longshore transport of coarse material under oblique wave attack. *Proceedings of the 15th International Conference on Coastal Engineering*. American Society of Civil Engineers, 1258-1276.
- van Hijum, E., & Pilarczyk, K.W. (1982), Equilibrium profile and longshore transport of coarse material under wave attack. *Delft Hydraulics Laboratory*. Netherlands, Pub. No., 274.
- Van Wellen, E., Chadwick, A.J., Bird, P.A.D., Bray, M., Lee, M. & Morfett, J. (1997), Coastal sediment transport on shingle beaches. *Coastal Dynamics '97: Proceedings of the Conference on Coastal Dynamics*. American Society of Civil Engineers, 38-47.
- Van Wellen, E., Chadwick, A.J., Lee, M., Baily, B. & Morfett, J. (1998), Evaluation of longshore sediment transport models on coarse grained beaches: A preliminary investigation. *Proceedings of the 26th International Conference on Coastal Engineering*. American Society of Civil Engineers, 2640-2653.
- Van Wellen, E., Chadwick, A.J., Mason, T. (2000a), A review and assessment of longshore sediment transport equations for coarse-grained beaches. *Coastal Engineering*, 40, 243-275.
- Van Wellen, E., Baldock, T.E., Chadwick, A.J., Simmonds, D. (2000b), STRAND – A model for longshore sediment transport in the swash zone. *Proceedings of the 27th International Conference on Coastal Engineering*. American Society of Civil Engineers, 3139-3150.
- Voulgaris, G., Workman, M. & Collins, M.B. (1999), Measurement techniques of shingle transport in the nearshore zone. *Journal of Coastal Research*, 15 (4), 1030-1039.

W

- Waal, J.P. & Van der Meer, J.W. (1992), Wave runup and overtopping on coastal structures. *Proceedings of the 23rd Coastal Engineering Conference*. American Society of Civil Engineers, 1758-1771.
- Wang, P., Davis, R.A. & Kraus, N.C. (1998), Cross-shore distribution of sediment texture under breaking waves along low-wave-energy coasts. *Journal of Sedimentary Research*, 68 (3), 497-506.
- Warren, G. (1967), *Geological Map of New Zealand: Sheet 17, Hokitika (1st ed.)*. 1:250 000. Department of Scientific and Industrial Research, Wellington, New Zealand.
- Wassing, F. (1958), Model investigations on wave run-up carried out in the Netherlands during the past twenty years. *Proceedings of the 6th Coastal Engineering Conference*. American Society of Civil Engineers, 700-714.
- Watts, G.M. (1953), *A Study of Sand Movement at South Lake Worth Inlet, Florida*. U.S. Army Corps of Engineers, Beach Erosion Board Technical Memorandum No. 42, 24pp.
- Wild, C.J. & Seber, G.A. (2000), *Chance Encounters: A First Course in Data Analysis and Inference*. John Wiley & Sons, New York, 611pp.

- Wentworth, C.K. (1922), A scale of grade and class terms for clastic sediments. *Journal of Geology*, 34 (5), 377-392.
- Wood, W.L., Stockberger, M.T. & Madalon, L.J. (1994), Modeling beach and nearshore profile response to lake level change. *Journal of Great Lakes Research*, 20 (1), 206-214.
- Woodroffe, C.D. (2002), *Coasts*. Cambridge University Press, Cambridge, U.K., 623pp.
- Workman, M.H., Smith, J., Boyce, P., Collins, M.B. (1994), *Electronic Pebble Development (Vol. 1). The Need for and Development of a New Tracer Technique to Study Shingle Beaches: The Electronic Pebble System*. Technical Report 94/9/C. Department of Oceanography, University of Southampton, 77pp.
- Worthington, A. (1989), *Longshore Sediment Transport on a Glacial Lake: Coleridge*. M.A. thesis, Department of Geography, University of Canterbury, Christchurch, New Zealand, 149pp.
- White, T.E. (1998), Status of measurement techniques for coastal sediment transport. *Coastal Engineering*, 35 (1), 17-45.
- Wright, L.D., Chappell, J., Thom, B.G., Bradshaw, M.P. & Cowell, P. (1979), Morphodynamics of reflective and dissipative beach and inshore systems: Southeast Australia. *Marine Geology*, 32, 105-140.
- Wright, L.D. & Short, A.D. (1983), Morphodynamics of beaches and surf zones in Australia. In Komar, P.D. (ed.), *Handbook of Coastal Processes and Erosion*, pp35-64. CRC Press.
- Wright, P. (1982), *Aspects of the Coastal Dynamics of Poole and Christchurch Bays*. Ph.D. thesis, Department of Civil Engineering, University of Southampton, Southampton, U.K., 201pp.

Y

- Yamamoto, Y. & Horikawa, K. (1992), New methods to evaluate wave run-up height and wave overtopping rate. *Proceedings of the 23rd Coastal Engineering Conference*, ASCE, 1734-1747.

Z

- Zar, J.H. (1984), *Biostatistical Analysis*. 2nd Edition. Prentice-Hall, New Jersey, 718pp.
- Zenkovich, V.P. (1967), *Processes of Coastal Development*. Oliver and Boyd, Edinburgh, 738pp.
- Zyserman, J.A. (1992), A critical review of available data for calibration and/or verification of sediment transport models. *Proceedings of the 23rd International Conference on Coastal Engineering*. American Society of Civil Engineers, 2567-2580.
- Zyserman, J.A., Hedegaard, I.B., Fredsøe, J. & Deigaard, R. (1991), Requirements to a sediment transport model for morphological modelling. *Proceedings of the 2nd International Conference on Computer Modelling in Ocean Engineering*, 261-270.

